The role of Septin9 in myogenic differentiation

A Dissertation

Submitted in Partial Fulfilment of the

Requirements for the Degree of

Doctor rerum naturalium (Dr. rer. nat.)

to the Department of Biology, Chemistry, Pharmacy

of Freie Universität Berlin

by

VLADIMIR UGORETS

Berlin, 2024

This thesis was carried out during the period of June 2016 and September 2024 under the supervision of Prof. Dr. Petra Knaus, Institute of Chemistry and Biochemistry, Freie Universität Berlin.

First reviewer: Prof. Dr. Petra Knaus
Institut für Chemie und Biochemie
Freie Universität Berlin
Thielallee 63, 14195 Berlin
E-Mail: petra.knaus@fu-berlin.de

Second reviewer: Prof. Dr. Sigmar Stricker
Institut für Chemie und Biochemie
Freie Universität Berlin
Thielallee 63, 14195 Berlin
E-Mail: sigmar.stricker@fu-berlin.de

Date of disputation: 13th of December 2024

Statement of authorship

I hereby declare that I alone am responsible for the content of my doctoral dissertation and that I have only used the sources or references cited in the dissertation.

Berlin, den 24. September 2024

_____

Vladimir Ugorets

In your reflection

They live in you

Acknowledgement

As I reflect on the beginning of my doctoral studies, which now feels like a distant yet formative chapter in my personal and professional development, I find it challenging to distinguish the countless events that shaped me during this journey. It has been over a decade since I arrived as an undergrad student at the **Institute of Biochemistry** at the **Freie Universität Berlin**, an institution that welcomed me with its timeless values—Veritas, Iustitia, Libertas. While these virtues may seem idealistic to some, I am profoundly grateful to be part of an institution that upholds principles the world needs now more than ever. The Institute quickly became more than just a place of study or work; it became my second home, and my true *alma mater*. It supported me through significant moments in my life, from navigating the challenges of the Covid-19 pandemic to my naturalization in Germany (and the addition of another letter to my surname), as well as the troubling political instability in my home country, which has, at times, unsettled my peace of mind. Yet, through it all, the Freie Universität embodied its guiding principles by offering me the chance for growth rooted in truth, justice, and intellectual freedom, as its motto so proudly declares. Of course, institutions are defined by the people within them, and it is those people who made my doctoral studies so fulfilling. To them, I extend my deepest gratitude.

First and foremost, I would like to thank my doctoral mother, **Prof. Dr. Petra Knaus**. Petra, thank you for trusting me with this project and for knowing when and how to step in with just the right amount of support. You've been there for the good and the bad, like the time you said, "Vladimir, today was your worst performance," or celebrated with me on other occasions. Both meant a lot and helped me grow. Your enthusiasm for science, especially in the often complex field of signal transduction, is contagious. It may be a challenging craft to transduce so much passion for cell signaling itself, but you've managed to do it. Joking aside, I'm immensely grateful for your long-lasting support, even as my sprint turned into more of a marathon. Thank you for all the "go-for-it", guiding my ideas and septating them from spiraling into aimlessness, while always encouraging me to explore further. You've inspired me to see the beauty in biology, especially experimental work. I hope your kind and generous nature continues to guide many more students with this remarkable energy, and that you supervise as many students as there are grains of oat in a müsli box! Further, I would like to express my gratitude to my second reviewer, **Prof. Dr. Sigmar Stricker**. Thank you for generously sharing your expertise in developmental and muscle biology, and for always keeping your door open to hear my, at times, questionable ruminations. I have learned a great deal from you, and your insightful guidance has been invaluable to both my project and its publication. I'm especially grateful for the access to your group's wealth of know-how, which has truly propelled my research to new heights.

I would like to acknowledge the **SFB958**, **SFB1444** and the **Sonnenfeld Stiftung** for their generous funding, which enabled me to conduct my research and provided opportunities to enhance my soft skills and network with inspiring individuals. The access to multiple institutes and facilities in Berlin has been pivotal to the completion of my project, and I am deeply thankful to all the collaboration partners who contributed profoundly to my work. First, a heartfelt thanks to the **FMP Berlin** for the outstanding support I received. Special thanks to **Dr. Martin Lehmann** and the imaging facility for their invaluable help with imaging acquisition—those live-cell videos made it not only into the final cut of my paper but also into a special place in my memories. I also extend my gratitude to **Heike Stephanowitz** from the MS facility for your support. Additionally, I would like to thank **Prof. Dr. Michael Krauss** for providing smooth access to the institute during my brief time in his lab. Your guidance in

septin biology and our engaging discussions were invaluable. A special thanks to **Dr. Giulia Russo** for your assistance with weekend imaging sessions, knock-in cloning strategies, septin expertise, and so much more. Working on this project opened up a fascinating dive into the world of septins. I am deeply grateful to the international septin community and the Berlin Septin Club members for fostering such a stimulating, open, and welcoming environment, especially for early-career researchers. In this light, I want to give special recognition to few more local septinologists **Nadja Hümpfner**, **Dr. Markus Müller**, and **Prof. Dr. Helge Ewers** for their fruitful, often informal discussions that were enlightening and supportive. A heartfelt thanks goes to **Dr. Thomas Gronemeyer** and **Benjamin Grupp** for their warm hospitality in Ulm, for engaging discussions over long dinners, and for the "coral factory" backup plan, in case our research ever went off track. I owe immense gratitude to **Annette** and **Ernst-Martin Füchtbauer**. Although most of our interactions preceded this dissertation project, your guidance on myoblast cultures, mouse models, and your early advisory support were foundational. There are so many moments I am thankful for, but I remain with a quiet wish to disappear every time a certain bicycle at the Aarhus dormitory comes to mind. Furthermore, I am grateful to **Dr. Thorsten Mielke**, **Dr. René Buschow**, and **Beatrix Fauler** from the imaging facility at the MPI of Molecular Genetics for their help in establishing imaging and quantification processes—you are an incredible group of people. I also appreciate **Dr. Yannic Kerkhoff** from the FU Berlin for the support with image analysis and quantification.

This work would not have been possible without the tremendous contributions from both current and former colleagues of the Knaus lab. First and foremost, a heartfelt thank you to **Dr. Jerome Jatzlau**—it has been a true pleasure to work with you. I am deeply grateful for everything professional in the lab: your guidance, motivation, unwavering support, and belief in me. Your wide-ranging knowledge of scientific topics and quick thinking have been invaluable. Co-teaching alongside you was a highlight, and your drive for innovation and constant desire to improve will surely challenge traditional teaching methods for years to come. Beyond the lab, I also want to thank you for everything else—for the much-needed distractions, the game nights, legendary memes and inside jokes, lunches and dinners, as well as our small chats and deep conversations. Working with you has been an enriching experience in every sense. I would also like to extend my sincere gratitude to **Dr. Paul Mendez** for your invaluable support and contributions to my project. Your bioinformatics magic was something I could hardly grasp, but I am immensely thankful that you made things happen without bogging me down with complicated explanations. Your expertise made an enormous difference, and I'm grateful for your seamless execution. A big thank you goes to **Nurcan Haştar**—I honestly don't know where to begin. Thank you for your boundless optimism and unwavering support. It has been a true pleasure sharing an office with you. Many days were brightened by your kindness, listening to my endless complaints and responding with a smile. Everything always seemed better after talking to you, and I now realize how much of my whining you endured, especially during that long stretch of writing! If it were up to me, I'd commission a life-size statue of you for your patience and perseverance, placing it between Ernst Beckmann and Lise Meitner in front of the lecture hall. Hang in there—you're almost at the finish line! I want to extend my heartfelt thanks to **Sonja Niedrig** and **Branka Kampfrath** for doing the essential work that keeps the lab running smoothly – it's truly appreciated. I also acknowledge the invaluable administrative support provided by **Isabella Mahlke**, and formerly, **Katharina Hoffman**. I'm grateful to all the current and former members of AG Knaus for creating such a warm, stimulating, and fun work environment that made every day a pleasure. Special thanks to **Nadine Großmann**, **Yunyun Xiao**, **Mounir Benamar**, **Wiktor**

Burdzinski, **Mustafa Ilhan**, **Leon Obendorf**, **Lion Raaz**, and **Michael Trumpp** for giving the lab its unique and pleasant character. I also thank former members **Dr. Martina Fischer**, **Dr. Gina Dörpholz**, **Dr. Maria Reichenbach**, **Dr. David Yadin**, **Dr. Christian Kähler** and **Dr. Christian Hiepen** for sharing their time and experiences in the lab. A big thank you goes to **Dr. Susanne Hildebrandt** - it was a true pleasure working alongside you, sharing an office, having long conversations, and enjoying off-lab activities together. To all my former students - **Andreas Lenk**, **Lara Gutsche**, **Jerry Chan**, **Jegor Velitski**, **Dr. Alexander Stockhammer**, **Dmitrii Zagrebin**, **Mariya Martiyenko**, and **Olena Grebenchuk** - I was honored to supervise such brilliant individuals. You often showed potential far beyond my own, leaving me with little else to teach. I'm grateful for what I learned about my project and myself during those times of mentorship.

Shifting one floor down in the institute, I'd find more amazing people to acknowledge - the full ensemble of Stricktastics. **Dr. Pedro Vallecillo-García**, thank you for your support with FACS sorting and your calm, reassuring presence. **Dr. Xiaoyan Wei** and **Dr. Arunima Murgai**, I'm grateful to both of you for your insights, experimental advice, and thought-provoking discussions. To the ever-energetic **Dr. Sophie Pöhle-Kronawitter**, thank you for being such a wonderful friend and colleague. You always saw through the irony and silliness and still laughed with us! I admire your dedication to everything you do, and I've always appreciated that I could drop into your office for a chat, whether lighthearted or serious. You made workdays so much brighter. **Dr. Georgios Kotsaris**, words hardly do justice to how much gratitude I feel towards you. Obviously, thank you for the scientific contribution to my project and for all the time spent together at the bench, which I now come to value even more. But primarily, thank you for everything outside the lab – the laughter, the conversations, the friendship. As the great Socrates (or was it George?) once mused, "true friendship binds two souls in a single body, so when one soul earns its degree, the other must follow, even if reluctantly". I'm deeply thankful for the chance to have crossed paths with you, and I'm so lucky to call you a friend.

A heartfelt shout-out goes to all my friends—both within the scientific world and beyond it, scattered across different countries—who have rooted for me in their own ways, each one perfect. **Dr. Mathias Girbig**, thank you, buddy, for always being there. **Dr. Ando Zehrer**, it's always a blast with you, no matter the format—though I still can't quite grasp the rugby rules! My dear **Tamir Cohen**, your directness and beautiful voice are like a ray of sunshine—thank you for brightening my days. A big thank you to my **Italian in-law friends**, who welcomed me into their circles and, thankfully, don't seem to regret it yet. And to my **cherished friends in Russia**, though distance and circumstances may have stretched our ties, every conversation takes me down a treasured memory lane, keeping me connected to the past, no matter what the future holds.

And finally, a deep expression of gratitude goes to **my family**. I've promised them I'd become a doctor for as long as I can remember, and though the twist might work in many languages I know, the disappointment among the adults is still tangible that I won't be a "real doctor". But they'll manage. **Мам**, спасибо for always supporting me and believing in me. You and **папа** saw a path for us long before I did, even as you navigated your own struggles during the rubble crisis. I still remember you taking my hand and bringing me to school on my first day, and now, you're ready to pick me up, as I walk out with a degree. I'm sad that both grandmas missed my promises of a timely graduation, as they were my самая искренняя группа поддержки. You cannot choose your family, but if I could, I would choose my brother **Victor** every time. I haven't been the easiest sibling with constant disappearances into the lab, but I couldn't have walked this path without you. Thank you and **Tamar** for the wonderful new

addition to the family and for making me Uncle Vladimir to **little Ben**. Cari **Adele** and **Michele**, grazie a voi for welcoming me into your family, radiating the warm Italian spirit, and for all the journeys we've shared- whether on foot, in cars, or in gommone, the adventures were always unforgettable. And lastly, to the most special person in my acknowledgments and my heart, **Giulia Russo**. Words fall short when it comes to expressing how much you mean to me. I could easily thank you in every section of this thesis- as a collaborator, colleague, friend and family member- and your influence is felt on every page. Your contributions are immeasurable. As Hemingway would put it "thank you". Ti voglio bene, my love.

Thank you for making it through this short version of my acknowledgments, trimmed for space but still bursting with gratitude. The full, unabridged version—likely to be the cheesiest memoir in human history—will be written when I'm old, and I'll be sure to send you a copy for your library (or shredder).

I hope I'll have the chance to repay your kindness and support someday.

With gratitude,
Vladimir

Contents

List of figures

List of tables

Summary

The formation, maintenance, and regeneration of skeletal muscle tissue depend on the interplay between muscle progenitor cells, known as myoblasts, and other local cell populations. Successful myogenesis requires precise regulation of multiple cellular processes, culminating in the formation of myofibers, multinuclear contractile syncytia from myoblasts. Proliferating myoblasts migrate to the muscle formation region, adhere to each other, express terminal differentiation markers, and eventually fuse their cytoplasmic contents. These processes are characterized by dynamic alterations in cytoskeletal architecture. The cytoskeleton comprises polymerizing proteins such as microfilaments, microtubules, intermediate filaments, and septins, forming an interconnected network of filaments. While the roles of actin, tubulin, and intermediate filaments are well studied, septins have only recently begun to emerge in the myogenic context.

In my thesis, I investigated the expression and organization of septin paralogues in dividing and differentiating myoblasts, describing septins as a necessary component of the myoblast cytoskeleton. I propose the existence of septin octamers in myoblasts consisting of Septin2-7-11 and 9, with Septin9 undergoing substantial changes in expression. Septin9 mRNA is induced as quiescent cells transition to activated progenitors in regenerating mouse muscle and is downregulated by the end of the regenerative process. Septin9 mRNA and protein expression were also reduced during *in vitro* differentiation in C2C12 and primary myoblasts. Cycling myoblasts incorporate Septin9 into actin-decorating septin filaments that form primarily near the nucleus, in close proximity to the plasma membrane. However, these filaments undergo substantial reorganization after myogenic differentiation is induced. I observed that a fraction of Myogenin-positive cells exhibits short, curved septin rods and filament remnants, with no co-localization with actin filaments. This reorganization potentially coincides with the accumulation of muscle specific actin and myosin proteins. These findings were confirmed via live-cell microscopy using an endogenously tagged eGFP-Septin9 C2C12 cell line. Furthermore, nascent myotubes showed septin filaments extending across the perinuclear area in the basal plane, while the rest of the sarcoplasm contained filamentous remnants and rings. Mature myotubes, which exhibit sarcomeric actin organization, were mostly devoid of septin structures.

SiRNA-mediated depletion of Septin9 resulted in the disruption of septin filaments and in a premature transition from proliferating to committed transcriptional signature in C2C12 and

primary myoblasts, as evident from RNASeq analysis. Additionally, Septin9-deficient myoblasts showed signs of premature cell cycle exit, increased apoptosis, and a precocious onset of myogenic differentiation during *in vitro* differentiation.

Taken together, my findings establish Septin9 as a critical regulator of myoblast differentiation during the initial commitment phase. We propose that filamentous septin structures are part of a temporal regulatory mechanism governing myogenic differentiation, with their reorganization marking the progress of unfolding myoblast differentiation.

Zusammenfassung

Die Bildung, Erhaltung und Regeneration von Skelettmuskelgewebe hängt vom Zusammenspiel zwischen Muskelvorläuferzellen, den sogenannten Myoblasten, und anderen lokalen Zellpopulationen ab. Eine erfolgreiche Myogenese erfordert eine präzise Regulation mehrerer zellulärer Prozesse, die schließlich zur Bildung multinukleärer kontraktiler Synzytien aus Myoblasten führt. Proliferierende Myoblasten wandern in die Region der Muskelbildung, haften aneinander, exprimieren terminale Differenzierungsmarker und vereinigen schließlich ihre zytoplasmatischen Inhalte. Diese Prozesse sind durch dynamische Veränderungen in der Zytoskelettarchitektur gekennzeichnet. Das Zytoskelett besteht aus polymerisierenden Proteinen wie Mikrofilamenten, Mikrotubuli, Intermediärfilamenten und Septinen, die ein miteinander verbundenes Netzwerk von Filamenten bilden. Während die Rollen von Aktin, Tubulin und Intermediärfilamenten gut untersucht sind, treten Septine erst in jüngster Zeit im myogenen Kontext in den Vordergrund.

In meiner Dissertation habe ich die Expression und Organisation von Septin-Paralogen in teilenden und differenzierenden Myoblasten untersucht und beschrieben, dass Septine eine notwendige Komponente des Myoblasten-Zytoskeletts darstellen. Ich schlage vor, dass in Myoblasten Septin-Oktamere existieren, die aus Septin2-7-11 und 9 bestehen, wobei Septin9 erhebliche Veränderungen in der Expression durchläuft. Septin9-mRNA wird induziert, wenn ruhende Zellen in aktivierte Vorläuferzellen in regenerierendem Mausmuskel übergehen, und am Ende des Regenerationsprozesses herunterreguliert wird. Die Expression von Septin9-mRNA und -Protein wurde auch während der *in vitro* Differenzierung in C2C12-Zellen und primären Myoblasten reduziert.

Proliferierende Myoblasten integrieren Septin9 in aktin-dekorierende Septinfilamente, die hauptsächlich in der Nähe des Zellkerns, in unmittelbarer Nähe zur Plasmamembran, gebildet werden. Diese Filamente unterliegen jedoch nach der Induktion der myogenen Differenzierung einer erheblichen Reorganisation. Ich beobachtete, dass ein Teil der Myogenin-positiven Zellen kurze, gebogene Septin-Stäbchen und Filamentreste aufweist, die nicht mit Aktinfilamenten kolokalisiert sind. Diese Reorganisation könnte möglicherweise mit der Akkumulation von muskelspezifischen Aktin- und Myosinproteinen zusammenfallen. Diese Befunde wurden durch Lebendzellmikroskopie mit einer endogen markierten eGFP-Septin9 C2C12-Zelllinie bestätigt. Darüber hinaus zeigten neu entstehende Myotuben Septinfilamente, die sich im basalen Bereich über den perinukleären Bereich erstreckten,

während der Rest des Sarkoplasmas filamentöse Reste und Ringe enthielt. Reife Myotuben, die eine sarcomerische Aktinorganisation aufweisen, waren größtenteils frei von Septinstrukturen.

Die siRNA-vermittelte Depletion von Septin9 führte zur Disruption der Septinfilamente und zu einem vorzeitigen Übergang von einem proliferativen zu einem differenzierten transkriptionellen Signaturprogramm in C2C12- und primären Myoblasten, wie aus der RNASeq-Analyse hervorgeht. Darüber hinaus zeigten Septin9-defiziente Myoblasten Anzeichen eines vorzeitigen Zellzyklusaustritts, erhöhter Apoptose und eines verfrühten Beginns der myogenen Differenzierung während der *in vitro* Differenzierung.

Zusammengefasst belegen meine Ergebnisse, dass Septin9 ein kritischer Regulator der Myoblastendifferenzierung in der initialen Commitment-Phase ist. Wir schlagen vor, dass filamentöse Septinstrukturen Teil eines zeitlich regulierten Mechanismus sind, der die myogene Differenzierung steuert, wobei ihre Reorganisation den Fortschritt, der sich entfaltenden Myoblastendifferenzierung markiert.

1. Introduction

1.1. Skeletal muscle: A hallmark of youth

The timeless desire for eternal life has captured the imagination of artists, storytellers and thinkers across cultures and epochs. From the ancient Epic of Gilgamesh to modern tales of immortal cells of Henrietta Lacks, the quest for perpetual youth echoes through myth and reality alike. Whether depicted as blessed like the mythological Phoenix or cursed like the Wandering Jew, painted dancing across the basin of the Fountain of Youth or immortalized in the lyrics of Bob Dylan's iconic song, our collective fascination with immortality persists, across literature, music, art, and folklore, transcending cultural boundaries. In contemporary discourse, the fascination has evolved into a focus on longevity and the broader public health implications of a rapidly aging global population. This preoccupation is likely to endure, especially considering projections from the World Health Organization (WHO) indicating that the number of individuals aged 60 and above will exceed 2 billion by 2050. This marks a substantial increase from the 600 million recorded in 2000 (www.who.int/health-topics/ageing, 2023). Additionally, it is anticipated that a significant portion of children born after 2000 in developed nations like Germany, Italy, France, Japan and USA will live to become centenarians (Christensen et al., 2009). Advancing age is characterized by reduced regenerative capacity, exhaustion of the stem cell pool and progressing skeletal muscle weakness (Brotto and Abreu, 2012; López-Otín et al., 2013). These hallmarks coupled with chronic metabolic and muscle associated diseases significantly impact quality of life (Conboy et al., 2005; Granic et al., 2023; Koopman and van Loon, 2009; López-Otín et al., 2013). Overcoming these challenges and promoting healthy aging to sustain mobility and preserve quality of life is a persistent scientific endeavor (McGregor et al., 2014). In this context, the study of skeletal muscle biology remains imperative for the understanding and addressing the complexities of aging and promoting healthy longevity in the future.

1.2. Adult skeletal muscle architecture

Skeletal muscle, is one of the biggest organs in human body, constitutes approximately 40% of lean body mass, slightly higher in males and a little less in females (Janssen et al., 2000). With about 640 individual muscles it functions as a biomechanical device crucial for various

physiological roles including voluntary contraction, force generation and motion (Mukund and Subramaniam, 2020). Moreover, it accounts for 30-50% of overall body protein turnover, rendering it particularly responsive to physiological triggers such as growth factors, nutritional status, hormones, exercise, and injury. Beyond its metabolic role and heat production, skeletal muscle exhibits high energy demands and susceptibility to fatigue. The basic contractile units, known as sarcomeres, generate force that transmits via tendons to bones. This organization of muscle fibers and diverse connective tissue highlights the well-described architecture of the tissue (Gillies and Lieber, 2011).

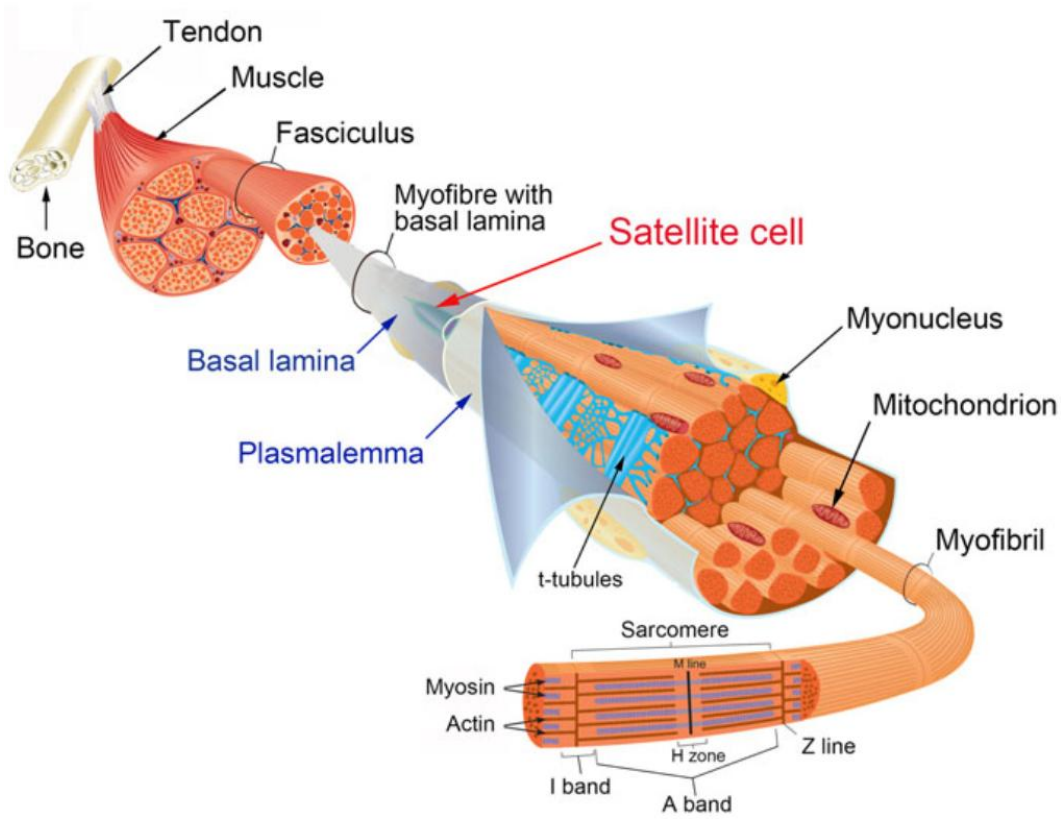

Figure 1-1. Skeletal muscle ultra-structure
A scheme depicting the musculoskeletal system comprising of bone, muscle and connective tendons. Skeletal muscle is composed of muscle cells, cylindrical myofibers that house intracellular organelles and contractile units, called sarcomeres. Muscle-resident stem cells (satellite cells) reside at the periphery of myofibers beneath the basal lamina- an extracellular matrix layer. These individual fibers aggregate into fascicles and fascicle bundles, all ensheathed by distinct connective tissue layers: endomysium, perimysium, and epimysium. The epimysium connects the overall ultrastructure to tendons (adapted from (Relaix and Zammit, 2012), originally from (Tajbakhsh, 2009)).

Individual muscle fibers, which are multinucleated and post-mitotic, house intracellular organelles, including the contractile machinery. Enveloping these fibers is an extracellular matrix layer called basal lamina, further enclosed by a connective tissue layer known as

endomysium. Bundles of fibers, called fascicles, are surrounded by perimysium, while an individual muscle is ultimately ensheathed into epimysium (Frontera and Ochala, 2015; Mukund and Subramaniam, 2020) (Fig. 1-1).

1.3. Embryonic origin of skeletal muscle

Skeletal muscle development initiates in transient embryonic structures termed somites, which arise from the paraxial mesoderm – a tissue forming during gastrulation and embryonic axis elongation (Fig. 1-2). The paraxial mesoderm subdivides into an immature posterior presomitic mesoderm and a committed anterior region, from which somites emerge, ultimately giving rise to multinucleated myofibers (Chal and Pourquié, 2017). The subsequent specification and differentiation of the paraxial mesoderm into somites, are processes tightly regulated by gradients of fibroblast growth factor (FGF), Wingless and Int-1 (WNT) and bone morphogenetic protein (BMP) signaling (Ciruna and Rossant, 2001; Reshef et al., 1998). Further regulation is achieved through the segmentation clock, a molecular oscillator mechanism (Hubaud and Pourquié, 2014). In brief, receding concentration thresholds (called determination front) for Notch, WNT and FGF deriving from the posterior tail region, is counteracted by specification- inducing retinoic acid (RA) produced in the anterior segment (Aulehla and Pourquié, 2008). This mechanism guides the transformation of the mesodermal structure toward somite development.

Freshly formed somites undergo dorsoventral segmentation, giving rise to the dorsal epithelial dermomyotome structure. In response to WNT, BMP and sonic hedgehog (Shh) signaling, the initial uncommitted cell populations within the dermomyotome become directed toward distinct somitic fates (Yusuf and Brand-Saberi, 2006). These nascent progenitor cells express the early myogenic factor paired-homeobox 3 (Pax3), while the dermomyotome subdivides further (Gros et al., 2005). Shortly after dermomyotome establishment, cells transition to expressing Myogenic factor 5 (Myf5) (Ott et al., 1991) and downregulating Pax3 (Bober et al., 1994), marking the formation of the myotome, a ventrally located cell layer in respect to the dermomyotome (Chal and Pourquié, 2017). Development of the myotome corresponds with appearance of first postmitotic cells called myocytes, characterized by the expression of specialized myogenic proteins such as cytoskeletal proteins slow (Myh7) and embryonic myosin heavy chains (*Myh3*), α-actin (*Acta1*), desmin (*Des*) (Babai et al., 1990; Lyons et al., 1990) and an enzyme carbonic anhydrase III (*Car3*)

(Tweedie et al., 1991). Additional Pax3^{+} cells migrate from the dermomyotome and integrate into the myotome, where they subsequently undergo fusion to generate first myofibers (Gros et al., 2005). Migration of those cells into the limb bud sets the stage for the eventual development of limb muscles (Buckingham et al., 2003). This foundational myogenic process is regulated by a network of muscle regulatory factors (MRF) consisting of Myf5, Myogenic determination protein 1 (Myod1), Mrf4 and Myogenin (the MRFs are introduced in detail in chapter 1.4.2) (Berkes and Tapscott, 2005; Chal and Pourquié, 2017).

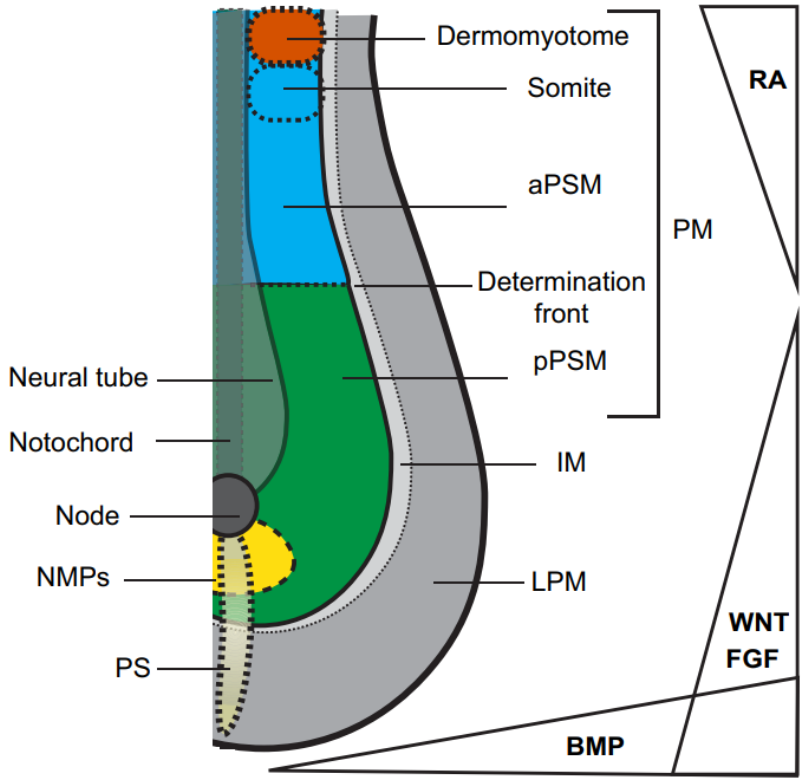

Figure 1-2. Embryonic origin of somites
An illustration of spatial organization of mesoderm development within the embryo's posterior region. Mesoderm subtypes - paraxial mesoderm (only in this figure indicated as PM), intermediate mesoderm (IM) and lateral plate mesoderm (LPM)- emerge progressively during development. Signaling gradients, including BMP, retinoic acid, WNT and FGF drive mesoderm patterning as depicted on the right side. Initial embryonal axis elongation (from top to bottom in this representation) is concomitant with the emergence of neuromesodermal progenitors (NPMs) constituting the first paraxial mesoderm progenitors. The determination front, a WNT/FGF signaling gradient, is countered by retinoic acid, partitioning the nascent mesoderm into anterior presomitic mesoderm (aPSM) and immature posterior presomitic mesoderm (pPMS). Subsequent somite formation occurs in the anterior region, differentiating into dermomyotome and myotome, culminating later in skeletal muscle generation. Mesodermal subtypes are color-coded. Axial mesoderm includes the neural tube, notochord and node. Mesoderm initially forms at the primitive streak (PS) level. Presented from dorsal view (modified from (Chal and Pourquié, 2017)).

1.4. The paradigm of myogenesis

Muscle development is a complex process involving several stages: the emergence of mesenchymal progenitors, their specification into myoblasts, the subsequent commitment of myoblasts and their cell cycle arrest, the fusion of myoblasts to multinucleated myotubes, and ultimately the maturation of myofibers (Bentzinger et al., 2012). This myogenic process can be subdivided into embryonic, fetal and adult phases.

1.4.1. Embryonic, fetal, and neonatal myogenesis

In mice, the initiation of somitogenesis takes place at embryonic day 8 (E8), generating distinct paraxial mesoderm segments that promptly differentiate into dermomyotome (Aulehla and Pourquié, 2008). By day E10.5, $Pax3^+$ cells from the dermomyotome delaminate, migrate ventrally and fuse to form the initial muscles of the primary myotome. This embryonic or primary phase of myogenesis persists until E14.5 (Buckingham and Relaix, 2007). Subsequently, during secondary or fetal myogenesis (E14.5-E17.5) $Pax3^+$ cells start expressing Pax7 and fuse either with each other or preformed primary myotubes, leading to formation of secondary fibers (Biressi et al., 2007a; Buckingham and Relaix, 2007). Primary and secondary fibers differ from each other expressing various sets of metabolic enzymes and structural proteins including specific myosins (Schiaffino and Reggiani, 2011). Formation of the basal lamina towards the end of the secondary myogenesis (E17) marks maturation of fibers and the emergence of satellite cells, a $Pax7^+$ cell pool residing uniquely between basal lamina and sarcolemma of myofibers (Relaix et al., 2005) (Fig. 1-3).

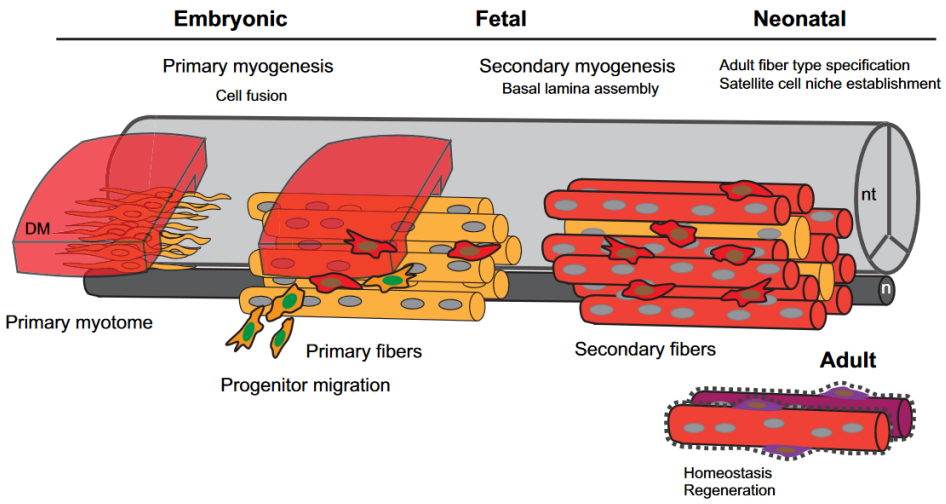

Figure 1-3. Stages of skeletal myogenesis
An illustration depicting dermomyotome (DM) development. Early myotome is comprised of primary myocytes (yellow) forming the initial muscles. In the primary myogenesis phase, $Pax3^{+}$ cells (yellow, middle panel) delaminate from DM and form primary myofibers. During secondary myogenesis, $Pax7^{+}$ cells (red middle and right panel) give rise to secondary myofibers (red, right panel). During this stage, some Pax7+ cells position beneath the nascent basal lamina, constituting a stem cell pool. nt- notochord, n- neural tube. (modified from (Chal and Pourquié, 2017)).

1.4.2. Genetic network controlling the progression of the myogenic lineage

The sine oculis–related homeobox 1 (*Six1*) and *Six4* are transcription factors that govern the whole cascade directing dermomyotomal progenitors toward myogenic lineage, and regulate expression of crucial transcription factors involved into developmental steps of myogenesis (Bentzinger et al., 2012; Grifone et al., 2005).

Next level of genetic hierarchy is regulated by *Pax3* and *Pax7* transcription factors that drive specification of myogenic progenitors. *Pax3* expression is detected in presomitic mesoderm at E8.5, while *Pax7* expression initiates in somites at E9 (Boudjadi et al., 2018; Kassar-Duchossoy et al., 2005). *Pax3* loss-of-function mutation inhibits formation of limb muscle among other defects (Bober et al., 1994). Specific ablation of *Pax3* lineage using Pax3-cre driver led to embryonic lethality, while Pax7 lineage depletion lead to defects in later stages of development (Hutcheson et al., 2009). Therefore, it is believed that Pax3-positive cells form a template of initial fibers, to which Pax7-positive cells contribute forming secondary fibers and the satellite cell pool, during secondary myogenesis (Bentzinger et al., 2012; Maqbool and Jagla, 2007).

The terminal specification of mesodermal progenitors is regulated by sequential activation of the basic helix-loop-helix (bHLH) myogenic regulatory factors (MRFs): Myf5, Myod1,

Myogenin and Mrf4 (Hernández-Hernández et al., 2017). These factors bind DNA through their basic domain utilize the helix-loop-helix motif to heterodimerize with E proteins. E proteins mediate binding to E boxes (CANNTG), regulatory cis elements found in promoters of muscle specific genes (Massari and Murre, 2000). Myod1 was the first MRF recognized to possess the ability to reprogram fibroblasts into myogenic cells (Davis et al., 1987; Lassar et al., 1986). Myf5 is the first MRF transiently upregulated in the paraxial mesoderm and later together with others MRFs during myotome formation (E10.5) (Buckingham, 1992). Shortly after Myf5, Myod1 is expressed, and both of them are involved into commitment and proliferation of myogenic cells, upstream of Myogenin and Mrf4 (Hernández-Hernández et al., 2017). Subsequently Myogenin (E11.5) and Mrf4 (E13.5) are expressed, guiding terminal differentiation and trigger the expression of myotube-specific genes (Buckingham and Relaix, 2007) (Fig. 1-4).

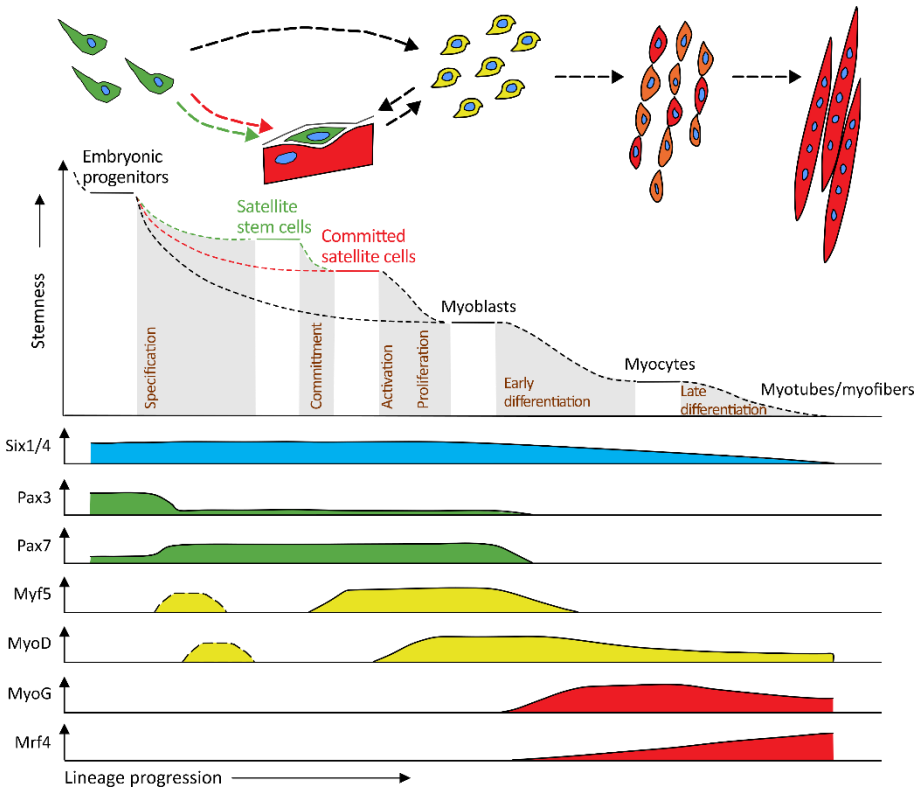

Figure 1-4. Transcription factors orchestrating myogenic lineage progression
Embryonic muscle progenitors give rise to initial myoblasts and establish a pool of postnatal stem cells. Committed stem cells retain the capacity to return to a quiescent state. Early lineage specification is governed by Six1, Six4, Pax3 and Pax7. Myf5 and Myod1 commit myoblasts, while myogenin (MyoG) and Mrf4 orchestrate late-stage differentiation, fusion and myotube formation. Modified from (Bentzinger et al., 2012).

1.4.3. Skeletal muscle stem cells

Skeletal muscle stem cells (MuSCs) play vital roles in the neonatal growth of skeletal muscle and regenerative process in adult organism. They were first described by Alexander Mauro in 1961 as cells possessing their own plasmalemma while sharing the basal lamina of the myofiber (Mauro, 1961). Mauro suggested their involvement in muscle regeneration, providing a source for fiber repair. These MuSCs originate from mesodermal progenitors of the embryonic dermomyotome and commit to myogenic fate during embryogenesis (Lepper and Fan, 2010). In the adult state, satellite cells remain in a quiescent state and reside in a specialized, polarized microenvironment referred to as the stem cell niche (Yin et al., 2013). The basal side of the cell makes close contact with the basal lamina and specifically expresses laminin receptor α7β1 integrin. In contrast, the apical side, adjacent to the myofiber, is enriched in the cell adhesion molecule (CAM) M-cadherin (Kuang et al., 2007). Studies involving the isolation and cultivation of single live myofibers have revealed that quiescent MuSCs can be activated, leading to proliferation and differentiation, ultimately resulting in the generation of new myofibers (Bischoff, 1986). This process is controlled by sequential expression of transcription factors, closely resembling the commitment and differentiation process observed during embryonic and fetal development (Schmidt et al., 2019) (Fig. 1-5).

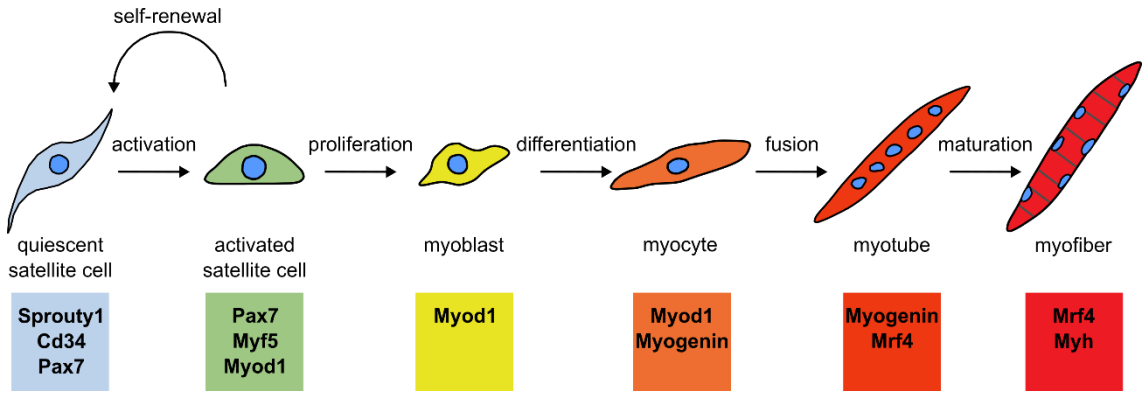

Figure 1-5. Transcription factor and marker expression during satellite cell activation, proliferation, differentiation, fusion and maturation
In the quiescent state, satellite cells express *Pax7* and reside in G0 phase of the cell cycle. Muscle injury or damage to the basal lamina triggers their activation, causing them to re-enter the cell cycle. Proliferating cells begin expressing *Myod1* and *Myf5*. They can choose to return to quiescence, maintaining the stem cell pool, or continue expanding as myoblasts. Myoblasts commit to myogenic differentiation, marked by the expression of *Myogenin*, exiting the cell cycle, while downregulating *Pax7* and *Myf5*. Differentiated myocytes subsequently express *Mrf4* and late myogenic marker proteins such as myosin heavy chain (*Myh*). They fuse either with each other or pre-existing myofibers, contributing to muscle regeneration or the formation of new myofibers. The process concludes with maturation and hypertrophy, which are regulated by *Mrf4*. Modified from (Schmidt et al., 2019).

Tissue-specific or adult stem cells poses the unique capability to both self-renew and differentiate into specialized cells (Wosczyna and Rando, 2018). The MuSCs are classified as adult stem cells due to their capacity for both generating proliferating progeny to repair injured muscle fibers and efficiently self-renew, although this ability tends to diminish with age (Chakkalakal and Brack, 2012). Satellite cells exhibit heterogeneity across various characteristics. All SCs express Pax7, and depleting of Pax7 results in a reduced number of SCs, early postnatal lethality, and absence of injury induced muscle regeneration (Lepper et al., 2011; Seale et al., 2000). However, studies using mouse models like Myf5-Cre reporter mice (Myf5-Cre/ Rosa-YFP) have demonstrated that approximately 10% of Pax7+ cells have never expressed Myf5 (Kuang et al., 2007). Additionally, investigations using Pax7-nGFP mouse line have revealed subpopulations of SCs with varying levels of Pax7 expression, distinguishing between $Pax7^{high}$ and $Pax7^{low}$ expressing cells. Notably, $Pax7^{high}$ cells exhibit a delayed entry into the cell cycle compared to $Pax7^{low}$ cells (Rocheteau et al., 2012). Furthermore, a subset of $Pax7^{high}$ cells segregates template DNA specifically to one of the daughter cells during asymmetric cell division (Rocheteau et al., 2012), a phenomenon first described by Shinin and colleagues (Shinin et al., 2006). Studies on satellite cells within cultured isolated myofibers have elucidated two types of cell division: symmetric and asymmetric. Symmetric division occurs along the plane perpendicular to the muscle fiber axis (a planar division mode) resulting in two identical cells, that can enter quiescence or commit to the myogenic lineage. In contrast, asymmetric division which is oriented basal-apically, yields distinct progeny. One cell, closer to basal lamina, exits the cell cycle to replenish the stem cell pool, while the other commits to the myogenic program (Kuang et al., 2007).

In addition to DNA strand segregation, organelles, signaling molecules, receptors and other determinants of cell fate exhibit a binary distribution during asymmetric cell division. Multiple signaling pathways, including the Notch pathway, have been implicated in the control of asymmetric cell division (Wen et al., 2012), with Notch effectors like Notch3 and Dll1 shown to asymmetrically segregate to satellite daughter cells (Kuang et al., 2007). Further evidence suggests that the Notch inhibitor Numb becomes preferentially enriched in one of daughter cells (Shinin et al., 2006). Numb, functioning as an intracellular adaptor protein, polarization agent and cell fate determinant, recruits E3 ubiquitin ligase Itch to the Notch1 receptor, priming it for degradation (George et al., 2013; Ortega-Campos and García-Heredia, 2023). It is noteworthy that although approximately 90% of satellite cells that segregate template DNA

also cosegregate Numb, it is unlikely that Numb directs this process, rather these processes are likely coregulated (Shinin et al., 2006). Additionally, the regulation of cell polarity through proteins involved in asymmetry breaking, such as Par, Numa and Dystrophin, plays a critical role in asymmetric cell division in satellite cells (Dumont et al., 2015; Troy et al., 2012; Hirth, 2013). Striking the right balance between self-renewal, expansion and differentiation is fundamental for maintaining the stem cell pool and ensuring an adequate supply of material for muscle repair and homeostasis.

1.4.4. Postnatal myogenesis

During the initial three weeks of murine growth, body size increases approximately eight-fold, with skeletal muscle contributing significantly to this growth, accounting for about 50% of the increase (Gokhin et al., 2008). Although the total number of myofibers is established between E18 and birth, the number of nuclei and the radial size of fibers continue to rapidly increase until slowing down after postnatal day 21 (Ontell et al., 1984; White et al., 2010). Postnatal muscle growth primarily results from the fusion of $Pax7^{+}$ satellite cells into the myofibers and sustained anabolic hypertrophy until adulthood. At birth, SCs represent around 30% of all sub-laminal nuclei in skeletal muscle (Allbrook et al., 1971). However, during the early postnatal period, the relative proportion of SCs drops to about 3%, a number that further decreases with age (Ontell et al., 1984; Sousa-Victor et al., 2014). Adult muscles exhibit a consistent SC density, indicating tight regulation of this process (Boldrin and Morgan, 2012). The radial growth, or hypertrophy of myofibers involves an increase in both the size and number of myofibrils. There is a positive correlation between the myonuclear accretion and myofiber volume (Pizza and Buckley, 2023). Skeletal muscle mass depends on the balance between anabolic protein synthesis and catabolic protein degradation, which can lead to muscle atrophy. Various signaling pathways control this balance. Negative control of protein synthesis is primarily achieved through the Myostatin-Smad2/3 pathway, while Igf1-Akt-mTOR acts as a principal positive regulator (Schiaffino et al., 2013). Insulin-like growth factor 1 (Igf1) activates Akt in a PI3K-dependent manner, which, in turn, activates mammalian target of rapamycin (mTOR) to stimulate protein synthesis through downstream effectors. Myostatin (*Mstn*), a Transforming growth factor beta (TGFβ) family ligand, binds to cell surface receptors and activates Smad2/3 transcription factors, which inhibit mTOR pathway and stimulate protein degradation via activation of specific E3 ubiquitin ligase Atrogin 1

(Sartori et al., 2014). Muscle loss is typically regulated by atrogenes or atrophy-related genes that mediate protein degradation through proteasomal and lysosomal pathways. Forkhead box O (FoxO) transcription factors are the primary regulator of muscle protein turnover, activating expression of E3 ubiquitin ligases such as Atrogin-1 and Muscle RING finger 1 (MuRF1). These ligases control the half-lives of many structural proteins. Notably, Akt can phosphorylate and inhibit FoxO, representing an intricate fine-tuning network that regulates muscle protein turnover (Schiaffino et al., 2013).

1.4.5. Muscle regeneration

Skeletal muscle possesses a remarkable capacity for regeneration. Daily activities can result in minor muscle fiber damage, which is effectively repaired intrinsically by patching the membrane using intracellular vesicles. This process relies on Dysferlin expression (Bansal et al., 2003). In response to more significant traumatic damage caused by factors like strenuous exercise, myotoxins, or genetic disorders leading to muscle degeneration, muscle tissue goes through a process of destruction and reconstruction. This process can be further divided into distinct phases, including necrosis, inflammation, regeneration, maturation and functional recovery (Forcina et al., 2020). The initial phase involves the necrosis of damaged fibers, characterized by the release of intracellular materials, including calcium, leading to proteolytic degradation (Forcina et al., 2020). The innate immune system acts as a first responder, recruiting inflammatory cells through chemotaxis within seconds of muscle injury (Yang and Hu, 2018). Neutrophils are among the first immune cells to invade the site of lesion, secreting enzymes, oxidative factors, chemokines, and pro-inflammatory signals like Tumor necrosis factor-α (TNF-α), Interferon-γ (IFN-γ) and Interleukin-1β (IL-1β). The next phase of regeneration is marked by the infiltration of pro-inflammatory ($CD68^+/CD163^-$) M1 macrophages and the activation of muscle stem cells within 24 hours of injury. Macrophages play a crucial role in clearing cellular debris and continue to secret early pro-inflammatory cytokines that attract MuSCs to the damaged site and induce their expansion. TNF-α, for instance, inhibits Notch1 and Pax7 expression, therefore promoting the commitment of MuSCs (Caballero-Sánchez et al., 2022). Between 2 to 4 days after initial damage, the number of myoblasts reaches its peak, and the pro-inflammatory environment transitions to an anti-inflammatory state, marked by the conversion of M1 macrophages to M2 macrophages ($CD68^-/CD163^+$). M2 macrophages secrete a wide range of pro-regenerative molecules,

including IGF1, which enhances tissue regeneration (Tonkin et al., 2015), and Interleukin-10 (IL-10), stimulating myoblast differentiation and fusion (Arnold et al., 2007). Newly formed myofibers express embryonic isoforms of myosin heavy chain and feature centrally localized myonuclei. In the final phase of muscle regeneration, new myofibers mature into functional, contractile myofibers with peripheral nuclei. This maturation process coincides with the restoration muscle function, ultimately re-establishing the adult muscle ecosystem, including the appropriate extracellular matrix, connective tissue, blood circulation, innervation, stem cell niche, and associated, muscle-residing cells (Qazi et al., 2019; Schmidt et al., 2019).

It is universally accepted that *de novo* formation of a myofiber depends on the proliferation and differentiation of muscle progenitor cells and the fusion of myoblasts. These fundamental processes are integral to both embryonic and postnatal myogenesis, as well as adult muscle regeneration. Progenitor cell proliferation, nuclei accretion, and hypertrophy of a new myofiber occur *in vitro*, during embryonic and fetal development, and in the regeneration of adult muscle (Fukada et al., 2022). Therefore, it is conceivable that the cellular and molecular mechanisms underlying fiber maturation appear analogous, if not identical, despite substantial morphological differences between newly formed muscle structures. The most remarkable differences include nuclei organization and myofiber size (Pizza and Buckley, 2023). For example, developing fibers assemble their own basal lamina, while regenerating fibers predominantly form within the lamina of the necrotic fiber (Webster et al., 2016). Embryonic myogenesis relies on embryonic and fetal myoblasts, whereas $Pax7^{+}$ satellite cells appear to be primarily, if not the sole, precursor of adult myofiber (Relaix and Zammit, 2012). Regenerating myofibers are regulated by different cells in the environment, such as macrophages, compared to developmental stages (Forcina et al., 2020). General questions as extrinsic and intrinsic need to obtain nuclei may differ between acute injury and development. Regenerating myofibers rapidly accumulate a higher-than-normal number of nuclei (per area) within the first 7 days after injury in an accelerated fashion, preceding hypertrophic growth. In contrast, developing myofibers reach the adult number of myonuclei and level of hypertrophy several months after birth (Buckley et al., 2022). Lastly, regenerating fibers feature centrally located nuclei, organized in nuclear chains, strings containing at least 10-20 nuclei that appear in contact. In contrast, during development, centrally positioned nuclei are consistently non-randomly separated from each other (Buckley et al., 2022; Wada et al., 2008). Despite these and other differences, developing and regenerating myogenesis

share common processes, with variations often explained by alterations in the soluble and cellular environment mediating maturation (Pizza and Buckley, 2023).

1.5. A synopsis of signaling pathways regulating myogenesis

Cellular responses are initiated by gradients of morphogens that emanate from a localized sources and orchestrate the organization of surrounding cells into specific pattern (Gurdon and Bourillot, 2001). Skeletal muscle formation is a highly regulated, multistep process governed by a complex genetic network of these morphogenic signals across all developmental stages. This intricate regulatory network also plays a role in maintaining homeostasis and guiding adult regenerative processes, although not always with a complete overlap (Bentzinger et al., 2012). Interestingly, Biressi and colleagues have proposed that embryonic and fetal myogenic progenitors may possess intrinsic genetic differences. Through cell-sorting techniques, they have demonstrated disparities between these two types of myoblasts in terms of proliferation, differentiation and fusion capabilities, and response to myogenic inhibitors like TGFβ and BMP4 *in vitro* (Biressi et al., 2007b). Overall, morphogenic signals are sensed and interpreted by myogenic precursors, influencing either the promotion or antagonism of myogenic commitment. Numerous well-studied developmental signaling pathways play pivotal roles in regulating myogenesis, including Sonic hedgehog (Shh), Notch, Hepatocyte growth factor (HGF), Fibroblast growth factors (FGFs), IGFs, RA, WNT, and TGFβ signaling among others (Chal and Pourquié, 2017). Here we will dive into greater detail on a few relevant pathways, specifically the TGFβ, or more precise Activin receptor signaling, and WNT pathways.

1.5.1. Activin receptor signaling

The TGFβ superfamily encompasses more than thirty soluble ligands that play vital roles in both developmental myogenesis and postnatal muscle growth (Horbelt et al., 2012; Moustakas and Heldin, 2009). In numerous preclinical mouse disease models, the inhibition of specific TGFβ ligands has demonstrated potent anabolic effects on muscle (Lee et al., 2023). Three of these ligands have garnered particular attention: myostatin, activins and growth differentiation factor 11 (GDF11). These proteins are initially synthesized as large precursor molecules comprising a signal peptide, N-terminal prodomain, and a C-terminal

mature domain. The mature growth factor is composed of a dimer formed by two carboxy-terminal domains held together by a single disulfide bond. The signal peptide is removed in the endoplasmic reticulum, and the remaining peptide undergoes further processing in the trans-Golgi network and extracellularly. The prodomain is cleaved by protein convertases, such as furin, converting the peptide into a “latent state”, where the prodomain remains non-covalently bound to the mature domain (Lee and McPherron, 2001; Wang et al., 2016). The final cleavage is mediated by metalloproteases of the BMP1/tolloid family, resulting in the release of the mature ligand (Wolfman et al., 2003).

Myostatin, activins, and GDF11 share a common set of activin transmembrane receptors to initiate their signaling pathways. This receptor complex consists of two type I and two type II receptors. Each activin receptor has a single-pass transmembrane domain flanked by an extracellular ligand-binding domain and an intracellular serine/threonine kinase domain. When ligands bind to the type II receptor, they form a complex that recruits and activates the type I receptors through transphosphorylation. This activation propagates intracellular signaling as the type I receptor activates transcription factors Smad2 and Smad3. These Smads then form multimers with Smad4 and translocate to the nucleus, where they bind to a DNA sequence known as the Smad-binding element (SBE) (Massagué et al., 2005). Within the TGFβ family, there are seven different type I receptors known as activin receptor-like kinase (ALK1-7). Activin A primarily utilizes ALK4, but can also form a non-signaling complex with Alk2, becoming a competitor of Alk4 signaling (Hildebrandt et al., 2021; Olsen et al., 2018; Quist-Løkken et al., 2023; Szilágyi et al., 2024). Myostatin and GDF11 signal through both ALK4 and ALK5 (Andersson et al., 2006; Rebbapragada et al., 2003). There are five different type II receptors in the TGFβ superfamily: TGFβ receptor type II (TβRII), bone morphogenetic protein receptor type II (BMPRII), anti-Müllerian hormone receptor type II (AMHR), activin receptor type IIA (ActRIIA), and activin receptor type IIB (ActRIIB). Activin A and GDF11 utilize both ActRIIA and ActRIIB, with similar affinity for these ligands. Myostatin primarily uses ActRIIB as its main type II receptor, with much lower affinity for ActRIIA (Goebel et al., 2019; Jatzlau et al., 2023; Walker et al., 2017). The TGFβ receptor signaling is notoriously promiscuous, with other ligand family members also binding to ActRIIA and ActRIIB, such as BMP10. This can sometimes lead to unexpected outcomes in studies that manipulate either growth factors or receptor complexes, potentially disrupting the pathway (Rodgers and Ward, 2021) (Fig. 1-6).

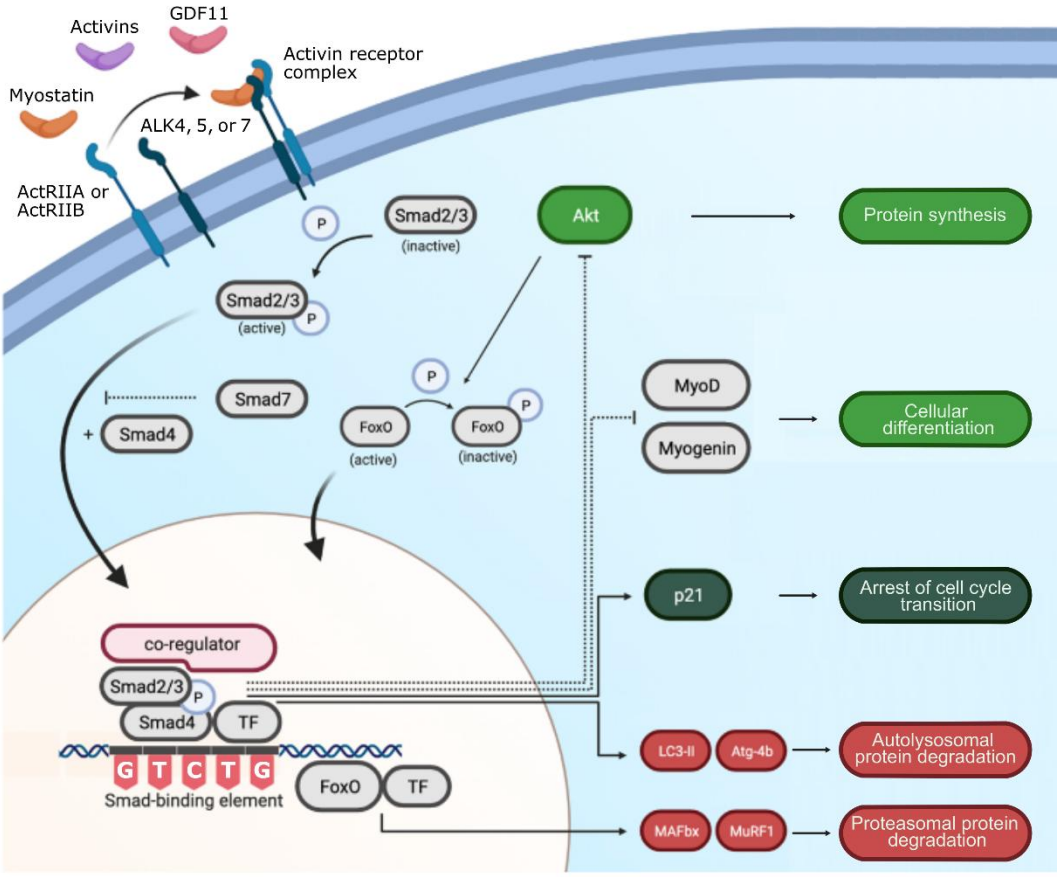

Figure 1-6. Activin receptor signaling pathway in skeletal muscle
This figure illustrates the promiscuous signaling of various ligands from TGFβ superfamily, including myostatin, GDF11 and Activin A, through the activin receptor complex. The activation of the receptor complex involves two pairs of receptors: type II (ActRIIA or ActRIIB) and type I (Alk4, Alk5, Alk7). Active type I receptors phosphorylate Smad2/3, which then form complexes with Smad4 and translocate to the nucleus. There, they bind to specific DNA sequences, driving the transcriptional response. Other transcription factors, chromatin- and histone modifying enzymes, collectively modulate Smad-dependent transcription to regulate essential cellular processes such as protein synthesis, degradation, cellular differentiation, and proliferation. Modified from (Lodberg, 2021).

Studying the impact of myostatin in C2C12 cells and primary human myoblasts has provided significant mechanistic insights into activin receptor signaling in muscle. Myostatin primarily affects four cellular programs: protein synthesis, protein degradation, cellular differentiation and proliferation (Lodberg, 2021). Myostatin has been shown in cell lines and mice to suppress protein synthesis by inhibiting Akt signaling in a Smad2/3-dependent manner, disrupting a critical signal for anabolic protein synthesis regulated by mTOR (Trendelenburg et al., 2009; Welle et al., 2009). Additionally, Akt inhibition increases the amount of active FoxO transcription factor, which controls the expression of E3 ubiquitin ligases Atrogin-1 and MuRF1. These ligases subsequently facilitate the proteasomal degradation of myogenic regulatory factors and structural muscle proteins (Lokireddy et al., 2011; McFarlane et al.,

2006). Myostatin has also been linked to the regulation of autolysosomal activity in C2C12 cells (Lee et al., 2011). In myoblasts primed for differentiation, myostatin exerts Smad3-dependent myostatin control over the expression of myogenic regulatory factors such as Myod1, Myf5 and Myogenin (Langley et al., 2002). However, in proliferating myoblasts, myostatin leads to the inhibition of cell cycle progression through a p21-mediated mechanism (McCroskery et al., 2003; Thomas et al., 2000) (Fig. 1-6). The myogenic impact of myostatin is nuanced and context specific, often leading to conflicting results particularly in studies involving immortalized mouse cell lines (Rodgers and Ward, 2021). The prevailing model suggests that during development and regeneration, myostatin arrests the cell cycle and initiates the myogenic program in proliferating muscle progenitors. In quiescent, contact inhibited satellite cells, myostatin maintains quiescence and inhibits terminal differentiation. In mature muscle, myostatin functions as a potent atrogene, stimulating protein degradation and inhibiting protein synthesis. Similar effects are assumed for Activin A and GDF11 (Rodgers and Ward, 2021). Myostatin is often depicted as a regulator of muscle precursor cell behavior, with a seemingly contradictory role in inhibiting both cell proliferation and differentiation (Rodgers and Ward, 2021). Although there are reports of increased proliferation following myostatin (Rodgers et al., 2014) and Activin A (Ma et al., 2021) stimulation in C2C12 cells, multiple vertebrate models such as ovine, porcine, chicken and trout myogenic precursors (Kamanga-Sollo et al., 2005; McFarland et al., 2007; Salabi et al., 2014; Seiliez et al., 2012), consistently demonstrate myostatin's role in the cell cycle inhibition through the upregulation of p21- Retinoblastoma1 (pRb1) axis. The conflicting data regarding myostatin's impact on myogenesis largely stem from studies in C2C12 cells, which have shown the downregulation of MRFs and p21 during differentiation (Langley et al., 2002). Furthermore, studies involving myostatin null mice have reported an increased number of satellite cells present in muscle (McCroskery et al., 2003). However, subsequent research using an ActRIIA and ACTRIIB antibody to inhibit Activin A, myostatin, and GDF11 indicated that hypertrophy can occur independently of satellite cell numbers (Lee et al., 2012). Fig. 1-7 provides a summary of myostatin and Activin A functions.

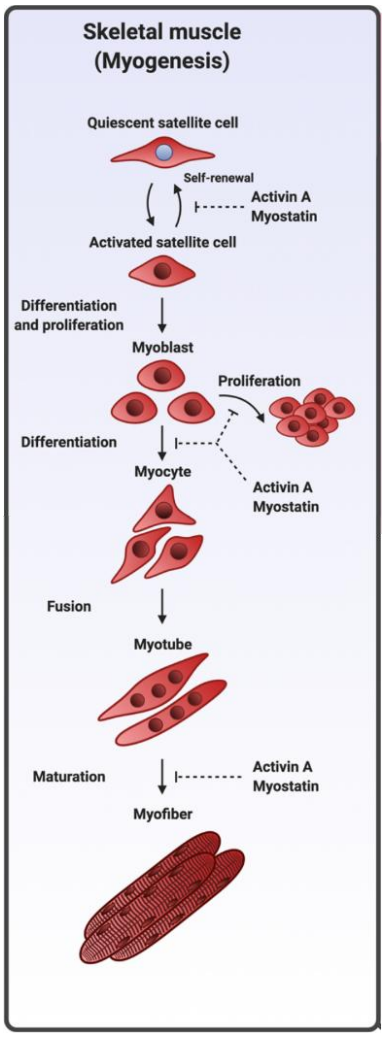

Figure 1-7. Cellular effects of Activin A and Myostatin in myogenesis
Myostatin, a well-investigated member of the activin receptor complex ligands, is thought to impede the proliferation of skeletal muscle progenitor cells and favor protein degradation during muscle maturation. The regulation of satellite cell self-renewal and cellular differentiation remains a subject of debate with context-dependent characteristics. Other TGFβ ligands such as Activin A and GDF11, are presumed to exert comparable functions. Modified from (Lodberg, 2021).

Future studies will likely provide clarity on the precise cellular functions of activin complex signaling in myoblasts and myogenic progenitor cells. Nevertheless, the grotesque hypertrophy observed in animal models lacking myostatin, such as cattle, dogs and trout, has intensified the interest in the TGFβ pathway. It serves as a paradigm, illustrating the intricacies of regulation within a signaling network and crosstalk (Rodgers and Ward, 2021). Notably, myostatin primarily signals directly to myofibers rather than satellite cells, as demonstrated by its specific depletion in fast-twitching fibers (Myl1-Cre), resulting in significant hypertrophy without satellite cell activation and fusion (Lee et al., 2020). Simultaneous inhibition of Activin A and myostatin (and GDF11) through the inhibition of both activin type II receptors using ActRII-Fc antibody (targeting ActRIIA and ActRIIB) greatly amplifies the increase in muscle mass observed with myostatin inhibition alone (Lee et al., 2005). Conversely, inhibiting BMP type II receptor (BMPRII) in conjunction with both activin type II receptors does not yield an additional increase in muscle mass. Surprisingly, inhibiting both type I receptors (Alk4 and Alk5) surpasses the effect of ActRII-Fc antibody treatment, nearly quadrupling muscle mass (Lee et al., 2020). These findings suggest the involvement of another type II receptor in myofibers, potentially bringing the TGFβ receptor type II (TBRII) into focus, although no binding of myostatin or Activin A binding to this receptor has been reported. The ActRIIA/IIB-neutralizing antibody represents one of 19 pharmaceutical strategies in the first generation of “first mover” biologicals that entered clinical trials to address muscle wasting conditions, including dystrophies, cachexia, sarcopenia and bone injuries. Regrettably, these “first movers” have not succeeded in achieving functional end

results and physiological benefits in patients during phase 2 trials, despite increasing lean muscle mass (Lee et al., 2023; Rodgers and Ward, 2021). The failure to translate from the potent muscle hypertrophy observed in mice following myostatin inhibition to humans may be attributed to differences in the circulating levels of these growth factors between species. Indeed, recent research in cynomolgus monkeys has revealed a superior effect of Activin A inhibition on muscle mass regulation (Latres et al., 2017). However, the complete absence of myostatin signaling does not provide the full picture, as simultaneous overexpression of the BMP antagonist noggin in the *Mstn* null mouse mitigated the hypertrophy (Sartori et al., 2013). This underscores the importance of crosstalk that involves the upregulation of anabolic BMP signaling, which shares the transcription factor Smad4 with the catabolic activin receptor pathway. The insights gained from recent research and clinical setbacks have enriched the TGFβ field with a deeper understanding of the complex regulation of this signaling pathway, paving the way for the development of novel treatment strategies.

1.5.2. WNT signaling

Signaling molecules from the WNT family play crucial roles in myogenesis during both embryonic development and adult tissue homeostasis by regulating muscle formation and maintenance. This pathway consists of canonical (β-catenin-dependent) and noncanonical (β-catenin-independent) branches (MacDonald et al., 2009). Upon binding of WNT ligands to Frizzled (Fzd) receptor and low-density lipoprotein receptor-related protein (LRP5/6) co-receptor, β-catenin accumulates in the cytoplasm and translocates to the nucleus. There, in conjunction with T cell factor (TCF) and Lymphoid enhancer factor (LEF), β-catenin stimulates the transcription of target genes. Conversely, in the absence of receptor activation, β-catenin is phosphorylated by the cytoplasmic destruction complex, comprising Axin, Adenomatous Polyposis Coli (APC), Casein Kinase I (CKI) and Glycogen Synthase Kinase 3β (GSK3β), leading to its ubiquitination and subsequent proteasomal degradation. Activation of the pathway results in the sequestration of Axin by a scaffold protein Dishevelled (Dvl), leading to the disassembly of the destruction complex (Liu et al., 2022).

Additionally, non-canonical pathways, such as the Planar Cell Polarity (WNT/PCP) and calcium-dependent (WNT/Ca^{2+}) pathways, can also be activated by WNT ligands. The WNT/PCP pathway activates small GTPases like Rho and Rac, which in turn activate Rho-associated protein kinase (Rock) and c-Jun N-terminal kinases (JNKs), ultimately leading to

cytoskeletal reorganization and activation of target genes. The WNT/Ca^{2+} pathway triggers the activation of phospholipase C (PLC) and inositol triphosphate (IP3)-dependent release of intracellular calcium (Ca^{2+}). Subsequently, this leads to the activation of calcineurin (CaN), Calcium/calmodulin-dependent kinase II (CAMKII), and protein kinase C (PKC), culminating in the activation of transcriptional regulators such as Nfat, Creb and Nf-κB (Shah and Kazi, 2022). WNT proteins serve as morphogens in various developmental processes, playing critical roles in embryonic segmentation and somitogenesis (Jensen et al., 2010). Active WNT signaling is essential for dermomyotome induction and maintaining the epithelial organization of the dermomyotome, as well as for myotome formation (Geetha-Loganathan et al., 2008; Marcelle et al., 1997). However, in mature skeletal muscle, the WNT pathway is notably less active, compared to development stages (Kuroda et al., 2013). Nevertheless, studies have shown that inhibition of WNT1 or GSK3β can enhance myogenic differentiation in adult muscle cells (Rochat et al., 2004; van der Velden et al., 2006). High levels of WNT/β-catenin signaling are required to drive the transition from proliferation to differentiation, as evidenced by mouse models, where exogenous activation of canonical WNT signaling leads to premature differentiation towards postmitotic myocytes (Brack et al., 2008). Conversely, limiting WNT activity is crucial to maintaining satellite cell expansion and preventing premature differentiation during early stages of muscle regeneration (Figeac and Zammit, 2015). Studies have also demonstrated that both loss-of-function and gain-of-function mutations in satellite cells can alter the regenerative process., with β-catenin signaling-deficient SCs showing reduced differentiation ability, while constitutively active β-catenin cascade leads to growth arrest and accelerated commitment of proliferating cells. These findings underscore the importance of temporal control of WNT signaling and the levels of pathway activation for effective muscle regeneration (Rudolf et al., 2016).

The molecular mechanisms underlying WNT-dependent muscle repair are not fully understood. WNT signaling may regulate the activity of MRFs or inhibit Pax7 in differentiating myoblasts (Hulin et al., 2016). Additionally, the non-canonical PCP pathway impacts cytoskeletal reorganization through activation of Rac1, enhancing satellite cell migration and improving engraftment *in vivo* (Bentzinger et al., 2014). Furthermore, studies in C2C12 cells have demonstrated WNT-dependent activation of the Akt/mTOR pathway, resulting in elevated hypertrophy of postmitotic myotubes (von Maltzahn et al., 2011), as well as WNT-

dependent expression of the TGFβ antagonist Follistatin (Fst) (Han et al., 2014). Fig. 1-8 provides an overview of the activity of WNT signaling during regeneration.

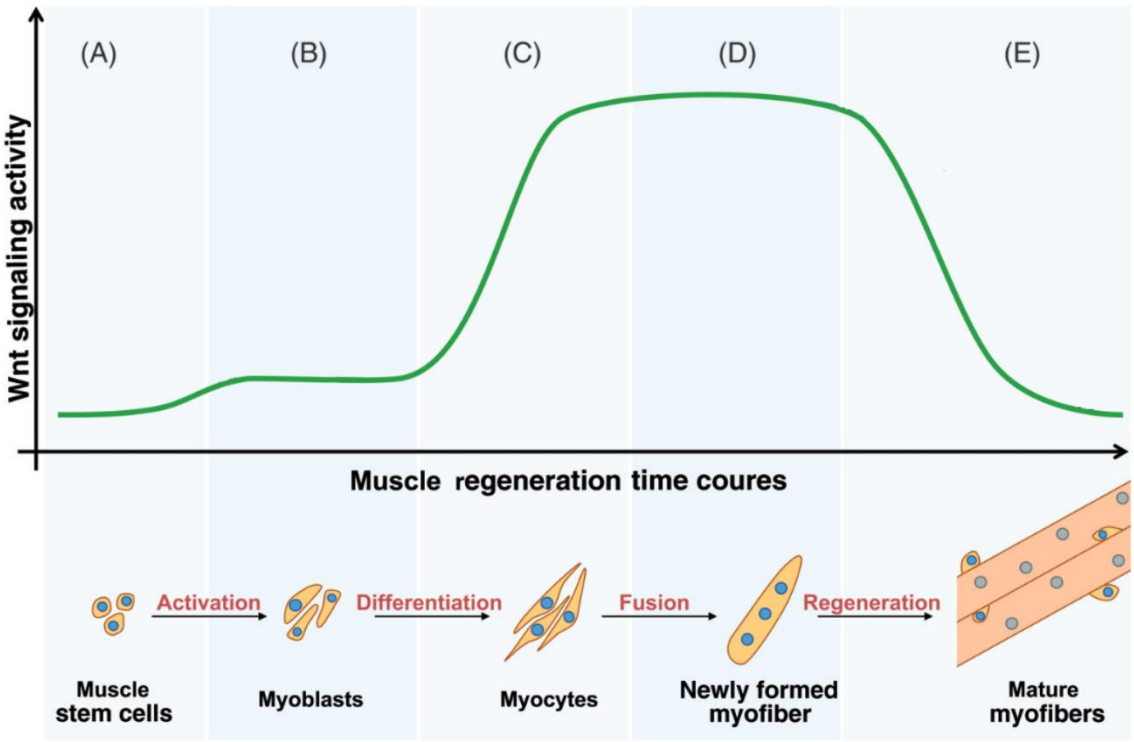

Figure 1-8. WNT pathway activity throughout muscle regeneration
Temporal regulation of canonical WNT signaling is vital for adult muscle regeneration. A. Quiescent MuSCs exhibit no active WNT signaling and require its inhibition to properly enter the cell cycle. B. WNT/PCP signaling stimulates symmetric cell division of activated satellite cells, while the inhibition of canonical WNT signaling is necessary for their proliferation. C. WNT/β-catenin facilitates the transition from proliferation to differentiation. D. Active WNT signaling promotes the differentiation and fusion of myoblasts, partially through the inhibition of Myostatin and activation of Follistatin expression. E. WNT signaling promotes the hypertrophic growth of muscle and is downregulated upon the completion of regeneration. Modified from (Girardi and Le Grand, 2018).

Experimental data suggests the existence of a dynamic interplay between WNT and TGFβ pathways (Girardi and Le Grand, 2018). WNT signaling has been shown to activate BMP4 expression, thereby facilitating the formation of slow myofibers (Kuroda et al., 2013). Additionally, a study in C2C12 cells has demonstrated that WNT4 antagonizes Smad2 phosphorylation caused by Myostatin, a negative regulator of muscle growth (Takata et al., 2007). Subsequent research in primary myoblasts has confirmed that WNT4 regulates cell fusion and myotube size, antagonizing myostatin function and upregulating MRF expression (Bernardi et al., 2011). However, contrasting findings have been reported, as another study demonstrated myostatin-dependent repression of WNT4 in proliferating C2C12 cells (Steelman et al., 2006).

Recent investigations in primary myoblasts have revealed that the canonical WNT pathway regulates the transcription of TGFβ2 and TGFβ3 (Rudolf et al., 2016). Moreover, WNT/ β-catenin signaling has been demonstrated to trigger the expression of Myogenin, a key regulator of myogenic differentiation, leading to the upregulation of Follistatin expression and premature myogenic differentiation (Jones et al., 2015). In summary, the reciprocal interplay between WNT and TGFβ signaling is complex and vital for the correct regeneration process (Girardi and Le Grand, 2018).

1.5.3. Signaling regulating the transition from proliferation to differentiation in myoblasts

Myoblasts continue dividing until they reach a fully differentiated state, where terminal differentiation typically aligns with the cessation of proliferation and a permanent exit from the cell cycle (Ruijtenberg and van den Heuvel, 2016; Wu and Yue, 2024). Cycle-promoting cyclin-dependent kinases (CDKs) and tissue-specific transcription factors such as Myod1 contribute to the temporal coordination of these mutually antagonistic processes (Wu and Yue, 2024). Mitogens and growth factors stimulate the sustained expression of cell cycle genes such as *CyclinD1* (*Ccnd1*), *CyclinE2* (*Ccne2*), *CyclinA2* (*Ccna2*), *Cdc25a*, *Thymidin kinase1* (*Tk1*) and *Dyhydrofolate reductase* (*Dhfr*) via the E2F/DP1 transcription factor duo (Bracken et al., 2004; Engeland, 2022; Rao et al., 2016; Wang et al., 1996). Active cyclin-CDK complexes phosphorylate the repressive tumor suppressor protein pRb1, which dissociates from E2F/DP1, promoting entry into the S-phase of the cell cycle (Dyson, 1998; Engeland, 2022; Stallaert et al., 2019; Trimarchi and Lees, 2002). Cell division inhibitors (CDIs) such as p21, p27, and p57 inhibit cyclin-CDK proteins, leading to cell cycle exit and inactivation of E2F/TFDP1, partially via pRb1 hypophosphorylation. The induction of myogenic differentiation also leads to pRb1 hypophosphorylation, directly promoting Myod1 activity and repressing CDK and E2F-dependent inhibition of Myod1 (Ruijtenberg and van den Heuvel, 2016). Additionally, several layers of redundant regulation of the proliferation-differentiation decision balance the effects of E2F/DP1 and Myod1 on myoblasts, including competition for shared proteins such as pRb1, transcriptional coactivators, and chromatin regulators (Ruijtenberg and van den Heuvel, 2016; Wu and Yue, 2024). Fig. 1-9 summarizes key factors participating in the proliferation-differentiation regulation in myoblasts.

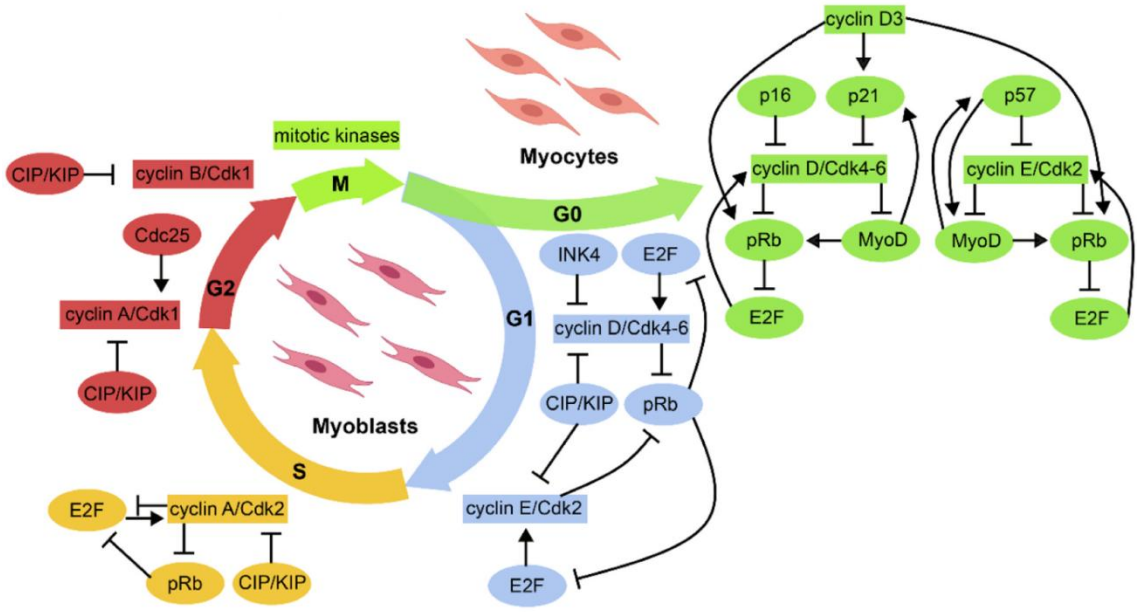

Figure 1-9. The crosstalk between myogenic regulatory factors and cell cycle regulators during myogenic differentiation

The initiation of myoblast differentiation involves an irreversible exit from the cell cycle into the G_0 phase, characterized by the persistent inhibition of the cell cycle regulators. This is followed by the expression of myogenic regulatory factors that activate a specific set of muscle-specific genes. The progression through the cell cycle is orchestrated by specific combinations of cyclin/CDK complexes that phosphorylate target proteins during the corresponding stage of the cycle. These complexes function alongside other cell cycle regulators, such as CDK inhibitors, which exert broader influence throughout the cell cycle. Two families of CDK inhibitors (INK4 and CDK interacting protein/Kinase inhibitory protein (CIP/KIP)) play crucial roles in preventing premature entry into any phase of the cell cycle. Some cell cycle regulators can influence cell differentiation independently of their role in cell division control, and several cell type-specific transcription factors can directly interact with cell cycle regulators to modulate gene expression related to the cell cycle. Modified from (Wu and Yue, 2024).

1.5.4. Mitochondrial signaling and apoptosis in myogenic differentiation

Mitochondria are highly dynamic organelles that play crucial roles in energy production, stress regulation, and cell survival (Lin et al., 2024). They can be *de novo* generated through mitochondrial biogenesis, known as mitogenesis, or removed and recycled via mitochondrial autophagy, known as mitophagy (Rahman and Quadrilatero, 2021). Additionally, their elongation and division, termed fusion and fission respectively, are tightly regulated processes that influence mitogenesis and mitophagy. Mitochondrial fusion prevents mitophagy, while the onset of mitophagy is typically preceded by fission (Rahman and Quadrilatero, 2021). Furthermore, mitochondrial apoptotic signaling is interconnected with mitophagy activation, with mitophagy reciprocally inhibiting apoptosis (Baechler et al., 2019; Jiang et al., 2021; McMillan and Quadrilatero, 2014). Mitochondrial remodeling is intricately

linked to myogenic differentiation and is involved throughout the entire process (Bloemberg and Quadrilatero, 2014; Kim et al., 2013; Lin et al., 2024; Rahman and Quadrilatero, 2021; Sin et al., 2016; Wagatsuma and Sakuma, 2013), as illustrated in Fig. 1-10.

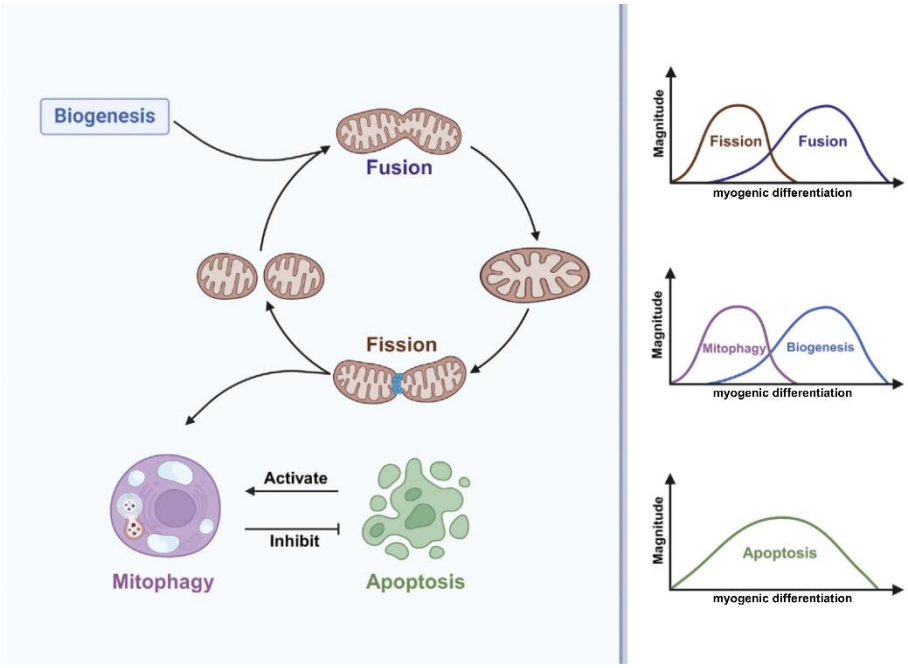

Figure 1-10. Mitochondrial remodeling during myogenic differentiation
The dynamic reorganization of the mitochondrial network during myogenic differentiation is illustrated. At the initial stages of differentiation, interconnected mitochondrial fission and autophagy predominate, while biogenesis and elongation through fusion occur during the middle and late stages. Fission initiates mitophagy, which in turn inhibits apoptosis. Apoptosis serves as a signal for the initiation of mitophagy and persists throughout the differentiation process, peaking in the middle stages. Modified from (Lin et al., 2024).

This process encompasses the metabolic reprograming associated with the mitophagy of old mitochondria and biogenesis of a mature mitochondrial network. The transition from the "underdeveloped" or undifferentiated sparse myoblast network to mature, tightly-coupled differentiated mitochondria (Rahman and Quadrilatero, 2021; Sin et al., 2016) drives the metabolic reprogramming necessary to complement and sustain the energy-demanding metabolism of myotubes and myofibers. This mature network supports efficient oxidative phosphorylation (OXPHOS) machinery, as myotubes primarily generate ATP through OXPHOS, in contrast to glycolytic myoblasts (Barbieri et al., 2011; Remels et al., 2010).

During early myogenesis, the induction of the fission protein Dynamin 1-like/ Dynamin-related protein 1 (Dnm1l/Drp1) and mitophagy receptors such as Sequestosome1 (Sqstm1/p62) leads to mitochondrial fragmentation followed by mitophagy-dependent clearance of old mitochondria (Huang et al., 2020; Sin et al., 2016). This process is followed

by mitochondrial biogenesis, driven by the peroxisome proliferator-activated receptor-gamma coactivator-1 (PGC-1) family of coactivators, which aligns with the mitochondrial fusion machinery, including dynamin-like GTPases such as Mitofusin 1 (Mfn1), Mfn2 and Optic-atrophy 1 (Opa1). This generation and elongation processes generate a new myotubal mitochondrial network characterized by increased mitochondrial enzyme activity (Duguez et al., 2002; Sin et al., 2016; Wagatsuma et al., 2011). The dynamic maintenance of mitochondrial morphology and function is essential for the initiation and progression of myogenic differentiation (Lin et al., 2024). For instance, the downregulation of mitogenesis through depletion of PGC-1α, or mitophagy through the depletion of Autophagy related 7 (Atg7) (Baechler et al., 2019), Atg5 (Sin et al., 2016) or of Bcl-2/adenovirus E1B interacting protein 3 (BNIP3) in C2C12 cells results in poor differentiation (Baechler et al., 2019; Sin et al., 2016). Additionally, both overactivation and inhibition of Drp1-mediated fission delay the *in vitro* differentiation of myoblasts (De Palma et al., 2010; Kim et al., 2013). Inhibition of myogenic differentiation has also been demonstrated through the inhibition of various other aspects of mitochondrial function and activity, such as mitochondrial DNA transcription, and RNA and protein synthesis, using agents like ethidium bromide, rifampicin and chloramphenicol, respectively, among others (Brunk and Yaffe, 1976; Korohoda et al., 1993; Seyer et al., 2011). Many other mitochondrial processes also contribute to this inhibition (Lin et al., 2024).

Induced myogenic differentiation is characterized by the generation of cellular stress signals, including the production of reactive oxygen species (ROS), upregulation of oxidative stress-related genes, and activation of the Caspase (cysteine-aspartic protease) cascade (Gugliuzza and Crist, 2022; Jahnke et al., 2009). In response to these and other signals, whether under physiological conditions or due to mitochondrial dysfunction, mitochondria engage in retrograde signaling crosstalk with the nucleus and cytoplasm to execute diverse mitochondrial stress responses (Lin et al., 2024). Depending on the duration and intensity of these responses, they can either contribute to cellular homeostasis or trigger apoptosis (Picard and Shirihai, 2022).

Apoptosis is a conserved mechanism that eliminates dysfunctional, damaged, and unnecessary cells (Galluzzi et al., 2018). The endogenous apoptosis is initiated by mitochondria under tight regulation of initiator proteins from the B-cell leukemia/lymphoma 2 (Bcl2) family, such as Bcl2 binding component 3 (Bbc3/Puma) and Bcl2 homology 3 (BH3)

interacting domain death agonist (Bid) (Rosa et al., 2022). Bbc3 or Bid directly activate pro-apoptotic effectors like Bcl2-associated X protein (Bax) and Bcl2-antagonist/killer 1 (Bak1), which translocate to the mitochondria and induce mitochondrial outer membrane permeabilization (MOMP) (H.-C. Chen et al., 2015). Upon mitochondrial membrane rupture, Cytochrome c (Cycs) is released into the cytoplasm and binds to apoptotic protease activator factor 1 (Apaf-1), initiating the activation of caspases through the cleavage of their zymogens (Donepudi and Grütter, 2002; Thornberry and Lazebnik, 1998). This cascade results in the cleavage of various cellular proteins, leading to cellular demise (Bock and Tait, 2020). Additionally, MOMP leads to the release of pro-apoptotic proteins from the mitochondria, such as second mitochondria-derived activator of caspase (Smac) (Du et al., 2000), High temperature requirement protein a2 (Htra2) (Hegde et al., 2002), and Arts (Gottfried et al., 2004). These proteins promote apoptosis by counteracting inhibitors of apoptosis (IAP), including the X-linked inhibitor of apoptosis (XIAP), which inhibits Caspase 3, 7, and 9, (Bock and Tait, 2020; Galbán and Duckett, 2010). Conversely, anti-apoptotic proteins such as Bcl2 and Bcl2-like 1 (Bcl2l1/Bclxl) counteract the activation of mitochondrial apoptotic signaling, thereby regulating the apoptotic process (Rahman and Quadrilatero, 2023a).

Besides elimination of dysfunctional cells, apoptotic signaling is essential for the orderly progression of myogenic differentiation (Lin et al., 2024; Rahman and Quadrilatero, 2023a). Both excessive or deficient apoptosis can adversely affect myogenic differentiation and myotube formation (Fernando et al., 2002). Early work from the Megeney Lab demonstrated the crucial role of Caspase 3 (Casp3) activity in myogenic differentiation (Fernando et al., 2002). Myoblasts derived from Casp3-null mice failed to reduce the expression of the cell cycle regulator cyclin D1 (Ccnd1), resulting in impaired differentiation. Under normal conditions, Casp3 activity peaks during early differentiation (Bloemberg and Quadrilatero, 2014; Dick et al., 2015; Fernando et al., 2002). Conversely, exogenous expression of Casp3 in C2C12 cells abolished Ccnd1 expression, suggesting a premature exit from the cell cycle(Fernando et al., 2002). Consistently, Casp3's function was further demonstrated in MuSCs (Dick et al., 2015). Inhibition of Casp3 promoted the self-renewal of MuSCs, impairing their differentiation and thereby affecting muscle regeneration. This inhibition was mediated by the cleavage of Pax7, which was identified to harbor aspartic cleavage sites (Dick et al., 2015). Additionally, depletion or inhibition of other components of the caspase signaling cascade, including Casp9 (Murray et al., 2008), Cycs, and Apaf1 (H. Dehkordi et al., 2020),

resulted in impaired differentiation or myotube formation. The involvement of Casp2 (Boonstra et al., 2018; H. Dehkordi et al., 2020) and Bcl2-family proteins in the regulation of myogenic differentiation has also been demonstrated. Notably, depletion of Peptidyl-tRNA hydrolase 2 (Ptrh2/Bit1), a transcriptional regulator of Bcl2, in C2C12 cells led to reduced Bcl2 levels and rapid onset of differentiation due to elevated levels of Casp3 and Caps9 (Griffiths et al., 2015). These findings emphasize the importance of mitochondrial apoptotic signaling for the orderly progression of myogenesis and suggest that moderate stress responses may be necessary to support differentiation.

1.6. Cytoskeleton as the crossroad for stem cell structure and function

Stem cells, by virtue of their presence, dynamically influence their mechanical microenvironment, while simultaneously being influenced by it. This bidirectional interaction of mechano-sensation and mechano-adaptation forms the basis for the establishment of structure-function relationships across various biological scale, from individual cells to entire organ systems (Knothe Tate et al., 2016; Michael, 2021). In addition to biochemical signals, the mechanome, which encompasses a collection of biomechanical cues, profoundly shapes the formation of biological structures. This process involves a feedback loop wherein cells regulate the generation of extracellular matrix externally and the cytoskeletal architecture internally, thereby contributing to the emergence of complex living architectures (Knothe Tate et al., 2016; Putra et al., 2023).

The cytoskeleton, comprising actin microfilaments, microtubules (MTs), intermediate filaments (IFs), and septins, functions as a dynamic network of filamentous polymers within cells, transmitting mechanical stimuli and conferring structural integrity, while regulating vital biological processes (Oses et al., 2023). Actin, MTs and IFs are well described components of this network, each serving distinct mechanical roles. Actin enable cells to sense and respond to their extracellular environment by facilitating cellular protrusions, maintaining cell shape, regulating motility, contractility and tension-sensing (Greene et al., 2009; Rivero and Cvrcková, 2013). MTs provide resistance to compressive load and serve as an intracellular directional transport system (Oses et al., 2023). IFs support organelle positioning in the cytoplasm (Lowery et al., 2015), protect cellular architecture, maintain nuclear integrity

(Patteson et al., 2019), and facilitate communication between actin and MTs (Gan et al., 2016; Wu et al., 2022). In addition to their roles as scaffolding elements and physical connectors between cells and substrates, the mechano-induced reorganization of actin (Sakai et al., 2011), MTs (Yang et al., 2018) and IFs (Stavenschi and Hoey, 2019) modulates the interaction between cytoskeleton-associated proteins, thereby regulating cytoskeletal behavior (Bieling et al., 2016) and mechano-adaptation to the microenvironment (Putra et al., 2023).

The growing body of evidence suggests that extracellular matrix (ECM) mechanics regulate cell adhesion and cytoskeletal organization, thereby influencing key cellular processes including proliferation, migration, self-renewal and differentiation (Engler et al., 2006; Nava et al., 2012). Cells possess the ability to recognize and respond to physical cues through the formation of multi-protein complexes known as focal adhesions (FAs). These FAs are anchored by transmembrane integrin proteins that bind ECM ligands and connect to the intracellular cytoskeleton via other FA proteins such as talin, vinculin and focal adhesion kinase (FAK) (Geiger and Yamada, 2011). The balance between external and internal forces gives rise to a cellular behavior that is best described by the “molecular clutch hypothesis”, which posits a metaphorical clutch mechanism enabling cells to sense the stiffness of their local environment (Putra et al., 2023). Briefly, actin polymerization drives a continuous flow of actin from the leading edge towards the cell center, known as retrograde flow. When engaged with the ECM, myosin-mediated contractility applies force against the ECM, resulting in the slowing down of retrograde flow, protrusion of the leading edge, and generation of rearward traction forces that propel the cell forward (Panzetta et al., 2023; Swaminathan and Waterman, 2016). Besides facilitating motility, the molecular clutch is proposed to provide cells and tissues with a molecular basis for adapting to the local environment, regulating the number and the behavior of clutches in response to the elastic properties of the matrix (Putra et al., 2023).

1.6.1. Mechanoadaptive remodeling of cytoskeletal components

Adaptation to dynamic environments hinges on cytoskeletal remodeling, a process crucial for cell survival (Putra et al., 2023). Various cytoskeletal elements undergo mechano-adaptation, with cell-cell and cell-matrix adhesions being mechanically modulated, leading to the maturation and evolution of FAs (Geiger and Yamada, 2011). Actin stress fibers (SFs), for instance, are structures subjected to isometric tension, with their local mechanical properties

believed to influence the strength of actin-integrin linkages, actin conformation, and interaction with actin-binding proteins (Burridge and Wittchen, 2013). Substrate tension regulates SF localization, as well as their de-/polymerization dynamics and FA maturation (Putra et al., 2023). Microtubules, on the other hand, are the stiffest filaments and function as compression-resisting components (Gittes et al., 1993). In the cytosol, MTs buckle into short-wavelength shapes, affording them the capacity to withstand compression and influence cell shape through pulling and pushing forces mediated by their dynamic polymerization and depolymerization (Brangwynne et al., 2006; Matis, 2020). IFs, like vimentin, contribute to force generation and transmission (Wang and Stamenovic, 2002), while also protecting intracellular space and nucleus from large deformations (Mendez et al., 2010). In migrating fibroblasts, vimentin aligns with actin branches to direct actomyosin contractile force orientation (Costigliola et al., 2017) and guide microtubule growth and cell polarity through spatial correlation with the end-binding protein Eb1 (Gan et al., 2016). IFs thus function as an intermediary cytoskeletal structure between MTs and microfilaments, contributing to cell shape organization and force transmission (Putra et al., 2023). Cooperative reorganization of actin and tubulin has been observed in various studies, including changes in mechanical properties and changes in gene expression of mesenchymal marker genes in response to seeding density and exposure to shear stress in multipotent murine embryonic fibroblasts C3H/10T1/2 (Chang and Knothe Tate, 2011; Song et al., 2012). These changes are accompanied by anisotropic remodeling in actin and tubulin, with compression-sensing tubulin buckling and bundling depending on cell density and substrate proximity, while tension-sensing actin remodeling is attributed to the direction and magnitude of force (Chang and Knothe Tate, 2011; Putra et al., 2023). Substrate rigidity regulates MT acetylation through MRTF-responsive α-tubulin acetyltransferase (αTAT1) (Seetharaman et al., 2022). The recruitment of αTAT1 to Talin in focal adhesions in a Rho-ROCK-dependent manner demonstrates the involvement of MTs in cell migration and actomyosin contractility (Seetharaman et al., 2022). Additionally, depletion of the actin-polymerizing formin Inf2 leads to the downregulation of αTAT1 and repression of MRTF signaling (Fernández-Barrera et al., 2018). Together, these findings underscore the synergistic role of the entire cytoskeletal machinery in achieving enhanced mechano-adaptation during emergent cytoskeletal responses (Putra et al., 2023).

1.6.2. Cytoskeletal remodeling during induced cell differentiation

The alterations in cytoskeletal architecture within mesenchymal stem cells (MSCs) serve as markers for identifying specific pathways of cellular differentiation. Upon induction with osteogenic, adipogenic, or chondrogenic media MSC-derived osteogenic, adipogenic, and chondrogenic cells exhibit distinct structural changes in actin and tubulin organization (Fig. 1-11) (Putra et al., 2023). Naïve MSCs typically display thin, unidirectional actin fibers, which transform into thicker, more disorganized stress fibers (SFs) with a perinuclear zig-zag pattern following osteogenic induction (Pablo Rodríguez et al., 2004; Yourek et al., 2007). In contrast, chondrogenic and adipogenic cells tend to exhibit a lower degree of cytoskeletal organization or tension. Chondrocytes, upon maturation from MCSs, organize thin cortical actin, while adipocytes show lack of organized actin, reflecting the depolymerization of microfilaments in the cytoplasm. However, chondrocytes exhibit a broader range of shapes *in vivo*, with no significant changes in cytoskeletal architecture, suggesting that additional chemical factors might be necessary to distinguish between chondrocyte and adipocyte differentiation based solely on actin organization (Lauer et al., 2021; Mathieu and Loboa, 2012; Pablo Rodríguez et al., 2004).

The reorganization of MTs is also well-documented throughout MSC differentiation. In naïve MSCs, MTs typically display a spindle-shaped cell organization, with linear MTs radiating from the perinuclear microtubule organizing center (MTOC). Interestingly, despite cell spreading characteristic of osteogenic lineage, MTs do not undergo substantial reorganization in osteogenic medium (Mathieu and Loboa, 2012). Chondrogenic cells derived from MCSs exhibit gradually non-radial, non-centrosomal arrays of disorganized microtubules (Putra et al., 2023; Tvorogova et al., 2018). Conversely, adipogenic conversion of MSCs results in an increased total tubulin density, thick perinuclear MTs, and thin cytoplasmic fibers that buckle at the cell periphery (Yang et al., 2013). Overall, observed cytoskeletal remodeling correlates with differentiation of mesenchymal stem cells.

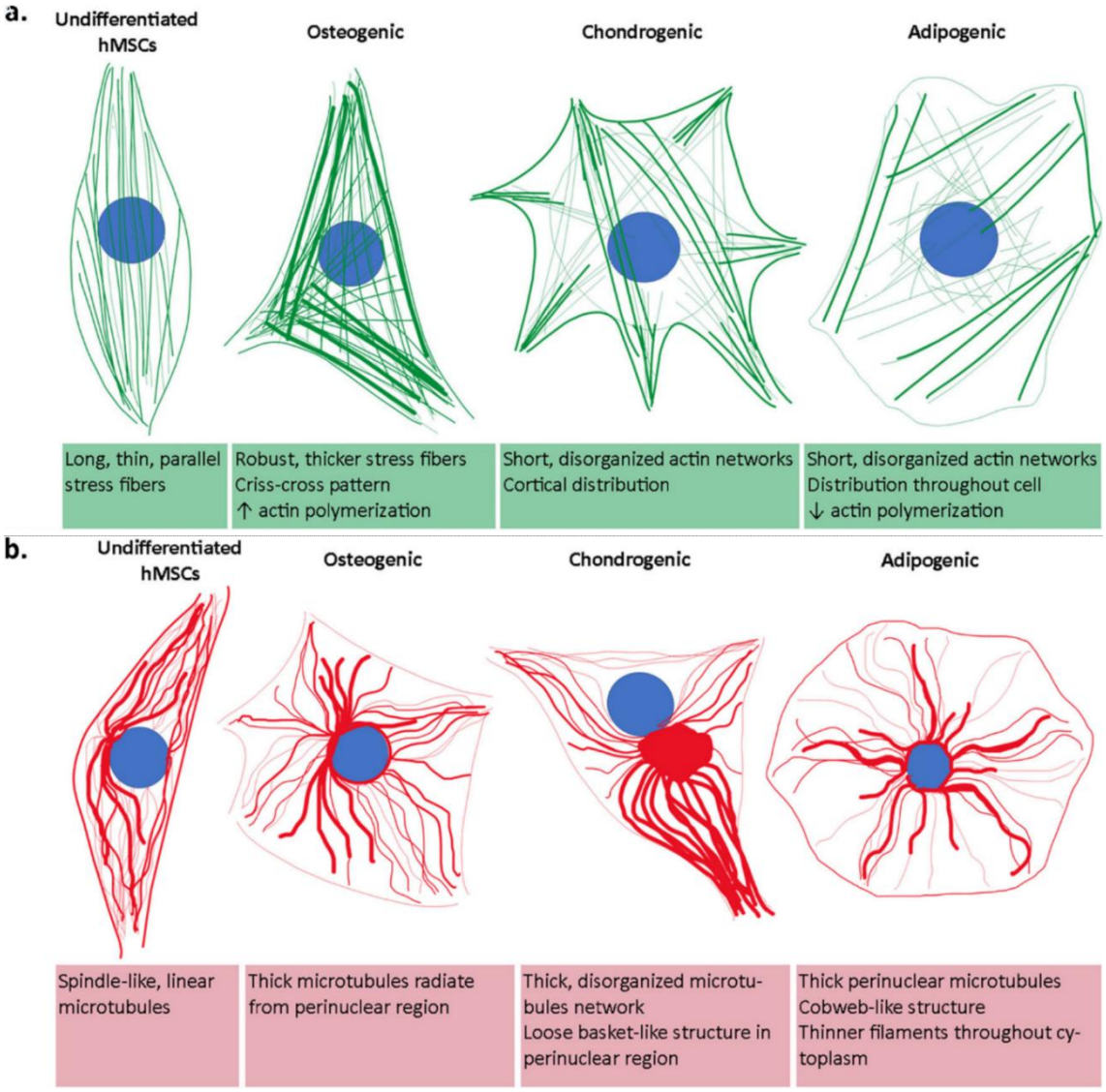

Figure 1-11. MSCs adapt to their local environment through cytoskeletal reorganization
Genetic markers offer a valuable tool for tracing the temporal progression of stem cell differentiation. Likewise, the reorganization of (a) actin and (b) tubulin cytoskeletons align with emergent differentiation of mesenchymal stem cells. Modified from (Putra et al., 2023).

A plethora of studies has explored the influence of cytoskeletal architecture and remodeling on the outcomes of stem cells differentiation. Kilian *et al.* demonstrated the impact of cytoskeletal tension on MSC differentiation by confining cells to various geometries, such as star or flower shapes. They found that thick concave stress fibers, larger FAs, and higher contractility formed on the star pattern promoted robust osteogenic differentiation, while flower shapes induced adipogenic commitment. Disruption of actin or MT polymerization with Cytochalasin D or Nocodazole, respectively, abolished the cell shape differences, leading to adipogenic differentiation when actin was disrupted and osteogenic differentiation when MTs were disrupted on both patterns (Kilian et al., 2010; Lee et al., 2015). Additionally, low-

intensity vibration (LIV) enhanced osteogenic fate selection in MSCs by aligning stress fibers with the primary axis of vibration (Pongkitwitoon et al., 2016). Cyclic hydrostatic pressure (CHP), induced actin expression, remodel vimentin IFs, and induced osteogenic differentiation in C3H/10T1/2 murine embryonic fibroblasts. Using the IF-disrupting agent Withaferin (WA), authors mimicked CHP-induced IF remodeling, highlighting its necessity for osteogenic differentiation (Putra et al., 2023; Stavenschi and Hoey, 2019). Other studies support the interplay between actin polymerization and lineage commitment. Depletion of actin depolymerizers Cofilin1 and Destrin increased F-actin polymerization and osteogenic differentiation in hMSCs (L. Chen et al., 2015). Advances in biomaterial fabrication and bioengineering have further elucidated the role of cytoskeleton remodeling in stem cell regulation(Putra et al., 2023). Fibronectin micropatterning on polydimethylsiloxane (PDMS) substrates revealed the influence of cell spreading and intracellular tension on adipogenic and osteogenic fate determination (McBeath et al., 2004). Adipogenesis was favored in roundish cells on small protein islands, whereas spread cells on large islands committed to osteogenic lineage. This regulatory effect of cell shape on lineage commitment was demonstrated to modulate RhoA-ROCK activity downstream of soluble factors (McBeath et al., 2004). Increasing the shape aspect ratio of rectangular patterns enhanced the osteogenic potential of MSCs (Kilian et al., 2010). Furthermore, stiffer, short silicone micropillars promoted cell spreading, SF thickness, and osteogenic differentiation of hMSCs in comparison to softer, higher pillars that favored adipogenesis (Fu et al., 2010). Culturing MSCs on highly disordered, randomly spaced nanotopographies promoted stress fiber polymerization and vimentin remodeling, thereby enhancing cell adhesion and promoting osteogenic differentiation (Allan et al., 2018; Dalby et al., 2007, 2006). Moreover, tilt dipping the substrate in a polyglycerol solution created a roughness gradient, with high roughness leading to a gradual reduction in cell spreading, organization, and bundling of stress fibers, and FA area. Notably, MCSs exhibited increased osteogenic differentiation through actin ordering until the roughness reached 50%, while cultivation on higher roughness promoted the adipogenesis (Hou et al., 2020). These findings collectively suggest that cytoskeletal remodeling may coincide with or actively regulate cell differentiation processes.

Recent advancements in fluorescence tagging and live-cell imaging techniques have significantly contributed to our understanding of cytoskeletal remodeling during stem cell machano-adaptation and lineage commitment (Putra et al., 2023). By combining fixed and

live-cell imaging with computational workflows, researchers can assess cytoskeletal remodeling and its roles in stem cell behavior. Analysis of structural features or cytoskeleton descriptors, such as architecture, intensity, and distribution, in hMSCs seeded on fibronectin-coated glass, has revealed early changes in actin organization, allowing for the detection and prediction of early time-dependent lineage divergence (Treiser et al., 2010). Fluorescence imaging of labeled actin combined with flow cytometry has enabled the discernment of distinct actin patterns in osteogenic and adipogenic differentiating cells within the initial 24 hours, preceding detectable changes in gene expression (Sonowal et al., 2013).

Mishra *et al.* have investigated the turnover dynamics of the fluorogenic F-actin probe, SiR-actin (SA), in differentiating hMSCs (Mishra et al., 2019). SA labels cells with high levels of actin polymerization or pronounced stress fibers, while low actin polymerization or high actin turnover results in a dim label. By employing a combination of live and fixed-sample imaging, the authors successfully predicted early MSC differentiation tendencies based on SA decay and actin turnover rate (Mishra et al., 2019). Subsequent modification of the analysis through cell fixation and phalloidin labeling, which visualizes the amount of newly synthesized actin, allowed the authors to discern MSC lineage divergence into osteogenic, adipogenic, or chondrogenic populations as early as 1h after differentiation induction through soluble factors (Mishra et al., 2021). These studies collectively suggest that cytoskeletal remodeling serves as a trackable morphological marker of cell differentiation.

Taken together, these research findings elucidate the intricate interplay between a cell's mechanical and chemical environment in shaping cellular behavior and facilitating the differentiation process. Actin and tubulin play crucial roles in regulating cellular ability to generate traction, contract and, change shape, leading to their assembly and disassembly, often resulting in anisotropic spatial distribution. This phenomenon is conductive to guiding lineage commitment. Thus, cytoskeletal remodeling serves as an indicator of the unfolding lineage commitment or stage of stem cell differentiation (Putra et al., 2023).

1.7. The cytoskeleton of the skeletal muscle

The muscle cytoskeleton undergoes major reorganization during myogenic differentiation, with myoblasts and myofibers sharing numerous cytoskeletal components that dynamically interact to govern cellular functions (Jabre et al., 2021). The cytoskeleton of myoblasts and myofibers is composed of actin filaments, microtubules, intermediate filaments, the linker of

nucleoskeleton and cytoskeleton (LINC) complex, which interconnects the nuclear cytoskeleton and nuclear envelope (NE) with the cytoplasmic cytoskeleton and associated proteins. Myoblast actin cytoskeleton exhibits radial organization reminiscent of naïve MSC, characterized by ventral stress fibers, a dorsal actin cap, and transmembrane actin-associated nuclear (TAN) lines (Jabre et al., 2021). Notably, the actin cap, a developmentally regulated structure absent in embryonic stem cells and myofibers (Khatau et al., 2012, 2009; Roman et al., 2017), plays a critical role in nuclear mechano-transduction (Shiu et al., 2018). During myogenesis, the muscle-specific isoform α-actin becomes the predominant isoform, localizing to sarcomeric thin filaments (Bains et al., 1984), while β and γ isoforms are downregulated and localize to the perinuclear area (Otey et al., 1988). β- and γ-actins reside in the cortical area, contributing to the formation of the paraxial costameric F-actin network, which facilitates radial force transmission (Ervasti, 2003; Jabre et al., 2021). However, the structure and function of the perinuclear actin cytoskeleton in myotubes remains poorly understood (Jabre et al., 2021).

In myoblasts, MTs are radially organized and show centrosome-dominated distribution, playing key roles in intracellular transport, transmission of external mechanical forces, and nuclear shape maintenance (Becker et al., 2020; Lucas and Cooper, 2023). Upon myogenic differentiation, there is a significant remodeling of centrosomal proteins, necessitating their relocation to the surface of the nucleus (Becker et al., 2021, 2020; Muroyama and Lechler, 2017). MT nucleation relies on centrosome proteins, leading to a remodeling of MT architecture into an ordered paraxial array of filaments within the myotube (Becker et al., 2020). Additionally, mature myofibers develop a network of perinuclear MTs characterized by a high-density cage-like structure and a collection of circular and radial-anisotropic filaments (Jabre et al., 2021; S. Wang et al., 2015).

Cytoplasmic intermediate filaments represent a flexible component the cytoskeleton that undergoes major remodeling during myogenesis (Jabre et al., 2021). Several IFs are expressed in myoblasts and are developmentally regulated in human muscle progenitors (Capetanaki et al., 2007). Among these, Vimentin and Nestin are non-muscle specific IFs in myoblasts, organized in dense networks linked to outer nuclear membrane, but are downregulated during myogenesis (Abe et al., 2004; Salmon and Zehner, 2009; Sejersen and Lendahl, 1993). Conversely, Desmin, one of muscle specific IFs, is barely expressed in myoblasts, but becomes prominently expressed in terminally differentiated myofibers and adult muscle. While

Desmin seems dispensable during myogenesis (Li et al., 1997), it plays crucial roles in muscle structural integrity, cellular integrity, force transmission, and mitochondrial homeostasis (Agnetti et al., 2022). In mature myotubes, Desmin forms a large three-dimensional network that connects the contractile apparatus, the ECM, and cellular organelles (Jabre et al., 2021). Within the perinuclear area of myotubes, Desmin filaments extend from the Z-lines to the nuclear envelopes. The primary features of the cytoskeletal remodeling during skeletal myogenesis are summarized in Fig. 1-12.

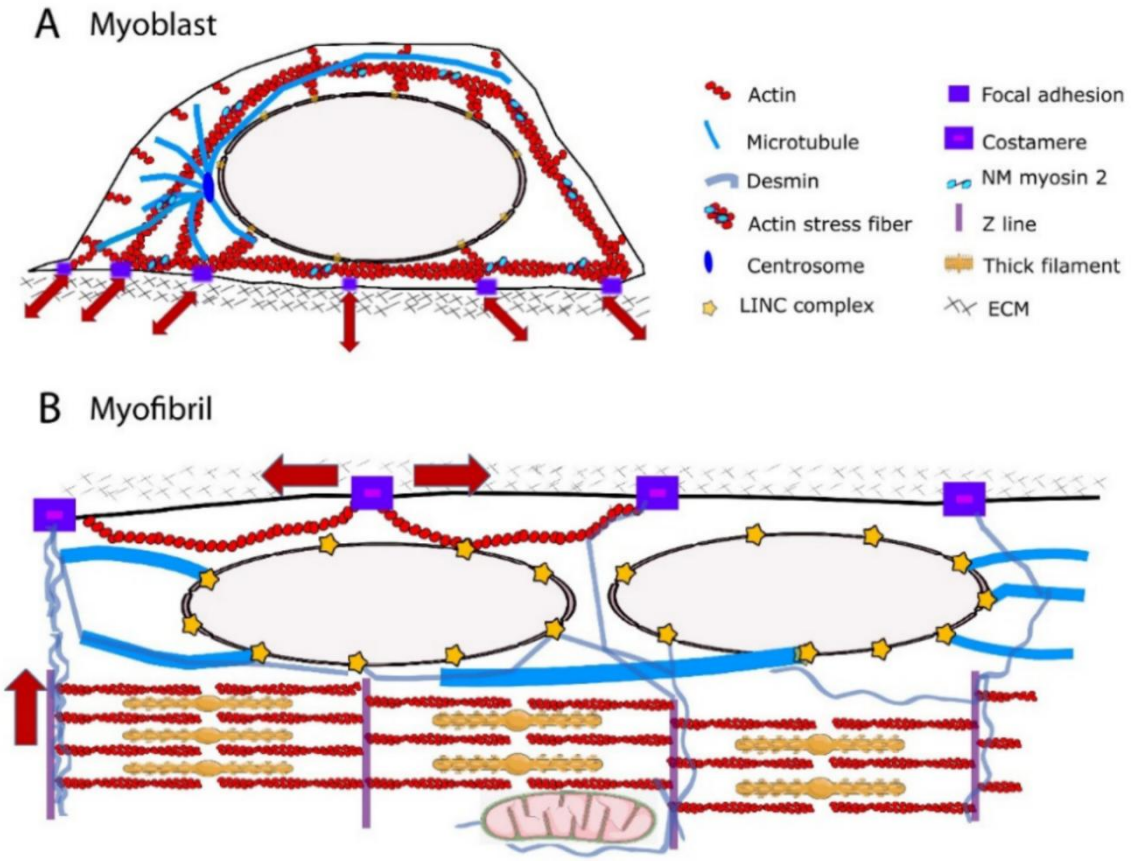

Figure 1-12. Cytoskeletal remodeling from myoblast to myofibril
A Myoblasts display a mesenchymal cytoskeletal organization characterized by primarily radial distribution of microfilaments (actin), microtubules, and intermediate filaments (Desmin). These cells form direct connections with the substrate via focal adhesion, facilitating the transmission of forces along actin filaments towards the nucleus and from the cell interior to the ECM (red arrows). The perinuclear cytoskeleton is linked to the nuclear envelope through the linker of nucleoskeleton and cytoskeleton complex (LINC). **B** Mature myotubes predominantly exhibit paraxial arrays of F-actin, MTs and IFs oriented in the direction of sarcomeric contraction. However, the radial distribution of cytoskeletal proteins also plays a crucial role in ensuring proper cellular function. Modified from (Jabre et al., 2021).

Cytoskeletal architecture possesses the ability to both influence and correlate with differentiation of cells (Mishra et al., 2021). Particularly in highly mechanosensitive cells like

myoblasts and myofibers (Engler et al., 2004; Olsen et al., 2019; Pang et al., 2023), cytoskeletal properties such as remodeling and contractility are essential for mechano-adaptation during myogenesis (Bruyère et al., 2019). Muscle cells respond to various biomechanical stimuli, including substrate stiffness, stretch, and topography (Pang et al., 2023). For instance, Engler *et al.* used atomic force microscopy (AFM) indentation to measure the rigidity of murine skeletal muscle and C2C12 cells, finding it to be approximately 12 kPa (Engler et al., 2004). Culturing C2C12 cells on collagen-coated polyacrylamide gels matching this intracellular stiffness (~12 kPa) led to enhanced myoblast differentiation, fusion, and striation(Engler et al., 2004). Similarly, the maintenance of mouse and human MuSCs stemness was achieved by culturing on engineered 3D micro scaffolds comprising collagen, recombinant laminin, and α4β1 integrin. Despite the lower stiffness of the scaffold (~1-2 kPa) compared to optimal muscle stiffness, replicating key biophysical and biochemical properties of the native niche, including geometry, elasticity, ECM composition, and structure, along with a cocktail of quiescence-modulating molecules, proved sufficient to preserve the quiescence signature of MuSCs (Quarta et al., 2016).

Furthermore, substrate rigidity regulates the self-renewal ability of mouse and human MuSCs. Murine MuSCs cultured on polyethylene glycol (PEG) hydrogels mimicking muscle elasticity (12 kPa) exhibited self-renewal *in vitro* and contributed to regeneration when transplanted into mice (Gilbert et al., 2010). Similarly, culturing human MuSCs on soft poly-L-lysine/hyaluronic acid films preserved their quiescence and stemness compared to stiffer substrates (Monge et al., 2017). Notably, muscle rigidity transiently increases during regeneration (Silver et al., 2021). Culturing C2C12 cells on hydrogels that mimic the stiffness of injured muscle resulted in heightened proliferation, migration and nuclear Yap/Taz accumulation (Silver et al., 2021). Similarly, when primary myoblasts were cultured on stiff hydrogels, Notch signaling was found to synergize with substrate stiffness to inhibit differentiation in a RhoA-ROCK-dependent manner (Safaee et al., 2017).

Lastly, Trensz *et al.* conducted a study measuring the stiffness of intact and collapsed myofibers (0.5 versus 2.0 kPa). Subsequent cultivation of myogenic progenitor cells (MPCs) on hydrogels mimicking collapsed myofibers inhibited spontaneous differentiation and promoted proliferation (Trensz et al., 2015). This finding is consistent with previous research indicating a strong correlation between MPC proliferation and substrate elasticity (Boonen et al., 2009). Additionally, numerous other biophysical stimuli have been shown to influence

myoblast behavior, contributing to skeletal muscle formation. This stimuli include substrate topography, electrical and magnetic stimulation, tensile strain, ultrasound and altered gravity (Iberite et al., 2022; Mueller et al., 2021; Pang et al., 2023; Wang et al., 2020). The wide array of cues that regulate the behavior of myogenic progenitor cells underscores the significance of cytoskeletal remodeling in mediating skeletal muscle formation, serving as primary mediator of cellular mechano-adaptation (Putra et al., 2023).

1.7.1. Rho GTPases and cytoskeletal dynamics

The Rho GTPases are widely recognized as key regulators of actin remodeling and related biological processes, including cell adhesion, migration, and polarity. However, their influence extends beyond actin dynamics to encompass MT dynamics, cell cycle progression and transcriptional regulation (Etienne-Manneville and Hall, 2002; Hall, 1998; Rodríguez-Fdez and Bustelo, 2021). Recent studies have underscored the critical roles played by Rho GTPases play in myogenesis (Bryan et al., 2005; Rodríguez-Fdez and Bustelo, 2021). Comprising 20 members, the canonical Rho GTPase family, exhibits predominantly ubiquitous expression, with RhoA, Rac, and Cdc42 being the most extensively studied subfamilies (Boureux et al., 2007). The Rho GTPases undergo cycles of activation and inactivation during cell signaling (Bourne et al., 1990). Activation is facilitated by GDP/GTP exchange factors (GEFs), which catalyze the release of GDP and the incorporation of the GTP molecules, leading to GTPases anchoring to the plasma membrane via C-terminal prenylation. Conversely, inactivation is mediated by GTPase activating proteins (GAPs), which promote GTP hydrolysis. Additionally, guanine nucleotide dissociation inhibitors (GDIs) bind to GDP-bound GTPases, rendering them inactive, and retaining them in the cytoplasm through sequestration of the C-terminal geranyl-geranyl group (Etienne-Manneville and Hall, 2002; Rodríguez-Fdez and Bustelo, 2021). Active Rho GTPases engage numerous downstream effectors, with over 200 identified to date (Bagci et al., 2020). These effectors include kinases such as Rho kinase (ROCK), p21-activated kinase (Pak) c-Jun N-terminal kinase (JNK), and scaffolding proteins such as mammalian Diaphanous related formin 1 (mDia1) and the Wiskott-Aldrich syndrome protein (WASP), as well as transcription factors such as serum response factor (SRF), the Yes-associated protein (YAP)/WW domain containing transcription regulator 1 (TAZ) complex (Rodríguez-Fdez and Bustelo, 2021). Moreover, the existence of 84 Rho GEFs, 66 Rho Gaps,

and 3 Rho GDIs in humans underscores the importance of intricate regulation in GTPase activity (Fort and Blangy, 2017; Mosaddeghzadeh and Ahmadian, 2021).

1.7.2. Rho GTPases in muscle differentiation

A rich body of research has shown the direct involvement of Rho GTPases in the regulation of both embryonic and adult myogenesis, where they exert influence over processes integral to cell fate determination and later myogenesis steps (Rodríguez-Fdez and Bustelo, 2021). The delineation of these functions is often complex, as different members of Rho family have been shown to act synergistically or exhibit opposing roles at specific stages of differentiation (Bryan et al., 2005). For instance, RhoA has been implicated in contributing downstream of IGF1 to the commitment of MSCs toward myogenic and adipogenic lineages. Elimination of ArhGAP5 leads to increased RhoA activity, promoting the spontaneous differentiation of murine embryonic fibroblasts into muscle cells in culture. It is speculated that RhoA coordinates both cytoskeletal remodeling and gene transcription required for cell differentiation (Sordella et al., 2003). Furthermore, RhoA has been demonstrated to be essential for the initial induction of the myogenic program, partially through its stimulation of SRF targets, and to maintain the proliferative state of myoblasts (Carnac et al., 1998; Castellani et al., 2006). Subsequent steps of myogenesis such as cell cycle exit and myoblast fusion, require RhoA signaling to be downregulated, a process possibly mediated by ArhGAP26 and ArhGAP35 (Rodríguez-Fdez and Bustelo, 2021). RhoA maintains myoblast identity through SRF-dependent Myod1 expression. Constitutively active RhoA blocks myogenesis, while inhibition of RhoA, achieved through C3 transferase-mediated inhibition or dominant negative mutants of RhoA, have no discernible effect on myogenic progression of C2C12 cells (Castellani et al., 2006; Gauthier-Rouviere et al., 1996). ROCK activity is also crucial in maintaining myoblast proliferation and preventing premature commitment, partly through the phosphorylation and cytoplasmic sequestration of the Foxo1 transcription factor. Foxo1, which in turn, binds and sequesters MRTF-A/Smad1 complex from Id3 promoter, thereby enhancing myogenic differentiation. Constitutively active ROCK mutant inhibits myogenic progression, whereas inhibition of the kinase through Y27632 small molecule greatly promotes it (Castellani et al., 2006; Iwasaki et al., 2008; Nishiyama et al., 2004). RhoA was shown to fluctuate between high and low activity *in vitro*, consistent with its role (Castellani et al., 2006).

Rac1 and Cdc42 play roles in the later stages of muscle differentiation, regulating myoblast fusion through their effector proteins Pak1 and Pak3 (Charrasse et al., 2007; Vasyutina et al., 2009). Levels of active Rac1 and Cdc42 increase during myogenesis in cell culture, opposing the pattern observed for RhoA (Travaglione et al., 2005). The GEF Dock1 activates Rac1, while the Rho GEF Trio is involved into Rho activation downstream of M-Cadherin before myoblast fusion (Laurin et al., 2008; Moore et al., 2007) . The known roles of Rho GTPases during myogenesis are summarized in Fig. 1-13.

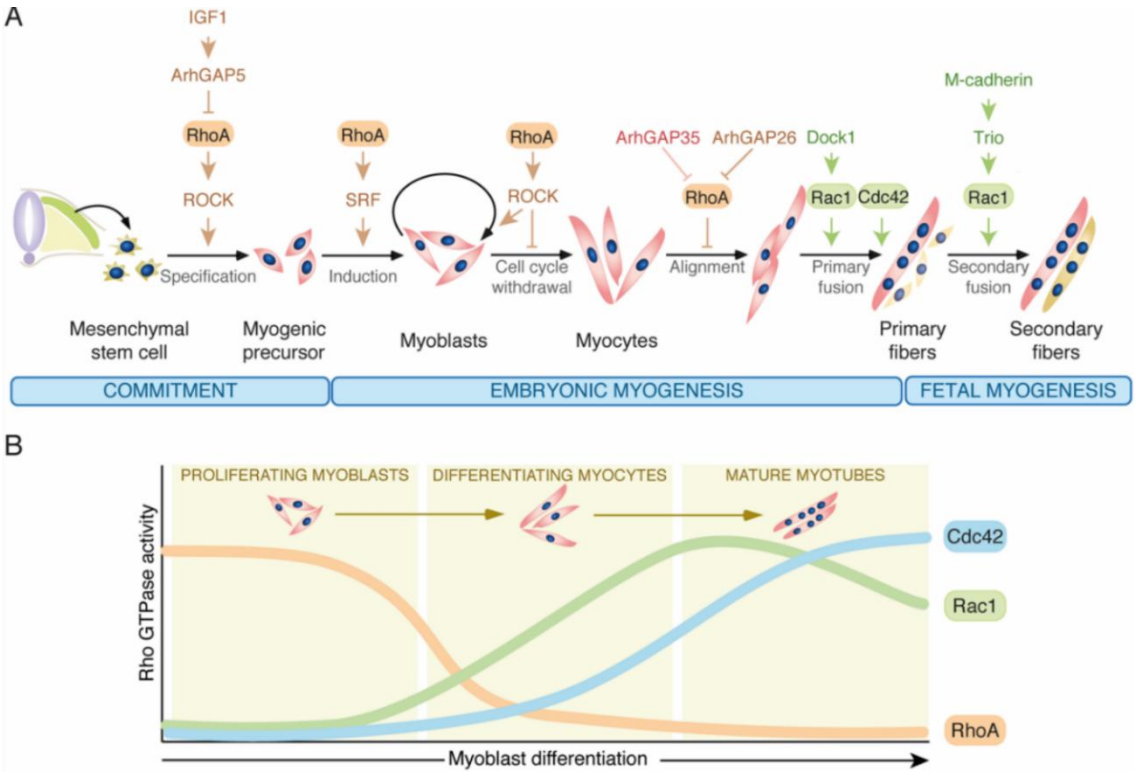

Figure 1-13. The roles and activity of Rho GTPases during myogenesis
A Current understanding suggests that Rho GTPases play crucial roles in the initial stages of myogenic development, regulating the commitment of mesenchymal progenitors, the appropriate expansion of muscle progenitor cells, as well as primary and secondary fusion. **B** The schematic line plot illustrates the dynamics of Rho GTPase activities throughout myogenic differentiation, primarily derived from *in vitro* experiments with C2C12 cells. Modified from (Rodríguez-Fdez and Bustelo, 2021).

In addition to their fundamental roles in muscle development, Rho GTPases are implicated in myofibrillogenesis, muscle mass regulation, muscle-related pathologies, and regenerative processes. Specifically, RhoA has been found to facilitate proper timing of the cell cycle re-entry in MuSCs during activation (Rodríguez-Fdez and Bustelo, 2021). In a quiescent state, satellite cells reside within the stem cell niche beneath the basal lamina, where Notch and WNT signaling pathways predominantly maintain their dormant state (Bjornson et al., 2012; Eliazer et al., 2022; Mourikis et al., 2012). Yap signaling, on the other hand, serves as a crucial

mediator breaking the quiescence (Esteves de Lima et al., 2016; Zhang et al., 2019). Satellite cells have been shown to sustain RhoA activity, primarily induced by WNT4 protein emanating from muscle fibers (Eliazer et al., 2019). Eliazer *et al.* demonstrated that the activated RhoA-ROCK axis, in turn, suppresses Yap activity in quiescent cells, thereby preventing their transition to an active state. Consequently, a reduction in WNT4 signaling during injury would inhibit RhoA activity, thereby promoting Yap-mediated quiescence break. These findings indicate the pivotal role of cytoskeletal signaling preceding cell cycle entry in regulating fate decisions and the dynamic transition of muscle stem cells during early activation (Eliazer et al., 2019).

In contrast to previous findings, Kann and colleagues present evidence that MuSCs exhibit Rac1-promoted cytoplasmic projections (Fig. 1-14), which respond to muscle injury by upregulating RhoA/ROCK signaling. This switch from Rac1 to RhoA facilitates the retraction of the projections and drives the downstream transition from quiescent to activated stem cells (Kann et al., 2022). These long and heterogenous quiescent projections resemble motile structures with active filopodia formation, presumed to act as sensors of the niche (Fig. 1-14A). The projections, capable of full retraction within 2-3 hours, consist of core tubulin structures flanked by a cortical actin cytoskeleton (Fig. 1-14B-C). Additionally, there is an anisotropic distribution of cell-cell adhesion molecules such as M- and N-Cadherins, with M-Cadherin equally distributed and N-Cadherin exclusively localizing to the quiescent projections (Fig. 1-14D-E). The RhoA-driven retraction of projections involves isotropic redistribution of N-Cadherin, substantial reorganization of microtubules and microfilaments, formation of the centrosomal MT organizing center (cMTOC), nuclear translocation of MRTF-A, and ultimately expression of Myod1. Interference with Rac1, RhoA or N-Cadherin activity or function results in morphological changes in muscle stem cells and premature quiescence break (Fig. 1-14F) (Kann et al., 2022). In summary, the authors propose a model in which the projections of muscle stem cells monitor the niche environment for signals of tissue damage, leading to a switch in GTPase activity and cytoskeletal remodeling associated with retraction. These cellular changes are necessary for the efficient temporal control of stem cell activation (Krauss and Kann, 2023).

The regulation of Rho GTPase levels in MuSCs remains an area requiring further investigation. However, studies conducted by Brack (Eliazer et al., 2019) and Krauss (Kann et al., 2022) labs have shed light on the importance of cytoskeletal signaling in the initial stages of myogenic

differentiation. These findings establish cytoskeletal remodeling as a crucial aspect of mechano-adaptation in MuSCs, driving the differentiation process.

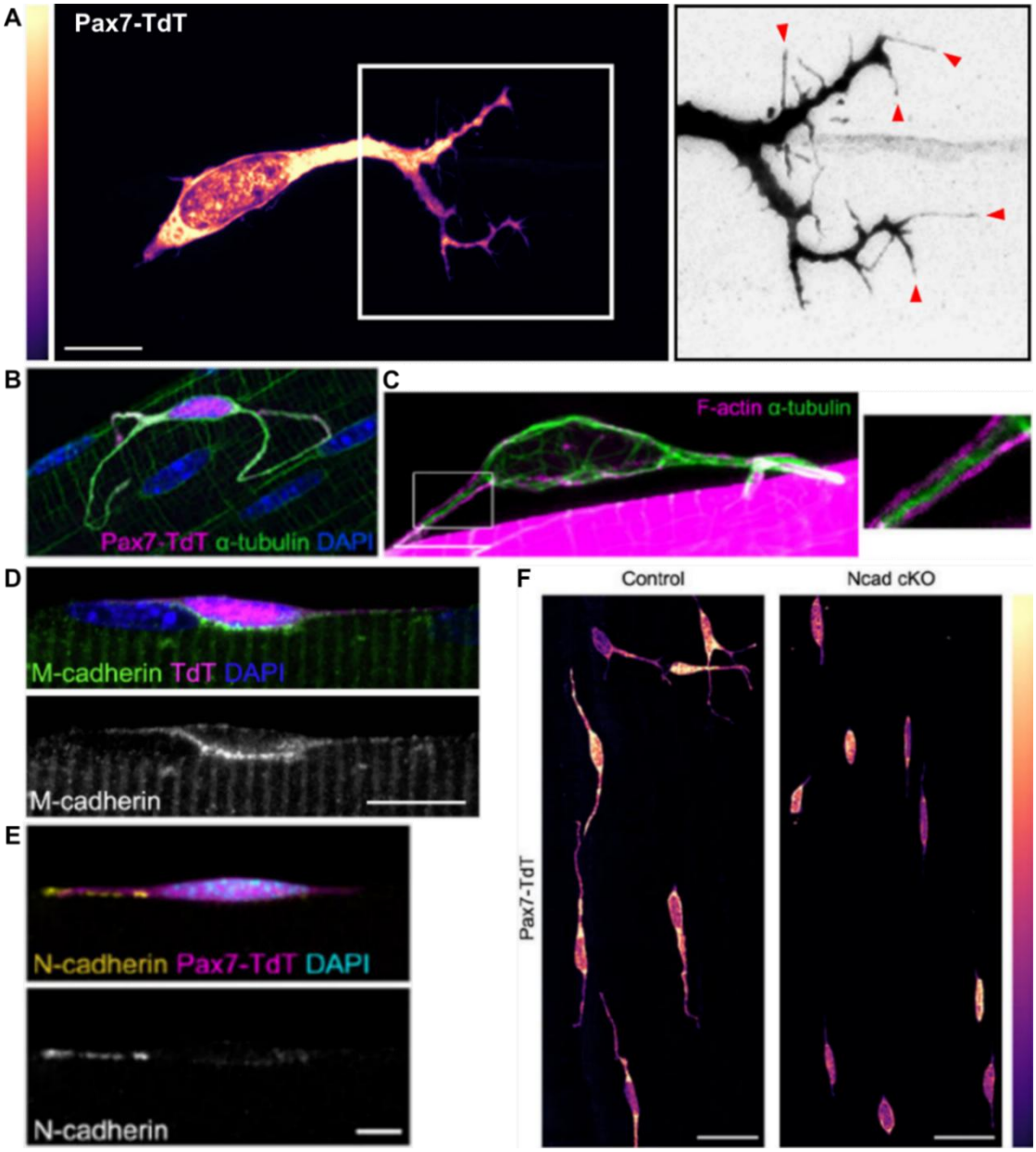

Figure 1-14. The cytoskeleton-based dynamic projections of satellite cells resemble motile structures

A Tissue clearing was performed on the EDL muscle, allowing visualization of the MuSC-specific Pax7-TdTomato reporter. Signal intensity is depicted using a Lookup Table. The magnified view on the right highlights filopodia indicated by red arrowheads at the end of the projections. **B-C** MuSCs show a dense α-tubulin network (B) and cortical actin structures (C) within the quiescent projections. The magnified image on the right illustrates the core tubulin structure flanked by cortical actin cytoskeleton. **D** Immunofluorescence images of the M-Cadherin show its uniform distribution in the apical adherens junctions facing the myofiber in quiescent MuSCs. **E** N-Cadherin specifically localizes to the quiescent projections in the MuSCs. **F** Pax7-TdT images in cleared EDL muscle from control and $Cdh2^{fl/fl}$;$Pax7^{CreERT2}$ (Ncad cKO) mice, showing genetic depletion of N-Cadherin. Depletion of N-Cadherin leads to the activation of quiescent MuSCs(Goel et al., 2017), underscoring the conserved feature of dynamic projections during muscle stem cell activation. Modified from (Kann et al., 2022; Krauss and Kann, 2023).

1.7.3. Cytoskeletal remodeling during myoblast migration

Muscle regeneration relies on the activation and mobilization of the resident stem cell population. Following activation, MuSCs initiate proliferating and migrate towards the injury site, where committed myoblasts align and fuse with each other or existing myofibers (Relaix et al., 2021). This process is best elucidated through studies conducted on freshly isolated murine myofibers, cultured *in vitro*, where activated MuSCs emerge from beneath the basal lamina (Bischoff, 1975; Brondolin et al., 2023). *In vitro* analysis shows that proliferating MuSCs initially exhibit a roundish morphology, and assume an elongated shape as they commence differentiation (Brondolin et al., 2023). High-resolution imaging further revealed that MuSCs undergo rapid migration on myofibers, employing an ameboid mode characterized by rapid cortical contraction and membrane blebbing (Collins-Hooper et al., 2012; Otto et al., 2011; Urciuolo et al., 2018). This mode relies on both actin remodeling to generate membrane protrusion and minimal interaction with the substrate (Charras and Paluch, 2008; Liu et al., 2015).

In contrast, Siegel *et al.* have demonstrated that MuSCs migrate via pseudopodia extension on myofibers embedded in a 3D collagen gel (Siegel et al., 2009). This mesenchymal mode of movement entails cell adhesion to the ECM and coordinated actin-driven leading-edge protrusion, along with posterior retraction of the cell (Petrie and Yamada, 2012). The process involves the formation of fan-shaped lamellipodia and slender hair-like filopodia, comprising branched actin and parallel, bundled actin filaments, respectively. Lamellipodia formation is primarily mediated by Rac1 activity and its downstream targets such as actin-related protein 2/3 (Arp2/3) and the WASP-family verprolin-homologous protein regulatory complex (WAVE), while Cdc42 regulates filopodia formation predominantly through diaphanous formins (Choi et al., 2020; Petrie and Yamada, 2016). Finally, RhoA-ROCK-driven anterior cell contractility propels cellular movement through a complex 3D environment (Doyle et al., 2021). Recent intravital microscopy (IVM) imaging studies in zebrafish and mouse muscle injury models have corroborated pseudopodia as the principal mode of satellite cell migration (Baghdadi et al., 2018; Gurevich et al., 2016; Webster et al., 2016).

It is notable that inhibition of RhoA-ROCK signaling in migrating zebrafish MuSCs led to alterations in cell shape, migration mode, and coincided with increased differentiation (Brondolin et al., 2023). Briefly, ROCK inhibition caused MuSCs to adopt more elongated shape with a posteriorly displayed nucleus and exhibit higher migration speed, recapitulating

phenotypic changes observed in C2C12 cells treated similarly with the Y-27632 inhibitor (Brondolin et al., 2023; Goetsch et al., 2014). Additionally, ROCK inhibition in zebrafish MuSCs lead to formation of smaller pPaxillin adhesions and loss of their polar distribution relative to the axis of migration, mimicking smaller adhesions and a more motile “gliding” phenotype observed in C2C12 cells with impaired ROCK signaling (Brondolin et al., 2023; Goetsch et al., 2014). Ultimately, Brondolin *et al.* demonstrated a reduction in genes associated with G2/M transition and Yap/Taz target genes, as well as an increase in Myod1 expression in zebrafish MuSCs treated with Y-27632, suggesting that the RhoA-ROCK-YAP axis prevents premature differentiation during migration to the injury site (Brondolin et al., 2023). Collectively, the authors propose that migration behavior can predict altered MuSCs outcomes, with higher adhesion and slower, punctuate migration associated with increased proliferation, while faster migration and reduced adhesion was indicative of increased myogenic differentiation (Brondolin et al., 2023).

1.7.4. Cytoskeletal remodeling during myoblast fusion

Myoblast fusion is essential for skeletal muscle development and regeneration (Tajbakhsh, 2009).Extensive cytoskeletal reorganization occurs before and after myoblast fusion, as demonstrated in various models, from flies to mice (Duan and Gallagher, 2009; Fulton et al., 1981; Richardson et al., 2007; Sens et al., 2010; Städler et al., 2010). In *Drosophila melanogaster*, fusion involves mononucleated founder cells (FCs) and fusion-competent myoblasts (FCMs), specified by the action of transcription factors (Tixier et al., 2010), leading tosyncytial myofibers (Rushton et al., 1995). Initial recognition and cell adhesion is mediated by proteins of the immunoglobulin (Ig) superfamily, where FCs express Nephrin-like proteins Dumbfounded (Duf or Kin-of-Irregular chiasm Kirre) and Roughest (Rst or IrreC), while FCMs express Nephrin homologs, Sticks-and-stones (Sns) and Hibris (Hbs) (Abmayr and Pavlath, 2012). Sns- Duf interactions facilitate adhesion and membrane apposition (Galletta et al., 2004), bringing their plasma membranes within close proximity, about 45 nm apart (Özkan et al., 2014), a distance insufficient for membrane fusion to occur (Petrany and Millay, 2019).Whether asymmetric myoblast fusion, reliant on distinct muscle cell types, occurs in vertebrates and if *Drosophila* CAMs play analogous roles in other systems remain unclear (Kim et al., 2015a). Further insights into these regulatory molecules are covered in elegant

detail elsewhere with an emphasis on vertebrae myoblast fusion (Galletta et al., 2004; Lee and Chen, 2019; Lehka and Rędowicz, 2020a; Willkomm and Bloch, 2015).

Cytoskeletal dynamics, particularly actin polymerization, are central to membrane fusion. In *Drosophila*, actin regulators and nucleation promoting factors (NPFs) such as WASP and Scar (*Drosophila* homolog of WAVE) (Berger et al., 2008; Richardson et al., 2007) and their partners WASP-interacting protein (WIP or Solitary, Sltr) (Massarwa et al., 2007) and Kette (the Nckap1 homolog) (Schröter et al., 2004) drive actin reorganization via the Arp2/3 complex. Upstream of Scar, *Drosophila* Rac GTPase, through its bipartite GEF Myoblast city (Mbc, homolog of Dock1) and Engulfment and cell motility (Elmo) (Geisbrecht et al., 2008), modulates actin polymeriazetion. Furthermore, small GTPase Arf6, together with its GEF Loner (homolog of Brag2) regulates Rac localization (Chen et al., 2003). This leads to the formation of an actin focus in FCMs, which protrudes into FCs, creating podosome-like structures (PLS) that assist in membrane deformation and potentially serves as a site for the accumulation of other fusion-promoting elements (Haralalka et al., 2014; Schejter, 2016; Sens et al., 2010). The interface between the PLS and the trans-interacting CAMs residing in the indented layer of both cell membranes is referred to as the fusogenic synapse (Chen, 2011). In response, FCs increase cortical tension via Myosin II (MyoII) accumulation, regulated by the Rho1-Rok axis, facilitating the creation of fusion pores (Kim et al., 2015a, 2015b).

In vertebrates, many actin-regulating molecules are conserved, including homologs of Mbc (Dock1/ Dock5), Rac1, and N-WASP.However, specific details of cytoskeletal asymmetry during fusion remain unclear in vertebrates (Kim et al., 2015a). Key proteins like the multi-pass transmembrane protein Myomaker (Millay et al., 2013) and the small protein Myomerger (Quinn et al., 2017) are essential for vertebrate myoblast fusion, regulating membrane hemifusion and pore formation, respectively. Though these proteins lack structural homologs in known fusogens, they are sufficient to induce fusion in non-fusogenic cells (Sampath et al., 2018).

Phospholipids, Particularly Phosphatidylserine (PS), play crucial roles in membrane fusion by interacting with effectors like Brain-specific angiogenesis inhibitor 1 (BAI1) and Stabilin-2, which promote Rac1-dependent actin polymerization (Hochreiter-Hufford et al., 2013; Park et al., 2016). Disruption of PS, phosphatidylinositol (4,5)bisphosphate or actin regulators like Annexin I and V and Dynamin can impair different stages of myoblast fusion (Leikina et al., 2013; Sampath et al., 2018).

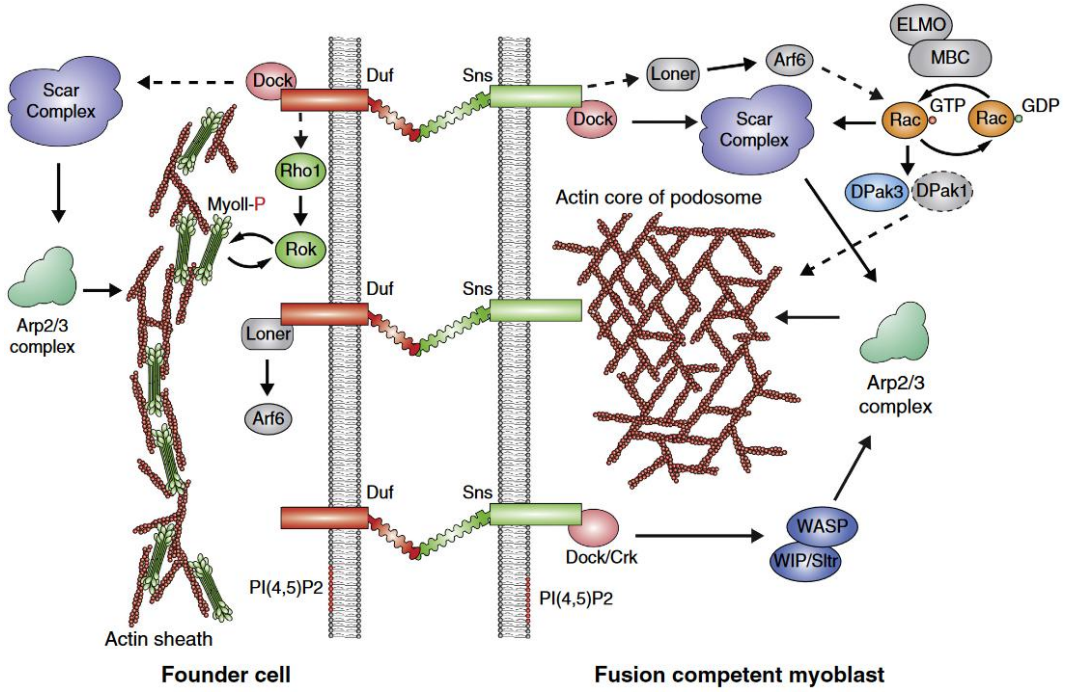

Figure 1-15. Asymmetric signaling pathways in Drosophila myoblast fusion
The process of cytoskeletal remodeling during myoblast fusion is extensively studied in the embryonic development of *Drosophila*, providing valuable insights into this asymmetric process. It involves two distinct populations of progenitor cells: the founder cells (FCs) and fusion competent myoblasts (FCMs). FCs, positioned at sites where mature muscle will form, attract migrating FCMs through trans-interactions of cell adhesion molecules (CAMs), facilitating their recognition and adhesion. The engaged of CAMs triggers cytoskeletal signaling resulting, resulting in the formation of a thin actin sheath in FCs and a dense, branched actin-enriched focus within the FCMs, forming part of a podosome-like structure. This actin-based mechanism generates pushing and resisting forces, promoting tight adhesion of plasma membranes between the fusion partners. Ultimately, protein machineries containing fusogens facilitate the fusion of cellular membranes and the mixing of cellular contents, culminating in the formation of a syncytial cell. Despite the low conservation observed in invertebrate and vertebrate myoblast fusion machineries, cytoskeletal remodeling remains a critical element required for myoblast fusion across these animal groups. For a comprehensive understanding of this process, further details can be found in the main text and are reviewed in greater detail in (Abmayr and Pavlath, 2012; Kim et al., 2015a; Sampath et al., 2018; Schejter, 2016). Modified from (Kim et al., 2015a).

Overall, myoblast fusion involves a conserved multi-step process of cell adhesion, actin-mediated membrane apposition, and membrane coalescence. However, some components of this process exhibit limited conservation between invertebrates and vertebrates, particularly in terms of adhesion effectors. For instance, in *Drosophila*, the Irre recognition Module (IRM) consisting of the Ig superfamily proteins like Duf, Rst, and Sns, plays a crucial role, whereas in zebrafish myogenesis, Junctional adhesion molecule B and C (Jamb, Jamc) are essential. However, the specific adhesion proteins pertinent to mammalian myoblast fusion remain elusive. In contrast, the process of branched actin polymerization and

remodeling appears to be more conserved during myoblast fusion across species, albeit with species-specific variations in protein composition and mechanistic details (Krauss et al., 2017; Sampath et al., 2018).

1.8. The septin cytoskeleton

As highlighted in previous sections, the anisotropic distribution and dynamic remodeling of cytoskeletal components including microtubules, microfilaments, and intermediate filaments, often play a pivotal role in guiding lineage commitment. Despite being identified over 50 years ago and recognized as integral elements of the cytoskeleton, septins have received limited attention in the field of muscle research. As of the time of writing, only a small number of publications have explored their involvement in the context of myogenesis. The following paragraphs will delve into the literature to introduce the principles of organization and function of mammalian septins, elucidate regulatory mechanisms governing their remodeling, and provide an overview of their involvement in the regulation of cellular differentiation processes.

1.8.1. The molecular building blocks for the cell

Septin GTPases are heteropolymeric cytoskeletal proteins (Mostowy and Cossart, 2012), first discovered in 1970 by Leeland H. Hartwell as four alleles in *Saccharomyces cerevisiae*, causing temperature-sensitive cytokinesis defect during the cell division cycle (cdc) mutant screen. Initially named based on their roles in cytokinesis (Cdc3, Cdc10, Cdc11 and Cdc12) (Hartwell et al., 1973, 1970), further studies revealed septins forming ring-like structures at the plasma membrane of the septate bud neck, confirming their role in recruiting essential players of cell division (Byers and Goetsch, 1976; Longtine et al., 2000). Recognizing their distinctive localization, the lab of John Pringle renamed this protein family “septins” in the early nineties (Sanders and Field, 1994). For a long time, believed to be limited to opisthokonts (the group of fungi, animals, and their close relative choanoflagellates), septins have since been identified in all clades of eukaryotes except of land plants (Nishihama et al., 2011; Shuman and Momany, 2022). It has been proposed that septins evolved from an ancestral bacterial GTPase and were present in a very early eukaryotic progenitor. However, their significant

expansion occurred during opisthokont diversification (Cao et al., 2007; Nishihama et al., 2011; Weirich et al., 2008).

In 2001, Momany lab classified fungal septins into five groups based on sequence homology, with most fungal septins falling into four groups consisting of core or prototypical yeast septins (Cdc3, 10, 11 and 12). Additionally, some fungal septins, that did not group with others were suggested to constitute a separate, fifth group (Momany et al., 2001). These group 4 septins were later discovered not only in filamentous fungi but also in protists and early diverged eukaryotes, leading to the contemporary belief of their ancestral role the evolution of septins (Auxier et al., 2019; Nishihama et al., 2011). Septins exhibit high structural conservation among species, but the number of genes per organism varies substantially. For example, there is only one septin gene in *Chlamydomonas*, two in *C. elegans*, five in *D. melanogaster*, seven in S. *cerevisiae*, thirteen each in *M. musculus* and *H. sapiens,* and seventeen in *D. rerio* (Pan et al., 2007; Shuman and Momany, 2022; Willis et al., 2016).

In 2002, Ian Macara and colleagues proposed a unified nomenclature for mammalian septins to address the confusion surrounding their naming conventions (Macara et al., 2002). Subsequently, Kinoshita and colleagues classified 13 human septins into four groups based on sequence similarity, which differed somewhat from the fungal classification proposed earlier (Kinoshita, 2003). Further analysis of metazoan species revealed that all septins fell into the four Kinoshita categories, leading to the widespread adoption of this nomenclature (Cao et al., 2007). Based on molecular interactions among paralogues, Kinoshita *et al.* proposed that group members were potentially interchangeable within heteropolymers, a concept now known as the “Kinoshita rule”, although the underlying molecular mechanisms of this phenomenon emerged only recently (Cavini et al., 2021).

The mammalian septin gene family comprises 13 members: Septin1 to Septin12 and Septin14, along with at least eleven pseudogenes (Ivanov et al., 2021; Kinoshita, 2003). This complexity is further diversified by tissue specific and ubiquitous expression of some paralogues, as well as an alternative splicing, which gives rise to multiple additional variants (Russell and Hall, 2011; Zuvanov et al., 2019). These septins are classified into four Kinoshita group, named after best studied paralogue: SEPT2 (including Septin1, 2, 4 and 5), SEPT3 (including Septin3, 9 and 12), SEPT6 (including Septin6, 8, 10, 11 and 14), and SEPT7 (only member of the subgroup) (Grupp and Gronemeyer, 2023). Structurally, all septins belong to

the GTPase superclass of phosphate-binding loop (P-loop) NTPases and possess a central G-domain homologous to the Ras-like, Dynamin, Myosin-Kinesin, and Translation factor superfamily of nucleosid triphosphate binding enzymes (Leipe et al., 2002). The G-domain of septins resembles a Rossmann-like fold, comprising repetitive αβ-units (Longo et al., 2020; Weirich et al., 2008), and contains all elements required for classification as active GTPases (Valadares et al., 2017). These elements include three GTPase boxes G1 (P-loop or Walker A motif), G3 (switch 2), and G4 (confers GTP specificity), which interact with the GTP nucleotide or its cofactor (Bourne et al., 1991; Leipe et al., 2002). Additionally, the G-domain features characteristic elements and insertions that distinguish septins from other members of P-loop NTPases and are primarily involved in forming contacts between septin monomers (Auxier et al., 2019). Notably, these motifs include a polybasic region PB2 (Shuman and Momany, 2022), four short Sep motifs (Sep1-Sep4), six specific residues (Pan et al., 2007), and a polyacidic region (PAR) all crucial for inter-monomer interaction (Castro et al., 2020; Valadares et al., 2017). Another distinctive feature is the C-terminal septin unique element (SUE) (Versele et al., 2004), which comprises approximately 60 residues and consists of three small β-strands and two helices (α5 and α6), essential for the dimerization at both G- and NC-interfaces (Cavini et al., 2021; Grupp and Gronemeyer, 2023). A representative view of a Septin6 GTPase domain with conserved elements is depicted in Fig. 1-16.

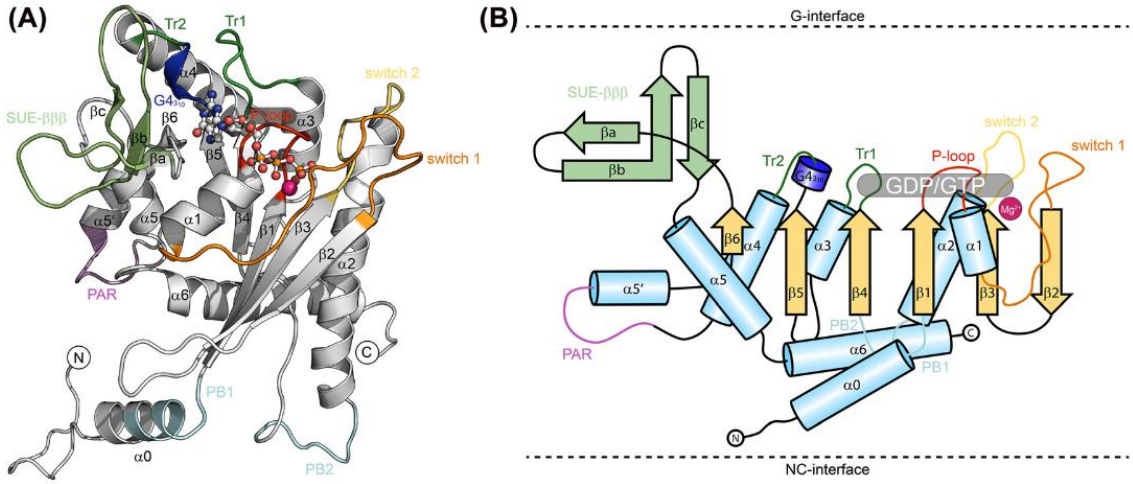

Figure 1-16. Representative crystal structure and a schematic topology of a septin subunit
A Septin6-GTP (PDB-ID 7M6J) is labeled based on the canonical G domain found in Ras-like proteins. **B** A general topology of a septin paralogue belonging to one of Kinoshita's subgroups. G-interface, GTP binding domain-interface; NC-interface, amino- and carboxyl-terminal interface; SUE, septin unique element; Tr, trans-loop; PB, polybasic motif; PAR, polyacidic region. From (Grupp and Gronemeyer, 2023).

In contrast to the highly conserved G-domain, the amino- and carboxyl-terminal extension (NTE and CTE) of septin paralogues exhibit significant variability. The N-terminal domain, the least studied and most variable region among septins (Cavini et al., 2021), typically harbors a structured α-helix, often accompanied by a polybasic region (PB1). This region is plays a crucial role in phosphoinositide binding and subsequent association with the plasma membrane (Bertin et al., 2010; J. Zhang et al., 1999). However, the region immediately upstream from this helix is considered intrinsically unstructured (Garcia et al., 2006), with some septins possessing substantial extensions, such as SEPTIN4 (~150 residues) and SEPTIN9 (~300 residues), compared to others rarely exceeding 50 amino acids (Cavini et al., 2021). Septins with long N-terminal extensions exhibit extensive alternative splicing, further enhancing functional diversity. For example, human SEPTIN9 presents more than 30 distinct isoforms with unique functions attributed to different variants (Connolly et al., 2014; Estey et al., 2010; Zuvanov et al., 2019).

The N-terminal domain of the longest isoforms of SEPTIN9 and SEPTIN4 can be roughly divided into two regions. The more N-terminal basic domain, containing a cytoskeletal binding region (CBR), interacts with acidic regions of cytoskeletal components like actin and tubulin (Bai et al., 2013; Cavini et al., 2021; Smith et al., 2015). Moreover, these extensions facilitate interactions with proteins such as dynactin (Kesisova et al., 2021) and Septin-associated RhoGEF (SA-RhoGEF) (Nagata and Inagaki, 2005). The second, more C-terminal region is notably acidic and encompasses a proline-rich motif positioned adjacent to the structural α-helix described above (Cavini et al., 2021). This region has been implicated in mediating interactions with various partners, including the SH3-containing CIN85 (Diesenberg et al., 2015), and harbors modulatory motifs and sites for posttranslational modifications (PTM) such as acetylation, phosphorylation, and SUMOylation (Hernández-Rodríguez and Momany, 2012; Ribet et al., 2017; Sharma and Menon, 2023). The unstructured region is thought to restrict aberrant filament assembly (Jiao et al., 2020; Weems and McMurray, 2017) and further fine-tune binding specificity among septins and their promiscuous binding partners, thereby broadening their ordinary interactome (Cavini et al., 2021; Devlin et al., 2021). Notably, septin isoforms lacking the basic CBR motif display increased affinity towards SH3 domain containing signaling factors (Cavini et al., 2021). Collectively, these findings suggest a modular nature of the N-terminal domain of septins,

potentially serving as regulatory switches modulating the effects of their adjacent regions and overall governing polymer organization (Cavini et al., 2021).

The CTE is located immediately downstream the G-domain and is present in all septins (except the SEPT3 group and ancestral septins). It typically contains at least one heptad repeat sequence, predicted to form a coiled-coil (CC) helix bundle. These coiled-coils are thought to form contacts within and across polymers, contributing to higher-order structure formation (Bertin et al., 2010; Leonardo et al., 2021). The coiled-coil domain is linked to the G-domain through a flexible hinge (Mendonça et al., 2021). Additionally, the very C-terminus of septins is generally believed to be unstructured, although SEPTIN6 and SEPTIN7 are thought to contain a structured domain, which likely forms an amphipathic helix, facilitating plasma membrane binding (Cannon et al., 2019; Shuman and Momany, 2022; Woods and Gladfelter, 2021).

1.8.2. Protofilament formation and higher-order structures

In stark contrast to other small GTPases, septins polymerize into filaments, and most of their functions are attributed to this ability (Spiliotis and McMurray, 2020). Septin filaments consist of core particles, also known as protofilaments, which contain linear hetero-oligomeric succession of monomers from each of the four Kinoshita groups, maintaining “positional orthology” across species (Shuman and Momany, 2022) (Fig. 1-17). Each monomer utilizes two alternate interfaces for oligomerization: N- and C-terminal domain, termed the NC interface and the G-domain, which reconstitutes the G interface (Sirajuddin et al., 2007). In mammals, the palindromic protomer forms a centrally symmetric filament with an order of SEPT2-6-7-7-6-2 for a hexamer and SEPT2-6-7-3-3-7-6-2 for an octamer (McMurray and Thorner, 2019; Mendonça et al., 2019; Soroor et al., 2021). Septin filament formation likely occurs through end-to-end collision of the core particles, presumably at the plasma membrane (Bridges et al., 2014). Recent research suggests that mammalian septin filaments predominantly exist as immobilized membrane-bound octamers, at least during the interphase (Martins et al., 2022).

These core particles are considered the building blocks of septin filaments due to their persistence in high ionic strength (over 300mM) solution *in vitro* (Cavini et al., 2021). Several studies have demonstrated the impact of varying salt concentrations on filament polymerization of yeast and human septins (Bertin et al., 2008; Fischer et al., 2022; Iv et al.,

2021). It is assumed that lowering the ionic strength permits end-to-end annealing of protofilaments (Grupp and Gronemeyer, 2023). Weems *et al.* have demonstrated a multi-step assembly of yeast protofilaments from monomers, predicting an active communication between G- and NC-interfaces. They combined the Biomolecular Fluorescence Complementation assay with depletion of cellular GDP and GTP levels (Weems and McMurray, 2017). Initially, the central dimer of Cdc10 is formed (NC-interface), followed by the dimerization of two outer septins, Cdc11-Cdc12 (G-interface). The Cdc11-Cdc12 dimer recruits the bridging Cdc3 to the NC-interface of Cdc12, inducing a conformational change in the exposed G-domain of Cdc3. Protofilament assembly concludes with the lateral association of Cdc11-Cdc12-Cdc3 trimers to the central Cdc10 dimer (G-domain) (Grupp and Gronemeyer, 2023; Weems and McMurray, 2017).

The formation of the mammalian protofilaments remains poorly understood. Additionally, septin filaments can assemble into high-order structures, including paired and stacked filaments, gauzes, and rings (Bertin et al., 2010, 2008; Mostowy and Cossart, 2012). C-terminal coiled coils are believed to mediate the connection between adjacent filaments. In both human and yeast, two types of spacings between filaments have been observed *in vitro*: loose (15-20 nm) and tight (~5 nm). These spacings correspond to the length of larger CC domains of SEPT6-SEPT7 (8-11 nm) group members and shorter SEPT2 (4-5 nm) group members, suggesting the potential involvement of septin CTEs in high-order filament formation (Bertin et al., 2010, 2008; Jiao et al., 2020; Leonardo et al., 2021).

While reconstituted septins exhibit high theoretical shape plasticity in solution, living cells likely utilize a more narrow set of geometries (Martins et al., 2022; Szuba et al., 2021). Kinoshita's rule, governing the position of monomers within a filament, restricts the potential number of octamers to 60, without considering known alternative splice variants. However, the existence of possible combinations, the simultaneous presence of multiple distinct complexes, or their *in vivo* relevance for mammalian cells have yet to be convincingly described (Mendonça et al., 2019). In 2022, Panagiotou *et al.* demonstrated the co-existence of two septin filament populations incorporating either SEPTIN11 or SEPTIN9. Both filaments were shown to associate with Anillin, either directly or through CIN85, respectively. Anillin anchors distinct populations of septins to the plasma membrane of the intracellular bridge in dividing cells (Panagiotou et al., 2022).

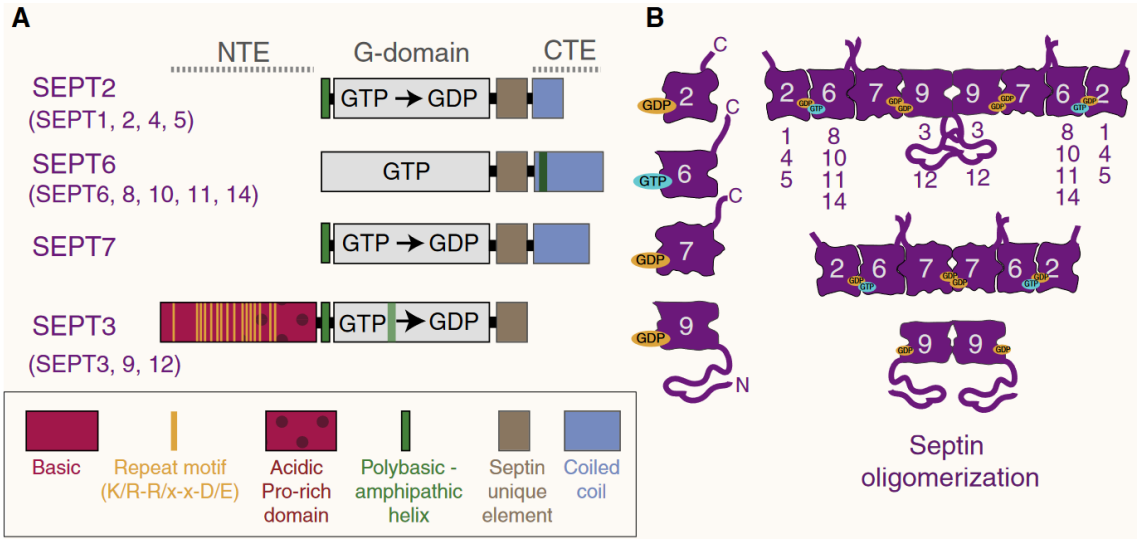

Figure 1-17. The domain architecture and protofilament assembly of septin GTPases
A Mammalian septins are divided into four subgroups (SEPT2, SEPT6, SEPT7, and SEPT3) through bioinformatical analysis. The septin fold comprises a central GTP-binding domain (G-domain) followed by a characteristic insertion known as the septin unique element (SUE). Members of the SEPT6 group remain constitutively bound to GTP due to the lack of the catalytic residue. Surrounding the central domain are highly variable amino- and carboxyl-terminal extensions (NTE and CTE). The CTE contains coiled-coil domains of varying length, except for the SEPT3 group. The NTE sequence is unique to SEPT3 septins and is largely unstructured. It includes a proximal acidic proline-rich motif and a distal basic motif that facilitate interactions with actin and tubulin. Additionally, septins feature polybasic and/or amphipathic helices that facilitate binding to lipid bilayers. **B** Septins form non-polar protofilaments through heteropolymerization via alternating G-domain and NC-domain interfaces. The smallest functional unit consists of a dimer of tetramers, comprising a paralog from each subgroup. According to the Kinoshita rule, septins from the same subgroup can interchange, leading to a variety of potential oligomer combinations. Modified from (Spiliotis and Nakos, 2021).

The cellular functions of cytoskeletal filaments, such as actin and tubulin NTPases, depend on the complete GDP-GTP cycle. NTP binding promotes filament polymerization, while hydrolysis and phosphate release induce disassembly (Bowne-Anderson et al., 2013; Kudryashov and Reisler, 2013). Although the dynamics, assembly, stability, and turnover of septin protofilaments are not fully understood, GTP activity likely regulates these processes (Valadares et al., 2017; Weems and McMurray, 2017; Zent and Wittinghofer, 2014). Unlike actin and tubulin, studies by the Wittinghofer lab have demonstrated that nucleotide hydrolysis stabilizes the dimeric interface between certain septins, such as Septin7 (Sirajuddin et al., 2009; Zent et al., 2011; Zent and Wittinghofer, 2014), while others like the SEPT6 subfamily, remain catalytically inactive and constitutively bound to GTP (Zent and Wittinghofer, 2014). A recent study by Weems and McMurray suggests that nucleotide-bound states influence interaction preferences in septin monomers, with enhanced stability observed at the dimeric interface between GDP- and constitutively GTP-bound paralogues

compared to two GDP-bound yeast septins (Weems and McMurray, 2017). Nucleotide binding and hydrolysis are likely early, one-time events that initiate septin protofilament formation (Grupp and Gronemeyer, 2023). However, the impact of very low GTP hydrolysis/exchange rates on subsequent septin dynamics following protomer assembly remains unclear (Abbey et al., 2019; Spiliotis, 2018). Fluorescence recovery after photobleaching (FRAP) assays revealed that septin heteropolymers exhibit 2 to 3 times slower turnover rates than average actin or tubulin polymers, indicating heightened stability of septins (Hagiwara et al., 2011; Hu et al., 2008; Schmidt and Nichols, 2004). Although monomeric septins hydrolyze GTP faster than signaling GTPases or monomeric actin and tubulin, the association of a GAP to small GTPases or cytoskeletal NTPase polymerization significantly increases their hydrolysis rates (Kanematsu et al., 2022; Mishra and Lambright, 2016; Paydar and Kwok, 2020; Roostalu et al., 2020). The absence of described mammalian GEFs or GAPs for septins (Abbey et al., 2019; Akhmetova et al., 2015) implies their dynamic remodeling might be regulated by post-translational modifications and other unidentified factors (Alonso et al., 2015; Hernández-Rodríguez and Momany, 2012; Sharma and Menon, 2023; Spiliotis, 2018).

1.8.3. The role of septins in actomyosin organization

Septin and actin filaments exhibit a remarkable structural interdependence, with disruptions in one filament system affecting the other (Spiliotis, 2018), though the nature of this interaction remains unclear. Early studies showed that recombinant human septin hexamers self-assemble into rings and do not interact with pre-polymerized phalloidin-stabilized actin filaments (Kinoshita et al., 2002). However, recent evidence suggests that human SEPTIN2-SEPTIN6-SEPTIN7 and SEPTIN9 can cross-link and bend actin filaments, depending on septin filament state (Dolat et al., 2014b; Mavrakis et al., 2014; Smith et al., 2015). This actin cross-linking ability has been attributed directly to human SEPTIN9 (Dolat et al., 2014b). In renal epithelial cells, SEPTIN9 orchestrates the organization of lamellar actin stress fibers, contributing to focal adhesion maturation and stability, which promotes epithelial motility. Studies employing low-speed actin sedimentation assays and negative stain electron microscopy (EM) have demonstrated the unique ability of SEPTIN9, but not the SEPTIN2-6-7 complex, to cross-link preformed actin filaments (Dolat et al., 2014b). Up to date, only the human SEPTIN9 is presumed to directly interact with actin filaments (Smith et al., 2015). *In*

vitro reconstruction assays and EM studies conducted by Smith and colleagues have revealed that the basic region of the NTE of SEPTIN9, shared among long isoforms 1, 2, and 3, can bind and bundle F-actin, occupying three distinct positions. Notably, two of those actin surfaces are also targeted by Myosin V and Cofilin, potentially competing with SEPTIN9 for binding sites (Smith et al., 2015). Recent studies using biochemical and biophysical assays propose an alternative binding mode for septin octamers. Specifically, mammalian octamers, containing the short isoform 5 (SEPTIN9_i5) can interact with and cross-link actin filaments (Iv et al., 2021). Moreover, despite an 18-residue difference, SEPTIN9-i2, but not SEPTIN9-i1, is downregulated in breast tumors. Reintroducing SEPTIN9-i2 remodeled septin structures into short rods, leading to the loss of perinuclear actin stress fibers and inhibiting of cancer cell migration (Verdier-Pinard et al., 2017).

The arrangement of septins along actin filaments has remained unclear, with uncertainties regarding whether they form filamentous polymers, short oligomers, or protofilaments. Recent work by Martins *et al.*, provided insight into this, suggesting that most human septins organize into octamer-based, paired filaments along actin stress fibers (Martins et al., 2022). Using split-GFP assays, single protein tracking andsuper-resolution microscopy, the study underscores the importance of octamer assembly for the integrity of both septin and actin filaments. These actin-bound septin filaments are largely immobile and located near the plasma membrane, anchoring actin (Martins et al., 2022). The role of specific paralogues or splice variants, such as SEPTIN9, in influencing actin organization remains an area for further investigation.

Septins indirectly associate with actin filaments through mediating proteins. For instance, the recombinant SEPTIN2-6-7 interacts with pre-polymerized actin only after its decoration by anillin (Kinoshita et al., 2002), which facilitates septin-actin interaction in the mitotic contractile ring (Panagiotou et al., 2022; Renshaw et al., 2014). During interphase, non-muscle myosin IIA serves as an adaptor protein linking septins to actin. Specifically, SEPTIN2 binds the myosin heavy chain, acting as a scaffold for kinases like citron kinase (CRIK) or ROCK, and disruption of this interaction disassembles septin filaments and reduces cytoplasmic actin filaments, linking septins to actomyosin contractility (Joo et al., 2007).

Furthermore, the binding of septins to actin is facilitated by Cdc42 effectors, such as binders of Rho GTPases BORG/ Cdc42EP (Spiliotis and Nakos, 2021). BORG proteins are largely unstructured and feature a Cdc42/Rac interactive binding (CRIB) domain that binds to Cdc42,

along with three characteristic BORG homology domains (BH1-3) (Joberty et al., 1999). Specifically, BORG 1-3 directly binds to septins, with the BD3 domain being responsible for this association. Overexpression of BORG3 in Madin-Darby canine kidney (MDCK) cells promotes the formation of thick perinuclear septin filament (Joberty et al., 2001). The BD3 domain of BORG3 was shown to bind SEPTIN6-7 dimers and to SEPTIN2-6-7 trimers, likely at the interface between SEPTIN6 and SEPTIN7 (Joberty et al., 2001; Sheffield et al., 2003). In breast cancer-associated fibroblasts, elevated BORG2 enhances actomyosin contractility and aligns thick septin filament, promoting YAP nuclear import, which is crucial for cancer-promoting abilities of CAFs (Calvo et al., 2015). Conversely, in melanoma cells, BORG3 facilitates metastasis through ameboid migration, and its depletion (or SEPTIN9) reduces invasion both *in vitro* and *in vivo*, highlighting the necessity of septin binding for the function of BORG3 in melanoma invasion (Farrugia et al., 2020). Moreover, Salameh *et al.* observed a decrease in BORG2 and BORG3 levels along with the disappearance of actin stress fibers in human hepatocyte line 16 (HHL16) cells during paclitaxel treatment or resistance aquisition (Salameh et al., 2021). This effect was linked to proteasomal degradation of BORG2/3 and the re-localization of septins to MTs (Salameh et al., 2021). Cdc42, a key regulator of actin remodeling (Nobes and Hall, 1995), influences BORG-dependent septin organization. *In vitro* studies show Cdc42 reduces BORG binding to septins, but cellular outcomes vary (Tomasso and Padrick, 2023). For instance, constitutively active Cdc42 (Q61L) disrupted septin filaments in MDCK cells and CAFs (Farrugia and Calvo, 2017; Joberty et al., 2001), while in HHL16 cells,it counteracted BORG2 degradation, preserving septins on actin stress fibers during paclitaxel treatment (Salameh et al., 2021). Dominant negative Cdc42 (T17N) also disrupted septin filaments in multiple cell lines (Burbelo et al., 1999; Farrugia and Calvo, 2017; Salameh et al., 2021). These findings suggest that Cdc42, cycling between active and inactive states, regulates septinstability by modulating BORGs (Tomasso and Padrick, 2023).

In addition to Cdc42 effectors, Rho effectors potentially mediate septin- actin interaction (Spiliotis and Nakos, 2021). SEPTIN9 interacts with the septin-associated Rho GEF 18 (SA-RhoGEF, ARHGEF18), and with Rhotekin, an effector of RhoA and RhoC (Ito et al., 2005; Nagata and Inagaki, 2005; Safavian et al., 2023). Sept9b (SEPTIN9_i3) binds SA-RhoGEF, assembling on actin filaments and inhibiting GEF activity, leading to reduced SF formation (Nagata and Inagaki, 2005). Furthermore, SEPTIN9 also plays a role in substrate stiffness sensing, regulating RhoA signaling via SA-RhoGEF-dependent mechanism in human umbilical

vein endothelial cells (HUVEC) (Yeh et al., 2012). HUVEC cells cultured on low-stiffness polyacrylamide (PA) gels upregulated expression of SEPTIN9 through an integrin αvβ3-dependent mechanism, resulting in perinuclear SF disassembly and actin re-localization to the cell periphery (Yeh et al., 2012). Conversely, Safavian *et al.* demonstrated that SEPTIN9 binds to and activates SA-RhoGEF, thereby promoting RhoA signaling at the base of a cilium in retinal pigment epithelial cells (hTERT-RPE1) (Safavian et al., 2023).

Moreover, SEPTIN9_i1 activates RhoA-ROCK and FAK-Src-paxillin signaling in MCF7 cells, although no involvement of SA-RhoGEF or direct septin participation in the phosphorylation of these proteins was investigated (Zeng et al., 2019). Rhotekin involved in switching Rho function from SF contractility to membrane ruffling and actin polymerization (Chen et al., 2013), binds SEPTIN9_i3 on actin SF in a Rho-dependent manner (Ito et al., 2005). The activated Rho disrupts septin filaments in REF52 cells, resembling the transfection of Rhotekin (Ito et al., 2018). Considering the role of SEPTIN2 in myosin phosphorylation cascade, septins modulate actin organization also directly, integrating signals from pathways that regulate actin remodeling (Spiliotis, 2018).

Two examples of signaling pathways linking septins to actin filament remodeling involve Yap and the non-catalytic region of tyrosine kinase 1 (Nck1) protein (Calvo et al., 2015; Fan et al., 2021; Kremer et al., 2007). Septins have been shown to regulate the cellular localization of YAP, a key transcriptional regulator, suggesting their involvement in mechanotransduction pathways (Lam and Calvo, 2019). Increased septin-actin association has been demonstrated to enhance the nuclear translocation of YAP in breast CAFs and hepatocellular carcinoma (HCC) cells, thereby promoting oncogenic progression (Calvo et al., 2015; Fan et al., 2021). Nck1 is an adaptor protein involved in signal transduction that stimulates actin polymerization through a N-WASp-Arp2/3-dependent mechanism (Buday et al., 2002; Ditlev et al., 2012). In HeLa cells, SEPTIN2-6-7 complexes associated with stress fibers maintain the cytoplasmic localization of Nck1. Depletion of septins results in the suppressor of cytokine signaling 7 (SOCS7)-dependent nuclear translocation of Nck1 and loss of actin stress fibers (Kremer et al., 2007). This finding suggests that septins may influence gene transcription by sequestering nucleoplasmic proteins to stress fibers in a mechanoresponsive manner (Spiliotis and Nakos, 2021).

Despite their functional interdependence, septins only partially overlap with actin, preferentially associating with contractile ventral actin structures, such as linear SFs

connected to focal adhesions on both ends, and transverse arcs at the interface with lamellae (Calvo et al., 2015; Dolat et al., 2014b; Kinoshita et al., 2002; Kremer et al., 2007; Spiliotis, 2018). Septins also localize at branched actin sites, as seen with SEPTIN1, 4 and 5 in lamellipodia of squamous cell carcinoma, seemingly in absence of other septins (Mizutani et al., 2013). Additionally, SEPTIN6 plays a role in collateral branching in the axon of sensory neurons, promoting the formation of filopodia and localizing to membrane actin patches consisting of branched actin filaments. This facilitates the recruitment of cortactin, an activator of Arp2/3-mediated polymerization (Hu et al., 2012). *In vitro* binding assays have shown that SEPTIN6 exhibits a preference for Arp2/3-nucleated branching points on actin filaments compared to linear actin, while SEPTIN7 showed no such preference and binds to linear segments (Hu et al., 2012). Another study demonstrated SEPTIN2 (and potentially SEPTIN7 and 9) accumulation at curved membrane tips of lamellipodia between two opposing endothelial cells (Kim and Cooper, 2018). Branched actin filaments are proposed to push membranes of endothelial cells in close proximity, promoting tight barrier formation via vascular endothelial (VE) cadherin interaction (Efimova and Svitkina, 2018). Loss of SEPTIN2 resulted in marked filopodia formation, gaps between cells, re-localization of cortical F-actin to the cytoplasm, and disruption of junctional integrity (Kim et al., 2023; Kim and Cooper, 2021, 2018).

1.8.4. The functions of MT-associated septins

Septins are known to associate with microtubules and play crucial roles in regulating MT organization, dynamics, post translational modifications, and interactions with MT-associated proteins (MAPs). They also regulate transport along MTs, earning them the status of *bona fide* MAPs themselves (Spiliotis and Kesisova, 2021; Spiliotis and Nakos, 2021). Septins often associate with subsets of bundled MTs in specific cellular regions, including the perinuclear cytoplasm, subcortex, Golgi nucleated MTs, as well as MTs of the primary cilium and the cytokinetic bridge (Bowen et al., 2011; Ghossoub et al., 2013; Nagata et al., 2003; Russo et al., 2024).

The current understanding of how septins associate with microtubules has been elucidated through investigations into human SEPTIN9, which possesses a long and disordered N-terminal extension (NTE), a feature unique among septins. Alternative splicing generates at least 5 isoforms, varying in size and functions (Connolly et al., 2011; Verdier-Pinard et al.,

2017). The NTE of SEPTIN9_i1 contains a motif (K/R-R/x-x-D/E) resembling the microtubule-binding repeat motifs found in microtubule-associated proteins (MAP) (Spiliotis and Kesisova, 2021). Competition assays reveal that this motif preferentially binds carboxy-terminal tails (CTT) of βII-tubulin (*TUBB2*) isotype (Bai et al., 2013). Furthermore, tyrosination of α-tubulin and polyglutamylation of CTTs promote the association of septins to tubulin (Froidevaux-Klipfel et al., 2015; Spiliotis et al., 2008). Initially, all three long isoforms of SEPTIN9 (SEPTIN9_i1, _i2, and _i3) were shown to interact with MTs *in vitro*(Bai et al., 2013). However, recent study has narrowed down the microtubule-binding domain (MBD) of SEPTIN9 to the first 25 amino acids of SEPTIN9_i1, identifying other common sequences of long isoforms as negative regulatory elements (Kuzmić et al., 2022). Other cellular and *in vitro* studies suggest potential interactions of SEPTIN6 and 7, SEPTIN9 dimers, and SEPTIN2-6-7 hexamers with MTs (Hu et al., 2012; Moon et al., 2013; Nakos et al., 2019b, 2019a). Nevertheless, the mechanistic nature of these associations remains poorly understood, and the *in vivo* presence is still controversial, as SEPTIN9 depletion leads to absence of septin hexamer-MT interaction in cells (Kuzmić et al., 2022; Verdier-Pinard et al., 2017).

Septins play crucial roles in promoting or regulating various aspects pf microtubule dynamics, including nucleation, growth, elongation and bundling (Spiliotis and Nakos, 2021). At the centrosome, SEPTIN7 interacts with the dynactin subunit $p150^{Glued}$, and depletion of SEPTIN7 leads to a disorganized MT network (Chen et al., 2021). On Golgi membranes, SEPTIN1 scaffolds γ-tubulin and the centrosomal protein CEP170, thereby promoting the nucleation of non-centrosomal MTs (Song et al., 2019). Although these studies suggest unique roles for specific septins, the contribution of other septins cannot be entirely ruled out. Additionally, *in vitro* reconstruction assays demonstrated that septins can directly bundle MTs and slow down MT depolymerization, thereby promoting their growth (Bai et al., 2013; Kuzmić et al., 2022; Nakos et al., 2019b, 2019a). Furthermore, mutations in SEPTIN9_i1 or SEPTIN2 that impair dimerization abolish the association of septins with MTs in U2OS cells, suggesting that incorporation of certain septin paralogues into filaments enables these septin filaments to exert regulatory functions on MTs (Kuzmić et al., 2022). Bowen *et al.* have demonstrated the role of septins in MT growth in MDCK cells, wherein septins capture, bundle, and guide the directionality of MT plus end movement (Bowen et al., 2011). Despite evidence of interaction between septins and the MT plus-end-binding protein EB1, septins were not observed to track on growing plus ends *in vivo* or *in vitro* (Bowen et al., 2011; Spiliotis and Nakos, 2021).

Additionally, septins influence the post-translational modifications of MTs. For instance, in murine neurons, Septin7 recruits the Histone deacetylase 6 (HDAC6), which deacetylates unpolymerized αβ-tubulin dimers in the cytoplasm, maintaining the dynamic equilibrium during neuritogenesis (Ageta-Ishihara et al., 2013). In MDA-MB 231 cells, SEPTIN9_i1-containing octamers recruit enzymes to the MT interface that modify the length of the polyglutamyl side chains at the CTT of tubulin, thereby conferring high dynamism (Froidevaux-Klipfel et al., 2015).

Septins have recently emerged as key regulators MT-dependent transport, influencing the movement of motor-cargo complexes and serving as membrane-associated scaffolds for motor proteins (Spiliotis and Kesisova, 2021). *In vitro* reconstruction assays has shown that SEPTIN9_i1 impedes the motility of Kinesin-1/KIF5 and Dynein-Dynactin motors, promotes the motility of Kinesin-3/KIF1A, and does not influence Kinesin-2/KIF17 (Karasmanis et al., 2018). Live-cell imaging in rat hippocampal neurons, combined with overexpression and depletion of SEPTIN9_i1, has further demonstrated the differential regulation of Kinesin-1 and Kinesin-3 and their cargo on dendritic MTs, consistent with *in vitro* studies (Karasmanis et al., 2018). Moreover, Kinesin-1 and Kinesin-3 exhibit movement in opposite directions due to their differential preferences towards antiparallel acetylated and tyrosinated dendritic MTs(Tas et al., 2017). Thus, septins are envisioned to contribute to the maintenance of axon-dendrite polarity through their differential affinity towards distinct subsets of MTs (Spiliotis and Kesisova, 2021). Furthermore, the interaction of septins with MTs is affected by MT-associated proteins (MAPs), such as MAP4, which compete with SEPTIN2 for binding. Conversely, SEPTIN2 has been shown to sequester MAP4 or occlude its binding sites, thereby modulating MT polyglutamylation, which in turn potentiates the activity MAP4 and regulates the motility of Kinesin-1 and -2 motors (Ghossoub et al., 2013; Kremer et al., 2005; Spiliotis et al., 2008).

Recent interactome studies suggest that septins play a crucial role in bridging the interaction between MT motors and membrane cargo (Spiliotis and Kesisova, 2021). Through human dynein interactome analysis using biotin ligase (BioID) and yeast-to-hybrid screen of human septins, along with cellular studies, SEPTIN2, 7 and 9 have been identified to associate with subunits of dynactin, as well as the dynein intermediate and light chains (DIC, DILC) (Chen et al., 2021; Kesisova et al., 2021; Nakahira et al., 2010; Redwine et al., 2017). Kesisova *et al.* demonstrated that SEPTIN9 acts as a scaffold for dynein motors on lysosomes, facilitating

retrograde traffic (Kesisova et al., 2021). This suggests that septins, at least SEPTIN9, may serve as cargo scaffolds for uni- or bidirectional movement of membrane organelles (Spiliotis and Kesisova, 2021).

In summary, septins emerge as crucial components of the cytoskeleton, selectively regulating motor interactions with cargo and MTs, thus contributing to the regulatory landscape of the "MT code" as *bona fide* microtubule-associated proteins (Janke and Magiera, 2020; Spiliotis and Nakos, 2021). With the recent discovery of septin association with processive myosins such as Myo1b, Myo1c, and Myo6 (MyoVI) (Hecht et al., 2019), septins may extend their regulatory functions to myosin-driven transport along actin filaments as well, supporting the hypothesis of a broader "septin code" (Spiliotis and Kesisova, 2021).

1.8.5. The functions of phospholipid membrane-associated septins

In addition to their interactions with actin and MTs, septins also interact with specific membrane domains, a process that is influenced by the lipid composition and shape of these domains.

Septins recognize various phosphoinositides, including phosphatidylinositol (PI) 5-posphate PI (5)P, PI (4,5)P_2 (will be referred to as PIP2), PI (3,5)P_2, and PI (3,4,5)P_3, as well as other cone-shaped lipids like cardiolipin and phosphatidic acid, within membrane domains (Akil et al., 2016; Dolat and Spiliotis, 2016; Krokowski et al., 2018; J. Zhang et al., 1999). The N-terminal polybasic region (PB1), absent SEPTIN6 family members, mediates septin interaction with phosphoinositoles (Cavini et al., 2021). Recent evidence suggests that distinct paralogue-specific septin domains exhibit varying affinities towards lipid membranes (Cannon et al., 2019; Omrane et al., 2019). Studies using lipid monolayer assays have demonstrated that yeast septins to preferentially interact with PIP2 over PI(3,4,5)P_3. Moreover, these interactions on lipid monolayers significantly promote filament polymerization, even under conditions that typically inhibit filament formation in solution, such as high salt buffers (300mM) or deleterious mutations (Bertin et al., 2010). Additionally, experiments using liposome sedimentation with SEPTIN4 (known as H5 at the time) have revealed that SEPTIN4 binds to PIP2 in the GDP-bound state, suggesting a role for this interaction in recruiting or anchoring septins to the areas of high PIP2 concentration (J. Zhang et al., 1999).

Septins exhibit a preference for assembling on membrane domains curved on the micrometer scale, with a particular accumulation on the saddle-shaped cytoplasmic layer (Beber et al.,

2019; Bridges et al., 2016; Cannon et al., 2019; Woods and Gladfelter, 2021). Studies have shown that septins can reshape membranes in giant unilamellar vesicles (GUVs) and liposomes, and septin filaments have been observed to associate with both positive and negative curvatures (Beber et al., 2019; Tanaka-Takiguchi et al., 2009). While there is evidence suggesting a preference for positive curvatures, as seen in tubulation of liposomes and adsorption on 1-5 µm beads in anionic lipid bead-binding assays (Bridges et al., 2016; Tanaka-Takiguchi et al., 2009), there are also findings indicating that septin filaments avoid positive curvature, instead lying flat in bundles along the hill axis of positive curvature, while bending negatively in the valleys of supported lipid monolayers on undulating solid templates (Beber et al., 2019). Despite these discrepancies observed *in vitro*, septins are more commonly found *in cellulo* at regions of positive curvature, often outlining protrusive structures, such as the base of lamellipodia, filopodia, dendritic spines, and the surface of larger organelles like mitochondria, lysosomes and lipid droplets (Akil et al., 2016; Dolat and Spiliotis, 2016; Kesisova et al., 2021; Sirianni et al., 2016). An evolutionary conserved amphipathic helix at the C-terminus of SEPTIN6 has been identified as necessary and sufficient for curvature sensing, highlighting the role of specific septin domains in membrane curvature regions (Cannon et al., 2019).

Septins, when associated with phospholipid bilayers, form tracks of paired parallel filaments that serve as scaffolds, confining the diffusion of proteins and lipids while rearranging the surrounding cytoskeleton architecture (Bridges et al., 2014; Hu et al., 2012; Martins et al., 2022; Pacheco et al., 2022; Szuba et al., 2021). For example, membrane-associated septins have been implicated in capturing and guiding the growth of MTs and crosslinking actin filaments at the base of nascent PM protrusions, as demonstrated by the essential role of SEPTIN6 and SEPTIN7 in filopodia formation during axon collateral branching (Hu et al., 2012; Spiliotis, 2018). In addition to their association with micrometric curvatures, septins are also capable of recognizing nanometer-scale domains, binding to smaller membrane patches potentially as oligomers (Dolat and Spiliotis, 2016; Kesisova et al., 2021). Thus, septins can interact with membrane domains both as high-order filaments and as oligomers, influencing protein localization and interactions, organizing other cytoskeletal components, and mediating their interaction with plasma membrane. This central role places septins at the forefront of cytoskeletal regulation (Ivanov et al., 2021).

1.8.6. Septins in morphogenesis

Septins are indispensable for the morphogenesis of various cell types, including neurons and epithelial cells, where proper organization of actin or microtubules dictates their polarized shapes (Spiliotis and McMurray, 2020). The cytoplasmic regulation of septins plays a crucial role in fine-tuning membrane traffic dependent on MTs during the development of apical-basal polarity or the differentiation of dendritic compartment (Bowen et al., 2011; Karasmanis et al., 2018; Radler et al., 2023). Septins's interaction with membranes and MTs is pivotal for guiding the morphogenesis of platelets and spermatozoa, highlighting their role in cellular development and function (Becker et al., 2024; Kim et al., 2022; Kuo et al., 2013; Lai et al., 2016; Martínez et al., 2006). Additionally, the interaction between septins and actin at the membrane interface regulates processes such as migration and podosome-dependent ECM invasion by endothelial cells, thereby influencing angiogenesis (Collins et al., 2019; Liu et al., 2014).

The association between septins and actin plays a crucial role in steering coordinated cell movement during embryonic development. Tissue and organ morphogenesis, particularly during convergent extension (CE), is regulated by planar cell polarity (PCP) proteins (Butler and Wallingford, 2017). In gastrulating *Xenopus laevis* embryos, Septin7-dependent cortical actomyosin coordination is essential for effective PCP function during CE (Butler and Wallingford, 2017). The PCP mediator Dishevelled (Dvl) regulates the localization of Septin7 to the vertices of mediolateral cell-cell contacts. Subsequently, Septin7 facilitates the enrichment of actin filaments and phosphorylated myosin II at anteroposterior junctions. Knockdown of Septin7 results in displacement of actin filaments, impaired membrane compartmentalization, and reduced cortical tension, ultimately leading to the failure of proper cell intercalation (Kim et al., 2010; Park et al., 2015; Shindo and Wallingford, 2014).

Septins are recognized as topologically and functionally specialized regulators of neuronal morphogenesis and plasticity (Radler and Spiliotis, 2022), finely orchestrating the spatiotemporal dynamics of division and differentiation in neuronal progenitors (Boubakar et al., 2017; Loyer and Januschke, 2018; Qiu et al., 2020). In *Drosophila*, septins (Sep1/2) localize at the basal contacts of neuroblasts with the last-born daughter cell, critically maintaining the division axis and potentially guiding the orientation of the mitotic spindle, while leaving cytokinesis unaffected (Loyer and Januschke, 2018). Additionally, Septin7 has been implicated in providing spatial memory for neurite re-emergence in chick neural crest cells (NCCs), which

undergo division and differentiation into sensory dorsal root ganglia (Boubakar et al., 2017). As NCCs divide, their bipolar neurites, marked by Septin7 at their base, retract. Disruption of Septin7 organization leads to the loss of the critical cell bipolarity that instructs the division axis of NCCs (Boubakar et al., 2017; Radler and Spiliotis, 2022). Controlling the axis of cell division might be an evolutionarily conserved feature as septins regulate the site of bud emergence and mitotic spindle position in budding yeast *S. cerevisiae* (Spiliotis and McMurray, 2020). Additionally, Septin7 has been demonstrated to temporally control the differentiation of murine neuronal progenitor cells (NPCs), which undergo cycles of division and differentiation into neurons and glia cells (Geng et al., 2018; Qiu et al., 2020). Researchers have identified an interaction between Septin7 and the kinesin motor Kif20A/Mklp2 at the intracellular bridge (ICB), connecting two daughter NPC cells. During late cytokinesis, the ICB harbors cell fate regulators crucial for maintaining NPC proliferative state or inducing differentiation. The mitotic kinesin Kif20a associates with the Ephrin-B/regulator of G-protein signaling (RGS) pathway, essential for NPC identity maintenance. Consequently, inducible depletion of Septin7 leads to the premature cell cycle exit and a switch in NPCs' mitotic state towards differentiation into neurons, being detrimental to proper brain development (Geng et al., 2018, 2018). This prompts speculation on whether Septin7 can influence the localization of cell-fate regulators during cytokinesis (Spiliotis and Nakos, 2021). Interestingly, while no cytokinetic defect was observed in murine NPCs upon Septin7 depletion, it seems indispensable for cytokinesis in human NPCs (Li et al., 2019; Radler and Spiliotis, 2022). Taken together, septins provide membrane cues for neuronal precursor cell division and differentiation across different species (Radler and Spiliotis, 2022).

1.8.7. Septins in skeletal muscle

Septins, acting as molecular scaffolds and lateral diffusion barriers, play integral roles in regulating a diverse array of intracellular and morphogenic processes across various cell types and tissues (Benoit et al., 2023; Dolat et al., 2014a; Spiliotis and Nakos, 2021). Surprisingly, our understanding of septins's functions in muscle-related processes remains limited, with recent reports from the Csernoch Lab shedding light on emerging functions, primarily focusing on Septin7 (De Gasperi et al., 2024; Gönczi et al., 2022, 2021; Ráduly et al., 2023; Szabó et al., 2023).

Gönczi *et al.* identified Septin7 as a key component of the muscle cytoskeleton in murine skeletal muscle (Gönczi et al., 2022). Most septin paralogues were expressed in murine muscle and C2C12 cells, except Septin12 and 14, with low levels of Septin1 and 3. In adult muscle fibers from *m. flexor digitorum brevis* (FDB), Septin7 localized near the sarcomeric Z-line, similar to α-actinin. Furthermore, age-dependent downregulation of Septin7 was observed, with lower mRNA levels in older hind limb muscles. Muscle-specific downregulation of Septin7 (human alpha-skeletal actin (ACTA1) promoter-driven Cre mouse), led to skeletal deformations, reduced body mass, altered myofibrillar structure, impaired mitochondrial function, and weakened force generation. Increased Septin7 expression following $BaCl_2$- induced injury to *m. tibialis anterior* (TA) indicated a role in muscle regeneration. Finally, knockdown of Septin7 in C2C12 cells reduced cell proliferation and myogenic differentiation, while CRISPR/Cas9 knockout completely halted cell division (Gönczi et al., 2022).

Ráduly *et al.* provide the initial evidence implicating Septin7 into C2C12 cell migration (Ráduly et al., 2023). Septin7 forms actin-associated filaments, distributed throughout the cell, with migrating myoblasts exhibiting organized Septin7 filaments in the perinuclear area and within membrane protrusions. Depletion of Septin7 via shRNA leads to reduced Ca2+ concentration in migrating cells and other alterations in cell migration dynamics. Knockdown (KD) myoblasts tend to migrate faster, cover greater distances, and follow more defined routes. Additionally, treating myoblasts with the septin-stabilizing plant cytokinin forchlorfenuron (FCF) (Hu et al., 2008) results in decreased migration speed and distance traveled by C2C12 cells. Overall, septins play a crucial role in myoblast migration, which is essential for muscle development, as directional cell migration critically regulates muscle morphogenesis, repair, and efficiency of engraftment in cell therapies (Choi et al., 2020; Ráduly et al., 2023).

Recent evidence further supports the role of Septin7 in skeletal muscle regeneration (Szabó et al., 2023). Partial depletion of Septin7 in adult muscle fibers leads to an increase in inflammatory cells and myofibers with centrally located nuclei 14 days after $BaCl_2$ injection. Moreover, Septin7-depleted muscles exhibit elevated levels of Myogenin protein 14 days after muscle injury, suggesting a delay in the ordered progression of the regenerative process (Szabó et al., 2023).

1.9. Aims of the study

The formation of a multinuclear muscle fiber necessitates the repeated fusion of muscle progenitor cells, known as myoblasts. This intricate process is preceded by coordinated cell migration, adhesion, and differentiation. The extensive cellular alterations that myoblasts undergo during muscle fiber formation demand profound adaptations in structure and function. An adaptive cytoskeleton is the foundation and driving force behind the morphological changes associated with cell migration and adhesion, undergoing marked reorganization during the myoblast-to-myotube transition. Furthermore, the cytoskeleton contributes to cell differentiation by integrating external and internal signaling inputs into a mechano-adaptive response.

While the roles of actin, tubulin, and intermediate filaments in myogenic differentiation are well established, the involvement of septins in muscle context remains largely unexplored. Septins, a large family of polymerizing GTPases, interact with other cytoskeletal components and are thus prime candidates for participating in regulatory mechanisms during myogenic differentiation.

This study aims to specifically understand the role of Septin9 during myoblast differentiation.

To achieve this, I will:

(i) Elucidate the expression patterns of septin gene family in myoblasts, identify the available septin paralogues, and propose a model for core septin complex oligomerization in muscle precursor cells.

(ii) Analyze the organization of Septin9 in myoblasts and myotubes, with a particular focus on septin architecture during myoblast differentiation.

(iii) Elucidate the contribution of the septin cytoskeleton to the myoblast differentiation process by challenging myoblasts with siRNA-mediated depletion of Septin9.

2. Materials and Methods

2.1. Materials

2.1.1. Chemicals and reagents

General chemicals and standard reagents were purchased from Carl Roth GmbH, Sigma-Aldrich, NEB and Invitrogen, unless stated otherwise in corresponding method section. All solutions and buffers were prepared using Mili-Q water, unless stated otherwise. The pH was adjusted using HCl or NaOH.

Table 2-1. Solutions and buffers for molecular biology and biochemistry methods

Solution or Buffer	Composition
10X TBE	121.1 g Tris Base, 61.8 g Boric acid, 27.5 g EDTA ad 1 l dH_2O, pH 8.0
Laemmli buffer (6x)	375 mM Tris-HCl, 25% SDS, 45% Glycerol, 12.5% 2-Mercaptoethanol, 0.01% Bromphenol blue in H_2O
Lysogenic broth (LB) medium	25 g LB-Medium in 1 L H_2O
ZYM-5052 auto-inducing medium	1% N-Z-amine AS, 0.5% yeast extract, 25 mM Na_2HPO_4, 25 mM KH_2PO_4, 50 mM NH_4Cl, 5 mM Na_2SO_4, 2 mM $MgSO_4$, 0.5% glycerol, 0.5% glucose, 0.2% α-lactose
LB agar plates	7.5 g LB-Medium, 4.5 g Agar-Agar, in 300 mL H_2O
Antibiotics (1000x)	100 mg/mL Ampicillin, sterile filtered 50 mg/mL Kanamycin, sterile filtered
4x SDS separation buffer (Lower Tris)	1.5 M Tris, 0.4% SDS in H_2O, pH 8.8
4x SDS stacking buffer (Upper Tris)	0.5 M Tris, 0.4% SDS in H_2O, pH 6.8
1x SDS-PAGE running buffer	10% Rotiphorese 10x SDS-PAGE in H_2O
1x Transfer buffer	24 mM Tris, 196 mM Glycine, 20% Methanol in H_2O
RIPA light (Radioimmunoprecipitation) lysis buffer	150 mM NaCl, 25 mM Tris, 0.1% SDS, 0.5% NP-40 Alternative. Freshly supplemented with 1 mM Phenylmethylsulfonyl fluoride (PMSF), 2 mM Sodium orthovanadate, 500 mM Sodium fluoride, 20 mM Sodium pyrophosphate, 1x Protease Inhibitor Cocktail in H_2O, pH 7.4
6x Laemmli SDS sample buffer	0.375 M Tris, 18% (w/v) SDS, 30% (v/v) β-Mercaptoethanol, 60% (v/v) Glycerol, Bromophenol blue (tip of a spatula)
TBS	100 mM Tris pH 7.5 150 mM NaCl
TBS-T (0.1%)	0.5% Tween 20, 5% 20x TBS buffer in H_2O
TNE Buffer	20 mM Tris-HCl, 150 mM NaCl, 1 mM EDTA in H_2O, pH 7.5
Blocking buffer	5% NGS, 3% BSA in DPBS

Table 2-2. Non-standard chemicals and commercial kits

Substance	Manufacturer
EZ-Link Sulfo-NHS-SS-Biotin	Thermo Fischer
rProtein A Sepharose Fast Flow	GE Healthcare
Streptavidin Sepharose High Performance	GE Healthcare
Fluoromount-G	Southern Biotech

Collagenase A	Roche
Dispase II	Merck
Proteinase K	Carl Roth
5x passive lysis buffer for Dual luciferase reporter gene assays	Promega
NucleoBond Xtra Midi	Machery-Nagel
NucleoSpin Plasmid EasyPure	Machery-Nagel
NucleoSpin Gel and PCR Clean-up	Macherey-Nagel
NucleoSpin RNA II isolation kit	Machery-Nagel
M-MLV Reverse Transcriptase:	Promega
Pierce BCA Protein Assay Kit	Thermo Fisher Scientific
DeadEnd Fluorometric TUNEL System	Promega
Click-iT EdU Cell Proliferation Kit, AF488	Thermo Fisher Scientific
Caspase-Glo 3/7 Assay	Promega
Proximity Ligation Assay DUOLINK Kit	Sigma Aldrich
NEBuilder® HiFi DNA Assembly Cloning Kit	New England Biolabs

2.1.2. Technical devices, software and online tools

Table 2-3. Technical devices

Device	Type	Manufacturer
Deionisation system	Milli-Q	Millipore Corporation
Cell counter	CASY Model TT	Roche
CCD-based detection system	FUSION FX7	Vilber Lourmat
Camera	Axiocam ERc 5s	Carl Zeiss Microscopy
Microscope (bright field)	Axiovert 40 CFL	Carl Zeiss Microscopy
Microscope (epifluorescence)	Axio Observer 7	Carl Zeiss Microscopy
Clean bench	Herasafe KS, Class II Biological Safety cabinet	Thermo Fischer Scientific
Cell culture incubator	Heracell 240i	Thermo Fischer Scientific
Electrophoresis power supply	PowerPac High Current	Bio-Rad
Electrophoresis chambers	Mini-PROTEAN Tetra Cell Systems	Bio-Rad
Wet/Tank Blotting system	Trans-Blot Cell	Bio-Rad
Luminometer	TECAN infinite f200	Tecan
Real-Time PCR System	Applied Biosystems StepOnePlus	Life Technologies
Spectrophotometer	NanoDrop ND-1000	NanoDrop Technologies
Swinging-Bucket Rotor	SW 41 Ti	Beckman Coulter
Thermal Cycler	PTC-200	MJ Research
Ultracentrifuge	Optima LE-80k	Beckman Coulter
Microplate reader	Sunrise	Tecan

Table 2-4. Online tools and software

Software	Application	Source
AxioVision	Image acquisition	Zeiss
BIO1D	Densitometric protein level quantification	Vilber Lourmat
Zotero	Bibliography managment	Corporation for Digital Scholarship. https://www.zotero.org/
FusionCapt Advance FX7	Immunoblot image acquisition	Vilber Lourmat
ImageJ FIJI	Image processing and quantification	Open Source
LAS-X 3.7	Image acquisition	Leica Microsystems
Microsoft Office	Text editing	Microsoft
Inkscape	Figure preparation	Open source, https://inkscape.org/
Prism9	Analysis and graphing of data	GraphPad
Snapgene	DNA viewer and digital cloning	Snapgene
StepOne Software2.3	qRT-PCR evaluation	Thermo Fisher Scientific
ZEN Microscopy Software 2.5	Image acquisition and quantification	Zeiss
Primer BLAST	Primer design	ncbi.nlm.nih.gov/tools/primerblast/
Ensembl genome browser	cDNA, genomic DNA, and mRNA sequences	http://www.ensembl.org/index.html
CRISPOR	sgRNA design	http://crispor.tefor.net/
NEBuilder Assembly Tool	Knock-in cloning strategy	New England BioLabs

2.1.3. Cell culture materials, reagents and media

Sterile cell culture materials and consumables were purchased from Greiner Bio-One GmbH (Frickenhausen, Germany), Corning (New York, USA) and Hartenstein Laborbedarf (Würzburg, Germany).

Table 2-5. Cell culture reagents and materials

Solution or Buffer	Supplier
Dulbecco's Modified Eagle Medium (DMEM), stable L-Glutamine, 4.5 g/L glucose	PAN Biotech
Dulbecco's Phosphate Buffered Saline (DPBS)	PAN Biotech
Fetal Bovine Serum (FBS)	PAN Biotech
Horse Serum (HS)	Gibco, Thermo Fisher Scientific
Gelatine from porcine skin, Type A	Sigma-Aldrich
Lipofectamine 2000	Life Technologies
Lipofextamine RNAiMax	Life Technologies
Trypsin 0,05%/ EDTA 0,02% in PBS w/o Ca, Mg	PAN Biotech
DMSO	Sigma-Aldrich
Collagen I, rat tail	Gibco, Thermo Fisher Scientific
Matrigel Growth Factor Reduced Basement Membrane Matrix	Corning

Penicillin 10.000U/ml /Streptomycin 10mg/ml (P/S)	PAN Biotech
Opti-MEM Reduced Serum Medium (OptiMEM)	Life Technologies
Chick Embryo Extract	LSP
Recombinant Human FGF-basic (154 a.a.)	PeproTech
µ-Slide 8 Well	Ibidi
µ-Slide 18 Well	Ibidi

Table 2-6. Cell culture medium

Medium	Composition
Growth medium for C2C12 (GM)	DMEM, 1%P/S, 10% (v/v) FBS
Myogenic differentiation medium for C2C12 (DM)	DMEM, 1%P/S, 2% (v/v) HS
Growth medium for primary myoblasts (mGM)	DMEM, 1%P/S, 20% (v/v) FBS, 10% (v/v) HS, 0.5% chicken embryo extract, 2.5 ng/ml bFGF
Myogenic differentiation medium for primary myoblasts (mDM)	DMEM, 1%P/S, 5% (v/v) HS
Freezing medium	10% FCS, 10% DMSO, 70% growth medium

2.1.4. Cell lines

Table 2-7. Cell lines

Cell line	Cell type	Tissue of origin	Source
C2C12	Myoblast	Satellite cells of the thigh muscle of a C3H mouse	AG Knaus cell bank
Primary myoblasts	Myoblast	Satellite cells of the hind limb muscles of C57BL/6 mouse	Freshly isolated in this study
NSC-34	Motor neuron progenitor	Hybridoma from fusion of embryonic spinal cord cells with neuroblastoma	AG Knaus cell bank
Septin9 $^{cond/cond}$ and Septin9 $^{del/del}$	Myoblast	Immortalized embryonic fibroblasts from Septin9$^{cond/cond}$ mouse lacking with Septin9 exons 2-5 flanked with loxP sites. Septin9$^{del/del}$ lacks exon 2-5 after Cre recombinase treatment	Kind gift from Dr. Ernst-Martin Füchtbauer, University of Aarhus, Denmark
Septin9-eGFP C2C12	Myoblast		Generated in this study
HEK293T	Embryonic kidney cells	Human embryonic kidney	Human embryonic kidney
C2C12 CAGA $_{12}$-luc cells	Myoblast	Satellite cells of the thigh muscle of a C3H mouse	AG Knaus cell bank
HEK293T CAGA $_{12}$-luc cells	Embryonic kidney cells	Human embryonic kidney	AG Knaus cell bank

2.1.5. Recombinant growth factors and inhibitors

Table 2-8. Recombinant growth factors and inhibitors

Growth factor	Comment	Source	Molecular weight
rhBMP6	produced in CHO cells	Gift from Slobodan Vukicevic (Simic et al., 2006)	31.36 kDa
rhTGFβ1	produced in CHO cells	PeproTech	25.0 kDa
rhActivin A (MH)	produced in *E. coli*	Gift from Marko Hyvönen	26 kDa
rhBMP2	produced in *E. coli*	Gift from Walter Sebald (Ruppert et al., 1996)	25.8 kDa

Table 2-9: Small molecule inhibitors

Inhibitor	Comment	Source
Staurosporine	Broad-spectrum ATP-competitive protein kinase inhibitor	Selleckchem
Z-DEVD-FMK	Specific, irreversible Caspase-3 inhibitor	Selleckchem

2.1.6. Antibodies and fluorescent dyes

Table 2-10. Antibodies and dyes

Antibody	Source	Identifier
Mouse monoclonal anti-MF20, dilution IF 1:100, WB 1:500	DHSB	Cat# MF 20; RRID:AB_2147781
Mouse monoclonal anti-Myog, dilution WB 1:100	Santa Cruz	Cat# sc-12732; RRID:AB_627980
Mouse monoclonal anti-Myog, dilution IF 1:100	DHSB	Cat# F5D; RRID:AB_2146602
Mouse monoclonal anti-Vinculin, dilution WB 1:1000	Sigma-Aldrich	Cat# V9131; RRID:AB_477629
Mouse monoclonal anti-Actinin-2, dilution IF 1:500	Sigma-Aldrich	Cat# A7811; RRID:AB_476766
Mouse monoclonal anti-Actin beta, dilution WB 1:5000	Sigma-Aldrich	Cat# A5441; RRID:AB_476744
Mouse monoclonal anti-alpha Tubulin, dilution IF 1:500	Cell Signaling	Cat# 3873; RRID:AB_1904178
Rabbit monoclonal anti-Gapdh, dilution WB 1:2000	Cell Signaling	Cat# 2118, RRID:AB_561053
Rabbit polyclonal anti-Septin9, dilution IF 1:500, WB 1:2500	Homemade; Kind gift from Prof. Dr. M. Krauss (Diesenberg et al., 2015)	N/A
Rabbit polyclonal anti-Septin2, dilution IF 1:500	Sigma-Aldrich	Cat# HPA018481, RRID:AB_1856684
Rabbit polyclonal anti-Septin7, dilution IF 1:500	IBL America; Kind gift from Prof. Dr. Helge Ewers	Cat# IMB-18991, RRID:AB_10700085
Rabbit polyclonal anti-GFP, dilution IF 1:1000	Abcam	Cat# ab6556, RRID:AB_305564
Mouse monoclonal anti-GFP, dilution IF 1:100, WB 1:100	Santa Cruz	Cat# sc-9996, RRID:AB_627695
Rabbit monoclonal anti-Cleaved Caspase, dilution WB 1:1000, IF 1:400	Cell Signaling	Cat# 9661 RRID:AB_2341188
Ki67 dilution IF: 1:100	BD Biosciences	Cat# 550609 RRID:AB_393778
Rabbit monoclonal anti-Phospho-Histone3, dilution IF 1:100	Cell Signaling	Cat# 3377 RRID:AB_1549592

Bmpr2 BD, dilution IF 1:200	BD Biosciences	Cat# 612292 RRID:AB_399609
Mouse monoclonal anti-Myc, dilution WB 1:1000	Clone 9E10, purified from hybridoma cell culture	homemade
Mouse monoclonal anti-HA, dilution WB 1:1000	Sigma-Aldrich	Cat# H3663 RRID:AB_262051
Rabbit monoclonal anti-pSMAD1/5 (Ser463/465), dilution WB 1:1000	Cell Signaling	Cat# 13820 RRID:AB_2493181
Rabbit monoclonal anti-pSMAD2 (Ser465/467), dilution WB 1:1000	Cell Signaling	Cat# 3108 RRID:AB_490941
Rabbit monoclonal anti-SMAD1, dilution WB 1:1000	Cell Signaling	Cat# 6944 RRID:AB_10858882
Rabbit monoclonal anti-SMAD2, dilution WB 1:1000	Cell Signaling	Cat# 8685 RRID:AB_10889933
Rabbit polyclonal anti-His probe, dilution WB 1:100	SCBT (discontinued)	Cat# sc-803 RRID:AB_631655
Mouse monoclonal anti-GST, dilution WB 1:100	SCBT	Cat# sc-138 RRID:AB_627677
Mouse monoclonal anti-Zyxin, dilution IF 1:100	Abcam	Cat# ab58210 RRID:AB_946255
Rabbit monoclonal anti-PARP1, dilution WB 1:1000	Cell Signaling	Cat# 9542 RRID:AB_2160739
Mouse monoclonal IgG1 Isotype Control	Cell Signaling	Cat# 5415 RRID:AB_10829607
Mouse monoclonal IgG Isotype Control	Cell Signaling	Cat# 3900 RRID:AB_1550038
Polyclonal goat anti-mouse IgG (H+ L), dilution WB 1:5000	Dianova	Cat# 115-035-068, RRID:AB_2338505
Polyclonal goat anti-rabbit IgG (H+ L), dilution WB 1:5000	Dianova	Cat# 111-035-144, RRID:AB_2307391
Polyclonal goat anti-rabbit IgG (H+ L) AF488, dilution IF 1:400	Thermo Fisher Scientific	Cat# A-11034, RRID:AB_2576217
Polyclonal goat anti-rabbit IgG (H+ L) AF594, dilution IF 1:400	Thermo Fisher Scientific	Cat# A-11012, RRID:AB_2534079
Polyclonal goat anti-mouse IgG (H+ L) AF488, dilution IF 1:400	Thermo Fisher Scientific	Cat# A-11001, RRID:AB_2534069
Polyclonal goat anti-mouse IgG (H+ L) AF594, dilution IF 1:400	Thermo Fisher Scientific	Cat# A-11005, RRID:AB_2534073
Polyclonal goat anti-rabbit IgG (H+ L) AF647, dilution IF 1:400	Thermo Fisher Scientific	Cat# A-21244 RRID:AB_2535812
Phalloidin CruzFluor™ 594 Conjugate, dilution IF 1:600	Santa Cruz	Cat# sc-363795
Phalloidin CruzFluor™ 647 Conjugate, dilution IF 1:600	Santa Cruz	Cat# sc-363797
4'6-Diamino-2-phenylindole dihydrochloride (DAPI), dilution IF 1:2000	Sigma-Aldrich	Cat# D9542

2.1.7. Oligonucleotides

Table 2-11. siRNA sequences

Target gene	Target sequence	Manufacturer
ON-TARGETplus Non-targeting Control siRNA #1	UGGUUUACAUGUCGACUAA	Dharmacon, Cat# D-001810-01-50
ON-TARGETplus Mouse Septin9 siRNA	CCAACGGCAUUGACGUGUA	Dharmacon, Cat# J-048947-11-0050

Table 2-12. Real-time PCR Primer

Target gene	Forwards	Reverse
Myog	CCAAGGTCTCCTGTGCTGATG	TTGGCAAAACCACACAATGC
Myh2	GGAGGCTGAGGAACAATCCA	GTCATTCCACAGCATCGGGA
Myh8	AATGATGTTTCACAGCTGCAGAG	CCATCATGGCGGCATCAGTA
Rna18s1	CGGCTACCACATCCAAGGAA	GCTGGAATTACCGCGGCT
Septin2	GCCTGTCATTGCGAAAGCTG	GGGATACTGGCCTTGAGGAG
Septin4	CATCGTGGAAGTGGAAAACCC	GACAGCAGGGATAGGGAAGTC
Septin5	CAAGCAGTACGTTGGCTTCG	GTTGATGCGTTCCTCAGCAC
Septin6	CCCGACAGGACATTCGCTTA	AGGTGGGCATTCATGGTTCC
Septin7	GCCAACCTCCCAAATCAAGTG	ACTTTGGATTGCTCCACCTGT
Septin8	AGAGCGAGCTCCACAAGTTC	CAAAAGGCAGGTGTGCGTTC
Septin9	GGCTATGTGGGGATCGACTC	CGGCTGATTTTGGACTTGAA
Septin10	GAGATAAAAGAGCATCCCCGC	AATTCCAGTCTCCCCCACAC
Septin11	AGCCAGTGTCGGTAAAGAGC	GTTTCGCAGCTCTTCATTAC
Wwtr1	TCCCCACAACTCCAGAAGAC	CAAAGTCCCGAGGTCAACAT
Fst	CTCTTCAAGTGGATGATTTTC	ACAGTAGGCATTATTGGTCTG
Septin9_v2	CTGGACGGGATCATTTCAGAC	CGGCTCAATCTCCTCGACTTC
Septin9_X5	TATCACCGACCACCCTGATTTC	ATCCCCACATAGCCGAACTC
Septin9_x1	GGAATGGAGAGAGATCGCATCA	CGGCTCAATCTCCTCGACTTC (as S9_v2)
Septin9_v1	AGGCTTGCGGATCCCACTG	CGGCTCAATCTCCTCGACTTC (as S9_v2)
Septin9_v3	AGGCAGCCCGACTTTCAGC	ATCCCCACATAGCCGAACTC (as S9_X5)
Septin9_v4	CTGGCTTCCTCTCTTGCTTCTC	ATCCCCACATAGCCGAACTC (as S9_X5)
Pax7	CCGTGTTTCTCATGGTTGTG	GAGCACTCGGCTAATCGAAC
Myod1	CGACACCGCCTACTACAGTGA	AGATGCGCTCCACTATGCTG
Actb	CACTGTCGAGTCGCGTCCA	TGACCCATTCCCACCATCAC
Acta1	TGCTGTCCCTCTATGCTTCC	CACGAAGGAATAGCCACGCT
Inhba	GGAGATAGAGGACGACATTGGC	CTGGTTCTGTTAGCCTTGGGG
Mgp	TGCGCTGGCCGTGGCAACCCT	CCTCTCTGTTGATCTCGTAGGCA
Mymk	ATCGCTACCAAGAGGCGTT	CACAGCACAGACAAACCAGG
Mymx	CTGAGCTGTCTGCTCTTTGT	TCTCCTTCCTCTGGGAGTG
Trim72	CCGGCAAGGCTAGATATCCA	CTTCTGGTCTGAGCACTCCA
Synpol2	CCTTACTGTGAGGAGGGTAACA	TGGCTTCTCTTGTGTGGCAG
Jspr1	GGAGGCTGTCGGTCTCTA	TCCTCCAGAAATGGGAGGTCA
Dysf	TTCTACCCTGAGCTTTGGCG	CGATGGCGTAGGGATCAGAG
Cdc42ep1	TCAACCAGGCCACCTATGAC	AGACTCCAGGCCGTAACCAG
Cdc42ep 2	CCTCAAGCTTCTCAACTCTGGAC	GCCAACAAAGACAGGGTGGT
Cdc42ep 3	CTCACCGACAACCCAGTTCC	AGCTCAGAGAAACCAGCAGTC
Cdc42ep 4.1	TGATTTAACCGCTGGCTTGG	CAATCAGAGGGCCACAGCAAC
Cdc42ep 4.2	GCCAGAGGAAACAAACGCCG	GGCAATCAGAGGGCTCGGTC
Cdc42ep 5	TAAGTCTGGACCACGAGATGCC	GTGGCGACTCAGGAATGAGG

2.1.8. DNA constructs

Table 2-13. DNA constructs

Plasmid name	Comment	Backbone	Source
BRE-Luc	BMP responsive element from Id1 promoter	pGL3-basic	obtained and modified from Peter ten Dijke (Korchynskyi and Dijke, 2002)
pRL-TK	Renilla luciferase expressed under constitutive active thymidine kinase promoter	pRL-TK	Promega
hBMPR2-LF-HA	full length human BMPR2-HA	pcDNA3.1	AG Knaus plasmid bank
hBMPR2-SF-HA	human BMPR2-HA lacking C-terminal tail	pcDNA3.1	AG Knaus plasmid bank
β-Gal	β-Galactosidase	pcDNA1	Kind gift from Dr. Serhiy Souchelnytksi, Karolinska Institute, Stockholm, Sweden
Septin9-Myc	full length human SEPTIN9-6xMyc	pcDNA3.1	Kind gift from Dr. Michael Krauß, FMP, Berlin, Germany
SEPTIN9-GST	Full length human SEPTIN9	pGEX-4T1	Kind gift from Dr. Michael Krauß, FMP, Berlin, Germany
His-BMPR2-Kinase-Tail	M189-L1038 human BMPR2	pLIC-SGC1	AG Knaus plasmid bank
GST	GST CDS	pGEX-4T1	Kind gift from Dr. Michael Krauß, FMP, Berlin, Germany
hALK2-HA	full length human ALK2-HA	pcDNA3	AG Knaus plasmid bank
hTbr2-HA	full length human TBR2-HA		AG Knaus plasmid bank
pSpCas9(BB)-2A-GFP (PX458)	Cas9 from S. pyogenes with 2A-EGFP, and cloning backbone for sgRNA	PX458	Kind gift from Dr. Feng Zhang, Cat# 48138; RRID:Addgene_48138

Table 2-14. Oligonucleotides used for cloning

Plasmid name	Comment
5'HA_fwd	taagctacaacaaggcaaggcttgaccgac*aattg*CGAAGTCACCAGGATGAGAGGGG
5'HA_rev	gcccttgctcaccatACCGCCGCTACCGCCCATC
GFP_fwd	ggcggtagcggcggtATGGTGAGCAAGGGCGAG
GFP_rev	aggaacgggacgcatTTACTTGTACAGCTCGTCCATG
3'HA_fwd	gagctgtacaagtaaATGCGTCCCGTTCCTGGAC
3'HA_rev	agcatttaggtgacactatagaatagggccc*GACCACGCGGATATGCCTTC*
gRNA for	CACCGATCTGGGGGTGGGGTCCAG
gRNA rev	AAACCTGGACCCCACCCCCAGATC

2.2. Molecular biology method

2.2.1. Extraction of genomic DNA

Mouse genomic DNA (gDNA) was extracted from C2C12 cells cultured in a 6 cm dish using the QuickExtract DNA extraction solution following the manufacturer's instructions. The isolated gDNA was subsequently stored at 4 °C until further use.

2.2.2. Cloning of DNA vectors for CRISPR-Cas9-based Septin9 knock-in

To clone the guide vector, the CRISPOR tool was employed to identify an appropriate guide sequence targeting the C terminal region of *Septin9* gene. The selected guide sequence was introduced into the guide vector by annealing the forward (5´-CACCGATCTGGGGGTGGGGTCCAG -3`) and reverse (5´- AAACCTGGACCCCACCCCCAGATC -3´) oligonucleotides. The annealing reaction was carried out in 20 µL of 1x T4 Ligase buffer, supplemented with 2.5 µM of each oligonucleotide. The mixture was incubated in a cycler (Peltier Thermal Cycler PTC-200) for 5 minutes at 95 °C, followed by a gradual temperature decrease to 25 °C at a rate of -0.1 °C/s. The px458-pSpCas9(BB)-2A-GFP backbone was digested with BpiI and dephosphorylated. Specifically, the vector was digested for 1 hour at 37 °C using 1 µL of the enzyme, followed by dephosphorylation with 1 unit of alkaline phosphatase (PhastAP, Thermo Fischer Scientific) during the last 15 minutes of restriction digestion. The linearized plasmid was then purified on an agarose gel. The annealed oligonucleotides, designed with overhangs, where ligated into the linearized vector by incubating the vector with a 3- to 7-fold molar excess of insert DNA using T4 DNA ligase (~ 40 Units) at 16 °C overnight. Subsequently, 4 µl of ligation reaction was used for transformation into TOP10 *E. coli*.

For the donor vector, the coding sequence of meGFP was flanked by two homology regions (HR): 904 bps upstream (5' HR) and 896 bp downstream (3' HR) of the stop codon of *Septin9*, and inserted into pcHA-MK backbone (derived from pcDNA3.1 (+), provided by Prof. Dr. Michael Krauß). The 5' HR was separated from meGFP by a Gly-Ser-Gly-Ser-Gly linker (15 bp), and the stop codon of Septin9 was removed. The design and cloning of the donor vector were performed using the NEBuilder assembly tool and NEBuilder HiFi DNA assembly cloning kit, according to the manufacturer's instructions. The backbone was digested with ApaI and MfeI, dephosphorylated, and the homology arms and me GFP were subcloned from gDNA and plasmid DNA, respectively. All fragments were ligated following the assembly kit protocol, using 0.05 pmoles of each component, and transformed into NEB 5-alpha *E. coli* (provided in the kit).

2.2.3. Quantitative real-time PCR

For sample collection, cells were rinsed twice with DPBS and lysed in 350 µl RA1 buffer, supplemented with 1% β-mercaptoethanol. The lysates were stored at -80 °C until further processing. Total RNA was isolated using the NucleoSpin RNA II isolation kit (Macherey-Nagel, Düren, Germany) following the manufacturer's protocol. Subsequently, 1 µg of total RNA was reverse transcribed using random primers (100 pmol µL–1, Invitrogen, Carlsbad, USA) and M-MuLV reverse transcriptase enzyme (200,000 U mL–1, New England Biolabs, Ispwich, USA). RT-PCR was conducted using a StepOnePlus Real-Time PCR System (Thermo Fisher Scientific) with specific primers listed in Table 2-12. Reactions were performed in triplicate in MicroAmp Optical 96-well reaction plates (Thermo Fisher Scientific), utilizing 2ng cDNA as a template per replicate and Luna PCR Master Mix (New England Biolabs). Fold induction was calculated by comparing relative gene expression to the housekeeping gene 18S RNA using the ΔΔCT method (Pfaffl, 2001).

Table 2-15. Mastermix for reverse transcription reaction

Reagent	Volume
RNA (total 500 – 1000ng)	0.5-1 µg
H_20	ad 14.5 µl
Random Primer	0.5 µl
10x M-MLV (buffer)	2.5 µl
dNTPS (10 µM)	1.25 µl
RNAsin	0.5 µl
M-MLV-RT (Reverse Transcriptase)	1.0 µl
H_20	19.25 µl

Table 2-16. PCR cycler program for cDNA synthesis

Steps	Process	Time	Temperature
Combine RNA, random primer mix and H_2O, total 15 µl			
1	Denaturation	5 min	70 °C
2	Oligo Annealing cool down	10 min	4 °C
Add the other ingredients as a mastermix, total 25 µl, mix and spin down			
3	cDNA synthesis	60 min	37 °C
4	cool down	∞	10 °C

2.2.4. Single-nucleus RNA-sequencing data analysis

Single-cell sequencing data analysis was conducted by Dr. Paul Mendez (FU Berlin, Germany). The data was retrieved from the Gene Expression Omnibus (GSE138826) as a pre-annotated data frame containing RNA counts values. Initially, the data was first log-normalized using a

scale factor of 10^4. The top 2000 variable genes were identified using the *FindVariableGenes()* function with default settings. Subsequently, centering and scaling of the data were performed on these 2000 variable features using a linear regression model. For clustering, a shared nearest neighbor graph was constructed based on the first 25 principal components (PCs), followed by Louvain clustering with a resolution set to 0.5. Overall cluster annotations were available in the data frame retrieved from GEO. For subclustering, cells attributed to "MuSC" were selected, and the resulting subgroup of cells was scaled, with a shared nearest neighbor graph constructed using the first 10 principal components (PCs). Louvain clustering was then performed with a clustering resolution of 0.4, and subclusters were annotated based on expressed marker genes. The top three marker genes used to assign cell identities were as follows: quiescent cells (Pax7, Sdc4, and Spry1); activated cells (Pax7, Islr, and Itm2a), dividing cells (Top2a, Cdk1, and Pax7), and differentiated cells (Myog, Ttn, and Myl4). Notably, two clusters that did not express essential myogenic markers were excluded for further analysis. Additionally, similar to the original publication, we identified a cluster of immuno-myoblasts marked by expression of C1qa, which we excluded from our plots for clarity.

2.2.5. Bulk mRNA-sequencing data analysis

For RNA-seq library preparation, cells were seeded at a density of 40.000 cells/cm^2 in a 12-well plate 24 hours after Septin9 knockdown in full myoblast proliferation medium. Two independent repetitions were performed. Cells were expanded for an additional 24 hours (48 hours after post-knockdown in total). Primary myoblasts were lysed, while C2C12 cells were differentiated for 12 hours before lysis. RNA was isolated following the manufacturer's instructions using the NucleoSpin RNA isolation kit (Macherey-Nagel). A total of 500ng RNA was sent for sequencing to Genewiz, Leipzig, Germany. mRNA sequencing data analysis was performed by Dr. Paul Mendez (FU Berlin, Germany). Paired-end, 300-bp reads generated by Illumina sequencing were mapped to the GRCm38.p6 reference genome using STAR (v2.7.2b) (Dobin et al., 2013) with default settings via the Galaxy platform (Afgan et al., 2018). Raw count matrices were generated using featureCounts (v2.0.1) with a GTF annotation file for GRCm38 from Gencode (vM15) (Liao et al., 2014).Batch effects in the raw count data were then modeled using ComBat-Seq (Zhang et al., 2020), and gene expression was quantified using DESeq2 (Love et al., 2014) by comparing wild-type versus knockdown samples, with batch effects removed from the ComBat-Seq adjusted count matrices. Gene ontology

enrichment analysis was conducted using Enrichr (Kuleshov et al., 2016). Data visualization was subsequently performed in R (v4.1.1) utilizing the pheatmap (Kolde, 2019), ggplot2 (Wickham, 2016), ggrepel (Slowikowski et al., 2023), and dplyr (Wickham et al., 2023) packages.

2.3. Cell biology methods

2.3.1. Mammalian cell culture

C2C12 were obtained from American Type Culture Collection (ATCC) and were not used beyond passage 25. Both, C2C12 and Septin9-GFP C2C12 cell lines (the generation of which is described below) were cultured in GM in a humidified atmosphere at 37 °C and 10% CO_2 (v/v). C2C12 were passaged every other day in uncoated T175 tissue culture flasks. To induce differentiation, the GM was replaced with DM. For myogenic differentiation assays, C2C12 were seeded 20-40 x10^4/ cm^2. Primary myoblasts were cultured in mGM in a humidified atmosphere at 37 °C and 5% CO_2 (v/v). All tissue culture surfaces used for primary myoblast cultivation were coated with Matrigel coating solution (10% (v/v) Matrigel in DPBS) for 10 min at 4 °C, then dried in the incubator before cell plating. To induce differentiation, the mGM was replaced with mDM. Primary myoblasts were seeded at a density of 20-40 x10^4/ cm^2 for myogenic differentiation assays. HEK293T cells were cultured and expanded in GM under a humidified atmosphere at 37 °C and 5% CO_2 (v/v). All cell lines were tested for mycoplasma contaminations. To detach cells, they were rinsed twice with DPBS and then incubated with one volume of Trypsin/EDTA (PAN Biotech, 2 ml for T175 flask) for 10-15 minutes at 37 °C. The cells then were gently resuspended in 10 volumes of GM. C2C12 and HEK293T cells were starved for 5h in GM without FCS.

2.3.2. Cell stimulation with growth factors and inhibitors

For cell stimulation, BMP2, BMP6, Activin A and TGFβ1 were added to the cells at the specified concentrations in PBS following a starvation period. Unless otherwise noted, cells were stimulated with 2 nM BMP2, 5 nM BMP6, or 0.2nM TGFβ1. The concentration of Activin A used in Figure 3-24 is indicated. Prior to ligand stimulation or the induction of myogenic differentiation, cells were pre-treated with 1 µM Staurosporine for 1 hour and 10 µM Z-DEVD-FMK for 3 hours.

2.3.3. Ligand activity measurements

C2C12 cells were seeded, transfected with siRNA, and reseeded as previously described. GM and DM were collected from proliferating and differentiating cells, respectively, and immediately frozen in liquid nitrogen. For the assay, 5 x 10^5 stable $CAGA_{12}$-luc HEK293T cells were seeded in 100 µl GM in a 96-well plate. The following day, cells were starved for 5 hours in 0% FCS and then stimulated with the collected conditioned medium. Cells were treated with eighter pure conditioned medium, or with 1:1 and 1:4 dilutions in starvation medium, for 24 hours. A rhActivin A concentration curve was used as a control. After the stimulation period, the medium was decanted, and cells were lysed and processed according to the Dual Luciferase Assay protocol described in chapter 2.2.6.

2.3.4. Isolation of primary myoblasts

Mice were maintained in compliance with European Union and German legislation under license number ZH120. Skeletal muscle progenitors were isolated from the hindlimbs of 5-week-old mice as described in (Shahini et al., 2018). Briefly, muscles were minced and digested with 2.5 mg/mL collagenase A (Roche) for 1 hour at 37 °C. Following digestion, the cells were centrifuged at 300g for 5 minutes, and the supernatant was discarded. The cell pellet was resuspended in mGM and placed on Matrigel- coated plates (Corning, working concentration of 0.9 mg/ml). Myoblast migration from the minced myofibers was observed on day 3 of culture. At this point, cells were trypsinized and plated for 1 hour on plates coated with type I rat tail collagen (Corning, working concentration 0.1 mg/ml) to remove fibroblastic and non-myogenic cells. The medium containing non-attached cells was then collected and transferred to Matrigel-coated plates for further expansion of the myoblast culture. This purification step was repeated after an additional 2 days in culture.

2.3.5. Transfection with siRNA and plasmid DNA

For gene silencing, cells were transfected with either scrambled (non-targeting #1) siRNA or Septin9 siRNA (J-048947-11-0050 ONTARGETplus) using Lipofectamine-RNAiMAX (ThermoFisher Scientific) following th manufacturer's instructions. Septin9 was silenced in C2C12 using a single round of 48-hour knockdown with 50 nM siRNA. Briefly, 1.5 x 10^5 cells were seeded in a 6 cm dish with 2 ml of P/S-free GM. The following day, the siRNA –

Lipofactamine mix was prepared in Opti-MEM and incubated for 20 minutes at RT. Cells were rinsed once with DPBS, and 1.7 mL Opti-MEM was added. Subsequently, 300 µl of the transfection mix was added dropwise to the cells, achieving an effective siRNA concentration of 100 nM for the first 5 hours. After 5 hours, 2 mL of 20% FCS P/S-free medium was added. After 24 hours, cells were trypsinized, re-plated for the experiment, and the medium was replaced with fresh GM. All experiments were conducted 48 hours after siRNA transfection. Primary myoblasts were handled at the recommended density of 3000/cm^2 (Shahini et al., 2018) and transfected in 3.7 mL of mGM with 300 µL of the Opti-MEM/siRNA mix. After 24 hours, the cells were re-plated for the experiment, and the medium was exchanged for fresh mGM.

For co-immunoprecipitation experiments, HEK293T cells were transfected with 3 µg DNA using polyethylenimne (PEI) at a 1:2 PEI-to-DNA ratio for 1.5 x 10^6 cells (Boussif et al., 1995). C2C12 cells were transfected with Lipofectamine 2000 according to the manufacturer's instructions, using 0.75 µg DNA and 1.5 µL Lipofectamine 2000 in a 12-well plate format. Cells were allowed to express protein for 48 hours prior to the experiment.

2.3.6. Generation of knock-in Septin9-eGFP C2C12 cell line

Endogenous tagging of the Septin9 C-terminus with meGFP was achieved using CRISPR/Cas9 technology (Ran et al., 2013). Briefly, the primers 5´-AAACCTGGACCCCACCCCCAGATC-3` and 5´- CACCGATCTGGGGGTGGGGTCCAG-3´ were annealed and cloned into the px458-pSpCas9(BB)-2A-GFP vector (Addgene, #48138) using the BpiI restriction site to generate the guide RNA. In the donor vector, the expression cassette was replaced with the coding sequence (CDS) of meGFP, which was inserted between two homology regions (HRs) consisting of ~ 1000 bp of the original genomic sequences upstream (5´HA) and downstream (3´HA) of the Septin9 stop codon. These regions were separated by a Gly-Ser-Gly-Ser-Gly linker (L). The stop codon of Septin9 was removed in the donor vector. The design and cloning of the donor vector were performed using the NEBuilder assembly tool and NEBuilder HiFi DNA assembly cloning kit, according to the manufacturer's instructions. C2C12 cells were transfected with both px458-pSpCas9(BB)-2A-GFP and the donor vector. 72 hours post-transfection, GFP-expressing C2C12 cells were sorted into 96-well plates at the density of one cell per well using a fluorescence-activated single cell sorter (BD FACSAriaII SORP, BD Biosciences) at MPI-MG Berlin. The growing colonies were expanded and screened for

Septin9-eGFP expression by immunofluorescence and Western blotting using anti-Septin9 and anti-GFP antibodies. The expression of Septin9-eGFP in selected clones was further validated by siRNA-mediated depletion of Septin9 followed by immunocytochemistry.

2.3.7. Dual Luciferase Assay

C2C12 stably expressing a SMAD2/3 sensitive $(CAGA)_{12}$ luciferase reporter, along with a constitutively expressed renilla luciferase construct (RL-TK; Promega) as an internal control, were transfected with Septin9 siRNA as described in 2.2.4. 48 hours post- transfection, the cells were starved in serum-free medium for 5 hours before being stimulated with TGFβ1 (0.1 pm) for 24 hours. HEK293T cells, also stably expressing the $(CAGA)_{12}$ luciferase reporter and RL-TK control, were similarly starved for 5 hours before stimulation with conditioned medium as indicated in Figure 3-24. Cell lysis was performed using passive lysis buffer (Promega), and luciferase activity was measurement according to the manufacturer's instructions using a TECAN initiate f200 Luminometer (TECAN).

2.3.8. Proximity Ligation Assay

The Proximity Ligation Assay (Duolink) was performed according to manufacturer's instructions to visualize the interaction between Bmpr2 and Septin9. A total of 2×10^4 C2C12 cells were seeded on glass coverslips. The following day, the cells were starved and then stimulated with BMP2 for the indicated times and at the specified temperatures. After stimulation, the cells were fixed with 4% PFA for 15 minutes at RT. Subsequently, the cells were washed three times with DPBS and permeabilized using 0.5% Triton-X100 in DPBS. The permeabilized cells were then blocked with the PLA blocking solution (provided with the Kit) for 1 hour at 37 °C. Primary antibodies were diluted in the Antibody diluent solution (provided) and incubated with the samples overnight at 4 °C in a humidity chamber. The following day, the samples were washed with wash buffer A (0.01 M Tris, 0.15 M NaCl, 0.05% Tween, pH 7.4) and then incubated for 1 hour at 37 °C with MINUS and PLUS secondary probes diluted in the antibody diluent. After washing with wash buffer A, the samples were incubated with a Ligation solution for 30 minutes at 37°C in a humidity chamber. Following ligation, the solution was removed, and the samples were washed twice with wash buffer A. The cells were then incubated with the Polymerase solution for 100 minutes at 37 °C. Finaly,

the samples were washed twice with wash buffer B (0.2 M Tris, 0.1 M NaCl, pH 7.5) and mounted with Mounting medium containing DAPI (provided).

2.3.9. Myogenic differentiation assay

For protein and RNA level analysis, 1.4 x 10^5 myoblasts (4 x 10^4/ cm^2) were seeded on day 0 into 12-well plates with 1 mL of GM. After 24 hours, the GM was replaced with 1 mL of DM, which was refreshed every other day. For the immunofluorescence assay, 4 x 10^4 myoblasts were seeded in 250 µl of GM in 8-well Ibidi chamber slides. After 24 hours, the medium was replaced with DM, which was also refreshed every other day. Seeding conditions for live-cell microscopy will be described below.

2.3.10. EdU and TUNEL assays

The Click-iT EdU Imaging Kit was used to visualize C2C12 cells in the S-phase of the cell cycle according to the manufacturer's instructions. Briefly, C2C12 cells were seeded, transfected with siRNA, and then reseeded at a density of 4 x 10^4 / cm^2 in 100 µl of GM in 18-well chamber slides (Ibidi). The following day, cells were incubated with 10 µM EdU solution for 2 hours at 37 °C, followed by fixation with 3.7% FA in DPBS for 15 minutes at RT. Cells were then washed twice with 3% BSA in DPBS and permeabilized with 0.5% Trixon-X100 in DPBS for 20 minutes RT. After two additional washes, 30 µl of the click reaction mix was added to the samples and incubated in the dark for 30 minutes at RT, followed by a single wash with BSA/DPBS. Subsequently, Hoechst staining was performed, followed by two washing steps in DPBS. Samples were imaged shortly thereafter.

To visualize DNA single strand breaks, the TUNEL DeadEnd assay was performed according to the manufacturer's instructions. Cells were seeded as described above in 18-well chamber slides (Ibidi) and allowed to undergo myogenic differentiation for 12 and 24 hours. Following differentiation, cells were fixed with 4% fresh FA (methanol-free) for 25 minutes at 4°C, then washed and permeabilized according to the standard protocol. Samples were incubated with 100 µL of equilibration buffer for 10 minutes at RT, followed by incubation with 30 µl rTdT mix for 1 hour at 37 °C. The reaction was quenched with SSC buffer for 15 minutes, followed by three washes with DPBS. Finally, cells were stained with DAPI and imaged shortly thereafter.

2.3.11. Caspase-Glo 3/7 assay

Caspase-3 and -7 activity was monitored using Caspase-Glo® 3/7 Assay according to the manufacturer's instructions, with volumes adjusted for a 96-well format. Briefly, C2C12 cells were reseeded into the 96-well plates following siRNA transfection, in 100 µl GM. The following day, myogenic differentiation was induced for eighter 12 or 24 hours, as indicated in the figure. At the end of the experiment, the medium in each well was replaced with 25 µl of starvation medium, and the plate cooled to RT. The reconstituted Caspase-Glo reagent was allowed to equilibrate to RT, and 25 µL was added to each well. The plate was shaken on an orbital shaker for 30 second to ensure homogenous cell lysis and reagent distribution, followed by a 30-minute incubation at RT. Bioluminescence was measured at both 30 minutes and 1 hour post-incubation using the TECAN infinite f200 luminometer in a white, flat-bottom 96-well plate. For the positive control, cells were incubated with 1 µM Staurosporine for 1 hour prior to lysis.

2.3.12. Tissue preparation

Muscle tissue sections were performed by Dr. Georgios Kotsaris (FU Berlin, Germany). After dissection, the muscle was embedded in 6% (w/v) gum tragacanth (Sigma-Aldrich) dissolved in H_2O and snap-frozen in liquid nitrogen-cooled isopentane. Tissues were sectioned at a thickness of 10 µm using a cryostat set to a chamber temperature of -20 °C and a blade temperature of -22 °C and mounted onto Superfrost Plus slides (Thermo Scientific). The prepared slides were stored in -80°C for further use.

2.3.13. Immunoytochemistry (ICC)

C2C12 cells (parental and knock-in) were seeded on glass coverslips or 8-well chamber slides (Ibidi), then fixed with 4% PFA for 15 minutes at RT and washed three times with DPBS. Cells were then permeabilized with 0.5 % Triton-X100 in DPBS for 20 minutes and blocked for 1 hour in a blocking buffer containing NGS. For staining with a primary antibody raised in goat, donkey serum was used as the blocking agent. Cells were incubated overnight at 4 °C with the indicated primary antibodies in blocking buffer. Following primary antibody incubation, cells were stained with secondary antibodies and Phalloidin (if applicable) for 1 hour at RT in blocking buffer, followed by three washes with DPBS. Fluorescence staining with DAPI (1:2000 in DPBS) was performed for 5 minutes at RT, followed by a final DPBS wash and a rinse with

H_2O. The coverslips were mounted on microscope glass slides with Fluoromont-G or Prolonged Gold (for STED microscopy). Cells seeded on Ibidi chamber slides were kept in PBS and imaged within a week.

2.3.14. Immunolabeling on muscle tissue sections

Frozen tissue sections were gradually brought to RT on a heated plate. Slides were immersed in DPBS for 5 min and subsequently fixed in 4% PFA for 10 min at RT. After fixation, the slides were washed in DPBS and permeabilized with 0.4% Triton X-100 in DPBS for 10 minutes. Tissue sections were then blocked with 5% BSA in 0,1% Triton X-100 in DPBS for 1 hour at RT. Primary antibodies were diluted in 5% BSA in 0,1% Triton X-100 in DPBS and incubated with the tissue sections overnight at 4°C. The following day, slides were washed three times in DPBS for 5 min. Secondary antibodies, diluted in 5% BSA in DPBS, were applied for 1 hour at RT, followed by three washes in DPBS. Nuclei were stained with DAPI, and the slides were mounted with Fluoromount-G.

2.3.15. Fluorescence microscopy

Epifluorescence images of fixed cells were routinely acquired using an Axiovert 200 inverted fluorescence microscope (Carl Zeiss Microimaging) with Cy2, FITC, Alexa594 and Cy5 excitation/emission filters. Signals were recorded using a CoolSNAP HQ2 EMCCD camera (Photometrics). Images were pseudocoloured and processed using the linear BestFit option in ZEN 2.5 (Carl Zeiss). Tile scan images were obtained with a Leica brightfield microscope (DMi8) equipped with an automated XY scanning stage, controlled by the LAS-X 3.7 interface. At least three independent experiments, each with three technical replicates from 8-well chamber slides (Ibidi), were performed. Tile scans of 6.4 μm^2 (4x4) or 3.6 (3x3) μm^2 were generated by automatically stitching together images acquired around a chosen point with a 20x objective. Four to five tile scans were acquired per condition. Confocal and STED data of fixed C2C12 cells were collected using the Expert Line STED Microscope from Abberior. Confocal images of Septin9-GFP C2C12 cells were captured using 485 nm (20% laser power) and 640 nm (20% laser power). STED images were acquired using 561 nm excitation for ATTO 594 (20% laser power) and 640 nm excitation for a 775 nm. STED laser at 10% laser power was used to deplete both dyes.

Live-cell imaging was performed in DM without phenol red at 37 °C and 5% CO2. Confocal live-cell imaging of Septin9-meGFP cells was conducted on a spinning disk Nikon Eclipse Ti microscope (Yokogawa CSU-X1 and EMCCD Camera), operated by NIS-Elements software, with a 40x air objective (0.75 NA). Imaging was initiated 72 hours after medium change and carried out overnight, with a frame rate of 30 minutes. Images were taken at two z-planes, set initially by focusing on septin fibers and 0.5 µm above, with an autofocus system maintaining focus. TIRF live-cell imaging was conducted using a Nikon Eclipse Ti microscope (illumination: TIRF laser 488, prime95B sCMOS camera) operated by Micromanager, with a 60x oil objective (1.49 NA). Imaging began after medium change and was carried out overnight, with a frame rate of 30 minutes.

2.3.16. Holotomography Microscopy (Nanolive)

Refractive index measurements were performed on Septin9-meGFP C2C12 cells cultured in 8-well chamber slides (ibidi). Holographic refractive index data were acquired using the 3D Cell Explorer system over a 24-hour period, with images captured every 20 minutes under humidified conditions with 5% CO_2.

2.3.17. Image analysis & semi-automated quantification

Original TIFF files were processed and analyzed using the open-source software Fiji (ImageJ). Quantification of cell numbers and nuclear staining was performed in Fiji. For DAPI-labeled nuclei, a median filter with a radius of 3 pixels was applied, followed by Otsu-based thresholding to distinguish nuclei from the background. Touching nuclei were segmented using a watershed algorithm. The particle analyzer tool was subsequently used to count nuclei and measure the intensity nuclear signals such as EdU, TUNEL, Ki-67 or pHH3. Myogenesis progression was assessed by counting nuclei within and outside of myotubes using a custom Fiji macro. Myotubes and nuclei were fluorescently labeled with MF20 and DAPI. A Gaussian blur with a sigma radius of 1 pixel was applied to smooth the fluorescence channels. The Otsu-based thresholding method was used to isolate nuclei from the background, and a watershed algorithm was employed to segment touching nuclei. Morphological operations, including despeckle, 4x dilate, close, fill holes, and 3x erode were applied to refine the myotube staining. Touching myotubes were segmented using a

watershed algorithm. Regions of interest (ROIs) were defined based on the processed myotube channel, and the number of nuclei within these regions was counted. Fiji's particle analyzer was used to quantify the total number of nuclei, both inside and outside of myotubes. To ensure the accuracy of the analysis, a composite image combining the fluorescence channels of the myotubes and nuclei was generated. The outlines of analyzed myotubes and nuclei were overlaid on this image, allowing for manual validation of the analysis. Line scans were performed in Fiji, followed by the plot profile function to cover the region of interest, and normalized intensity values were plotted in Exel.

2.4. Biochemistry methods

2.4.1. Preparation of protein extracts, sodium dodecyl sulfate polyacrylamide gel electrophoresis (SDS-PAGE) and Immunoblotting

For SDS-PAGE, treated cells were trypsinized, washed with DPBS, and lysed on ice for 15 minutes in RIPA light lysis buffer, supplemented with protease inhibitor cocktail (Roche) and 1mM PMSF. The lysates were passed through a 20-gauge syringe and cleared by centrifugation at 11.000 g for 15 minutes at 4°C. Protein concentrations were determined using Pierce BCA Protein Assay Kit, following the manufacturer's instructions, and normalized with 1x sample buffer. Lysates were then denatured by boiling in Laemmli buffer for 5 minutes at 95 °C. Pre-cast 10% or 12,5% polyacrylamide gels, stored at 4°C until use, were employed for protein separation. For each sample, 10-30 µg of protein were loaded and separated by molecular weight, and 4 µL of PageRuler Plus Protein standard (Thermo Fischer Scientific) was included as a molecular weight marker. Following electrophoresis, proteins were transferred onto nitrocellulose membranes via Western blot. Membranes were blocked for 1 hour in 0.1% TBS-T containing 5% w/v skim milk, followed by three washes in 0.1% TBS-T, and then incubated overnight at 4°C with primary antibodies diluted in 3% w/v bovine serum albumin (BSA)/fraction V in TBS-T. For HRP-based detection, goat anti-mouse or goat anti-rabbit IgG HRP conjugates (± 0.8 mg/ml) were applied in 3% TBS-T. Chemiluminescent signals were developed using WesternBright Quantum HRP substrate (Advansta) and visualized on a FUSION FX7 digital imaging system.

2.4.2. Surface biotinylation

For surface biotinylation of transiently transfected HEK293T cells, 1.5 x 10^6 cells were seeded in a 6 cm dish and transfected with the indicated plasmids. 48 hours post-transfection, the cells were starved and subsequently stimulated. Biotinylation solution was prepared by dissolving 0.5 mg/mL EZ-Link Sulfo-NHS-SS-Biotin in DPBS, supplemented with 10 mM MgCl2 (PBSM), at 37°C. The culture medium was decanted, and the cells were carefully rinsed twice with ice-cold PBSM before being incubated with the biotin solution for 50 minutes on ice. After incubation, the biotin solution was removed, and the cells were quenched with 50 mM Tris (pH 8.0) for 10 minutes. The cells were then washed once with PBSM and lysed in RIPA light buffer. Cell debris were removed by centrifugation at maximum speed, and the supernatant was incubated overnight with streptavidin beads at 4°C. The samples were washed up to five times with fresh lysis buffer, eluted in 40 µL 2x Laemmli buffer, and subsequently analyzed via Western blotting.

2.4.3. Immunoprecipitation

For immunoprecipitation, 1.5 x 10^6 HEK293T cells were seeded in a 6 cm dish, transfected with the indicated plasmids, and allowed to express exogenous proteins for 48 hours. After transfection, cells were starved for 5 hours and subsequently stimulated with the specified ligands before lysis. Cells were lysed in RIPA light buffer supplemented with protease and phosphatase inhibitors. Tissue culture dishes (10 cm) were washed with ice-cold DPBS, and cells were scraped in 800 µL lysis buffer. The lysates were cleared by centrifugation at 11000 x g for 30 minutes at 4 °C. Total cell lysate was collected, and the supernatant was incubated overnight with either 3 µg of primary antibody or control IgG1 under rotation at 4°C. Immunocomplexes were precipitated by incubating with protein A-coupled sepharose beads for 1 hour at 4 °C. The beads were then washed up to seven times with RIPA light buffer. Proteins were eluted by boiling the beads in 2x SDS sample buffer for 15 min, followed by the addition of 1 mM dithiothreitol (DTT) as a reducing agent. Samples were subsequently analyzed by SDS-PAGE and Western blotting.

2.4.4. Septin2 interactome

For identification of Septin2 interaction partners, immunoprecipitation of Septin2 in C2C12 was coupled with Maldi/LC-MS analysis. Immunoprecipitation was performed as outlined in section 2.4.3. Briefly, 2.3 x 10^6 C2C12 cells were seeded in 10 cm tissue culture dish. The following day, myogenic differentiation was induced, and the cells were allowed to differentiate for five days (D5 sample). On day 4, additional cells were seeded for the day 0 sample (D0). On day 5, D0 and D5 samples were harvested and lysed in 600 µl RIPA light buffer (with inhibitors) for 30 minutes at 4 °C on a rotating wheel. Cell debris was removed by centrifugation, and the protein concentration of the supernatant was determined using the BCA assay. Protein concentrations were normalized to the lowest sample (D0, 3 mg/mL). Next, 3 µg Septin2 antibody and 60 µl Protein A Sepharose beads were added to each sample and incubated for 2 hours at 4 °C on the wheel. The beads were washed five times with RIPA light buffer, and 60 µL 1x SDS-PAGE sample buffer was added. The samples were then alkylated with 15 mM iodoacetamide for 30 minutes at RT in the dark. Proteins were separated on gradient pre-cast gels (Biorad) for approximately 1 cm, stained with freshly prepared Comassie solution, and destained overnight at 4 °C. The gel was given in water to FMP Mass Spectrometry facility (Berlin-Buch, Germany) for Maldi/LC-MS analysis. The resulting data were analyzed using the Perseus software (https://maxquant.net/perseus/). Three independent experiments were performed and analyzed together in a single gel.

2.4.5. Expression and purification of SEPTIN9-GST from *E. coli*

BL21 *E. coli* were used to express glutathione-S-transferase (GST)-SEPTIN9 or GST alone. A 40 mL overnight culture of BL21 cells, transformed with pGEX-4T-1 expression constructs, was diluted into 1L of 2x YT medium containing the appropriate antibiotics. Cultures were grown to an OD600 of 0.7-0.8, then transferred to 4 °C for 15 minutes. Protein expression was induced by adding 0.5 mM isopropyl thio-β-d-galactoside (IPTG), and the induced cultures were incubated overnight at 18 °C, shaking at 180 rpm. Bacteria were harvested by centrifugation at 6000 x *g* for 10 minutes at 4°C, and the resulting pellets were resuspended in 15 mL DPBS, transferred to 50 mL Falcon tubes, and stored at -20 °C.

To purify the GST-fused proteins, the bacterial pellets were thawed on ice and supplemented with 0.5 mL of 1x proteinase inhibitor cocktail (Roche) per 1 L bacterial culture. DTT was added to a final concentration of 1 mM, along with 10 mM of arginine and glutamate. Samples were then sonicated on ice (5 minutes total or until complete lysis, maximum

temperature 15 °C, 30 % power, using Branson Sonifier 250, Branson Ultrasonics, Germany). To remove DNA, 1 mL of 1 mg/mL DNAse was added and incubated for 15 minutes on ice. The lysates were cleared by centrifugation at 40000 *x g* for 30 minutes at 4 °C. The supernatant was then filtered using a 0.45 or 0.8 µm syringe filter and stored on ice. Glutathion- Sepharose 4B beads (GE-Healthcare) were prepared by washing 2 mL of beads with 10 column volumes (CV) of H_2O and equilibrating them with 5 CV of GST binding buffer (50 mM HEPES pH 7.5, 300 mM NaCl, 5% glycerol, 1 mM DTT). The bacterial lysate was loaded onto the column 2-3 times to ensure protein binding, followed by washing with 15 CV of binding buffer. Bound proteins were eluted with 5 CV of elution buffer (50 mM HEPES pH 7.5, 300 mM NaCl, 5% glycerol, 15 mM glutathione, 1 mM DTT) in two rounds. For overnight storage, protein samples were supplemented with 5 mM DTT. Lysate, supernatant, wash fraction, and elution fractions were analyzed via SDS-PAGE followed by Coomassie staining. The purified proteins were stored at 4 °C and used for pulldown experiments within 24h.

2.4.6. Expression and purification of His-tagged BMPR2 kinase domain from *E. coli*

The initial steps for protein purification were identical to those described for SEPTIN9-GST in section 2.3.4. The bacterial pellet was thawed on ice and resuspend in 30 mL lysis buffer (50 mM HEPES pH 7.5, 500 mM NaCl, 5% glycerol, 5 mM imidazole), supplemented with 0.5 mL 1x proteinase inhibitor (Roche), 0.5 mM TCEP, 10 mM arginine and glutamate. The cells were sonicated, treated with DNAse to remove DNA, and the lysate was cleared by centrifugation and filtered as previously described. For protein purification via immobilized metal affinity chromatography (IMAC), 2 mL of Fast Flow Chelating Sepharose (GE Healthcare) were washed with 10 column volumes (CV) of H_2O. The column was then washed with 5 mL 1 M $NiSO_4$ and 15 CV of H_2O, followed by equilibration with 5 CV lysis buffer. The cleared lysate was loaded onto the column to bind the His-tagged proteins, followed by washing with 5 CV lysis buffer. Further washing was performed with 15 CV of wash buffer (50 mM HEPES pH 7.5, 500 mM NaCl, 5% glycerol, 30 mM imidazole). Bound proteins were eluted using 5 CV of elution buffer (50 mM HEPES pH 7.5, 300 mM NaCl, 5% glycerol, 250 mM imidazole). For overnight storage, the eluted protein was supplemented with 5 mM DTT. Lysate, supernatant, wash fraction and elution fractions were analyzed via SDS-PAGE followed by Coomassie staining. The purified proteins were stored at 4 °C and used for pulldown experiments within 24 hours.

2.4.7. GST Pulldown and His-tag Pulldown Assay

To evaluate the direct interaction between SEPTIN9 and the BMPR2 kinase domain, GST and His-tag pulldowns were performed. For the GST pulldown, 20 µL Glutathione magnetic beads (Thermo Fisher Scientific) per sample were washed three times with wash buffer (50 mM HEPES pH 7.5, 150 mM NaCl, 0.05% Tween-20), and once with binding buffer (50 mM HEPES pH 7.5, 150 mM NaCl, 0.05% Tween-20, 1% BSA) before being resuspended in the binding buffer. The beads were then equally distributed among the samples and resuspended in 200 µl binding buffer. Next, 25 µg of SEPTIN9-GST or GST alone was incubated with the beads for 30-60 minutes, with rotation at 4 °C. After the initial incubation, 20 µg of His-BMPR2-kinase domain was added, and the samples were further incubated for 60 minutes at 4 °C with rotation. After incubation, the beads were washed three times with wash buffer and resuspended in 40 µL 2x SDS-PAGE sample buffer. Both the samples and purified proteins (as controls) were analyzed by SDS-PAGE, followed by Western blotting. For the His-tag pulldown assay, 40 µL of Chelating Sepharose Fast Flow beads were used per sample. The beads were washed with wash buffer (50 mM Tris-HCl pH 7.5, 150 mM NaCl, 0.05% (v/v) Tween-20, 20 mM imidazole) and equilibrated in binding buffer (50 mM Tris-HCl pH 7.5, 150 mM NaCl, 0.05% (v/v) Tween-20, 20 mM imidazole, 1% BSA, 1mM TCEP). Subsequently, 15 µg of His-tagged protein was incubated with the beads on a rotating wheel for 30 minutes at 4 °C. Aftrward, 20 µg GST-tagged protein was added, and the samples were incubated for 1 hour at 4 °C on the wheel. Following the incubation, the beads were washed three times with binding buffer and three times with wash buffer. Finally, the beads were resuspended in 40 µL 2x SDS-PAGE sample buffer. Both, the samples and purified proteins (as controls) were analyzed via SDS-PAGE, followed by Western blotting.

2.4.8. Statistical analysis

All data, except for RNA-seq, were derived from at least three independent experiments and are represented as means ± standard deviation (SD). Statistical analyses were conducted using GraphPad Prism (v9.3) software. The specific statistical tests used are detailed in the figure legends. To assess normality, datasets were subjected to the Shapiro-Wilk test. For comparisons between two conditions, a two-tailed Student’s t-test was applied. When

comparing more than two conditions, one-way ANOVA followed by Dunnett's post hoc test was employed to evaluate statistical significance, assuming normality. Statistical significance is denoted by asterisks in the figures as follows: *P < 0.05; **P < 0.01; ***P < 0.001; ****P < 0.0001.

3. Results

Expression and functional contribution of septins during critical phases of skeletal muscle development, homeostasis and regeneration remain largely unknown. The central focus of this work revolves around understanding septin contribution to myogenic differentiation and fusion, including (i) mapping the expression of septins during early muscle regeneration and throughout the myoblast differentiation process, (ii) describing the morphology of septin filaments in myoblasts and myotubes and focus on the changes septin filaments undergo during this transition, and (iii) scrutinizing the consequences of septin filament perturbation in regulating the proliferation and differentiation in myogenic context. This work was published in iScience under the title “Dynamic remodeling of septin structures fine-tunes myogenic differentiation” in 2024, sheds light on the dynamic interplay between cytoskeletal components and their critical roles in controlled myogenic differentiation.

3.1. Expression pattern of septins during muscle regeneration and differentiation

Expression pattern of septin paralogues in skeletal muscle are not well characterized. Which septins are relevant during embryonic development of muscle progenitors, in dormant versus activated satellite cells, myoblast expansion, myocyte differentiation, nascent vs mature myotubes and adult muscle fibers are open questions. Here we focus on defining core myogenic filaments and on characterizing murine septin expression during adult muscle regeneration (publicly available data set (Oprescu et al., 2020)) and *in vitro* myogenic differentiation.

3.1.1. Core myogenic septins

The presence of 13 distinct mammalian septin paralogs exhibits a dual nature of ubiquity and tissue-restricted expression. While implying redundancy, it also suggests a specificity of certain septins within each tissue. We analyzed the relative expression of all murine septin paralogs in C2C12 cells and primary myoblasts seeking to identify the expressed septins and potential combination thereof, available for the polymer formation in line with the Kinoshita hypothesis (Kinoshita, 2003). We used the control Transcripts Per Million (TPM) values of all

septin paralogs in early differentiating C2C12 cells (12 hours after induction) and proliferating primary myoblasts from the RNASeq experiments performed in this study (details of RNASeq are discussed in chapter 3.4) (Fig. 3-1). Normalization to the highest expressing septin (Septin2 in C2C12 and Septin11 in myoblasts) revealed a consistent trend, where the four most prominently expressed septins (2-11-7-9) were observed across both cell types (Fig. 3-1A-B). Those septins will be referred to as core myogenic paralogs in this study (Fig. 3-1C). While Septin1, 3, 5, 6, 8 and 10 were detected, their expression levels were approximately one order (Septin5, 6, 8 and 10) and two to three orders (Septin1 and 3) of magnitude less, than core septins. Septin12 was solely detected in C2C12 cells. Notably, some alternative septins (5, 6, 8 and 10) reach substantial expression levels in C2C12 cells (with Septin8 at 36%) and are less abundant in myoblasts. The expression of Septin4 and 14 was not found under tested conditions.

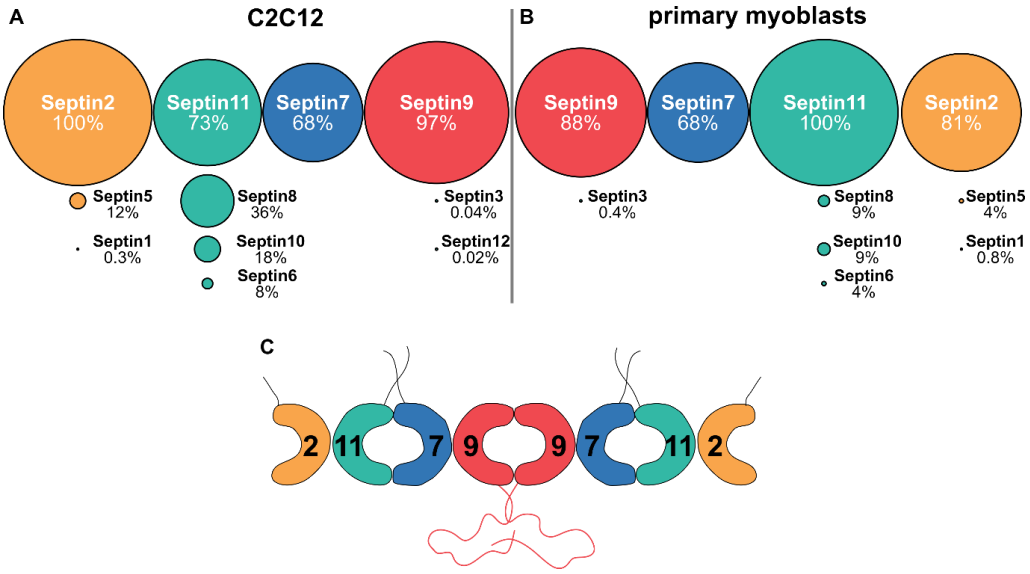

Figure 3-1. Septin paralogs in C2C12 and primary myoblasts
Comparison of relative expression levels of septin genes in **A** C2C12 cells and **B** freshly isolated primary myoblasts. TPM values from control cells are shown, averaged from two independent experiments, normalized to the highest expressed paralog (Septin2 in C2C12 and Septin11 in myoblasts). **C** Depiction of a potential core myogenic octamer, based on the expression level of all septin paralog.

3.1.2. Transcriptional landscape of septins during mouse musculature regeneration

To explore the expression dynamics of core and alternative myogenic septins in myogenic progenitors, we analyzed muscle stem cells (MuSCs) using single-cell RNA-sequencing (scRNA-seq) data obtained from regenerating tibialis anterior (TA) muscle samples collected

at various time points post cardiotoxin (CTX) injury (Oprescu et al., 2020). Unsupervised clustering identified four distinct sub-clusters: quiescent, activated, dividing, and differentiated MuSCs, distinguished by their expression of marker genes such as *Pax7*, *Myod1*, *Cdk1* and *Myogenin*, respectively (Fig. 3-2A-B).

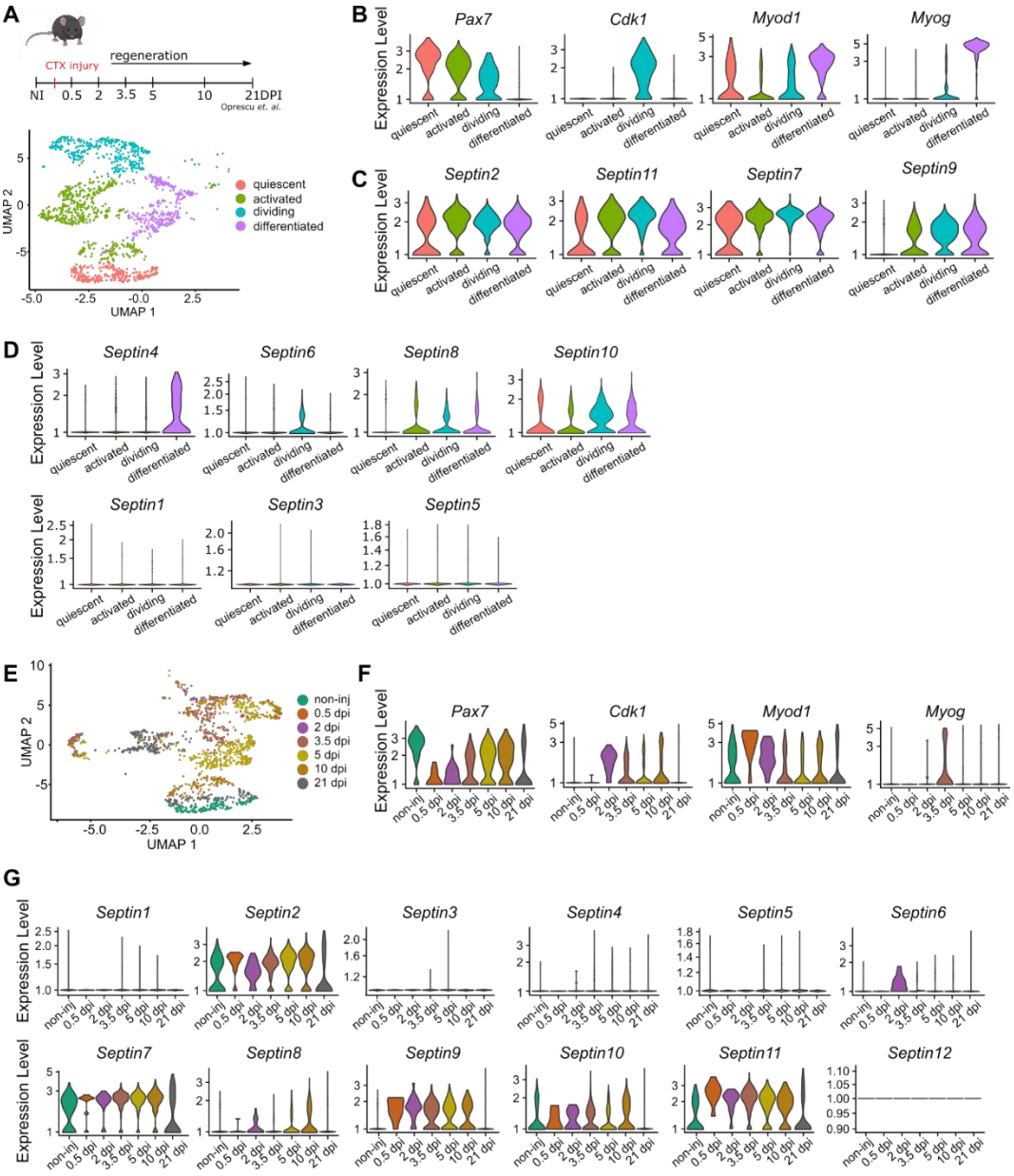

Figure 3-2. Transcriptional landscape of septins during muscle regeneration
Single cell RNA sequencing data of non-injured tibialis anterior muscle and additional six time points following cardiotoxin injury (CTX) (Oprescu et al., 2020). **A** UMAP visualization of the sub-cluster MuSC in regenerating musculature colored by identified cell populations within the sub-clusters. MuSC labelled cells were extracted from annotated single cell dataset available from GSE138826. **B** Violin plots representing subcluster-specific gene expression colored by cluster identity. **C** Violin plots representing gene expression profiles of *Septin2, 7, 9* and *11* in MuSC subclusters. **D** Violin plots representing gene expression profiles of *Septin1, 3, 4, 5, 6, 8* and *10* in MuSC subclusters. **E** UMAP visualization of the sub-cluster MuSC in regenerating musculature colored by time points within the sub-cluster. **F** Violin plots representing subcluster-specific gene expression colored by time points. **G** Violin plots representing subcluster-specific gene expression of all septins colored by experimental time points. Modified from (Ugorets et al., 2024).

This *in silico* analysis revealed consistent expression of *Septin2*, *7*, *10* and *11* across all MuSC populations, while *Septin8* and *Septin9* were absent in quiescent cells (Fig. 3-2C-D). Additionally, among other expressed septins, *Septin6* marked the proliferating cell population, while *Septin4* marked the differentiated population (Fig. 3-2D). *Septin2, 7*, and *11* were the most highly expressed septins within each septin homology group, particularly in quiescent MuSCs, and *Septin2, 7, 9* and *11* were prominent in all other myogenic sub-clusters, providing insights into potential promoter assembly during myogenic lineage progression. Analyzing gene expression over the course of muscle regeneration, revealed that the expression of core septin paralogues (2, 7, 9, 11) was induced concurrently with the onset of muscle regeneration, declining steadily over time, and largely downregulated by day 21 (Fig. 3-2E-G). At this time point the regeneration is assumed to be nearly complete (Baghdadi and Tajbakhsh, 2018). Notably, *Septin9* expression completely diminished by day 21 (Fig. 3-2G).

3.1.3. Expression of septins during *in vitro* differentiation within publicly available datasets

Myogenic differnetiation, initiated by serum deprivation, orchestrates the transition from myoblasts to contractile myotubes, characterized by dynamic changes in expression of myogenic regulatory factors, cell morphology, and cytoskeletal architecture (Bentzinger et al., 2012; Peckham, 2008; Swailes et al., 2006, 2004). Zhang *et al.* previously employed robust rank aggregation (RRA) algorithm to identify ‘key and robust’ differentially expressed genes (DEGs) during C2C12 myogenesis. This analysis integrated data from nine publicly available RNA-seq datasets in differentiating C2C12 cell into one meta study (Zhang et al., 2022). In this study upregulated *Septin4* and downregulated *Septin6* emerged as robust DEGs, as highlighted by the authors. Considering these findings, we aimed to explore the expression of all other septin paralogues besides *Septin4* and *6* and sought to investigate potential parallels in septin expression during muscle regeneration and *in vitro* differentiation (Fig. 3-3).

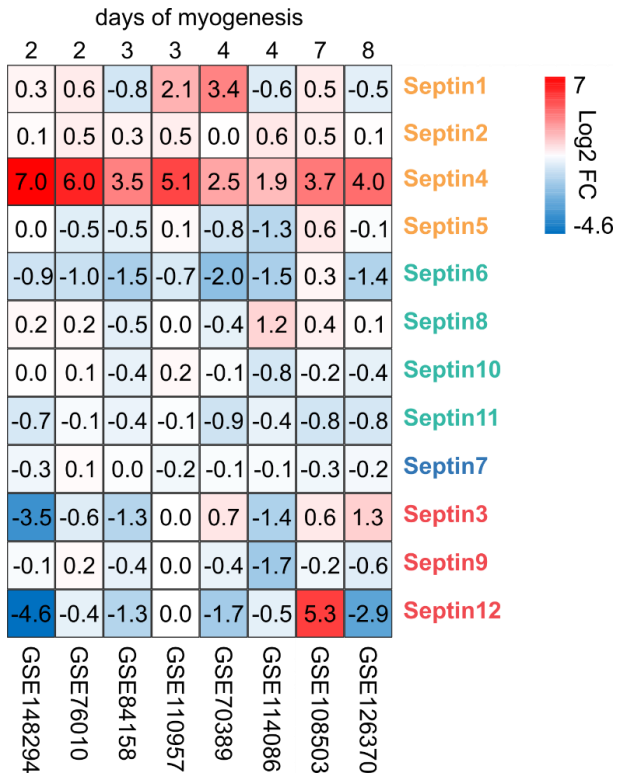

Figure 3-3. Expression of septins during myogenic differentiation across 8 publicly available RNA-Seq datasets

Expression of septins was re-analyzed in all available RNA-seq experiments on differentiating C2C12 cells from (Zhang et al., 2022). Noteworthy, original RNA-seq experiments were performed at different times during myogenic differentiation and are represented in columns (GSE numbers are labeled at the bottom, days of differentiation are labeled at the top). Heatmap depicting Log2 Fold Changes of all expressed mammalian septins derived from DESeq2 analysis across all RNA-seq datasets.

Remarkably, the Septin2 subgroup exhibited consistent expression with rather modest upregulation across different RNA-seq experiments. Similarly, *Septin7* demonstrated a stable expression profile. In contrast, the remaining septin subgroups displayed a mild downregulation in the tested conditions. Collectively, these insights underscore a similarity of expression profiles of septins in publicly available data for C2C12 cells and in the regenerating muscule.

3.1.4. Expression of septins during *in vitro* myogenic differentiation

We analyzed the expression of all septin paralogues at both RNA and protein levels in differentiating C2C12 cells. Accompanying the process of *in vitro* differentiation (Fig. 3-4 A), the upregulation of *Myog, Myh2, Myh8* and muscle specific *Acta1* genes, alongside the downregulation of *Actb* outlines the advancing process (Fig. 3-4B). We confirmed the expression of septins (except *Septin1, 3*, *12* and *14*, not detectable) during 7 days of *in vitro*

differentiation in C2C12 cells (Fig. 3-4C-E) showing consistent downregulation of *Septin6, 9* and *11* from 3 days onwards (Fig. 3-4C). Notably, *Septin2* exhibited stable expression while *Septin5,* and *7* were downregulated after 5 and 7 days, respectively (Fig. 3-4C, D). Analogous to adult regeneration process, *Septin4* is distinctively upregulated in C2C12 cells (Fig. 3-4E).

To complement our study, we analyzed protein levels of Septin9 during 7 days of differentiation. Protein levels partially mirror the RNA levels, where Septin9 initially exhibits an increase followed by subsequent downregulation, quantified over several experiments (Fig. 3-4F-G).

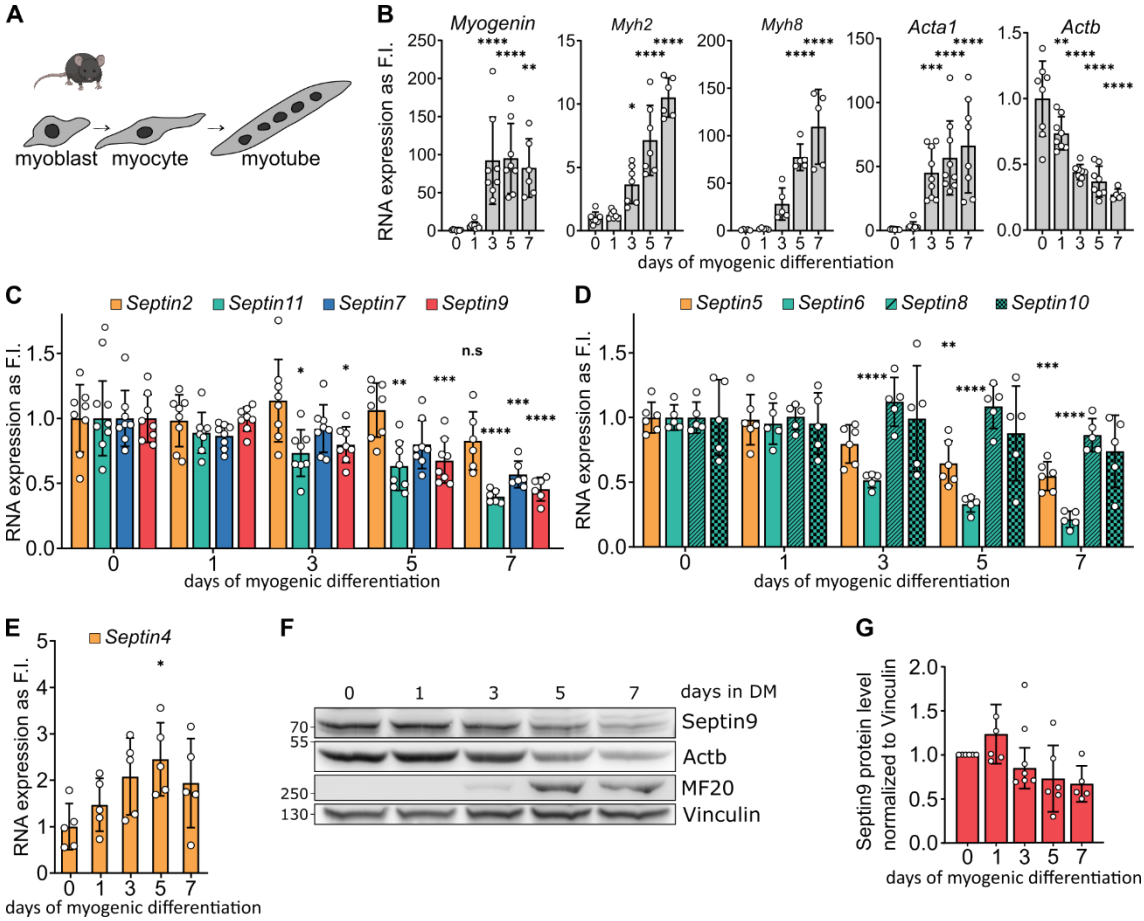

Figure 3-4. Expression of septins during in vitro myogenesis in C2C12
A Schematic illustration of murine *in vitro* myogenesis. **B** mRNA expression levels of myogenic marker genes during 7 days of myogenic differentiation of C2C12 cells. **C** mRNA expression levels of core septins (2, 7, 9 and 11) during C2C12 differentiation. **D-E** mRNA levels of other expressed septin paralogs. **F** Protein level Septin9 during C2C12 differentiation. **G** Summarizing quantification of Septin9 signal normalized to Vinculin during myogenic differentiation in C2C12 cells. Septins are color-coded based on subgroups of core myogenic protomers as proposed in Fig. 3-1. Data represent mean ± standard deviation (SD), *p<0.05, **p<0.01, ***p<0.001, ****p<0.0001, n.s – not significant from one way ANOVA followed by Dunnett's multiple comparison test. Data from (Ugorets et al., 2024).

Next, we investigated the expression of *Septin9* splice variants in C2C12 cells over a 7-day differentiation. *Septin9* undergoes alternative splicing resulting in up to three N-terminal long variants in mice, alongside an additional alternative start site leading to a short variant (Fig. 3-5A). To identify expressed isoforms, manual RT-PCR was performed using isoform-specific primers validated on whole embryo RNA (Fig. 3-5B). Furthermore, we used myoblasts isolated from homozygous *Sept9*$^{cond/cond}$ mice (Füchtbauer et al., 2011), Cre-recombinase treated *Sept9*$^{del/del}$ Septin9-null myoblasts and murine neuronal cell line NSC34 as controls. Within C2C12 cells only transcript variant 2 encoding for the long isoform b was detected. Additionally, we detected mRNA for two potential isoforms: (i) transcript variant X5 resulting in a short isoform c and (ii) transcript variant X1, resulting in a long isoform distinct from b, without an established name up to date (Fig. 3-5B).

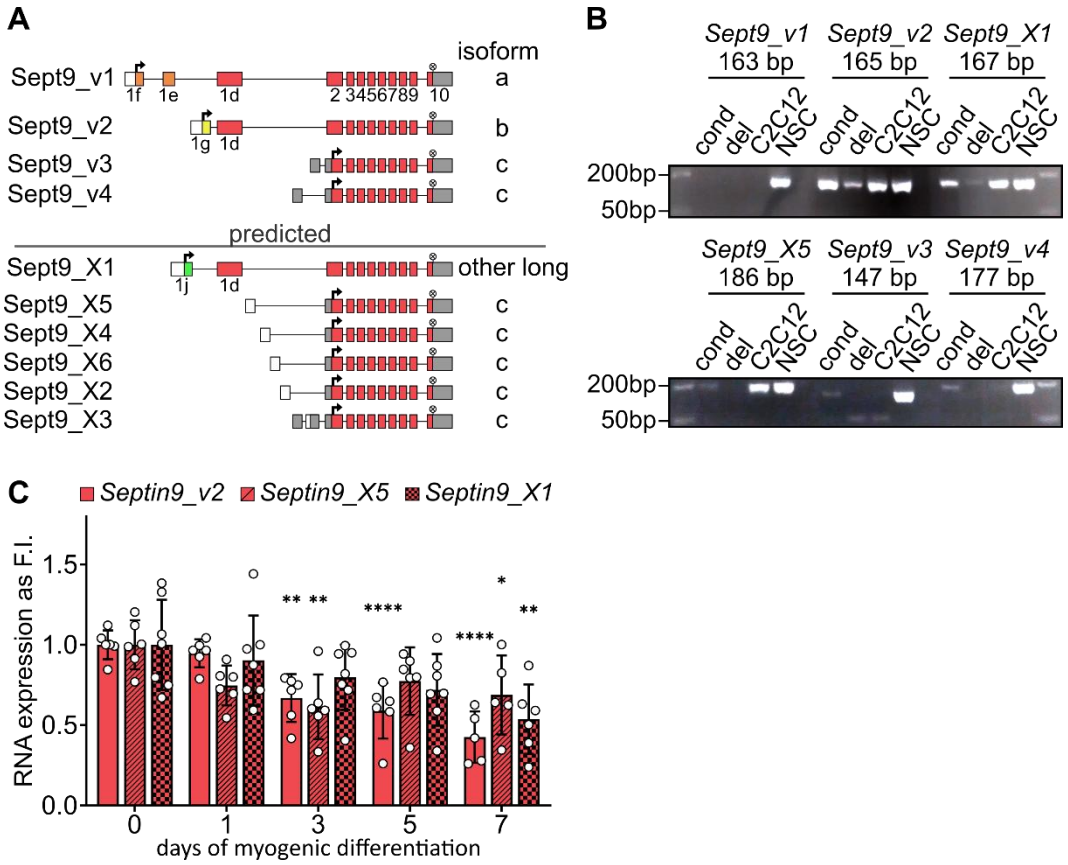

Figure 3-5. Expression of Septin9 transcripts during in vitro differentiation in C2C12
A Diagram depicting different *Septin9* transcript variants. The translation start site is indicated by an arrow, the stop codon by a cross, isoform-specific sequences by colored boxes, unique noncoding regions by open boxes and shared noncoding sequences by grey boxes (Füchtbauer et al., 2011; McDade et al., 2007). **B** Manual RT-PCR analysis of *Septin9* isoforms in Septin9^{CKO} myoblasts (cond), Sept9^{null} myoblasts (del), C2C12 and immortalized mouse neuron NSC34 cells. **C** Normalized mRNA expression profiles of three *Septin9* isoforms in C2C12 during 7 days of differentiation. Data represent mean ± standard deviation (SD), *p<0.05, **p<0.01, ***p<0.001, ****p<0.0001, n.s – not significant from one way ANOVA followed by Dunnett's multiple comparison test.

To elucidate isoform expression dynamics during myogenic differentiation, qRT-PCR was employed (Fig. 3-5C). The long isoform b (v2) exhibited reduced expression from day 3 onwards, while the short isoform X5 displayed an early downregulation, becoming significantly downregulated on day 7. Surprisingly, X5 returned to proliferation levels at day 5 before the subsequent decline. The predicted long isoform X1 remained relatively stable during early myogenesis but was significantly downregulated on day 7 (Fig. 3-5C).

We proceeded by analyzing the expression of septins in freshly isolated primary myoblasts, which exhibit a similar behavior to C2C12 cells in terms of myogenic regulatory factor expression. Tracking myogenesis through the upregulation of *Myog* and *Myh8,* coupled with the downregulation of *Pax7*, *Myf5*, and *Actb*, we characterized the progression of myogenic differentiation (Fig. 3-6A). In this context, three core muscle septins showed a robust and consistent downregulation trend over a 5-day differentiation period, with *Septin2, 7* and *9* being significantly downregulated (Fig. 3-6B). It is noteworthy, *Septin2* was not regulated in C2C12 cells while *Septin11* showed a downregulation in C2C12 cells, which is not observed in primary myoblasts. Resembling observations in C2C12 cells, the remaining septins exhibited a downregulation trend, with significant downregulation of *Septin6* (Fig. 3-6C). *Septin4* displayed a notable although not a significant upregulation (Fig. 3-6D). The transient upregulation of Septin9 protein followed by a marked downregulation are further evident through western blot, performed in primary myoblasts myogenically differentiating over 9-day period and quantified over several biological repetitions (Fig. 3-6E-F).

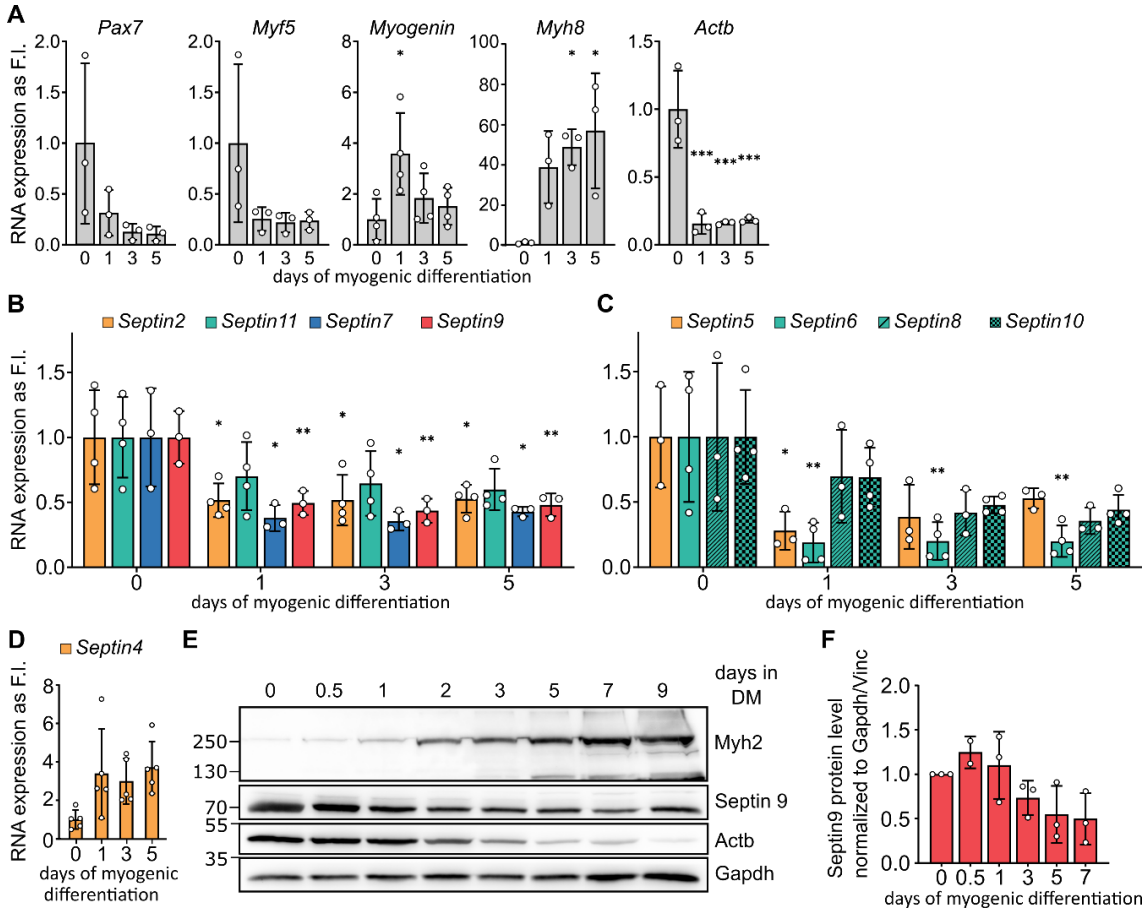

Figure 3-6. Expression of septins during myogenic differentiation in primary myoblasts
A mRNA expression of myogenic marker genes during 5 days of myogenic differentiation of primary myoblasts. **B** mRNA levels of core myogenic septins and **C-D** other septin paralogues. **E** Representative western blot depicting Septin9 expression over 9-day myogenic differentiation period in primary myoblasts. **F** Summarizing quantification of Septin9 signal normalized to Gapdh or Vinculin during myogenic differentiation in primary myoblasts. Septins are color-coded based on subgroups of core myogenic protomers as proposed in Fig. 3-1. Data represent mean ± standard deviation (SD), *p<0.05, **p<0.01, ***p<0.001, ****p<0.0001 from one way ANOVA followed by Dunnett's multiple comparison test. Data from (Ugorets et al., 2024).

3.1.5. Interaction of Septin2 with other septin paralogs in proliferating and differentiating C2C12 cells

We investigated the interaction of Septin2 with other septin paralogs in proliferating and differentiating C2C12 cells to assess potential changes in septin oligomer composition. Immunoprecipitation of Septin2 coupled with Maldi/LC-MS analysis revealed co-precipitation of core myogenic septins (7, 9 and 11) along with less abundant paralogs including Septin 5, 6, 8 and 10 (Table 3-1, Table 6-2). We compared the septin interactomes of Septin2 in proliferating and for 5 days differentiating C2C12 cells. Notably, core myogenic septins exhibited approximately 10-fold higher total intensity compared to Septin5, 8 and 10, and approximately 100-fold higher than Septin6. The interaction profiles of all identified septins

with Septin2 remained consistent during differentiation, with no significant changes observed (Table 3-1). Septin1, 3 and 4, being less abundant, were not identified as Septin2 interactors under tested conditions. Further details regarding additional interactors will be provided in a subsequent chapter 3.4.5.

Table 3-1. Septin2 interactors among septin family members in proliferating and differentiating C2C12 cells.

Gene names	Intensity	Log2 IgG_d0 avg	Log2 S2IP_d0 avg	Log2 IgG_d5 avg	Log2 S2IP_d5 avg	-Log10 p-value S2IP/ IgG d0	Log2 FC difference S2IP/ IgG d0	-Log10 p-value S2IP/ IgG d5	Log2 FC difference S2IP/ IgG d5	-Log10 p-value S2IP d5/ S2IP d0	Log2 FC difference S2IP d5/ S2IP d0
Septin2	1.7E+12	25.54	30.89	28.62	31.28	1.77	**5.35**	2.27	**2.66**	0.72	**0.39**
Septin7	1.5E+12	25.11	31.03	28.42	31.35	1.77	**5.92**	2.49	**2.93**	0.54	**0.33**
Septin9	1.3E+12	23.50	29.14	26.72	29.39	1.73	**5.63**	2.21	**2.66**	0.42	**0.25**
Septin11	9.2E+11	24.13	29.43	26.79	29.89	1.92	**5.30**	2.64	**3.10**	1.17	**0.45**
Septin8	1.6E+11	20.87	27.48	24.55	27.97	1.93	**6.61**	3.08	**3.42**	0.99	**0.49**
Septin5	1.6E+11	19.92	26.75	23.85	27.00	1.77	**6.83**	1.93	**3.15**	0.65	**0.25**
Septin10	7.3E+10	20.72	26.81	24.02	27.43	1.72	**6.09**	2.32	**3.41**	1.15	**0.62**
Septin6	4.E+10	19.80	26.68	23.42	26.34	3.51	**6.89**	3.19	**2.92**	0.38	**-0.34**

This section of the study identifies a possible composition of the core myogenic septin oligomer potentially comprising Septin2-11-7-9 in proliferating myoblasts. It delivers a thorough analysis of septin expression kinetics during *in vitro* differentiation in C2C12 cells, primary myoblasts, and during adult muscle regeneration. Notably, within the core septin subset, a consistent reduction in Septin9 expression during differentiation is discerned across diverse myogenesis models.

3.2. Dynamic organization of Septin9 in proliferating and differentiating myoblasts

Septins primarily function as polymers organized into higher ordered structures (Martins et al., 2022; Spiliotis and Nakos, 2021). We therefore aimed to (i) characterize the arrangement of septin filaments under proliferating conditions and (ii) monitor the changes in septin morphology during myoblast differentiation. Our study is centered on Septin9, guided by the insights from preceding chapters, the availability of specific antibodies, and certain attributes, such as a central position in the protomer (Soroor et al., 2021), the embryonic lethality (Füchtbauer et al., 2011), and unique N-terminal extensions that facilitate interactions with actin and microtubules (Spiliotis and Nakos, 2021).

3.2.1. The reorganization of endogenous Septin9 during differentiation and fusion

We investigated the organization of Septin9 structures in proliferating C2C12 cells using immunofluorescence microscopy. Septin9 filaments were observed in every myoblast in culture (data not shown), its organization showed a pronounced colocalization with actin filaments, strongly decorating the perinuclear area (Fig. 3-7A). Subsequently, we differentiated the cells for four days and compared the morphology of the myotubal cytoskeleton (Fig. 3-7B).

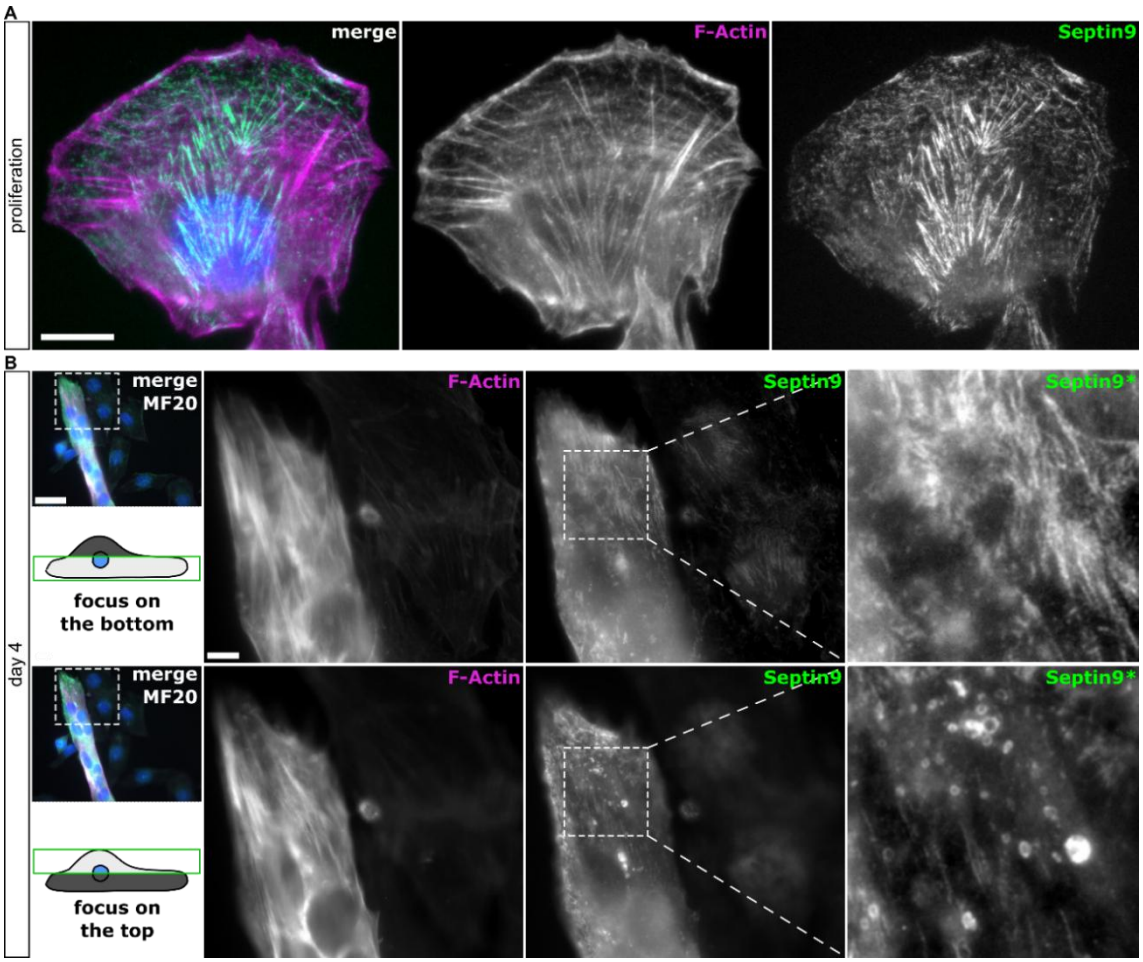

Figure 3-7. Septins reorganize and lose actin-based organization during differentiation in C2C12
A Representative epifluorescence images of proliferating C2C12 cells illustrating substantial colocalization between Actin and Septin9. Septin structures decorated both ventral and transversal actin filaments, as indicated by phalloidin staining. **B** Representative epifluorescence micrographs depicting a myotube after 4 days of differentiation, focusing on either the lower or the upper cellular region. The contrast in the inset was modified (marked as Septin9*). In the ventral part of the cell, Septin9 structures exhibit a relatively independent distribution from actin filaments. Conversely, the upper cellular region mainly displays residual septin filaments, including ring-like structures. Scale bar 10 µm, modified inset 5 µm.

Employing epifluorescence microscopy and focusing on both the basal and apical regions of the myotube, we observed Septin9 structures differentially distributed on a sub-cellular level. Notably, the basal Septin9 structures exhibited a loss of organization, in contrast to the filamentous structures observed in proliferating cells. These structures were composed of short, curvy filaments, occasionally colocalizing with actin structures (Fig. 3-7B, upper panel). Conversely, apical septin structures assumed short rod-like structure, ring form, remnants of collapsed filaments, with apparent random distribution (Fig. 3-7B, lower panel). Collectively, these observations indicate a profound reorganization of septin filaments and their dissociation from actin filaments during myoblast differentiation.

To investigate when the reorganization of Septin9 is happening during early or late differentiation or fusion, we co-stained Septin9 with Myogenin an early myogenic marker after one day of differentiation (Fig. 3-8). Myogenin-negative cells (Fig. 3-8B, inset i) showed no discernible difference in Septin9 organization at day 1 compared to proliferating cells. In these cells Septin9 decorates presumably contractile actin fibers. Most of Myogenin-positive cells (Fig. 3-8B, inset ii-iii) showed similar actin-based Septin9 structures, that resembled those observed in proliferating cells. These structures may appear more discontinuous and patchier, and few septin rings were observed (Fig. 3-8B, inset iii, arrowhead).

Additionally, a subset of Myogenin-positive cells displayed marked reorganization of Septin9 structures into curvy, short rods, seemingly no longer associating with actin filaments (Fig. 3-8B, inset iv). Notably, these cells stained stronger for actin compared to undifferentiated or other Myogenin-positive cells, suggesting a higher degree of differentiation. Aligned and differentiated pre-fusion myoblasts have been demonstrated to stain stronger for actin compared to undifferentiated cells (Swailes et al., 2006). Therefore, this subset of Myogenin-positive cells with the substantial Septin9 reorganization potentially represents more differentiated myoblasts.

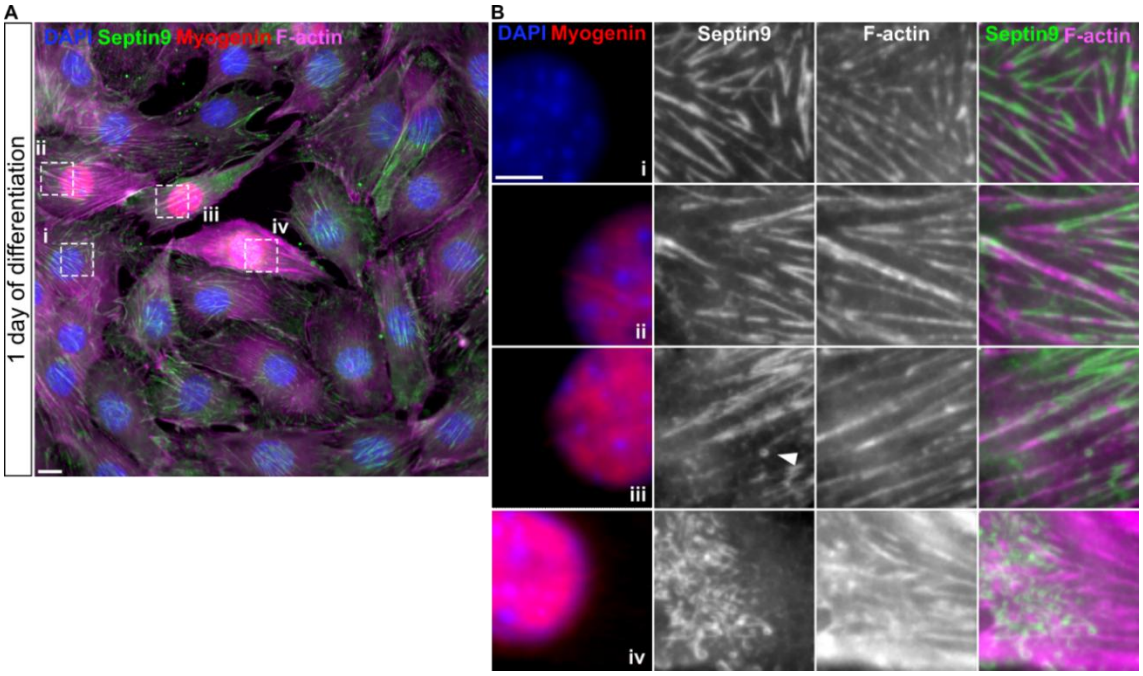

Figure 3-8. Septin9 reorganization is subsequent to Myogenin expression
A Representative epifluorescence micrograph of C2C12 cells differentiated for 1 day. Septin9, Myogenin and F-Actin via phalloidin are visualized. **B** Magnified areas from A depict organization of Septin9 structures in Myogenin-negative (inset i) and Myogenin positive cells (insets ii-iv). White arrowhead shows a septin ring. Scale bar 10 µm, inset 5 µm. Data from (Ugorets et al., 2024).

Furthermore, we investigated the potential displacement of septins from actin filaments by sarcomeric protein α-actinin-2 and its impact on septin reorganization, examining the distribution of α-actinin-2 in both proliferating and differentiating myoblasts (Fig. 3-9). In proliferating cells, α-actinin-2 localizes to focal adhesions and colocalizes with actin filaments, while septins are excluded from these structures (Fig. 3-9A). During myoblast differentiation, there is an upregulation in the expression of sarcomeric α-actinin-2, which progressively decorates actin fibers (Salucci et al., 2015). This increased expression of α-actinin-2 coincides with remarkable reorganization of Septin9 in myoblasts undergoing differentiation (Fig. 3-9B-C). Specifically, we observed long and straight Septin9 filaments found in proliferating myoblasts to undergo a transition into shorter, curved rods, metaphorically “peeling off” of actin structures. This change in morphology suggests a potential detachment and collapse of septin filaments, possibly due to reduced support from actin on a larger scale (Fig. 3-9C). Notably, despite their spatial proximity, α-actinin-2 and Septin9 do not exhibit colocalization in either proliferating or differentiating myoblasts, even though both proteins have the capacity to bind actin.

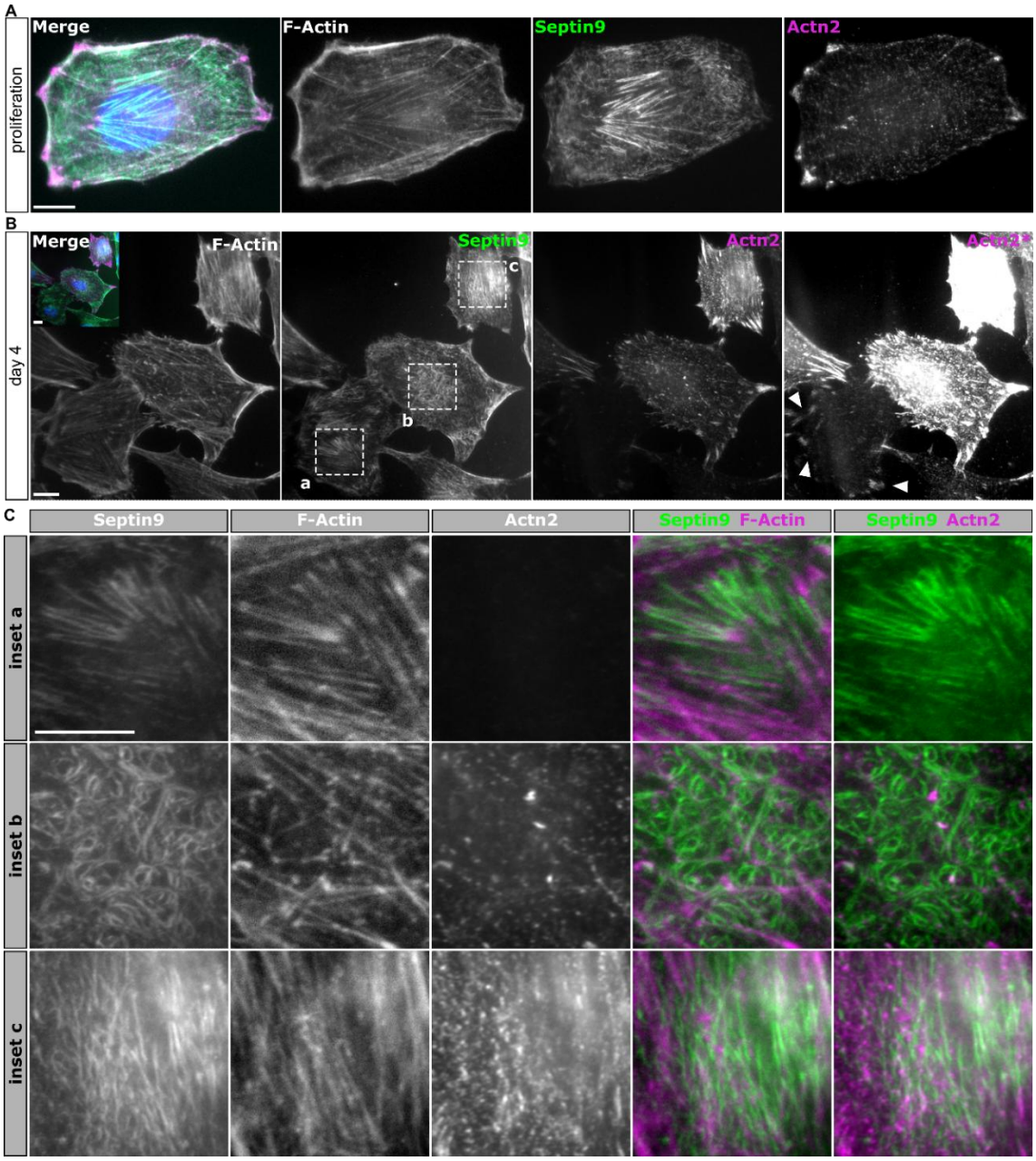

Figure 3-9. Septin9 does not colocalize with α-actinin-2 during in vitro differentiation
A Representative epifluorescence images of proliferating C2C12 cells, visualizing α-actinin-2 (Actn2) in focal adhesions, Septin9 and F-Actin via phalloidin staining. **B** Representative epifluorescence images of mononucleated myoblasts differentiating for 4 days. Undifferentiated myoblasts express low levels of α-actinin-2 localized to focal adhesions (arrow heads). Committed myoblasts increase α-actinin-2 expression in preparation for sarcomere assembly. Septin9 dissociates from actin and does not colocalize with α-actinin-2 during this transition. The contrast in the Actn2 channel was modified (marked as Actn2*) for better visibility of the cell with the low Actn2 level. **C** Magnified insets from (B), emphasizing Septin9 reorganization and the absence of Septin9- α-actinin-2 colocalization in differentiating myoblasts. Scale bar 10 µm.

3.2.2. Generation and validation of the Septin9-GFP C2C12 cell line

To enhance our understanding of Septin9 reorganization during myogenesis and facilitate visualization of this prominent process, we employed a fluorescent labeling strategy by tagging the endogenous Septin9 locus with a C-terminal mEGFP using CRISPR/Cas9- mediated gene editing in C2C12 cells (Fig. 3-10A). This approach results in visualization of all potential splice variants of Septin9, including the short variant c, which is not recognized with available anti-Septin9 antibodies. Multiple clones were generated (not shown) and tested primarily through western blotting following small interfering RNA-mediated *Septin9* depletion (Fig. 3-10B). Detection using anti-GFP antibodies in conjunction with antibodies against endogenous Septin9 revealed at least one long isoform and the short isoform, characterized by the anticipated shift in molecular weight due to the EGFP tag. The right panel of Fig. 3-10B illustrates the endogenous Septin9, a 62 kDa protein migrating at around 70 kDa, and the expected 30 kDa band shift attributed to mEGFP. The left panel indicates the long isoform (~100 kDa) and potentially the short isoform (indicated by black arrowheads), both exhibiting downregulation upon siSeptin9 treatment.

Furthermore, we investigated whether Septin9-GFP is incorporated into endogenous septin structures. We stained for endogenous Septin9, 7, and 2 under proliferating (Fig. 3-10C) and for Septin7 and 2 under differentiating conditions (Fig. 3-10D, Septin2 not shown). Septin9-GFP forms distinctive perinuclear and distal filamentous structures, which may colocalize with ventral and transversal stress fibers, resembling the ones observed in WT cells (actin visualization not included) (Fig. 3-10C). Complete overlap of endogenous Septin9, 7, and 2 signal with Septin9-GFP was observed in the gene-edited cells during proliferation and five-day myogenic differentiation. The observed myogenesis-associated disruption of Septin9 corresponded with analogous alterations in Septin7, likely residing in the same filaments.

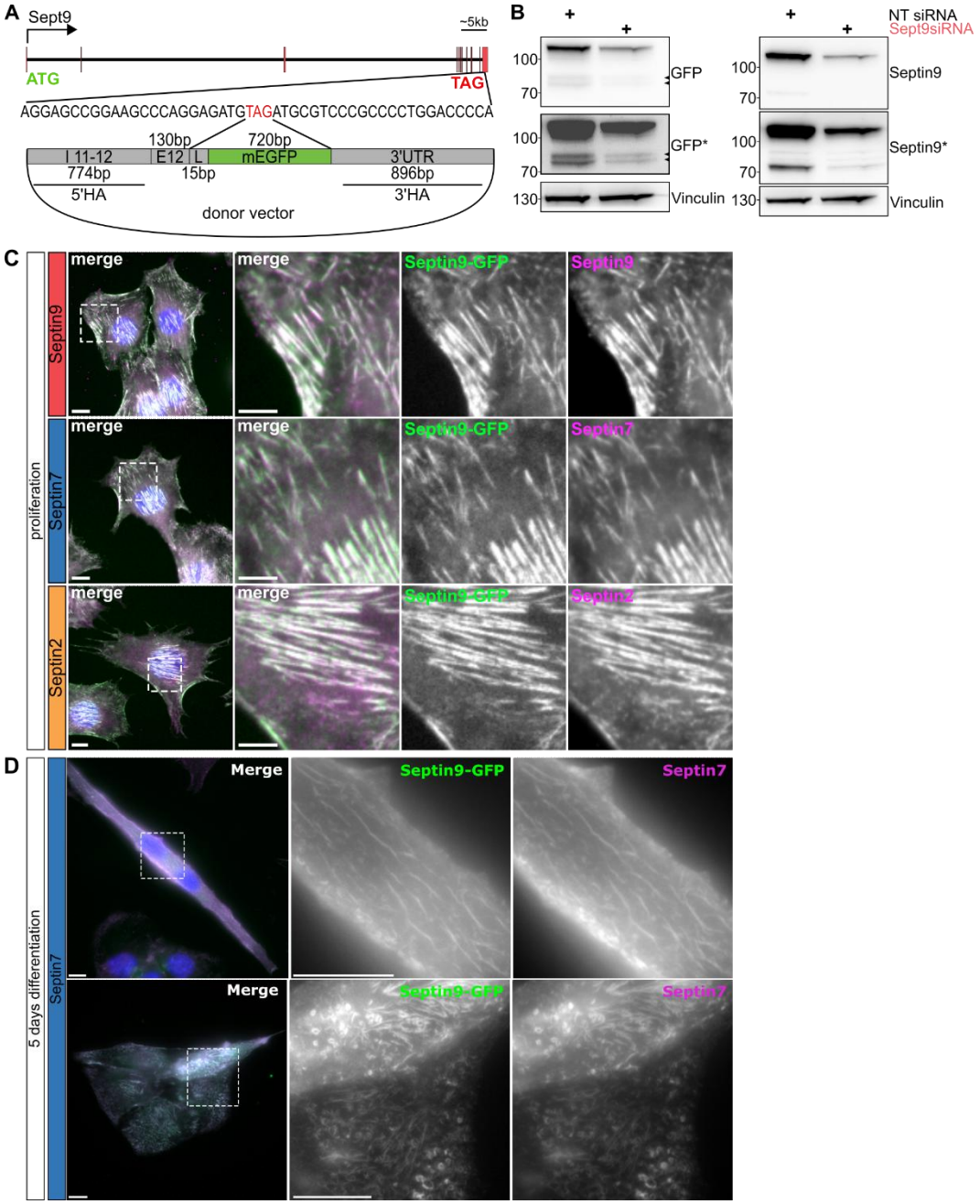

Figure 3-10. Generation and validation of a Septin9-GFP C2C12 cell line

A Schematic representation of the cloning strategy introducing a 15bp linker and an mEGFP sequence in place of the stop codon of *Septin9* in C2C12 cells. The C-terminal strategy targets all Septin9 isoforms. Multiple clones were generated and tested. **B** Clone 32 was transfected with either non-targeting siRNA or Septin9 siRNA, followed by SDS PAGE analysis and western blotting. Antibodies against long endogenous Septin9 isoforms (above 70kDa) and GFP were used to confirm knock-in. The shift of approximately 30kDa is observed with both antibodies. Detection using anti-GFP antibody may reveal expression of short isoforms (black arrowheads). **C** Representative epifluorescent images of proliferating Septin9-GFP C2C12 cells (clone#32). Septin9-GFP is incorporated into endogenous septin structures. **D** Representative epifluorescence images of Septin9-GFP clone#32 after 5 days of myogenic differentiation. Sepin9-GFP shows knock-in GFP signal, Septin9, Septin7 and Septin2 are stained with antibodies. Scale bar 10 µm, insets 5 µm. Modified from (Ugorets et al., 2024).

Septin9 occupies central positions within palindromic septin filaments (Mendonça et al., 2019; Soroor et al., 2021). Therefore, depletion of Septin9 may adversely affect the expression of other septins or organization of septin polymers in the myogenic context, in accordance with the Kinoshita hypothesis of septin paralogue incorporation and availability. To investigate this, we depleted Septin9 in Septin9-GFP cells and visualized other core myogenic septins, Septin2 and 7 (Fig 3-11). The absence of Septin9 is visible as reduced fluorescent signal (Fig 3-11 inset b and c). While the intensity of Septin2 and Septin7 remained relatively unchanged (not quantified), their appearance changed from filamentous towards diffusely cytoplasmic. Furthermore, we tested mRNA expression levels of all septins after 48 hours of Septin9 depletion in proliferating wild type C2C12 cells (n=8) (Fig. 3-11C-D). No septin exhibited significantly altered expression level, while only Septin6 showed approximately 20%, although not significant, upregulation in every experiment (Fig. 3-11D). Taken together, Septin9 enables myoblasts to organize Septin2- or Septin7-containing filaments, visible through conventional light microscope.

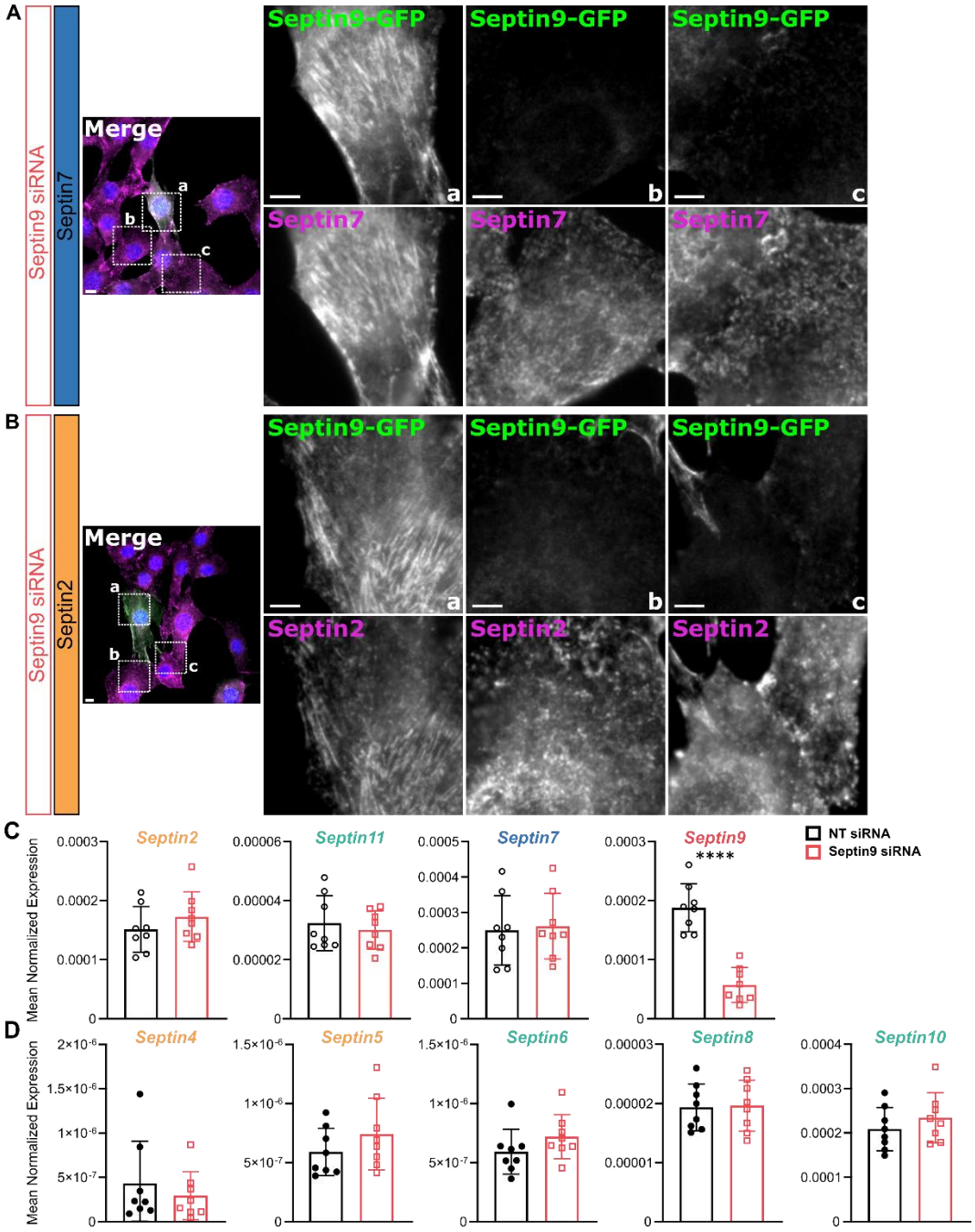

Figure 3-11. Septin9 is essential for macroscopic myoblast septin structures
Expression of Septin9 is crucial for the maintenance of core septin structures in C2C12 cells. Depletion of Septin9 through siRNA results in the breakdown of Septin2 and Septin7 structures revealing their mutual dependence. Septin9-GFP C2C12 cells treated with Septi9 siRNA for 48 hours were fixed under proliferating conditions. Fluorescent micrographs depict co-staining of Septin9-GFP with eighter **A** Septin7 or **B** Septin2 in Septin9-deficient cells. C-D Expression of core (C) and other (D) septin paralogues in WT C2C12 cells 48 hours after siRNA-mediated depletion of Septin9. Data represent mean ± standard deviation (SD), ****p<0.0001 from two-sided unpaired t test. Scale bar 10 µm, insets 5 µm. Modified from (Ugorets et al., 2024).

3.2.3. The reorganization of Septin9-GFP during differentiation and fusion in high resolution

In preparation for live cell microscopy, we subjected the Septin9-GFP cell line to the confocal and STED microscopy, validating the observed endogenous septin reorganization during myogenic differentiation in wild type cells (Fig. 3-12 - Fig. 3-14). First, we compared the colocalization of Septin9-GFP with actin using anti-GFP antibodies and phalloidin staining. In the bottom plane of proliferating myoblasts, the Septin9-GFP organization closely resembled that of the wild type C2C12 cells, with robust perinuclear and ventral septin fibers decorating actin stress fibers (Fig. 3-12A). Notably, the Septin9-GFP signal remained excluded from focal adhesions, indicative of its non-colocalization with focal adhesion markers (Fig. 3-14). Focusing on the prominent septin structures in the mid plane of the myotube, we consistently observed septin rings and few thin filaments that no longer colocalized with actin filaments (Fig. 3-12B).

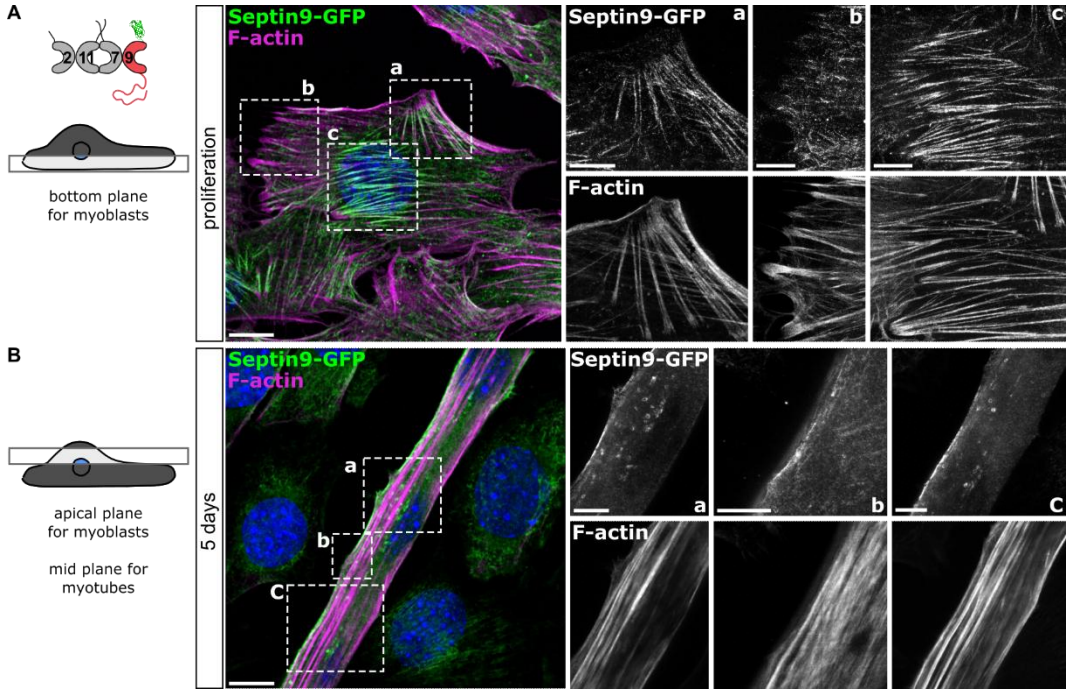

Figure 3-12. Septin9-GFP reorganization resembles the endogenous behavior during in vitro differentiation

A Representative confocal (merge) and STED (insets) images of proliferating Septin9-GFP knock-in cells. Strong colocalization is observed between Septin9-GFP and F-Actin, detected using anti-GFP antibodies and phalloidin. **B** Nascent myotubes reorganize actin cytoskeleton into parallel, bundled filaments, with Septin9-GFP exhibiting strongly reduced colocalization. Multinucleated tubes retain residual Septin9-GFP filaments scattered throughout the cell body. Scale bar 10 µm, insets 5 µm. Data from (Ugorets et al., 2024).

In contrast to flattened myoblasts, myotubes displayed increased size and diameter, accompanied by notable changes in the distribution of Septin9 (Fig. 3-13). Within myotubes, Septin9 appeared to dissociate from actin filaments, forming residual filament structures like spirals, short rods, and rings. These structures were irregularly distributed in regions proximal to the plasma membrane along the myotube (Fig. 3-13). Smaller myotubes lacking ordered sarcomeric actin that organized in thick filaments, showed a higher abundance of Septin9 structures in the basal plane. However, these structures appeared thinner, less organized, and exhibited limited colocalization with actin (Fig. 3-13A). In mature myotubes with sarcomeres, patches of disorganized Septin9 were visible in the basal plane (Fig. 3-13B). The remaining space within the myotubes was primarily occupied by actin-independent rings and membrane-associated patches of Septin9.

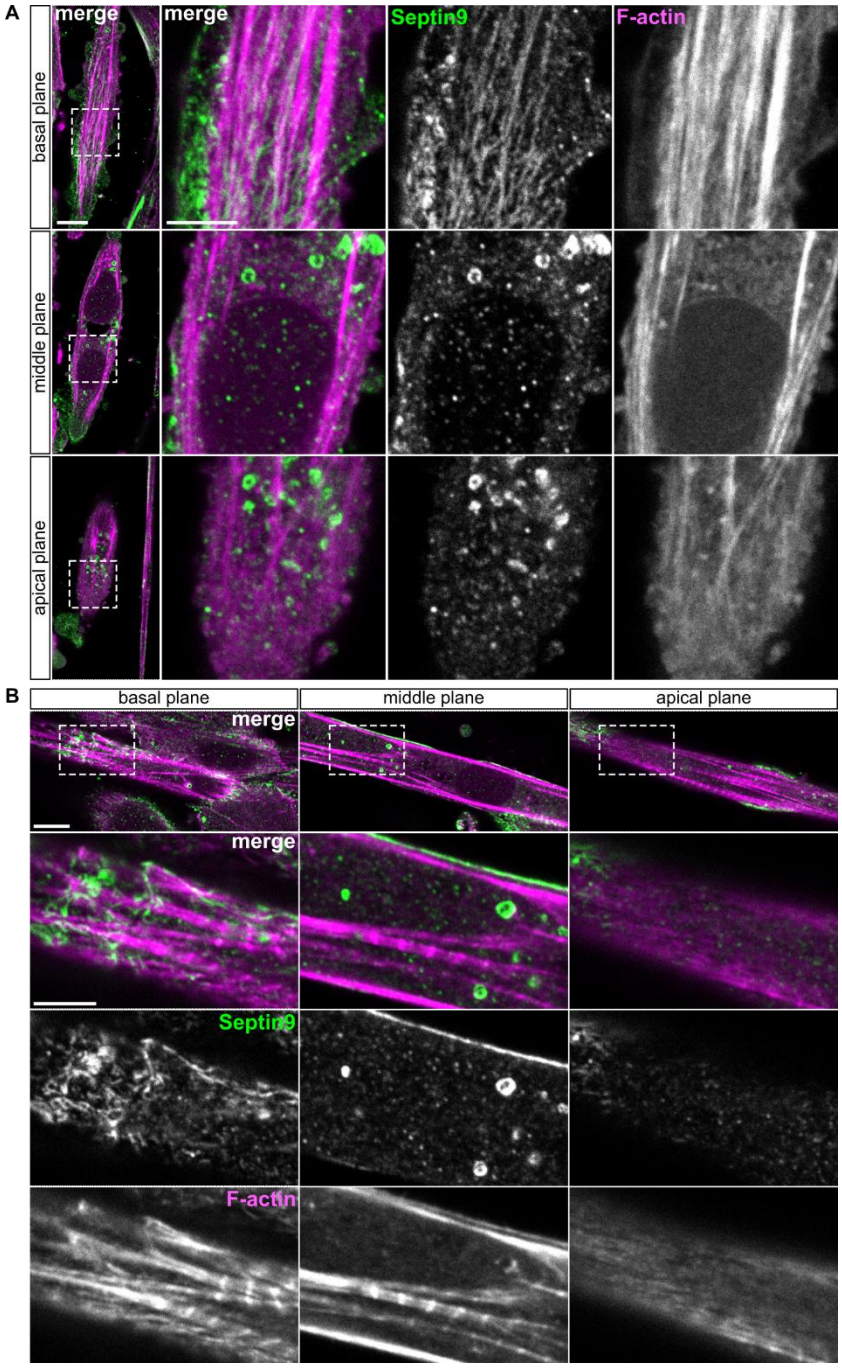

Figure 3-13. Sub-cellular distribution of endogenous Septin9 in a myotube
Sub-cellular distribution of endogenous Septin9 after prolonged differentiation (5 days) in three confocal planes. **A** Representative confocal images of a nascent myotube without sarcomers visible with phalloidin. Planes represent steps of 6µm at the bottom, middle (6µm) and upper (12µm) plane of WT C2C12 cells. **B** Representative confocal images of a mature myotube with apparent sarcomeric structures visualized with phalloidin. The bottom, middle (5µm) and upper (11µm) plane in of WT C2C12 cells. Insets show Septin9 and Actin (phalloidin) organization in the boxed area of the myotube. Scale bar 10 µm, inset 5 µm. Data from (Ugorets et al., 2024).

To confirm the exclusion of Septin9 from focal adhesions, we conducted co-staining with skeletal α-actinin-2 (Fig. 3-14). In proliferating Septin9-GFP cells, a clear spatial separation between actin-based Septin9 and focal adhesion-associated α-actinin-2 was evident (Fig. 3-

14A). Upon focusing on the bottom plane of a nascent myotube, reorganized Septin9 structures and elevated Actinin expression were observed, indicating sarcomeric machinery formation (Fig. 3-14B). Following five days of differentiation in Septin9-GFP cells, a global loss of organized septin structures was apparent (Fig. 3-14C). Septin9 and Actn2, two actin binding proteins, were abundant during nascent myotubular stage, positioned proximal to actin and each other. However, they exhibited no interaction and retained to their mutually exclusive compartments throughout every stage of *in vitro* differentiation (Fig. 3-14).

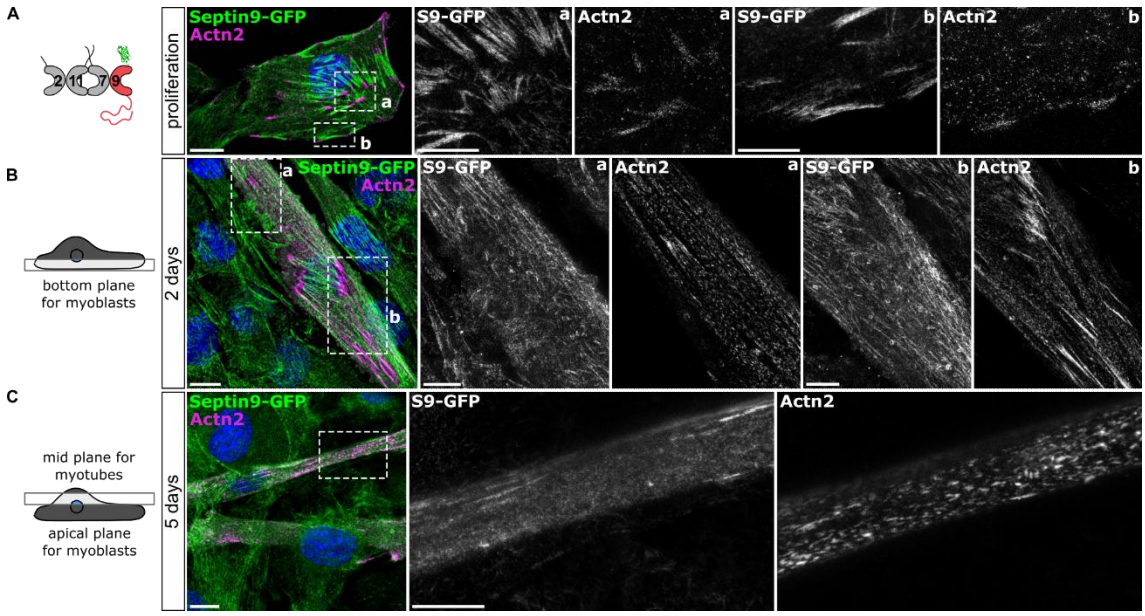

Figure 3-14. High resolution of Septin9-GFP does not show a colocalization with skeletal alpha actinin 2 during myogenic differentiation
A Confocal (merge) and STED (insets) fluorescence micrographs of proliferating Septin9-GFP knock-in myoblasts. Skeletal α-actinin 2 (Actn2) localizes to focal adhesions, while Septin9-GFP is excluded from these structures. **B** Cytoskeletal reorganization in nascent myotube after 2 days of differentiation. Septin9-GFP transitions from long, straight filaments, to short rods and rings, displaying no colocalization with Actn2. **C** In mature myotube, residual Septin9-GFP does not colocalize with Actn2, that resembles primitive sarcomeres. Scale bar 10 µm, insets 5 µm. Data from (Ugorets et al., 2024).

3.2.4. The dynamic reorganization of Septin9-GFP during differentiation and fusion in live cell microscopy

Live cell microscopy was employed in Septin9-GFP C2C12 cells to capture the dynamic changes in septin reorganization during the transition from proliferating myoblasts to differentiated myocytes. Using the TIRF microscopy, we focused on basal septin structures proximal to the plasma membrane during initial steps of differentiation (Fig. 3-15). Cells were differentiated in the incubator for 12 hours, before transferring to the microscope. At the

onset of differentiation (time stamp 0:00), cells displayed linear and straight septin filaments, potentially colocalizing with actin filaments (Fig. 3-15, inset a). Subsequently, at 18 hours of differentiation, septin filament exhibited a shift towards shorter, thinner, and visibly curvier formations, resembling short septin rods previously observed in differentiated cells in fixed samples (Fig. 3-15. Inset b).

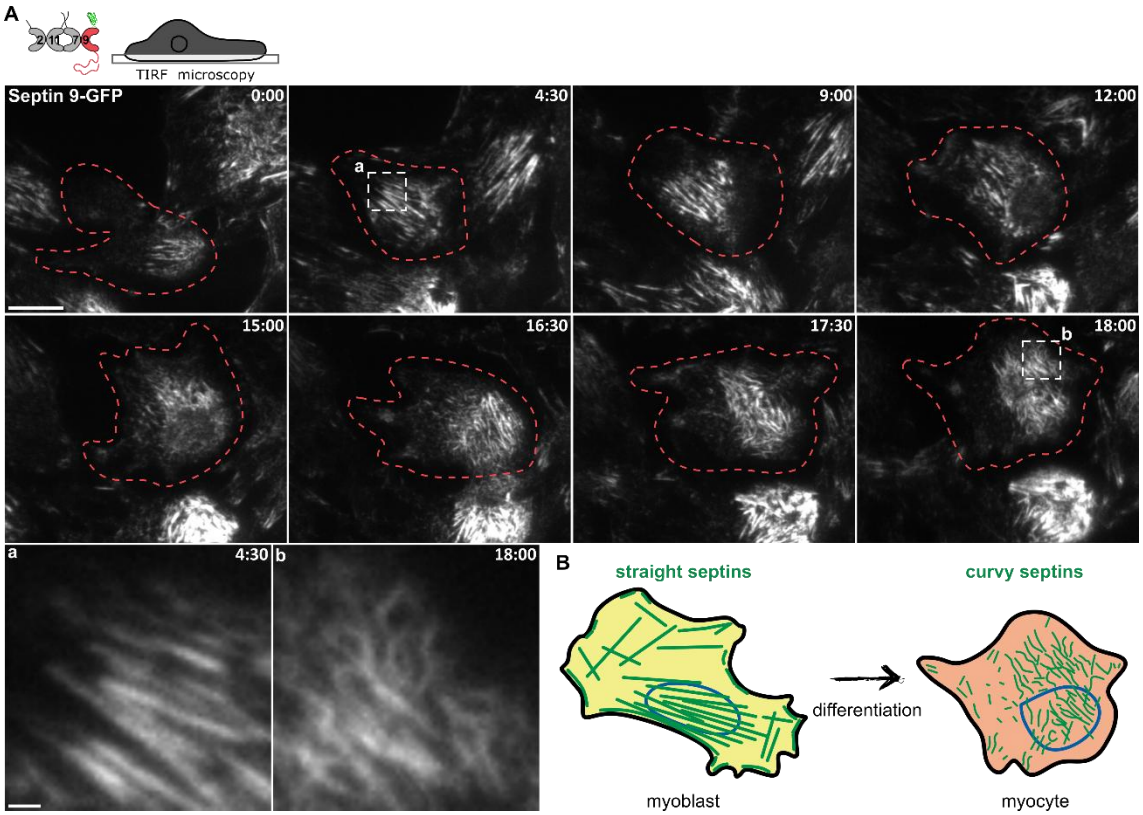

Figure 3-15. Septin9-GFP reorganization during myogenic differentiation
A Live cell TIRF experiment images of differentiating Septin9-GFP myoblasts on Ibidi polymer surface. Imaging began 12 hours after the initiation of myogenic differentiation, with time stamps provided in hours and minutes. Insets highlight changes in septin filament organization. **B** Schematic depiction of myoblast differentiation into myocyte, accompanied by changes in septin morphology. Scale bar 10 µm, insets 1 µm. Modified from (Ugorets et al., 2024).

Differentiated myoblasts exhibit changes in morphology and behavior as they advance towards fusion (Swailes et al., 2004). We extended our TIRF microscopy experiments to 3 days of differentiation prior to imaging, to shed light on septin reorganization around myocyte fusion (Fig. 3-16). The myogenesis onset lacks synchronization in cell culture, allowing examination of both differentiated and undifferentiated mononucleated cells. While most cells exhibit short and straight septin filaments (Fig. 3-16, inset iii), still distinct from proliferating myoblasts (Fig. 3-12A), a central representative myocyte demonstrated septin

structures reminiscent of differentiated cells, with short and curvy filaments near the nucleus (Fig. 3-16, inset ii) and remnants of filaments in proximal regions (Fig. 3-16, inset i).

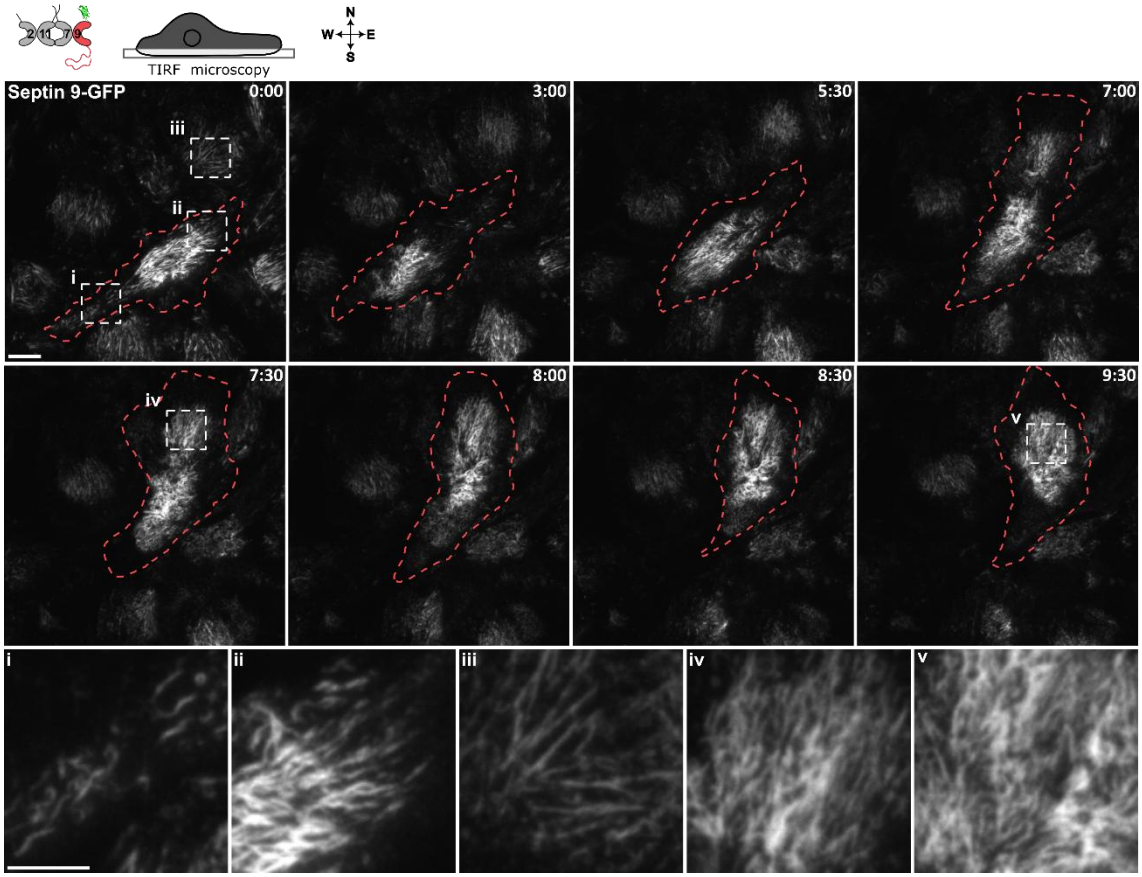

Figure 3-16. Reorganization of ventral Septin9-GFP filaments during myocyte fusion
Representative images from live cell TIRF experiment featuring differentiating Septin9-GFP C2C12 cells on Ibidi polymer surface. Imaging began72 hours after the initiation of myogenic differentiation, with time stamps indicated in hours and minutes. Insets (i-v) highlight changes in septin filament morphology. Scale bar 10 µm, inset 5 µm.

During the initial 6-hour period of image acquisition, the highly dynamic myocyte undergoes a notable change in direction of migration, transitioning from North- East to South- West and back to North- East, concomitant with rearrangements in septin filaments. (Fig. 3-16 0:00, 3:00 and 5:30 hours). The myocyte engages in fusion with a neighboring cell after approximately 7 hours (Fig. 3-16 inset iii and iv). TIRF microscopy limitations hinder clear visualization of cellular outlines, nuclei, and membrane fusion. Therefore, after the presumed fusion event at 7,5 hours, the emerging myotube appears to mix and integrate the short, curly and dynamic septin filaments (Fig. 3-16). Following fusion, the nascent myotube displays reduced mobility and Septin9 reorganization, as frequently observed in long-imaged myoblasts that anticipate cellular demise. Unfortunately, the acquisition ends around 6 hours later, possibly due to myotube detachment or apoptosis (frames not depicted).

Finally, using confocal microscopy, we tracked basal and apical septin reorganization in Septin9-GFP C2C12 cells during myocyte fusion and nascent myotube formation. After initial 48 hours of differentiation in the incubator (time stamp 0:00, t= 0), we observed successful fusion events during 16 hours of imaging (Fig. 3-17). At fusion onset, the invading and receiving cell exhibited distinct ventral septin organization (Fig. 3-17A). The invading cell lacked higher- ordered septin structures, extending Septin9-free lamellipodia towards the receiving cell. The receiving cells had only short and curvy perinuclear Septin9 filaments (Fig. 3-17 0:00; 1:00, 3:00 hours and inset i). Upon fusion, membranes merged, and the invading cell developed short, curvy septin filaments (Fig. 3-17 4:00 and inset ii). Short perinuclear Septin9 rods from two different cells converged, potentially alongside nucleus movement, resulting in filament mixing (Fig. 3-17 5:00, 7:30 and inset iii). Next, the nascent myotube prepared for more fusion events, while Septin9 appeared to form long, straight filaments alongside to the previously described short rods and rings (Fig. 3-17 10:00 and inset iv). A new cycle of fusion reproduced Septin9 reorganization, cellular content mixing and septin structure retraction from the cell periphery as described in earlier (Fig. 3-17 12:00, 14:00, 15:30 and inset v). Dynamic Septin9 organization follows the fusion site of the myotube, while the myotube's distal site contained only septin rings and filament remnants (Fig. 3-17 5:00-15:30 and inset vi).

Taken together, we utilized a range of microscopy techniques to investigate the dynamic reorganization of Septin9 during myogenic differentiation in C2C12 cells, uncovering a transition from long filaments to shorter, curved rods, detached from actin stress fibers. Live cell imaging of Septin9-GFP highlighted its dynamic rearrangement during myoblast differentiation and fusion, offering insights into its potential role in regulating myogenic differentiation and fusion processes.

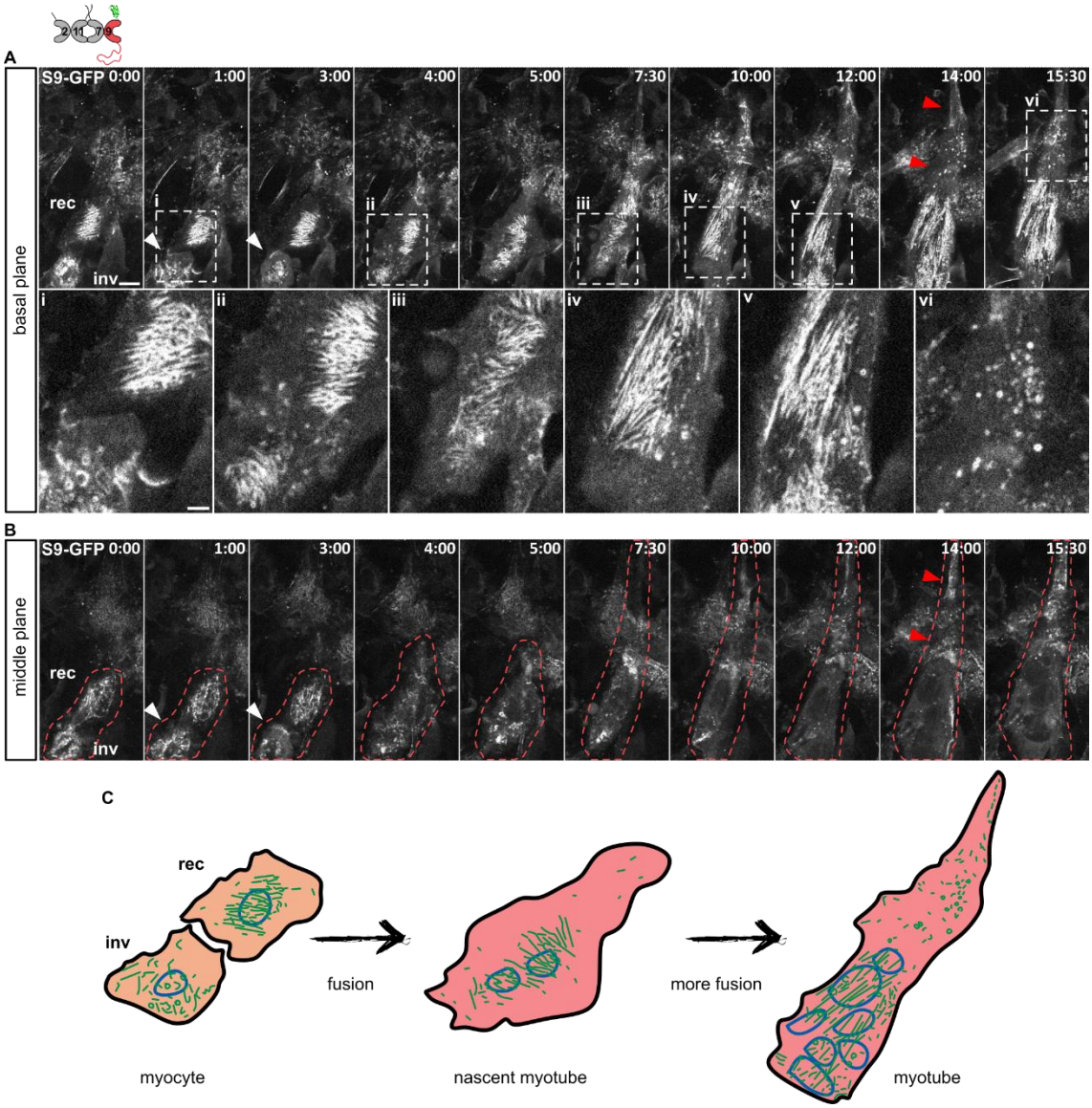

Figure 3-17. Septin9-GFP reorganization during myocyte fusion
Representative confocal images from a live cell experiment depicting the **A** basal and **B** 0.5µm higher apical plane of fusing Septin9-GFP myocytes on an Ibidi polymer surface. Acquisition started 72 hours after the onset of myogenic differentiation (time stamp in hours and minutes), Zoom-in insets i-vi from panel A highlight specific details. **C** Schematic depiction of a fusion event between to myocytes and the subsequent maturation of the nascent myotube, accompanied by changes in septin morphology. Scale bar 10 µm, inset 5 µm. Rec- receiving cells, inv- invading cell. Modified from (Ugorets et al., 2024).

3.2.5. The reorganization of plasma membrane in Septin9-GFP myoblasts during fusion in live cell microscopy

Cytoskeletal reorganization during later stages of myogenic differentiation coordinates architectural rearrangement in cells, membrane dynamics and formation of functional myotubes through fusion (Pajcini et al., 2008). Integral to the process of mammalian fusion

is the participation of conventional blebs and smaller bubbling blebs, representing distinct forms of membrane protrusions (Lian et al., 2020). We traced fusing Septin9-GFP cells after 3 days of differentiation, focused on the membrane dynamics and investigated septin reorganization using holotomographic imaging (Fig. 3-18). Notably, during the fusion process, committed progenitor cells exhibited the presence of large blebs and smaller bubbling membrane blebs throughout majority of the fusion event (Fig. 3-18A, lower panels). Following the fusion, the cells exhibited reduced active blebbing, which could potentially signify readiness for subsequent fusion event (Fig. 3-18B, insets vii-viii). As observed using other microscopy methods, Septin9 morphology is changed in myoblasts cultured under differentiation permissive conditions. Committed progenitors displayed a reorganization of Septin9, leading to formation of domains with either shorter, curvier structures or remnants and rings (Fig. 3-18A-B, insets i-iii). Myoblasts undergoing fusion displayed a near absence of long, straight septin filaments. Septin9 appeared to co-localize with vacuoles, generated during membrane blebbing, suggesting potential participation in the process (Fig. 3-18B, insets v-vi). Despite limitations in resolution, Septin9-rich domains were observed at the interface between fusing cells, implying septin involvement (Fig. 3-18A 8:40, arrowhead). Notably, we captured only one fusion event through holotomography, requiring caution during interpretation.

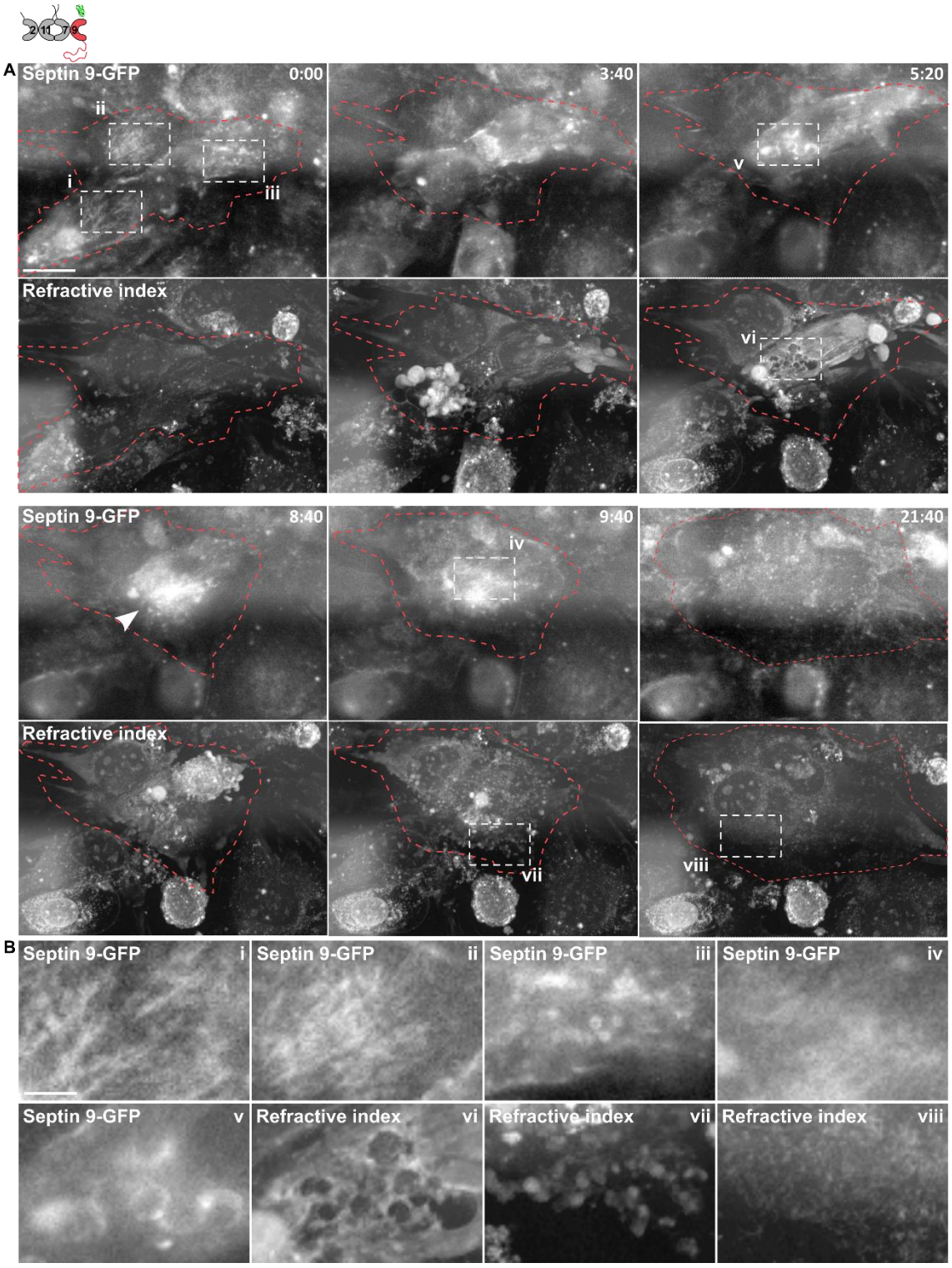

Figure 3-18. Membrane dynamics during myoblast fusion
Holotomography images acquired with the 3D Cell Explorer (Nanolive) depicting Septin9-GFP myoblasts after 3 days of myogenesis. Imaging was performed every 20 minutes over a 24-hour period, maintained under humidified conditions at 37°C with 5% CO2 on an Ibidi polymer surface. **A** Representative images from a live cell experiment showing the reorganization of Septin9-GFP and the pronounced membrane dynamics observed during myoblast fusion event. **B** Magnifications from boxed areas in panel (A). Scale bar 10 µl, insets 2 µm. n=1.

3.3. Expression and localization of Septin9 in adult mouse muscle

The expression pattern and spatial organization of septins in adult muscle tissue remains largely unknown (Gönczi et al., 2021). During the preparation of this manuscript (Ugorets et al., 2024) first a study was published, reporting the crucial role of Septin7 for skeletal muscle architecture and function. Additionally, Gönczi et al. has shown the expression of most septin paralogues in adult skeletal muscle (Gönczi et al., 2022). Therefore, we characterized the subcellular localization of Septin9 within adult muscle tissue. We immunostained for skeletal α-actinin-2 (Actn2) and slow-twitching Myh7 in sagittal sections of TA muscle, revealing sarcomeric organization of the contractile machinery (Fig. 3-19). Actn2 marks the Z-line, a structural component within the sarcomere, while Myh7 labels the contractile M-line. Upon examination, Septin9 co-localized with α-actinin-2 fraction (Fig. 3-19A-B) and is distinctly segregated from the contractile compartment, as evident through its lack of overlap with Myh7 (Fig. 3-19C-D). A closer look at the Z-line organization shows no colocalization between Septin9 and α-actinin-2. Actn2 is a marker of the T-tubule, a plasma membrane invagination into the Z-line, that is surrounded by terminal cisternae of the sarcoplasmic reticulum (Al-Qusairi and Laporte, 2011; Kawaguchi and Fujita, 2024). Septin9 appeared to flank the Actinin2 from two sides, resembling a pattern characteristic to the sarcoplasmic reticulum at the Z-line. (Fig. 3-19A, inset i). This distinctive organization is further supported by a linescan analysis performed across multiple sarcomeres, which revealed the presence of two intensity peaks corresponding to the Septin9 signal surrounding a single α-actinin-2 peak (Fig. 3-19B).

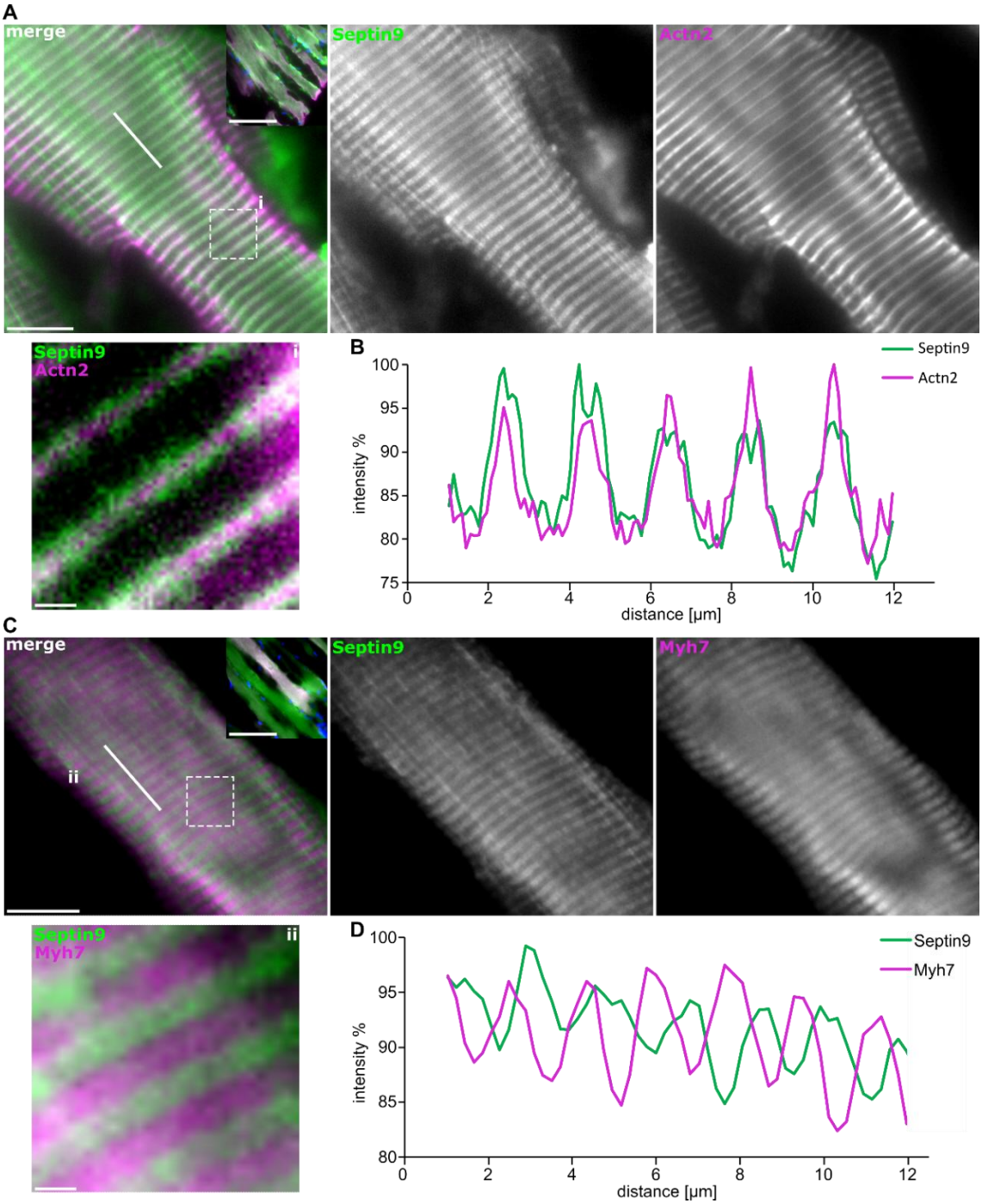

Figure 3-19. Septin9 localization in adult mouse muscle

Longitudinal sections of the Tibialis anterior (TA) muscle from 3-month-old mice. **A** Immunofluorescence staining illustrating Septin9 and Actinin2 distribution, with DAPI staining for nuclei (in the big image). Inset i shows a magnified view with modified brightness and contrast. **B** Linescan analysis of Septin9 and Actn2 signals from panel (A). **C** Immunofluorescence staining depicting Septin9 and slow twitching Myosin heavy chain 7 (Myh7), with DAPI-labeled nuclei (in the big image). **D** Linescan analysis of Septin9 and Myh7 signals from panel C. Scale bar 100 µm, central insets 10 µm, smallest insets i and ii 1 µm.

3.4. Altered dynamics of myogenic differentiation in response to Septin9 knockdown

Building upon the dynamic adaptation of septin cytoskeleton during *in vitro* differentiation, we sought to test the interrelation between these changes and the myogenic process by addressing the impact of Septin9 knockdown and therefore its causative or "bystander" nature. We depleted Septin9 using mRNA interference and documented changes in myoblast proliferation, survival, differentiation, and fusion.

3.4.1. Transcriptional landscape upon Septin9 knockdown in myoblasts

Septin9 plays a pivotal role in determining the subcellular localization of the septin cytoskeleton and in governing cytoarchitecture regulation (Kuzmić et al., 2022; Martins et al., 2022). This prompted us to investigate whether downregulation of Septin9 merely removes a vestigial cytoskeletal component rendered dispensable during late myogenesis or serves a potentially instructive purpose regulating the progression through myogenesis. To address this, we effectively depleted *Septin9* using siRNA approach (Fig. 3-20A, lack of septin structures upon Septin9 depletion as visualized in Fig. 3-11). We then performed transcriptomic analysis of Septin9-depleted differentiating C2C12 cells (after 12h of differentiation, detailed in Fig. 3-21) and proliferating primary myoblasts (detailed in Fig. 3-22). Both data sets had a high overlap in expressed genes (Fig. 3-20B). To gain further insights, we compared the expression profiles of Septin9-deficient C2C12 cells and primary myoblasts with those of proliferating and committed muscle stem cells (MuSCs), as defined through correlation with an external single-cell RNA-sequencing dataset (top 25 genes for each cluster (De Micheli et al., 2020)) (Fig. 3-20C). Both Septin9-deficient C2C12 cells and primary myoblasts exhibited a shared upregulation of genes associated with the "committed progenitors" cluster (such as *Myog* and *Cdkn1c* (p57)), coupled with a modest downregulation of genes linked to "cycling progenitors" cluster (such as *Cdk1* and *Ccnb2*). This intriguing pattern suggests a precocious transition of the Septin9-deficient cycling progenitor population towards the state of committed progenitors.

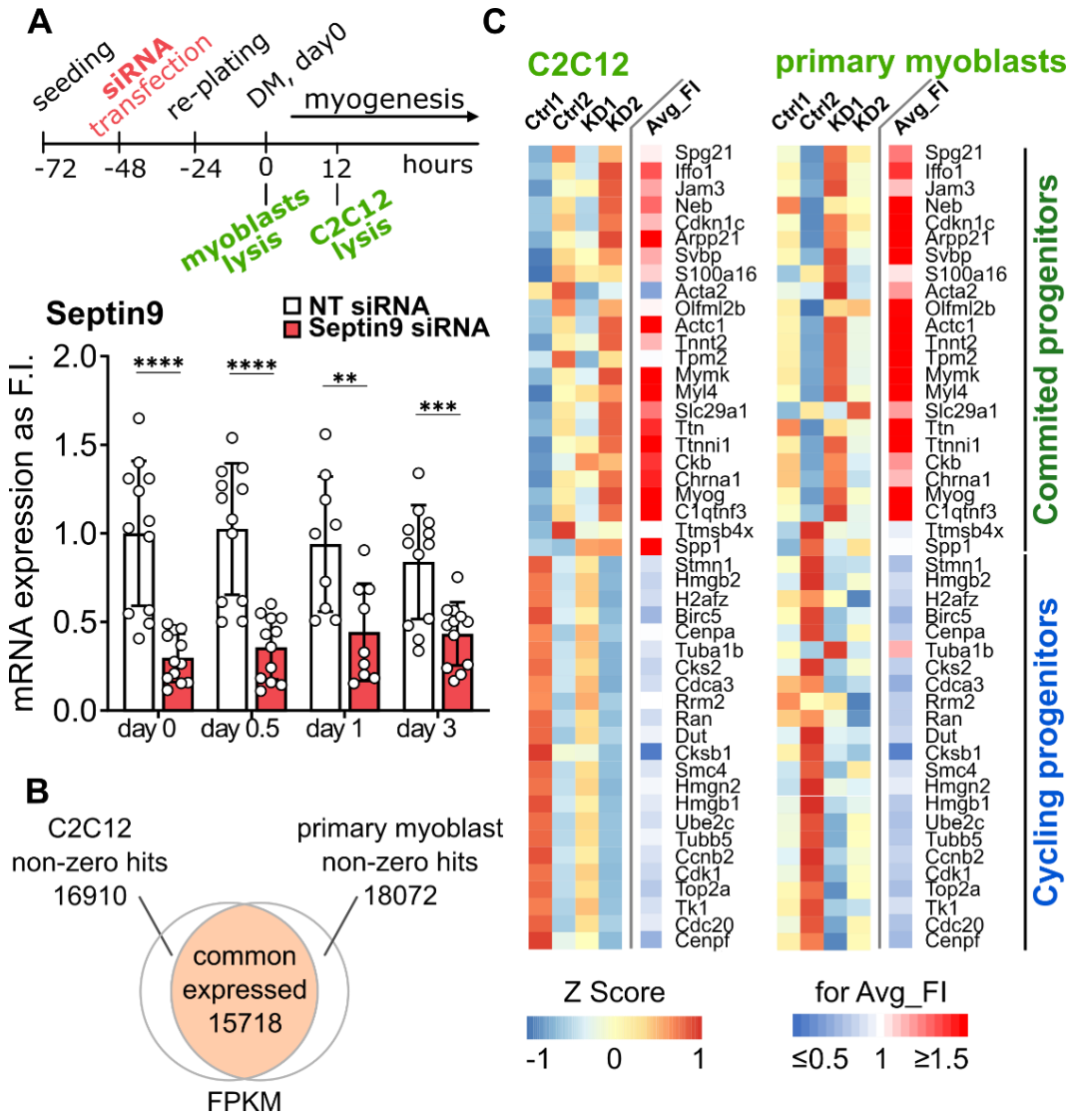

Figure 3-20. Septin9 depletion induces transition from cycling towards committed progenitors
A Experimental design overview. Total RNA was extracted from proliferating myoblasts 48 hours post-Septin9 knockdown and from differentiating C2C12 cells (12 hours into differentiation, 60 hours post-knockdown). Validation of Septin9 knockdown efficiency over 3 days of differentiation by qRT-PCR in C2C12 cells. **B** Venn diagram comparing expressed genes in C2C12 and primary myoblasts. **C** Heat map depicting 47 genes in C2C12 (left panel) and in primary myoblasts (right panel) grouped into 'cycling progenitors' and 'committed progenitors' clusters based on annotation adapted from (De Micheli et al., 2020) (except Gm7325, 2810417h13rik, 2700094k13rik not expressed in C2C12 and in primary myoblasts and excluded from the heatmap). Septin9 depletion leads to accelerated switch towards the committed myogenic progenitor state, evident by overall upregulation of genes in the "committed progenitors" cluster and slight downregulation of genes in the "cycling progenitors" cluster. Avg_FI represents average between two experiments measuring KD to Ctrl ratio. Data represent mean ± standard deviation (SD), *p<0.05, **p<0.01, ***p<0.001, ****p<0.0001 from two-sided unpaired t test.

Next, we investigated the early myogenic potential influenced by Septin9 knockdown through total transcriptome analysis in C2C12 cells (Fig. 3-21). Following a 48-hour knockdown, differentiation was induced for 12 hours, and total RNA was collected and subjected to a transcriptomic analysis. (Fig. 3-21A). Differential expression analysis (DESeq2) revealed 201 differentially expressed genes (DEGs) in C2C12 cells (65 up- and 136 downregulated) (Fig. 3-21B). Gene ontology (GO) annotation analysis of DEGs in Septin9-deficient C2C12 cells revealed association of upregulated genes with the terms 'Myod1 targets', 'hallmark myogenesis', 'positive regulation of skeletal muscle tissue development', 'positive regulation of myoblast differentiation', and 'E box binding' (Fig. 3-21D). Downregulated DEGs are associated with reduced cellular response to certain stimuli (TGFβ, TNFα, mTORC1), 'cell cycle regulation (G2M transition, mitotic spindle)', 'cholesterol homeostasis' and 'reduced cell adhesion (cadherin binding, adherens junction assembly)' (Fig. 3-21D). Taken together, depletion of Septin9 in C2C12 cells via siRNA leads to changes in gene expression that are reflect accelerated progression through myogenic differentiation or a premature onset thereof.

To test the potential of Septin9 depletion to induce changes resembling the initiation of differentiation in proliferating cells, we conducted a total transcriptome analysis on primary myoblast following 48 hours of robust Septin9 knockdown under proliferating conditions (Fig. 3-22A). The DESeq2 analysis revealed a total of 213 DEGs, comprising 168 up- and 45 downregulated genes (Fig. 3-22B-C). GO annotation analysis revealed association of upregulated genes with the terms 'Myod1 targets', 'hallmark myogenesis', 'muscle contraction', 'acto-myosin filament sliding', 'sarcomere organization', 'positive regulation of skeletal muscle tissue development' and 'positive regulation of myoblast differentiation'. The downregulated DEGs are annotated as Fos, Myc and PPARg targets. Downregulated genes further associated with EMT, reduced cellular response to certain stimuli (TGFβ, TNFα) and exit from the cell cycle (G2M transition) (Fig. 3-22D). Notably, the transcriptional changes observed in proliferating myoblasts lacking Septin9 generally resembled those occurring during the initial stages of myogenic differentiation in Setpin9-deficient C2C12 cells.

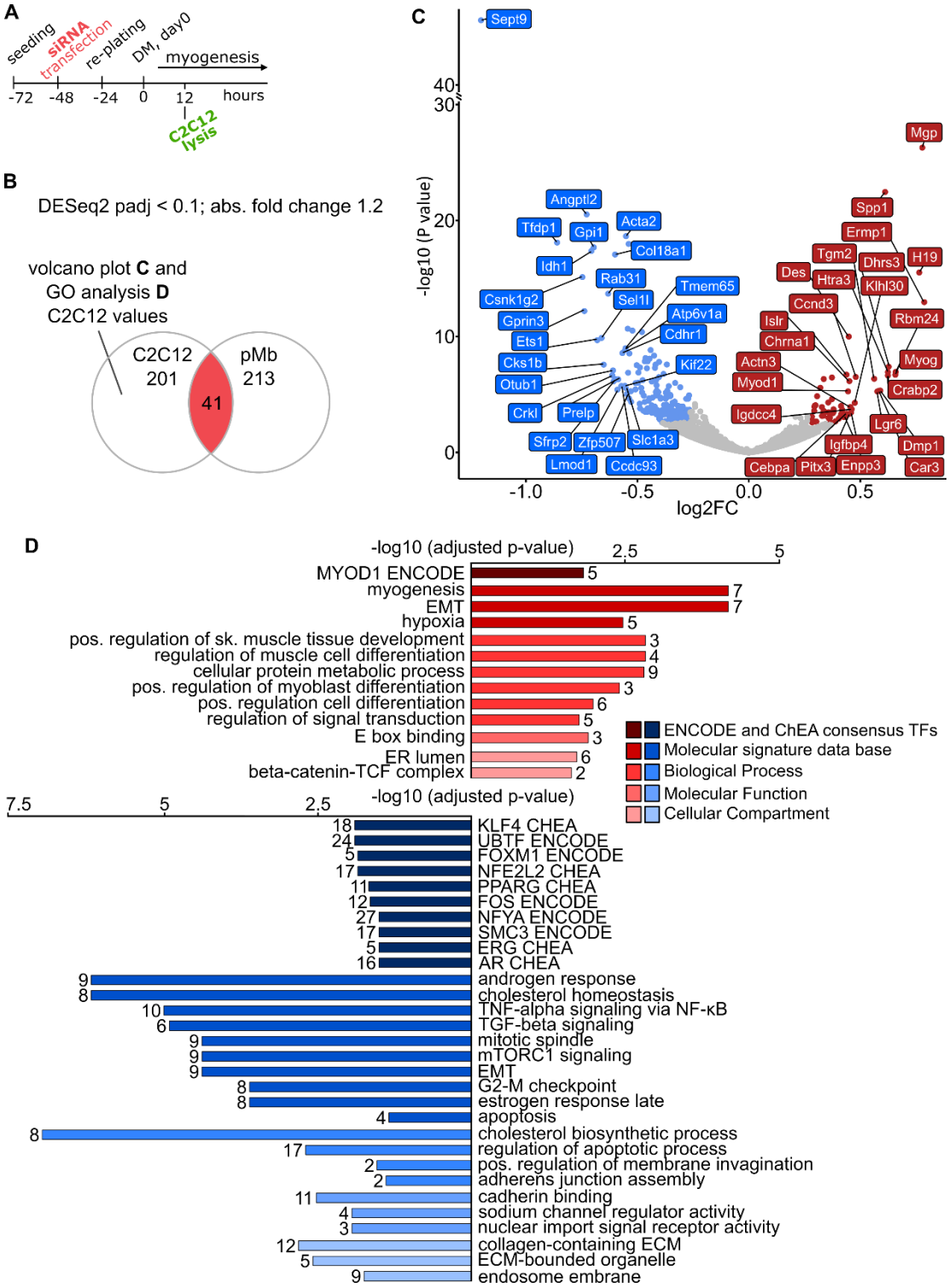

Figure 3-21. Septin9 depletion accelerates myogenic differentiation in C2C12 cells

A Schematic representation of the experimental setup. Total RNA was isolated from C2C12 cells 60 hours after Septin9 knockdown and 12 hours of myogenic differentiation. **B** Venn diagram depicting DEGs calculated using DESeq2 algorithm (adjusted p value < 0.1; -0,322 ≤ log2FC ≤ 0,263). **C** Volcano plot of DE genes (adjusted p value <0.1; -0,322 ≤ log2FC ≤ 0,263) of C2C12 cells transfected with either non-targeting siRNA (control) or Septin9 siRNA after 12 hours of myogenic differentiation, 50 most regulated DEGs are highlighted. **D** GO enrichment analysis of genes upregulated (red) or downregulated (blue) in Septin9-deficient C2C12 cells.

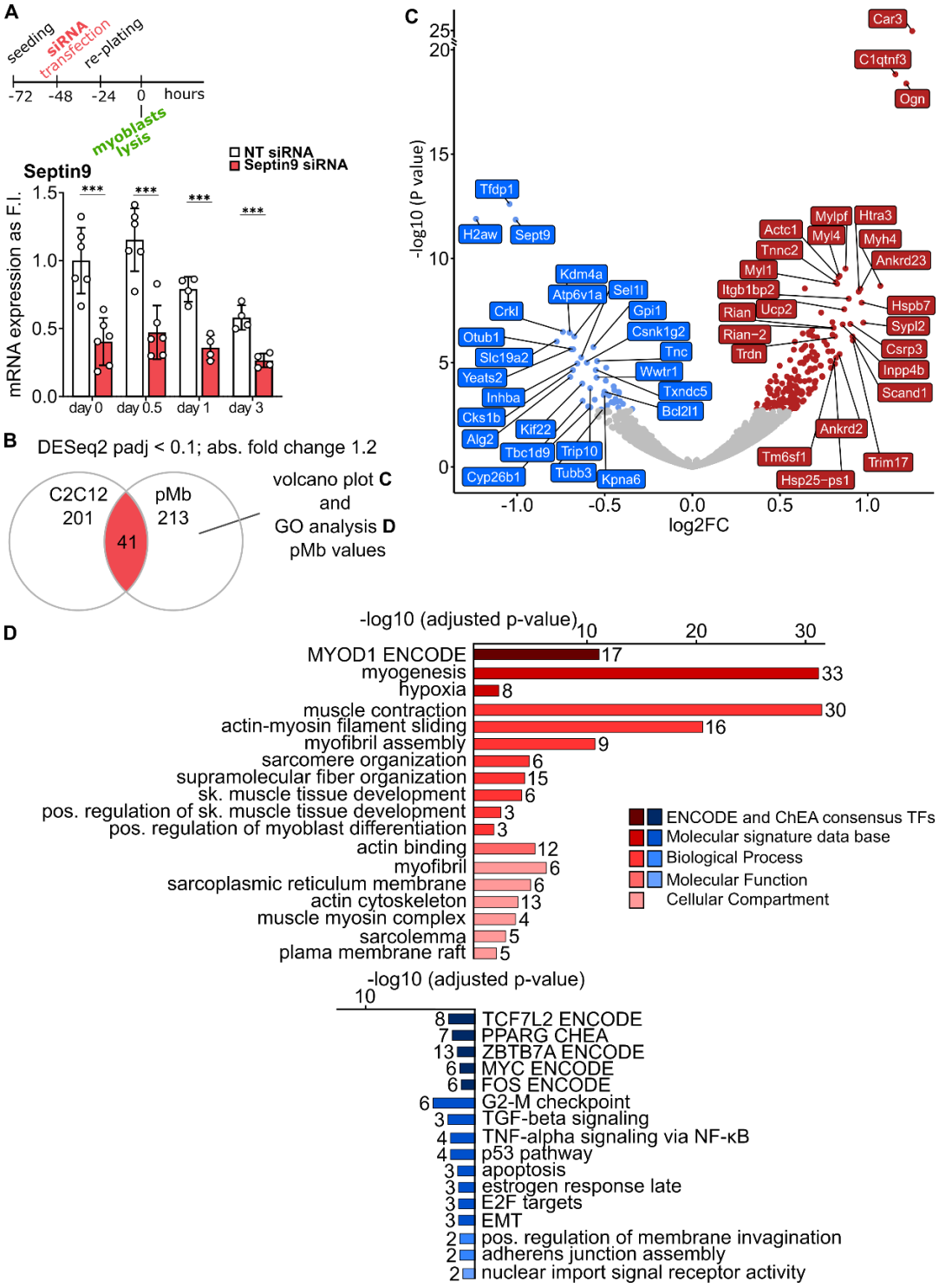

Figure 3-22. Septin9 depletion accelerates myogenic differentiation in proliferating primary myoblasts

A Schematic representation of the experimental setup. Total RNA was isolated from proliferating myoblasts 48 hours after Septin9 knockdown. Septin9 knockdown efficiency validation over 3 days of differentiation by qRT-PCR in primary myoblasts. **B** Venn diagram comparing DEGs calculated using DESeq2 algorithm (adjusted p value < 0.1; -0,322 ≤ log2FC ≤ 0,263). **C** Volcano plot of DE genes (adjusted p value <0.1; -0,322 ≤ log2FC ≤ 0,263) in primary myoblasts transfected with either non-targeting siRNA (control) or Septin9 siRNA, 50 most regulated DEGs are highlighted. **D** GO enrichment analysis of genes upregulated (red) or downregulated (blue) in Septin9-deficient myoblasts. Data represent mean ± standard deviation (SD), *p<0.05, **p<0.01, ***p<0.001, from two-sided unpaired t test.

In addition, we scrutinized the pool of differentially expressed genes that were shared and consistently up- or downregulated in Septin9-deficient C2C12 and primary myoblasts (Fig. 3-23). We employed two distinct analysis methods, each yielding a specific subset of DEGs, characterized mainly by differences in stringency thresholds. The first set comprised 41 DEG identified through the DESeq2 algorithm, with padj < 0.1 and fold induction of 1.2 (Fig. 3-23B). Conversely, the second set consisted of 164 genes manually derived from TPM values, utilizing a fold induction threshold of 1.5 (Fig. 3-23C). Furthermore, we segregated the DEGs into distinct categories: one comprised of genes uniquely influenced by Septin9-depletion, and another comprising robustly regulated myogenic genes as defined in a comparative study involving nine RNA sequencing datasets by Zhang *et al* (Zhang et al., 2022). This meta study encompassed both cycling and differentiating C2C12 cells and spanned a minimum differentiation period of two days. We emphasize the DEGs absent from the cohort of 'robust myogenic genes', designating them as 'not robust genes', thereby potentially signifying their specificity in response to Septin9 depletion.

Upon examination of the 41 DEG from DESeq2 analysis, it becomes evident that most of the upregulated genes belong to the category of 'robust myogenic genes', with a subset belonging to the 'hallmark myogenesis' GO term (marked red). Notable representatives of this group include *Myog*, *Actn3*, *Des* and *Cdkn1a (p21)*, collectively suggesting an overall elevation in myogenic differentiation (Fig. 3-23B). Among the 'not robust' upregulated genes we found (i) Carbonic anhydrase 3 (*Car3*), an intracellular pH regulator and an early myogenesis marker (Feng and Jin, 2016) and (ii) Matrix GLA protein (*Mgp*) an ECM protein inhibiting myostatin receptor binding (Ahmad et al., 2017). In contrast, most downregulated genes do not belong to 'robust myogenic targets' and comprise a heterogenous selection of genes. The cohort of downregulated genes comprises (i) *Kpna6* and *Kpnb1* a dimerizing nuclear import karyopherin pair, (ii) actin binding proteins Destrin (*Dstn*) and (*Amotl2*), (iii) myogenic lysin demethylase 4a (*Kdm4a*), (iv) SH2/SH3 containing adapter *Crkl*, involved in growth factor signaling (v) the soluble TGFβ ligand Activin A (*Inhba*), (vi) transcription factors DP1 (*Tfdp1*) and Taz (*Wwtr1*) and (vii) beta-catenin (*Ctnnb1*) among others. In sum, an examination of the stringent DESeq2 analysis points towards an accelerated myogenic process in cells lacking Septin9.

The second gene set derives from the TPM values and lacks thorough statistical cutoff applied by DESeq2 algorithm This leads to the identification of a larger pool of deregulated genes

encompassing 164 genes. We have composed a heat map out of these DEGs, shared between C2C12 and primary myoblasts lacking Septin9 (Fig. 3-23C). A set of 80 'robust myogenic DEGs' is excluded from the heat map and is detailed in the Table 3-2. This table highlights genes (marked in red) which are associated with the 'hallmark myogenesis' GO term. Notably, only three 'robust' downregulated genes such as WNT10b, Slc26a10, Prr5l, displayed an inverse regulation pattern upon Septin9 depletion. Together, these 'robust' upregulated myogenic markers further support the propensity towards premature myogenic progression in absence of Septin9.

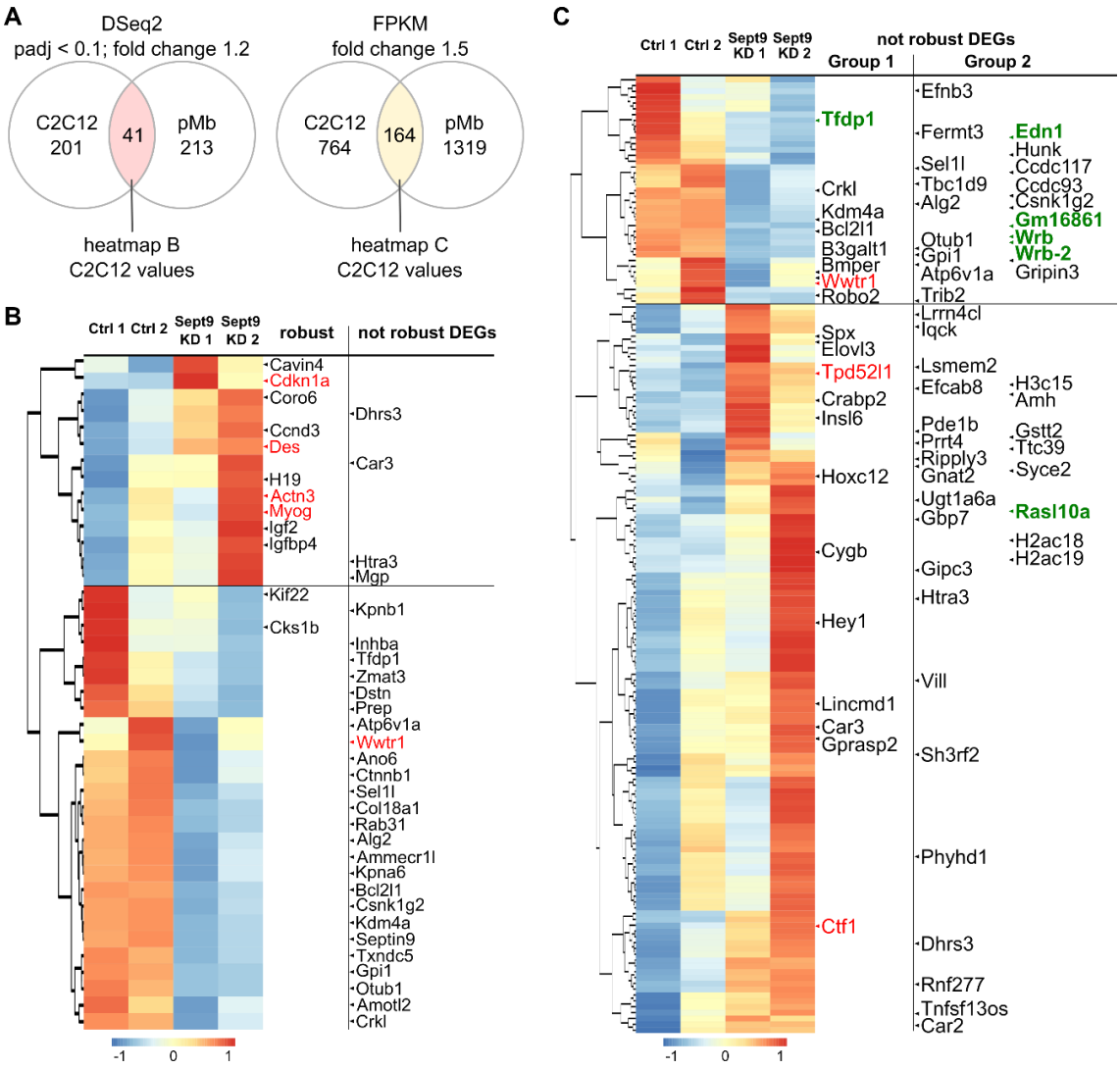

Figure 3-23. Transcriptional changes in C2C12 cells upon Septin9 depletion
A Comparative Venn diagram displaying DEGs obtained through DESeq2 algorithm (adjusted p value < 0.1; -0,322 ≤ log2FC ≤ 0,263) and those identified manually using FPKM values (-0,58 ≤ log2FC ≤ 0,58). **B** Heat map depicting 41 DEGs in C2C12 cells with Fold Increase (F.I.) > 1.2 from DESeq2 analysis. **C** Heat map depicting 164 DEGs in C2C12 cells with F.I. > 1.5 calculated from FPKM values. Labeled DEGs belong to 'non-robust' myogenic genes identified by Zhang *et. al* (Zhang et al., 2022). Group1 comprises established markers and regulators of myogenesis, while Group2 includes genes uncharacterized in the context of myogenic. Red highlighted- genes from Molecular Signature Database (MSigDB) "Hallmark MYOGENESIS", green highlighted- genes with fold change >2.

Table 3-2. 'Robust' myogenic genes regulated upon Septin9 depletion, in addition to Fig. 3-23C The table highlights 'robust and key' myogenic genes affected by Septin9 depletion. Notably, the gene names listed here were not among the 164 DEGs presented in Figure 3-21 C.

	Robust myogenic genes from (Zhang et al., 2022)
upregulated genes	*0610009L18Rik, 4833422C13Rik, Actc1, Actn3, Arpp21, Atp1a2, Atp2a1, C1qtnf3, Cacna1s, Casq2, Ccdc141, Chst13, Cilp2, Clic5, Colca2, Coro6, Ctrb1, Fgf21, Flrt1, Fndc5, Fxyd1, Galnt6, H19, Heyl, Hjv, Hsf2bp, Igf2, Igfbp4, Il12a, Inpp4b, Irgm2, Itgb1bp2, Klhl30, Klhl31, Klhl40, Klhl41, Mb, Mdfi, Mybph, Myh3, Myh8, Myl1, Mylk4, Mylpf, Mymk, Mymx, Myog, Myom1, Myom3, Pcbd1, Plpp7, Ppfia4, Pstpip1, Serping1, Smim1, Smyd1, Sntb1, Sugct, Susd5, Tesmin, Tgm2, Tmem182, Tnnc1, Tnnc2, Tnni1, Tnnt3, Traf3ip3, Trim63 ,Trim72.*
downregulated genes	*Kif22, Ccnb1-ps, Cks1b, Slc2a9, C530008M17Rik, Nanos1, Fgfr2, Gm7390, WNT10b*, Slc26a10*, Prr5l*.*

* inverse regulation, red highlighted- from Molecular Signature Data Base "Hallmark MYOGENESIS".

The remaining 84 Septin9-depletion specific 'not robust' myogenic DEGs are represented in the heat map, and this subset holds potential insights into the underlying mechanism by which Septin9 depletion impairs myogenesis (Fig. 3-23C). We have divided these genes in two distinct groups. Group 1 includes genes that have been implicated in the context of myogenesis. Among the downregulated genes in group 1 are BMP binding endothelial regulator (*Bmper*) and Roundabout guidance receptor 2 (*Robo2*), among others. Conversely, the upregulated genes in this group are Spexin hormone (*Spx*), Cytoglobin (*Cygb*), Hes related family BHLH transcription factor with YRPW motif 1 (*Hey1*) and Long intergenic non-protein coding RNA, muscle differentiation 1 (*Lincmd1*) among others. Distinct from group 1, DEGs within the second group serve diverse cellular functions, although many remain uncharacterized in the myogenic context. Among the highest regulated genes (marked in green, fold induction >2) are downregulated transcription factor DP 1 (*Tfdp1*), Endothelin 1 (*Edn1*), Tryptophan-rich basic protein (Wrb), a *Wrb-2* pseudogene, *Gm16861*, and upregulated Ras like family 10 member a (*Rasl10a*) (Fig. 3-23C).

In summary, evaluation of DEGs points towards the premature switch from proliferating to differentiating myogenic progenitors in both cellular contexts lacking Septin9. Additionally, this assessment provides insights into several potential key DEGs that could contribute to the observed effect.

3.4.2. Impact of Septin9 depletion on Activin A expression and Smad2/3 signaling in myoblasts

Certain identified DEGs from the RNA-seq analysis hold significant interest as potential contributors to the phenomenon of premature myogenic differentiation, potentially serving as hallmarks thereof. Initially, we investigated the expression and activity of Activin A, a member of the TGFβ family, involved in myogenesis (Lodberg, 2021), along with the potential extracellular inhibitor Mgp (Ahmad et al., 2017) (Fig. 3-24). RNA-Seq analysis revealed a consistent downregulation of *Inhba* RNA expression coupled with an upregulation of *Mgp* expression in both Septin9-deficient cell lines (Fig.3-23 B). To confirm and substantiate these findings, we conducted qRT-PCR analysis for *Inhba* and *Mgp* expression in Septin9-deficient C2C12 cells (Fig. 3-24A). This analysis revealed a reduced expression trend for *Inhba*, accompanied by a mild induction in *Mgp* expression (Fig. 3-24B-C). Next, we analyzed the Activin A-dependent Smad2 phosphorylation levels in Septin9-deficient C2C12 cells (Fig. 3-24D). Stimulation of these cells with Activin A at varying concentrations (0.24, o,27 and 1.92 nM) revealed diminished Smad2 phosphorylation (pSmad2) levels compared to control cells. It is noteworthy, that no discernible differences in pSmad2 levels were observed when utilizing medium containing 10% FCS. Further, we tested the responsiveness of the Septin9-deficient C2C12 cells containing the Smad3-sensitive $CAGA_{12}$-luciferase promoter (Fig. 3-24E). Under starvation conditions, depletion of Septin9 appeared to dampen the basal responsiveness of the CAGA reporter-gene. Notably, in the presence of a high concentration of TGFβ1 (100 pM), Septin depletion seemed to be dispensable for the reporter gene activity (Fig. 3-24F). Finally, we analyzed the capacity of Septin9-deficient cells to secrete ligands capable of activating the $CAGA_{12}$-reporter gene. To elucidate this, conditioned medium was collected from Septin9-deficient C2C12 cells during proliferation and 12 and 24 hours of myogenic differentiation. Subsequent stimulation of highly sensitive HEK cells, stably expressing $CAGA_{12}$-luciferase reporter gene, was conducted using the conditioned medium (diluted at 1:1 with 0% FCS DMEM) derived from C2C12 cells (Fig. 3-24G). Notably the medium derived from Septin9-deficient C2C12 cells demonstrated a tendency towards reduced basal activity compared to control cells. This observed difference was mitigated upon supplementation of the conditioned medium with 0.5 nM Activin A (Fig. 3-24G-H).

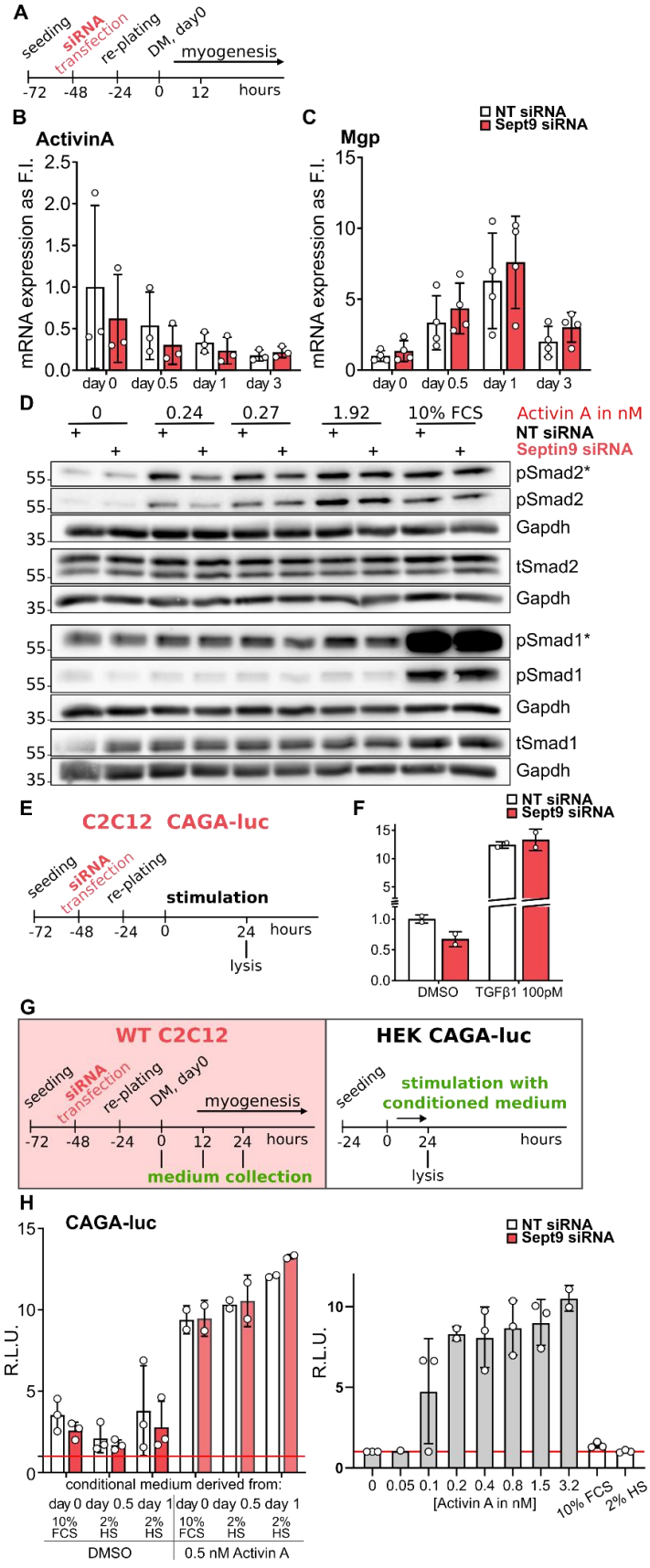

Figure 3-24. Septin9 depletion dampens basal TGFβ signaling potentially via modulation of Activin A availability
Differential expression analysis of genes upon Septin9 depletion indicates lower levels of Activin A (Fig. 3-21B). **A** Schematic representation of Septin9 knockdown strategy in C2C12 cells. **B-C** qRT-PCR analysis revealed a trend towards reduced mRNA levels for *Inhba* and a concurrent upregulation trend of its potential antagonist *Mgp* upon Septin9 depletion. **D** Western blot analysis of Smad1 and Smad2 phosphorylation upon Septin9 depletion. C2C12 cells were subjected to a 6-hour starvation followed by 1-hour stimulation with indicated concentration of Activin A or 10% FCS (n=1). **E** Schematic depiction of the dual luciferase assay utilizing Septin9-deficient C2C12 $CAGA_{12}$-luc cells. **F** Dual luciferase assay in stable $CAGA_{12}$-luc cells showed a dampened basal responsiveness of CAGA-reporter gene (n=2). **G** Experimental layout involving HEK cells with stable CAGA-luciferase construct, exposed to conditional medium supplemented or not with 0.5 nM Activin A from proliferating or differentiating (12 and 24 hours) Septin9-deficient C2C12 cells. **H** Dual luciferase assay shows $CAGA_{12}$ promoter activity in HEK cells. Medium from Septin9-depleted cells showed reduced tendency to activate the CAGA promoter in absence of exogenous Activin A.

Taken together, the depletion of Septin9 potentially results in diminished levels of Activin A transcription and less secretion thereof, potentially leading to subsequent attenuation of downstream signaling response.

3.4.3. Impact of Septin9 depletion on expression of selected WNT target genes

In light of our identification of β-catenin (*Ctnnb1*) as a downregulated DEG in the RNA-seq analysis, we explored some β-catenin target genes (Cui et al., 2019), aiming to understand the regulatory landscape of the *Ctnnb1* gene in Septin9-deficint myoblasts. Several of these genes were simultaneously identified as interactors of minion (*Mymx*, except *Ctnnb1*), thereby potentially playing a role in myoblast fusion and later stages of myogenic differentiation (Zhang et al., 2017) (Fig. 3-25A-B). In addition to the observed downregulation of *Ctnnb1*, our findings reveal the upregulation of Myomaker (*Mymk*), Minion (*Mymx*), Tripartite motif containing 72 (*Trim72*), Junctional Sarcoplasmic Reticulum Protein 1 (*Jspr1*), Synaptopodin 2 Like (Synpo2l, observed in C2C12 only) and Dysferlin (*Dysf*, significantly upregulated only in one repetition in each cell type) in Septin9-deficient myoblasts (Fig. 3-25B).

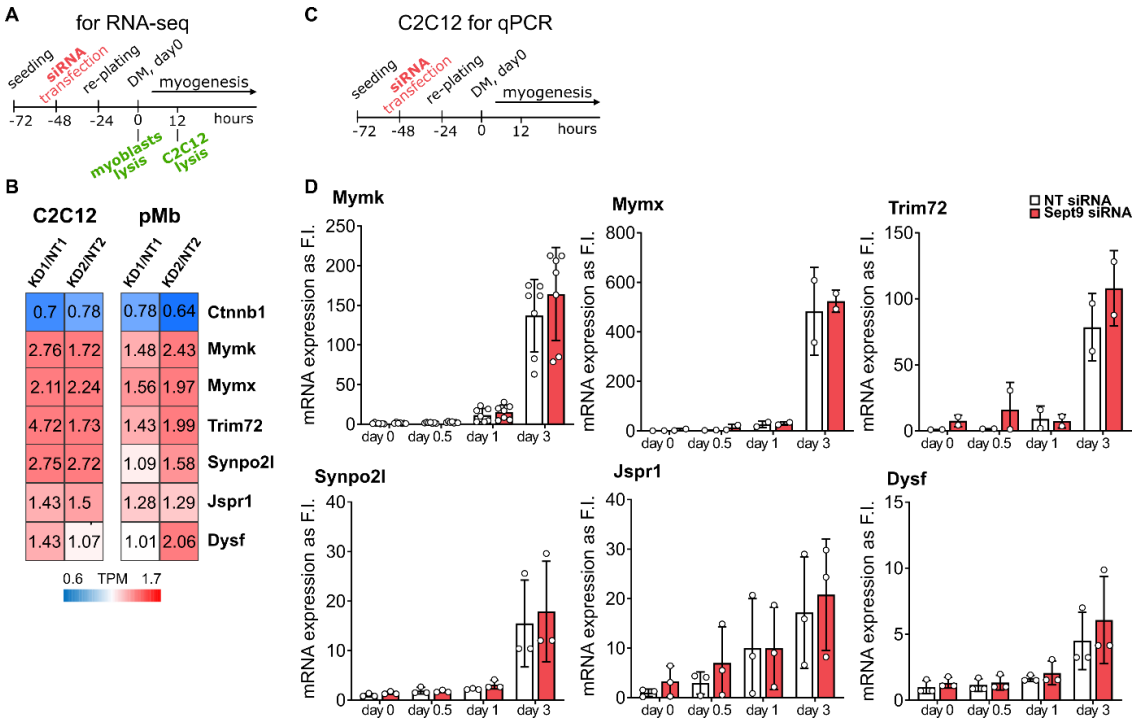

Figure 3-25. Depletion of Septin9 leads to upregulation of some WNT/ β-catenin targets and downregulation of β-catenin

Differential expression analysis of genes upon Septin9 depletion indicates higher levels of WNT/ β-catenin target genes and the downregulation of β-catenin itself. **A** Experimental setup for RNA-seq analysis in Septin9-deficient myoblasts. **B** Heatmap representing the TPV values of *Ctnnb1* and its target genes from Septin9-deficient C2C12 and primary myoblasts. The values represent knockdown-to-control ratio, obtained from TPM values in each RNASeq experiment. **C** Schematic representation of the Septin9 knockdown in C2C12 cells for subsequent qRT-PCR validation. **D** Validation of mRNA expression levels through qPCR for the genes selected in (B) (excluding *Ctnnb1*). Most tested genes (except *Mymx*) exhibited an upregulation trend on day 3 of myogenesis, with several genes also demonstrating premature expression during other time points. Notably, the early gene *Jspr1* displayed a distinct difference trend on day 0 and after 12 hours of differentiation.

Subsequent validation of the expression levels of these target genes (excluding *Ctnnb1*) at the mRNA level was conducted via qRT-PCR (Fig. 3-25C). Evidently, all tested genes (except *Mymx*) showed an inclination towards upregulation during day 3 of myogenic differentiation upon Septin9 depletion. Furthermore, a premature elevation in expression was discerned under both proliferative and early myogenic (12-hour) conditions (Fig. 3-25D). Together, Septin9 depletion is potentially associated with reduced β-catenin levels and heightened expression of some of its target genes, further contributing to the disruption of signaling pathways following septin loss.

3.4.4. Accelerated early myogenic differentiation in C2C12 cells upon Septin9 knockdown

To further validate the observed accelerated early myogenic progression resulting from Septin9 depletion, we conducted a series of experiments, employing siRNA-mediated Septin9 knockdown, C2C12 cells were subjected to myogenic differentiation for a period of up to 3 days (Fig.3-26 A). Following mRNA extraction, we analyzed the expression of pivotal myogenic targets, including *Myog* as well as other marker genes such as Taz (*Wwtr1*), Follistatin (*Fst*), Myosin heavy chain 2 and 8 (*Myh2* and *Myh8*) using qRT PCR (Fig. 3-26 B, C). Notably, M*yog*, an early marker of myogenesis, was upregulated upon Septin9 knockdown during the initial stages of myogenic differentiation (Fig. 3-26B). Moreover, we validated the downregulation of *Wwtr1*, consistent with previous RNA-seq findings. Late myogenic genes (*Fst*, *Myh2* and *8*), that are not expressed in the first day, were observed to undergo upregulation after 3 days of myogenic differentiation in Septin9-deficient C2C12 cells (Fig. 3-26C). Additionally, we verified the augmented expression of Myogenin (at 24 hours) and Myh2 (at 72 hours) at the protein level following Septin9 depletion (Fig. 3-26D).

Next, the immunostaining of undifferentiated and differentiated C2C12 cells (day3) with MF20 antibodies, recognizing all Myosin heavy chain isoforms (Fig. 3-26E-G). By day 3 of myogenesis, Septin9-deficient myoblasts displayed elevated level of MF20 staining, confirming an initial increase in early myogenic differentiation (Fig. 3-26E). The myogenic differentiation index (MDI), calculated from the ratio of total DAPI-positive cell count to MF20-positive myoblast, highlights cellular differentiation capacity. Notably, on day 3 of myogenic differentiation, Septin9-deficient cells exhibited a twofold increase in MDI compared to control cells (Fig. 3-26F). Next, we evaluated the ability of septin-deficient

myoblasts to undergo fusion. Quantification of nuclei within MF20-positive myoblasts and myotubes, denoted as the myogenic fusion index (MFI), indicated a substantial rise in mono-, bi- and trinucleated Septin9-deficient myoblasts compared to controls. Additionally, a trend towards increased presence of multinucleated cells was observed (Fig. 3-26G). Hence, myoblasts lacking Septin9 did not display evident early fusion defects, as addressed by the myogenic fusion index (Fig. 3-26G). In sum, Septin9 depletion indicates increased differentiation capacity in C2C12 cells.

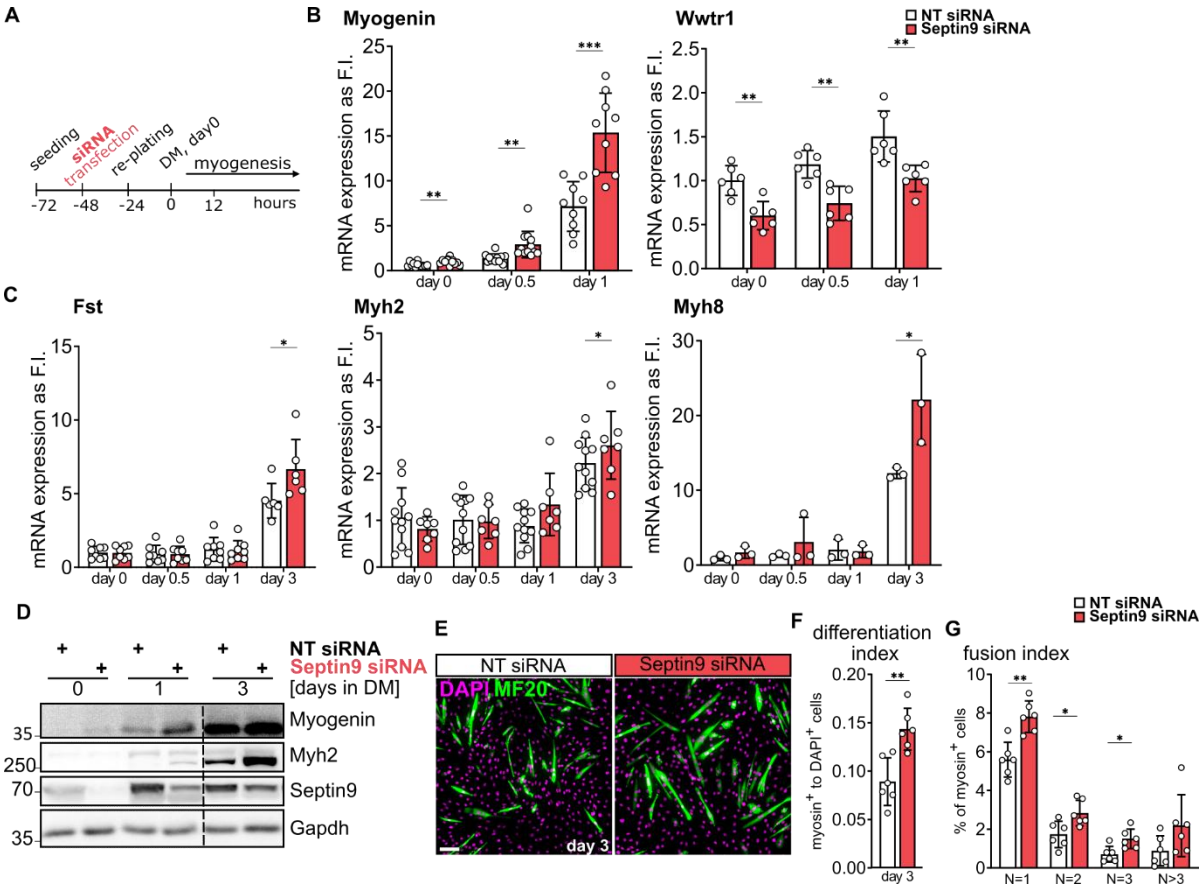

Figure 3-26. Septin9 depletion accelerates early myogenic differentiation
A Schematic representation of Septin9 knockdown in C2C12 cells. **B** Quantification of mRNA levels of *Myog* and *Wwtr1* through qRT-PCR analysis in C2C12 cells following Septin9 knockdown. **C** qRT-PCR of late myogenic target genes *Fst, Myh2* and *Myh8* Septin9-deficient C2C12 cells. **D** Western blot analysis of myogenic markers Myogenin and Myosin heavy chain 2 in Septin9 deficient myoblasts. **E** Immunofluorescence staining of myosin heavy chain 2 (MF20) after 3 days of differentiation. **F** The myogenic differentiation index, reflecting the count of MF20-positive cells (from (E)). **G** The myogenic fusion index, reflecting the number of nuclei per myotube (from (E)). 'N' denotes the number of nuclei. Data represent mean ± standard deviation (SD), *p<0.05, **p<0.01, ***p<0.001, ****p<0.0001 from two-sided unpaired t test. Scale bar 50 µm. Data from (Ugorets et al., 2024).

3.4.5. Reduced cell proliferation in myoblasts upon Septin9 knockdown

Given the potential impact of impaired differentiation on cycling myoblasts growth and viability, we assessed Septin9-deficient myoblast proliferation. First, we quantified the

expansion of proliferating myoblasts through immunofluorescence-based counting of nuclei-labeled C2C12 cells. To avoid potential knockdown-induced proliferation differences, cells were re-plated 24 hours before the experiment and allowed to differentiate after for the specific duration (Fig. 3-27A). Following Septin9 depletion, a notable reduction in myoblast cell numbers was observed after 24 hours of differentiation (Fig. 3-27B). Despite efforts to ensure consistent initial cell densities through automated cell counting before seeding, variations were observed. Categorizing experiments based on initial cell density revealed a density-dependent hindrance in the expansion of Septin9-deficient myoblasts. Specifically, myoblasts with higher initial densities exhibited less efficient expansion compared to sparsely seeded counterparts. (Fig. 3-27C-E).

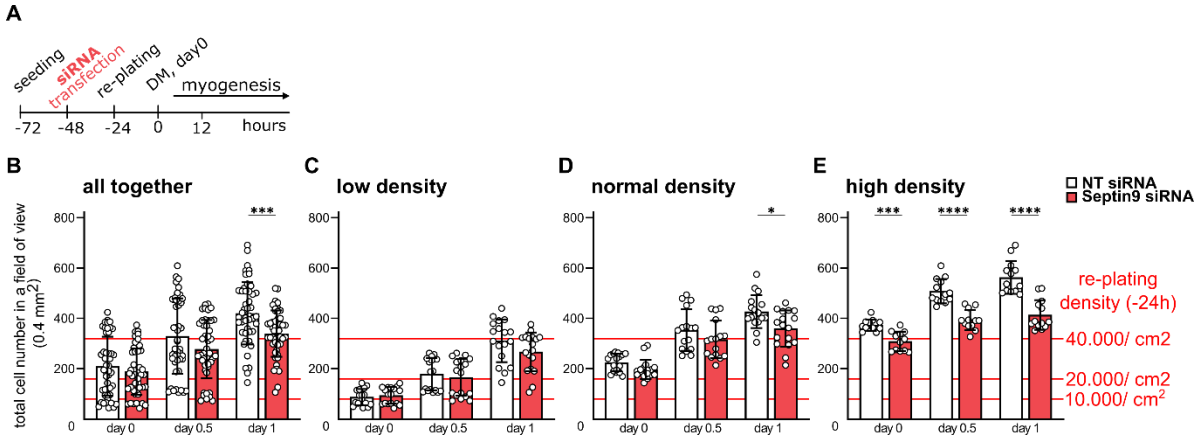

Figure 3-27. Septin9 knockdown impairs expansion of myoblasts in a density-dependent manner
A Schematic representation of Septin9 knockdown in C2C12 cells. **B** Quantitative assessment of total cell numbers using DAPI nuclear staining in both proliferating and differentiating C2C12 cells upon Septin9 knockdown (number of experiments >45). To account for differences in initial cell densities in the beginning of the experiment, the experiments were grouped based on the initial cell count of proliferating control cells (first white bar). Consequently, red lines arbitrary divide experiments into three categories: **C** low density- below 160 cells per field of view (less than 20.000 cells per cm^2), **D** normal density- below 320 cells per field of view (less than 40.000 cells per cm^2) and **E** high density- above 320 cells per field of view (more than 40.000 cells per cm^2). Data represent mean ± standard deviation (SD), *p<0.05, **p<0.01, ***p<0.001, ****p<0.0001 from Mann-Whitney-U-test.

To elucidate the basis for the decreased cell numbers, we investigated whether Septin9 depletion impacts progression through specific cell cycle stages. We employed the proliferation marker Ki67, the mitotic phospho-Histone H3 (pHH3) marker, and a 5-Ethynyl-2'-deoxyuridine (EdU) incorporation assay highlighting DNA synthesis (Fig. 3-28). Notably, Septin9 depletion did not substantially alter myoblast expansion under the tested conditions, as evidenced by Ki67 and pHH3 staining in C2C12 (Fig. 3-28A-B). However, a reduction in Septin9-deficient cells during the DNA synthesis phase (S-phase) of the cell cycle was

observed through the EdU assay. This impairment in transitioning through the DNA synthesis phase was reversed once myoblasts were exposed to myogenesis permissive conditions (Fig. 3-28C). Collectively, these findings indicate a modest decline in cell cycle progression in absence of Septin9.

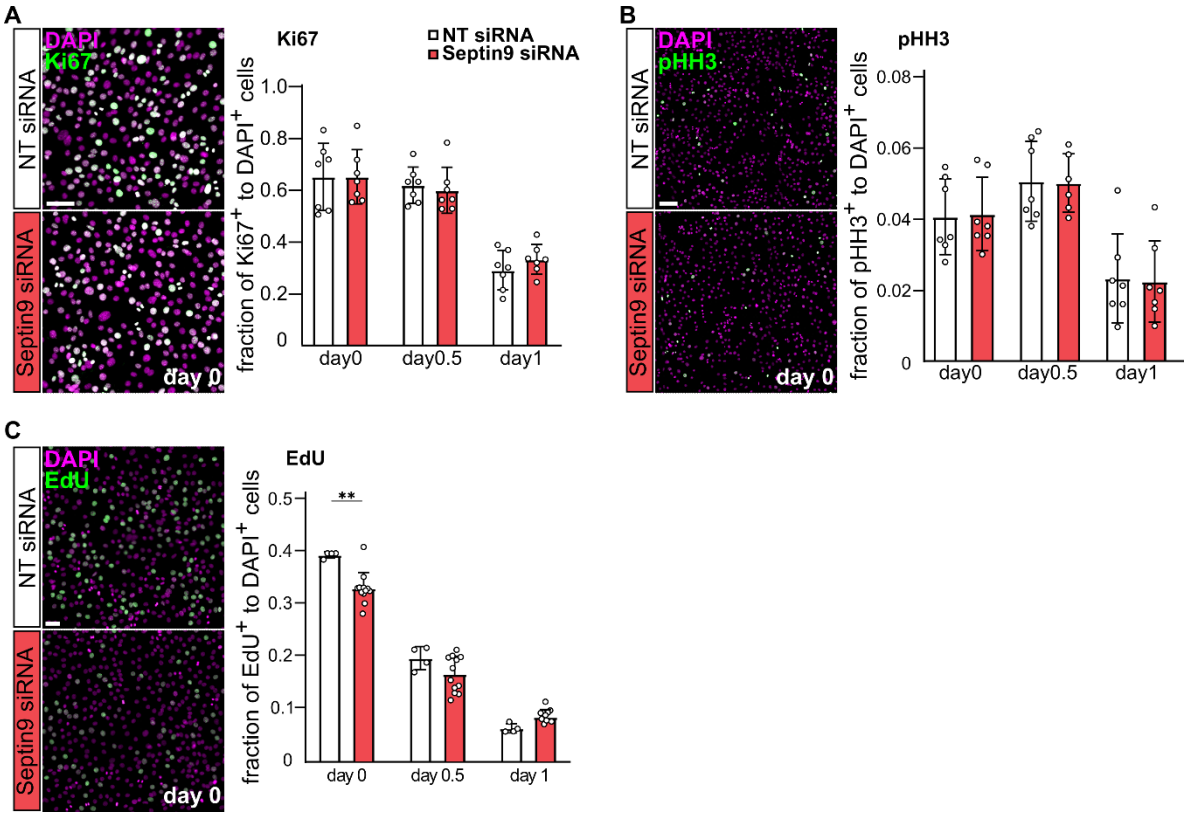

Figure 3-28. Mild reduction in S phase of the cell cycle upon Septin9 depletion
Fluorescent proliferation assays conducted on both proliferating and differentiating C2C12 cells deficient in functional septins. **A** Representative images captured on day 0 depicting Ki67 proliferation marker labeling, along with imaging-based quantification. **B** Visualization of the mitotic marker phospho-Histone H3 (pHH3) on day 0 along, with imaging-based quantification of dividing cells. **C** Representative micrographs showing the fluorescent EdU incorporation assay on day 0, alongside quantification of cells residing within the DNA synthesis (S) phase of the cell cycle. Data represent mean ± standard deviation (SD), *p<0.05, **p<0.01, ***p<0.001, ****p<0.0001 from two-sided unpaired t test. Scale bar 50 µm in a-b, 20 µm in c.

3.4.6. Increased apoptosis in myoblasts upon Septin9 knockdown

The decline in cell numbers may also arise from augmented cell death. To explore this, we investigated apoptosis rates upon Septin9 knockdown. Specifically, we focused on the execution pathway of the programmed cell death, centering on the activation of caspase 3 (Fig. 3-29). Western blot analysis of cleaved caspase 3 protein levels was conducted in C2C12 cells lacking functional septin filaments. Notably, Septin9 depletion induced an upregulation of caspase 3 cleavage in both proliferating and early differentiating myoblasts (Fig. 3-29A-B).

Furthermore, we assessed the activity of the cleaved executioner caspase 3 and 7 using a luminescent assay based on the cleavage of a proluminescent caspase substrate. This analysis revealed an augmentation in executioner caspase activity following Septin9 knockdown in both proliferating cells and those undergoing 12 hours of myogenic differentiation. It is noteworthy that no significant variation in cleaved caspase 3/7 activity was observed in cells differentiating for 24 hours (Fig. 3-29C-D). Next, we examined the levels of cleaved caspase 3 in Septin9 deficient cells using immunofluorescence. The frequency of cells exhibiting cleaved caspase 3 staining upon Septin9 knockdown displayed a tendency towards elevation across all tested conditions, mirroring the observations from protein levels analysis. However, this increase did not attain statistical significance in this assay (Fig. 3-29E).

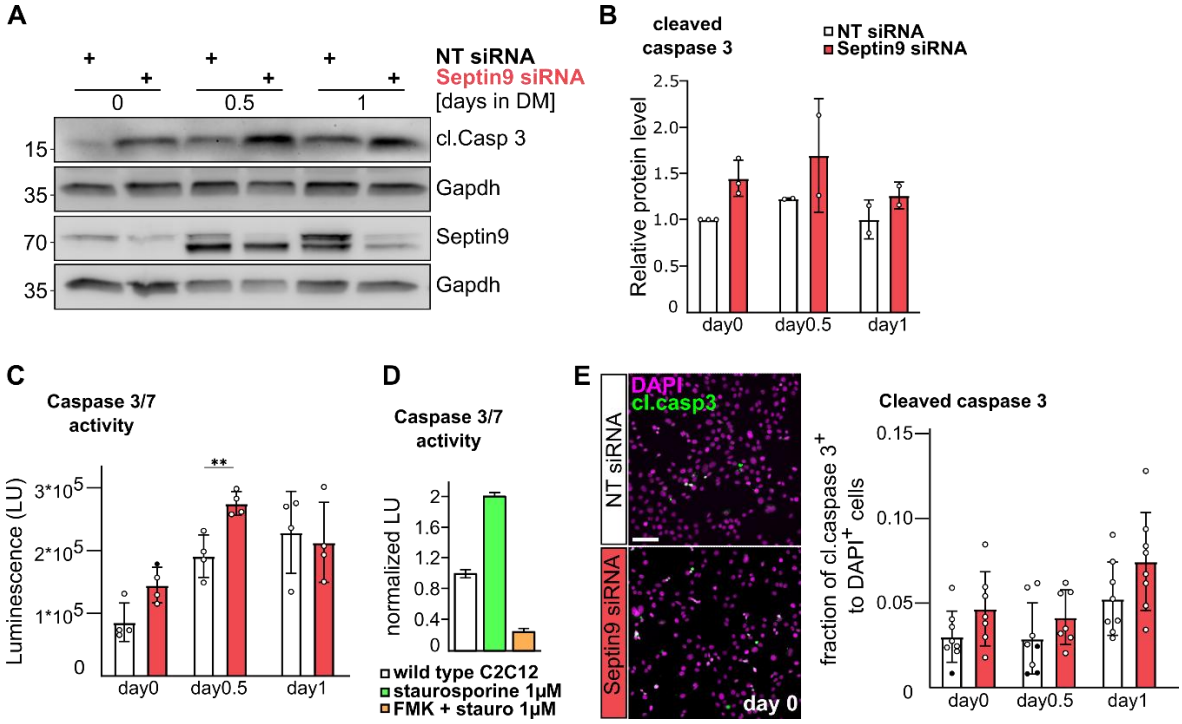

Figure 3-29. Septin9 knockdown activates Caspase3 and 7

A Septin9 depletion induced elevated protein levels of active cleaved Caspase3 protein in both proliferating and differentiating C2C12 cells. **B** Quantitative assessment of cleaved Caspase3 levels, normalized to Gapdh from panel (A). **C** Luminescent Caspase-Glo 3/7 assay revealed increased activity of executioner caspases 3 and 7 upon Septin9 depletion in early differentiating C2C12 cells. **D** Validation of Caspase-Glo 3/7 assay with positive and negative control in wild type C2C12 cells. Positive control involved 3-hour incubation with 1µM apoptosis-inducing agent staurosporine, while the negative control included pre-treatment with irreversible Caspase3 inhibitor FMK for 1 hour, followed by staurosporine incubation. **E** Representative epifluorescence images illustrating control and Septin9 knockdown C2C12 cells labeled for cleaved Caspase3, accompanied by quantification of the cleaved Caspase3-positive cells. Data represent mean ± standard deviation (SD), *p<0.05, **p<0.01, ***p<0.001, ****p<0.0001 from two-sided unpaired t test. Scale bar 50 µm.

Next, we investigated the levels of cleaved caspase 3 in Septin9 deficient cells via immunofluorescence. The number of cells with cleaved caspase upon Septin9 knockdown shows a tendency towards an increase under all tested conditions as in case of the protein levels, but the increase is not significant in this assay (Fig. 3-29E).

Moreover, we investigated the downstream effects of the executioner caspase pathway. Specifically, Caspase 3-mediated cleavage of Parp-1 and subsequent activation of endonucleases that induce DNA strand breaks (Elmore, 2007). In the context of Septin9 depletion, we observed an increase in total Parp-1 protein cleavage in differentiating, but not proliferating C2C12 cells (Fig. 3-30A). To evaluate endonuclease cleavage products, we used the TdT-mediated dUTP-biotin nick end labeling (TUNEL) assay, revealing an increase in DNA single strand breaks in cells lacking functional septin filaments. Notably, C2C12 exhibited a trend toward increased TUNEL signal in proliferating cells, with significant upregulation detected only in cells undergoing differentiation for 12 and 24 hours (Fig. 3-30B). Together, Septin9 is potentially involved in regulation of myoblast survival, as its depletion leads to enhanced apoptosis.

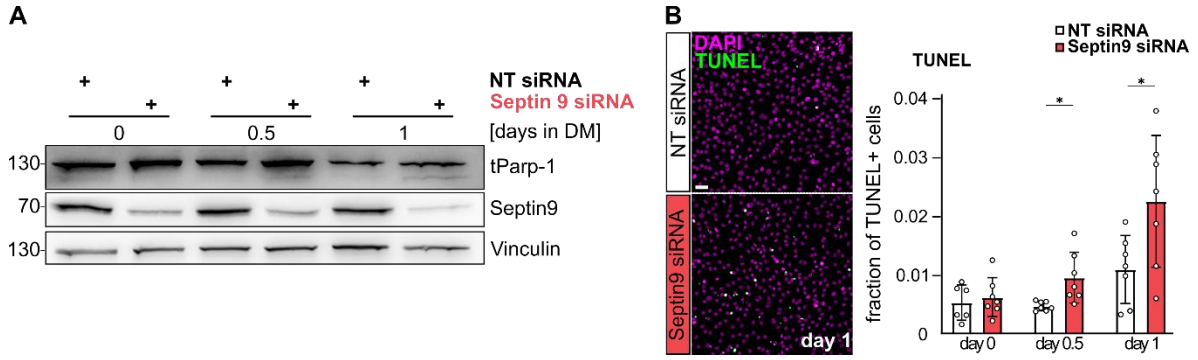

Figure 3-30. Septin9 depletion increased apoptosis
A Septin9 depletion results in augmented apoptosis, as indicated by the accumulation of apoptosis-associated Parp-1 cleavage in both proliferating and differentiating C2C12 cells. Total Parp-1 levels are represented, with antibodies that also recognize cleaved protein. **B** Epifluorescence images display nuclei labeled with DAPI and apoptotic cells labeled using the Terminal deoxynucleotidyl transferase dUTP nick end labeling (TUNEL) assay. Quantification of TUNEL-positive cells revealed an increase in apoptotic events in differentiating C2C12 cells lacking Septin9. Data represent mean ± standard deviation (SD), *p<0.05, **p<0.01, ***p<0.001, ****p<0.0001 from two-sided unpaired t test. Scale bar 20 µm.

3.4.7. Septin2 interactome in proliferating and differentiating C2C12 cells

In pursuit of identifying interaction partners of septin oligomers, we performed an immunoprecipitation of Septin2 coupled with Maldi/LC-MS analysis in both proliferating and 5-day differentiating C2C12 cells (Fig. 3-31 and Table 3-3 – 3-6 and Table 6-2) (MS facility FMP

Berlin, Heike Stephanowitz, Prof. Dr. Michael Krauss). We identified 67 interaction partners exhibiting specific enrichment through anti-Septin2 antibodies in proliferating cells, and 29 proteins interacting with Septin2 in differentiating cells (Fig. 3-31A-B). Notably, several septin paralogs emerged as consistent Septin2 interactors under both experimental conditions (discussed in detail in chapter 3.1.5). Moreover, we found Septin2 to interact with a myogenic transcription factor Nuclear factor of activated T cells 5 (Nfat5) (O'Connor et al., 2007) and the inhibitory component of the positive transcription elongation factor b (P-TEFb) complex, hexamethylene bisacetamide inducible 1 (Hexim1 or Clp-1), which modulates the expansion of satellite cells (Hong et al., 2012) (Fig. 3-31A-B). Most of the identified proteins exhibited specific enrichment by anti-Septin2 antibodies exclusively in proliferating cells. Noteworthy, among these interactors was Protein arginine methyltransferase 5 (Prmt5), a crucial factor in Myod1-induced myogenesis (Dacwag et al., 2007) along with its associated adaptor protein WD domain 77 (Wdr77) (Mulvaney et al., 2021) (Fig. 3-31A). Furthermore, we compared enrichment strength of the identified interaction partners across different conditions (Fig. 3C-D). Our results highlighted eight proteins that displayed significantly reduced enrichment with anti-Septin2 antibodies in differentiating cells, including Nfat5 (Fig. 3-31C). We employed control IgGs as a negative control for proteins exhibiting differential enrichment by control IgGs and beads across experimental conditions, revealing four proteins, such as Nascent polypeptide associated complex subunit alpha (Naca) among others, that need to be evaluated carefully (Fig. 3-31D). Overall, our findings point to a select group of proteins potentially influencing the course of myogenic differentiation through interactions with septin complexes.

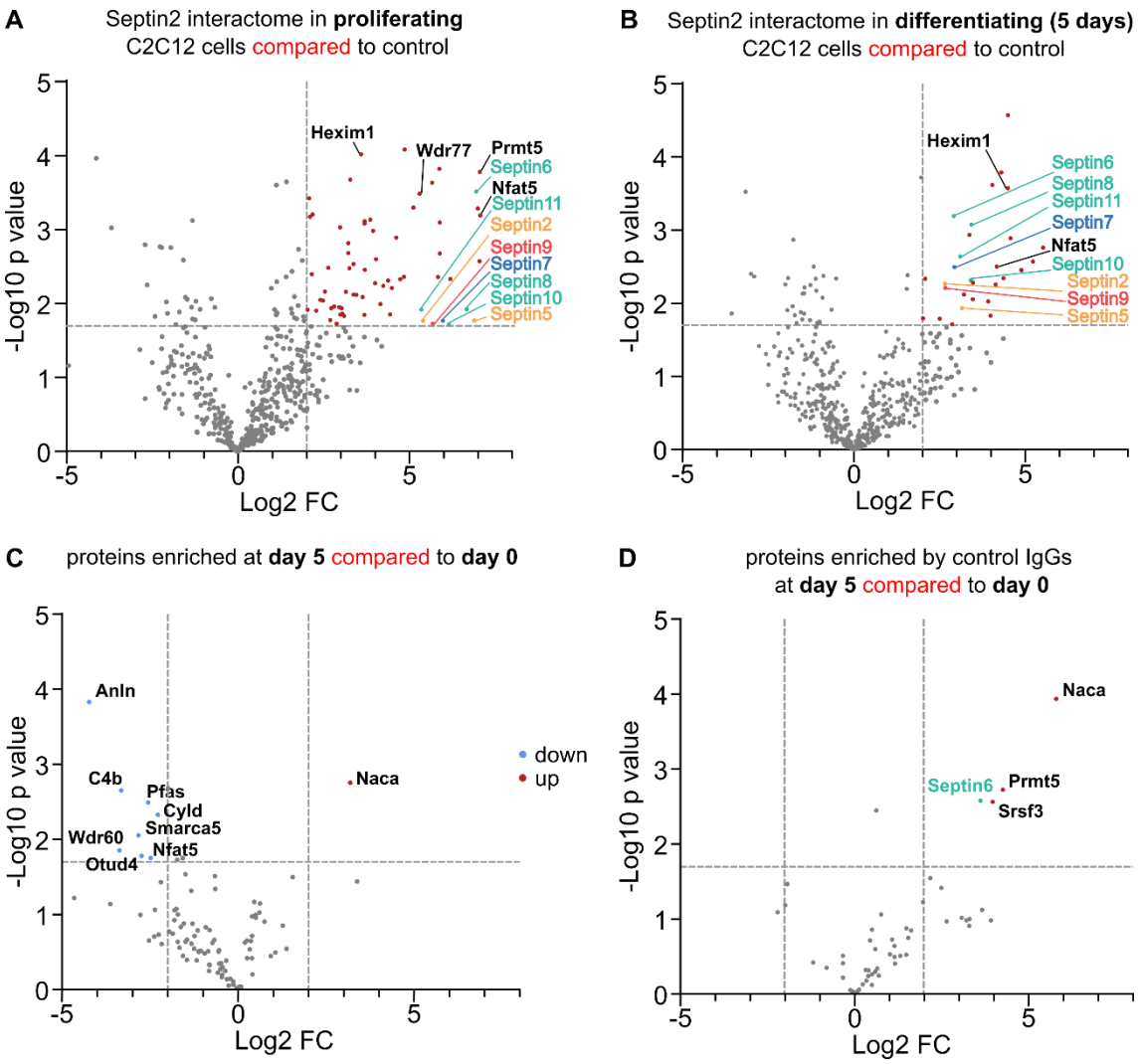

Figure 3-31. Septin2 interactome in proliferating and differentiating C2C12 cells identified by affinity purification mass spectrometry

A Volcano plot depicting Septin2 interactors identified in proliferating C2C12 cells. Meaningful interactors are represented by significant and specific hits (enrichment > 2 Log2FC, p value < 0.05). **B** Volcano plot highlights significant specific Septin2 interactors (enrichment > 2 Log2FC, p value < 0.05) in C2C12 cells undergoing 5 days of myogenic differentiation. **C-D** Comparative analysis of Septin2 interacting partners enriched with Septin2 IgG and control IgGs during proliferation and differentiation. **C** Volcano plots representing meaningful (specific interactors from A and B) and significant Septin2 interactors (enrichment > 2 Log2FC, p value < 0.05) in differentiating cells compared to proliferating cells. Downregulation signifies potentially reduced interaction with Septin2 during differentiation, while upregulation indicates increased interaction with Septin2. **D** Enrichment of meaningful interactors (specific interactors from A and B) by control IgGs. Significant hits (enrichment > 2 Log2FC, p value < 0.05) show enhanced specific enrichment with control IgGs in differentiating cells.

Table 3-3. Selected interactors of Septin2 in proliferating C2C12 cells

Gene name	Log2 IgG_d0_avg	Log2 S2IP_d0_avg	-Log10 p-value	Log2 FC difference S2IP/ IgG day 0
Neurl4	19.67	24.48	**4.08**	**4.82**
Hexim1	18.66	22.23	**4.02**	**3.56**
Herc2	19.34	25.17	**3.82**	**5.82**
Prmt5	19.03	26.02	**3.78**	**6.99**
Aebp1	18.48	21.73	**3.68**	**3.25**
Arhgap17	19.23	24.85	**3.63**	**5.61**
Wdr77	19.51	24.76	**3.49**	**5.25**
Dhx36	18.97	24.04	**3.30**	**5.07**
Nfat5	18.96	25.96	**3.19**	**7.00**

Table 3-4. Selected interactors of Septin2 in C2C12 cells differentiating for 5 days

Gene name	Log2 IgG_d5_avg	Log2 S2IP_d5_avg	-Log10 p-value	Log2 FC difference S2IP/ IgG day 5
Neurl4	19.34	23.83	**4.57**	**4.49**
Map7d1	23.54	27.58	**3.62**	**4.03**
Hexim1	18.34	22.83	**3.57**	**4.49**
Herc2	19.02	23.59	**2.89**	**4.57**
Nfat5	19.31	23.47	**2.50**	**4.17**

Table 3-5. Interactors of Septin2 that exhibit differences in enrichment during differentiation

Gene name	Log2 IgG_d0_avg	Log2 S2IP_d0_avg	Log2 IgG_d5_avg	Log2 S2IP_d5_avg	-Log10 p-value	Log2 FC difference S2IP d5/ S2IP d0
Anln	19.71	23.06	19.04	18.83	**3.83**	**-4.23**
Naca	19.51	23.34	25.31	26.52	**2.75**	**3.18**
Nfat5	18.96	25.96	19.31	23.47	**1.75**	**-2.49**

Table 3-6. Proteins that exhibit increased enrichment by control IgG during differentiation

Gene name	Log2 IgG_d0_avg	Log2 S2IP_d0_avg	Log2 IgG_d5_avg	Log2 S2IP_d5_avg	-Log10 p-value	Log2 FC difference IgG d5/ IgG d0
Naca	19.51	23.34	25.31	26.52	**3.94**	**5.80**
Prmt5	19.03	26.02	23.30	25.53	**2.73**	**4.27**
Septin6	19.80	26.68	23.42	26.34	**2.58**	**3.63**
Srsf3	19.01	23.46	22.98	23.41	**2.56**	**3.98**

4. Discussion

With the exception of sensory and neuronal functions, skeletal muscle enables animals to perform nearly all daily activities, from walking and running to lifting and breathing. Given its vital roles, understanding the biology of skeletal muscle—how it forms, maintains itself, regenerates, and functions—is crucial. Basic research on muscle cell differentiation, the process by which dormant stem cells transform into contractile muscle fibers, helps us grasp these essential processes. Such research can ultimately provide new methods to enhance the beneficial characteristics of healthy muscle, with the aim of extending a healthy lifespan.

In this study, it was examined how the cytoskeleton, the cell's structural framework, influences the orderly progression of muscle cell differentiation. I found that cytoskeletal reorganization is crucial during the early stages of myoblast differentiation and fusion, which aligns with previous knowledge. The focus was on a lesser-known family of cytoskeletal proteins, called septins. Septins were once thought to be passive scaffolding elements in biological processes, and their importance in muscle biology has only recently come to light. For instance, Septin7 is postulated to be essential for the structure and function of mammalian skeletal muscle (Gönczi et al., 2022, 2021).

This newfound interest in septins led us to explore their dynamic expression pattern in adult MuSCs and myoblasts. I observed a significant reorganization of septin filaments during early myoblast differentiation. Moreover, I discovered that depleting Septin9, a *passive cytoskeletal component,* accelerates the onset of the myogenic differentiation program. In summary, septins were identified as an integral part of the muscle cell cytoskeleton, ensuring the orderly progression through myogenic differentiation.

4.1. Septins in muscle cells

To comprehensively understand septin function in specific cell lines or tissues, it is crucial to characterize the expression profile of all septins within the chosen model. Due to the extensive number of septin genes in mammals, comparative expression profiles of all septins in a particular cell type or tissue are still lacking. In this study, we examined the expression profiles of septins in proliferating and differentiating myoblasts, as well as MuSCs during adult muscle regeneration.

Quiescent MuSCs displayed a minimal set of septins, consisting of *Septin2*, *7*, *10,* and *11*, which are sufficient to form a hexamer, with *Septin10* and *11* potentially competing for the same position within the filament (Fig. 3-2). In contrast, non-quiescent MuSC populations, along with *in vitro* cycling myoblasts and myotubes, expressed *Septin8* and Septin9 in addition to the core septins. Furthermore, the expression of *Septin4* and *Septin6* was also temporally regulated. Notably, *Septin5* expression was exclusive to myoblasts (Fig. 3-2). Our findings revealed that *Septin2*, *7*, *9* and *11* were the most highly expressed septins at both the RNA (in C2C12 and primary myoblasts) and protein levels (in C2C12 cells). We termed these septins the "core myogenic septins" (Fig. 3-1 – 3-6 and Table 3-1). This expression profile suggests the formation of octameric complexes, which are the smallest functional units of the septin cytoskeleton (Martins et al., 2022) (consequences of Septin9 incorporation are discussed in chapter 4.1.3). The expression levels of other septins ranged from trace amounts to approximately 10% of the levels observed for the core septins.

Our findings align with earlier reports demonstrating the expression of various septin paralogues in C2C12 cells, as well as in neonatal and adult TA muscle (Gönczi et al., 2022). Using semi-quantitative PCR, they identified the presence of most septins, excluding Septin1, 3, 12, and 14. Our data, alongside their findings, indicate that myoblasts (and potentially muscle fibers) express the same set of septin paralogues as activated MuSCs (Fig. 3-1 and 3-2). This conclusion is further supported by the expression of septin paralogues in adult MuSC population from the 3-month-old TA muscle, analyzed within the framework of Tabula Muris compendium (Schaum et al., 2018). Examination of Tabula Muris revealed high expression levels of various septins, including *Septin2*, *7*, *8*, *9*, *10* and *11*, with lower levels of *Septin4*, *5*, and *6* (data not shown).

Information on septin expression in adult murine muscle is limited. Gönczi *et al*. showed mRNA expression of most septin paralogues, including Septin7, in adult TA muscle (Gönczi et al., 2022). Our study also reports Septin9 expression in adult TA muscle (Fig. 3-19), with both Septin7 and Septin9 localizing to the contractile compartment of the sarcomere. To support this data, we explored the expression of septin paralogues in the Myoatlas, a single-nucleus RNASeq data repository from the Millay Lab (Petrany et al., 2020) that analyzes different post-natal stages of murine TA and Soleus muscle. Our search revealed that only *Septin7* and *Septin11* were abundantly expressed in a subset of adult myonuclei according to Myoatlas (data not shown). The Myoatlas repository may overlook septins due to its focus on highly

expressed genes, suggesting that other septin paralogues could be present in adult mouse muscle. Since multiple paralogues are needed for functional septin complexes, further research is required to explore their differential distribution and coordinated expression in adult muscle tissue, clarifying septin complex composition and function.

The expression of septin paralogues in murine myoblasts is generally consistent with those of human septins expressed in skeletal muscle, as analyzed via bulk RNASeq from tissue biopsies (Carithers et al., 2015) within the framework of The Adult Genotype Tissue Expression (GTEx) Project. According to the expressions levels derived from the GTEx Analysis v7 (https://gtexportal.org/home/ datasets), human skeletal muscle septins - including *SEPTIN2*, *4*, *5*, *6*, *7*, *8*, *9*, *10* and *11* - are expressed at one or two orders of magnitude lower than in a paradigm septin tissue such as spinal cord (Fig. 4-1). Therefore, it is conceivable that murine muscle fibers express a selection of septin paralogues similar to human tissue.

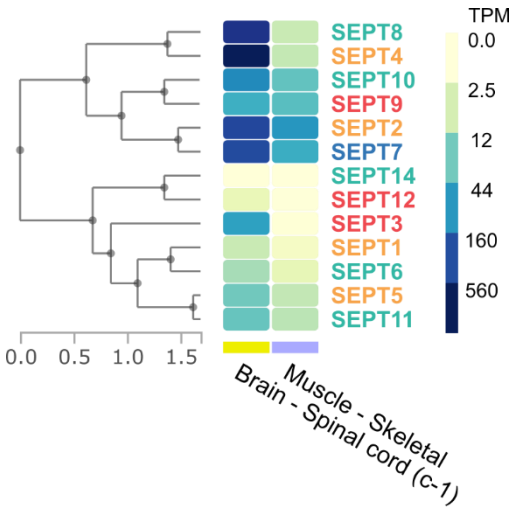

Figure 4-1. Septin expression in human spinal cord and skeletal muscle tissues
Using septin median TPM values we performed hierarchical clustering of gene expression profiles from the human spinal cord and skeletal muscle tissues. Septins are color-coded based on subgroups of core myogenic protomers as proposed in Fig. 3-1. Data is derived from GTEx portal (THE GTEX CONSORTIUM et al., 2015).

This comprehensive profiling underscores the significance of core septins in myogenic processes and provides a foundation for further studies on their specific roles in muscle cell biology. Additionally, myogenic differentiation and muscle injury resulted in alterations of septin expression in myoblasts *in vitro* and quiescent MuSCs, respectively. This highlights the dynamic nature of septin regulation in response to physiological changes, warranting further investigation into their expression and organization in myoblasts, myotubes and adult muscle.

4.1.1. Insights into Septin6 role in myoblast cell division

Septin6 expression was observed exclusively in dividing MuSCs, particularly at the 2dpi time point, marked by the expression of *Cdk1* (Fig. 3-2). While dividing cells express *Septin6*, differentiating myoblasts showed a significant downregulation of this septin following induction (Fig. 3-4 and 3-6). This observation aligns with the meta-analysis findings that identify *Septin6* as a robustly downregulated gene during C2C12 differentiation (Fig. 3-3, extracted from (Zhang et al., 2022)). These data suggest a potential role for *Septin6* in regulating myoblast cell division.

The detailed understanding of septin paralogue-specific functions and of the mechanisms regulating septin expression remains limited. A recent study by Simi *et al.* identified a putative binding site for Snail1, an EMT-promoting transcription factor, in a G/C-rich E-box sequence (CAGGTG) located 1kb upstream of the *Septin6* promoter (Simi et al., 2018). TGFβ1-dependent upregulation of Snail1 resulted in increased Septin6 expression in mammary epithelial cells undergoing epithelial-mesenchymal transition (EMT), promoting the EMT phenotype and multinucleation through increased persistence of the intracellular bridge (Simi et al., 2018). This effect was enhanced on a stiff ECM substrate and mediated via β1-integrin-integrin-linked kinase (ILK) signaling, while a soft ECM substrate protected against Septin6-mediated multinucleation (Rabie et al., 2021).

While EMT reprograms myogenic progenitors to migrate during developmental myogenesis, its role in post-natal myogenic differentiation is less understood (Dill et al., 2020). Snail1-driven EMT opposes *in vitro* myogenic differentiation by competing for E-box sequences of differentiation targets with Myod1. Depletion of Snail1 leads to precocious differentiation (Soleimani et al., 2012). Interestingly, our RNASeq data showed that depletion of Septin9 mildly increases (approximately by 20%) the expression of Snail1 and Septin6 in both C2C12 and primary myoblasts (data not shown). Additionally, Septin9 depletion led to a non-significant trend towards *Septin6* mRNA upregulation in proliferating C2C12 cells (Fig. 3-11D). Thus, Septin6 upregulation might play a role in myoblast differentiation downstream of EMT-promoting agents, although enhanced EMT would contradict the observed precocious differentiation in the absence of Septin9. Alternatively, upregulation of Septin6 may represent a compensation mechanism, counteracting precocious differentiation upon Septin9-depletion.

Snail1 exhibits complex regulation at multiple levels, and its gene expression does not always correlate with its functionality (Baulida et al., 2019). For instance, Snail1 could potentially be sequestered by interacting proteins such as Protein arginine methyltransferase 5 (Prmt5) (Gao et al., 2021), which we identified as an interaction partner of Septin2 along with its adaptor protein Wdr77 in myoblasts but not in myotubes (Fig. 3-31). Septins are essential for progression through cytokinesis (Menon and Gaestel, 2015; Russo and Krauss, 2021), and Septin6 expression may be regulated by Snail, an MRF, or other unidentified mechanisms to facilitate myoblast cell division as a cytokinesis-specialized septin paralogue. Alternatively, Septin6 may also be involved in the regulation of myogenic differentiation. Visualization of Septin6 in myoblasts and Septin6-depletion experiments during myogenic differentiation may shed light on the function of this septin paralogue in the differentiation process.

4.1.2. Septin4 and its isoforms: implications for myogenic and mitochondrial processes

We identified Septin4 as a differentiation-specific septin paralogue (Fig. 3-2, 3-4, and 3-6), not expressed in quiescent MuSCs or proliferating myoblasts, but upregulated during myogenic differentiation. This aligns with findings from *Gönczi et al.* (Gönczi et al., 2022), and *Zhang et al.* (Zhang et al., 2022) (Fig. 3-3), suggesting that *Septin4* may regulate myoblast differentiation. It's upregulation during differentiation and fusion stages may reflect responses to mitochondrial signaling, such as biogenesis or apoptosis (Abbas and Larisch, 2020; Larisch et al., 2000). Mitochondrial dynamics, including mitogenesis, mitochondrial fission (mitokinesis), fusion, mitophagy, and apoptosis, are tightly linked to myogenic differentiation (Lin et al., 2024; Rahman and Quadrilatero, 2023b, 2023a, 2021; Sin et al., 2016; Wagatsuma and Sakuma, 2013). Since disrupted apoptosis impairs differentiation and fusion of myoblasts (Lin et al., 2024; Rahman and Quadrilatero, 2023a), Septin4 expression may be crucial for orderly myogenic progression.

Studies show septins interact with the cytosolic GTPase Dnm1l/Drp1 to promote mitochondrial fission, and depletion of SEPTIN2 and 7 impairs fission, leading to elongated mitochondria in HeLa cells and *C. elegans* (Pagliuso et al., 2016; Sirianni et al., 2016). Moreover, Gönczi *et al.* observed impaired mitochondrial dynamics in skeletal muscle following the conditional knockdown of Septin7. They observed the formation of elongated mitochondrial networks with reduced mitochondrial DNA content, suggesting impaired

mitochondrial function in murine TA muscle. Additionally, Septin7 knockdown in C2C12 cells led to disrupted mitochondrial network organization in myoblasts (Gönczi et al., 2022). This highlights the role of septins in regulating mitochondrial dynamics in both myoblasts and adult mouse muscle. Together, these studies suggest a conserved role for septins in mitochondrial dynamics and provide evidence for mitochondria-assisted septin assembly, although the precise mechanisms remain unclear.

For a long time, Septin4 was the only septin linked to mitochondria (Takahashi et al., 2003). In rat brain, a mitochondrial variant of Septin4 (termed M-septin) is upregulated during neuronal differentiation. It transiently localizes to mitochondria during neurite outgrowth, aiding protein recruitment for axon guidance in embryonal carcinoma P19 cells (Takahashi et al., 2003). Similarly, upregulated Septin4 during myogenic differentiation and muscle regeneration may help recruit septins to dynamically reorganizing mitochondrial network in myoblasts, facilitating differentiation.

Another mitochondria-associated splice variant of *Septin4*, the apoptosis-related protein in TGF-β signaling pathway (Arts/Septin4_i2), results from intron retention in *Septin4* (Mandel-Gutfreund et al., 2011). This variant localizes to the mitochondrial outer membrane (Edison et al., 2012) and serves as a pro-apoptotic protein (Abbas et al., 2024, p. 20; Larisch et al., 2000). Not yet reported in skeletal muscle, Arts exhibits a distinct tissue expression pattern and has a separate transcription start site compared to *Septin4_i1* (Larisch et al., 2000). It lacks the first 20 amino-terminal residues and carries a Siah consensus motif for binding to the E3 ligase Siah-1 (Mandel-Gutfreund et al., 2011). The intron retention event between exon 6 and 7 results in a premature stop codon and 27 unique unstructured amino acids at the C-terminus that confer binding to Xiap, another E3 ligase (Bian et al., 2022; Mandel-Gutfreund et al., 2011). The premature stop within the G domain of Arts leads to the loss of the G4 element, which confers nucleotide specificity (Cavini et al., 2021; Larisch et al., 2000), and of the coiled-coil sequences, typical for Septin2 subgroup (Cavini et al., 2021). Consequently, Arts is presumed to be incapable of exchanging or even binding nucleotide, and potentially unable to oligomerize with other septins, as the G4 element is essential for inter-septin interaction at the G-interface (Cavini et al., 2021). The absence of the coiled coil sequences can further destabilize interactions with other septins, as these sequences stabilize the NC-interface, although polymerization is not entirely prevented without them (Sirajuddin et al., 2007; Szuba et al., 2021). Interestingly, mutations in the P-loop domain of

Arts abolish its apoptosis-inducing capability (Gottfried et al., 2004). Therefore, it remains unclear whether Arts functions as a septin-like protein with septin-independent roles or is functionally related to filament-forming septins.

Enhanced *Septin4* expression during myogenic differentiation may indicate increased expression of the pro-apoptotic Arts isoform or a shift in the Septin4 isoform ratio. This upregulation may compensate for the increased apoptotic resistance in myotubes, driven by mitochondrial signaling adjustments (Bloemberg and Quadrilatero, 2014; McMillan and Quadrilatero, 2014; Salucci et al., 2013; Sandri and Carraro, 1999; Smith et al., 2009). Myotubes exhibit enhanced anti-apoptotic ability through Apaf1 downregulation (Smith et al., 2009) and Bcl2 upregulation (Baechler et al., 2019; Dominov et al., 1998; Schöneich et al., 2014), while Xiap levels remain stable (Smith et al., 2009). The *Septin4_i2/Arts* isoform promotes apoptosis by inhibiting Xiap and Bcl2 via the proteasomal pathway and cooperating with the Transformation-related protein 53 (p53) to inhibit Bcl-Xl (Bcl2l1) (Bian et al., 2022; Hao et al., 2022). Arts overexpression induces apoptosis in various cancer cell lines by binding to Xiap (Bornstein et al., 2011; Larisch et al., 2000; Reingewertz et al., 2011), leading to its degradation and the release of active caspases (Abbas et al., 2024). Abbas *et al.* also described a feedback loop where p53 enhances Arts expression, resulting in Xiap degradation and robust apoptotic signaling (Abbas et al., 2024).

The expression of *Septin4_i2/Arts* in muscle cells or during myogenic differentiation has not been reported. It remains unclear which *Septin4* isoforms are expressed in differentiating myoblasts. The primers used in our study detect all Septin4 splice variants, without distinguishing between them. Targeting the unique C-terminal tail of Arts could differentiate it from the *Septin4_i1*. Moreover, the relationship between changes in other paralogues' expression and Septin4 upregulation, as well as Septin4's integration into filamentous structures in muscle cells, remains to be investigated.

Septin4 is also implicated in pro-apoptotic signaling. *Septin4_i2/Arts* was initially the only mammalian septin linked to apoptosis, with early research on *Tetrahymena thermophila* suggesting septin-like proteins had anti-apoptotic functions (Aravind et al., 1999; Larisch et al., 2000; Włoga et al., 2008). More recently, Wu and colleagues demonstrated that Septin4 promotes cardiomyocyte apoptosis by targeting the E3 ubiquitin ligase von Hippel-Lindau protein (VHL) to the cardioprotective HIF-1α, worsening hypoxia-induced cell death (S. Wu et

al., 2021). Septin4 interacts with HIF-1α via its GTP domain, suggesting its involvement in apoptosis regulation without excluding any isoform (S. Wu et al., 2021).

Research by the Mostowy Lab showed that Septin2 and 7 facilitate Cytochrome C release and Casp3, 7 and 9 activation in Hela cells and zebrafish larvae, highlighting the role of septins in mitochondrial apoptosis (Van Ngo et al., 2023). They proposed that septin polymers, rather than smaller entities or Arts, stabilize mitochondrial membranes during fission or apoptosis by scaffolding other interactions partners. (Van Ngo et al., 2023). This suggests that septin paralogues beyond Septin4 participate in apoptosis at the mitochondrial membrane. Further research is needed to determine if any Septin4 isoform is involved in mammalian apoptosis and whether its expression regulates myogenic differentiation.

4.1.3. Septin9: Indicator of myoblast activity and differentiation

In regenerating MuSCs Septin6 and 4 distinctly mark dividing and differentiated populations, respectively, whereas most other septins show broader expression since they are present in several MuSC populations (Fig. 3-2). Activated MuSCs begin to express additional septin paralogues such as Septin8 and 9 (Fig. 3-2). Septin8, belonging to the same subfamily of Septin10 and 11, may diversify the second outer position in the filament occupied by this subgroup (Mendonça et al., 2019; Soroor et al., 2021). Septin9 mediates the binding of septins to actin (Mavrakis et al., 2014; Smith et al., 2015) and microtubules (Bai et al., 2013; Kuzmić et al., 2022), significantly shifting the functionality and behavior of septin complexes within the cell. Notably, Septin9 expression diminishes to undetectable levels 21 days post-injury, when MuSCs are expected to return to quiescence after successful regeneration (Baghdadi and Tajbakhsh, 2018), highlighting the dynamic nature of septin expression.

This downregulation raises important questions about how septin expression changes during other transitions along the full myogenic trajectory in developing or regenerating muscle, for instance during transition from quiescent to activated MuSC state (Cao et al., 2019; De Micheli et al., 2020; Oprescu et al., 2020; Porpiglia et al., 2017). Furthermore, it is important to examine whether the protein expression of Septin9 mirrors the RNA level changes observed in regenerating MuSCs? Additionally, it is of great interest to understand septins expression in adult muscle across different ages. Advances and tools from the muscle research community offer unique opportunities to study septins in detail during both transitions along the myogenic trajectory and in stable branch points. These branch points

are represented by quiescent MuSCs, muscle fibers, and a heterogenous population of transiently amplifying progenitors (myoblasts) (Motohashi and Asakura, 2014; Tierney and Sacco, 2016). Elucidating the role of septins in stem cells is ambitious and remains an open area for future research.

We examined Septin9 expression in adult mouse TA muscle and found it localized in sarcomeres, potentially in the immobile fraction and terminal cisternae of the sarcoplasmic reticulum, but not in the Myh-positive contractile fraction (Fig. 3-19). Septin7 expression and sarcomeric organization in adult mouse muscles, correlating with muscle contractility, has previously been reported, alongside with age-dependent downregulation over four-month period (Gönczi et al., 2022). The presence of both Septin9 and Septin7 in adult muscle suggests that these septins likely form complexes within muscle fibers, as their monomeric functions have not been documented. Similarly, postnatal downregulation of septins in cardiomyocytes was noted by Ahuja *et al.*, with the hypothesis that septins may be used less in post-mitotic tissue (Ahuja et al., 2006). Furthermore, De Gasperi *et al.* demonstrated that Septin7 partially co-localizes with the adaptor protein Numb in skeletal muscle sarcomeres and interacts with Numb in C2C12 cells (De Gasperi et al., 2024). Numb levels are reduced in older individuals (Carey et al., 2007) and in muscles from 24-month-old mice (De Gasperi et al., 2022), and disrupting Numb expression leads to disorganized sarcomeres and mitochondrial networks, as well as Septin7 organization (De Gasperi et al., 2024). The authors speculate that the aging-related reduction of Numb expression may perturb Septin7 organization and impair overall physical function (De Gasperi et al., 2024). Our findings, demonstrating Septin9 expression localized to the sarcomers in adult muscle, suggest a potential structural role for Septin9 alongside Septin7 in maintaining sarcomeric organization and mitochondrial function. Given the age-dependent downregulation of Septin7 and its interaction with the adaptor protein Numb, it is plausible that similar mechanisms could regulate Septin9 in aging muscle. Investigating the expression and localization of Septin9 in aged muscle may provide deeper insights into how septins contribute to sarcomeric integrity and muscle function during aging.

Additionally, we observed a general downregulation of all septins during myogenic differentiation in C2C12 cells and primary myoblasts, raising intriguing questions about the extent of septin downregulation during muscle formation. It seems implausible that septin expression is so low as to be undetectable at the end of the differentiation process, and

myonuclei must re-express at least Septin7 and 9 in adult muscle. Currently available public data and our study cannot adequately answer this question. The transition from mononucleated MuSCs to syncytial myonuclei is challenging to target in a single-cell approach, as myonuclei, although detected, are typically bioinformatically excluded due to difficulty in distinguishing between non-injured and newly incorporated ones. Data on developmental myogenesis, such as presented by *Cao et al* (Cao et al., 2019), offer a possibility to elucidate this issue, as muscle fibers do not exist at early developmental stages like E9.5 (Biressi et al., 2007a). Lastly, an age-dependent decrease in expression in brain tissue has been demonstrated for SEPTIN3 and 5, human septins paralogues highly co-expressed in various brain tissues (Zuvanov et al., 2019). The authors speculate that these septins may be involved in cognitive decline and neurodegenerative diseases associated with advanced age (Zuvanov et al., 2019). Collectively, this underscores the potential regulatory roles of septins in myogenic contexts beyond just myogenic differentiation.

4.1.4. Early Sepitn9 protein induction and isoform variability during differentiation

The dynamics of Septin9 expression during myogenic differentiation are of particular interest, as the mechanisms of transcriptional and translational control over septin expression are largely unknown. Regenerating muscle datasets have shown an early induction of core septins expression to varying degrees (Fig. 3-2). Specifically, septins are induced at 0.5 dpi, a highly dynamic stage of regeneration characterized by a marked immune response and subsequent steps of MuSC activation, cell cycle entry, and terminal differentiation (Relaix and Zammit, 2012). The profound changes in Septin9 expression profile suggest that some factors may stimulate its expression during the early stages of regeneration. Notably, core septins maintain high expression levels until 21 dpi, when MRFs and inflammatory signaling diminish, indicating the completion of the regeneration process (Baghdadi and Tajbakhsh, 2018). This supports the involvement of factors driving regeneration in the transcriptional modulation of septin expression.

In this study we identified two long isoforms of Septin9 alongside one short splice variant, which lacks the unstructured N-terminal extension. It will be important to investigate the prevalence of these alternatively spliced Septin9 variants during changes in expression observed in regeneration datasets. While many septin genes produce several splice variants,

Zuvanov *et al*. argue for the coordinated expression of the predominant isoform (Zuvanov et al., 2019). By analyzing human septin expression in the GTEx database, the authors calculated the average proportion of each isoform across various tissues, concluding that most steady-state complexes formed in a cell are expected to be uniform in isoform composition (Zuvanov et al., 2019).

There is some conflicting evidence regarding which specific Septin9 N-terminal extension enables septins to cross-link actin filaments *in vitro* (Iv et al., 2021; Smith et al., 2015). Moreover, Martins *et al.* demonstrated that a non-dimerizing Septin9 mutant (or a Septin9 knockdown) abolishes the association of septins with actin stress fibers in U2OS cells (Martins et al., 2022). While these findings suggest that distinct Septin9 variants contribute differently to septin filament organization, it remains to be elucidated how Septin9 isoforms affect septin complex formation and interaction with actin filaments in myoblasts.

The dynamic expression of Septin9 at the protein level during myogenic differentiation in both C2C12 cells and primary myoblasts further supports its regulatory role in myogenic differentiation (Fig. 3-4G and Fig. 3-6F). Both cell lines exhibit increased Septin9 expression 12 hours after induction of differentiation (Fig. 3-S1). However, due to the absence of comprehensive RNA data at this 12-hour time point, it is unclear whether protein regulation mirrors RNA changes. The induction of Septin9 in regenerating MuSCs suggests a potential link to factors regulating myogenic differentiation, although the expression of Septin9 mRNA in myoblasts needs to be investigated separately. We hypothesize that enhanced expression of Septin9 mRNA must occurs rapidly, within the first 12 hours of differentiation. Moreover, a translational or protein stabilizing effect at the beginning of differentiation might be responsible, although this has not been previously demonstrated for septins, to the best of my knowledge.

Understanding the early upregulation of Septin9 could enhance our mechanistic knowledge of regulatory processes behind septin expression and tissue distribution. Overall, we observed a global downregulation of multiple ubiquitous septins during myogenic differentiation, except of Septin4 (Fig. 3-4 and 3-6). Less abundant myoblast septins, including Septin5, 8, and 10, may play redundant roles or help diversify and fine-tune the core septin protomer composition, likely consisting of Septin2-11-7-9 paralogues. They may also engage in core filament-independent functions, although hetero-oligomerization appears to be an obligatory mechanism of septin activity (Ivanov et al., 2021). Septins represent an

understudied family of proteins in the myogenic context, potentially playing regulatory roles during and beyond myogenic differentiation. They could maintain the homeostasis and organization of MuSCs or of the adult muscle tissue, and could regulate orderly progression during transition states, such as muscle cell development and regeneration, hence it is of crucial to elucidate their expression and subcellular organization.

4.2. First insights into septin reorganization during myogenic differentiation

Myogenic differentiation induces not only changes in gene expression but also distinct alterations in the morphology of proliferating myoblasts as they transition into terminally differentiated contractile fibers (Chal and Pourquié, 2017; Relaix and Zammit, 2012). Initially, myoblasts transform into fusion-competent myocytes, and their subsequent fusion gives rise to new myotubes. These complex cellular transitions are accompanied by the reorganization of various cytoskeletal proteins (Sampath et al., 2018; Schejter, 2016), including actin (Bruyère et al., 2019; Duan and Gallagher, 2009; Nowak et al., 2009; Städler et al., 2010; Swailes et al., 2006, 2004) and tubulin (Becker et al., 2020; Lu et al., 2001; Lucas and Cooper, 2023; Musa et al., 2003; Tassin et al., 1985). In this study, we investigated the organization of Septin9 in myoblasts, elucidating the dynamic changes in Sepint9 distribution during the progression from proliferating to differentiated muscle cells.

To characterize these dynamic changes in septin reorganization, we generated a C-terminal meGFP-Septin9 C2C12 cell line, which enables visualization of all endogenous Septin9 splice variants produced via N-terminal alternative splicing (Connolly et al., 2011; Verdier-Pinard et al., 2017). Using live confocal and TIRF microscopy, we examined the subcellular reorganization of septins during myogenic differentiation with high resolution. Our observations revealed that in proliferating myoblasts, septins primarily associate with contractile actin structures near the plasma membrane (Fig. 3-7, 3-12 and 3-15). As cells transition to fusion-competent myocytes, septins gradually dissociate from these actin structures (Fig. 3-8, 3-9 and 3-15). In myotubes, septins are found in membrane proximity as filamentous remnants, and mostly as short rods and rings dispersed throughout the sarcoplasm (Fig. 3-7, 3-12 and 3-13).

In the following chapters, I will discuss the potential regulatory mechanisms that could influence septin organization in myoblasts and explore the possible cellular consequences of septin reorganization.

4.3. Putative causes of Septin9 reorganization during myogenic differentiation

Understanding the causes of the remarkable reorganization of septins during myoblast differentiation is complex, as the knowledge about upstream regulators of septin organization is limited. The following chapters discuss potential regulators of the septin cytoskeleton.

4.3.1. Rho GTPases

Rho GTPases are key regulators of cytoskeletal organization (Etienne-Manneville and Hall, 2002; Narumiya and Thumkeo, 2018), and may influence septin reorganization. Dominant-negative mutants of RhoA, Cdc42 and Rac1 disrupt both actin and septin organization (Schmidt and Nichols, 2004). While, RhoA has not been shown to directly regulate septins, it's reduced activity could lead to septin disassembly via actin stress fiber downregulation (Brunton et al., 2004; Burridge and Guilluy, 2016). Additionally, acute activation of photoactivatable Rac1 recruited Septin7 to the cell periphery in NRK cells, although the underlying mechanism remains unclear (Merenich et al., 2022). Cdc42, however, has been convincingly shown to affect septin localization through Borg proteins (Tomasso and Padrick, 2023), which directly bind to septins (Joberty et al., 2001; Sheffield et al., 2003). With some exceptions (Salameh et al., 2021), Cdc42 displaces Borg proteins from thick septin filaments, which Borgs promote, thereby regulating actin stress fiber organization in cells (Tomasso and Padrick, 2023). Cdc42, and to lesser extend RhoA, appear to be potential upstream effectors of septin reorganization during myoblast differentiation.

The role of Cdc42 in myogenic differentiation is debated. Constitutively active Rac1/Cdc42 has been shown to activate the Myogenin promoter (Takano et al., 1998), while dominant negative Rac1/Cdc42 mutants impair Myogenin expression and p38 activity, indicating that these GTPases are necessary for differentiation (Meriane et al., 2000). However, most studies suggest a negative role for Rac1/Cdc42 in differentiation, based on activating mutations in various models (Gallo et al., 1999; Heller et al., 2001; Meriane et al., 2002, 2000; Travaglione

et al., 2005). Interestingly, depletion of Rac1/Cdc42 did not affect the *in vivo* differentiation of myogenic progenitors derived from Lbx1cre mice, which undergo recombination in myogenic progenitor cells migrating to targets such as limbs (Jagla et al., 1995; Vasyutina et al., 2009). Instead, Cdc42 appears crucial in later stages of differentiation, with its activity increasing towards myoblast fusion in cultured myoblasts (Travaglione et al., 2005). Indeed, Cdc42, Rac1, and their effectors Pak1 and Pak3 are essential for myoblast fusion (Charrasse et al., 2007; Joseph et al., 2017; Vasyutina et al., 2009). Therefore, the observed reorganization of Septin9 in this study may be driven by Cdc42, as C2C12 cells express at least Borg2, 4, and 5, which can mediate Cdc42-induced septin disassembly (Fig. 6-1 and 6-2). We also observed interactions between Septin9 and exogenous rat Borg1-5 proteins, as well as wild type, constitutively active or dominant negative Cdc42. Additionally, Borg1-5 localize to septin filaments in C2C12 cells (Fig. 6-1 and 6-2). While Cdc42's influence was not explored in depth here, it likely plays a role in septin reorganization during differentiation.

The role of RhoA in myogenic differentiation is not fully understood. Early studies, primarily conducted in C2C12 cells, demonstrated that introduction of constitutive active (ca) or wild type RhoA promotes muscle-specific gene expression (Dhawan and Helfman, 2004; Meriane et al., 2000; Takano et al., 1998; Wei et al., 2000, 1998). In contrast, later studies reported that caRhoA is dispensable for the progression of myogenic differentiation (Castellani et al., 2006; Nishiyama et al., 2004). Nevertheless, dominant negative RhoA (dnRhoA) mutant or RhoA inhibitor C3 have been shown to block myogenic differentiation (Takano et al., 1998; Wei et al., 1998), which conflicts with studies reporting no impaired myogenic differentiation upon dnRhoA introduction (Dhawan and Helfman, 2004).

Recent research has shown that RhoA is crucial for muscle development and regeneration, highlighting its significant role in regulating both embryonic and adult myogenesis (Noviello et al., 2023, 2022; Saclier et al., 2020; Taglietti et al., 2018). Despite the initial controversial findings, RhoA is considered essential for initiating the myogenic program by stimulating Serum response factor (Srf)-mediated muscle-specific gene expression, actin remodeling, and by maintaining myoblasts in a proliferative state (Burridge et al., 2019; Carnac et al., 1998; Dhawan and Helfman, 2004; Meriane et al., 2000; Miralles et al., 2003; Sotiropoulos et al., 1999; Takano et al., 1998; Wei et al., 1998). Later, RhoA exhibits an activity pattern opposite to that of Cdc42 and Rac1 and must be inhibited to induce cell cycle exit and efficient fusion (Castellani et al., 2006; Iwasaki et al., 2008; Meriane et al., 2000). These oscillations between

high and low RhoA activity in dividing and differentiating myoblasts have been demonstrated *in vitro* (Charrasse et al., 2006; Nishiyama et al., 2004).

One of the principal effectors of Rho GTPase is the Rho-associated kinase (Rock) (Bishop and Hall, 2000; Guan et al., 2023; Watanabe et al., 1997). RhoA utilizes Rock to regulate the actin cytoskeleton in myoblasts, but recent research suggests that Rock has also RhoA-independent roles in myogenesis (Castellani et al., 2006). Notably, Rock1 functions as a negative regulator of myogenic differentiation, preventing myoblast fusion (Castellani et al., 2006; Charrasse et al., 2006; Iwasaki et al., 2008; Nishiyama et al., 2004). Rock1 activity maintains myoblasts in a proliferative state and decreased as myoblast fusion approaches (Castellani et al., 2006). Despite some controversy (Pelosi et al., 2007; Wei et al., 2000), constitutively active Rock1 (but not caRhoA) inhibits Myogenin expression, while its inhibition through Y27632, siRNA, or miR-148a promotes lineage progression and myoblast fusion (Castellani et al., 2006; Iwasaki et al., 2008; Zhang et al., 2012). Although not directly tested in our study, the decreased activity of RhoA-Rock axis in differentiating myoblasts could potentially offer another, albeit indirect, mechanism for septin reorganization via actin stress fiber disassembly.

Rather than acting individually, Cdc42 and RhoA could converge in myoblasts and act in concert to facilitate septin reorganization. In studies of non-muscle cell types, Rho GTPase pathways often counteract each other. Specifically, cellular responses mediated by Rac1/Cdc42 are usually antagonistic to those of RhoA (Bryan et al., 2005). For instance, Cdc42 and Rac1 promote cellular protrusion formation, while RhoA mediates cell retraction in 3T3 fibroblasts (Hall, 1998; Maddox and Burridge, 2003; Ridley et al., 1992; Ridley and Hall, 1992). Similarly, in neurons, RhoA promotes growth cone collapse, while Cdc42 and Rac1 stimulate neurite outgrowth (Etienne-Manneville and Hall, 2002; Mackay et al., 1995; Nikolic, 2002). In contrast, focal adhesion formation is characterized by increased Rac1 activity, while RhoA activity is reduced (Lawson and Burridge, 2014). Then, FA maturation requires increase of RhoA activity to mediate stress fiber assembly and actomyosin contractility (Lawson and Ridley, 2018; Salloum et al., 2020). This highlights the sequential action, rather than antagonism, of Rac1 and RhoA in FA formation and maturation. In myotubes, Rac1 acts upstream of RhoA and its transient activation leads to the initial localization of acetylcholine receptors (AChR), while RhoA facilitates condensation and maturation of AChR clusters (Weston et al., 2003).

The dynamic activity of Rho-GTPases during myogenic differentiation was elucidated by Travaglione *et al* (Travaglione et al., 2005). They detected active form of RhoA in dividing C2C12 cells and demonstrated a loss of activation during the first day of differentiation, with activation levels returning to those observed in proliferating cells three days after myogenic induction. Active Rac1 was detected in proliferating and differentiating myoblasts, declining only after 24 hours of differentiation. Active Cdc42 was not detected in dividing myoblasts but accumulated after the onset of differentiation and remained high for three days. This evidence implies that the functions of GTPases during differentiation are not sharply opposed. Furthermore, Travaglione *et al.* argue that free cycling Rac1,Cdc42 and Rho from inactive to active states is crucial for myogenic differentiation (Bryan et al., 2005; Travaglione et al., 2005).

Further studies should elucidate whether concerted changes in Rho GTPase activities, such as during FA formation and maturation, or their separate actions, could impact septin reorganization during terminal differentiation of myoblasts.

4.3.2. Relocalization between different subcellular compartments, a peculiarity of septins

Septins can switch between various interaction partners, such as other cytoskeletal components or phospholipid membranes, depending on the physical proximity and abundance of the interaction substrates (Spiliotis, 2018). Septin reorganization during myogenic differentiation may be caused, at least in part, by changes in actin organization or by the detachment of septins from plasma membrane-bound actin fibers. Septins can shift away from actin under the influence of various actin depolymerizing toxins, such as C3 exoenzyme, Cytochalasin D (Kinoshita et al., 1997), Latrunculin (Kinoshita et al., 2002), or *Clostridium difficile* transferase (CDT) (Nölke et al., 2016). Treatment with CDT, and to a lesser extent with latrunculin, results in the formation of MT-based protrusions and membrane translocation of septins, which accumulate at the base of the protrusion and guide the MT growth into the emerging protrusions (Nölke et al., 2016). These toxin—induced protrusions share basic functional and structural features with microtentacles - MT-based protrusions formed upon detachment and rounding of adherent tumor cells (Østevold et al., 2017). Østevold *et al.* demonstrated that septins localize to actin in adherent cells; however, upon detachment of tumor cells, actin and septin structures reorganized substantially. Specifically,

changes in actin included initial contraction of actin filaments, followed by reduced perinuclear density and increased cortical density. Septin filaments, instead, lost localization to actin, disassembled and redistributed to the plasma membrane. Given that toxin-indued protrusions and microtentacles are hypothesized to be driven by Cdc42 activity, and that septins can transition from associating with actin to the plasma membrane to initiate protrusion formation, it is plausible that Cdc42 may play a role in facilitating the detachment of septins from actin filaments (Nölke et al., 2016; Østevold et al., 2017).

Previous research demonstrated that octamer-based septin complexes anchor actin filaments to the plasma membrane (Martins et al., 2022). Using TIRF microscopy, we observed long, straight septin filaments in proliferating cells, while in differentiating myoblasts, septins appeared as short, curvy rods in close proximity to the plasma membrane (Fig. 3-15 and 3-16). Furthermore, in differentiating myoblasts, septins dissociated from actin filaments (Fig. 3-8). These findings suggest that septins may only anchor actin to the plasma membrane in dividing myoblasts. It is conceivable that septin filaments co-localizing with actin in cycling myoblasts could either dissociate from actin and translocate to the plasma membrane or release the membrane-bound actin filaments during differentiation, subsequently transforming into curvy rather than long, straight filaments.

Additionally, septins have been shown to shift onto MTs from other cellular compartments. For instance, septins translocate onto MT from actin stress fibers in hepatocyte HHL16 cells upon treatment with the taxol-based drug paclitaxel (Salameh et al., 2021). Akil *et al.* demonstrated the association of septins with phosphatidylinositol 5-phophate (PI5P)-containing lipid droplets, and that this association may result in the switch of septins to MTs, due to the spatial proximity of these two organelles (Akil et al., 2016). Furthermore, it has been proposed that septins translocate onto cytokinetic bridge MTs from the proximal plasma membrane during the constriction of the cleavage furrow in cytokinetic cells; however, the decoration of bridge microtubules by a newly assembled pool of septin filaments cannot be ruled out (Russo et al., 2024). Although, we cannot exclude the possibility of septins switching onto MTs during myogenic differentiation, it seems unlikely, as we observed only poor colocalization of septins with MTs in myoblasts and myotubes (Ugorets et al., 2024).

Instead of hopping onto MT, septins could potentially switch to intermediate filaments (IFs). Interestingly, this type of septin relocalization has not yet been demonstrated. Besides actin and tubulin, intermediate filaments undergo profound reorganization during myogenic

differentiation (Hakibilen et al., 2022; Jabre et al., 2021) and represent another extensive network of cytoskeletal polymers (Abe et al., 2004; Charrier et al., 2018). Devlin *et al.* identified IFs as interaction partners of several SEPTIN9 isoforms through proteomic profiling in MCF-7 cells (Devlin et al., 2021). Furthermore, SEPTIN12 has been shown to interact with the nucleo-cytoskeleton LAMINB1 and the nuclear membrane linker SUN4 during human spermatogenesis, with its exogenous expression interfering with LAMINA/C distribution during sperm morphogenesis (Yeh et al., 2019, 2015). Whether septins interact or co-localize with IFs in myoblasts or myotubes remains to be elucidated in future experiments.

4.3.3. A change of actin filament decoration

The observed dissociation of Septin9 from actin may be attributed to increasing competition from muscle-specific actin binding proteins or changes in actin expression levels. Notably, changes in septin organization were observed only in a subset of Myogenin-positive cells at the onset of myogenic differentiation (Fig. 3-8), suggesting that these organization changes could follow the initial transcriptional changes in myoblasts expressing terminal differentiation markers. Several actin-binding proteins have been reported to change expression and organization during the transition from myoblasts to myotubes, including conventional and unconventional myosins (Hoh, 2023; Lehka et al., 2020; Swailes et al., 2006; Wells et al., 1997), and α-actinin (Salucci et al., 2015). Therefore, it is plausible that Septin9 may encounter competition from muscle-specific actin binders during differentiation.

We and others (Salucci et al., 2015; Ugorets et al., 2024) have described skeletal α-actinin as localizing to FAs in myoblasts and co-aligning with actin in myocytes and myotubes, facilitating the formation of sarcomeres (Fig. 3-9 and 3-14). Notably, α-actinin did not exhibit colocalization with Septin9 throughout differentiation, despite the close proximity observed between these two proteins. This is consistent with the lack of direct interaction between septins and actinins.

Skeletal myosins represent another protein family that could interfere with the septin-actin interaction. Skeletal muscle expresses up to twelve myosin heavy chain proteins that bind to sarcomeric and sarcoplasmic actin filaments (Hoh, 2023), as opposed to the seven myosins previously described for myoblasts (Wells et al., 1997). This increased amount of myosin proteins could translate into higher occupation of actin binding sites in differentiated muscle cells. Although initially demonstrated to require anillin (Kinoshita et al., 2002) or myosin II(Joo

et al., 2007) for binding to actin, septins are now shown to directly bind and bundle actin in flies (Mavrakis et al., 2014) and mice (Dolat et al., 2014b). Furthermore, Septin9 has been demonstrated *in vitro* to bind actin in several modes, including a myosin-independent mode and a mode where Septin9 competes with myosin for the binding site. Binding to the F-actin site shared with myosin could inhibit myosin ATPase activity and modulate acto-myosin activity (Smith et al., 2015). Notably, besides myosin II (Joo et al., 2007), proteomic analysis suggest septins to interact with processive myosins such as Myo6 (Hecht et al., 2019; O'Loughlin et al., 2018). It would be of interest to unravel the nature of interaction between septins and muscle-specific non-processive and processive myosins. In our study, we did not address interactions with skeletal nor non-muscle myosins directly, and it remains to be elucidated if these proteins can outcompete septins from actin during myogenic differentiation.

As mentioned above, the interaction of septins with actin could be modulated by the prevalence of different actin isoforms. Undifferentiated myoblasts are characterized by the expression of cytoplasmic β- and γ-actin, which are gradually downregulated during differentiation. Elongated prefusion myoblasts express α- cardiac (αCAA, Actc1) and α-smooth muscle actin (αSMA, Acta2), while α-skeletal muscle actin (αSKA, Acta1) is detected only in multinucleated cells (Dwyer et al., 2011; Lancioni et al., 2007; Tondeleir et al., 2009). Despite high conservation, skeletal and non-skeletal actins exhibit different conformations in their N-termini due to sequence variations (Arora et al., 2023). These variations dictate different biochemical interactions with actin-binding proteins (Arora et al., 2023), myosin motors, and. and fine-tune the enzymatic output of the motors, allowing them to perform specialized functions. For instance, non-sarcomeric myosins exhibit faster ATPase activity and increased *in vitro* sliding velocity along non-muscle actins compared to muscle actins (Müller et al., 2013). This isoform-specific regulatory mechanism may also extend to other actin-binding proteins (Arora et al., 2023). Work from the Mavrakis lab demonstrated the co-polymerization of skeletal rabbit actin with human SEPTIN2/6/7 (Mavrakis et al., 2014). In contrast, sedimentation assays using pre-polymerized muscle or non-muscle actin from human platelets showed no interaction with septin complexes; only monomeric SEPTIN9 co-sedimented and bundled these actin filaments (Dolat et al., 2014b; Kinoshita et al., 2002; Smith et al., 2015). This discrepancy may be attributed to septins' preference for co-polymerizing with actin rather than binding to pre-formed filaments. However, the possibility

that the sequential expression of sarcomeric actins during myogenic differentiation influences the nature of septin-actin interaction cannot be excluded.

Moreover, the reorganization of septins during myogenic differentiation could be also caused by changes in the composition of septin filaments and the prevalence of alternatively spliced variants. Research indicates that the type of Septin9 isoforms present within the octamer dictates the septin filaments subcellular localization and organization into long or short structures (Iv et al., 2021; Kuzmić et al., 2022; Martins et al., 2022; Verdier-Pinard et al., 2017). Sequence differences between splice variants could also diversify the interactions with binding partners, and the post-translational modification profile of the filament. For instance, long SEPTIN9_i1 harbors serines, threonines, and lysines for phosphorylation, ubiquitylation, sumoylation, acetylation, and methylation (Devlin et al., 2021; Estey et al., 2013; Hernández-Rodríguez and Momany, 2012; Sharma and Menon, 2023). Acetylation and methylation sites are absent from the short variants SEPTIN_i4 and SEPTIN_i5. Additionally, the shortest variant, SEPTIN9_i5, lacks also phosphorylation and sumoylation sites (Devlin et al., 2021). Moreover, Devlin *et al.* demonstrated that SEPTIN9 splice variants exhibit different affinities for other septin paralogues, with shorter SEPTIN9 isoforms showing more promiscuous binding with septins from the SEPT6 group (Devlin et al., 2021). Specifically, all isoforms exhibited binding to SEPTIN8, SEPTIN9_i4 and SEPTIN9_i5 interacted also with SEPTIN11, while only SEPTIN9_i5 strongly coprecipitated with SEPTIN6 as well. The authors speculate that the length of the NTE of SEPTIN9 could modulate the binding to other paralogues, as truncations could expose more promiscuous binding sites. This is consistent with previous findings for the NTE of the yeast septin Cdc3, which influenced interaction with other septins through allosteric inhibitory interaction with its own G-domain (Devlin et al., 2021; Weems and McMurray, 2017).

In this study, we described changes in septin organization that occur 12-24 hours after the induction of differentiation, appearing in some Myogenin-positive cells (Fig. 3-8). During this brief window, we would not expect profound transcriptional changes associated with myogenic differentiation to result in substantial stochiometric shifts in septin paralogue expression, leading to septin reorganization. However, some immediate transcriptional regulation cannot be entirely excluded. This conclusion is supported by our analysis of Septin2 interaction partners in myoblasts and myotubes, which showed no significant change in inter-septin interactions despite observed transcriptional changes at the mRNA level for

various septins (Fig. 3-4 and Table 3-1). The lack of changes in interaction preference could be attributed to a low differentiation index of C2C12 cells, even though myotube formation is readily observed after five days. Notably, septin mRNA and protein levels do not necessarily correlate directly, as seen with actin isoforms, where discrepancies between relative protein and mRNA levels suggest the involvement of transcriptional or translational stabilization mechanisms (Tondeleir et al., 2009). Additionally, Zuvanov *et al.*, after analyzing the expression of human *SEPTIN* genes in the GTeX atlas, propose a rather uniform and monotonous composition of septin filaments within each cell type, despite vast theoretical possibilities for variation (Zuvanov et al., 2019). This observation argues against significant stochiometric shifts in septin complex composition. However, the expression profiles of septin paralogues during different stages of development, regeneration, or aging, which encompass various states of a tissue, remain largely unexplored.

Together, investigating the expression patterns of Septin9 isoforms in muscle cells could provide valuable insights into the diversity of interactions between septin paralogues and between septins and other proteins during myogenic differentiation. Understanding these interactions could further elucidate how Septin9 isoforms specifically regulate filament integrity and actin organization. It remains to be determined whether and how the septin interactome adapts during the transition from proliferating myoblasts to differentiated myocytes, reflecting changes associated with myogenic differentiation.

4.4. Organization of septins during myoblast fusion

Fusion-competent myocytes undergo profound cytoskeletal reorganization during the steps leading to fusion, including migration, cell-cell adhesion, and membrane coalescence (Bruyère et al., 2019; Lehka and Rędowicz, 2020b). We observed a pronounced reorganization of septins during myoblast fusion (Fig. 3-17). Indeed, differentiated myotubes exhibit a distinct septin organization compared to proliferating myoblasts (Fig. 3-12 and 3-13). The mechanisms hypothesized in the previous chapter may also contribute to septin organization during myoblast fusion and could possibly act in concert with additional factors orchestrating myotube formation.

For example, Rho GTPases are also prominent regulators of myoblast migration and fusion, as elegantly reviewed in detail in (Bryan et al., 2005; Lehka and Rędowicz, 2020b; Rodríguez-Fdez and Bustelo, 2021). However, given the limited knowledge about the upstream

regulation of septin organization and the limited resolution of the fusion process investigated here, the discussion on this aspect of septin organization will be combined with the following chapter. The following chapter will focus on the putative role of septin reorganization during differentiation and fusion.

4.5. Putative roles of Septin9 during myoblast differentiation

Depletion of Septin9 in myoblasts resulted in complete disruption of septin filaments, as observed through conventional light microscope (Fig. 3-11). Surprisingly, proliferating Septin9-deficient myoblasts exhibited a precocious onset of myogenic differentiation. This was detected by a premature switch from the proliferating to the differentiating program via bulk mRNA-sequencing (Fig. 3-20), premature expression of terminal differentiation markers (Fig. 3-26), and an increased differentiation index (Fig. 3-26). These alterations were accompanied by signs of reduced viability, including lower cell expansion (Fig. 3-27 and 3-28) and increased apoptosis (Fig. 3-29 and 3-30). This chapter will discuss these effects in detail and reconcile them with available literature on the contribution of septins to myogenic differentiation.

4.5.1. Septin9 is essential for septin oligomerization in myoblasts

According to the “Kinoshita Hypothesis”, which proposes preassigned positions of septin subgroups within a septin oligomer, there could be up to 60 possible combinations of septin octamers (Cavini et al., 2021; Kinoshita, 2003). However, due to the predominant expression of myoblast-specific paralogues (Fig. 3-1, 3-2 and Table 1) and to the temporal regulation of others, this number is likely reduced to only eight possible combinations of octamers. However, the actual formation of these combinations and their physiological relevance remain to be elucidated. Zuvanov *et al.* performed an analysis of co-expression of all possible septin pairs in human tissues, reporting SEPTIN2, 7 and 10 (and to a lesser extent SEPTIN11) as consistently co-expressed paralogues in tissues other than brain. Interestingly, the authors identified also a limited number of specialized complexes, as those containing Septin3 and Septin5 in the brain (Zuvanov et al., 2019). Here, based on our data, we propose that Septin2-7-11 and 9 are good candidates for myogenic protomer formation, and the depletion of one of these core paralogues may lead to the disruption of myogenic septin complexes.

In this study, we demonstrated the lack of higher-order septin structures in myoblasts deficient of Septin9. Upon Septin9 knockdown, Septin2 and Septin7 were diffusely distributed in the cytosol (Fig. 3-11A-B). This disruption is not due to the downregulation of other core septins, as their mRNA levels remain unchanged (Fig. 3-11C-D, protein levels not shown). Given that the length of a hexamer is approximately 25nm (Sirajuddin et al., 2007), the theoretical possibility of forming septin hexamers and small rods, which cannot be resolved using conventional microscopy, remains. However, these short structures may unlikely be able to compensate for octamer-dependent functions. Recent work argues for Septin9-containing complexes as the prevalent form of septin complexes that interact with actin filaments at the plasma membrane, as well as disruption of Septin9 dimerization abolished association of septins with actin filaments (Martins et al., 2022). Therefore, we hypothesize that Septin9 is an integral part of the myoblast septin cytoskeleton and that it potentially mediates actin decoration with septin complexes.

The observed changes in expression of certain paralogues during myogenic differentiation pose another interesting question. It remains to be elucidated whether other septins such as Septin4, 5, 6, 8, and 10 are incorporated into the core complex and how their stoichiometry varies throughout the process, if at all. Particularly, the stoichiometry of curved septin filaments observed during differentiation (Fig. 3-15) is another intriguing question. This can potentially be addressed using a split-GFP system, as described by Martins *et al* (Martins et al., 2022), to probe inter-septin interactions.

4.5.2. The role of Septin9 as a RhoGTPase scaffold in myogenic differentiation

This study demonstrates that Septin9 plays a crucial role in maintaining the orderly progression of myoblast differentiation. Disrupting septin reorganization leads to premature *in vitro* differentiation. This chapter discusses the potential physiological consequences of septin reorganization and elucidates potential deregulated mechanisms that lead to accelerated differentiation upon Septin9 depletion.

Septin9 may enable septin filaments to integrate RhoA signaling in proliferating or differentiating prefusion myoblasts. The role of RhoA in myogenic differentiation is controversial. The RhoA/Rock1 axis is critical for maintaining MuSC quiescence by preserving cellular tension, shape, and niche retention (Eliazer et al., 2019), and is also crucial in muscle development and regeneration by repressing JunB and Nuclear factor I X (Nfix) expression,

while regulating Erk activity (Saclier et al., 2020; Taglietti et al., 2018). In C2C12 cells, RhoA/Rock1 is essential for initiating the myogenic program via Srf-mediated gene expression (Burridge et al., 2019; Carnac et al., 1998; Miralles et al., 2003; Sotiropoulos et al., 1999; Wei et al., 1998). Although some studies in C2C12 report endogenous RhoA not to be required for attaining terminal differentiation (Castellani et al., 2006). A recent study in sorted MuSCs found that RhoA is dispensable for terminal differentiation, as myoblasts lacking RhoA showed even increased differentiation index, although the mechanism remains unclear (Noviello et al., 2023).

Septins may scaffold RhoA signaling in myoblasts, as Septin9 depletion increases myogenic differentiation (Fig. 3-26), partially phenocopying the absence of RhoA. The link between Rho GTPases and septins has been previously reported (Hickson and O'Farrell, 2008; Ito et al., 2005; Piatti, 2020; N. Wang et al., 2015). Additionally, SEPTIN11 promotes the phosphorylation of RhoA-specific GEF-H1, activating RhoA and downstream pathways like ROCK1, LIMK/Cofilin, and FAK/Src, driving cell migration and invasion in Hepatocellular carcinoma (HCC) (Fu et al., 2023). Furthermore, SEPTIN9 binds septin-associated RhoGEF (saRhoGEF)/ ARHGEF18 (Nagata and Inagaki, 2005; Safavian et al., 2023), initially thought to inhibit RhoA signaling (Nagata and Inagaki, 2005). However, Trimble's lab showed that this inhibition is likely due to SEPTIN9 overexpression alone, while overexpression of the whole septin complex promotes ARHGEF18 activation and RhoA signaling in hTERT-RPE1 cells (Safavian et al., 2023). Thus, intact septin complexes may scaffold RhoA-specific GEFs, targeting RhoA signaling to actin stress fibers near the plasma membrane, preventing premature differentiation. The precocious myogenic differentiation observed in this study (Fig. 3-26) may result from disrupted RhoA signaling due Septin9 depletion, causing dissociation of RhoA-specific GEFs from actin, mimicking the increased myogenic differentiation in RhoA absence.

While RhoA signaling is crucial for myoblast fusion, its activity must be reduced for efficient fusion to occur (Castellani et al., 2006; Nishiyama et al., 2004; Noviello et al., 2023; Takano et al., 1998). Despite this, fusion in Septin9-deficient myoblast proceeds normally (Fig. 3-26E-G). This may be explained by the presence of cycling RhoA that can be inhibited as myocytes approach fusion, or by differing roles of RhoA or its interaction partners during fusion compared to differentiation or proliferation (Noviello et al., 2023). Interestingly, inhibiting RhoA/Rock1 during proliferation suppresses myotube formation, whereas inhibition during

differentiation enhances the myogenic potential of C2C12 cells (Iwasaki et al., 2008). In proliferating myoblasts, RhoA maintains myoblast identity by regulating Myod1 expression and promoter activity through Srf. In contrast, inhibition of RhoA but not Rock1, reduces Myod1 expression, suggesting a Rock1-independent roles for RhoA (Carnac et al., 1998; Dhawan and Helfman, 2004; Gauthier-Rouviere et al., 1996). Furthermore, an active Rock1 mutant, but not caRhoAV14, inhibited Myogenin expression, suggesting that RhoA and Rock1 do not always act in a cascade and that Rock1 may integrate signals from other pathways, such as Raf1 kinase (Castellani et al., 2006). Interestingly, Y27632 treatment mimics the cell shape changes caused by C3 transferase and inhibits stress fiber formation by caRhoA, indicating that Rock acts downstream of RhoA in regulating cytoskeletal organization in C2C12 cells (Castellani et al., 2006; Dhawan and Helfman, 2004). Surprisingly, however, RhoA-deficient myoblasts showed no defects in F-actin organization or changes in expression for fusion-related genes like *Myomaker* (*Mymk*) and *Myomerger (Mymx)*. Moreover, expression of *Srf*, the RhoA-dependent fusion regulator, remained unchanged, potentially explaining the lack of actin disruption. Indeed, Srf depletion disrupts actin organization and impairs fusion but not differentiation (Randrianarison-Huetz et al., 2017). Since RhoA- and Srf-depleted cells showed distinct gene regulation, Noviello *et al.* suggest that impaired fusion following RhoA depletion is independent of cytoskeletal failure and of the RhoA-Srf axis. This supports the notion that RhoA may interact with different partners and effectors in dividing and fusing myoblasts (Noviello et al., 2023).

Notably, RhoA depletion did not affect Myogenin expression (Castellani et al., 2006; Noviello et al., 2023), while partial depletion of Septin9 increased *Myogenin* mRNA levels in both dividing and differentiating myoblasts (Fig. 3-26B). This may be linked to altered signaling downstream of RhoA. RhoA signaling, mainly through Rock1 and mDia, promotes actin polymerization, contractility, and filament bundling (Burridge et al., 2019), while the Srf/Mrtf-A complex, inhibited by G-actin, transduces RhoA signals into the nucleus (Esnault et al., 2014; Randrianarison-Huetz et al., 2017; Selvaraj and Prywes, 2003). Moreover, Rock1-dependent phosphorylation of Foxo1 sequesters it in the cytoplasm, allowing Myocardin-related transcription factor A (Mrtf-A) / Smad complex formation and preventing premature myoblast differentiation (Iwasaki et al., 2008). Studies showed that inhibiting or depleting Rock1 (Castellani et al., 2006; Iwasaki et al., 2008; Nishiyama et al., 2004; Zhang et al., 2012) or depleting Mrtf-A (Holstein et al., 2020; Song et al., 2021) increases Myogenin expression.

Thus, Septin9 depletion may reduce Rock1 or Srf/Mrtf-A activity, increasing Myogenin expression, and disrupting only these specific branches of RhoA signaling. Septin9 depletion may impair Rock1 activity through both RhoA-dependent and -independent mechanisms. For instance, Septin2 scaffolds Myosin II activation by CRIC and ROCK during cytokinesis in CHO-K1 cells (Joo et al., 2007),while, SEPTIN9_i1 and SEPTIN11 activate the RHOA/ROCK1 cascade in MCF7 and HCC cells, respectively (Fu et al., 2023; Zeng et al., 2019). Septin depletion could also lead to increased G-actin accumulation due to reduced stress fiber bundling and stability (Dolat et al., 2014b; Mavrakis et al., 2014), which inhibits MRTF-A transcriptional activity (Olson and Nordheim, 2010). Indeed, a recent study showed a reduced F/G-actin ratio upon SEPTIN11 depletion (Fu et al., 2023). Notably, we observed changes in perinuclear actin fiber organization upon Septin9 depletion (Fig. 6-4), suggesting that loss of Septin9 may inhibit Srf/Mrtf-A signaling. This could lead to increased Myogenin expression via an Mrtf-A-dependent mechanism.

It is crucial to examine the activity levels of RhoA, Rock1, and Srf/Mrtf-A following Septin9 depletion, as well as monitor actin organization, the F/G-actin ratio, and RhoA/Srf-dependent signaling to clarify the link between septins and Rho GTPases during myogenic differentiation. Tools such as RhoA activity assays, mutants for RhoA, Rock1, and Mrtf-A, along with specific inhibitors of RhoA and Rock1, and promoter activity measurements for Srf and Mrtf-A can address these questions. Applying these tools will be essential for understanding the mechanistic relationship between septin dynamics and Rho GTPase signaling in myogenic differentiation.

4.5.3. The role of Septin9 in modulating myoblast cell cycle dynamics

The reorganization of septins observed at the onset of myogenic differentiation may either be a direct consequence of a general cytoarchitectural adaptation during the process, or it could play an instructive role in the orderly transition from proliferating to differentiating myoblasts. In this study, we described an increase in terminal differentiation marker expression in Septin9-deficient myoblasts (Fig. 3-26), alongside a density-dependent loss of cells (Fig. 3-27), and a reduction in proliferating EdU-positive cells (Fig. 3-28). These findings suggest an active participation of septins in the process of myogenic differentiation.

The mild reduction in DNA-synthetizing cells and overall cell number may result from enhanced myogenic differentiation (Fig. 3-26), coinciding with, or due to, a premature cell

cycle exit upon Septin9 depletion (Fig. 6-3). Alternatively, these changes could indicate defects in cell cycle progression, consisting of a reduced S-phase prevalence or extension of the G_1 phase, providing more time to respond to extracellular stimuli and allowing myogenic regulators to accumulate (Lange and Calegari, 2010; Salomoni and Calegari, 2010). The role of septins in regulating cell division is well documented, focusing prominently on the orchestration of the mitotic phase and associated kinases, however, whether septins regulate progression through other cell cycle stages is not well understood (Estey et al., 2010; Panagiotou et al., 2022; Russo and Krauss, 2021; Zheng et al., 2024).

Interestingly, cell cycle arrest can be uncoupled from myogenic differentiation by interfering with actomyosin contractility (Dhawan and Helfman, 2004). Dhawan *et al.* showed that a reduced cell contractility, following the use of myosin inhibitors, reduced BrdU incorporation, indicating an reversible growth arrest in C2C12 cells (Dhawan and Helfman, 2004). This cell cycle arrest resembled the G_0 arrest seen upon adhesion abolishment in C2C12 cells (Dhawan and Helfman, 2004; Milasincic et al., 1996). While these myosin inhibitors disrupted stress fibers and focal adhesion complexes, they did not induce muscle-specific gene expression, similar to findings in suspension-arrested myoblasts. Notably, treatment with MI resulted in reduced Myod1 expression and inhibited fusion, indicating RhoA's involvement in the contractility-dependent phenotype (Dhawan and Helfman, 2004). Indeed, dnRhoA and C3 transferase treatments resulted in decreased DNA synthesis and lower Myod1 levels, while Myogenin and p21 levels remained unchanged, thus compromising both proliferation and differentiation. Furthermore, inhibition of Rock via Y27632 suppressed S-phase prevalence but did not affect Myod1 expression, repeatedly indicating divergent roles of RhoA and Rock (Dhawan and Helfman, 2004). Collectively, these data suggest that coupling cell cycle exit with differentiation requires actomyosin contractility. As highlighted in the previous chapter 4.5.2, Septin9 may regulate myoblast contractility via the Rho/Rock pathway, underscoring the importance of characterizing actin organization and actomyosin contractility upon Septin9 depletion. Overall, Septin9 depletion may interfere with cell contractility, affecting myoblast cell division, which can be uncoupled from myogenic differentiation. Whether the reduced myoblast number and the ratio of EdU-positive cells is connected to precocious differentiation upon Septin9 depletion will require further investigation.

Despite the observed mild decrease in proliferation (Fig. 3-27 and 3-28), we did not observe signs of cytokinetic failure, such as the accumulation of bi- or multinucleated undifferentiated

cells (Normand and King, 2010). Nevertheless, future detailed live cell experiments should focus on the proliferation-differentiation transition to ensure that binucleated cells result from fusion rather than failed cytokinesis of differentiated cells, which would be crucial for interpreting the myogenic differentiation index. The existence of tri- and multinucleated Septin9-deficient cells (Fig. 3-26) argues against a severe cell division phenotype. The lack of cell division defects in the absence of Septin9 (not shown) and the apparently unaffected cytokinesis in myoblasts make it puzzling to understand how Septin9 depletion could skew other phases of cell division, particularly the G_1 phase or G_1 to S transition, and lead to a premature cell cycle exit.

During the G_1 to S transition, proliferating myoblasts express E2F/DP1 target genes that are indicative of cell cycle progression (Bracken et al., 2004; Fu et al., 2023; Ruijtenberg and van den Heuvel, 2016). Notably, upon depletion of Septin9 in both C2C12 and primary myoblasts, we observed a decrease in the expression of E2F/DP1 target genes such as *Dhfr*, *Tk1*, *Cdk1* and *Ccna2*, coupled with an increase in Myod1 target genes, including *Myogenin* and *Cdkn1a* (*p21*). Additionally, *pRb1* was upregulated specifically in primary myoblasts (Table 6-5). These findings indicate a transcriptional switch from the proliferative E2F program to the differentiative Myod1 program. This observation is further supported by the premature transition towards a differentiating progenitor transcriptome observed in Septin9-deficient C2C12 cells and primary myoblasts (Fig. 3-20), as well as by the GO enrichment analysis (Fig. 3-21D and Fig. 3-22D). The effect is more striking in primary myoblasts cultivated in proliferation medium, compared to C2C12 cells differentiated for 12 hours.

Interestingly, inactivation of E2F transcription can promote Myod1-driven myogenic differentiation in various ways (Ruijtenberg and van den Heuvel, 2016; Wu and Yue, 2024). First, E2F1 transcriptional activity directly inhibits Myod1 and Myogenin function in a pRB1-independent manner (Wang et al., 1996, 1995). Next, E2F target genes such as *CyclinD1* and *c-myc* can directly inhibit *Myod1* activity (Wang et al., 1996). Moreover, downregulation of E2F target genes like *Cyclin A2*, *D1,* and *E2* can result in hypophosphorylation and activation of pRb1 (Lim and Kaldis, 2013; Wang et al., 1996). PRb1 is essential for E2F-mediated inhibition of the proliferative transcription program (Puri et al., 2001) and associates with Myod1 to potentiate its transcriptional activity (Gu et al., 1993; Guo et al., 2003). Lastly, the G_1/S transition-regulating Cdk2-CyclinE complex phosphorylates Myod1 downstream of E2F proteins, increasing Myod1 turnover and inhibiting myogenic differentiation (Kitzmann et al.,

1999; Ruijtenberg and van den Heuvel, 2016; Tintignac et al., 2000). Inhibition of differentiation exerted by Cdk2-CyclinE may represent a conserved effect, as the absence of CyclinE, an E2F target gene, results in premature differentiation of *Drosophila* neuroblasts (Berger et al., 2005) and loss of quiescence in somatic gonads that become differentiated distal tip cells in *C. elegans* (Fujita et al., 2007; Ruijtenberg and van den Heuvel, 2016). Therefore, the observed increased expression of Myod1 targets such as p21 and pRb1 and downregulation of various E2F target genes upon Septin9 knockdown (Fig. 3-23B, 6-3 and Table 6-5) further supports the decision shift from E2F-driven proliferation towards myogenic differentiation (Gérard and Goldbeter, 2014; Stallaert et al., 2019; P. Zhang et al., 1999). This supports the idea, that reduced cell proliferation and premature differentiation upon Septin9 depletion are connected, although a coincidental effect cannot be entirely ruled out. Whether the reduced proliferation induces the differentiation in absence of Septin9 remains to be elucidated.

Our data strongly indicate a coinciding exit from the cell cycle and precocious differentiation of Septin9-deficient myoblast. However it is challenging to elucidate the mechanistic details and the “cause or consequence” question of the proliferation-differentiation decision due to complex and partially redundant regulation (Ruijtenberg and van den Heuvel, 2016; Wu and Yue, 2024). Notably, E2F activity is reduced during myogenic differentiation in C2C12 cells (Luo et al., 2016). While most of the above mentioned E2F target genes (*Dhfr1*, *Tk1*, *Cdk1*, *Ccna2*, *Ccnd1*, *Ccnde2*, *Cdc25a*) and Myod1 target genes (*Myog*, *Cdkn1a*, *Cdkn1c*, *Rb1*) are robustly down- and upregulated, respectively, in differentiating C2C12 cells as identified in a meta-study by Zhang *et al* (Zhang et al., 2022), the E2F target gene DP1 (*Tfdp1*) is not. In this study, we observed a marked downregulation of DP1 (*Tfdp1*), a sibling factor of E2F and a key component of the E2F/DP1 transcription duo (Trimarchi and Lees, 2002), in both C2C12 and primary myoblasts following the depletion of Septin9 (Fig. 3-23B). This finding may offer one potential explanation for the premature cell cycle exit and early onset of differentiation observed in these cells. Unlike nuclear E2F, Tfdp1 shuttles between the cytoplasm and nucleus and is subject to ubiquitination when it lacks heterodimerization with E2F (Gong et al., 2015; Magae et al., 1999). This ubiquitination is mediated by Kelch repeat and BTB domain containing protein 5 (Kbtbd5)/ Kelch-like protein 40 (Klhl40) (Gong et al., 2015; Magae et al., 1999). Klhl40, a Myod1 target gene (Bowlin et al., 2013), acts as a substrate-specific adaptor for the Cullin3 (Cul3) E3 ubiquitin ligase (Garg et al., 2014). Interestingly, Klhl40 mRNA

expression is upregulated following Septin9 depletion in both C2C12 cells and primary myoblasts (Table 3-2). The increased expression of Klhl40 could represent both a consequence and a feed-forward mechanism of myogenic differentiation, potentially aimed at reducing proliferative E2F activity. Additionally, it might lower Tfdp1 protein levels through cellular degradation pathways, although it does not account for the substantial decrease in Tfdp1 mRNA expression. Therefore, this observation may address the question of premature cell cycle exit and precocious differentiation, but it is unlikely to cause them.

Lastly, Tfdp1 is retained in the cytoplasm by Suppressor of cytokine signaling 3 (Socs3), resulting in negative regulation of E2F activity (Masuhiro et al., 2008). Kremer *et al.* reported that SEPTIN2, 6 and 7 associate with SOCS7 and thereby regulate cytoplasmic retention of the adaptor protein NCK1 (Kremer et al., 2007). Similarly, septins could mediate Socs3-dependent Tfdp1 cytoplasmic retention or ubiquitination in myoblasts, serving as a Socs3 cytoplasmic interaction platform, in a mechanism like the SOCS7- mediated NCK1 retention. However, cytoplasmic retention of Tfdp1 serves as a negative regulator of E2F activity (Masuhiro et al., 2008). Therefore, Septin9 must either serve a positive role in E2F/Tfdp1 activity, or a negative role in Tfdp1 cytoplasmic retention and ubiquitination, or Tfdp1 expression/ subcellular localization must have a feedback mechanism tied into its transcription. Notably, E2F1 and Tfdp1 are subject to autoregulatory transcription control mechanisms and bind their own promoter sequences (Bracken et al., 2004; Johnson et al., 1994; Luo et al., 2016; Nakajima et al., 2023). Hypothetically, a reduction in Tfdp1 protein or mRNA levels upon Septin9 depletion would be sufficient to drive the biphasic E2F-pRb1 switch towards cell cycle exit and, potential, myogenic differentiation. Further research focusing on cell cycle progression, E2F and pRb1 activity, and on the subcellular localization of Tfdp1 upon Septin9 depletion, will provide more information for a better understanding of the mechanism behind Septin9-dependent cell cycle regulation in myoblasts.

Only a subset of Myogenin-positive cells exhibited reorganization of Septin9 structures (Fig. 3-8), suggesting that septin reorganization occurs after the initiation of the myogenic program and subsequent cell cycle exit. This observation implies that the reduced proliferation and decreased prevalence of cells in the S-phase may simply result from fewer cells available for expansion as differentiation progresses. However, if Septin9 depletion disrupts the same functions of septins during differentiation, the observed changes in cell cycle dynamics raise important cause-and-effect questions. Specifically, how do septins that regulate myoblast

differentiation also influence proliferation? One possibility is that Septin9 depletion introduces a temporally distinct defect that affects cell cycle decisions independently of its role in septin reorganization during differentiation. Yet, if Septin9 depletion causes an early defect in dividing myoblasts, it remains unclear why only a limited subset of cells shows early-onset differentiation. One explanation could be that the Septin9 knockdown does not affect every cell equally, leaving some cells with sufficient Septin9 protein or allowing them to rely on Septin9-independent complex formation. Additionally, some observed defects might be related to other septin paralogues, such as Septin7. Indeed, we do not observe the cell division failure seen with Septin7 depletion, as described by Gönczi et al (Gönczi et al., 2022), but disruption of septin filaments may still influence Septin7-dependent division. It would be valuable to use super resolution microscopy to examine Septin9-deficient cells during cell division, particularly to investigate whether Septin7-containing complexes are sufficient to rescue cytokinetic failure. Alternatively, some Septin9-deficient cells may counteract premature differentiation, which should manifest in signs of anti-myogenic programs. This line of inquiry touches on the broader question of cell cycle exit and its relationship to terminal differentiation- whether myoblasts should maintain the ability to proliferate until they reach a terminally differentiated state or if they exit the division cycle immediately following myogenic induction. Addressing this issue directly is challenging and remains an open question. To gain deeper insights, it will be essential to thoroughly analyze the cell cycle of Septin9 deficient cells and the transcriptomic changes at the single-cell level following Septin9 depletion, addressing proliferation- differentiation phenotype. Additionally, combining live reporters for cell cycle progression, myogenic differentiation, and septin reorganization could help to temporally dissect the sequence of events associated with septin reorganization and the consequences of septin depletion.

4.5.4. The role of Septin9 in myoblast survival: Balancing differentiation and apoptosis

Depletion of Septin9 resulted in increased expression of terminal myoblast differentiation markers and coincided with an increase in mitochondrial apoptotic signaling (Fig. 3-29 and 3-30). Interestingly, although differentiating myoblasts progressively acquire apoptosis resistance (Walsh and Perlman, 1997), they share overt phenotypic and signaling similarities with apoptotic cells (Bell and Megeney, 2017). This is the case of exposure of

phosphatidylserine to the outer membrane leaflet (van den Eijnde et al., 2001), appearance of transient DNA single strand breaks (Larsen et al., 2010), mitochondrial remodeling and mitophagy (Baechler et al., 2019; Rahman and Quadrilatero, 2023b), and transient activation of Caspase-3 (Fernando et al., 2002).

We observed a mild increase in Caspase3/7 activity and an accumulation of active Caspase3 protein in Septin9-deficient C2C12 cells, which may indicate precocious differentiation (Fig. 3-29). Strict temporal control over caspase signaling activation is a feature of many differentiating cell types, including muscle cells (Bell and Megeney, 2017; Fernando and Megeney, 2007). Typically, Cytochrome C release and Caspase3/7 activation occur more slowly, usually postponed by 24 hours, and with a dampened amplitude in differentiating cells compared to apoptotic cells (Akbari-Birgani et al., 2014; Fernando et al., 2002; Weber and Menko, 2005). It will be necessary to further elucidate the level of cytosolic Cytochrome C and subcellular localization of active Caspase3 to properly discern between death and differentiation signaling. The timing and intensity of these factors appear to be critical in determining the outcome (Akbari-Birgani et al., 2014; Bell and Megeney, 2017; Fernando et al., 2002; Fernando and Megeney, 2007).

Interestingly, p21 has been demonstrated to confer apoptosis resistance to differentiating myogenic progenitors (Wang and Walsh, 1996). In differentiating myoblast cultures, Myogenin-negative/p21-positive cells are not observed, indicating that Myogenin expression precedes p21 expression. Only cells double-positive for Myogenin and p21, and not Myogenin-positive only, acquire apoptotic resistance. This suggests that apoptotic resistance is connected with cell cycle withdrawal, rather than with an earlier step of commitment to terminal differentiation (Andrés and Walsh, 1996; Wang and Walsh, 1996). We observed increased mRNA expression of *Cdkn1a* (p21) upon Septin9 depletion in both cell lines, potentially indicating increased apoptotic resistance. It would be of interest to precisely analyze Septin9 reorganization in relation to Myogenin, p21, and Myosin heavy chain expression to better resolve the cellular stages and processes preceding septin reorganization. Given the observed reorganization of septin filaments only in a subset of Myogenin-positive cells (Fig. 3-8), we hypothesize that septin reorganization is independent of commitment and associated with subsequent events.

Nonetheless, other signs of apoptosis are considered more specific to cell death, such as Parp-1 cleavage, which is a hallmark of apoptosis (Elmore, 2007; Kaufmann et al., 1993;

Soldani and Scovassi, 2002). Hence, the increased levels of cleaved Parp1, a ”death only” target of executioner caspases (Fernando and Megeney, 2007; Pirrotta, 2004), observed in C2C12 depleted of Septin9 (Fig. 3-30), may indicate progressive cellular demise. It is conceivable that Septin9 deficiency may compromise myoblast viability and survival, although the effect appears to be mild and accumulates slowly during prolonged myogenic differentiation, as no Parp1 cleavage and TUNEL-positive cells were observed in proliferating cells. Furthermore, we observed an increase in pro-apoptotic serine protease *Htra3* (L. Wu et al., 2021) and a decrease in anti-apoptotic *Bcl2l1* (Loo et al., 2020) in both C2C12 and primary myoblasts lacking Septin9 (Fig. 3-23), further supporting potential susceptibility for apoptosis.

Collectively, the mild transient increase in Caspase3 activation and the heightened apoptotic signaling observed in Septin9-deficient cells may represent independent or at least temporally distinct events. If the increase in apoptosis is directly caused by Septin9 depletion and occurs independently of myogenic differentiation, it raises important questions about how organized septins modulate executioner caspase signaling to prevent apoptosis and promote myoblast survival. Interfering with G_1-S transition and S-phase checkpoint upon Septin9 depletion, as described in previous chapter (4.5.2), may lead to a E2F-dependent S-phase-coupled apoptosis (Cho and Liang, 2011; Polager and Ginsberg, 2009). Moreover, septins are demonstrated to participate in mitochondrial dynamics (Pagliuso et al., 2016; Sirianni et al., 2016) and, therefore, deficient septin organization may interfere with physiological mitochondrial maturation and result in the release of cytosolic apoptogenic agents. Nonetheless, it will be crucial to determine whether the cells showing increased apoptotic signaling are the same ones undergoing early-onset differentiation.

Taken together, Septin9-depletion accelerates cell cycle exit and induces precocious differentiation, accompanied by a decrease in myoblast number and an increase in apoptotic cells. Interestingly, all these phenotypes are rather mild and potentially, but not necessarily, connected. Observing the viability of Septin9-depleted cells during myogenic differentiation through live cell imaging may help to decipher the origin of the reduced myoblast number: whether it is due to reduced proliferation, induced differentiation, or apoptosis.

4.5.5. The role of Septin9 in modulating key signaling pathways during myoblast differentiation

Numerous signaling pathways regulate the process of myogenic differentiation, including the TGFβ and WNT signaling cascades, which antagonize or promote myogenesis in a highly regulated fashion (Chal and Pourquié, 2017). Upon depletion of Septin9, we observed changes in the expression of central transcription factors, ligands, and target genes of several pathways, including downregulation of *Inhba* (Activin A), *Ctnnb1* (β-catenin), and *Wwtr1* (Taz) (Fig. 3-23). Among the deregulated pathways, the most prominent is Activin A signaling, which belongs to the TGFβ family of growth factors and negatively regulates myogenesis (Horbelt et al., 2012; Lodberg, 2021; Moustakas and Heldin, 2009). Specifically, we observed reduced secretion of Activin A into the medium, reduced phosphorylation of the downstream transcription factor Smad2 upon stimulation with low concentration of Activin A (0.25 nM), and reduced basal activity of the $CAGA_{12}$-luciferase reporter (Fig. 3-24). Furthermore, we observed an upregulated expression of Matrix gla protein (Mgp) (Fig. 3-23 and 3-24), which positively correlates with myogenic differentiation and potentially interferes with the binding of Myostatin and its AcvRIIB receptor (Ahmad et al., 2017). Collectively, these data indicate reduced signaling activity downstream of Activin A.

Similar to Myostatin, Activin A contributes to atrophy, negatively regulating skeletal muscle mass by attenuating protein synthesis via Akt/mTOR pathway (Chen et al., 2016, 2014; Loumaye et al., 2022). Furthermore, *in vitro* studies suggest that Activin A impairs myogenic differentiation and fusion (Bloise et al., 2019; Trendelenburg et al., 2009). Therefore, the downregulation of Activin A signaling may offer an additional explanation for the precocious myogenic differentiation observed upon Septin9 depletion.

So far, the knowledge about the role of septins in the regulation of growth factor signaling is scarce. In our study, we found that Septin9 interacts with receptors from the TGFβ and BMP family of proteins, such as Alk2, Bmpr2, and Tgfbr2 in a ligand-enhancing manner (Fig. 6-6). However, the interaction with Activin A specific Alk4, ActRIIA or ActRIIB was not tested. Moreover, using proximity ligation assays and surface biotinylation, we demonstrated that Septin9 interacts with Bmpr2 at the plasma membrane and is recruited to the membrane in a ligand-dependent manner (Fig. 6-7 and 6-8). Therefore, septins may play a role in stabilizing the signaling outcome downstream of Activin A by organizing a permissive environment as protein scaffolds. Specifically, septin complexes may promote membrane or sub-

membranous localization of receptors TGFβ and BMP family receptors, promote their clustering, protect them from degradation, facilitate their association with effector molecules, and facilitate the secretion of signaling-relevant molecules.

Notably, Diesenberg *et al.* demonstrated that SEPTIN9 is recruited to active EGF receptors in a CIN85-dependent manner and protects them from Cbl-dependent ubiquitination and sorting into the degradative pathway (Diesenberg et al., 2015). Furthermore, Mostowy *et al.* showed that SEPTIN2 and 11 regulate surface levels and anchorage to the sub-membranous actin cytoskeleton of the Hepatocyte growth factor (HGF) receptor (HGFR/MET) (Mostowy et al., 2011). Similarly, septins may scaffold Activin A signaling. Nevertheless, future studies will need to elucidate whether a deregulation of Activin A production and secretion is indeed the cause of the enhanced differentiation of Septin9-deficient myoblasts. A rescue experiment in Septin9-depleted cells, consisting in titrating Activin A to control levels, may provide an answer to this question.

The other downregulated genes,*Wwtr1* (Taz, Fig. 3-23, Fig. 3-24) and *Ctnnb1* (β-catenin, Fig. 3-23, Fig. 3-25), are a central transcription co-factor from Hippo signaling (Fu et al., 2022) and a transcription factor from WNT signaling (Liu et al., 2022), respectively. How septins could regulate the expression of these proteins remains to be elucidated in future studies. Nonetheless, the downregulation of these factors appears counterintuitive, as both Taz (Jeong et al., 2010; Mohamed et al., 2016) and β-catenin (Jones et al., 2015) promote myogenic differentiation in myoblasts. Indeed, Jones *et al.* demonstrated that ectopic activation of WNT/ β-catenin signaling results in premature differentiation of myoblasts during regeneration (Cui et al., 2019; Jones et al., 2015). In addition to reduced expression of *Ctnnb1*, we reported upregulation of β-catenin target genes (Cui et al., 2019) involved in terminal differentiation and myoblast fusion, such as *Mymk*, *Myomx*, *Trim72*, *Jspr1* (Fig. 3-25). The upregulation of β-catenin target genes and downregulation of β-catenin may suggest a feedback mechanism counteracting premature or excessive activation of β-catenin signaling, although it cannot be excluded that these genes are also regulated by alternative factors. Moreover, while promoting differentiation during the terminal phase, Taz has been shown to also promote myoblast proliferation (Mohamed et al., 2016; Sun et al., 2017). Thus, reduced Taz levels may reflect the reduced proliferation observed upon Septin9-depletion. Alternatively, reduced levels of Taz may also represent a compensation mechanism counteracting precocious differentiation.

Given the complex, cross-regulated nature of signaling pathways, it is not simple to clearly dissect their independent roles. Hippo and WNT signaling can interfere with the expression of each other's signaling mediators and activity (Konsavage and Yochum, 2013). Additionally, there is evidence of positively corelated expression of Taz and β-catenin (Sun et al., 2014). Interestingly, Activin A stimulation induces Taz expression in different cellular models (Ma et al., 2017; Radhakrishnan et al., 2023), emphasizing the intricate crosstalk between TGFβ, Hippo, and WNT signaling (Chen et al., 2020; LeBlanc et al., 2021; Piersma et al., 2015).
To understand whether Septin9 depletion affects any of these signaling pathways directly or indirectly, and if this regulation leads to premature differentiation, activities of the pathways and target gene expressions would need to be studied in detail. Many available luciferase constructs could be used to test the transcriptional activity of Hippo, WNT, and TGFβ signaling upon Septin9-depletion. This may ultimately lead to a better understanding of the mechanistic details and signaling alterations behind premature myogenic differentiation following Septin9 depletion.

4.5.6. A potential synergy between Septin9 and myosin motors during myogenesis

Myoblasts express various non-muscle myosin motors from at least six different classes, including NMIIA, and NMIIB, unconventional myosin Iα, and VI (Myo6). All these non-skeletal myosin motors decrease in myotubes, undergoing downregulation after the onset of differentiation (Karolczak et al., 2015; Wells et al., 1997). This is essential for reorganizing the cytoskeleton during myoblast differentiation and fusion (Karolczak et al., 2015; Lehka et al., 2020; Swailes et al., 2006). Notably, core septins are known to interact with NMIIA, NMIIB, and Myo6 in non-muscle cells (Hecht et al., 2019; Joo et al., 2007; Wasik et al., 2017). The similar expression pattern of septins and myosin motors suggest they may synergize in regulating myogenic differentiation. The association between class II non-muscle myosins and actin is crucial for the morphology of myoblasts and for the acquisition of a spindle shape in prefusion myoblasts (Swailes et al., 2006). These myosins reorganize alongside actin to the cell periphery at the onset of differentiation, and their depletion results in the failure of myoblast alignment and fusion (Swailes et al., 2006, 2004). Additionally, differentiating myoblasts exhibit reduced adherence to the substrate and increased cell-cell adhesion (Peckham, 2008; Swailes et al., 2006; Wells et al., 1997). Moreover, Brondolin *et al.*

demonstrated the role of actomyosin contractility in adhesion-dependent migration of zebrafish MuSCs (Brondolin et al., 2023). Specifically, Rock1 inhibition led to changes in cortical tension, focal adhesion dynamics, migration, and increased myogenic differentiation, suggesting a connection between migration and differentiation of MuSCs. The authors observed that Y-27632 treatment resulted in smaller, less polarized FAs and reduced cell polarity, which indicated diminished cortical tension. Following previous research demonstrating Septin9's role in stabilizing focal adhesions (Dolat et al., 2014b), depletion of Septin9 impaired focal adhesion maturation in C2C12 cells (Fig. 6-5). In accordance with this, reduced contractility or tension is associated with myoblast differentiation (Boontheekul et al., 2007; Brondolin et al., 2023; Engler et al., 2004; Gilbert et al., 2010; Romanazzo et al., 2012; Trensz et al., 2015). Collectively, septins may synergize with actomyosin ensuring cytoskeletal integrity, focal adhesion dynamics, and substrate adherence in proliferating and differentiating myoblast. Therefore, the enhanced myogenic potential observed in the absence of Septin9 could be caused by the partial phenocopy of actomyosin reorganization and the precocious acquisition of differentiating phenotype, such as decreased substrate adhesion.

Notably, due to their interaction with actomyosin cortex and plasma membrane phospholipids, septins are considered emerging regulators of cellular mechano-transduction (Lam and Calvo, 2019). Septins stabilize the cell cortex of lymphocytes, which otherwise undergo substantial blebbing in absence of septins (Gilden et al., 2012; Tooley et al., 2009). It is therefore conceivable that changes in myoblast actomyosin-mediated cortical elasticity upon Septin9 knockdown could skew myoblast fates towards differentiation. The viscoelastic properties of Septin9-depleted myoblasts will need to be elucidated in future studies.

Recent work has identified SEPTIN9 as direct interaction partner of Myo6 (Hecht et al., 2019; O'Loughlin et al., 2018), validating the interaction for SEPTIN9 in 1306 fibroblasts and through *in vitro* pulldown assays (Hecht et al., 2019). Myo6 is a weakly processive motor protein that can act as a scaffold protein with many specialized functions (de Jonge et al., 2019; O'Loughlin et al., 2018; Tumbarello et al., 2013). Recent evidence suggests that myosin motors not only track along actin filaments but also actively induce filament formation (de Jonge et al., 2019; Lee et al., 2000; Pylypenko et al., 2016). Moreover, Myo6 associates with a RhoGEF complex, potentially linking actin and septin cytoskeleton (de Jonge et al., 2019). Proximity labeling identified actin-binding proteins Leucine-Rich repeats Calponin Homology domain 1 and 3

(LRCH1 and LRCH3) as associating with Myo6 and with the Rac1/Cdc42 GEF, DOCK7, in neuronal PC12 cells (Majewski et al., 2012; O'Loughlin et al., 2018). These proteins form a DISP (DOCK7-induced septin displacement) complex, likely via the interaction of LRCH3 with SEPTIN7, 8, 9, 10 and 11 (O'Loughlin et al., 2018). Notably, exogenous expression of DISP components displaces septins from actin and results in cytosolic septin ring formation, potentially coordinating septin removal via competition and actin reorganization through Rac1/Cdc42 activation (O'Loughlin et al., 2018). These findings provide an additional layer of a dynamic actin-septin interaction regulation and may provide another mechanism for septin reorganization during myogenic differentiation.

The depletion of Myo6 induces changes in cytoskeletal organization, cell adhesion, spreading, and leads to transient increase in the myogenic differentiation index in C2C12 cells and myoblasts derived from Snell's waltzer mice, that naturally lack Myo6 (Karolczak et al., 2015; Lehka et al., 2020). Notably, a substantial pool of Myo6 depleted myoblasts formed sac-like myotubes (myosac), characterized by enlarged aberrant morphology and misaligned, centrally positioned nuclei indicative of disrupted myosin thick filaments during sarcomere formation (Lehka et al., 2020; Lin and Holtzen, 1990; McGrath et al., 2006). Myo6 depletion led to an increase in Myod1 expression but did not affect Myogenin levels (Karolczak et al., 2015; Lehka et al., 2020). Given, Myo6 organizes the actin cytoskeleton in numerous cell lines, and this is required, for instance, during spermatogenesis and neuritogenesis (Lehka et al., 2020; Lv et al., 2015; Sobczak et al., 2016; Zakrzewski et al., 2020), it is conceivable that septins may facilitate the interaction between Myo6 and actin filaments in myoblasts. Thus, disruption of this interaction may lead to a partial Myo6-dependent increase in myogenic fusion index after Septin9 depletion. We did not focus on the morphology of Septin9-depleted myotubes, nor investigate septin interactions with Myo6; therefore, it remains to be elucidated if septin-deficient myoblasts form disorganized myosac-like myotubes in a Myo6-dependent manner.

A potential interaction with a processive myosin motor opens the possibility for septins to participate in the actin-mediated secretory pathway regulating the transport of cell surface receptors or differentiation-inducing factors to the PM or towards the cell body. Thus, Septin9 may participate in the regulation of intracellular trafficking in myoblasts and therefore a depletion of Septin9 may result in a disbalance between anterograde and retrograde traffic in a Myo6-dependent or independent manner. Notably, the inhibition of ER-Golgi transport

via brefeldin A severely impairs myogenic differentiation and lowers fusion potential in chicken and mouse myoblasts (Ichikawa et al., 1993; Possidonio et al., 2014), indicating the significance of vesicles trafficking for successful myogenesis. Yi *et al.* reported the involvement of intracellular transport in regulating myogenesis (Yi et al., 2015). The authors demonstrated that kinesin KIF5B plays an essential role in the myogenic differentiation of C2C12 cells by transporting the adaptor protein Bcl-2/adenovirus E1B interacting protein 2 (BNIP-2) to the membrane. Subsequently, BNIP-2 facilitates p38MAPK activation, thus promoting myogenesis (Yi et al., 2015).Moreover, depletion of Myo6 (Warner et al., 2003) and SEPTIN1 (Song et al., 2019) results in disrupted Golgi organization, indicating potential synergy in maintaining Golgi architecture. Furthermore, Septin9 is also implicated in the stabilization of bidirectional MT-based transport through interactions with dynein and several kinesin motors (Spiliotis and Kesisova, 2021). Specifically, Karasmanis *et al.* reported that SEPTIN9_i1 impedes the motility of KIF5 *in vitro* (Karasmanis et al., 2018). Based on these findings, it is conceivable that septins may be involved into the regulation of vesicle trafficking during myogenic differentiation. Additionally, Myo6 interacts with the RhoA-specific ARHGEF12 (Leukemia-associated RhoGEF, LARG), which activates RhoA downstream of Gα12/13 G protein subunits of surface receptors. In complex with adaptor proteins SH3BP4 and GIPC PDZ Domain Containing Family Member 1 (GIPC1), LARG and Myo6 regulate actin organization at early endosomes as part of the LARG-induced F-actin for tethering (LIFT) complex (O'Loughlin et al., 2018). Myo6 and GIPC1 transport receptors and endocytic vesicles from the actin rich cell periphery toward the cell body (Aschenbrenner et al., 2003; Naccache et al., 2006). This collectively implies a possibility for a septin-Myo6 axis to regulate cargo transport during myogenic differentiation. It remains speculative whether Septin9 depletion could skew transport toward the plasma membrane or result in a more severe defect in vesicle transport upon the collapse of septin structures. Furthermore, it is not clear which myosin motor would be involved into this regulation. Nonetheless, it remains to be elucidated whether and how septins are involved in actin- or tubulin-based cargo transport in myoblasts and whether this interaction has functional relevance for homeostatic processes or during differentiation and fusion.

4.5.7. The putative role of Septin9 as a cell fate regulator during myoblast cytokinesis

Due to their ability to break cellular symmetry (Schuster and Geiger, 2021), septins are emerging as regulators of the stem cell division mode (whether symmetric or asymmetric) and as balancers between self-renewal and differentiation. In hematopoietic stem cells, Septin7 is crucial for regulating hematopoietic differentiation by compartmentalizing cytoplasmic polarity markers such as Cdc42 and Borg4 (Kandi et al., 2021). Additionally, Septin7 is essential for maintaining the motor protein Kif20a/Mklp2 at the intracellular bridge in neuronal progenitor cells (NPCs), and the loss of Septin7 results in premature neuronal differentiation, disrupting the regulation of asymmetric cell division (Qiu et al., 2020). Since Kif20a interacts with the regulator of G-protein signaling Rgs3, the depletion of which phenocopies the absence of Septin7 and Kif20a, authors suggest that Septin7 may help to control the inheritance of neuronal cell fate determinants by daughter cells during cytokinesis (Geng et al., 2018).

Recent studies indicate that in myotubes derived from C2C12 cells, Septin7 interacts with Numb (Gasperi et al., 2023), another asymmetric cell fate determinant, although its role in vertebrates is not completely understood (Betschinger and Knoblich, 2004; Knoblich, 2008). Numb segregates asymmetrically during cytokinesis in many cell types, such as murine neuronal (Zhong et al., 1996) and retinal (Cayouette et al., 2001) progenitors, hematopoietic stem cells (Wu et al., 2007), MuSCs (Conboy and Rando, 2002; Shinin et al., 2006), and dermomyotome (Jory et al., 2009; Venters and Ordahl, 2005). However, the role of Numb in regulating binary fate decisions and differentiation remains controversial. For instance, the loss of Numb was initially demonstrated to result in precocious differentiation and loss of NPCs, while later studies found it to induce over-proliferation and impaired neuronal differentiation (Li et al., 2003; Petersen et al., 2002). Instead, the Rando lab initially reported that increased Numb expression in myofiber explant system, or cultured myoblasts, promotes myoblast differentiation (Conboy and Rando, 2002). Later, the Tajbakhsh lab provided conflicting evidence utilizing spatiotemporal misexpression of Numb in myogenic progenitor cells prior to cell fate decision in dermomyotome (Jory et al., 2009). The authors used a transgenic mouse line stably overexpressing Numb-GFP in Pax3+/Pax7+ population using the epaxial enhancer of *Myf5,* driving the expression of the reporter gene in the dorsal somite (Jory et al., 2009). Surprisingly, the overexpression of asymmetrically distributed Numb led to

symmetric divisions and an increase in the dermomyotomal progenitor pool size, without altering their rate of proliferation or differentiation, suggesting involvement in the self-renewal of progenitor cells (Jory et al., 2009).

Nonetheless, in keeping with the roles of septins in asymmetry breaking (Schuster and Geiger, 2021; Spiliotis and McMurray, 2020) and cell division (Russo and Krauss, 2021), the association between septin filaments and a protein involved in cell fate choice in metazoans is highly intriguing. The interaction between Septin9 and Numb will require validation in myoblasts. Nevertheless, we speculate that myoblasts possess a mechanism for balancing proliferation and differentiation, which could be regulated by septins to assure orderly progression through cell division. Specifically, in myogenic cells septin complexes may compartmentalize cell fate determinants through a mechanism like that described for neuronal or hematopoietic progenitors. It is plausible that the role of septins in determining cell fate is conserved across various cell types.

4.5.8. Septin9 as a putative, antimyogenic scaffold

Septins could affect actin organization and gene transcription during myoblast differentiation by sequestering nucleocytoplasmic shuttling proteins. This may ultimately modulate mechano-transduction in myoblasts. In cancer-associated fibroblasts, Calvo *et al.* demonstrated that septins assist actin stress fibers formation and the remodeling of extracellular matrix into a pro-tumorigenic structure by supporting actomyosin contractility (Calvo et al., 2015). They further showed that the upregulated actin-binding protein BORG2 interacts with SEPTIN2 and 7 on stress fibers and contributes to maintaining filamentous actin. Given that the expression of SEPTIN6 (Simi et al., 2018) and 9 (Yeh et al., 2012) can change in an ECM stiffness-dependent manner, it is possible that septin presence on actin may be modulated as a part of a regulatory mechano-transduction loop. In turn, septins may assist in mechano-transduction of extracellular cues to the nucleus, stabilizing the actomyosin network and mediating force exertion on focal adhesions (Spiliotis and Nakos, 2021). Accordingly, a stiff ECM instructs BORG2- and SEPTIN2-dependent nuclear translocation of YAP1, leading to further upregulation of BORG2 and SEPTIN2, which increasingly localize to actin filaments (Calvo et al., 2015).

Furthermore, septins associated with stress fibers ensure cytoplasmic localization of the adaptor protein NCK1 in HeLa cells (Kremer et al., 2007). NCK1, an SH2/SH3 domain-

containing protein, links tyrosine kinase signaling hubs, such as growth factor receptors and FAs, to changes in cytoskeletal dynamics (Alfaidi et al., 2021; Buday et al., 2002). Interestingly, NCK1 also has an anti-apoptotic function and translocates to the nucleus following DNA damage in a SOCS7-dependent manner (Errington and Macara, 2013). Unlike NCK1, SOCS7possesses a nuclear localization sequence (NLS) but is retained in the cytoplasm through its interaction with septin complexes. Kremer et al. demonstrated that depletion of SEPTIN2,6, or 7 leads to the release of SOCS7, which then translocates to the nucleus along with NCK1, resulting in the loss of actin stress fibers. They further showed that expressing NCK1 fused with a nuclear export sequence (NES) could rescued the disruption of actin stress fibers caused by septin depletion (Kremer et al., 2007). These findings suggest that septins may sequester proteins in the cytoplasm that are required for the onset of differentiation, and that septin reorganization may facilitate the mobilization of these factors. Depleting Septin9 could lead to the release of such proteins, potentially explaining the premature differentiation observed.

Interestingly, using a MS-based approach, we identified Nfat5 as an interactor of Septin2 in proliferating and differentiating C2C12 cells. This interaction significantly decreased after five days of differentiation (Fig. 3-31 and Table 5). Nfat5 is a member of the Nfat family of Ca2+-activated transcription factors acting in various tissues, including skeletal muscle (Horsley and Pavlath, 2002). Nfat5 exhibits predominant nuclear localization in myoblasts and myotubes, and the mechanism regulating its nuclear translocation in muscle context is not well understood (Lopez-Rodríguez et al., 1999; O'Connor et al., 2007). Nonetheless, O'Connor *et al.* reported that NFAT5$^{+/-}$ mice display impaired muscle regeneration, and myoblasts expressing dominant-negative Nfat5 exhibited impaired migration and differentiation (O'Connor et al., 2007). The identification of Nfat5 as a putative septin interaction partner supports the intriguing possibility that septins could sequester a pro-myogenic factor on stress fibers, to be subsequently released during cytoskeletal reorganization, before myoblast fusion. Depletion of Septin9 would release this factor from stress fibers, leading to its premature activation. The interaction between Nfat5 and septins will need to be validated in future studies to determine whether Nfat5 associates with septin filaments during proliferation or differentiation of myoblasts.

4.5.9. The impact of Septin9 depletion on actin

A potential consequence of septin depletion is the cellular availability of a large portion of monomeric or filamentous actin. Disruption of septin-actin interaction primarily affects ventral contractile stress fibers, while peripheral actin fibers or fibers associated with non-protrusive cell edges are less affected (Calvo et al., 2015; Dolat et al., 2014b; Joo et al., 2007; Kinoshita et al., 2002; Kremer et al., 2007). Furthermore, Verdier-Pinard *et al.* demonstrated that SEPTIN9_i2 overexpression specifically disrupts the perinuclear actin network (Verdier-Pinard et al., 2017). Thus, septins are believed to associate with spatially and functionally distinct actin filaments (Spiliotis, 2018), and disrupting septins may release these actin pools and alter the ratio between monomeric and filamentous actin. Given that septins compete with actin binding proteins (Smith et al., 2015), the disruption of the septin cytoskeleton may favor the access to actin of actin-severing and depolymerizing proteins, such as cofilin, gelsolin and Molecule interacting with CasL (MICAL) (Frémont et al., 2017; Rajan et al., 2023), and this could potentially lead to stress fiber disassembly. This modification of actin filaments potentially following Septin9 knock-down, would align with the discussion on actin reorganization (chapter 4.5.6), accelerating the acquisition of a fusion-competent phenotype. Furthermore, destabilized actin filaments may increase the fraction of monomeric G-actin, leading to changes in cytoskeletal organization and cell behavior. For instance, Peckham *et al.* demonstrated that β-actin overexpression in myoblasts results in a marked increase in motility and excessive protrusion formation, accompanied by β-actin accumulation in the nascent protrusions (Peckham et al., 2001). New evidence suggests that γ-actin organizes as a cortical meshwork and associates with lamellipodia, indicating its role in cell motility, in contrast to the contractile functions of stress fiber-localized β-actin (Dugina et al., 2009; Simiczyjew et al., 2014). Despite the minor difference of only four amino acids, these actin isoforms show different functions, and the unique contributions of these non-muscle actin isoforms are not yet well understood (Vanslembrouck et al., 2020). Moreover, since the expression of β- and γ-actin is regulated by SRF transcriptional activity (Posern et al., 2002; Sotiropoulos et al., 1999), the release of monomeric actin upon Septin9 depletion would lead to feedback inhibition of SRF signaling, which is sensitive to the polymer status of actin. Therefore, it is conceivable that Septin9 depletion in myoblasts may trigger a profound reorganization of actin, liberating actin binding sites, and potentially resulting in changes in

cell behavior and gene transcription. Future studies to investigate the regulatory role of the septin cytoskeleton on actin organization during myogenic differentiation are needed.

4.6. Septin9 and Septin7: adjacent paralogues with opposite functions in myogenic differentiation

Our study strongly indicates an enhancement of myogenic potential following the depletion of Septin9 during the early stages of myogenic differentiation in both C2C12 cells and primary myoblasts. This finding contrasts with previous studies that showed a negative effect on myogenic differentiation when Septin7 was depleted in C2C12 cells (Gönczi et al., 2022). Reconciling the notion that depletion of two adjacent septin paralogues in the septin protomer yields opposing outcomes is challenging. Potential explanations are limited by the current knowledge of septin paralogue-specific functions and interaction partners.

One potential explanation for the differing results may be the distinct impact of Septin7 and Septin9 on cell division. Septin2, 7, 9, and 11 play crucial roles in adherent cell division (Estey et al., 2010; Karasmanis et al., 2019; Renshaw et al., 2014), while certain hematopoietic cells rely on septin-independent methods for cytokinesis (Menon and Gaestel, 2015). In line with the uniqueness of Septin7 in its subgroup, Gönczi *et al.* reported that the depletion of Septin7 results in the failure to form any septin structures, leading to cytokinesis failure and to a range of cellular defects. These defects likely affected myoblast expansion and viability, thereby impacting myogenic differentiation (Gönczi et al., 2022). On the other hand, Septin9 is critical only for the late stages of cytokinesis in HeLa and MDCK cells (Estey et al., 2010; Karasmanis et al., 2019; Renshaw et al., 2014) while it appears dispensable for the initial steps of cell division. In this study we did not observe cytokinesis defects, such as bi- and multinucleated cells or chromatin-bridges (Hong et al., 2021; Normand and King, 2010), upon depleting Septin9 in C2C12 cells and primary myoblasts. This is similar to findings in murine fibroblasts where Septin9 depletion led to a slight increase in polynucleation but did not affect cell proliferation (Füchtbauer et al., 2011).

More in detail, the discrepancy between the phenotypes following Septin9 and Septin7 depletion may be attributed to distinct options for septin complex formation upon the lack of Septin9 or Septin7. The ubiquitous Septin7 is a unique paralogue in its subgroup and is an obligatory member of septin hexamers and octamers, while Septin9 is excluded from

hexamers (Kinoshita, 2003). The functional significance of septin hexamers in cellular processes is disputed. In our study, we demonstrated the absence of Septin2- or Septin7-containing macroscopic septin structures upon Septin9 depletion in C2C12 cells (Fig. 3-11). However, it cannot be excluded that these myoblasts still overcome cell division failure by engaging the remaining levels of Septin9 protein, or by switching to a hexamer-based protofilament. As mentioned above, Septin9 is dispensable for most of the cytokinesis. Moreover, Panagiotou *et al.* demonstrated the existence of Septin9-devoid septin hexamers at the intracellular bridge, which mediate the initial phases of furrow constriction and bridge maturation (Panagiotou et al., 2022). Thus, Septin9 may be dispensable for myoblast cell division. Furthermore, as discussed in the chapter 4.5.3, Septin9-deficient myoblasts may even circumvent cytokinetic defects by avoiding cytokinesis altogether. This could occur through premature differentiation, apoptosis, irreversible cell cycle exit, or arrest in G_1 or G_2 phase. This is supported by increased terminal differentiation marker expression (Fig. 3-26), Parp1-cleavage (Fig. 3-29), and reduction in Edu-positive cells (Fig. 3-28), respectively.

The observed discrepancies in outcomes could also be linked to changes in migratory behaviors resulting from the depletion of Septin9 or Septin7. It has been shown that inhibiting myoblast migration can enhance myoblast fusion, which may subsequently affect differentiation (Bondesen et al., 2007; Szabo et al., 2022). However, *in vitro* differentiation is typically studied in contact inhibited, confluent myoblasts, making it difficult to understand how prefusion events and alterations in migratory behavior could affect fusion and myotube formation. Gönczi *et al.* found that Septin7 depletion boosts myoblast migration, which supports the reduction in myogenic differentiation seen in Septin7-deficient myoblasts (Gönczi et al., 2022). Septin9, instead, has been shown to enhance migration in renal and mammary epithelial cells due to its actin-crosslinking activity (Chacko et al., 2005; Connolly et al., 2011; Dolat et al., 2014b). Additionally, Farrugia *et al.* observed paralogue-specific differences in melanoma cells undergoing ameboid migration, where Septin9, but not Septin7, affected the migration phenotype (Farrugia et al., 2020).

Previous work in our lab (PhD thesis, Dr. Agnieszka Denkis) analyzed the migratory behavior of Septin9-deficient C2C12 cells via wound scratch and Transwell migration assays, revealing no change in basal migration properties. Since Septin9-depletion did not change basal migration, it is fair to assume that this aspect did not contribute to precocious onset of myogenic differentiation. However, Septin9 depletion drastically reduced semi-directional

migration towards a BMP2 source through the Transwell membrane, indicating Septin9 involvement in chemotaxis-regulated migration. This aspect will need to be elucidated in greater detail, incorporating the analysis of directional migration under various seeding densities. Live cell imaging experiments focusing on monitoring the organization of Septin9 and Septin7 during myoblast proliferation and differentiation may help to understand the differences in observed phenotypes upon their depletion.

4.7. Working model and conclusions

Based on our data and discussion, we propose that Septin9 is a crucial component of myoblast septin complexes, which reorganizes as myogenic differentiation unfolds, ensuring the orderly progression through the differentiation process. Proliferating myoblasts predominantly exhibit actin-associated straight septin fibers in the perinuclear area. Induction of myogenic differentiation results in substantial reorganization of septins and dissociation from actin structures. SiRNA-mediated Septin9 depletion leads to the disruption of septin organization and triggers the premature onset of myogenic differentiation in cultured myoblasts (Fig. 4-3A-B). The central question of how exactly Septin9 safeguards against precocious differentiation requires further detailed investigation. However, we propose several potential cellular processes that may link septins with cell fate decisions (Fig. 4-3C).

First, septins may regulate actomyosin organization in differentiating myoblasts, as cytoskeletal remodeling is essential during early steps of differentiation, such as myoblast alignment (Swailes et al., 2006, 2004). This regulation may influence actomyosin integrity and contractility, actin decoration, bundling, and polymerization states, further regulating the physical properties of the cell cortex and nucleus (Bruyère et al., 2019; Gilden et al., 2012; Karolczak et al., 2015; Swailes et al., 2006; Tooley et al., 2009). This regulation may result from Septin9 binding to actin filaments (Smith et al., 2015) or changes in associated Rho GTPase signaling (Ito et al., 2005; Nagata and Inagaki, 2005; Safavian et al., 2023; Tomasso and Padrick, 2023).

Second, polymerized septins may support extracellular myokine signal transduction or facilitate the propagation of mechanical cues, as septins have been shown to regulate surface levels of transmembrane receptors and are considered emerging components of mechano-transduction pathways (Diesenberg et al., 2015; Lam and Calvo, 2019; Mostowy et al., 2011).

For instance, in the absence of Septin9, we observed changes in Activin A signaling and reduced expression of Taz co-transcription factor. As these two factors regulate myogenic differentiation (Jeong et al., 2010; Lodberg, 2021; Mohamed et al., 2016; Moustakas and Heldin, 2009), their altered signaling pathways may disrupt the orderly progression of the differentiation process.

Third, septins may influence cell fate decisions, such as the proliferation-differentiation decision, regulate intracellular protein transport, or ensure the homeostatic regulation of mitochondrial biogenesis. Septins play a prominent role in the mitotic phase of eukaryotic cell division (Russo and Krauss, 2021; Spiliotis and Nakos, 2021), but their influence on other phases of the cell cycle is not well understood. Following Septin9 knock-down, we reported decreased expression of Tfdp1, which is essential for the G_1/S transition (Engeland, 2022; Trimarchi and Lees, 2002), and a reduced prevalence of Septin9-deficient cells in the S-phase of the cell cycle. Thus, septins might lead to premature differentiation by regulating cell cycle progression. Furthermore, septins have been shown to bind mitochondria and participate in mitochondrial dynamics (Pagliuso et al., 2016; Sirianni et al., 2016). Therefore, the release of apoptogenic agents and an erroneous mitochondrial adaptation to myogenic differentiation upon Septin9 depletion may contribute to enhanced myogenic signaling.

This summary of the putative consequences of Septin9 depletion provides a framework for future investigations aimed at deciphering the exact contribution of the septin cytoskeleton to myoblast biology.

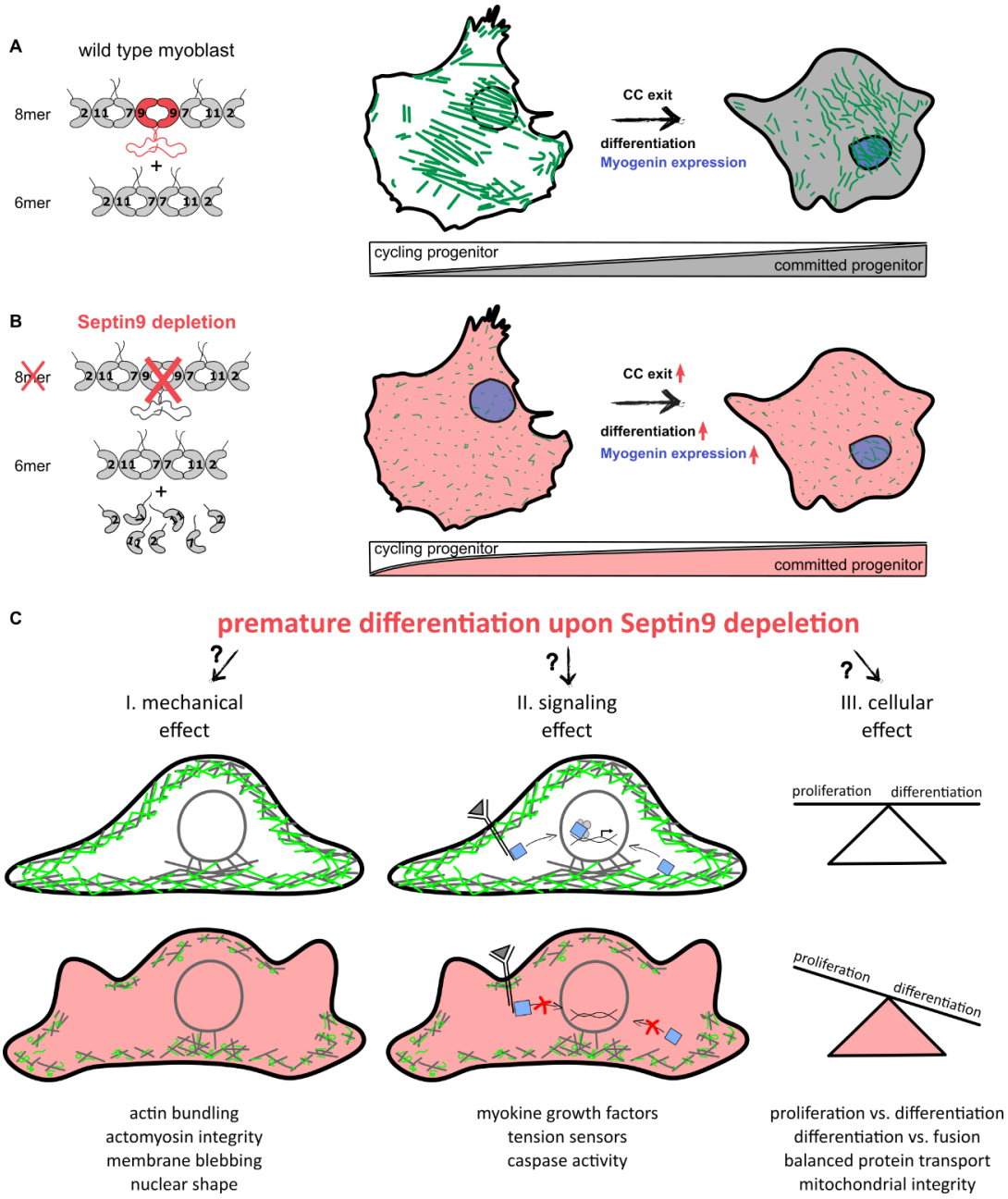

Figure 4-*2.* Working model and putative consequences of Septin9 depletion
A Septin9 incorporation into septin filaments ensures the orderly transition from proliferating to differentiating myoblasts. Myoblasts expressing terminal differentiation markers exhibit substantial reorganization of septin structures prior to fusion events. **B** Septin9 depletion disrupts myoblastal septin complexes and results in premature myogenic differentiation. **C** Putative consequences (I-III) of disrupted septin cytoskeleton in myoblast: (I) In dividing and differentiating prefusion myoblasts, Septin9 depletion may affect actomyosin integrity and, consequently, the physical properties of cortical membranes or the nucleus. Reducing actin decoration and interfering with the abundance of actin monomers may further impact the differentiation process. (II) Septin9 may enable septin complexes to scaffold components of myogenic signaling (e.g. receptors for extracellular myokine signals), intracellular homeostatic regulation, and mechanotransduction. (III) Septin complexes may assist in cellular proliferation-differentiation or differentiation-fusion decisions by regulating global processes such as protein transport towards the plasma membrane and ensuring organelle integrity, thereby maintaining the orderly transition from proliferation to differentiation.

4.8. Future perspectives

Despite sustained efforts over the past three decades by the prolific septin research community, our detailed understanding of septin functions in cellular processes remains incomplete and lags behind the knowledge accumulated about other cytoskeletal polymers. The understanding of septin-dependent regulatory mechanisms in muscle cells has only recently begun to emerge. As scientific discovery accelerates with the advent of new fields and tools, it is often driven by headline-grabbing breakthroughs. However, it is the foundational research, though less glamorous, that ultimately makes these advances possible.

Our study has introduced septins as a crucial component of the myoblast cytoskeleton, demonstrating their role in preventing premature differentiation onset. However, the detailed mechanisms behind this role remain unclear. Therefore, my short-term outlook radiates to explore various aspects of septin biology, including their stoichiometry, expression, polymer state, sub-cellular localization, and interactions in myoblasts. Addressing the questions formulated in the discussion section will be instrumental in promoting a broader understanding of these mechanisms.

Key questions include:

- How do septin paralogues express and localize in quiescent and activated MuSCs?
- What is the organization of the putative myogenic septin promoter? Are suggested septin proteins expressed and incorporated into the filament?
- To what extent do septin protein level changes correlate with mRNA level alterations observed in this study, and how do these changes influence protomer stoichiometry?
- In what processes and signaling pathways do septins act as scaffolds in myoblasts, and why must they reorganize so substantially?
- How does septin organization temporally correlate with myogenic lineage progression, and what triggers their reorganization?
- Is septin presence essential for the myoblast proliferation-differentiation decision?
- How do organized septin filaments exert their anti-apoptotic functions, and does the increase in apoptosis correlate with differentiation following disruption of septins?
- How is the actin cytoskeleton organized and functionally linked with septins in myoblasts?

- What roles do septins play in actomyosin contractility in myoblasts, and how do they influence formation of focal adhesions?
- How do septins affect actin-based cytoskeletal signaling and the propagation of signals to the nucleus of myoblasts?
- Is there an interconnected RhoA-actin-septin regulatory module that dynamically regulates cytoskeleton organization and maintains the undifferentiated state of myoblasts?

Addressing these questions will significantly enhance our understanding of septin roles in myoblasts.

Broader long-term questions addressing adjacent topics would examine how septin reorganization scales with the formation of contractile muscle tissue. Do septins reform in the contractile muscle after disorganization in myotubes, or do they continue their gradual reorganization along the myogenic trajectory under physiologic conditions, maintaining sustained upstream regulation lacking *in vitro*?

The protein expression of septins in adult muscle tissue prompts further questions about their roles in homeostasis, regeneration, and pathological conditions such as aging, sarcopenia, and cachexia. Moreover, it is essential to investigate whether septins are involved in the biology of smooth and cardiac muscle cells. Understanding whether the essential role of septins is conserved across different myogenic contexts is of great interest.

Furthermore, it is intriguing to examine whether the roles of septins in cell differentiation are conserved beyond myogenic context. Do septins play a role in differentiation processes of other cell types beyond those reported and discussed here? Exploring these aspects will improve our understanding of septin biology and of its implications across various physiological and pathological conditions.

5. Bibliography

Abbas, R., Larisch, S., 2020. Targeting XIAP for Promoting Cancer Cell Death—The Story of ARTS and SMAC. Cells 9, 663. https://doi.org/10.3390/cells9030663

Abbas, Ruqaia, Hartmann, O., Asiss, D.T., Abbas, Rabab, Kagan, J., Kim, H.-T., Oren, M., Diefenbacher, M., Orian, A., Larisch, S., 2024. ARTS and small-molecule ARTS mimetics upregulate p53 levels by promoting the degradation of XIAP. Apoptosis. https://doi.org/10.1007/s10495-024-01957-2

Abbey, M., Gaestel, M., Menon, M.B., 2019. Septins: Active GTPases or just GTP-binding proteins? Cytoskeleton 76, 55–62. https://doi.org/10.1002/cm.21451

Abe, T., Takano, K., Suzuki, A., Shimada, Y., Inagaki, M., Sato, N., Obinata, T., Endo, T., 2004. Myocyte differentiation generates nuclear invaginations traversed by myofibrils associating with sarcomeric protein mRNAs. Journal of Cell Science 117, 6523–6534. https://doi.org/10.1242/jcs.01574

Abmayr, S.M., Pavlath, G.K., 2012. Myoblast fusion: lessons from flies and mice. Development 139, 641–656. https://doi.org/10.1242/dev.068353

Afgan, E., Baker, D., Batut, B., van den Beek, M., Bouvier, D., Čech, M., Chilton, J., Clements, D., Coraor, N., Grüning, B.A., Guerler, A., Hillman-Jackson, J., Hiltemann, S., Jalili, V., Rasche, H., Soranzo, N., Goecks, J., Taylor, J., Nekrutenko, A., Blankenberg, D., 2018. The Galaxy platform for accessible, reproducible and collaborative biomedical analyses: 2018 update. Nucleic Acids Res 46, W537–W544. https://doi.org/10.1093/nar/gky379

Ageta-Ishihara, N., Miyata, T., Ohshima, C., Watanabe, M., Sato, Y., Hamamura, Y., Higashiyama, T., Mazitschek, R., Bito, H., Kinoshita, M., 2013. Septins promote dendrite and axon development by negatively regulating microtubule stability via HDAC6-mediated deacetylation. Nat Commun 4, 2532. https://doi.org/10.1038/ncomms3532

Agnetti, G., Herrmann, H., Cohen, S., 2022. New roles for desmin in the maintenance of muscle homeostasis. The FEBS Journal 289, 2755–2770. https://doi.org/10.1111/febs.15864

Ahmad, S., Jan, A.T., Baig, M.H., Lee, E.J., Choi, I., 2017. Matrix gla protein: An extracellular matrix protein regulates myostatin expression in the muscle developmental program. Life Sciences 172, 55–63. https://doi.org/10.1016/j.lfs.2016.12.011

Ahuja, P., Perriard, E., Trimble, W., Perriard, J.-C., Ehler, E., 2006. Probing the role of septins in cardiomyocytes. Experimental Cell Research 312, 1598–1609. https://doi.org/10.1016/j.yexcr.2006.01.029

Akbari-Birgani, S., Hosseinkhani, S., Mollamohamadi, S., Baharvand, H., 2014. Delay in Apoptosome Formation Attenuates Apoptosis in Mouse Embryonic Stem Cell Differentiation. Journal of Biological Chemistry 289, 16905–16913. https://doi.org/10.1074/jbc.M113.536730

Akhmetova, K., Balasov, M., Huijbregts, R.P.H., Chesnokov, I., 2015. Functional insight into the role of Orc6 in septin complex filament formation in Drosophila. MBoC 26, 15–28. https://doi.org/10.1091/mbc.e14-02-0734

Akil, A., Peng, J., Omrane, M., Gondeau, C., Desterke, C., Marin, M., Tronchère, H., Taveneau, C., Sar, S., Briolotti, P., Benjelloun, S., Benjouad, A., Maurel, P., Thiers, V., Bressanelli, S., Samuel, D., Bréchot, C., Gassama-Diagne, A., 2016. Septin 9 induces lipid droplets growth by a phosphatidylinositol-5-phosphate and microtubule-dependent mechanism hijacked by HCV. Nat Commun 7, 12203. https://doi.org/10.1038/ncomms12203

Alfaidi, M., Scott, M.L., Orr, A.W., 2021. Sinner or Saint?: Nck Adaptor Proteins in Vascular Biology. Front. Cell Dev. Biol. 9. https://doi.org/10.3389/fcell.2021.688388

Allan, C., Ker, A., Smith, C.-A., Tsimbouri, P.M., Borsoi, J., O'Neill, S., Gadegaard, N., Dalby, M.J., Dominic Meek, R.M., 2018. Osteoblast response to disordered nanotopography. J Tissue Eng 9, 2041731418784098. https://doi.org/10.1177/2041731418784098

Allbrook, D.B., Han, M.F., Hellmuth, A.E., 1971. Population of muscle satellite cells in relation to age and mitotic activity. Pathology 3, 233–243. https://doi.org/10.1080/00313027109073739

Alonso, A., Greenlee, M., Matts, J., Kline, J., Davis, K.J., Miller, R.K., 2015. Emerging roles of sumoylation in the regulation of actin, microtubules, intermediate filaments, and septins. Cytoskeleton (Hoboken) 72, 305–339. https://doi.org/10.1002/cm.21226

Al-Qusairi, L., Laporte, J., 2011. T-tubule biogenesis and triad formation in skeletal muscle and implication in human diseases. Skeletal Muscle 1, 26. https://doi.org/10.1186/2044-5040-1-26

Andersson, O., Reissmann, E., Ibáñez, C.F., 2006. Growth differentiation factor 11 signals through the transforming growth factor-β receptor ALK5 to regionalize the anterior–posterior axis. EMBO reports 7, 831–837. https://doi.org/10.1038/sj.embor.7400752

Andrés, V., Walsh, K., 1996. Myogenin expression, cell cycle withdrawal, and phenotypic differentiation are temporally separable events that precede cell fusion upon myogenesis. J Cell Biol 132, 657–666. https://doi.org/10.1083/jcb.132.4.657

Aravind, L., Dixit, V.M., Koonin, E.V., Aravind, L., Dixit, V.M., Koonin, E.V., Aravind, L., Dixit, V.M., Koonin, E.V., 1999. The domains of death: evolution of the apoptosis machinery. Trends in Biochemical Sciences 24, 47–53. https://doi.org/10.1016/S0968-0004(98)01341-3

Arnold, L., Henry, A., Poron, F., Baba-Amer, Y., van Rooijen, N., Plonquet, A., Gherardi, R.K., Chazaud, B., 2007. Inflammatory monocytes recruited after skeletal muscle injury switch into antiinflammatory macrophages to support myogenesis. Journal of Experimental Medicine 204, 1057–1069. https://doi.org/10.1084/jem.20070075

Arora, A.S., Huang, H.-L., Singh, R., Narui, Y., Suchenko, A., Hatano, T., Heissler, S.M., Balasubramanian, M.K., Chinthalapudi, K., 2023. Structural insights into actin isoforms. eLife 12, e82015. https://doi.org/10.7554/eLife.82015

Aschenbrenner, L., Lee, T., Hasson, T., 2003. Myo6 Facilitates the Translocation of Endocytic Vesicles from Cell Peripheries. Mol Biol Cell 14, 2728–2743. https://doi.org/10.1091/mbc.E02-11-0767

Aulehla, A., Pourquié, O., 2008. Oscillating signaling pathways during embryonic development. Current Opinion in Cell Biology 20, 632–637. https://doi.org/10.1016/j.ceb.2008.09.002

Auxier, B., Dee, J., Berbee, M.L., Momany, M., 2019. Diversity of opisthokont septin proteins reveals structural constraints and conserved motifs. BMC Evolutionary Biology 19, 4. https://doi.org/10.1186/s12862-018-1297-8

Babai, F., Musevi-Aghdam, J., Schurch, W., Royal, A., Gabbiani, G., 1990. Coexpression of α-sarcomeric actin, α-smooth muscle actin and desmin during myogenesis in rat and mouse embryos I. Skeletal muscle. Differentiation 44, 132–142. https://doi.org/10.1111/j.1432-0436.1990.tb00546.x

Baechler, B.L., Bloemberg, D., Quadrilatero, J., 2019. Mitophagy regulates mitochondrial network signaling, oxidative stress, and apoptosis during myoblast differentiation. Autophagy 15, 1606–1619. https://doi.org/10.1080/15548627.2019.1591672

Bagci, H., Sriskandarajah, N., Robert, A., Boulais, J., Elkholi, I.E., Tran, V., Lin, Z.-Y., Thibault, M.-P., Dubé, N., Faubert, D., Hipfner, D.R., Gingras, A.-C., Côté, J.-F., 2020. Mapping the proximity interaction network of the Rho-family GTPases reveals signalling pathways and regulatory mechanisms. Nat Cell Biol 22, 120–134. https://doi.org/10.1038/s41556-019-0438-7

Baghdadi, M.B., Firmino, J., Soni, K., Evano, B., Girolamo, D.D., Mourikis, P., Castel, D., Tajbakhsh, S., 2018. Notch-Induced miR-708 Antagonizes Satellite Cell Migration and Maintains Quiescence. Cell Stem Cell 23, 859-868.e5. https://doi.org/10.1016/j.stem.2018.09.017

Baghdadi, M.B., Tajbakhsh, S., 2018. Regulation and phylogeny of skeletal muscle regeneration. Developmental Biology, Regeneration: from cells to tissues to organisms 433, 200–209. https://doi.org/10.1016/j.ydbio.2017.07.026

Bai, X., Bowen, J.R., Knox, T.K., Zhou, K., Pendziwiat, M., Kuhlenbäumer, G., Sindelar, C.V., Spiliotis, E.T., 2013. Novel septin 9 repeat motifs altered in neuralgic amyotrophy bind and bundle microtubules. Journal of Cell Biology 203, 895–905. https://doi.org/10.1083/jcb.201308068

Bains, W., Ponte, P., Blau, H., Kedes, L., 1984. Cardiac actin is the major actin gene product in skeletal muscle cell differentiation in vitro. Mol Cell Biol 4, 1449–1453. https://doi.org/10.1128/mcb.4.8.1449-1453.1984

Bansal, D., Miyake, K., Vogel, S.S., Groh, S., Chen, C.-C., Williamson, R., McNeil, P.L., Campbell, K.P., 2003. Defective membrane repair in dysferlin-deficient muscular dystrophy. Nature 423, 168–172. https://doi.org/10.1038/nature01573

Barbieri, E., Battistelli, M., Casadei, L., Vallorani, L., Piccoli, G., Guescini, M., Gioacchini, A.M., Polidori, E., Zeppa, S., Ceccaroli, P., Stocchi, L., Stocchi, V., Falcieri, E., 2011. Morphofunctional and Biochemical Approaches for Studying Mitochondrial Changes during Myoblasts Differentiation. J Aging Res 2011, 845379. https://doi.org/10.4061/2011/845379

Baulida, J., Díaz, V.M., García de Herreros, A., 2019. Snail1: A Transcriptional Factor Controlled at Multiple Levels. J Clin Med 8, 757. https://doi.org/10.3390/jcm8060757

Beber, A., Taveneau, C., Nania, M., Tsai, F.-C., Di Cicco, A., Bassereau, P., Lévy, D., Cabral, J.T., Isambert, H., Mangenot, S., Bertin, A., 2019. Membrane reshaping by micrometric curvature sensitive septin filaments. Nat Commun 10, 420. https://doi.org/10.1038/s41467-019-08344-5

Becker, I.C., Wilkie, A.R., Unger, B.A., Sciaudone, A.R., Fatima, F., Tsai, I.-T., Xu, K., Machlus, K.R., Italiano, J.E., 2024. Dynamic actin/septin network in megakaryocytes coordinates proplatelet elaboration. Haematologica 109, 915–928. https://doi.org/10.3324/haematol.2023.283369

Becker, R., Leone, M., Engel, F.B., 2020. Microtubule Organization in Striated Muscle Cells. Cells 9, 1395. https://doi.org/10.3390/cells9061395

Becker, R., Vergarajauregui, S., Billing, F., Sharkova, M., Lippolis, E., Mamchaoui, K., Ferrazzi, F., Engel, F.B., 2021. Myogenin controls via AKAP6 non-centrosomal microtubule-organizing center formation at the nuclear envelope. eLife 10, e65672. https://doi.org/10.7554/eLife.65672

Bell, R.A.V., Megeney, L.A., 2017. Evolution of caspase-mediated cell death and differentiation: twins separated at birth. Cell Death Differ 24, 1359–1368. https://doi.org/10.1038/cdd.2017.37

Benoit, B., Poüs, C., Baillet, A., 2023. Septins as membrane influencers: direct play or in association with other cytoskeleton partners. Frontiers in Cell and Developmental Biology 11.

Bentzinger, C.F., von Maltzahn, J., Dumont, N.A., Stark, D.A., Wang, Y.X., Nhan, K., Frenette, J., Cornelison, D., Rudnicki, M.A., 2014. Wnt7a stimulates myogenic stem cell motility and engraftment resulting in improved muscle strength. J Cell Biol 205, 97–111. https://doi.org/10.1083/jcb.201310035

Bentzinger, C.F., Wang, Y.X., Rudnicki, M.A., 2012. Building muscle: molecular regulation of myogenesis. Cold Spring Harb Perspect Biol 4, a008342. https://doi.org/10.1101/cshperspect.a008342

Berger, C., Pallavi, S.K., Prasad, M., Shashidhara, L.S., Technau, G.M., 2005. A critical role for Cyclin E in cell fate determination in the central nervous system of Drosophila melanogaster. Nat Cell Biol 7, 56–62. https://doi.org/10.1038/ncb1203

Berger, S., Schäfer, G., Kesper, D.A., Holz, A., Eriksson, T., Palmer, R.H., Beck, L., Klämbt, C., Renkawitz-Pohl, R., Önel, S.-F., 2008. WASP and SCAR have distinct roles in activating the Arp2/3 complex during myoblast fusion. Journal of Cell Science 121, 1303–1313. https://doi.org/10.1242/jcs.022269

Berkes, C.A., Tapscott, S.J., 2005. MyoD and the transcriptional control of myogenesis. Seminars in Cell & Developmental Biology, Biology of Hypoxia and Myogenesis and Muscle Disease 16, 585–595. https://doi.org/10.1016/j.semcdb.2005.07.006

Bernardi, H., Gay, S., Fedon, Y., Vernus, B., Bonnieu, A., Bacou, F., 2011. Wnt4 activates the canonical β-catenin pathway and regulates negatively myostatin: functional implication in myogenesis. Am J Physiol Cell Physiol 300, C1122-1138. https://doi.org/10.1152/ajpcell.00214.2010

Bertin, A., McMurray, M.A., Grob, P., Park, S.-S., Garcia, G., Patanwala, I., Ng, H., Alber, T., Thorner, J., Nogales, E., 2008. Saccharomyces cerevisiae septins: Supramolecular organization of heterooligomers and the mechanism of filament assembly. Proceedings of the National Academy of Sciences 105, 8274–8279. https://doi.org/10.1073/pnas.0803330105

Bertin, A., McMurray, M.A., Thai, L., Garcia, G., Votin, V., Grob, P., Allyn, T., Thorner, J., Nogales, E., 2010. Phosphatidylinositol-4,5-bisphosphate Promotes Budding Yeast Septin Filament

Assembly and Organization. Journal of Molecular Biology 404, 711–731. https://doi.org/10.1016/j.jmb.2010.10.002

Betschinger, J., Knoblich, J.A., 2004. Dare to Be Different: Asymmetric Cell Division in Drosophila, C. elegans and Vertebrates. Current Biology 14, R674–R685. https://doi.org/10.1016/j.cub.2004.08.017

Bian, C., Su, J., Zheng, Z., Wei, J., Wang, H., Meng, L., Xin, Y., Jiang, X., 2022. ARTS, an unusual septin, regulates tumorigenesis by promoting apoptosis. Biomedicine & Pharmacotherapy 152, 113281. https://doi.org/10.1016/j.biopha.2022.113281

Bieling, P., Li, T.-D., Weichsel, J., McGorty, R., Jreij, P., Huang, B., Fletcher, D.A., Mullins, R.D., 2016. Force Feedback Controls Motor Activity and Mechanical Properties of Self-Assembling Branched Actin Networks. Cell 164, 115–127. https://doi.org/10.1016/j.cell.2015.11.057

Biressi, S., Molinaro, M., Cossu, G., 2007a. Cellular heterogeneity during vertebrate skeletal muscle development. Developmental Biology 308, 281–293. https://doi.org/10.1016/j.ydbio.2007.06.006

Biressi, S., Tagliafico, E., Lamorte, G., Monteverde, S., Tenedini, E., Roncaglia, E., Ferrari, Sergio, Ferrari, Stefano, Cusella-De Angelis, M.G., Tajbakhsh, S., Cossu, G., 2007b. Intrinsic phenotypic diversity of embryonic and fetal myoblasts is revealed by genome-wide gene expression analysis on purified cells. Dev Biol 304, 633–651. https://doi.org/10.1016/j.ydbio.2007.01.016

Bischoff, R., 1986. Proliferation of muscle satellite cells on intact myofibers in culture. Developmental Biology 115, 129–139. https://doi.org/10.1016/0012-1606(86)90234-4

Bischoff, R., 1975. Regeneration of single skeletal muscle fibers in vitro. The Anatomical Record 182, 215–235. https://doi.org/10.1002/ar.1091820207

Bishop, A.L., Hall, A., 2000. Rho GTPases and their effector proteins. Biochem J 348, 241–255.

Bjornson, C.R.R., Cheung, T.H., Liu, L., Tripathi, P.V., Steeper, K.M., Rando, T.A., 2012. Notch signaling is necessary to maintain quiescence in adult muscle stem cells. Stem Cells 30, 232–242. https://doi.org/10.1002/stem.773

Bloemberg, D., Quadrilatero, J., 2014. Mitochondrial pro-apoptotic indices do not precede the transient caspase activation associated with myogenesis. Biochimica et Biophysica Acta (BBA) - Molecular Cell Research 1843, 2926–2936. https://doi.org/10.1016/j.bbamcr.2014.09.002

Bloise, E., Ciarmela, P., Dela Cruz, C., Luisi, S., Petraglia, F., Reis, F.M., 2019. Activin A in Mammalian Physiology. Physiological Reviews 99, 739–780. https://doi.org/10.1152/physrev.00002.2018

Bober, E., Franz, T., Arnold, H.-H., Gruss, P., Tremblay, P., 1994. Pax-3 is required for the development of limb muscles: a possible role for the migration of dermomyotomal muscle progenitor cells. Development 120, 603–612. https://doi.org/10.1242/dev.120.3.603

Bock, F.J., Tait, S.W.G., 2020. Mitochondria as multifaceted regulators of cell death. Nat Rev Mol Cell Biol 21, 85–100. https://doi.org/10.1038/s41580-019-0173-8

Boldrin, L., Morgan, J.E., 2012. Human satellite cells: identification on human muscle fibres. PLoS Curr 3, RRN1294. https://doi.org/10.1371/currents.RRN1294

Bondesen, B.A., Jones, K.A., Glasgow, W.C., Pavlath, G.K., 2007. Inhibition of myoblast migration by prostacyclin is associated with enhanced cell fusion. FASEB J 21, 3338–3345. https://doi.org/10.1096/fj.06-7070com

Boonen, K.J.M., Rosaria-Chak, K.Y., Baaijens, F.P.T., van der Schaft, D.W.J., Post, M.J., 2009. Essential environmental cues from the satellite cell niche: optimizing proliferation and differentiation. American Journal of Physiology-Cell Physiology 296, C1338–C1345. https://doi.org/10.1152/ajpcell.00015.2009

Boonstra, K., Bloemberg, D., Quadrilatero, J., 2018. Caspase-2 is required for skeletal muscle differentiation and myogenesis. Biochim Biophys Acta Mol Cell Res 1865, 95–104. https://doi.org/10.1016/j.bbamcr.2017.07.016

Boontheekul, T., Hill, E.E., Kong, H.-J., Mooney, D.J., 2007. Regulating Myoblast Phenotype Through Controlled Gel Stiffness and Degradation. Tissue Engineering 13, 1431–1442. https://doi.org/10.1089/ten.2006.0356

Bornstein, B., Gottfried, Y., Edison, N., Shekhtman, A., Lev, T., Glaser, F., Larisch, S., 2011. ARTS binds to a distinct domain in XIAP-BIR3 and promotes apoptosis by a mechanism that is different from other IAP-antagonists. Apoptosis 16, 869–881. https://doi.org/10.1007/s10495-011-0622-0

Boubakar, L., Falk, J., Ducuing, H., Thoinet, K., Reynaud, F., Derrington, E., Castellani, V., 2017. Molecular Memory of Morphologies by Septins during Neuron Generation Allows Early Polarity Inheritance. Neuron 95, 834-851.e5. https://doi.org/10.1016/j.neuron.2017.07.027

Boudjadi, S., Chatterjee, B., Sun, W., Vemu, P., Barr, F.G., 2018. The expression and function of PAX3 in development and disease. Gene 666, 145–157. https://doi.org/10.1016/j.gene.2018.04.087

Boureux, A., Vignal, E., Faure, S., Fort, P., 2007. Evolution of the Rho family of ras-like GTPases in eukaryotes. Mol Biol Evol 24, 203–216. https://doi.org/10.1093/molbev/msl145

Bourne, H.R., Sanders, D.A., McCormick, F., 1991. The GTPase superfamily: conserved structure and molecular mechanism. Nature 349, 117–127. https://doi.org/10.1038/349117a0

Bourne, H.R., Sanders, D.A., McCormick, F., 1990. The GTPase superfamily: a conserved switch for diverse cell functions. Nature 348, 125–132. https://doi.org/10.1038/348125a0

Boussif, O., Lezoualc'h, F., Zanta, M.A., Mergny, M.D., Scherman, D., Demeneix, B., Behr, J.P., 1995. A versatile vector for gene and oligonucleotide transfer into cells in culture and in vivo: polyethylenimine. Proceedings of the National Academy of Sciences 92, 7297–7301. https://doi.org/10.1073/pnas.92.16.7297

Bowen, J.R., Hwang, D., Bai, X., Roy, D., Spiliotis, E.T., 2011. Septin GTPases spatially guide microtubule organization and plus end dynamics in polarizing epithelia. Journal of Cell Biology 194, 187–197. https://doi.org/10.1083/jcb.201102076

Bowlin, K.M., Embree, L.J., Garry, M.G., Garry, D.J., Shi, X., 2013. Kbtbd5 is regulated by MyoD and restricted to the myogenic lineage. Differentiation 86, 184–191. https://doi.org/10.1016/j.diff.2013.08.002

Bowne-Anderson, H., Zanic, M., Kauer, M., Howard, J., 2013. Microtubule dynamic instability: A new model with coupled GTP hydrolysis and multistep catastrophe. BioEssays 35, 452–461. https://doi.org/10.1002/bies.201200131

Brack, A.S., Conboy, I.M., Conboy, M.J., Shen, J., Rando, T.A., 2008. A Temporal Switch from Notch to Wnt Signaling in Muscle Stem Cells Is Necessary for Normal Adult Myogenesis. Cell Stem Cell 2, 50–59. https://doi.org/10.1016/j.stem.2007.10.006

Bracken, A.P., Ciro, M., Cocito, A., Helin, K., 2004. E2F target genes: unraveling the biology. Trends in Biochemical Sciences 29, 409–417. https://doi.org/10.1016/j.tibs.2004.06.006

Bragdon, B., Moseychuk, O., Saldanha, S., King, D., Julian, J., Nohe, A., 2011. Bone Morphogenetic Proteins: A critical review. Cellular Signalling 23, 609–620. https://doi.org/10.1016/j.cellsig.2010.10.003

Brangwynne, C.P., MacKintosh, F.C., Kumar, S., Geisse, N.A., Talbot, J., Mahadevan, L., Parker, K.K., Ingber, D.E., Weitz, D.A., 2006. Microtubules can bear enhanced compressive loads in living cells because of lateral reinforcement. J Cell Biol 173, 733–741. https://doi.org/10.1083/jcb.200601060

Bridges, A.A., Jentzsch, M.S., Oakes, P.W., Occhipinti, P., Gladfelter, A.S., 2016. Micron-scale plasma membrane curvature is recognized by the septin cytoskeleton. Journal of Cell Biology 213, 23–32. https://doi.org/10.1083/jcb.201512029

Bridges, A.A., Zhang, H., Mehta, S.B., Occhipinti, P., Tani, T., Gladfelter, A.S., 2014. Septin assemblies form by diffusion-driven annealing on membranes. Proceedings of the National Academy of Sciences 111, 2146–2151. https://doi.org/10.1073/pnas.1314138111

Brondolin, M., Herzog, D., Sultan, S., Warburton, F., Vigilante, A., Knight, R.D., 2023. Migration and differentiation of muscle stem cells are coupled by RhoA signalling during regeneration. Open Biol 13, 230037. https://doi.org/10.1098/rsob.230037

Brotto, M., Abreu, E.L., 2012. Sarcopenia: pharmacology of today and tomorrow. J Pharmacol Exp Ther 343, 540–546. https://doi.org/10.1124/jpet.112.191759

Brunk, C.F., Yaffe, D., 1976. The reversible inhibition of myoblast fusion by ethidium bromide (EB). Exp Cell Res 99, 310–318. https://doi.org/10.1016/0014-4827(76)90588-7

Brunton, V.G., MacPherson, I.R.J., Frame, M.C., 2004. Cell adhesion receptors, tyrosine kinases and actin modulators: a complex three-way circuitry. Biochim Biophys Acta 1692, 121–144. https://doi.org/10.1016/j.bbamcr.2004.04.010

Bruyère, C., Versaevel, M., Mohammed, D., Alaimo, L., Luciano, M., Vercruysse, E., Gabriele, S., 2019. Actomyosin contractility scales with myoblast elongation and enhances differentiation through YAP nuclear export. Sci Rep 9, 15565. https://doi.org/10.1038/s41598-019-52129-1

Bryan, B.A., Li, D., Wu, X., Liu, M., 2005. The Rho family of small GTPases: crucial regulators of skeletal myogenesis. CMLS, Cell. Mol. Life Sci. 62, 1547–1555. https://doi.org/10.1007/s00018-005-5029-z

Buckingham, M., 1992. Making muscle in mammals. Trends in Genetics 8, 144–149. https://doi.org/10.1016/0168-9525(92)90373-C

Buckingham, M., Bajard, L., Chang, T., Daubas, P., Hadchouel, J., Meilhac, S., Montarras, D., Rocancourt, D., Relaix, F., 2003. The formation of skeletal muscle: from somite to limb. Journal of Anatomy 202, 59–68. https://doi.org/10.1046/j.1469-7580.2003.00139.x

Buckingham, M., Relaix, F., 2007. The Role of Pax Genes in the Development of Tissues and Organs: Pax3 and Pax7 Regulate Muscle Progenitor Cell Functions. Annual Review of Cell and Developmental Biology 23, 645–673. https://doi.org/10.1146/annurev.cellbio.23.090506.123438

Buckley, K.H., Nestor-Kalinoski, A.L., Pizza, F.X., 2022. Positional Context of Myonuclear Transcription During Injury-Induced Muscle Regeneration. Frontiers in Physiology 13.

Buday, L., Wunderlich, L., Tamás, P., 2002. The Nck family of adapter proteins: Regulators of actin cytoskeleton. Cellular Signalling 14, 723–731. https://doi.org/10.1016/S0898-6568(02)00027-X

Burbelo, P.D., Snow, D.M., Bahou, W., Spiegel, S., 1999. MSE55, a Cdc42 effector protein, induces long cellular extensions in fibroblasts. Proceedings of the National Academy of Sciences 96, 9083–9088. https://doi.org/10.1073/pnas.96.16.9083

Burridge, K., Guilluy, C., 2016. Focal adhesions, stress fibers and mechanical tension. Experimental cell research 343, 14. https://doi.org/10.1016/j.yexcr.2015.10.029

Burridge, K., Monaghan-Benson, E., Graham, D.M., 2019. Mechanotransduction: from the cell surface to the nucleus via RhoA. Philosophical Transactions of the Royal Society B: Biological Sciences 374, 20180229. https://doi.org/10.1098/rstb.2018.0229

Burridge, K., Wittchen, E.S., 2013. The tension mounts: Stress fibers as force-generating mechanotransducers. J Cell Biol 200, 9–19. https://doi.org/10.1083/jcb.201210090

Butler, M.T., Wallingford, J.B., 2017. Planar cell polarity in development and disease. Nat Rev Mol Cell Biol 18, 375–388. https://doi.org/10.1038/nrm.2017.11

Byers, B., Goetsch, L., 1976. A highly ordered ring of membrane-associated filaments in budding yeast. Journal of Cell Biology 69, 717–721. https://doi.org/10.1083/jcb.69.3.717

Caballero-Sánchez, N., Alonso-Alonso, S., Nagy, L., 2022. Regenerative inflammation: When immune cells help to re-build tissues. The FEBS Journal n/a. https://doi.org/10.1111/febs.16693

Calvo, F., Ranftl, R., Hooper, S., Farrugia, A.J., Moeendarbary, E., Bruckbauer, A., Batista, F., Charras, G., Sahai, E., 2015. Cdc42EP3/BORG2 and Septin Network Enables Mechano-transduction and the Emergence of Cancer-Associated Fibroblasts. Cell Reports 13, 2699–2714. https://doi.org/10.1016/j.celrep.2015.11.052

Cannon, K.S., Woods, B.L., Crutchley, J.M., Gladfelter, A.S., 2019. An amphipathic helix enables septins to sense micrometer-scale membrane curvature. Journal of Cell Biology 218, 1128–1137. https://doi.org/10.1083/jcb.201807211

Cao, J., Spielmann, M., Qiu, X., Huang, X., Ibrahim, D.M., Hill, A.J., Zhang, F., Mundlos, S., Christiansen, L., Steemers, F.J., Trapnell, C., Shendure, J., 2019. The single cell transcriptional landscape of mammalian organogenesis. Nature 566, 496–502. https://doi.org/10.1038/s41586-019-0969-x

Cao, L., Ding, X., Yu, W., Yang, X., Shen, S., Yu, L., 2007. Phylogenetic and evolutionary analysis of the septin protein family in metazoan. FEBS Letters 581, 5526–5532. https://doi.org/10.1016/j.febslet.2007.10.032

Capetanaki, Y., Bloch, R.J., Kouloumenta, A., Mavroidis, M., Psarras, S., 2007. Muscle intermediate filaments and their links to membranes and membranous organelles. Experimental Cell Research, Special Issue - Intermediate Filaments 313, 2063–2076. https://doi.org/10.1016/j.yexcr.2007.03.033

Carey, K.A., Farnfield, M.M., Tarquinio, S.D., Cameron-Smith, D., 2007. Impaired expression of Notch signaling genes in aged human skeletal muscle. J Gerontol A Biol Sci Med Sci 62, 9–17. https://doi.org/10.1093/gerona/62.1.9

Carithers, L.J., Ardlie, K., Barcus, M., Branton, P.A., Britton, A., Buia, S.A., Compton, C.C., DeLuca, D.S., Peter-Demchok, J., Gelfand, E.T., Guan, P., Korzeniewski, G.E., Lockhart, N.C., Rabiner, C.A., Rao, A.K., Robinson, K.L., Roche, N.V., Sawyer, S.J., Segrè, A.V., Shive, C.E., Smith, A.M., Sobin, L.H., Undale, A.H., Valentino, K.M., Vaught, J., Young, T.R., Moore, H.M., on behalf of the GTEx Consortium, 2015. A Novel Approach to High-Quality Postmortem Tissue Procurement: The GTEx Project. Biopreservation and Biobanking 13, 311–319. https://doi.org/10.1089/bio.2015.0032

Carnac, G., Primig, M., Kitzmann, M., Chafey, P., Tuil, D., Lamb, N., Fernandez, A., 1998. RhoA GTPase and Serum Response Factor Control Selectively the Expression of MyoD without Affecting Myf5 in Mouse Myoblasts. Mol Biol Cell 9, 1891–1902.

Castellani, L., Salvati, E., Alemà, S., Falcone, G., 2006. Fine Regulation of RhoA and Rock Is Required for Skeletal Muscle Differentiation*. Journal of Biological Chemistry 281, 15249–15257. https://doi.org/10.1074/jbc.M601390200

Castro, D.K.S.V., da Silva, S.M.O., Pereira, H.M., Macedo, J.N.A., Leonardo, D.A., Valadares, N.F., Kumagai, P.S., Brandão-Neto, J., Araújo, A.P.U., Garratt, R.C., 2020. A complete compendium of crystal structures for the human SEPT3 subgroup reveals functional plasticity at a specific septin interface. IUCrJ 7, 462–479. https://doi.org/10.1107/S2052252520002973

Castro, D.K.S.V., Rosa, H.V.D., Mendonça, D.C., Cavini, I.A., Araujo, A.P.U., Garratt, R.C., 2023. Dissecting the Binding Interface of the Septin Polymerization Enhancer Borg BD3. Journal of Molecular Biology 435, 168132. https://doi.org/10.1016/j.jmb.2023.168132

Cavini, I.A., Leonardo, D.A., Rosa, H.V.D., Castro, D.K.S.V., D'Muniz Pereira, H., Valadares, N.F., Araujo, A.P.U., Garratt, R.C., 2021. The Structural Biology of Septins and Their Filaments: An Update. Frontiers in Cell and Developmental Biology 9.

Cayouette, M., Whitmore, A.V., Jeffery, G., Raff, M., 2001. Asymmetric Segregation of Numb in Retinal Development and the Influence of the Pigmented Epithelium. J. Neurosci. 21, 5643–5651. https://doi.org/10.1523/JNEUROSCI.21-15-05643.2001

Chacko, A.D., Hyland, P.L., McDade, S.S., Hamilton, P.W., Russell, S.H., Hall, P.A., 2005. SEPT9_v4 expression induces morphological change, increased motility and disturbed polarity. The Journal of Pathology 206, 458–465. https://doi.org/10.1002/path.1794

Chakkalakal, J., Brack, A., 2012. Extrinsic Regulation of Satellite Cell Function and Muscle Regeneration Capacity during Aging. J Stem Cell Res Ther Suppl 11, 001. https://doi.org/10.4172/2157-7633.S11-001

Chal, J., Pourquié, O., 2017. Making muscle: skeletal myogenesis in vivo and in vitro. Development 144, 2104–2122. https://doi.org/10.1242/dev.151035

Chang, H., Knothe Tate, M.L., 2011. Structure - Function Relationships in the Stem Cell's Mechanical World B: Emergent Anisotropy of the Cytoskeleton Correlates to Volume and Shape Changing Stress Exposure. Mol Cell Biomech 8, 297–318.

Charras, G., Paluch, E., 2008. Blebs lead the way: how to migrate without lamellipodia. Nat Rev Mol Cell Biol 9, 730–736. https://doi.org/10.1038/nrm2453

Charrasse, S., Comunale, F., Fortier, M., Portales-Casamar, E., Debant, A., Gauthier-Rouvière, C., 2007. M-Cadherin Activates Rac1 GTPase through the Rho-GEF Trio during Myoblast Fusion. Mol Biol Cell 18, 1734–1743. https://doi.org/10.1091/mbc.E06-08-0766

Charrasse, S., Comunale, F., Grumbach, Y., Poulat, F., Blangy, A., Gauthier-Rouvière, C., 2006. RhoA GTPase Regulates M-Cadherin Activity and Myoblast Fusion. MBoC 17, 749–759. https://doi.org/10.1091/mbc.e05-04-0284

Charrier, E.E., Montel, L., Asnacios, A., Delort, F., Vicart, P., Gallet, F., Batonnet-Pichon, S., Hénon, S., 2018. The desmin network is a determinant of the cytoplasmic stiffness of myoblasts. Biology of the Cell 110, 77–90. https://doi.org/10.1111/boc.201700040

Chen, E.H., 2011. Invasive Podosomes and Myoblast Fusion. Curr Top Membr 68, 235–258. https://doi.org/10.1016/B978-0-12-385891-7.00010-6

Chen, E.H., Pryce, B.A., Tzeng, J.A., Gonzalez, G.A., Olson, E.N., 2003. Control of Myoblast Fusion by a Guanine Nucleotide Exchange Factor, Loner, and Its Effector ARF6. Cell 114, 751–762. https://doi.org/10.1016/S0092-8674(03)00720-7

Chen, H.-C., Kanai, M., Inoue-Yamauchi, A., Tu, H.-C., Huang, Y., Ren, D., Kim, H., Takeda, S., Reyna, D.E., Chan, P.M., Ganesan, Y.T., Liao, C.-P., Gavathiotis, E., Hsieh, J.J., Cheng, E.H., 2015. An interconnected hierarchical model of cell death regulation by the BCL-2 family. Nat Cell Biol 17, 1270–1281. https://doi.org/10.1038/ncb3236

Chen, J.L., Walton, K.L., Qian, H., Colgan, T.D., Hagg, A., Watt, M.J., Harrison, C.A., Gregorevic, P., 2016. Differential Effects of IL6 and Activin A in the Development of Cancer-Associated Cachexia. Cancer Res 76, 5372–5382. https://doi.org/10.1158/0008-5472.CAN-15-3152

Chen, J.L., Walton, K.L., Winbanks, C.E., Murphy, K.T., Thomson, R.E., Makanji, Y., Qian, H., Lynch, G.S., Harrison, C.A., Gregorevic, P., 2014. Elevated expression of activins promotes muscle wasting and cachexia. The FASEB Journal 28, 1711–1723. https://doi.org/10.1096/fj.13-245894

Chen, L., Shi, K., Frary, C.E., Ditzel, N., Hu, H., Qiu, W., Kassem, M., 2015. Inhibiting actin depolymerization enhances osteoblast differentiation and bone formation in human stromal stem cells. Stem Cell Res 15, 281–289. https://doi.org/10.1016/j.scr.2015.06.009

Chen, M., Bresnick, A.R., O'Connor, K.L., 2013. Coupling S100A4 to Rhotekin alters Rho signaling output in breast cancer cells. Oncogene 32, 3754–3764. https://doi.org/10.1038/onc.2012.383

Chen, T.-Y., Lin, T.-C., Kuo, P.-L., Chen, Z.-R., Cheng, H., Chao, Y.-Y., Syu, J.-S., Lu, F.-I., Wang, C.-Y., 2021. Septin 7 is a centrosomal protein that ensures S phase entry and microtubule nucleation by maintaining the abundance of p150glued. Journal of Cellular Physiology 236, 2706–2724. https://doi.org/10.1002/jcp.30037

Chen, X., Yuan, W., Li, Y., Luo, J., Hou, N., 2020. Role of Hippo-YAP1/TAZ pathway and its crosstalk in cardiac biology. Int J Biol Sci 16, 2454–2463. https://doi.org/10.7150/ijbs.47142

Cho, Y., Liang, P., 2011. S-phase-coupled apoptosis in tumor suppression. Cell. Mol. Life Sci. 68, 1883–1896. https://doi.org/10.1007/s00018-011-0666-x

Choi, S., Ferrari, G., Tedesco, F.S., 2020. Cellular dynamics of myogenic cell migration: molecular mechanisms and implications for skeletal muscle cell therapies. EMBO Mol Med 12, e12357. https://doi.org/10.15252/emmm.202012357

Christensen, K., Doblhammer, G., Rau, R., Vaupel, J.W., 2009. Ageing populations: the challenges ahead. Lancet 374, 1196–1208. https://doi.org/10.1016/S0140-6736(09)61460-4

Ciruna, B., Rossant, J., 2001. FGF Signaling Regulates Mesoderm Cell Fate Specification and Morphogenetic Movement at the Primitive Streak. Developmental Cell 1, 37–49. https://doi.org/10.1016/S1534-5807(01)00017-X

Collins, K.B., Kang, H., Matsche, J., Klomp, J.E., Rehman, J., Malik, A.B., Karginov, A.V., 2019. Septin2 mediates podosome maturation and endothelial cell invasion associated with angiogenesis. Journal of Cell Biology 219, e201903023. https://doi.org/10.1083/jcb.201903023

Collins-Hooper, H., Woolley, T.E., Dyson, L., Patel, A., Potter, P., Baker, R.E., Gaffney, E.A., Maini, P.K., Dash, P.R., Patel, K., 2012. Age-Related Changes in Speed and Mechanism of Adult Skeletal Muscle Stem Cell Migration. Stem Cells 30, 1182–1195. https://doi.org/10.1002/stem.1088

Conboy, I.M., Conboy, M.J., Wagers, A.J., Girma, E.R., Weissman, I.L., Rando, T.A., 2005. Rejuvenation of aged progenitor cells by exposure to a young systemic environment. Nature 433, 760–764. https://doi.org/10.1038/nature03260

Conboy, I.M., Rando, T.A., 2002. The regulation of Notch signaling controls satellite cell activation and cell fate determination in postnatal myogenesis. Dev Cell 3, 397–409. https://doi.org/10.1016/s1534-5807(02)00254-x

Connolly, D., Hoang, H.G., Adler, E., Tazearslan, C., Simmons, N., Bernard, V.V., Castaldi, M., Oktay, M.H., Montagna, C., 2014. Septin 9 amplification and isoform-specific expression in peritumoral and tumor breast tissue. Biological Chemistry 395, 157–167. https://doi.org/10.1515/hsz-2013-0247

Connolly, D., Yang, Z., Castaldi, M., Simmons, N., Oktay, M.H., Coniglio, S., Fazzari, M.J., Verdier-Pinard, P., Montagna, C., 2011. Septin 9 isoform expression, localization and epigenetic changes during human and mouse breast cancer progression. Breast Cancer Research 13, R76. https://doi.org/10.1186/bcr2924

Costa, M.L., 2014. Cytoskeleton and Adhesion in Myogenesis. International Scholarly Research Notices 2014, e713631. https://doi.org/10.1155/2014/713631

Costigliola, N., Ding, L., Burckhardt, C.J., Han, S.J., Gutierrez, E., Mota, A., Groisman, A., Mitchison, T.J., Danuser, G., 2017. Vimentin fibers orient traction stress. Proceedings of the National Academy of Sciences 114, 5195–5200. https://doi.org/10.1073/pnas.1614610114

Cui, S., Li, L., Yu, R.T., Downes, M., Evans, R.M., Hulin, J.-A., Makarenkova, H.P., Meech, R., 2019. β-Catenin is essential for differentiation of primary myoblasts via cooperation with MyoD and α-catenin. Development 146, dev167080. https://doi.org/10.1242/dev.167080

Dacwag, C.S., Ohkawa, Y., Pal, S., Sif, S., Imbalzano, A.N., 2007. The Protein Arginine Methyltransferase Prmt5 Is Required for Myogenesis because It Facilitates ATP-Dependent Chromatin Remodeling. Mol Cell Biol 27, 384–394. https://doi.org/10.1128/MCB.01528-06

Dalby, M.J., Gadegaard, N., Tare, R., Andar, A., Riehle, M.O., Herzyk, P., Wilkinson, C.D.W., Oreffo, R.O.C., 2007. The control of human mesenchymal cell differentiation using nanoscale symmetry and disorder. Nature Mater 6, 997–1003. https://doi.org/10.1038/nmat2013

Dalby, M.J., McCloy, D., Robertson, M., Wilkinson, C.D.W., Oreffo, R.O.C., 2006. Osteoprogenitor response to defined topographies with nanoscale depths. Biomaterials 27, 1306–1315. https://doi.org/10.1016/j.biomaterials.2005.08.028

Davis, R.L., Weintraub, H., Lassar, A.B., 1987. Expression of a single transfected cDNA converts fibroblasts to myoblasts. Cell 51, 987–1000. https://doi.org/10.1016/0092-8674(87)90585-X

De Gasperi, R., C, M., D, A., Z, W., Lm, H., Y, D., Z, G., J, P., Xh, L., L, G., B, Z., F, K., Am, R., Wa, B., Cn, G., W, Z., M, B., Cp, C., 2022. Numb is required for optimal contraction of skeletal muscle. Journal of cachexia, sarcopenia and muscle 13. https://doi.org/10.1002/jcsm.12907

De Gasperi, R., Csernoch, L., Dienes, B., Gonczi, M., Chakrabarty, J.K., Goeta, S., Aslan, A., Toro, C.A., Karasik, D., Brown, L.M., Brotto, M., Cardozo, C.P., 2024. Septin 7 interacts with Numb to preserve sarcomere structural organization and muscle contractile function. eLife 12, RP89424. https://doi.org/10.7554/eLife.89424

de Jonge, J.J., Batters, C., O'Loughlin, T., Arden, S.D., Buss, F., 2019. The MYO6 interactome: selective motor-cargo complexes for diverse cellular processes. FEBS Letters 593, 1494–1507. https://doi.org/10.1002/1873-3468.13486

De Micheli, A.J., Laurilliard, E.J., Heinke, C.L., Ravichandran, H., Fraczek, P., Soueid-Baumgarten, S., De Vlaminck, I., Elemento, O., Cosgrove, B.D., 2020. Single-Cell Analysis of the Muscle Stem Cell Hierarchy Identifies Heterotypic Communication Signals Involved in Skeletal Muscle Regeneration. Cell Rep 30, 3583-3595.e5. https://doi.org/10.1016/j.celrep.2020.02.067

De Palma, C., Falcone, S., Pisoni, S., Cipolat, S., Panzeri, C., Pambianco, S., Pisconti, A., Allevi, R., Bassi, M.T., Cossu, G., Pozzan, T., Moncada, S., Scorrano, L., Brunelli, S., Clementi, E., 2010. Nitric oxide inhibition of Drp1-mediated mitochondrial fission is critical for myogenic differentiation. Cell Death Differ 17, 1684–1696. https://doi.org/10.1038/cdd.2010.48

Devlin, L., Okletey, J., Perkins, G., Bowen, J.R., Nakos, K., Montagna, C., Spiliotis, E.T., 2021. Proteomic profiling of the oncogenic septin 9 reveals isoform-specific interactions in breast cancer cells. PROTEOMICS 21, 2100155. https://doi.org/10.1002/pmic.202100155

Dhawan, J., Helfman, D.M., 2004. Modulation of acto-myosin contractility in skeletal muscle myoblasts uncouples growth arrest from differentiation. Journal of Cell Science 117, 3735–3748. https://doi.org/10.1242/jcs.01197

Dick, S.A., Chang, N.C., Dumont, N.A., Bell, R.A.V., Putinski, C., Kawabe, Y., Litchfield, D.W., Rudnicki, M.A., Megeney, L.A., 2015. Caspase 3 cleavage of Pax7 inhibits self-renewal of satellite cells. Proc Natl Acad Sci U S A 112, E5246-5252. https://doi.org/10.1073/pnas.1512869112

Diesenberg, K., Beerbaum, M., Fink, U., Schmieder, P., Krauss, M., 2015. SEPT9 negatively regulates ubiquitin-dependent downregulation of EGFR. Journal of Cell Science 128, 397–407. https://doi.org/10.1242/jcs.162206

Dill, T.L., Carroll, A., Gao, J., Naya, F.J., 2020. The long noncoding RNA Meg3 regulates myoblast plasticity and muscle regeneration through epithelial-mesenchymal transition. https://doi.org/10.1101/2020.06.15.152884

Ditlev, J.A., Michalski, P.J., Huber, G., Rivera, G.M., Mohler, W.A., Loew, L.M., Mayer, B.J., 2012. Stoichiometry of Nck-dependent actin polymerization in living cells. Journal of Cell Biology 197, 643–658. https://doi.org/10.1083/jcb.201111113

Dobin, A., Davis, C.A., Schlesinger, F., Drenkow, J., Zaleski, C., Jha, S., Batut, P., Chaisson, M., Gingeras, T.R., 2013. STAR: ultrafast universal RNA-seq aligner. Bioinformatics 29, 15–21. https://doi.org/10.1093/bioinformatics/bts635

Dolat, L., Hu, Q., Spiliotis, E.T., 2014a. Septin functions in organ system physiology and pathology. Biological Chemistry 395, 123–141. https://doi.org/10.1515/hsz-2013-0233

Dolat, L., Hunyara, J.L., Bowen, J.R., Karasmanis, E.P., Elgawly, M., Galkin, V.E., Spiliotis, E.T., 2014b. Septins promote stress fiber-mediated maturation of focal adhesions and renal epithelial motility. J Cell Biol 207, 225–235. https://doi.org/10.1083/jcb.201405050

Dolat, L., Spiliotis, E.T., 2016. Septins promote macropinosome maturation and traffic to the lysosome by facilitating membrane fusion. Journal of Cell Biology 214, 517–527. https://doi.org/10.1083/jcb.201603030

Dominov, J.A., Dunn, J.J., Miller, J.B., 1998. Bcl-2 expression identifies an early stage of myogenesis and promotes clonal expansion of muscle cells. J Cell Biol 142, 537–544. https://doi.org/10.1083/jcb.142.2.537

Donepudi, M., Grütter, M.G., 2002. Structure and zymogen activation of caspases. Biophys Chem 101–102, 145–153. https://doi.org/10.1016/s0301-4622(02)00151-5

Doyle, A.D., Sykora, D.J., Pacheco, G.G., Kutys, M.L., Yamada, K.M., 2021. 3D mesenchymal cell migration is driven by anterior cellular contraction that generates an extracellular matrix prestrain. Developmental Cell 56, 826-841.e4. https://doi.org/10.1016/j.devcel.2021.02.017

Du, C., Fang, M., Li, Y., Li, L., Wang, X., 2000. Smac, a mitochondrial protein that promotes cytochrome c-dependent caspase activation by eliminating IAP inhibition. Cell 102, 33–42. https://doi.org/10.1016/s0092-8674(00)00008-8

Duan, R., Gallagher, P.J., 2009. Dependence of myoblast fusion on a cortical actin wall and nonmuscle myosin IIA. Dev Biol 325, 374–385. https://doi.org/10.1016/j.ydbio.2008.10.035

Dugina, V., Zwaenepoel, I., Gabbiani, G., Clément, S., Chaponnier, C., 2009. β- and γ-cytoplasmic actins display distinct distribution and functional diversity. Journal of Cell Science 122, 2980–2988. https://doi.org/10.1242/jcs.041970

Duguez, S., Féasson, L., Denis, C., Freyssenet, D., 2002. Mitochondrial biogenesis during skeletal muscle regeneration. Am J Physiol Endocrinol Metab 282, E802-809. https://doi.org/10.1152/ajpendo.00343.2001

Dumont, N.A., Wang, Y.X., von Maltzahn, J., Pasut, A., Bentzinger, C.F., Brun, C.E., Rudnicki, M.A., 2015. Dystrophin expression in muscle stem cells regulates their polarity and asymmetric division. Nat Med 21, 1455–1463. https://doi.org/10.1038/nm.3990

Dwyer, J., Iskratsch, T., Ehler, E., 2011. Actin in striated muscle: recent insights into assembly and maintenance. Biophys Rev 4, 17–25. https://doi.org/10.1007/s12551-011-0062-7

Dyson, N., 1998. The regulation of E2F by pRB-family proteins. Genes Dev. 12, 2245–2262. https://doi.org/10.1101/gad.12.15.2245

Edison, N., Zuri, D., Maniv, I., Bornstein, B., Lev, T., Gottfried, Y., Kemeny, S., Garcia-Fernandez, M., Kagan, J., Larisch, S., 2012. The IAP-antagonist ARTS initiates caspase activation upstream of cytochrome C and SMAC/Diablo. Cell Death Differ 19, 356–368. https://doi.org/10.1038/cdd.2011.112

Efimova, N., Svitkina, T.M., 2018. Branched actin networks push against each other at adherens junctions to maintain cell–cell adhesion. Journal of Cell Biology 217, 1827–1845. https://doi.org/10.1083/jcb.201708103

Eliazer, S., Muncie, J.M., Christensen, J., Sun, X., D'Urso, R.S., Weaver, V.M., Brack, A.S., 2019. Wnt4 from the Niche Controls the Mechano-Properties and Quiescent State of Muscle Stem Cells. Cell Stem Cell 25, 654-665.e4. https://doi.org/10.1016/j.stem.2019.08.007

Eliazer, S., Sun, X., Barruet, E., Brack, A.S., 2022. Heterogeneous levels of delta-like 4 within a multinucleated niche cell maintains muscle stem cell diversity. Elife 11, e68180. https://doi.org/10.7554/eLife.68180

Elmore, S., 2007. Apoptosis: A Review of Programmed Cell Death. Toxicol Pathol 35, 495–516. https://doi.org/10.1080/01926230701320337

Engeland, K., 2022. Cell cycle regulation: p53-p21-RB signaling. Cell Death Differ 29, 946–960. https://doi.org/10.1038/s41418-022-00988-z

Engler, A.J., Griffin, M.A., Sen, S., Bönnemann, C.G., Sweeney, H.L., Discher, D.E., 2004. Myotubes differentiate optimally on substrates with tissue-like stiffness: pathological implications for soft or stiff microenvironments. J Cell Biol 166, 877–887. https://doi.org/10.1083/jcb.200405004

Engler, A.J., Sen, S., Sweeney, H.L., Discher, D.E., 2006. Matrix Elasticity Directs Stem Cell Lineage Specification. Cell 126, 677–689. https://doi.org/10.1016/j.cell.2006.06.044

Errington, T.M., Macara, I.G., 2013. Depletion of the Adaptor Protein NCK Increases UV-Induced p53 Phosphorylation and Promotes Apoptosis. PLOS ONE 8, e76204. https://doi.org/10.1371/journal.pone.0076204

Ervasti, J.M., 2003. Costameres: the Achilles' heel of Herculean muscle. J Biol Chem 278, 13591–13594. https://doi.org/10.1074/jbc.R200021200

Esnault, C., Stewart, A., Gualdrini, F., East, P., Horswell, S., Matthews, N., Treisman, R., 2014. Rho-actin signaling to the MRTF coactivators dominates the immediate transcriptional response to serum in fibroblasts. Genes Dev. 28, 943–958. https://doi.org/10.1101/gad.239327.114

Esteves de Lima, J., Bonnin, M.-A., Birchmeier, C., Duprez, D., 2016. Muscle contraction is required to maintain the pool of muscle progenitors via YAP and NOTCH during fetal myogenesis. eLife 5, e15593. https://doi.org/10.7554/eLife.15593

Estey, M.P., Ciano-Oliveira, C.D., Froese, C.D., Fung, K.Y.Y., Steels, J.D., Litchfield, D.W., Trimble, W.S., 2013. Mitotic Regulation of SEPT9 Protein by Cyclin-dependent Kinase 1 (Cdk1) and Pin1 Protein Is Important for the Completion of Cytokinesis *. Journal of Biological Chemistry 288, 30075–30086. https://doi.org/10.1074/jbc.M113.474932

Estey, M.P., Di Ciano-Oliveira, C., Froese, C.D., Bejide, M.T., Trimble, W.S., 2010. Distinct roles of septins in cytokinesis: SEPT9 mediates midbody abscission. Journal of Cell Biology 191, 741–749. https://doi.org/10.1083/jcb.201006031

Etienne-Manneville, S., Hall, A., 2002. Rho GTPases in cell biology. Nature 420, 629–635. https://doi.org/10.1038/nature01148

Fan, Y., Du, Z., Ding, Q., Zhang, J., Winkel, M.O.D., Gerbes, A.L., Liu, M., Steib, C.J., 2021. SEPT6 drives hepatocellular carcinoma cell proliferation, migration and invasion via the Hippo/YAP signaling pathway. Int J Oncol 58, 25. https://doi.org/10.3892/ijo.2021.5205

Farrugia, A.J., Calvo, F., 2017. Cdc42 regulates Cdc42EP3 function in cancer-associated fibroblasts. Small GTPases 8, 49–57. https://doi.org/10.1080/21541248.2016.1194952

Farrugia, A.J., Calvo, F., 2016. The Borg family of Cdc42 effector proteins Cdc42EP1–5. Biochem Soc Trans 44, 1709–1716. https://doi.org/10.1042/BST20160219

Farrugia, A.J., Rodríguez, J., Orgaz, J.L., Lucas, M., Sanz-Moreno, V., Calvo, F., 2020. CDC42EP5/BORG3 modulates SEPT9 to promote actomyosin function, migration, and invasion. Journal of Cell Biology 219, e201912159. https://doi.org/10.1083/jcb.201912159

Feng, H.-Z., Jin, J.-P., 2016. Carbonic Anhydrase III Is Expressed in Mouse Skeletal Muscles Independent of Fiber Type-Specific Myofilament Protein Isoforms and Plays a Role in Fatigue Resistance. Front Physiol 7, 597. https://doi.org/10.3389/fphys.2016.00597

Fernández-Barrera, J., Bernabé-Rubio, M., Casares-Arias, J., Rangel, L., Fernández-Martín, L., Correas, I., Alonso, M.A., 2018. The actin-MRTF-SRF transcriptional circuit controls tubulin acetylation via α-TAT1 gene expression. Journal of Cell Biology 217, 929–944. https://doi.org/10.1083/jcb.201702157

Fernando, P., Kelly, J.F., Balazsi, K., Slack, R.S., Megeney, L.A., 2002. Caspase 3 activity is required for skeletal muscle differentiation. Proceedings of the National Academy of Sciences 99, 11025–11030. https://doi.org/10.1073/pnas.162172899

Fernando, P., Megeney, L.A., 2007. Is caspase-dependent apoptosis only cell differentiation taken to the extreme? FASEB J 21, 8–17. https://doi.org/10.1096/fj.06-5912hyp

Figeac, N., Zammit, P.S., 2015. Coordinated action of Axin1 and Axin2 suppresses β-catenin to regulate muscle stem cell function. Cell Signal 27, 1652–1665. https://doi.org/10.1016/j.cellsig.2015.03.025

Fischer, M., Frank, D., Rösler, R., Johnsson, N., Gronemeyer, T., 2022. Biochemical Characterization of a Human Septin Octamer. Frontiers in Cell and Developmental Biology 10.

Forcina, L., Cosentino, M., Musarò, A., 2020. Mechanisms Regulating Muscle Regeneration: Insights into the Interrelated and Time-Dependent Phases of Tissue Healing. Cells 9, 1297. https://doi.org/10.3390/cells9051297

Fort, P., Blangy, A., 2017. The Evolutionary Landscape of Dbl-Like RhoGEF Families: Adapting Eukaryotic Cells to Environmental Signals. Genome Biol Evol 9, 1471–1486. https://doi.org/10.1093/gbe/evx100

Frémont, S., Romet-Lemonne, G., Houdusse, A., Echard, A., 2017. Emerging roles of MICAL family proteins – from actin oxidation to membrane trafficking during cytokinesis. Journal of Cell Science 130, 1509–1517. https://doi.org/10.1242/jcs.202028

Froidevaux-Klipfel, L., Targa, B., Cantaloube, I., Ahmed-Zaïd, H., Poüs, C., Baillet, A., 2015. Septin cooperation with tubulin polyglutamylation contributes to cancer cell adaptation to taxanes. Oncotarget 6, 36063. https://doi.org/10.18632/oncotarget.5373

Frontera, W.R., Ochala, J., 2015. Skeletal muscle: a brief review of structure and function. Calcif Tissue Int 96, 183–195. https://doi.org/10.1007/s00223-014-9915-y

Fu, J., Wang, Y.-K., Yang, M.T., Desai, R.A., Yu, X., Liu, Z., Chen, C.S., 2010. Mechanical regulation of cell function with geometrically modulated elastomeric substrates. Nat Methods 7, 733–736. https://doi.org/10.1038/nmeth.1487

Fu, L., Wang, X., Yang, Y., Chen, M., Kuerban, A., Liu, H., Dong, Y., Cai, Q., Ma, M., Wu, X., 2023. Septin11 promotes hepatocellular carcinoma cell motility by activating RhoA to regulate cytoskeleton and cell adhesion. Cell Death Dis 14, 1–15. https://doi.org/10.1038/s41419-023-05726-y

Fu, M., Hu, Y., Lan, T., Guan, K.-L., Luo, T., Luo, M., 2022. The Hippo signalling pathway and its implications in human health and diseases. Sig Transduct Target Ther 7, 1–20. https://doi.org/10.1038/s41392-022-01191-9

Füchtbauer, A., Lassen, L.B., Jensen, A.B., Howard, J., Quiroga, A. de S., Warming, S., Sørensen, A.B., Pedersen, F.S., Füchtbauer, E.-M., 2011. Septin9 is involved in septin filament formation and cellular stability. Biol Chem 392, 769–777. https://doi.org/10.1515/BC.2011.088

Fujita, M., Takeshita, H., Sawa, H., 2007. Cyclin E and CDK2 Repress the Terminal Differentiation of Quiescent Cells after Asymmetric Division in C. elegans. PLOS ONE 2, e407. https://doi.org/10.1371/journal.pone.0000407

Fukada, S., Higashimoto, T., Kaneshige, A., 2022. Differences in muscle satellite cell dynamics during muscle hypertrophy and regeneration. Skelet Muscle 12, 17. https://doi.org/10.1186/s13395-022-00300-0

Fulton, A.B., Prives, J., Farmer, S.R., Penman, S., 1981. Developmental reorganization of the skeletal framework and its surface lamina in fusing muscle cells. J Cell Biol 91, 103–112. https://doi.org/10.1083/jcb.91.1.103

Galbán, S., Duckett, C.S., 2010. XIAP as a ubiquitin ligase in cellular signaling. Cell Death Differ 17, 54–60. https://doi.org/10.1038/cdd.2009.81

Galletta, B.J., Chakravarti, M., Banerjee, R., Abmayr, S.M., 2004. SNS: Adhesive properties, localization requirements and ectodomain dependence in S2 cells and embryonic myoblasts. Mech Dev 121, 1455–1468. https://doi.org/10.1016/j.mod.2004.08.001

Gallo, R., Serafini, M., Castellani, L., Falcone, G., Alemà, S., 1999. Distinct Effects of Rac1 on Differentiation of Primary Avian Myoblasts. MBoC 10, 3137–3150. https://doi.org/10.1091/mbc.10.10.3137

Galluzzi, L., Vitale, I., Aaronson, S.A., Abrams, J.M., Adam, D., Agostinis, P., Alnemri, E.S., Altucci, L., Amelio, I., Andrews, D.W., Annicchiarico-Petruzzelli, M., Antonov, A.V., Arama, E., Baehrecke, E.H., Barlev, N.A., Bazan, N.G., Bernassola, F., Bertrand, M.J.M., Bianchi, K., Blagosklonny, M.V., Blomgren, K., Borner, C., Boya, P., Brenner, C., Campanella, M., Candi, E., Carmona-Gutierrez, D., Cecconi, F., Chan, F.K.-M., Chandel, N.S., Cheng, E.H., Chipuk, J.E., Cidlowski, J.A., Ciechanover, A., Cohen, G.M., Conrad, M., Cubillos-Ruiz, J.R., Czabotar, P.E., D'Angiolella, V., Dawson, T.M., Dawson, V.L., De Laurenzi, V., De Maria, R., Debatin, K.-M., DeBerardinis, R.J., Deshmukh, M., Di Daniele, N., Di Virgilio, F., Dixit, V.M., Dixon, S.J., Duckett, C.S., Dynlacht, B.D., El-Deiry, W.S., Elrod, J.W., Fimia, G.M., Fulda, S., García-Sáez, A.J., Garg, A.D., Garrido, C., Gavathiotis, E., Golstein, P., Gottlieb, E., Green, D.R., Greene, L.A., Gronemeyer, H., Gross, A., Hajnoczky, G., Hardwick, J.M., Harris, I.S., Hengartner, M.O., Hetz, C., Ichijo, H., Jäättelä, M., Joseph, B., Jost, P.J., Juin, P.P., Kaiser, W.J., Karin, M., Kaufmann, T., Kepp, O., Kimchi, A., Kitsis, R.N., Klionsky, D.J., Knight, R.A., Kumar, S., Lee, S.W., Lemasters, J.J., Levine, B., Linkermann, A., Lipton, S.A., Lockshin, R.A., López-Otín, C., Lowe, S.W., Luedde, T., Lugli, E., MacFarlane, M., Madeo, F., Malewicz, M., Malorni, W., Manic, G., Marine, J.-C., Martin, S.J., Martinou, J.-C., Medema, J.P., Mehlen, P., Meier, P., Melino, S., Miao, E.A., Molkentin, J.D., Moll, U.M., Muñoz-Pinedo, C., Nagata, S., Nuñez, G., Oberst, A., Oren, M., Overholtzer, M., Pagano, M., Panaretakis, T., Pasparakis, M., Penninger, J.M., Pereira, D.M., Pervaiz, S., Peter, M.E., Piacentini, M., Pinton, P., Prehn, J.H.M., Puthalakath, H., Rabinovich, G.A., Rehm, M., Rizzuto, R., Rodrigues, C.M.P., Rubinsztein, D.C., Rudel, T., Ryan, K.M., Sayan, E., Scorrano, L., Shao, F., Shi, Y., Silke, J., Simon, H.-U., Sistigu, A., Stockwell, B.R., Strasser, A., Szabadkai, G., Tait, S.W.G., Tang, D., Tavernarakis, N., Thorburn, A., Tsujimoto, Y., Turk, B., Vanden Berghe, T., Vandenabeele, P., Vander Heiden, M.G., Villunger, A., Virgin, H.W., Vousden, K.H., Vucic, D., Wagner, E.F., Walczak, H., Wallach, D., Wang, Y., Wells, J.A., Wood, W., Yuan, J., Zakeri, Z., Zhivotovsky, B., Zitvogel, L., Melino, G., Kroemer, G., 2018. Molecular mechanisms of cell death: recommendations of the Nomenclature Committee on Cell Death 2018. Cell Death Differ 25, 486–541. https://doi.org/10.1038/s41418-017-0012-4

Gan, Z., Ding, L., Burckhardt, C.J., Lowery, J., Zaritsky, A., Sitterley, K., Mota, A., Costigliola, N., Starker, C.G., Voytas, D.F., Tytell, J., Goldman, R.D., Danuser, G., 2016. Vimentin Intermediate Filaments Template Microtubule Networks to Enhance Persistence in Cell Polarity and Directed Migration. Cell Systems 3, 252-263.e8. https://doi.org/10.1016/j.cels.2016.08.007

Gao, J., Liu, R., Feng, D., Huang, W., Huo, M., Zhang, J., Leng, S., Yang, Y., Yang, T., Yin, X., Teng, X., Yu, H., Yuan, B., Wang, Y., 2021. Snail/PRMT5/NuRD complex contributes to DNA hypermethylation in cervical cancer by TET1 inhibition. Cell Death Differ 28, 2818–2836. https://doi.org/10.1038/s41418-021-00786-z

Garcia, W., de Araújo, A.P.U., de Oliveira Neto, M., Ballestero, M.R.M., Polikarpov, I., Tanaka, M., Tanaka, T., Garratt, R.C., 2006. Dissection of a Human Septin: Definition and Characterization of Distinct Domains within Human SEPT4. Biochemistry 45, 13918–13931. https://doi.org/10.1021/bi061549z

Garg, A., O'Rourke, J., Long, C., Doering, J., Ravenscroft, G., Bezprozvannaya, S., Nelson, B.R., Beetz, N., Li, L., Chen, S., Laing, N.G., Grange, R.W., Bassel-Duby, R., Olson, E.N., 2014. KLHL40 deficiency destabilizes thin filament proteins and promotes nemaline myopathy. J Clin Invest 124, 3529–3539. https://doi.org/10.1172/JCI74994

Gasperi, R.D., Csernoch, L., Dienes, B., Gonczi, M., Chakrabarty, J.K., Goeta, S., Aslan, A., Toro, C.A., Karasik, D., Brown, L.M., Brotto, M., Cardozo, C.P., 2023. Septin 7 Interacts with Numb to Preserve Sarcomere Structural Organization and Muscle Contractile Function. https://doi.org/10.1101/2023.05.11.540467

Gauthier-Rouviere, C., Vandromme, M., Tuil, D., Lautredou, N., Morris, M., Soulez, M., Kahn, A., Fernandez, A., Lamb, N., 1996. Expression and activity of serum response factor is required for expression of the muscle-determining factor MyoD in both dividing and differentiating mouse C2C12 myoblasts. Mol Biol Cell 7, 719–729. https://doi.org/10.1091/mbc.7.5.719

Geetha-Loganathan, P., Nimmagadda, S., Scaal, M., 2008. Wnt signaling in limb organogenesis. Organogenesis 4, 109–115.

Geiger, B., Yamada, K.M., 2011. Molecular Architecture and Function of Matrix Adhesions. Cold Spring Harb Perspect Biol 3, a005033. https://doi.org/10.1101/cshperspect.a005033

Geisbrecht, E.R., Haralalka, S., Swanson, S.K., Florens, L., Washburn, M.P., Abmayr, S.M., 2008. Drosophila ELMO/CED-12 interacts with Myoblast city to direct myoblast fusion and ommatidial organization. Dev Biol 314, 137–149. https://doi.org/10.1016/j.ydbio.2007.11.022

Geng, A., Qiu, R., Murai, K., Liu, J., Wu, X., Zhang, H., Farhoodi, H., Duong, N., Jiang, M., Yee, J., Tsark, W., Lu, Q., 2018. KIF20A/MKLP2 regulates the division modes of neural progenitor cells during cortical development. Nat Commun 9, 2707. https://doi.org/10.1038/s41467-018-05152-1

George, R.M., Biressi, S., Beres, B.J., Rogers, E., Mulia, A.K., Allen, R.E., Rawls, A., Rando, T.A., Wilson-Rawls, J., 2013. Numb-deficient satellite cells have regeneration and proliferation defects. Proceedings of the National Academy of Sciences 110, 18549–18554. https://doi.org/10.1073/pnas.1311628110

Gérard, C., Goldbeter, A., 2014. The balance between cell cycle arrest and cell proliferation: control by the extracellular matrix and by contact inhibition. Interface Focus 4, 20130075. https://doi.org/10.1098/rsfs.2013.0075

Ghossoub, R., Hu, Q., Failler, M., Rouyez, M.-C., Spitzbarth, B., Mostowy, S., Wolfrum, U., Saunier, S., Cossart, P., James Nelson, W., Benmerah, A., 2013. Septins 2, 7 and 9 and MAP4 colocalize along the axoneme in the primary cilium and control ciliary length. Journal of Cell Science 126, 2583–2594. https://doi.org/10.1242/jcs.111377

Gilbert, P.M., Havenstrite, K.L., Magnusson, K.E.G., Sacco, A., Leonardi, N.A., Kraft, P., Nguyen, N.K., Thrun, S., Lutolf, M.P., Blau, H.M., 2010. Substrate Elasticity Regulates Skeletal Muscle Stem Cell Self-Renewal in Culture. Science 329, 1078–1081. https://doi.org/10.1126/science.1191035

Gilden, J.K., Peck, S., M. Chen, Y.-C., Krummel, M.F., 2012. The septin cytoskeleton facilitates membrane retraction during motility and blebbing. J Cell Biol 196, 103–114. https://doi.org/10.1083/jcb.201105127

Gillies, A.R., Lieber, R.L., 2011. Structure and function of the skeletal muscle extracellular matrix. Muscle & Nerve 44, 318–331. https://doi.org/10.1002/mus.22094

Girardi, F., Le Grand, F., 2018. Chapter Five - Wnt Signaling in Skeletal Muscle Development and Regeneration, in: Larraín, J., Olivares, G. (Eds.), Progress in Molecular Biology and Translational Science, WNT Signaling in Health and Disease. Academic Press, pp. 157–179. https://doi.org/10.1016/bs.pmbts.2017.11.026

Gittes, F., Mickey, B., Nettleton, J., Howard, J., 1993. Flexural rigidity of microtubules and actin filaments measured from thermal fluctuations in shape. Journal of Cell Biology 120, 923–934. https://doi.org/10.1083/jcb.120.4.923

Goebel, E.J., Hart, K.N., McCoy, J.C., Thompson, T.B., 2019. Structural biology of the TGFβ family. Exp Biol Med (Maywood) 244, 1530–1546. https://doi.org/10.1177/1535370219880894

Goel, A.J., Rieder, M.-K., Arnold, H.-H., Radice, G.L., Krauss, R.S., 2017. Niche Cadherins Control the Quiescence-to-Activation Transition in Muscle Stem Cells. Cell Reports 21, 2236–2250. https://doi.org/10.1016/j.celrep.2017.10.102

Goetsch, K. p., Snyman, C., Myburgh, K. h., Niesler, C. u., 2014. ROCK-2 Is Associated With Focal Adhesion Maturation During Myoblast Migration. Journal of Cellular Biochemistry 115, 1299–1307. https://doi.org/10.1002/jcb.24784

Gokhin, D.S., Ward, S.R., Bremner, S.N., Lieber, R.L., 2008. Quantitative analysis of neonatal skeletal muscle functional improvement in the mouse. Journal of Experimental Biology 211, 837–843. https://doi.org/10.1242/jeb.014340

Gönczi, M., Dienes, B., Dobrosi, N., Fodor, J., Balogh, N., Oláh, T., Csernoch, L., 2021. Septins, a cytoskeletal protein family, with emerging role in striated muscle. J Muscle Res Cell Motil 42, 251–265. https://doi.org/10.1007/s10974-020-09573-8

Gönczi, M., Ráduly, Z., Szabó, L., Fodor, J., Telek, A., Dobrosi, N., Balogh, N., Szentesi, P., Kis, G., Antal, M., Trencsenyi, G., Dienes, B., Csernoch, L., 2022. Septin7 is indispensable for proper skeletal muscle architecture and function. eLife 11, e75863. https://doi.org/10.7554/eLife.75863

Gong, W., Gohla, R.M., Bowlin, K.M., Koyano-Nakagawa, N., Garry, D.J., Shi, X., 2015. Kelch Repeat and BTB Domain Containing Protein 5 (Kbtbd5) Regulates Skeletal Muscle Myogenesis through the E2F1-DP1 Complex*. Journal of Biological Chemistry 290, 15350–15361. https://doi.org/10.1074/jbc.M114.629956

Gottfried, Y., Rotem, A., Lotan, R., Steller, H., Larisch, S., 2004. The mitochondrial ARTS protein promotes apoptosis through targeting XIAP. The EMBO Journal 23, 1627–1635. https://doi.org/10.1038/sj.emboj.7600155

Granic, A., Suetterlin, K., Shavlakadze, T., Grounds, M.D., Sayer, A.A., 2023. Hallmarks of ageing in human skeletal muscle and implications for understanding the pathophysiology of sarcopenia in women and men. Clin Sci (Lond) 137, 1721–1751. https://doi.org/10.1042/CS20230319

Greene, G.W., Anderson, T.H., Zeng, H., Zappone, B., Israelachvili, J.N., 2009. Force amplification response of actin filaments under confined compression. Proceedings of the National Academy of Sciences 106, 445–449. https://doi.org/10.1073/pnas.0812064106

Griffiths, G.S., Doe, J., Jijiwa, M., Van Ry, P., Cruz, V., de la Vega, M., Ramos, J.W., Burkin, D.J., Matter, M.L., 2015. Bit-1 is an essential regulator of myogenic differentiation. J Cell Sci 128, 1707–1717. https://doi.org/10.1242/jcs.158964

Grifone, R., Demignon, J., Houbron, C., Souil, E., Niro, C., Seller, M.J., Hamard, G., Maire, P., 2005. Six1 and Six4 homeoproteins are required for Pax3 and Mrf expression during myogenesis in the mouse embryo. Development 132, 2235–2249. https://doi.org/10.1242/dev.01773

Gros, J., Manceau, M., Thomé, V., Marcelle, C., 2005. A common somitic origin for embryonic muscle progenitors and satellite cells. Nature 435, 954–958. https://doi.org/10.1038/nature03572

Grupp, B., Gronemeyer, T., 2023. A biochemical view on the septins, a less known component of the cytoskeleton. Biological Chemistry 404, 1–13. https://doi.org/10.1515/hsz-2022-0263

Gu, W., Schneider, J.W., Condorelli, G., Kaushal, S., Mahdavi, V., Nadal-Ginard, B., 1993. Interaction of myogenic factors and the retinoblastoma protein mediates muscle cell commitment and differentiation. Cell 72, 309–324. https://doi.org/10.1016/0092-8674(93)90110-C

Guan, G., Cannon, R.D., Coates, D.E., Mei, L., 2023. Effect of the Rho-Kinase/ROCK Signaling Pathway on Cytoskeleton Components. Genes 14, 272. https://doi.org/10.3390/genes14020272

Gugliuzza, M.V., Crist, C., 2022. Muscle stem cell adaptations to cellular and environmental stress. Skeletal Muscle 12, 5. https://doi.org/10.1186/s13395-022-00289-6

Guo, C.S., Degnin, C., Fiddler, T.A., Stauffer, D., Thayer, M.J., 2003. Regulation of MyoD activity and muscle cell differentiation by MDM2, pRb, and Sp1. J Biol Chem 278, 22615–22622. https://doi.org/10.1074/jbc.M301943200

Gurdon, J.B., Bourillot, P.-Y., 2001. Morphogen gradient interpretation. Nature 413, 797–803. https://doi.org/10.1038/35101500

Gurevich, D.B., Nguyen, P.D., Siegel, A.L., Ehrlich, O.V., Sonntag, C., Phan, J.M.N., Berger, S., Ratnayake, D., Hersey, L., Berger, J., Verkade, H., Hall, T.E., Currie, P.D., 2016. Asymmetric division of clonal muscle stem cells coordinates muscle regeneration in vivo. Science 353, aad9969. https://doi.org/10.1126/science.aad9969

H. Dehkordi, M., Tashakor, A., O'Connell, E., Fearnhead, H.O., 2020. Apoptosome-dependent myotube formation involves activation of caspase-3 in differentiating myoblasts. Cell Death Dis 11, 308. https://doi.org/10.1038/s41419-020-2502-4

Hagiwara, A., Tanaka, Y., Hikawa, R., Morone, N., Kusumi, A., Kimura, H., Kinoshita, M., 2011. Submembranous septins as relatively stable components of actin-based membrane skeleton. Cytoskeleton 68, 512–525. https://doi.org/10.1002/cm.20528

Hakibilen, C., Delort, F., Daher, M.-T., Joanne, P., Cabet, E., Cardoso, O., Bourgois-Rocha, F., Tian, C., Rivas, E., Madruga, M., Ferreiro, A., Lilienbaum, A., Vicart, P., Agbulut, O., Hénon, S., Batonnet-Pichon, S., 2022. Desmin Modulates Muscle Cell Adhesion and Migration. Front. Cell Dev. Biol. 10. https://doi.org/10.3389/fcell.2022.783724

Hall, A., 1998. Rho GTPases and the Actin Cytoskeleton. Science 279, 509–514. https://doi.org/10.1126/science.279.5350.509

Han, X.H., Jin, Y.-R., Tan, L., Kosciuk, T., Lee, J.-S., Yoon, J.K., 2014. Regulation of the follistatin gene by RSPO-LGR4 signaling via activation of the WNT/β-catenin pathway in skeletal myogenesis. Mol Cell Biol 34, 752–764. https://doi.org/10.1128/MCB.01285-13

Hao, Q., Chen, J., Lu, H., Zhou, X., 2022. The ARTS of p53-dependent mitochondrial apoptosis. Journal of Molecular Cell Biology 14, mjac074. https://doi.org/10.1093/jmcb/mjac074

Haralalka, S., Shelton, C., Cartwright, H.N., Guo, F., Trimble, R., Kumar, R.P., Abmayr, S.M., 2014. Live Imaging Provides New Insights on Dynamic F-Actin Filopodia and Differential Endocytosis during Myoblast Fusion in Drosophila. PLoS One 9, e114126. https://doi.org/10.1371/journal.pone.0114126

Hartwell, L.H., Culotti, J., Reid, B., 1970. Genetic Control of the Cell-Division Cycle in Yeast, I. Detection of Mutants. Proc Natl Acad Sci U S A 66, 352–359.

Hartwell, L.H., Mortimer, R.K., Culotti, J., Culotti, M., 1973. GENETIC CONTROL OF THE CELL DIVISION CYCLE IN YEAST: V. GENETIC ANALYSIS OF cdc MUTANTS. Genetics 74, 267–286. https://doi.org/10.1093/genetics/74.2.267

Hecht, M., Rösler, R., Wiese, S., Johnsson, N., Gronemeyer, T., 2019. An Interaction Network of the Human SEPT9 Established by Quantitative Mass Spectrometry. G3: Genes|Genomes|Genetics 9, 1869. https://doi.org/10.1534/g3.119.400197

Hegde, R., Srinivasula, S.M., Zhang, Z., Wassell, R., Mukattash, R., Cilenti, L., DuBois, G., Lazebnik, Y., Zervos, A.S., Fernandes-Alnemri, T., Alnemri, E.S., 2002. Identification of Omi/HtrA2 as a mitochondrial apoptotic serine protease that disrupts inhibitor of apoptosis protein-caspase interaction. J Biol Chem 277, 432–438. https://doi.org/10.1074/jbc.M109721200

Heller, H., Gredinger, E., Bengal, E., 2001. Rac1 Inhibits Myogenic Differentiation by Preventing the Complete Withdrawal of Myoblasts from the Cell Cycle *. Journal of Biological Chemistry 276, 37307–37316. https://doi.org/10.1074/jbc.M103195200

Hernández-Hernández, J.M., García-González, E.G., Brun, C.E., Rudnicki, M.A., 2017. The myogenic regulatory factors, determinants of muscle development, cell identity and regeneration. Seminars in Cell & Developmental Biology, Skeletal Muscle Development on the 30th Anniversary of MyoD 72, 10–18. https://doi.org/10.1016/j.semcdb.2017.11.010

Hernández-Rodríguez, Y., Momany, M., 2012. Posttranslational modifications and assembly of septin heteropolymers and higher-order structures. Current Opinion in Microbiology, Growth and development: eukaryotes/prokaryotes 15, 660–668. https://doi.org/10.1016/j.mib.2012.09.007

Hickson, G.R.X., O'Farrell, P.H., 2008. Rho-dependent control of anillin behavior during cytokinesis. J Cell Biol 180, 285–294. https://doi.org/10.1083/jcb.200709005

Hildebrandt, S., Kampfrath, B., Fischer, K., Hildebrand, L., Haupt, J., Stachelscheid, H., Knaus, P., 2021. ActivinA Induced SMAD1/5 Signaling in an iPSC Derived EC Model of Fibrodysplasia Ossificans Progressiva (FOP) Can Be Rescued by the Drug Candidate Saracatinib. Stem Cell Rev and Rep 17, 1039–1052. https://doi.org/10.1007/s12015-020-10103-9

Hirth, F., 2013. Stem Cells and Asymmetric Cell Division, in: Steinhoff, G. (Ed.), Regenerative Medicine: From Protocol to Patient. Springer Netherlands, Dordrecht, pp. 107–127. https://doi.org/10.1007/978-94-007-5690-8_4

Hochreiter-Hufford, A.E., Lee, C.S., Kinchen, J.M., Sokolowski, J.D., Arandjelovic, S., Call, J.A., Klibanov, A.L., Yan, Z., Mandell, J.W., Ravichandran, K.S., 2013. Phosphatidylserine receptor BAI1 and apoptotic cells as new promoters of myoblast fusion. Nature 497, 263–267. https://doi.org/10.1038/nature12135

Hoh, J.F.Y., 2023. Developmental, physiologic and phylogenetic perspectives on the expression and regulation of myosin heavy chains in mammalian skeletal muscles. J Comp Physiol B 193, 355–382. https://doi.org/10.1007/s00360-023-01499-0

Holstein, I., Singh, A.K., Pohl, F., Misiak, D., Braun, J., Leitner, L., Hüttelmaier, S., Posern, G., 2020. Post-transcriptional regulation of MRTF-A by miRNAs during myogenic differentiation of myoblasts. Nucleic Acids Res 48, 8927–8942. https://doi.org/10.1093/nar/gkaa596

Hong, P., Chen, K., Huang, B., Liu, M., Cui, M., Rozenberg, I., Chaqour, B., Pan, X., Barton, E.R., Jiang, X.-C., Siddiqui, M.A.Q., 2012. HEXIM1 controls satellite cell expansion after injury to regulate skeletal muscle regeneration. J Clin Invest 122, 3873–3887. https://doi.org/10.1172/JCI62818

Hong, Y., Zhang, H., Gartner, A., 2021. The Last Chance Saloon. Front. Cell Dev. Biol. 9. https://doi.org/10.3389/fcell.2021.671297

Horbelt, D., Denkis, A., Knaus, P., 2012. A portrait of Transforming Growth Factor β superfamily signalling: Background matters. The International Journal of Biochemistry & Cell Biology 44, 469–474. https://doi.org/10.1016/j.biocel.2011.12.013

Horsley, V., Pavlath, G.K., 2002. Nfat : ubiquitous regulator of cell differentiation and adaptation. Journal of Cell Biology 156, 771–774. https://doi.org/10.1083/jcb.200111073

Hou, Y., Xie, W., Yu, L., Camacho, L.C., Nie, C., Zhang, M., Haag, R., Wei, Q., 2020. Surface Roughness Gradients Reveal Topography-Specific Mechanosensitive Responses in Human Mesenchymal Stem Cells. Small 16, 1905422. https://doi.org/10.1002/smll.201905422

Hu, J., Bai, X., Bowen, J.R., Dolat, L., Korobova, F., Yu, W., Baas, P.W., Svitkina, T., Gallo, G., Spiliotis, E.T., 2012. Septin-Driven Coordination of Actin and Microtubule Remodeling Regulates the Collateral Branching of Axons. Current Biology 22, 1109–1115. https://doi.org/10.1016/j.cub.2012.04.019

Hu, Q., Nelson, W.J., Spiliotis, E.T., 2008. Forchlorfenuron Alters Mammalian Septin Assembly, Organization, and Dynamics. J Biol Chem 283, 29563–29571. https://doi.org/10.1074/jbc.M804962200

Huang, S., Wang, X., Yu, J., Tian, Y., Yang, C., Chen, Y., Chen, H., Ge, H., 2020. LonP1 regulates mitochondrial network remodeling through the PINK1/Parkin pathway during myoblast differentiation. Am J Physiol Cell Physiol 319, C1020–C1028. https://doi.org/10.1152/ajpcell.00589.2019

Hubaud, A., Pourquié, O., 2014. Signalling dynamics in vertebrate segmentation. Nat Rev Mol Cell Biol 15, 709–721. https://doi.org/10.1038/nrm3891

Hulin, J.-A., Nguyen, T.D.T., Cui, S., Marri, S., Yu, R.T., Downes, M., Evans, R.M., Makarenkova, H., Meech, R., 2016. Barx2 and Pax7 regulate Axin2 expression in myoblasts by interaction with β-catenin and chromatin remodelling. Stem Cells 34, 2169–2182. https://doi.org/10.1002/stem.2396

Hutcheson, D.A., Zhao, J., Merrell, A., Haldar, M., Kardon, G., 2009. Embryonic and fetal limb myogenic cells are derived from developmentally distinct progenitors and have different requirements for beta-catenin. Genes Dev 23, 997–1013. https://doi.org/10.1101/gad.1769009

Iberite, F., Gruppioni, E., Ricotti, L., 2022. Skeletal muscle differentiation of human iPSCs meets bioengineering strategies: perspectives and challenges. npj Regen Med 7, 1–30. https://doi.org/10.1038/s41536-022-00216-9

Ichikawa, K., Mimura, N., Asano, A., 1993. Brefeldin A inhibits muscle-specific gene expression during differentiation in C2C12 myoblasts. Exp Cell Res 209, 333–341. https://doi.org/10.1006/excr.1993.1318

Ito, H., Iwamoto, I., Morishita, R., Nozawa, Y., Narumiya, S., Asano, T., Nagata, K., 2005. Possible role of Rho/Rhotekin signaling in mammalian septin organization. Oncogene 24, 7064–7072. https://doi.org/10.1038/sj.onc.1208862

Ito, H., Morishita, R., Nagata, K., 2018. Functions of Rhotekin, an Effector of Rho GTPase, and Its Binding Partners in Mammals. Int J Mol Sci 19, 2121. https://doi.org/10.3390/ijms19072121

Iv, F., Martins, C.S., Castro-Linares, G., Taveneau, C., Barbier, P., Verdier-Pinard, P., Camoin, L., Audebert, S., Tsai, F.-C., Ramond, L., Llewellyn, A., Belhabib, M., Nakazawa, K., Di Cicco, A., Vincentelli, R., Wenger, J., Cabantous, S., Koenderink, G.H., Bertin, A., Mavrakis, M., 2021. Insights into animal septins using recombinant human septin octamers with distinct SEPT9 isoforms. J Cell Sci 134, jcs258484. https://doi.org/10.1242/jcs.258484

Ivanov, A.I., Le, H.T., Naydenov, N.G., Rieder, F., 2021. Novel Functions of the Septin Cytoskeleton: Shaping Up Tissue Inflammation and Fibrosis. The American Journal of Pathology 191, 40–51. https://doi.org/10.1016/j.ajpath.2020.09.007

Iwasaki, K., Hayashi, K., Fujioka, T., Sobue, K., 2008. Rho/Rho-associated Kinase Signal Regulates Myogenic Differentiation via Myocardin-related Transcription Factor-A/Smad-dependent Transcription of the Id3 Gene. J Biol Chem 283, 21230–21241. https://doi.org/10.1074/jbc.M710525200

Jabre, S., Hleihel, W., Coirault, C., 2021. Nuclear Mechanotransduction in Skeletal Muscle. Cells 10, 318. https://doi.org/10.3390/cells10020318

Jagla, K., Dollé, P., Mattei, M.G., Jagla, T., Schuhbaur, B., Dretzen, G., Bellard, F., Bellard, M., 1995. Mouse Lbx1 and human LBX1 define a novel mammalian homeobox gene family related to the Drosophila lady bird genes. Mech Dev 53, 345–356. https://doi.org/10.1016/0925-4773(95)00450-5

Jahnke, V.E., Sabido, O., Freyssenet, D., 2009. Control of mitochondrial biogenesis, ROS level, and cytosolic Ca2+ concentration during the cell cycle and the onset of differentiation in L6E9 myoblasts. Am J Physiol Cell Physiol 296, C1185-1194. https://doi.org/10.1152/ajpcell.00377.2008

Janke, C., Magiera, M.M., 2020. The tubulin code and its role in controlling microtubule properties and functions. Nat Rev Mol Cell Biol 21, 307–326. https://doi.org/10.1038/s41580-020-0214-3

Janssen, I., Heymsfield, S.B., Wang, Z.M., Ross, R., 2000. Skeletal muscle mass and distribution in 468 men and women aged 18-88 yr. J Appl Physiol (1985) 89, 81–88. https://doi.org/10.1152/jappl.2000.89.1.81

Jatzlau, J., Burdzinski, W., Trumpp, M., Obendorf, L., Roßmann, K., Ravn, K., Hyvönen, M., Bottanelli, F., Broichhagen, J., Knaus, P., 2023. A versatile Halo- and SNAP-tagged BMP/TGFβ receptor library for quantification of cell surface ligand binding. Commun Biol 6, 1–15. https://doi.org/10.1038/s42003-022-04388-4

Jensen, P.B., Pedersen, L., Krishna, S., Jensen, M.H., 2010. A Wnt Oscillator Model for Somitogenesis. Biophys J 98, 943–950. https://doi.org/10.1016/j.bpj.2009.11.039

Jeong, H., Bae, S., An, S.Y., Byun, M.R., Hwang, J.-H., Yaffe, M.B., Hong, J.-H., Hwang, E.S., 2010. TAZ as a novel enhancer of MyoD-mediated myogenic differentiation. The FASEB Journal 24, 3310–3320. https://doi.org/10.1096/fj.09-151324

Jiang, A., Guo, H., Wu, W., Liu, H., 2021. The Crosstalk between Autophagy and Apoptosis Is Necessary for Myogenic Differentiation. J Agric Food Chem 69, 3942–3951. https://doi.org/10.1021/acs.jafc.1c00140

Jiao, F., Cannon, K.S., Lin, Y.-C., Gladfelter, A.S., Scheuring, S., 2020. The hierarchical assembly of septins revealed by high-speed AFM. Nat Commun 11, 5062. https://doi.org/10.1038/s41467-020-18778-x

Joberty, G., Perlungher, R.R., Macara, I.G., 1999. The Borgs, a New Family of Cdc42 and TC10 GTPase-Interacting Proteins. Molecular and Cellular Biology 19, 6585–6597. https://doi.org/10.1128/MCB.19.10.6585

Joberty, G., Perlungher, R.R., Sheffield, P.J., Kinoshita, M., Noda, M., Haystead, T., Macara, I.G., 2001. Borg proteins control septin organization and are negatively regulated by Cdc42. Nat Cell Biol 3, 861–866. https://doi.org/10.1038/ncb1001-861

Johnson, D.G., Ohtani, K., Nevins, J.R., 1994. Autoregulatory control of E2F1 expression in response to positive and negative regulators of cell cycle progression. Genes Dev 8, 1514–1525. https://doi.org/10.1101/gad.8.13.1514

Jones, A.E., Price, F.D., Le Grand, F., Soleimani, V.D., Dick, S.A., Megeney, L.A., Rudnicki, M.A., 2015. Wnt/β-catenin controls follistatin signalling to regulate satellite cell myogenic potential. Skelet Muscle 5, 14. https://doi.org/10.1186/s13395-015-0038-6

Joo, E., Surka, M.C., Trimble, W.S., 2007. Mammalian SEPT2 Is Required for Scaffolding Nonmuscle Myosin II and Its Kinases. Developmental Cell 13, 677–690. https://doi.org/10.1016/j.devcel.2007.09.001

Jory, A., Le Roux, I., Gayraud-Morel, B., Rocheteau, P., Cohen-Tannoudji, M., Cumano, A., Tajbakhsh, S., 2009. Numb Promotes an Increase in Skeletal Muscle Progenitor Cells in the Embryonic Somite. Stem Cells 27, 2769–2780. https://doi.org/10.1002/stem.220

Joseph, G.A., Lu, M., Radu, M., Lee, J.K., Burden, S.J., Chernoff, J., Krauss, R.S., 2017. Group I Paks Promote Skeletal Myoblast Differentiation In Vivo and In Vitro. Mol Cell Biol 37, e00222-16. https://doi.org/10.1128/MCB.00222-16

Kamanga-Sollo, E., Pampusch, M.S., White, M.E., Hathaway, M.R., Dayton, W.R., 2005. Insulin-like growth factor binding protein (IGFBP)-3 and IGFBP-5 mediate TGF-beta- and myostatin-induced suppression of proliferation in porcine embryonic myogenic cell cultures. Exp Cell Res 311, 167–176. https://doi.org/10.1016/j.yexcr.2005.09.003

Kandi, R., Senger, K., Grigoryan, A., Soller, K., Sakk, V., Schuster, T., Eiwen, K., Menon, M.B., Gaestel, M., Zheng, Y., Florian, M.C., Geiger, H., 2021. Cdc42-Borg4-Septin7 axis regulates HSC polarity and function. EMBO reports 22, e52931. https://doi.org/10.15252/embr.202152931

Kanematsu, Y., Narita, A., Oda, T., Koike, R., Ota, M., Takano, Y., Moritsugu, K., Fujiwara, I., Tanaka, K., Komatsu, H., Nagae, T., Watanabe, N., Iwasa, M., Maéda, Y., Takeda, S., 2022. Structures and mechanisms of actin ATP hydrolysis. Proceedings of the National Academy of Sciences 119, e2122641119. https://doi.org/10.1073/pnas.2122641119

Kann, A.P., Hung, M., Wang, W., Nguyen, J., Gilbert, P.M., Wu, Z., Krauss, R.S., 2022. An injury-responsive Rac-to-Rho GTPase switch drives activation of muscle stem cells through rapid cytoskeletal remodeling. Cell Stem Cell 29, 933-947.e6. https://doi.org/10.1016/j.stem.2022.04.016

Karasmanis, E.P., Hwang, D., Nakos, K., Bowen, J.R., Angelis, D., Spiliotis, E.T., 2019. A Septin Double Ring Controls the Spatiotemporal Organization of the ESCRT Machinery in Cytokinetic Abscission. Current Biology 29, 2174-2182.e7. https://doi.org/10.1016/j.cub.2019.05.050

Karasmanis, E.P., Phan, C.-T., Angelis, D., Kesisova, I.A., Hoogenraad, C.C., McKenney, R.J., Spiliotis, E.T., 2018. Polarity of Neuronal Membrane Traffic Requires Sorting of Kinesin Motor Cargo during Entry into Dendrites by a Microtubule-Associated Septin. Developmental Cell 46, 204-218.e7. https://doi.org/10.1016/j.devcel.2018.06.013

Karolczak, J., Pavlyk, I., Majewski, Ł., Sobczak, M., Niewiadomski, P., Rzhepetskyy, Y., Sikorska, A., Nowak, N., Pomorski, P., Prószyński, T., Ehler, E., Rędowicz, M.J., 2015. Involvement of unconventional myosin VI in myoblast function and myotube formation. Histochem Cell Biol 144, 21–38. https://doi.org/10.1007/s00418-015-1322-6

Kassar-Duchossoy, L., Giacone, E., Gayraud-Morel, B., Jory, A., Gomès, D., Tajbakhsh, S., 2005. Pax3/Pax7 mark a novel population of primitive myogenic cells during development. Genes Dev 19, 1426–1431. https://doi.org/10.1101/gad.345505

Kaufmann, S.H., Desnoyers, S., Ottaviano, Y., Davidson, N.E., Poirier, G.G., 1993. Specific proteolytic cleavage of poly(ADP-ribose) polymerase: an early marker of chemotherapy-induced apoptosis. Cancer Res 53, 3976–3985.

Kawaguchi, K., Fujita, N., 2024. Shaping transverse-tubules: central mechanisms that play a role in the cytosol zoning for muscle contraction. The Journal of Biochemistry 175, 125–131. https://doi.org/10.1093/jb/mvad083

Kesisova, I.A., Robinson, B.P., Spiliotis, E.T., 2021. A septin GTPase scaffold of dynein–dynactin motors triggers retrograde lysosome transport. Journal of Cell Biology 220, e202005219. https://doi.org/10.1083/jcb.202005219

Khatau, S.B., Hale, C.M., Stewart-Hutchinson, P.J., Patel, M.S., Stewart, C.L., Searson, P.C., Hodzic, D., Wirtz, D., 2009. A perinuclear actin cap regulates nuclear shape. Proceedings of the National Academy of Sciences 106, 19017–19022. https://doi.org/10.1073/pnas.0908686106

Khatau, S.B., Kusuma, S., Hanjaya-Putra, D., Mali, P., Cheng, L., Lee, J.S.H., Gerecht, S., Wirtz, D., 2012. The Differential Formation of the LINC-Mediated Perinuclear Actin Cap in Pluripotent and Somatic Cells. PLOS ONE 7, e36689. https://doi.org/10.1371/journal.pone.0036689

Kilian, K.A., Bugarija, B., Lahn, B.T., Mrksich, M., 2010. Geometric cues for directing the differentiation of mesenchymal stem cells. Proceedings of the National Academy of Sciences 107, 4872–4877. https://doi.org/10.1073/pnas.0903269107

Kim, B., Kim, J.-S., Yoon, Y., Santiago, M.C., Brown, M.D., Park, J.-Y., 2013. Inhibition of Drp1-dependent mitochondrial division impairs myogenic differentiation. Am J Physiol Regul Integr Comp Physiol 305, R927-938. https://doi.org/10.1152/ajpregu.00502.2012

Kim, J., Cooper, J.A., 2021. Junctional Localization of Septin 2 Is Required for Organization of Junctional Proteins in Static Endothelial Monolayers. Arteriosclerosis, Thrombosis, and Vascular Biology 41, 346–359. https://doi.org/10.1161/ATVBAHA.120.315472

Kim, J., Cooper, J.A., 2018. Septins regulate junctional integrity of endothelial monolayers. MBoC 29, 1693–1703. https://doi.org/10.1091/mbc.E18-02-0136

Kim, J., Mooren, O.L., Onken, M.D., Cooper, J.A., 2023. Septin and actin contributions to endothelial cell–cell junctions and monolayer integrity. Cytoskeleton 80, 228–241. https://doi.org/10.1002/cm.21732

Kim, J.H., Jin, P., Duan, R., Chen, E.H., 2015a. Mechanisms of myoblast fusion during muscle development. Current Opinion in Genetics & Development, Developmental mechanisms, patterning and organogenesis 32, 162–170. https://doi.org/10.1016/j.gde.2015.03.006

Kim, J.H., Ren, Y., Ng, W.P., Li, S., Son, S., Kee, Y.-S., Zhang, S., Zhang, G., Fletcher, D.A., Robinson, D.N., Chen, E.H., 2015b. Mechanical tension drives cell membrane fusion. Dev Cell 32, 561–573. https://doi.org/10.1016/j.devcel.2015.01.005

Kim, O.V., Litvinov, R.I., Mordakhanova, E.R., Bi, E., Vagin, O., Weisel, J.W., 2022. Contribution of septins to human platelet structure and function. iScience 25. https://doi.org/10.1016/j.isci.2022.104654

Kim, S.K., Shindo, A., Park, T.J., Oh, E.C., Ghosh, S., Gray, R.S., Lewis, R.A., Johnson, C.A., Attie-Bittach, T., Katsanis, N., Wallingford, J.B., 2010. Planar Cell Polarity Acts Through Septins to Control Collective Cell Movement and Ciliogenesis. Science 329, 1337–1340. https://doi.org/10.1126/science.1191184

Kinoshita, M., 2003. Assembly of Mammalian Septins. The Journal of Biochemistry 134, 491–496. https://doi.org/10.1093/jb/mvg182

Kinoshita, M., Field, C.M., Coughlin, M.L., Straight, A.F., Mitchison, T.J., 2002. Self- and Actin-Templated Assembly of Mammalian Septins. Developmental Cell 3, 791–802. https://doi.org/10.1016/S1534-5807(02)00366-0

Kinoshita, M., Kumar, S., Mizoguchi, A., Ide, C., Kinoshita, A., Haraguchi, T., Hiraoka, Y., Noda, M., 1997. Nedd5, a mammalian septin, is a novel cytoskeletal component interacting with actin-based structures. Genes Dev. 11, 1535–1547. https://doi.org/10.1101/gad.11.12.1535

Kitzmann, M., Vandromme, M., Schaeffer, V., Carnac, G., Labbé, J.-C., Lamb, N., Fernandez, A., 1999. cdk1- and cdk2-Mediated Phosphorylation of MyoD Ser200 in Growing C2 Myoblasts: Role in Modulating MyoD Half-Life and Myogenic Activity. Molecular and Cellular Biology 19, 3167–3176. https://doi.org/10.1128/MCB.19.4.3167

Knoblich, J.A., 2008. Mechanisms of Asymmetric Stem Cell Division. Cell 132, 583–597. https://doi.org/10.1016/j.cell.2008.02.007

Knothe Tate, M.L., Gunning, P.W., Sansalone, V., 2016. Emergence of form from function—Mechanical engineering approaches to probe the role of stem cell mechanoadaptation in

sealing cell fate. Bioarchitecture 6, 85–103. https://doi.org/10.1080/19490992.2016.1229729
Kolde, R., 2019. pheatmap: Pretty Heatmaps.
Konsavage, W.M., Jr, Yochum, G.S., 2013. Intersection of Hippo/YAP and Wnt/β-catenin signaling pathways. Acta Biochimica et Biophysica Sinica 45, 71–79. https://doi.org/10.1093/abbs/gms084
Koopman, R., van Loon, L.J.C., 2009. Aging, exercise, and muscle protein metabolism. Journal of Applied Physiology 106, 2040–2048. https://doi.org/10.1152/japplphysiol.91551.2008
Korchynskyi, O., Dijke, P. ten, 2002. Identification and Functional Characterization of Distinct Critically Important Bone Morphogenetic Protein-specific Response Elements in the Id1 Promoter *. Journal of Biological Chemistry 277, 4883–4891. https://doi.org/10.1074/jbc.M111023200
Korohoda, W., Pietrzkowski, Z., Reiss, K., 1993. Chloramphenicol, an inhibitor of mitochondrial protein synthesis, inhibits myoblast fusion and myotube differentiation. Folia Histochem Cytobiol 31, 9–13.
Krauss, R.S., Joseph, G.A., Goel, A.J., 2017. Keep Your Friends Close: Cell-Cell Contact and Skeletal Myogenesis. Cold Spring Harb Perspect Biol 9, a029298. https://doi.org/10.1101/cshperspect.a029298
Krauss, R.S., Kann, A.P., 2023. Muscle stem cells get a new look: Dynamic cellular projections as sensors of the stem cell niche. BioEssays 45, 2200249. https://doi.org/10.1002/bies.202200249
Kremer, B.E., Adang, L.A., Macara, I.G., 2007. Septins Regulate Actin Organization and Cell-Cycle Arrest through Nuclear Accumulation of NCK Mediated by SOCS7. Cell 130, 837–850. https://doi.org/10.1016/j.cell.2007.06.053
Kremer, B.E., Haystead, T., Macara, I.G., 2005. Mammalian Septins Regulate Microtubule Stability through Interaction with the Microtubule-binding Protein MAP4. MBoC 16, 4648–4659. https://doi.org/10.1091/mbc.e05-03-0267
Krokowski, S., Lobato-Márquez, D., Chastanet, A., Pereira, P.M., Angelis, D., Galea, D., Larrouy-Maumus, G., Henriques, R., Spiliotis, E.T., Carballido-López, R., Mostowy, S., 2018. Septins Recognize and Entrap Dividing Bacterial Cells for Delivery to Lysosomes. Cell Host & Microbe 24, 866-874.e4. https://doi.org/10.1016/j.chom.2018.11.005
Kuang, S., Kuroda, K., Le Grand, F., Rudnicki, M.A., 2007. Asymmetric self-renewal and commitment of satellite stem cells in muscle. Cell 129, 999–1010. https://doi.org/10.1016/j.cell.2007.03.044
Kudryashov, D.S., Reisler, E., 2013. ATP and ADP Actin States. Biopolymers 99, 245–256. https://doi.org/10.1002/bip.22155
Kuleshov, M.V., Jones, M.R., Rouillard, A.D., Fernandez, N.F., Duan, Q., Wang, Z., Koplev, S., Jenkins, S.L., Jagodnik, K.M., Lachmann, A., McDermott, M.G., Monteiro, C.D., Gundersen, G.W., Ma'ayan, A., 2016. Enrichr: a comprehensive gene set enrichment analysis web server 2016 update. Nucleic Acids Res 44, W90–W97. https://doi.org/10.1093/nar/gkw377
Kuo, P.-L., Chiang, H.-S., Wang, Y.-Y., Kuo, Y.-C., Chen, M.-F., Yu, I.-S., Teng, Y.-N., Lin, S.-W., Lin, Y.-H., 2013. SEPT12-Microtubule Complexes Are Required for Sperm Head and Tail Formation. International Journal of Molecular Sciences 14, 22102–22116. https://doi.org/10.3390/ijms141122102
Kuroda, K., Kuang, S., Taketo, M.M., Rudnicki, M.A., 2013. Canonical Wnt signaling induces BMP-4 to specify slow myofibrogenesis of fetal myoblasts. Skeletal Muscle 3, 5. https://doi.org/10.1186/2044-5040-3-5
Kuzmić, M., Castro Linares, G., Leischner Fialová, J., Iv, F., Salaün, D., Llewellyn, A., Gomes, M., Belhabib, M., Liu, Y., Asano, K., Rodrigues, M., Isnardon, D., Tachibana, T., Koenderink, G.H., Badache, A., Mavrakis, M., Verdier-Pinard, P., 2022. Septin-microtubule association via a motif unique to isoform 1 of septin 9 tunes stress fibers. Journal of Cell Science 135, jcs258850. https://doi.org/10.1242/jcs.258850

Lai, T.-H., Wu, Y.-Y., Wang, Y.-Y., Chen, M.-F., Wang, P., Chen, T.-M., Wu, Y.-N., Chiang, H.-S., Kuo, P.-L., Lin, Y.-H., 2016. SEPT12–NDC1 Complexes Are Required for Mammalian Spermiogenesis. International Journal of Molecular Sciences 17, 1911. https://doi.org/10.3390/ijms17111911

Lam, M., Calvo, F., 2019. Regulation of mechanotransduction: Emerging roles for septins. Cytoskeleton 76, 115–122. https://doi.org/10.1002/cm.21485

Lancioni, H., Lucentini, L., Palomba, A., Fulle, S., Micheli, M.R., Panara, F., 2007. Muscle actin isoforms are differentially expressed in human satellite cells isolated from donors of different ages. Cell Biol Int 31, 180–185. https://doi.org/10.1016/j.cellbi.2006.10.002

Lange, C., Calegari, F., 2010. Cdks and cyclins link G1 length and differentiation of embryonic, neural and hematopoietic stem cells. Cell Cycle 9, 1893–1900. https://doi.org/10.4161/cc.9.10.11598

Langley, B., Thomas, M., Bishop, A., Sharma, M., Gilmour, S., Kambadur, R., 2002. Myostatin Inhibits Myoblast Differentiation by Down-regulating MyoD Expression*. Journal of Biological Chemistry 277, 49831–49840. https://doi.org/10.1074/jbc.M204291200

Larisch, S., Yi, Y., Lotan, R., Kerner, H., Eimerl, S., Tony Parks, W., Gottfried, Y., Birkey Reffey, S., de Caestecker, M.P., Danielpour, D., Book-Melamed, N., Timberg, R., Duckett, C.S., Lechleider, R.J., Steller, H., Orly, J., Kim, S.-J., Roberts, A.B., 2000. A novel mitochondrial septin-like protein, ARTS, mediates apoptosis dependent on its P-loop motif. Nat Cell Biol 2, 915–921. https://doi.org/10.1038/35046566

Larsen, B.D., Rampalli, S., Burns, L.E., Brunette, S., Dilworth, F.J., Megeney, L.A., 2010. Caspase 3/caspase-activated DNase promote cell differentiation by inducing DNA strand breaks. Proceedings of the National Academy of Sciences 107, 4230–4235. https://doi.org/10.1073/pnas.0913089107

Lassar, A.B., Paterson, B.M., Weintraub, H., 1986. Transfection of a DNA locus that mediates the conversion of 10T12 fibroblasts to myoblasts. Cell 47, 649–656. https://doi.org/10.1016/0092-8674(86)90507-6

Latres, E., Mastaitis, J., Fury, W., Miloscio, L., Trejos, J., Pangilinan, J., Okamoto, H., Cavino, K., Na, E., Papatheodorou, A., Willer, T., Bai, Y., Hae Kim, J., Rafique, A., Jaspers, S., Stitt, T., Murphy, A.J., Yancopoulos, G.D., Gromada, J., 2017. Activin A more prominently regulates muscle mass in primates than does GDF8. Nat Commun 8, 15153. https://doi.org/10.1038/ncomms15153

Lauer, J.C., Selig, M., Hart, M.L., Kurz, B., Rolauffs, B., 2021. Articular Chondrocyte Phenotype Regulation through the Cytoskeleton and the Signaling Processes That Originate from or Converge on the Cytoskeleton: Towards a Novel Understanding of the Intersection between Actin Dynamics and Chondrogenic Function. International Journal of Molecular Sciences 22, 3279. https://doi.org/10.3390/ijms22063279

Laurin, M., Fradet, N., Blangy, A., Hall, A., Vuori, K., Côté, J.-F., 2008. The atypical Rac activator Dock180 (Dock1) regulates myoblast fusion in vivo. Proceedings of the National Academy of Sciences 105, 15446–15451. https://doi.org/10.1073/pnas.0805546105

Lawson, C.D., Burridge, K., 2014. The on-off relationship of Rho and Rac during integrin-mediated adhesion and cell migration. Small GTPases 5, e27958. https://doi.org/10.4161/sgtp.27958

Lawson, C.D., Ridley, A.J., 2018. Rho GTPase signaling complexes in cell migration and invasion. J Cell Biol 217, 447–457. https://doi.org/10.1083/jcb.201612069

LeBlanc, L., Ramirez, N., Kim, J., 2021. Context-dependent roles of YAP/TAZ in stem cell fates and cancer. Cell. Mol. Life Sci. 78, 4201–4219. https://doi.org/10.1007/s00018-021-03781-2

Lee, D.M., Chen, E.H., 2019. Drosophila Myoblast Fusion: Invasion and Resistance for the Ultimate Union. Annual Review of Genetics 53, 67–91. https://doi.org/10.1146/annurev-genet-120116-024603

Lee, J., Abdeen, A.A., Tang, X., Saif, T.A., Kilian, K.A., 2015. Geometric guidance of integrin mediated traction stress during stem cell differentiation. Biomaterials 69, 174–183. https://doi.org/10.1016/j.biomaterials.2015.08.005

Lee, J.Y., Hopkinson, N.S., Kemp, P.R., 2011. Myostatin induces autophagy in skeletal muscle in vitro. Biochem Biophys Res Commun 415, 632–636. https://doi.org/10.1016/j.bbrc.2011.10.124

Lee, S.-J., Bhasin, S., Klickstein, L., Krishnan, V., Rooks, D., 2023. Challenges and Future Prospects of Targeting Myostatin/Activin A Signaling to Treat Diseases of Muscle Loss and Metabolic Dysfunction. The Journals of Gerontology: Series A 78, 32–37. https://doi.org/10.1093/gerona/glad033

Lee, S.-J., Huynh, T.V., Lee, Y.-S., Sebald, S.M., Wilcox-Adelman, S.A., Iwamori, N., Lepper, C., Matzuk, M.M., Fan, C.-M., 2012. Role of satellite cells versus myofibers in muscle hypertrophy induced by inhibition of the myostatin/activin signaling pathway. Proc Natl Acad Sci U S A 109, E2353-2360. https://doi.org/10.1073/pnas.1206410109

Lee, S.-J., Lehar, A., Liu, Y., Ly, C.H., Pham, Q.-M., Michaud, M., Rydzik, R., Youngstrom, D.W., Shen, M.M., Kaartinen, V., Germain-Lee, E.L., Rando, T.A., 2020. Functional redundancy of type I and type II receptors in the regulation of skeletal muscle growth by myostatin and activin A. Proceedings of the National Academy of Sciences 117, 30907–30917. https://doi.org/10.1073/pnas.2019263117

Lee, S.J., McPherron, A.C., 2001. Regulation of myostatin activity and muscle growth. Proc Natl Acad Sci U S A 98, 9306–9311. https://doi.org/10.1073/pnas.151270098

Lee, S.-J., Reed, L.A., Davies, M.V., Girgenrath, S., Goad, M.E.P., Tomkinson, K.N., Wright, J.F., Barker, C., Ehrmantraut, G., Holmstrom, J., Trowell, B., Gertz, B., Jiang, M.-S., Sebald, S.M., Matzuk, M., Li, E., Liang, L., Quattlebaum, E., Stotish, R.L., Wolfman, N.M., 2005. Regulation of muscle growth by multiple ligands signaling through activin type II receptors. Proceedings of the National Academy of Sciences 102, 18117–18122. https://doi.org/10.1073/pnas.0505996102

Lee, W.-L., Bezanilla, M., Pollard, T.D., 2000. Fission Yeast Myosin-I, Myo1p, Stimulates Actin Assembly by Arp2/3 Complex and Shares Functions with Wasp. J Cell Biol 151, 789–800.

Lehka, L., Rędowicz, M.J., 2020a. Mechanisms regulating myoblast fusion: A multilevel interplay. Seminars in Cell & Developmental Biology, Differentiation of skeletal muscles 104, 81–92. https://doi.org/10.1016/j.semcdb.2020.02.004

Lehka, L., Rędowicz, M.J., 2020b. Mechanisms regulating myoblast fusion: A multilevel interplay. Seminars in Cell & Developmental Biology 104, 81–92. https://doi.org/10.1016/j.semcdb.2020.02.004

Lehka, L., Topolewska, M., Wojton, D., Karatsai, O., Alvarez-Suarez, P., Pomorski, P., Rędowicz, M.J., 2020. Formation of Aberrant Myotubes by Myoblasts Lacking Myosin VI Is Associated with Alterations in the Cytoskeleton Organization, Myoblast Adhesion and Fusion. Cells 9, 1673. https://doi.org/10.3390/cells9071673

Leikina, E., Melikov, K., Sanyal, S., Verma, S.K., Eun, B., Gebert, C., Pfeifer, K., Lizunov, V.A., Kozlov, M.M., Chernomordik, L.V., 2013. Extracellular annexins and dynamin are important for sequential steps in myoblast fusion. J Cell Biol 200, 109–123. https://doi.org/10.1083/jcb.201207012

Leipe, D.D., Wolf, Y.I., Koonin, E.V., Aravind, L., 2002. Classification and evolution of P-loop GTPases and related ATPases. J Mol Biol 317, 41–72. https://doi.org/10.1006/jmbi.2001.5378

Leonardo, D.A., Cavini, I.A., Sala, F.A., Mendonça, D.C., Rosa, H.V.D., Kumagai, P.S., Crusca Jr, E., Valadares, N.F., Marques, I.A., Brandão-Neto, J., Munte, C.E., Kalbitzer, H.R., Soler, N., Usón, I., André, I., Araujo, A.P.U., D'Muniz Pereira, H., Garratt, R.C., 2021. Orientational Ambiguity in Septin Coiled Coils and its Structural Basis. Journal of Molecular Biology 433, 166889. https://doi.org/10.1016/j.jmb.2021.166889

Lepper, C., Fan, C.-M., 2010. Inducible lineage tracing of Pax7-descendant cells reveals embryonic origin of adult satellite cells. genesis 48, 424–436. https://doi.org/10.1002/dvg.20630

Lepper, C., Partridge, T.A., Fan, C.-M., 2011. An absolute requirement for Pax7-positive satellite cells in acute injury-induced skeletal muscle regeneration. Development 138, 3639–3646. https://doi.org/10.1242/dev.067595

Li, H., Saucedo-Cuevas, L., Yuan, L., Ross, D., Johansen, A., Sands, D., Stanley, V., Guemez-Gamboa, A., Gregor, A., Evans, T., Chen, S., Tan, L., Molina, H., Sheets, N., Shiryaev, S.A., Terskikh, A.V.,

Gladfelter, A.S., Shresta, S., Xu, Z., Gleeson, J.G., 2019. Zika Virus Protease Cleavage of Host Protein Septin-2 Mediates Mitotic Defects in Neural Progenitors. Neuron 101, 1089-1098.e4. https://doi.org/10.1016/j.neuron.2019.01.010

Li, H.-S., Wang, D., Shen, Q., Schonemann, M.D., Gorski, J.A., Jones, K.R., Temple, S., Jan, L.Y., Jan, Y.N., 2003. Inactivation of Numb and Numblike in Embryonic Dorsal Forebrain Impairs Neurogenesis and Disrupts Cortical Morphogenesis. Neuron 40, 1105–1118. https://doi.org/10.1016/S0896-6273(03)00755-4

Li, Z., Mericskay, M., Agbulut, O., Butler-Browne, G., Carlsson, L., Thornell, L.-E., Babinet, C., Paulin, D., 1997. Desmin Is Essential for the Tensile Strength and Integrity of Myofibrils but Not for Myogenic Commitment, Differentiation, and Fusion of Skeletal Muscle. J Cell Biol 139, 129–144.

Lian, Y.-L., Chen, K.-W., Chou, Y.-T., Ke, T.-L., Chen, B.-C., Lin, Y.-C., Chen, L., 2020. PIP3 depletion rescues myoblast fusion defects in human rhabdomyosarcoma cells. Journal of Cell Science 133, jcs240325. https://doi.org/10.1242/jcs.240325

Liao, Y., Smyth, G.K., Shi, W., 2014. featureCounts: an efficient general purpose program for assigning sequence reads to genomic features. Bioinformatics 30, 923–930. https://doi.org/10.1093/bioinformatics/btt656

Lim, S., Kaldis, P., 2013. Cdks, cyclins and CKIs: roles beyond cell cycle regulation. Development 140, 3079–3093. https://doi.org/10.1242/dev.091744

Lin, F., Sun, L., Zhang, Y., Gao, W., Chen, Z., Liu, Y., Tian, K., Han, X., Liu, R., Li, Y., Shen, L., 2024. Mitochondrial stress response and myogenic differentiation. Front Cell Dev Biol 12, 1381417. https://doi.org/10.3389/fcell.2024.1381417

Lin, Z., Holtzen, H., 1990. Studies on the role of microtubules in myofibrillogenesis. Cell Res 1, 119–129. https://doi.org/10.1038/cr.1990.12

Liu, J., Xiao, Q., Xiao, J., Niu, C., Li, Y., Zhang, X., Zhou, Z., Shu, G., Yin, G., 2022. Wnt/β-catenin signalling: function, biological mechanisms, and therapeutic opportunities. Sig Transduct Target Ther 7, 1–23. https://doi.org/10.1038/s41392-021-00762-6

Liu, Y.-J., Le Berre, M., Lautenschlaeger, F., Maiuri, P., Callan-Jones, A., Heuzé, M., Takaki, T., Voituriez, R., Piel, M., 2015. Confinement and Low Adhesion Induce Fast Amoeboid Migration of Slow Mesenchymal Cells. Cell 160, 659–672. https://doi.org/10.1016/j.cell.2015.01.007

Liu, Z., Vong, Q.P., Liu, C., Zheng, Y., 2014. Borg5 is required for angiogenesis by regulating persistent directional migration of the cardiac microvascular endothelial cells. MBoC 25, 841–851. https://doi.org/10.1091/mbc.e13-09-0543

Lodberg, A., 2021. Principles of the activin receptor signaling pathway and its inhibition. Cytokine & Growth Factor Reviews 60, 1–17. https://doi.org/10.1016/j.cytogfr.2021.04.001

Lokireddy, S., Mouly, V., Butler-Browne, G., Gluckman, P.D., Sharma, M., Kambadur, R., McFarlane, C., 2011. Myostatin promotes the wasting of human myoblast cultures through promoting ubiquitin-proteasome pathway-mediated loss of sarcomeric proteins. American Journal of Physiology-Cell Physiology 301, C1316–C1324. https://doi.org/10.1152/ajpcell.00114.2011

Longo, L.M., Jabłońska, J., Vyas, P., Kanade, M., Kolodny, R., Ben-Tal, N., Tawfik, D.S., 2020. On the emergence of P-Loop NTPase and Rossmann enzymes from a Beta-Alpha-Beta ancestral fragment. eLife 9, e64415. https://doi.org/10.7554/eLife.64415

Longtine, M.S., Theesfeld, C.L., McMillan, J.N., Weaver, E., Pringle, J.R., Lew, D.J., 2000. Septin-Dependent Assembly of a Cell Cycle-Regulatory Module in Saccharomyces cerevisiae. Molecular and Cellular Biology 20, 4049–4061. https://doi.org/10.1128/MCB.20.11.4049-4061.2000

Loo, L.S.W., Soetedjo, A.A.P., Lau, H.H., Ng, N.H.J., Ghosh, S., Nguyen, L., Krishnan, V.G., Choi, H., Roca, X., Hoon, S., Teo, A.K.K., 2020. BCL-xL/BCL2L1 is a critical anti-apoptotic protein that promotes the survival of differentiating pancreatic cells from human pluripotent stem cells. Cell Death Dis 11, 1–18. https://doi.org/10.1038/s41419-020-2589-7

López-Otín, C., Blasco, M.A., Partridge, L., Serrano, M., Kroemer, G., 2013. The Hallmarks of Aging. Cell 153, 1194–1217. https://doi.org/10.1016/j.cell.2013.05.039

Lopez-Rodríguez, C., Aramburu, J., Rakeman, A.S., Rao, A., 1999. NFAT5, a constitutively nuclear NFAT protein that does not cooperate with Fos and Jun. Proc Natl Acad Sci U S A 96, 7214–7219. https://doi.org/10.1073/pnas.96.13.7214

Loumaye, A., Lause, P., Zhong, X., Zimmers, T.A., Bindels, L.B., Thissen, J.-P., 2022. Activin A Causes Muscle Atrophy through MEF2C-Dependent Impaired Myogenesis. Cells 11, 1119. https://doi.org/10.3390/cells11071119

Love, M.I., Huber, W., Anders, S., 2014. Moderated estimation of fold change and dispersion for RNA-seq data with DESeq2. Genome Biology 15, 550. https://doi.org/10.1186/s13059-014-0550-8

Lowery, J., Kuczmarski, E.R., Herrmann, H., Goldman, R.D., 2015. Intermediate Filaments Play a Pivotal Role in Regulating Cell Architecture and Function. J Biol Chem 290, 17145–17153. https://doi.org/10.1074/jbc.R115.640359

Loyer, N., Januschke, J., 2018. The last-born daughter cell contributes to division orientation of Drosophila larval neuroblasts. Nat Commun 9, 3745. https://doi.org/10.1038/s41467-018-06276-0

Lu, Z., Joseph, D., Bugnard, E., Zaal, K.J.M., Ralston, E., 2001. Golgi Complex Reorganization during Muscle Differentiation: Visualization in Living Cells and Mechanism. Mol Biol Cell 12, 795–808.

Lucas, L., Cooper, T.A., 2023. Insights into Cell-Specific Functions of Microtubules in Skeletal Muscle Development and Homeostasis. International Journal of Molecular Sciences 24, 2903. https://doi.org/10.3390/ijms24032903

Luo, W., Li, G., Yi, Z., Nie, Q., Zhang, X., 2016. E2F1-miR-20a-5p/20b-5p auto-regulatory feedback loop involved in myoblast proliferation and differentiation. Sci Rep 6, 27904. https://doi.org/10.1038/srep27904

Lv, K., Chen, L., Li, Y., Li, Z., Zheng, P., Liu, Y., Chen, J., Teng, J., 2015. Trip6 Promotes Dendritic Morphogenesis through Dephosphorylated GRIP1-Dependent Myosin VI and F-Actin Organization. J. Neurosci. 35, 2559–2571. https://doi.org/10.1523/JNEUROSCI.2125-14.2015

Lyons, G.E., Ontell, M., Cox, R., Sassoon, D., Buckingham, M., 1990. The expression of myosin genes in developing skeletal muscle in the mouse embryo. Journal of Cell Biology 111, 1465–1476. https://doi.org/10.1083/jcb.111.4.1465

Ma, L., Li, C., Lian, S., Xu, B., Yuan, J., Lu, J., Yang, H., Guo, J., Ji, H., 2021. ActivinA activates Notch1-Shh signaling to regulate proliferation in C2C12 skeletal muscle cells. Molecular and Cellular Endocrinology 519, 111055. https://doi.org/10.1016/j.mce.2020.111055

Ma, R., Morshed, S.A., Latif, R., Davies, T.F., 2017. TAZ Induction Directs Differentiation of Thyroid Follicular Cells from Human Embryonic Stem Cells. Thyroid 27, 292–299. https://doi.org/10.1089/thy.2016.0264

Macara, I.G., Baldarelli, R., Field, C.M., Glotzer, M., Hayashi, Y., Hsu, S.-C., Kennedy, M.B., Kinoshita, M., Longtine, M., Low, C., Maltais, L.J., McKenzie, L., Mitchison, T.J., Nishikawa, T., Noda, M., Petty, E.M., Peifer, M., Pringle, J.R., Robinson, P.J., Roth, D., Russell, S.E.H., Stuhlmann, H., Tanaka, M., Tanaka, T., Trimble, W.S., Ware, J., Zeleznik-Le, N.J., Zieger, B., 2002. Mammalian Septins Nomenclature. Mol Biol Cell 13, 4111–4113. https://doi.org/10.1091/mbc.E02-07-0438

MacDonald, B.T., Tamai, K., He, X., 2009. Wnt/β-catenin signaling: components, mechanisms, and diseases. Dev Cell 17, 9–26. https://doi.org/10.1016/j.devcel.2009.06.016

Mackay, D.J., Nobes, C.D., Hall, A., 1995. The Rho's progress: a potential role during neuritogenesis for the Rho family of GTPases. Trends Neurosci 18, 496–501. https://doi.org/10.1016/0166-2236(95)92773-j

Maddox, A.S., Burridge, K., 2003. RhoA is required for cortical retraction and rigidity during mitotic cell rounding. Journal of Cell Biology 160, 255–265. https://doi.org/10.1083/jcb.200207130

Magae, J., Illenye, S., Chang, Y.-C., Mitsui, Y., Heintz, N.H., 1999. Association with E2F-1 governs intracellular trafficking and polyubiquitination of DP-1. Oncogene 18, 593–605. https://doi.org/10.1038/sj.onc.1202345

Majewski, Ł., Sobczak, M., Havrylov, S., Jóźwiak, J., Rędowicz, M.J., 2012. Dock7: a GEF for Rho-family GTPases and a novel myosin VI-binding partner in neuronal PC12 cells. Biochem Cell Biol 90, 565–574. https://doi.org/10.1139/o2012-009

Mandel-Gutfreund, Y., Kosti, I., Larisch, S., 2011. ARTS, the unusual septin: structural and functional aspects 392, 783–790. https://doi.org/10.1515/BC.2011.089

Maqbool, T., Jagla, K., 2007. Genetic control of muscle development: learning from Drosophila. J Muscle Res Cell Motil 28, 397–407. https://doi.org/10.1007/s10974-008-9133-1

Marcelle, C., Stark, M.R., Bronner-Fraser, M., 1997. Coordinate actions of BMPs, Wnts, Shh and noggin mediate patterning of the dorsal somite. Development 124, 3955–3963. https://doi.org/10.1242/dev.124.20.3955

Martínez, C., Corral, J., Dent, J.A., Sesma, L., Vicente, V., Ware, J., 2006. Platelet septin complexes form rings and associate with the microtubular network. Journal of Thrombosis and Haemostasis 4, 1388–1395. https://doi.org/10.1111/j.1538-7836.2006.01952.x

Martins, C.S., Taveneau, C., Castro-Linares, G., Baibakov, M., Buzhinsky, N., Eroles, M., Milanović, V., Omi, S., Pedelacq, J.-D., Iv, F., Bouillard, L., Llewellyn, A., Gomes, M., Belhabib, M., Kuzmić, M., Verdier-Pinard, P., Lee, S., Badache, A., Kumar, S., Chandre, C., Brasselet, S., Rico, F., Rossier, O., Koenderink, G.H., Wenger, J., Cabantous, S., Mavrakis, M., 2022. Human septins organize as octamer-based filaments and mediate actin-membrane anchoring in cells. Journal of Cell Biology 222, e202203016. https://doi.org/10.1083/jcb.202203016

Massagué, J., Seoane, J., Wotton, D., 2005. Smad transcription factors. Genes Dev. 19, 2783–2810. https://doi.org/10.1101/gad.1350705

Massari, M.E., Murre, C., 2000. Helix-Loop-Helix Proteins: Regulators of Transcription in Eucaryotic Organisms. Molecular and Cellular Biology 20, 429–440. https://doi.org/10.1128/MCB.20.2.429-440.2000

Massarwa, R., Carmon, S., Shilo, B.-Z., Schejter, E.D., 2007. WIP/WASp-Based Actin-Polymerization Machinery Is Essential for Myoblast Fusion in Drosophila. Developmental Cell 12, 557–569. https://doi.org/10.1016/j.devcel.2007.01.016

Masuhiro, Y., Kayama, K., Fukushima, A., Baba, K., Soutsu, M., Kamiya, Y., Gotoh, M., Yamaguchi, N., Hanazawa, S., 2008. SOCS-3 Inhibits E2F/DP-1 Transcriptional Activity and Cell Cycle Progression via Interaction with DP-1 *. Journal of Biological Chemistry 283, 31575–31583. https://doi.org/10.1074/jbc.M800328200

Mathieu, P.S., Loboa, E.G., 2012. Cytoskeletal and Focal Adhesion Influences on Mesenchymal Stem Cell Shape, Mechanical Properties, and Differentiation Down Osteogenic, Adipogenic, and Chondrogenic Pathways. Tissue Eng Part B Rev 18, 436–444. https://doi.org/10.1089/ten.teb.2012.0014

Matis, M., 2020. The Mechanical Role of Microtubules in Tissue Remodeling. BioEssays 42, 1900244. https://doi.org/10.1002/bies.201900244

Mauro, A., 1961. SATELLITE CELL OF SKELETAL MUSCLE FIBERS. The Journal of Biophysical and Biochemical Cytology 9, 493–495. https://doi.org/10.1083/jcb.9.2.493

Mavrakis, M., Azou-Gros, Y., Tsai, F.-C., Alvarado, J., Bertin, A., Iv, F., Kress, A., Brasselet, S., Koenderink, G.H., Lecuit, T., 2014. Septins promote F-actin ring formation by crosslinking actin filaments into curved bundles. Nat Cell Biol 16, 322–334. https://doi.org/10.1038/ncb2921

McBeath, R., Pirone, D.M., Nelson, C.M., Bhadriraju, K., Chen, C.S., 2004. Cell Shape, Cytoskeletal Tension, and RhoA Regulate Stem Cell Lineage Commitment. Developmental Cell 6, 483–495. https://doi.org/10.1016/S1534-5807(04)00075-9

McCroskery, S., Thomas, M., Maxwell, L., Sharma, M., Kambadur, R., 2003. Myostatin negatively regulates satellite cell activation and self-renewal. Journal of Cell Biology 162, 1135–1147. https://doi.org/10.1083/jcb.200207056

McDade, S.S., Hall, P.A., Russell, S.E.H., 2007. Translational control of SEPT9 isoforms is perturbed in disease. Hum Mol Genet 16, 742–752. https://doi.org/10.1093/hmg/ddm003

McFarland, D.C., Velleman, S.G., Pesall, J.E., Liu, C., 2007. The role of myostatin in chicken (Gallus domesticus) myogenic satellite cell proliferation and differentiation. Gen Comp Endocrinol 151, 351–357. https://doi.org/10.1016/j.ygcen.2007.02.006

McFarlane, C., Plummer, E., Thomas, M., Hennebry, A., Ashby, M., Ling, N., Smith, H., Sharma, M., Kambadur, R., 2006. Myostatin induces cachexia by activating the ubiquitin proteolytic system through an NF-κB-independent, FoxO1-dependent mechanism. Journal of Cellular Physiology 209, 501–514. https://doi.org/10.1002/jcp.20757

McGrath, M.J., Cottle, D.L., Nguyen, M.-A., Dyson, J.M., Coghill, I.D., Robinson, P.A., Holdsworth, M., Cowling, B.S., Hardeman, E.C., Mitchell, C.A., Brown, S., 2006. Four and a half LIM protein 1 binds myosin-binding protein C and regulates myosin filament formation and sarcomere assembly. J Biol Chem 281, 7666–7683. https://doi.org/10.1074/jbc.M512552200

McGregor, R.A., Cameron-Smith, D., Poppitt, S.D., 2014. It is not just muscle mass: a review of muscle quality, composition and metabolism during ageing as determinants of muscle function and mobility in later life. Longev Healthspan 3, 9. https://doi.org/10.1186/2046-2395-3-9

McMillan, E.M., Quadrilatero, J., 2014. Autophagy is required and protects against apoptosis during myoblast differentiation. Biochem J 462, 267–277. https://doi.org/10.1042/BJ20140312

McMurray, M.A., Thorner, J., 2019. Turning it inside out: the organization of human septin hetero-oligomers. Cytoskeleton (Hoboken) 76, 449–456. https://doi.org/10.1002/cm.21571

Mendez, M.G., Kojima, S.-I., Goldman, R.D., 2010. Vimentin induces changes in cell shape, motility, and adhesion during the epithelial to mesenchymal transition. The FASEB Journal 24, 1838–1851. https://doi.org/10.1096/fj.09-151639

Mendonça, D.C., Guimarães, S.L., Pereira, H.D., Pinto, A.A., de Farias, M.A., de Godoy, A.S., Araujo, A.P.U., van Heel, M., Portugal, R.V., Garratt, R.C., 2021. An atomic model for the human septin hexamer by cryo-EM. Journal of Molecular Biology 433, 167096. https://doi.org/10.1016/j.jmb.2021.167096

Mendonça, D.C., Macedo, J.N., Guimarães, S.L., Barroso da Silva, F.L., Cassago, A., Garratt, R.C., Portugal, R.V., Araujo, A.P.U., 2019. A revised order of subunits in mammalian septin complexes. Cytoskeleton 76, 457–466. https://doi.org/10.1002/cm.21569

Menon, M.B., Gaestel, M., 2015. Sep(t)arate or not – how some cells take septin-independent routes through cytokinesis. Journal of Cell Science 128, 1877–1886. https://doi.org/10.1242/jcs.164830

Merenich, D., Nakos, K., Pompan, T., Donovan, S.J., Gill, A., Patel, P., Spiliotis, E.T., Myers, K.A., 2022. Septins guide noncentrosomal microtubules to promote focal adhesion disassembly in migrating cells. Mol Biol Cell 33, ar40. https://doi.org/10.1091/mbc.E21-06-0334

Meriane, M., Charrasse, S., Comunale, F., Gauthier-Rouvière, C., 2002. Transforming growth factor beta activates Rac1 and Cdc42Hs GTPases and the JNK pathway in skeletal muscle cells. Biol Cell 94, 535–543. https://doi.org/10.1016/s0248-4900(02)00023-0

Meriane, M., Roux, P., Primig, M., Fort, P., Gauthier-Rouvière, C., 2000. Critical Activities of Rac1 and Cdc42Hs in Skeletal Myogenesis: Antagonistic Effects of JNK and p38 Pathways. Mol Biol Cell 11, 2513–2528.

Michael, J., 2021. What do we mean when we talk about “structure/function” relationships? Advances in Physiology Education 45, 880–885. https://doi.org/10.1152/advan.00108.2021

Milasincic, D.J., Dhawan, J., Farmer, S.R., 1996. Anchorage-dependent control of muscle-specific gene expression in C2C12 mouse myoblasts. In Vitro Cell Dev Biol Anim 32, 90–99. https://doi.org/10.1007/BF02723040

Millay, D.P., O’Rourke, J.R., Sutherland, L.B., Bezprozvannaya, S., Shelton, J.M., Bassel-Duby, R., Olson, E.N., 2013. Myomaker is a membrane activator of myoblast fusion and muscle formation. Nature 499, 301–305. https://doi.org/10.1038/nature12343

Miralles, F., Posern, G., Zaromytidou, A.-I., Treisman, R., 2003. Actin Dynamics Control SRF Activity by Regulation of Its Coactivator MAL. Cell 113, 329–342. https://doi.org/10.1016/S0092-8674(03)00278-2

Mishra, A.K., Lambright, D.G., 2016. Small GTPases and their GAPs. Biopolymers 105, 431–448. https://doi.org/10.1002/bip.22833

Mishra, P., Cohen, R.I., Zhao, N., Moghe, P.V., 2021. Fluorescence-based actin turnover dynamics of stem cells as a profiling method for stem cell functional evolution, heterogeneity and phenotypic lineage parsing. Methods, Methods and Advances in High-throughput Screening for Regenerative Medicine 190, 44–54. https://doi.org/10.1016/j.ymeth.2020.05.020

Mishra, P., Martin, D.C., Androulakis, I.P., Moghe, P.V., 2019. Fluorescence Imaging of Actin Turnover Parses Early Stem Cell Lineage Divergence and Senescence. Sci Rep 9, 10377. https://doi.org/10.1038/s41598-019-46682-y

Mizutani, Y., Ito, H., Iwamoto, I., Morishita, R., Kanoh, H., Seishima, M., Nagata, K., 2013. Possible role of a septin, SEPT1, in spreading in squamous cell carcinoma DJM-1 cells. Biological Chemistry 394, 281–290. https://doi.org/10.1515/hsz-2012-0258

Mohamed, A., Sun, C., De Mello, V., Selfe, J., Missiaglia, E., Shipley, J., Murray, G.I., Zammit, P.S., Wackerhage, H., 2016. The Hippo effector TAZ (WWTR1) transforms myoblasts and TAZ abundance is associated with reduced survival in embryonal rhabdomyosarcoma. J Pathol 240, 3–14. https://doi.org/10.1002/path.4745

Momany, M., Zhao, J., Lindsey, R., Westfall, P.J., 2001. Characterization of the Aspergillus nidulans septin (asp) gene family. Genetics 157, 969–977.

Monge, C., DiStasio, N., Rossi, T., Sébastien, M., Sakai, H., Kalman, B., Boudou, T., Tajbakhsh, S., Marty, I., Bigot, A., Mouly, V., Picart, C., 2017. Quiescence of human muscle stem cells is favored by culture on natural biopolymeric films. Stem Cell Research & Therapy 8, 104. https://doi.org/10.1186/s13287-017-0556-8

Moon, I.S., Lee, H., Walikonis, R.S., 2013. Septin 6 localizes to microtubules in neuronal dendrites. Cytotechnology 65, 179–186. https://doi.org/10.1007/s10616-012-9477-7

Moore, C.A., Parkin, C.A., Bidet, Y., Ingham, P.W., 2007. A role for the Myoblast city homologues Dock1 and Dock5 and the adaptor proteins Crk and Crk-like in zebrafish myoblast fusion. Development 134, 3145–3153. https://doi.org/10.1242/dev.001214

Mosaddeghzadeh, N., Ahmadian, M.R., 2021. The RHO Family GTPases: Mechanisms of Regulation and Signaling. Cells 10, 1831. https://doi.org/10.3390/cells10071831

Mostowy, S., Cossart, P., 2012. Septins: the fourth component of the cytoskeleton. Nat Rev Mol Cell Biol 13, 183–194. https://doi.org/10.1038/nrm3284

Mostowy, S., Janel, S., Forestier, C., Roduit, C., Kasas, S., Pizarro-Cerdá, J., Cossart, P., Lafont, F., 2011. A Role for Septins in the Interaction between the Listeria monocytogenes Invasion Protein InlB and the Met Receptor. Biophysical Journal 100, 1949–1959. https://doi.org/10.1016/j.bpj.2011.02.040

Motohashi, N., Asakura, A., 2014. Muscle satellite cell heterogeneity and self-renewal. Frontiers in Cell and Developmental Biology 2.

Mourikis, P., Sambasivan, R., Castel, D., Rocheteau, P., Bizzarro, V., Tajbakhsh, S., 2012. A critical requirement for notch signaling in maintenance of the quiescent skeletal muscle stem cell state. Stem Cells 30, 243–252. https://doi.org/10.1002/stem.775

Moustakas, A., Heldin, C.-H., 2009. The regulation of TGFβ signal transduction. Development 136, 3699–3714. https://doi.org/10.1242/dev.030338

Mueller, C., Trujillo-Miranda, M., Maier, M., Heath, D.E., O'Connor, A.J., Salehi, S., 2021. Effects of External Stimulators on Engineered Skeletal Muscle Tissue Maturation. Advanced Materials Interfaces 8, 2001167. https://doi.org/10.1002/admi.202001167

Mukund, K., Subramaniam, S., 2020. Skeletal muscle: A review of molecular structure and function, in health and disease. Wiley Interdiscip Rev Syst Biol Med 12, e1462. https://doi.org/10.1002/wsbm.1462

Müller, M., Diensthuber, R.P., Chizhov, I., Claus, P., Heissler, S.M., Preller, M., Taft, M.H., Manstein, D.J., 2013. Distinct Functional Interactions between Actin Isoforms and Nonsarcomeric Myosins. PLOS ONE 8, e70636. https://doi.org/10.1371/journal.pone.0070636

Mulvaney, K.M., Blomquist, C., Acharya, N., Li, R., Ranaghan, M.J., O'Keefe, M., Rodriguez, D.J., Young, M.J., Kesar, D., Pal, D., Stokes, M., Nelson, A.J., Jain, S.S., Yang, A., Mullin-Bernstein,

Z., Columbus, J., Bozal, F.K., Skepner, A., Raymond, D., LaRussa, S., McKinney, D.C., Freyzon, Y., Baidi, Y., Porter, D., Aguirre, A.J., Ianari, A., McMillan, B., Sellers, W.R., 2021. Molecular basis for substrate recruitment to the PRMT5 methylosome. Mol Cell 81, 3481-3495.e7. https://doi.org/10.1016/j.molcel.2021.07.019

Muroyama, A., Lechler, T., 2017. Microtubule organization, dynamics and functions in differentiated cells. Development 144, 3012–3021. https://doi.org/10.1242/dev.153171

Murray, T.V.A., McMahon, J.M., Howley, B.A., Stanley, A., Ritter, T., Mohr, A., Zwacka, R., Fearnhead, H.O., 2008. A non-apoptotic role for caspase-9 in muscle differentiation. J Cell Sci 121, 3786–3793. https://doi.org/10.1242/jcs.024547

Musa, H., Orton, C., Morrison, E.E., Peckham, M., 2003. Microtubule assembly in cultured myoblasts and myotubes following nocodazole induced microtubule depolymerisation. J Muscle Res Cell Motil 24, 301–308.

Naccache, S.N., Hasson, T., Horowitz, A., 2006. Binding of internalized receptors to the PDZ domain of GIPC/synectin recruits myosin VI to endocytic vesicles. Proceedings of the National Academy of Sciences 103, 12735–12740. https://doi.org/10.1073/pnas.0605317103

Nagata, K., Kawajiri, A., Matsui, S., Takagishi, M., Shiromizu, T., Saitoh, N., Izawa, I., Kiyono, T., Itoh, T.J., Hotani, H., Inagaki, M., 2003. Filament Formation of MSF-A, a Mammalian Septin, in Human Mammary Epithelial Cells Depends on Interactions with Microtubules*. Journal of Biological Chemistry 278, 18538–18543. https://doi.org/10.1074/jbc.M205246200

Nagata, K.-I., Inagaki, M., 2005. Cytoskeletal modification of Rho guanine nucleotide exchange factor activity: identification of a Rho guanine nucleotide exchange factor as a binding partner for Sept9b, a mammalian septin. Oncogene 24, 65–76. https://doi.org/10.1038/sj.onc.1208101

Nakahira, M., Macedo, J.N.A., Seraphim, T.V., Cavalcante, N., Souza, T.A.C.B., Damalio, J.C.P., Reyes, L.F., Assmann, E.M., Alborghetti, M.R., Garratt, R.C., Araujo, A.P.U., Zanchin, N.I.T., Barbosa, J.A.R.G., Kobarg, J., 2010. A Draft of the Human Septin Interactome. PLOS ONE 5, e13799. https://doi.org/10.1371/journal.pone.0013799

Nakajima, R., Deguchi, R., Komori, H., Zhao, L., Zhou, Y., Shirasawa, M., Angelina, A., Goto, Y., Tohjo, F., Nakahashi, K., Nakata, K., Iwanaga, R., Bradford, A.P., Araki, K., Warita, T., Ohtani, K., 2023. The TFDP1 gene coding for DP1, the heterodimeric partner of the transcription factor E2F, is a target of deregulated E2F. Biochemical and Biophysical Research Communications 663, 154–162. https://doi.org/10.1016/j.bbrc.2023.04.092

Nakos, K., Radler, M.R., Spiliotis, E.T., 2019a. Septin 2/6/7 complexes tune microtubule plus-end growth and EB1 binding in a concentration- and filament-dependent manner. MBoC 30, 2913–2928. https://doi.org/10.1091/mbc.E19-07-0362

Nakos, K., Rosenberg, M., Spiliotis, E.T., 2019b. Regulation of microtubule plus end dynamics by septin 9. Cytoskeleton 76, 83–91. https://doi.org/10.1002/cm.21488

Narumiya, S., Thumkeo, D., 2018. Rho signaling research: history, current status and future directions. FEBS Letters 592, 1763–1776. https://doi.org/10.1002/1873-3468.13087

Nava, M.M., Raimondi, M.T., Pietrabissa, R., 2012. Controlling Self-Renewal and Differentiation of Stem Cells via Mechanical Cues. J Biomed Biotechnol 2012, 797410. https://doi.org/10.1155/2012/797410

Nickel, J., Mueller, T.D., 2019. Specification of BMP Signaling. Cells 8, 1579. https://doi.org/10.3390/cells8121579

Nikolic, M., 2002. The role of Rho GTPases and associated kinases in regulating neurite outgrowth. Int J Biochem Cell Biol 34, 731–745. https://doi.org/10.1016/s1357-2725(01)00167-4

Nishihama, R., Onishi, M., Pringle, J.R., 2011. New Insights into the Phylogenetic Distribution and Evolutionary Origins of the Septins. Biol Chem 392, 681–687. https://doi.org/10.1515/BC.2011.086

Nishiyama, T., Kii, I., Kudo, A., 2004. Inactivation of Rho/ROCK Signaling Is Crucial for the Nuclear Accumulation of FKHR and Myoblast Fusion*. Journal of Biological Chemistry 279, 47311–47319. https://doi.org/10.1074/jbc.M403546200

Nobes, C.D., Hall, A., 1995. Rho, rac, and cdc42 GTPases regulate the assembly of multimolecular focal complexes associated with actin stress fibers, lamellipodia, and filopodia. Cell 81, 53–62. https://doi.org/10.1016/0092-8674(95)90370-4

Nölke, T., Schwan, C., Lehmann, F., Østevold, K., Pertz, O., Aktories, K., 2016. Septins guide microtubule protrusions induced by actin-depolymerizing toxins like Clostridium difficile transferase (CDT). Proc Natl Acad Sci U S A 113, 7870–7875. https://doi.org/10.1073/pnas.1522717113

Normand, G., King, R.W., 2010. Understanding Cytokinesis Failure. Adv Exp Med Biol 676, 27–55.

Noviello, C., Kobon, K., Delivry, L., Guilbert, T., Britto, F., Julienne, F., Maire, P., Randrianarison-Huetz, V., Sotiropoulos, A., 2022. RhoA within myofibers controls satellite cell microenvironment to allow hypertrophic growth. iScience 25. https://doi.org/10.1016/j.isci.2021.103616

Noviello, C., Kobon, K., Randrianarison-Huetz, V., Maire, P., Pietri-Rouxel, F., Falcone, S., Sotiropoulos, A., 2023. RhoA Is a Crucial Regulator of Myoblast Fusion. Cells 12, 2673. https://doi.org/10.3390/cells12232673

Nowak, S.J., Nahirney, P.C., Hadjantonakis, A.-K., Baylies, M.K., 2009. Nap1-mediated actin remodeling is essential for mammalian myoblast fusion. J Cell Sci 122, 3282–3293. https://doi.org/10.1242/jcs.047597

O'Connor, R.S., Mills, S.T., Jones, K.A., Ho, S.N., Pavlath, G.K., 2007. A combinatorial role for NFAT5 in both myoblast migration and differentiation during skeletal muscle myogenesis. Journal of Cell Science 120, 149–159. https://doi.org/10.1242/jcs.03307

O'Loughlin, T., Masters, T.A., Buss, F., 2018. The MYO6 interactome reveals adaptor complexes coordinating early endosome and cytoskeletal dynamics. EMBO reports 19, e44884. https://doi.org/10.15252/embr.201744884

Olsen, L.A., Nicoll, J.X., Fry, A.C., 2019. The skeletal muscle fiber: a mechanically sensitive cell. Eur J Appl Physiol 119, 333–349. https://doi.org/10.1007/s00421-018-04061-x

Olsen, O.E., Sankar, M., Elsaadi, S., Hella, H., Buene, G., Darvekar, S.R., Misund, K., Katagiri, T., Knaus, P., Holien, T., 2018. BMPR2 inhibits activin and BMP signaling via wild-type ALK2. Journal of Cell Science 131, jcs213512. https://doi.org/10.1242/jcs.213512

Olson, E.N., Nordheim, A., 2010. Linking actin dynamics and gene transcription to drive cellular motile functions. Nat Rev Mol Cell Biol 11, 353–365. https://doi.org/10.1038/nrm2890

Omrane, M., Camara, A.S., Taveneau, C., Benzoubir, N., Tubiana, T., Yu, J., Guérois, R., Samuel, D., Goud, B., Poüs, C., Bressanelli, S., Garratt, R.C., Thiam, A.R., Gassama-Diagne, A., 2019. Septin 9 has Two Polybasic Domains Critical to Septin Filament Assembly and Golgi Integrity. iScience 13, 138–153. https://doi.org/10.1016/j.isci.2019.02.015

Ontell, M., Feng, K.C., Klueber, K., Dunn, R.F., Taylor, F., 1984. Myosatellite cells, growth, and regeneration in murine dystrophic muscle: A quantitative study. The Anatomical Record 208, 159–174. https://doi.org/10.1002/ar.1092080203

Oprescu, S.N., Yue, F., Qiu, J., Brito, L.F., Kuang, S., 2020. Temporal Dynamics and Heterogeneity of Cell Populations during Skeletal Muscle Regeneration. iScience 23. https://doi.org/10.1016/j.isci.2020.100993

Ortega-Campos, S.M., García-Heredia, J.M., 2023. The Multitasker Protein: A Look at the Multiple Capabilities of NUMB. Cells 12, 333. https://doi.org/10.3390/cells12020333

Oses, C., De Rossi, M.C., Bruno, L., Verneri, P., Diaz, M.C., Benítez, B., Guberman, A., Levi, V., 2023. From the membrane to the nucleus: mechanical signals and transcription regulation. Biophys Rev 15, 671–683. https://doi.org/10.1007/s12551-023-01103-3

Østevold, K., Meléndez, A.V., Lehmann, F., Schmidt, G., Aktories, K., Schwan, C., 2017. Septin remodeling is essential for the formation of cell membrane protrusions (microtentacles) in detached tumor cells. Oncotarget 8, 76686–76698. https://doi.org/10.18632/oncotarget.20805

Otey, C.A., Kalnoski, M.H., Bulinski, J.C., 1988. Immunolocalization of muscle and nonmuscle isoforms of actin in myogenic cells and adult skeletal muscle. Cell Motil Cytoskeleton 9, 337–348. https://doi.org/10.1002/cm.970090406

Ott, M.-O., Bober, E., Lyons, G., Arnold, H., Buckingham, M., 1991. Early expression of the myogenic regulatory gene, myf-5, in precursor cells of skeletal muscle in the mouse embryo. Development 111, 1097–1107. https://doi.org/10.1242/dev.111.4.1097

Otto, A., Collins-Hooper, H., Patel, A., Dash, P.R., Patel, K., 2011. Adult Skeletal Muscle Stem Cell Migration Is Mediated by a Blebbing/Amoeboid Mechanism. Rejuvenation Research 14, 249–260. https://doi.org/10.1089/rej.2010.1151

Özkan, E., Chia, P.H., Wang, R., Goriatcheva, N., Borek, D., Otwinowski, Z., Walz, T., Shen, K., Garcia, K.C., 2014. Extracellular architecture of the SYG-1/SYG-2 adhesion complex instructs synaptogenesis. Cell 156, 482–494. https://doi.org/10.1016/j.cell.2014.01.004

Pablo Rodríguez, J., González, M., Ríos, S., Cambiazo, V., 2004. Cytoskeletal organization of human mesenchymal stem cells (MSC) changes during their osteogenic differentiation. Journal of Cellular Biochemistry 93, 721–731. https://doi.org/10.1002/jcb.20234

Pacheco, J., Cassidy, A.C., Zewe, J.P., Wills, R.C., Hammond, G.R.V., 2022. PI(4,5)P2 diffuses freely in the plasma membrane even within high-density effector protein complexes. Journal of Cell Biology 222, e202204099. https://doi.org/10.1083/jcb.202204099

Pagliuso, A., Tham, T.N., Stevens, J.K., Lagache, T., Persson, R., Salles, A., Olivo-Marin, J., Oddos, S., Spang, A., Cossart, P., Stavru, F., 2016. A role for septin 2 in Drp1-mediated mitochondrial fission. EMBO reports 17, 858–873. https://doi.org/10.15252/embr.201541612

Pajcini, K.V., Pomerantz, J.H., Alkan, O., Doyonnas, R., Blau, H.M., 2008. Myoblasts and macrophages share molecular components that contribute to cell–cell fusion. Journal of Cell Biology 180, 1005–1019. https://doi.org/10.1083/jcb.200707191

Pan, F., Malmberg, R.L., Momany, M., 2007. Analysis of septins across kingdoms reveals orthology and new motifs. BMC Evolutionary Biology 7, 103. https://doi.org/10.1186/1471-2148-7-103

Panagiotou, T.C., Chen, A., Wilde, A., 2022. An anillin-CIN85-SEPT9 complex promotes intercellular bridge maturation required for successful cytokinesis. Cell Reports 40, 111274. https://doi.org/10.1016/j.celrep.2022.111274

Pang, K.T., Loo, L.S.W., Chia, S., Ong, F.Y.T., Yu, H., Walsh, I., 2023. Insight into muscle stem cell regeneration and mechanobiology. Stem Cell Res Ther 14, 129. https://doi.org/10.1186/s13287-023-03363-y

Panzetta, V., De Clemente, C., Russo, M., Fusco, S., Netti, P.A., 2023. Insight to motor clutch model for sensing of ECM residual strain. Mechanobiology in Medicine 100025. https://doi.org/10.1016/j.mbm.2023.100025

Park, S.-Y., Yun, Y., Lim, J.-S., Kim, M.-J., Kim, S.-Y., Kim, J.-E., Kim, I.-S., 2016. Stabilin-2 modulates the efficiency of myoblast fusion during myogenic differentiation and muscle regeneration. Nat Commun 7, 10871. https://doi.org/10.1038/ncomms10871

Park, T.J., Kim, S.K., Wallingford, J.B., 2015. The planar cell polarity effector protein Wdpcp (Fritz) controls epithelial cell cortex dynamics via septins and actomyosin. Biochem Biophys Res Commun 456, 562–566. https://doi.org/10.1016/j.bbrc.2014.11.078

Patteson, A.E., Vahabikashi, A., Pogoda, K., Adam, S.A., Mandal, K., Kittisopikul, M., Sivagurunathan, S., Goldman, A., Goldman, R.D., Janmey, P.A., 2019. Vimentin protects cells against nuclear rupture and DNA damage during migration. Journal of Cell Biology 218, 4079–4092. https://doi.org/10.1083/jcb.201902046

Paydar, M., Kwok, B.H., 2020. Evidence for conformational change-induced hydrolysis of β-tubulin-GTP. https://doi.org/10.1101/2020.09.08.288019

Peckham, M., 2008. Engineering a multi-nucleated myotube, the role of the actin cytoskeleton. J Microsc 231, 486–493. https://doi.org/10.1111/j.1365-2818.2008.02061.x

Peckham, M., Miller, G., Zicha, D., Dunn, G.A., 2001. Specific changes to the mechanism of cell locomotion induced by overexpression of β-actin. Journal of Cell Science 114, 1367–1377. https://doi.org/10.1242/jcs.114.7.1367

Pelosi, M., Marampon, F., Zani, B.M., Prudente, S., Perlas, E., Caputo, V., Cianetti, L., Berno, V., Narumiya, S., Kang, S.W., Musarò, A., Rosenthal, N., 2007. ROCK2 and its alternatively

spliced isoform ROCK2m positively control the maturation of the myogenic program. Mol Cell Biol 27, 6163–6176. https://doi.org/10.1128/MCB.01735-06

Petersen, P.H., Zou, K., Hwang, J.K., Jan, Y.N., Zhong, W., 2002. Progenitor cell maintenance requires numb and numblike during mouse neurogenesis. Nature 419, 929–934. https://doi.org/10.1038/nature01124

Petrany, M.J., Millay, D.P., 2019. Cell Fusion: Merging Membranes and Making Muscle. Trends Cell Biol 29, 964–973. https://doi.org/10.1016/j.tcb.2019.09.002

Petrany, M.J., Swoboda, C.O., Sun, C., Chetal, K., Chen, X., Weirauch, M.T., Salomonis, N., Millay, D.P., 2020. Single-nucleus RNA-seq identifies transcriptional heterogeneity in multinucleated skeletal myofibers. Nat Commun 11, 6374. https://doi.org/10.1038/s41467-020-20063-w

Petrie, R.J., Yamada, K.M., 2016. Multiple Mechanisms of 3D Migration: The Origins of Plasticity. Curr Opin Cell Biol 42, 7–12. https://doi.org/10.1016/j.ceb.2016.03.025

Petrie, R.J., Yamada, K.M., 2012. At the leading edge of three-dimensional cell migration. J Cell Sci 125, 5917–5926. https://doi.org/10.1242/jcs.093732

Pfaffl, M.W., 2001. A new mathematical model for relative quantification in real-time RT–PCR. Nucleic Acids Res 29, e45.

Piatti, S., 2020. Cytokinesis: An Anillin-RhoGEF Module Sets the Stage for Septin Double Ring Assembly. Curr Biol 30, R347–R349. https://doi.org/10.1016/j.cub.2020.02.035

Picard, M., Shirihai, O.S., 2022. Mitochondrial signal transduction. Cell Metab 34, 1620–1653. https://doi.org/10.1016/j.cmet.2022.10.008

Piersma, B., Bank, R.A., Boersema, M., 2015. Signaling in Fibrosis: TGF-β, WNT, and YAP/TAZ Converge. Front. Med. 2. https://doi.org/10.3389/fmed.2015.00059

Pirrotta, V., 2004. The Ways of PARP. Cell 119, 735–736. https://doi.org/10.1016/j.cell.2004.12.002

Pizza, F.X., Buckley, K.H., 2023. Regenerating Myofibers after an Acute Muscle Injury: What Do We Really Know about Them? Int J Mol Sci 24, 12545. https://doi.org/10.3390/ijms241612545

Polager, S., Ginsberg, D., 2009. p53 and E2f: partners in life and death. Nat Rev Cancer 9, 738–748. https://doi.org/10.1038/nrc2718

Pongkitwitoon, S., Uzer, G., Rubin, J., Judex, S., 2016. Cytoskeletal Configuration Modulates Mechanically Induced Changes in Mesenchymal Stem Cell Osteogenesis, Morphology, and Stiffness. Sci Rep 6, 34791. https://doi.org/10.1038/srep34791

Porpiglia, E., Samusik, N., Ho, A.T.V., Cosgrove, B.D., Mai, T., Davis, K.L., Jager, A., Nolan, G.P., Bendall, S.C., Fantl, W.J., Blau, H.M., 2017. High-resolution myogenic lineage mapping by single-cell mass cytometry. Nat Cell Biol 19, 558–567. https://doi.org/10.1038/ncb3507

Posern, G., Sotiropoulos, A., Treisman, R., 2002. Mutant Actins Demonstrate a Role for Unpolymerized Actin in Control of Transcription by Serum Response Factor. MBoC 13, 4167–4178. https://doi.org/10.1091/mbc.02-05-0068

Possidonio, A.C.B., Soares, C.P., Portilho, D.M., Midlej, V., Benchimol, M., Butler-Browne, G., Costa, M.L., Mermelstein, C., 2014. Differences in the Expression and Distribution of Flotillin-2 in Chick, Mice and Human Muscle Cells. PLOS ONE 9, e103990. https://doi.org/10.1371/journal.pone.0103990

Puri, P.L., Iezzi, S., Stiegler, P., Chen, T.-T., Schiltz, R.L., Muscat, G.E.O., Giordano, A., Kedes, L., Wang, J.Y.J., Sartorelli, V., 2001. Class I Histone Deacetylases Sequentially Interact with MyoD and pRb during Skeletal Myogenesis. Molecular Cell 8, 885–897. https://doi.org/10.1016/S1097-2765(01)00373-2

Putra, V.D.L., Kilian, K.A., Knothe Tate, M.L., 2023. Biomechanical, biophysical and biochemical modulators of cytoskeletal remodelling and emergent stem cell lineage commitment. Commun Biol 6, 75. https://doi.org/10.1038/s42003-022-04320-w

Pylypenko, O., Welz, T., Tittel, J., Kollmar, M., Chardon, F., Malherbe, G., Weiss, S., Michel, C.I.L., Samol-Wolf, A., Grasskamp, A.T., Hume, A., Goud, B., Baron, B., England, P., Titus, M.A., Schwille, P., Weidemann, T., Houdusse, A., Kerkhoff, E., 2016. Coordinated recruitment of Spir actin nucleators and myosin V motors to Rab11 vesicle membranes. eLife 5, e17523. https://doi.org/10.7554/eLife.17523

Qazi, T.H., Duda, G.N., Ort, M.J., Perka, C., Geissler, S., Winkler, T., 2019. Cell therapy to improve regeneration of skeletal muscle injuries. J Cachexia Sarcopenia Muscle 10, 501–516. https://doi.org/10.1002/jcsm.12416

Qiu, R., Runxiang, Q., Geng, A., Liu, J., Xu, C.W., Menon, M.B., Gaestel, M., Lu, Q., 2020. SEPT7 Interacts with KIF20A and Regulates the Proliferative State of Neural Progenitor Cells During Cortical Development. Cereb Cortex 30, 3030–3043. https://doi.org/10.1093/cercor/bhz292

Quarta, M., Brett, J.O., DiMarco, R., De Morree, A., Boutet, S.C., Chacon, R., Gibbons, M.C., Garcia, V.A., Su, J., Shrager, J.B., Heilshorn, S., Rando, T.A., 2016. An artificial niche preserves the quiescence of muscle stem cells and enhances their therapeutic efficacy. Nat Biotechnol 34, 752–759. https://doi.org/10.1038/nbt.3576

Quinn, M.E., Goh, Q., Kurosaka, M., Gamage, D.G., Petrany, M.J., Prasad, V., Millay, D.P., 2017. Myomerger induces fusion of non-fusogenic cells and is required for skeletal muscle development. Nat Commun 8, 15665. https://doi.org/10.1038/ncomms15665

Quist-Løkken, I., Andersson-Rusch, C., Kastnes, M.H., Kolos, J.M., Jatzlau, J., Hella, H., Olsen, O.E., Sundan, A., Knaus, P., Hausch, F., Holien, T., 2023. FKBP12 is a major regulator of ALK2 activity in multiple myeloma cells. Cell Communication and Signaling 21, 25. https://doi.org/10.1186/s12964-022-01033-9

Rabie, E.M., Zhang, S.X., Dunn, C.E., Nelson, C.M., 2021. Substratum stiffness signals through integrin-linked kinase and β1-integrin to regulate midbody proteins and abscission during EMT. MBoC 32, 1664–1676. https://doi.org/10.1091/mbc.E21-02-0072

Radhakrishnan, K., Luu, M., Iaria, J., Sutherland, J.M., McLaughlin, E.A., Zhu, H.-J., Loveland, K.L., 2023. Activin and BMP Signalling in Human Testicular Cancer Cell Lines, and a Role for the Nucleocytoplasmic Transport Protein Importin-5 in Their Crosstalk. Cells 12, 1000. https://doi.org/10.3390/cells12071000

Radler, M.R., Liu, X., Peng, M., Doyle, B., Toyo-Oka, K., Spiliotis, E.T., 2023. Pyramidal neuron morphogenesis requires a septin network that stabilizes filopodia and suppresses lamellipodia during neurite initiation. Current Biology 33, 434-448.e8. https://doi.org/10.1016/j.cub.2022.11.043

Radler, M.R., Spiliotis, E.T., 2022. Right place, right time - spatial guidance of neuronal morphogenesis by septin GTPases. Curr Opin Neurobiol 75, 102557. https://doi.org/10.1016/j.conb.2022.102557

Ráduly, Z., Szabó, L., Dienes, B., Szentesi, P., Bana, Á.V., Hajdú, T., Kókai, E., Hegedűs, C., Csernoch, L., Gönczi, M., 2023. Migration of Myogenic Cells Is Highly Influenced by Cytoskeletal Septin7. Cells 12, 1825. https://doi.org/10.3390/cells12141825

Rahman, F.A., Quadrilatero, J., 2023a. Mitochondrial Apoptotic Signaling Involvement in Remodeling During Myogenesis and Skeletal Muscle Atrophy. Semin Cell Dev Biol 143, 66–74. https://doi.org/10.1016/j.semcdb.2022.01.011

Rahman, F.A., Quadrilatero, J., 2023b. Emerging role of mitophagy in myoblast differentiation and skeletal muscle remodeling. Seminars in Cell & Developmental Biology, Special Issue: Mitochondria: Key Modulators of Skeletal Muscle Remodeling 143, 54–65. https://doi.org/10.1016/j.semcdb.2021.11.026

Rahman, F.A., Quadrilatero, J., 2021. Mitochondrial network remodeling: an important feature of myogenesis and skeletal muscle regeneration. Cell. Mol. Life Sci. 78, 4653–4675. https://doi.org/10.1007/s00018-021-03807-9

Rajan, S., Kudryashov, D.S., Reisler, E., 2023. Actin Bundles Dynamics and Architecture. Biomolecules 13, 450. https://doi.org/10.3390/biom13030450

Ran, F.A., Hsu, P.D., Wright, J., Agarwala, V., Scott, D.A., Zhang, F., 2013. Genome engineering using the CRISPR-Cas9 system. Nat Protoc 8, 2281–2308. https://doi.org/10.1038/nprot.2013.143

Randrianarison-Huetz, V., Papaefthymiou, A., Herledan, G., Noviello, C., Faradova, U., Collard, L., Pincini, A., Schol, E., Decaux, J.F., Maire, P., Vassilopoulos, S., Sotiropoulos, A., 2017. Srf controls satellite cell fusion through the maintenance of actin architecture. Journal of Cell Biology 217, 685–700. https://doi.org/10.1083/jcb.201705130

Rao, V.K., Ow, J.R., Shankar, S.R., Bharathy, N., Manikandan, J., Wang, Y., Taneja, R., 2016. G9a promotes proliferation and inhibits cell cycle exit during myogenic differentiation. Nucleic Acids Res 44, 8129–8143. https://doi.org/10.1093/nar/gkw483

Rebbapragada, A., Benchabane, H., Wrana, J.L., Celeste, A.J., Attisano, L., 2003. Myostatin Signals through a Transforming Growth Factor β-Like Signaling Pathway To Block Adipogenesis. Molecular and Cellular Biology 23, 7230–7242. https://doi.org/10.1128/MCB.23.20.7230-7242.2003

Redwine, W.B., DeSantis, M.E., Hollyer, I., Htet, Z.M., Tran, P.T., Swanson, S.K., Florens, L., Washburn, M.P., Reck-Peterson, S.L., 2017. The human cytoplasmic dynein interactome reveals novel activators of motility. eLife 6, e28257. https://doi.org/10.7554/eLife.28257

Reingewertz, T.H., Shalev, D.E., Sukenik, S., Blatt, O., Rotem-Bamberger, S., Lebendiker, M., Larisch, S., Friedler, A., 2011. Mechanism of the Interaction between the Intrinsically Disordered C-Terminus of the Pro-Apoptotic ARTS Protein and the Bir3 Domain of XIAP. PLOS ONE 6, e24655. https://doi.org/10.1371/journal.pone.0024655

Relaix, F., Bencze, M., Borok, M.J., Der Vartanian, A., Gattazzo, F., Mademtzoglou, D., Perez-Diaz, S., Prola, A., Reyes-Fernandez, P.C., Rotini, A., Taglietti, 2021. Perspectives on skeletal muscle stem cells. Nat Commun 12, 692. https://doi.org/10.1038/s41467-020-20760-6

Relaix, F., Rocancourt, D., Mansouri, A., Buckingham, M., 2005. A Pax3/Pax7-dependent population of skeletal muscle progenitor cells. Nature 435, 948–953. https://doi.org/10.1038/nature03594

Relaix, F., Zammit, P.S., 2012. Satellite cells are essential for skeletal muscle regeneration: the cell on the edge returns centre stage. Development 139, 2845–2856. https://doi.org/10.1242/dev.069088

Remels, A.H.V., Langen, R.C.J., Schrauwen, P., Schaart, G., Schols, A.M.W.J., Gosker, H.R., 2010. Regulation of mitochondrial biogenesis during myogenesis. Molecular and Cellular Endocrinology 315, 113–120. https://doi.org/10.1016/j.mce.2009.09.029

Renshaw, M.J., Liu, J., Lavoie, B.D., Wilde, A., 2014. Anillin-dependent organization of septin filaments promotes intercellular bridge elongation and Chmp4B targeting to the abscission site. Open Biology 4, 130190. https://doi.org/10.1098/rsob.130190

Reshef, R., Maroto, M., Lassar, A.B., 1998. Regulation of dorsal somitic cell fates: BMPs and Noggin control the timing and pattern of myogenic regulator expression. Genes Dev. 12, 290–303.

Ribet, D., Boscaini, S., Cauvin, C., Siguier, M., Mostowy, S., Echard, A., Cossart, P., 2017. SUMOylation of human septins is critical for septin filament bundling and cytokinesis. Journal of Cell Biology 216, 4041–4052. https://doi.org/10.1083/jcb.201703096

Richardson, B.E., Beckett, K., Nowak, S.J., Baylies, M.K., 2007. SCAR/WAVE and Arp2/3 are crucial for cytoskeletal remodeling at the site of myoblast fusion. Development 134, 4357–4367. https://doi.org/10.1242/dev.010678

Ridley, A.J., Hall, A., 1992. The small GTP-binding protein rho regulates the assembly of focal adhesions and actin stress fibers in response to growth factors. Cell 70, 389–399. https://doi.org/10.1016/0092-8674(92)90163-7

Ridley, A.J., Paterson, H.F., Johnston, C.L., Diekmann, D., Hall, A., 1992. The small GTP-binding protein rac regulates growth factor-induced membrane ruffling. Cell 70, 401–410. https://doi.org/10.1016/0092-8674(92)90164-8

Rivero, F., Cvrcková, F., 2013. Origins and Evolution of the Actin Cytoskeleton, in: Madame Curie Bioscience Database [Internet]. Landes Bioscience.

Rochat, A., Fernandez, A., Vandromme, M., Molès, J.-P., Bouschet, T., Carnac, G., Lamb, N.J.C., 2004. Insulin and wnt1 pathways cooperate to induce reserve cell activation in differentiation and myotube hypertrophy. Mol Biol Cell 15, 4544–4555. https://doi.org/10.1091/mbc.e03-11-0816

Rocheteau, P., Gayraud-Morel, B., Siegl-Cachedenier, I., Blasco, M.A., Tajbakhsh, S., 2012. A subpopulation of adult skeletal muscle stem cells retains all template DNA strands after cell division. Cell 148, 112–125. https://doi.org/10.1016/j.cell.2011.11.049

Rodgers, B.D., Ward, C.W., 2021. Myostatin/Activin Receptor Ligands in Muscle and the Development Status of Attenuating Drugs. Endocr Rev 43, 329–365. https://doi.org/10.1210/endrev/bnab030

Rodgers, B.D., Wiedeback, B.D., Hoversten, K.E., Jackson, M.F., Walker, R.G., Thompson, T.B., 2014. Myostatin Stimulates, Not Inihibits, C2C12 Myoblast Proliferation. Endocrinology 155, 670–675. https://doi.org/10.1210/en.2013-2107

Rodríguez-Fdez, S., Bustelo, X.R., 2021. Rho GTPases in Skeletal Muscle Development and Homeostasis. Cells 10, 2984. https://doi.org/10.3390/cells10112984

Roman, W., Martins, J.P., Carvalho, F.A., Voituriez, R., Abella, J.V.G., Santos, N.C., Cadot, B., Way, M., Gomes, E.R., 2017. Myofibril contraction and crosslinking drive nuclear movement to the periphery of skeletal muscle. Nat Cell Biol 19, 1189–1201. https://doi.org/10.1038/ncb3605

Romanazzo, S., Forte, G., Ebara, M., Uto, K., Pagliari, S., Aoyagi, T., Traversa, E., Taniguchi, A., 2012. Substrate stiffness affects skeletal myoblast differentiation in vitro. Sci Technol Adv Mater 13, 064211. https://doi.org/10.1088/1468-6996/13/6/064211

Roostalu, J., Thomas, C., Cade, N.I., Kunzelmann, S., Taylor, I.A., Surrey, T., 2020. The speed of GTP hydrolysis determines GTP cap size and controls microtubule stability. eLife 9, e51992. https://doi.org/10.7554/eLife.51992

Rosa, N., Speelman-Rooms, F., Parys, J.B., Bultynck, G., 2022. Modulation of Ca2+ signaling by antiapoptotic Bcl-2 versus Bcl-xL: From molecular mechanisms to relevance for cancer cell survival. Biochim Biophys Acta Rev Cancer 1877, 188791. https://doi.org/10.1016/j.bbcan.2022.188791

Rudolf, A., Schirwis, E., Giordani, L., Parisi, A., Lepper, C., Taketo, M.M., Le Grand, F., 2016. β-Catenin Activation in Muscle Progenitor Cells Regulates Tissue Repair. Cell Rep 15, 1277–1290. https://doi.org/10.1016/j.celrep.2016.04.022

Ruijtenberg, S., van den Heuvel, S., 2016. Coordinating cell proliferation and differentiation: Antagonism between cell cycle regulators and cell type-specific gene expression. Cell Cycle 15, 196–212. https://doi.org/10.1080/15384101.2015.1120925

Ruppert, R., Hoffmann, E., Sebald, W., 1996. Human bone morphogenetic protein 2 contains a heparin-binding site which modifies its biological activity. Eur J Biochem 237, 295–302. https://doi.org/10.1111/j.1432-1033.1996.0295n.x

Rushton, E., Drysdale, R., Abmayr, S.M., Michelson, A.M., Bate, M., 1995. Mutations in a novel gene, myoblast city, provide evidence in support of the founder cell hypothesis for Drosophila muscle development. Development 121, 1979–1988. https://doi.org/10.1242/dev.121.7.1979

Russell, S.E.H., Hall, P.A., 2011. Septin genomics: a road less travelled 392, 763–767. https://doi.org/10.1515/BC.2011.079

Russo, G., Hümpfer, N., Jaensch, N., Restel, S., Schmied, C., Heyd, F., Lehmann, M., Haucke, V., Ewers, H., Krauss, M., 2024. Septin-associated PIPKIγ splice variants drive centralspindlin association with the midbody via PI(4,5)P2. https://doi.org/10.1101/2024.02.22.581562

Russo, G., Krauss, M., 2021. Septin Remodeling During Mammalian Cytokinesis. Front Cell Dev Biol 9, 768309. https://doi.org/10.3389/fcell.2021.768309

Saclier, M., Lapi, M., Bonfanti, C., Rossi, G., Antonini, S., Messina, G., 2020. The Transcription Factor Nfix Requires RhoA-ROCK1 Dependent Phagocytosis to Mediate Macrophage Skewing during Skeletal Muscle Regeneration. Cells 9, 708. https://doi.org/10.3390/cells9030708

Safaee, H., Bakooshli, M.A., Davoudi, S., Cheng, R.Y., Martowirogo, A.J., Li, E.W., Simmons, C.A., Gilbert, P.M., 2017. Tethered Jagged-1 Synergizes with Culture Substrate Stiffness to Modulate Notch-Induced Myogenic Progenitor Differentiation. Cell Mol Bioeng 10, 501–513. https://doi.org/10.1007/s12195-017-0506-7

Safavian, D., Kim, M.S., Xie, H., El-Zeiry, M., Palander, O., Dai, L., Collins, R.F., Froese, C., Shannon, R., Nagata, K., Trimble, W.S., 2023. Septin-mediated RhoA activation engages the exocyst complex to recruit the cilium transition zone. Journal of Cell Biology 222, e201911062. https://doi.org/10.1083/jcb.201911062

Sakai, D., Kii, I., Nakagawa, K., Matsumoto, H.N., Takahashi, M., Yoshida, S., Hosoya, T., Takakuda, K., Kudo, A., 2011. Remodeling of Actin Cytoskeleton in Mouse Periosteal Cells under Mechanical Loading Induces Periosteal Cell Proliferation during Bone Formation. PLoS One 6, e24847. https://doi.org/10.1371/journal.pone.0024847

Salabi, F., Nazari, M., Chen, Q., Nimal, J., Tong, J., Cao, W.G., 2014. Myostatin knockout using zinc-finger nucleases promotes proliferation of ovine primary satellite cells in vitro. J Biotechnol 192 Pt A, 268–280. https://doi.org/10.1016/j.jbiotec.2014.10.038

Salameh, J., Cantaloube, I., Benoit, B., Poüs, C., Baillet, A., 2021. Cdc42 and its BORG2 and BORG3 effectors control the subcellular localization of septins between actin stress fibers and microtubules. Curr Biol 31, 4088-4103.e5. https://doi.org/10.1016/j.cub.2021.07.004

Salloum, G., Jaafar, L., El-Sibai, M., 2020. Rho A and Rac1: Antagonists moving forward. Tissue and Cell 65, 101364. https://doi.org/10.1016/j.tice.2020.101364

Salmon, M., Zehner, Z.E., 2009. The transcriptional repressor ZBP-89 and the lack of Sp1/Sp3, c-Jun and Stat3 are important for the down-regulation of the vimentin gene during C2C12 myogenesis. Differentiation 77, 492–504. https://doi.org/10.1016/j.diff.2008.12.005

Salomoni, P., Calegari, F., 2010. Cell cycle control of mammalian neural stem cells: putting a speed limit on G1. Trends in Cell Biology 20, 233–243. https://doi.org/10.1016/j.tcb.2010.01.006

Salucci, S., Baldassarri, V., Falcieri, E., Burattini, S., 2015. α-Actinin involvement in Z-disk assembly during skeletal muscle C2C12 cells in vitro differentiation. Micron 68, 47–53. https://doi.org/10.1016/j.micron.2014.08.010

Salucci, S., Sabrina Burattini, Valentina Baldassarri, Michela Battistelli, Barbara Canonico, Aurelio Valmori, Stefano Papa, Elisabetta Falcier, first, 2013. The peculiar apoptotic behavior of skeletal muscle cells. Histology and Histopathology 1073–1087. https://doi.org/10.14670/HH-28.1073

Sampath, Srihari C., Sampath, Srinath C., Millay, D.P., 2018. Myoblast fusion confusion: the resolution begins. Skeletal Muscle 8, 3. https://doi.org/10.1186/s13395-017-0149-3

Sanders, S.L., Field, C.M., 1994. Cell Division: Septins in common? Current Biology 4, 907–910. https://doi.org/10.1016/S0960-9822(00)00201-3

Sandri, M., Carraro, U., 1999. Apoptosis of skeletal muscles during development and disease. The International Journal of Biochemistry & Cell Biology 31, 1373–1390. https://doi.org/10.1016/S1357-2725(99)00063-1

Sartori, R., Gregorevic, P., Sandri, M., 2014. TGFβ and BMP signaling in skeletal muscle: potential significance for muscle-related disease. Trends in Endocrinology & Metabolism 25, 464–471. https://doi.org/10.1016/j.tem.2014.06.002

Sartori, R., Schirwis, E., Blaauw, B., Bortolanza, S., Zhao, J., Enzo, E., Stantzou, A., Mouisel, E., Toniolo, L., Ferry, A., Stricker, S., Goldberg, A.L., Dupont, S., Piccolo, S., Amthor, H., Sandri, M., 2013. BMP signaling controls muscle mass. Nat Genet 45, 1309–1318. https://doi.org/10.1038/ng.2772

Schaum, N., Karkanias, J., Neff, N.F., May, A.P., Quake, S.R., Wyss-Coray, T., Darmanis, S., Batson, J., Botvinnik, O., Chen, M.B., Chen, S., Green, F., Jones, R.C., Maynard, A., Penland, L., Pisco, A.O., Sit, R.V., Stanley, G.M., Webber, J.T., Zanini, F., Baghel, A.S., Bakerman, I., Bansal, I., Berdnik, D., Bilen, B., Brownfield, D., Cain, C., Chen, M.B., Chen, S., Cho, M., Cirolia, G., Conley, S.D., Darmanis, S., Demers, A., Demir, K., de Morree, A., Divita, T., du Bois, H., Dulgeroff, L.B.T., Ebadi, H., Espinoza, F.H., Fish, M., Gan, Q., George, B.M., Gillich, A., Green, F., Genetiano, G., Gu, X., Gulati, G.S., Hang, Y., Hosseinzadeh, S., Huang, A., Iram, T., Isobe, T., Ives, F., Jones, R.C., Kao, K.S., Karnam, G., Kershner, A.M., Kiss, B.M., Kong, W., Kumar, M.E., Lam, J.Y., Lee, D.P., Lee, S.E., Li, G., Li, Q., Liu, L., Lo, A., Lu, W.-J., Manjunath, A., May, A.P., May, K.L., May, O.L., Maynard, A., McKay, M., Metzger, R.J., Mignardi, M., Min, D., Nabhan, A.N., Neff, N.F., Ng, K.M., Noh, J., Patkar, R., Peng, W.C., Penland, L., Puccinelli, R., Rulifson, E.J., Schaum, N., Sikandar, S.S., Sinha, R., Sit, R.V., Szade, K., Tan, W., Tato, C., Tellez, K., Travaglini, K.J., Tropini, C., Waldburger, L., van Weele, L.J., Wosczyna, M.N., Xiang, J., Xue, S., Youngyunpipatkul, J., Zanini, F., Zardeneta, M.E., Zhang, F., Zhou, L., Bansal, I., Chen, S., Cho, M., Cirolia, G., Darmanis, S., Demers, A., Divita, T., Ebadi, H., Genetiano, G., Green, F.,

Hosseinzadeh, S., Ives, F., Lo, A., May, A.P., Maynard, A., McKay, M., Neff, N.F., Penland, L., Sit, R.V., Tan, W., Waldburger, L., Youngyunpipatkul, J., Batson, J., Botvinnik, O., Castro, P., Croote, D., Darmanis, S., DeRisi, J.L., Karkanias, J., Pisco, A.O., Stanley, G.M., Webber, J.T., Zanini, F., Baghel, A.S., Bakerman, I., Batson, J., Bilen, B., Botvinnik, O., Brownfield, D., Chen, M.B., Darmanis, S., Demir, K., de Morree, A., Ebadi, H., Espinoza, F.H., Fish, M., Gan, Q., George, B.M., Gillich, A., Gu, X., Gulati, G.S., Hang, Y., Huang, A., Iram, T., Isobe, T., Karnam, G., Kershner, A.M., Kiss, B.M., Kong, W., Kuo, C.S., Lam, J.Y., Lehallier, B., Li, G., Li, Q., Liu, L., Lu, W.-J., Min, D., Nabhan, A.N., Ng, K.M., Nguyen, P.K., Patkar, R., Peng, W.C., Penland, L., Rulifson, E.J., Schaum, N., Sikandar, S.S., Sinha, R., Szade, K., Tan, S.Y., Tellez, K., Travaglini, K.J., Tropini, C., van Weele, L.J., Wang, B.M., Wosczyna, M.N., Xiang, J., Yousef, H., Zhou, L., Batson, J., Botvinnik, O., Chen, S., Darmanis, S., Green, F., May, A.P., Maynard, A., Pisco, A.O., Quake, S.R., Schaum, N., Stanley, G.M., Webber, J.T., Wyss-Coray, T., Zanini, F., Beachy, P.A., Chan, C.K.F., de Morree, A., George, B.M., Gulati, G.S., Hang, Y., Huang, K.C., Iram, T., Isobe, T., Kershner, A.M., Kiss, B.M., Kong, W., Li, G., Li, Q., Liu, L., Lu, W.-J., Nabhan, A.N., Ng, K.M., Nguyen, P.K., Peng, W.C., Rulifson, E.J., Schaum, N., Sikandar, S.S., Sinha, R., Szade, K., Travaglini, K.J., Tropini, C., Wang, B.M., Weinberg, K., Wosczyna, M.N., Wu, S.M., Yousef, H., Barres, B.A., Beachy, P.A., Chan, C.K.F., Clarke, M.F., Darmanis, S., Huang, K.C., Karkanias, J., Kim, S.K., Krasnow, M.A., Kumar, M.E., Kuo, C.S., May, A.P., Metzger, R.J., Neff, N.F., Nusse, R., Nguyen, P.K., Rando, T.A., Sonnenburg, J., Wang, B.M., Weinberg, K., Weissman, I.L., Wu, S.M., Quake, S.R., Wyss-Coray, T., The Tabula Muris Consortium, Overall coordination, Logistical coordination, Organ collection and processing, Library preparation and sequencing, Computational data analysis, Cell type annotation, Writing group, Supplemental text writing group, Principal investigators, 2018. Single-cell transcriptomics of 20 mouse organs creates a Tabula Muris. Nature 562, 367–372. https://doi.org/10.1038/s41586-018-0590-4

Schejter, E.D., 2016. Myoblast fusion: Experimental systems and cellular mechanisms. Seminars in Cell & Developmental Biology, The Rhomboid Superfamily in Development and Disease 60, 112–120. https://doi.org/10.1016/j.semcdb.2016.07.016

Schiaffino, S., Dyar, K.A., Ciciliot, S., Blaauw, B., Sandri, M., 2013. Mechanisms regulating skeletal muscle growth and atrophy. FEBS J 280, 4294–4314. https://doi.org/10.1111/febs.12253

Schiaffino, S., Reggiani, C., 2011. Fiber Types in Mammalian Skeletal Muscles. Physiological Reviews 91, 1447–1531. https://doi.org/10.1152/physrev.00031.2010

Schmidt, K., Nichols, B.J., 2004. Functional interdependence between septin and actin cytoskeleton. BMC Cell Biology 5, 43. https://doi.org/10.1186/1471-2121-5-43

Schmidt, M., Schüler, S.C., Hüttner, S.S., von Eyss, B., von Maltzahn, J., 2019. Adult stem cells at work: regenerating skeletal muscle. Cell. Mol. Life Sci. 76, 2559–2570. https://doi.org/10.1007/s00018-019-03093-6

Schöneich, C., Dremina, E., Galeva, N., Sharov, V., 2014. Apoptosis in differentiating C2C12 muscle cells selectively targets Bcl-2-deficient myotubes. Apoptosis 19, 42–57. https://doi.org/10.1007/s10495-013-0922-7

Schröter, R.H., Lier, S., Holz, A., Bogdan, S., Klämbt, C., Beck, L., Renkawitz-Pohl, R., 2004. kette and blown fuse interact genetically during the second fusion step of myogenesis in Drosophila. Development 131, 4501–4509. https://doi.org/10.1242/dev.01309

Schuster, T., Geiger, H., 2021. Septins in Stem Cells. Front Cell Dev Biol 9, 801507. https://doi.org/10.3389/fcell.2021.801507

Seale, P., Sabourin, L.A., Girgis-Gabardo, A., Mansouri, A., Gruss, P., Rudnicki, M.A., 2000. Pax7 is required for the specification of myogenic satellite cells. Cell 102, 777–786. https://doi.org/10.1016/s0092-8674(00)00066-0

Seetharaman, S., Vianay, B., Roca, V., Farrugia, A.J., De Pascalis, C., Boëda, B., Dingli, F., Loew, D., Vassilopoulos, S., Bershadsky, A., Théry, M., Etienne-Manneville, S., 2022. Microtubules tune mechanosensitive cell responses. Nat. Mater. 21, 366–377. https://doi.org/10.1038/s41563-021-01108-x

Seiliez, I., Sabin, N., Gabillard, J.-C., 2012. Myostatin inhibits proliferation but not differentiation of trout myoblasts. Mol Cell Endocrinol 351, 220–226. https://doi.org/10.1016/j.mce.2011.12.011

Sejersen, T., Lendahl, U., 1993. Transient expression of the intermediate filament nestin during skeletal muscle development. Journal of Cell Science 106, 1291–1300. https://doi.org/10.1242/jcs.106.4.1291

Selvaraj, A., Prywes, R., 2003. Megakaryoblastic Leukemia-1/2, a Transcriptional Co-activator of Serum Response Factor, Is Required for Skeletal Myogenic Differentiation *. Journal of Biological Chemistry 278, 41977–41987. https://doi.org/10.1074/jbc.M305679200

Sens, K.L., Zhang, S., Jin, P., Duan, R., Zhang, G., Luo, F., Parachini, L., Chen, E.H., 2010. An invasive podosome-like structure promotes fusion pore formation during myoblast fusion. Journal of Cell Biology 191, 1013–1027. https://doi.org/10.1083/jcb.201006006

Seyer, P., Grandemange, S., Rochard, P., Busson, M., Pessemesse, L., Casas, F., Cabello, G., Wrutniak-Cabello, C., 2011. P43-dependent mitochondrial activity regulates myoblast differentiation and slow myosin isoform expression by control of Calcineurin expression. Exp Cell Res 317, 2059–2071. https://doi.org/10.1016/j.yexcr.2011.05.020

Shah, K., Kazi, J.U., 2022. Phosphorylation-Dependent Regulation of WNT/Beta-Catenin Signaling. Frontiers in Oncology 12.

Shahini, A., Vydiam, K., Choudhury, D., Rajabian, N., Nguyen, T., Lei, P., Andreadis, S.T., 2018. Efficient and high yield isolation of myoblasts from skeletal muscle. Stem Cell Research 30, 122–129. https://doi.org/10.1016/j.scr.2018.05.017

Sharma, K., Menon, M.B., 2023. Decoding post-translational modifications of mammalian septins. Cytoskeleton 80, 169–181. https://doi.org/10.1002/cm.21747

Sheffield, P.J., Oliver, C.J., Kremer, B.E., Sheng, S., Shao, Z., Macara, I.G., 2003. Borg/Septin Interactions and the Assembly of Mammalian Septin Heterodimers, Trimers, and Filaments*. Journal of Biological Chemistry 278, 3483–3488. https://doi.org/10.1074/jbc.M209701200

Shindo, A., Wallingford, J.B., 2014. PCP and Septins Compartmentalize Cortical Actomyosin to Direct Collective Cell Movement. Science 343, 649–652. https://doi.org/10.1126/science.1243126

Shinin, V., Gayraud-Morel, B., Gomès, D., Tajbakhsh, S., 2006. Asymmetric division and cosegregation of template DNA strands in adult muscle satellite cells. Nat Cell Biol 8, 677–682. https://doi.org/10.1038/ncb1425

Shiu, J.-Y., Aires, L., Lin, Z., Vogel, V., 2018. Nanopillar force measurements reveal actin-cap-mediated YAP mechanotransduction. Nat Cell Biol 20, 262–271. https://doi.org/10.1038/s41556-017-0030-y

Shuman, B., Momany, M., 2022. Septins From Protists to People. Frontiers in Cell and Developmental Biology 9.

Siegel, A.L., Atchison, K., Fisher, K.E., Davis, G.E., Cornelison, D., 2009. 3D Timelapse Analysis of Muscle Satellite Cell Motility. Stem Cells 27, 2527–2538. https://doi.org/10.1002/stem.178

Silver, J.S., Günay, K.A., Cutler, A.A., Vogler, T.O., Brown, T.E., Pawlikowski, B.T., Bednarski, O.J., Bannister, K.L., Rogowski, C.J., Mckay, A.G., DelRio, F.W., Olwin, B.B., Anseth, K.S., 2021. Injury-mediated stiffening persistently activates muscle stem cells through YAP and TAZ mechanotransduction. Sci Adv 7, eabe4501. https://doi.org/10.1126/sciadv.abe4501

Simi, A.K., Anlaş, A.A., Stallings-Mann, M., Zhang, S., Hsia, T., Cichon, M., Radisky, D.C., Nelson, C.M., 2018. A Soft Microenvironment Protects from Failure of Midbody Abscission and Multinucleation Downstream of the EMT-Promoting Transcription Factor Snail. Cancer Research 78, 2277–2289. https://doi.org/10.1158/0008-5472.CAN-17-2899

Simic, P., Culej, J.B., Orlic, I., Grgurevic, L., Draca, N., Spaventi, R., Vukicevic, S., 2006. Systemically administered bone morphogenetic protein-6 restores bone in aged ovariectomized rats by increasing bone formation and suppressing bone resorption. J Biol Chem 281, 25509–25521. https://doi.org/10.1074/jbc.M513276200

Simiczyjew, A., Mazur, A.J., Popow-Woźniak, A., Malicka-Błaszkiewicz, M., Nowak, D., 2014. Effect of overexpression of β- and γ-actin isoforms on actin cytoskeleton organization and migration

of human colon cancer cells. Histochem Cell Biol 142, 307–322. https://doi.org/10.1007/s00418-014-1199-9

Sin, J., Andres, A.M., Taylor, D.J.R., Weston, T., Hiraumi, Y., Stotland, A., Kim, B.J., Huang, C., Doran, K.S., Gottlieb, R.A., 2016. Mitophagy is required for mitochondrial biogenesis and myogenic differentiation of C2C12 myoblasts. Autophagy 12, 369–380. https://doi.org/10.1080/15548627.2015.1115172

Sirajuddin, M., Farkasovsky, M., Hauer, F., Kühlmann, D., Macara, I.G., Weyand, M., Stark, H., Wittinghofer, A., 2007. Structural insight into filament formation by mammalian septins. Nature 449, 311–315. https://doi.org/10.1038/nature06052

Sirajuddin, M., Farkasovsky, M., Zent, E., Wittinghofer, A., 2009. GTP-induced conformational changes in septins and implications for function. Proceedings of the National Academy of Sciences 106, 16592–16597. https://doi.org/10.1073/pnas.0902858106

Sirianni, A., Krokowski, S., Lobato-Márquez, D., Buranyi, S., Pfanzelter, J., Galea, D., Willis, A., Culley, S., Henriques, R., Larrouy-Maumus, G., Hollinshead, M., Sancho-Shimizu, V., Way, M., Mostowy, S., 2016. Mitochondria mediate septin cage assembly to promote autophagy of Shigella. EMBO Rep 17, 1029–1043. https://doi.org/10.15252/embr.201541832

Slowikowski, K., Schep, A., Hughes, S., Dang, T.K., Lukauskas, S., Irisson, J.-O., Kamvar, Z.N., Ryan, T., Christophe, D., Hiroaki, Y., Gramme, P., Abdol, A.M., Barrett, M., Cannoodt, R., Krassowski, M., Chirico, M., Aphalo, P., 2023. ggrepel: Automatically Position Non-Overlapping Text Labels with “ggplot2.”

Smith, C., Dolat, L., Angelis, D., Forgacs, E., Spiliotis, E.T., Galkin, V.E., 2015. Septin 9 Exhibits Polymorphic Binding to F-Actin and Inhibits Myosin and Cofilin Activity. J Mol Biol 427, 3273–3284. https://doi.org/10.1016/j.jmb.2015.07.026

Smith, M.I., Huang, Y.Y., Deshmukh, M., 2009. Skeletal Muscle Differentiation Evokes Endogenous XIAP to Restrict the Apoptotic Pathway. PLOS ONE 4, e5097. https://doi.org/10.1371/journal.pone.0005097

Sobczak, M., Chumak, V., Pomorski, P., Wojtera, E., Majewski, Ł., Nowak, J., Yamauchi, J., Rędowicz, M.J., 2016. Interaction of myosin VI and its binding partner DOCK7 plays an important role in NGF-stimulated protrusion formation in PC12 cells. Biochimica et Biophysica Acta (BBA) - Molecular Cell Research 1863, 1589–1600. https://doi.org/10.1016/j.bbamcr.2016.03.020

Soldani, C., Scovassi, A.I., 2002. Poly(ADP-ribose) polymerase-1 cleavage during apoptosis: an update. Apoptosis 7, 321–328. https://doi.org/10.1023/a:1016119328968

Soleimani, V.D., Yin, H., Jahani-Asl, A., Ming, H., Kockx, C.E.M., van Ijcken, W.F.J., Grosveld, F., Rudnicki, M.A., 2012. Snail Regulates MyoD Binding-Site Occupancy to Direct Enhancer Switching and Differentiation-Specific Transcription in Myogenesis. Mol Cell 47, 457–468. https://doi.org/10.1016/j.molcel.2012.05.046

Song, K., Gras, C., Capin, G., Gimber, N., Lehmann, M., Mohd, S., Puchkov, D., Rödiger, M., Wilhelmi, I., Daumke, O., Schmoranzer, J., Schürmann, A., Krauss, M., 2019. A SEPT1-based scaffold is required for Golgi integrity and function. Journal of Cell Science 132, jcs225557. https://doi.org/10.1242/jcs.225557

Song, M.J., Brady-Kalnay, S.M., McBride, S.H., Phillips-Mason, P., Dean, D., Tate, M.L.K., 2012. Mapping the Mechanome of Live Stem Cells Using a Novel Method to Measure Local Strain Fields In Situ at the Fluid-Cell Interface. PLOS ONE 7, e43601. https://doi.org/10.1371/journal.pone.0043601

Song, R., Zhao, S., Xu, Yue, Hu, J., Ke, S., Li, F., Tian, G., Zheng, X., Li, J., Gu, L., Xu, Yao, 2021. MRTF-A regulates myoblast commitment to differentiation by targeting PAX7 during muscle regeneration. J Cell Mol Med 25, 8645–8661. https://doi.org/10.1111/jcmm.16820

Sonowal, H., Kumar, A., Bhattacharyya, J., Gogoi, P.K., Jaganathan, B.G., 2013. Inhibition of actin polymerization decreases osteogeneic differentiation of mesenchymal stem cells through p38 MAPK pathway. Journal of Biomedical Science 20, 71. https://doi.org/10.1186/1423-0127-20-71

Sordella, R., Jiang, W., Chen, G.-C., Curto, M., Settleman, J., 2003. Modulation of Rho GTPase Signaling Regulates a Switch between Adipogenesis and Myogenesis. Cell 113, 147–158. https://doi.org/10.1016/S0092-8674(03)00271-X

Soroor, F., Kim, M.S., Palander, O., Balachandran, Y., Collins, R.F., Benlekbir, S., Rubinstein, J.L., Trimble, W.S., 2021. Revised subunit order of mammalian septin complexes explains their in vitro polymerization properties. MBoC 32, 289–300. https://doi.org/10.1091/mbc.E20-06-0398

Sotiropoulos, A., Gineitis, D., Copeland, J., Treisman, R., 1999. Signal-regulated activation of serum response factor is mediated by changes in actin dynamics. Cell 98, 159–169. https://doi.org/10.1016/s0092-8674(00)81011-9

Sousa-Victor, P., Gutarra, S., García-Prat, L., Rodriguez-Ubreva, J., Ortet, L., Ruiz-Bonilla, V., Jardí, M., Ballestar, E., González, S., Serrano, A.L., Perdiguero, E., Muñoz-Cánoves, P., 2014. Geriatric muscle stem cells switch reversible quiescence into senescence. Nature 506, 316–321. https://doi.org/10.1038/nature13013

Spiliotis, E.T., 2018. Spatial effects − site-specific regulation of actin and microtubule organization by septin GTPases. Journal of Cell Science 131, jcs207555. https://doi.org/10.1242/jcs.207555

Spiliotis, E.T., Hunt, S.J., Hu, Q., Kinoshita, M., Nelson, W.J., 2008. Epithelial polarity requires septin coupling of vesicle transport to polyglutamylated microtubules. Journal of Cell Biology 180, 295–303. https://doi.org/10.1083/jcb.200710039

Spiliotis, E.T., Kesisova, I.A., 2021. Spatial regulation of microtubule-dependent transport by septin GTPases. Trends in Cell Biology 31, 979–993. https://doi.org/10.1016/j.tcb.2021.06.004

Spiliotis, E.T., McMurray, M.A., 2020. Masters of asymmetry – lessons and perspectives from 50 years of septins. MBoC 31, 2289–2297. https://doi.org/10.1091/mbc.E19-11-0648

Spiliotis, E.T., Nakos, K., 2021. Cellular functions of actin- and microtubule-associated septins. Curr Biol 31, R651–R666. https://doi.org/10.1016/j.cub.2021.03.064

Städler, B., Blättler, T.M., Franco-Obregón, A., 2010. Time-lapse imaging of in vitro myogenesis using atomic force microscopy. J Microsc 237, 63–69. https://doi.org/10.1111/j.1365-2818.2009.03302.x

Stallaert, W., Kedziora, K.M., Chao, H.X., Purvis, J.E., 2019. Bistable switches as integrators and actuators during cell cycle progression. FEBS Letters 593, 2805–2816. https://doi.org/10.1002/1873-3468.13628

Stavenschi, E., Hoey, D.A., 2019. Pressure-induced mesenchymal stem cell osteogenesis is dependent on intermediate filament remodeling. The FASEB Journal 33, 4178–4187. https://doi.org/10.1096/fj.201801474RR

Steelman, C.A., Recknor, J.C., Nettleton, D., Reecy, J.M., 2006. Transcriptional profiling of myostatin-knockout mice implicates Wnt signaling in postnatal skeletal muscle growth and hypertrophy. FASEB J 20, 580–582. https://doi.org/10.1096/fj.05-5125fje

Sun, C., De Mello, V., Mohamed, A., Ortuste Quiroga, H.P., Garcia-Munoz, A., Al Bloshi, A., Tremblay, A.M., von Kriegsheim, A., Collie-Duguid, E., Vargesson, N., Matallanas, D., Wackerhage, H., Zammit, P.S., 2017. Common and Distinctive Functions of the Hippo Effectors Taz and Yap in Skeletal Muscle Stem Cell Function. Stem Cells 35, 1958–1972. https://doi.org/10.1002/stem.2652

Sun, L., Chen, F., Shi, W., Qi, L., Zhao, Z., Zhang, J., 2014. Prognostic impact of TAZ and β-catenin expression in adenocarcinoma of the esophagogastric junction. Diagn Pathol 9, 125. https://doi.org/10.1186/1746-1596-9-125

Surka, M.C., Tsang, C.W., Trimble, W.S., 2002. The Mammalian Septin MSF Localizes with Microtubules and Is Required for Completion of Cytokinesis. MBoC 13, 3532–3545. https://doi.org/10.1091/mbc.e02-01-0042

Svitkina, T., 2018. The Actin Cytoskeleton and Actin-Based Motility. Cold Spring Harb Perspect Biol 10, a018267. https://doi.org/10.1101/cshperspect.a018267

Swailes, N.T., Colegrave, M., Knight, P.J., Peckham, M., 2006. Non-muscle myosins 2A and 2B drive changes in cell morphology that occur as myoblasts align and fuse. Journal of Cell Science 119, 3561–3570. https://doi.org/10.1242/jcs.03096

Swailes, N.T., Knight, P.J., Peckham, M., 2004. Actin filament organization in aligned prefusion myoblasts. J Anat 205, 381–391. https://doi.org/10.1111/j.0021-8782.2004.00341.x

Swaminathan, V., Waterman, C.M., 2016. The molecular clutch model for mechanotransduction evolves. Nat Cell Biol 18, 459–461. https://doi.org/10.1038/ncb3350

Szabo, K., Varga, D., Vegh, A.G., Liu, N., Xiao, X., Xu, L., Dux, L., Erdelyi, M., Rovo, L., Keller-Pinter, A., 2022. Syndecan-4 affects myogenesis via Rac1-mediated actin remodeling and exhibits copy-number amplification and increased expression in human rhabdomyosarcoma tumors. Cell. Mol. Life Sci. 79, 122. https://doi.org/10.1007/s00018-021-04121-0

Szabó, L., Telek, A., Fodor, J., Dobrosi, N., Dócs, K., Hegyi, Z., Gönczi, M., Csernoch, L., Dienes, B., 2023. Reduced Expression of Septin7 Hinders Skeletal Muscle Regeneration. International Journal of Molecular Sciences 24, 13536. https://doi.org/10.3390/ijms241713536

Szilágyi, S.S., Burdzinski, W., Jatzlau, J., Ehrlich, M., Knaus, P., Henis, Y.I., 2024. The Activation of the Fibrodysplasia Ossificans Progressiva-Inducing ALK2-R206H Mutant Depends on the Distinct Homo-Oligomerization Patterns of ACVR2B and ACVR2A. Cells 13, 221. https://doi.org/10.3390/cells13030221

Szuba, A., Bano, F., Castro-Linares, G., Iv, F., Mavrakis, M., Richter, R.P., Bertin, A., Koenderink, G.H., 2021. Membrane binding controls ordered self-assembly of animal septins. eLife 10, e63349. https://doi.org/10.7554/eLife.63349

Taglietti, V., Angelini, G., Mura, G., Bonfanti, C., Caruso, E., Monteverde, S., Le Carrou, G., Tajbakhsh, S., Relaix, F., Messina, G., 2018. RhoA and ERK signalling regulate the expression of the transcription factor Nfix in myogenic cells. Development 145, dev163956. https://doi.org/10.1242/dev.163956

Tajbakhsh, S., 2009. Skeletal muscle stem cells in developmental versus regenerative myogenesis. Journal of Internal Medicine 266, 372–389. https://doi.org/10.1111/j.1365-2796.2009.02158.x

Takahashi, S., Inatome, R., Yamamura, H., Yanagi, S., 2003. Isolation and expression of a novel mitochondrial septin that interacts with CRMP/CRAM in the developing neurones. Genes Cells 8, 81–93. https://doi.org/10.1046/j.1365-2443.2003.00617.x

Takano, H., Komuro, I., Oka, T., Shiojima, I., Hiroi, Y., Mizuno, T., Yazaki, Y., 1998. The Rho family G proteins play a critical role in muscle differentiation. Mol Cell Biol 18, 1580–1589. https://doi.org/10.1128/MCB.18.3.1580

Takata, H., Terada, K., Oka, H., Sunada, Y., Moriguchi, T., Nohno, T., 2007. Involvement of Wnt4 signaling during myogenic proliferation and differentiation of skeletal muscle. Dev Dyn 236, 2800–2807. https://doi.org/10.1002/dvdy.21327

Tanaka-Takiguchi, Y., Kinoshita, M., Takiguchi, K., 2009. Septin-Mediated Uniform Bracing of Phospholipid Membranes. Current Biology 19, 140–145. https://doi.org/10.1016/j.cub.2008.12.030

Tas, R.P., Chazeau, A., Cloin, B.M.C., Lambers, M.L.A., Hoogenraad, C.C., Kapitein, L.C., 2017. Differentiation between Oppositely Oriented Microtubules Controls Polarized Neuronal Transport. Neuron 96, 1264-1271.e5. https://doi.org/10.1016/j.neuron.2017.11.018

Tassin, A.M., Maro, B., Bornens, M., 1985. Fate of microtubule-organizing centers during myogenesis in vitro. Journal of Cell Biology 100, 35–46. https://doi.org/10.1083/jcb.100.1.35

THE GTEX CONSORTIUM, Ardlie, K.G., Deluca, D.S., Segrè, A.V., Sullivan, T.J., Young, T.R., Gelfand, E.T., Trowbridge, C.A., Maller, J.B., Tukiainen, T., Lek, M., Ward, L.D., Kheradpour, P., Iriarte, B., Meng, Y., Palmer, C.D., Esko, T., Winckler, W., Hirschhorn, J.N., Kellis, M., MacArthur, D.G., Getz, G., Shabalin, A.A., Li, G., Zhou, Y.-H., Nobel, A.B., Rusyn, I., Wright, F.A., Lappalainen, T., Ferreira, P.G., Ongen, H., Rivas, M.A., Battle, A., Mostafavi, S., Monlong, J., Sammeth, M., Mele, M., Reverter, F., Goldmann, J.M., Koller, D., Guigó, R., McCarthy, M.I., Dermitzakis, E.T., Gamazon, E.R., Im, H.K., Konkashbaev, A., Nicolae, D.L., Cox, N.J., Flutre, T., Wen, X., Stephens, M., Pritchard, J.K., Tu, Z., Zhang, B., Huang, T., Long, Q., Lin, L., Yang, J., Zhu, J., Liu, J., Brown, A., Mestichelli, B., Tidwell, D., Lo, E., Salvatore, M., Shad, S., Thomas, J.A., Lonsdale, J.T., Moser, M.T., Gillard, B.M., Karasik, E., Ramsey, K., Choi, C., Foster, B.A., Syron, J., Fleming, J., Magazine, H., Hasz, R., Walters, G.D., Bridge, J.P., Miklos, M., Sullivan, S.,

Barker, L.K., Traino, H.M., Mosavel, M., Siminoff, L.A., Valley, D.R., Rohrer, D.C., Jewell, S.D., Branton, P.A., Sobin, L.H., Barcus, M., Qi, L., McLean, J., Hariharan, P., Um, K.S., Wu, S., Tabor, D., Shive, C., Smith, A.M., Buia, S.A., Undale, A.H., Robinson, K.L., Roche, N., Valentino, K.M., Britton, A., Burges, R., Bradbury, D., Hambright, K.W., Seleski, J., Korzeniewski, G.E., Erickson, K., Marcus, Y., Tejada, J., Taherian, M., Lu, C., Basile, M., Mash, D.C., Volpi, S., Struewing, J.P., Temple, G.F., Boyer, J., Colantuoni, D., Little, R., Koester, S., Carithers, L.J., Moore, H.M., Guan, P., Compton, C., Sawyer, S.J., Demchok, J.P., Vaught, J.B., Rabiner, C.A., Lockhart, N.C., Ardlie, K.G., Getz, G., Wright, F.A., Kellis, M., Volpi, S., Dermitzakis, E.T., 2015. The Genotype-Tissue Expression (GTEx) pilot analysis: Multitissue gene regulation in humans. Science 348, 648–660. https://doi.org/10.1126/science.1262110

Thomas, M., Langley, B., Berry, C., Sharma, M., Kirk, S., Bass, J., Kambadur, R., 2000. Myostatin, a Negative Regulator of Muscle Growth, Functions by Inhibiting Myoblast Proliferation*. Journal of Biological Chemistry 275, 40235–40243. https://doi.org/10.1074/jbc.M004356200

Thornberry, N.A., Lazebnik, Y., 1998. Caspases: Enemies Within. Science 281, 1312–1316. https://doi.org/10.1126/science.281.5381.1312

Tierney, M.T., Sacco, A., 2016. Satellite Cell Heterogeneity in Skeletal Muscle Homeostasis. Trends Cell Biol 26, 434–444. https://doi.org/10.1016/j.tcb.2016.02.004

Tintignac, L.A., Leibovitch, M.P., Kitzmann, M., Fernandez, A., Ducommun, B., Meijer, L., Leibovitch, S.A., 2000. Cyclin E–Cdk2 Phosphorylation Promotes Late G1-Phase Degradation of MyoD in Muscle Cells. Experimental Cell Research 259, 300–307. https://doi.org/10.1006/excr.2000.4973

Tixier, V., Bataillé, L., Jagla, K., 2010. Diversification of muscle types: Recent insights from Drosophila. Experimental Cell Research, Special Issue: Myogenesis 316, 3019–3027. https://doi.org/10.1016/j.yexcr.2010.07.013

Tomasso, M.R., Padrick, S.B., 2023. BORG family proteins in physiology and human disease. Cytoskeleton 80, 182–198. https://doi.org/10.1002/cm.21768

Tondeleir, D., Vandamme, D., Vandekerckhove, J., Ampe, C., Lambrechts, A., 2009. Actin isoform expression patterns during mammalian development and in pathology: insights from mouse models. Cell Motil Cytoskeleton 66, 798–815. https://doi.org/10.1002/cm.20350

Tonkin, J., Temmerman, L., Sampson, R.D., Gallego-Colon, E., Barberi, L., Bilbao, D., Schneider, M.D., Musarò, A., Rosenthal, N., 2015. Monocyte/Macrophage-derived IGF-1 Orchestrates Murine Skeletal Muscle Regeneration and Modulates Autocrine Polarization. Mol Ther 23, 1189–1200. https://doi.org/10.1038/mt.2015.66

Tooley, A.J., Gilden, J., Jacobelli, J., Beemiller, P., Trimble, W.S., Kinoshita, M., Krummel, M.F., 2009. Amoeboid T lymphocytes require the septin cytoskeleton for cortical integrity and persistent motility. Nat Cell Biol 11, 17–26. https://doi.org/10.1038/ncb1808

Travaglione, S., Messina, G., Fabbri, A., Falzano, L., Giammarioli, A.M., Grossi, M., Rufini, S., Fiorentini, C., 2005. Cytotoxic necrotizing factor 1 hinders skeletal muscle differentiation in vitro by perturbing the activation/deactivation balance of Rho GTPases. Cell Death Differ 12, 78–86. https://doi.org/10.1038/sj.cdd.4401522

Treiser, M.D., Yang, E.H., Gordonov, S., Cohen, D.M., Androulakis, I.P., Kohn, J., Chen, C.S., Moghe, P.V., 2010. Cytoskeleton-based forecasting of stem cell lineage fates. Proceedings of the National Academy of Sciences 107, 610–615. https://doi.org/10.1073/pnas.0909597107

Trendelenburg, A.U., Meyer, A., Rohner, D., Boyle, J., Hatakeyama, S., Glass, D.J., 2009. Myostatin reduces Akt/TORC1/p70S6K signaling, inhibiting myoblast differentiation and myotube size. Am J Physiol Cell Physiol 296, C1258-1270. https://doi.org/10.1152/ajpcell.00105.2009

Trensz, F., Lucien, F., Couture, V., Söllrald, T., Drouin, G., Rouleau, A.-J., Grandbois, M., Lacraz, G., Grenier, G., 2015. Increased microenvironment stiffness in damaged myofibers promotes myogenic progenitor cell proliferation. Skeletal Muscle 5, 5. https://doi.org/10.1186/s13395-015-0030-1

Trimarchi, J.M., Lees, J.A., 2002. Sibling rivalry in the E2F family. Nat Rev Mol Cell Biol 3, 11–20. https://doi.org/10.1038/nrm714

Troy, A., Cadwallader, A.B., Fedorov, Y., Tyner, K., Tanaka, K.K., Olwin, B.B., 2012. Coordination of satellite cell activation and self-renewal by Par-complex-dependent asymmetric activation of p38α/β MAPK. Cell Stem Cell 11, 541–553. https://doi.org/10.1016/j.stem.2012.05.025

Tumbarello, D.A., Kendrick-Jones, J., Buss, F., 2013. Myosin VI and its cargo adaptors – linking endocytosis and autophagy. Journal of Cell Science 126, 2561. https://doi.org/10.1242/jcs.095554

Tvorogova, A.A., Kovaleva, A.V., Saidova, A.A., 2018. Reorganization of Actin Cytoskeleton and Microtubule Array during the Chondrogenesis of Bovine MSCs. Annual Research & Review in Biology 1–14. https://doi.org/10.9734/ARRB/2018/45687

Tweedie, S., Morrison, K., Charlton, J., Edwards, Y.H., 1991. CAIII a marker for early myogenesis: Analysis of expression in cultured myogenic cells. Somat Cell Mol Genet 17, 215–228. https://doi.org/10.1007/BF01232818

Ugorets, V., Mendez, P.-L., Zagrebin, D., Russo, G., Kerkhoff, Y., Kotsaris, G., Jatzlau, J., Stricker, S., Knaus, P., 2024. Dynamic remodeling of Septin structures fine-tunes myogenic differentiation. iScience 0. https://doi.org/10.1016/j.isci.2024.110630

Urciuolo, A., Urbani, L., Perin, S., Maghsoudlou, P., Scottoni, F., Gjinovci, A., Collins-Hooper, H., Loukogeorgakis, S., Tyraskis, A., Torelli, S., Germinario, E., Fallas, M.E.A., Julia-Vilella, C., Eaton, S., Blaauw, B., Patel, K., De Coppi, P., 2018. Decellularised skeletal muscles allow functional muscle regeneration by promoting host cell migration. Sci Rep 8, 8398. https://doi.org/10.1038/s41598-018-26371-y

Valadares, N.F., d' Muniz Pereira, H., Ulian Araujo, A.P., Garratt, R.C., 2017. Septin structure and filament assembly. Biophys Rev 9, 481–500. https://doi.org/10.1007/s12551-017-0320-4

van den Eijnde, S.M., van den Hoff, M.J.B., Reutelingsperger, C.P.M., van Heerde, W.L., Henfling, M.E.R., Vermeij-Keers, C., Schutte, B., Borgers, M., Ramaekers, F.C.S., 2001. Transient expression of phosphatidylserine at cell-cell contact areas is required for myotube formation. Journal of Cell Science 114, 3631–3642. https://doi.org/10.1242/jcs.114.20.3631

van der Velden, J.L.J., Langen, R.C.J., Kelders, M.C.J.M., Wouters, E.F.M., Janssen-Heininger, Y.M.W., Schols, A.M.W.J., 2006. Inhibition of glycogen synthase kinase-3beta activity is sufficient to stimulate myogenic differentiation. Am J Physiol Cell Physiol 290, C453-462. https://doi.org/10.1152/ajpcell.00068.2005

Van Ngo, H., Robertin, S., Brokatzky, D., Bielecka, M.K., Lobato-Márquez, D., Torraca, V., Mostowy, S., 2023. Septins promote caspase activity and coordinate mitochondrial apoptosis. Cytoskeleton 80, 254–265. https://doi.org/10.1002/cm.21696

Vanslembrouck, B., Ampe, C., van Hengel, J., 2020. Time for rethinking the different β-actin transgenic mouse models? Cytoskeleton 77, 527–543. https://doi.org/10.1002/cm.21647

Vasyutina, E., Martarelli, B., Brakebusch, C., Wende, H., Birchmeier, C., 2009. The small G-proteins Rac1 and Cdc42 are essential for myoblast fusion in the mouse. Proceedings of the National Academy of Sciences 106, 8935–8940. https://doi.org/10.1073/pnas.0902501106

Venters, S.J., Ordahl, C.P., 2005. Asymmetric cell divisions are concentrated in the dermomyotome dorsomedial lip during epaxial primary myotome morphogenesis. Anat Embryol 209, 449–460. https://doi.org/10.1007/s00429-005-0461-2

Verdier-Pinard, P., Salaun, D., Bouguenina, H., Shimada, S., Pophillat, M., Audebert, S., Agavnian, E., Coslet, S., Charafe-Jauffret, E., Tachibana, T., Badache, A., 2017. Septin 9_i2 is downregulated in tumors, impairs cancer cell migration and alters subnuclear actin filaments. Sci Rep 7, 44976. https://doi.org/10.1038/srep44976

Versele, M., Gullbrand, B., Shulewitz, M.J., Cid, V.J., Bahmanyar, S., Chen, R.E., Barth, P., Alber, T., Thorner, J., 2004. Protein–Protein Interactions Governing Septin Heteropentamer Assembly and Septin Filament Organization in Saccharomyces cerevisiae. MBoC 15, 4568–4583. https://doi.org/10.1091/mbc.e04-04-0330

von Maltzahn, J., Bentzinger, C.F., Rudnicki, M.A., 2011. Wnt7a/Fzd7 Signalling Directly Activates the Akt/mTOR Anabolic Growth Pathway in Skeletal Muscle. Nat Cell Biol 14, 186–191. https://doi.org/10.1038/ncb2404

Wada, K.-I., Katsuta, S., Soya, H., 2008. Formation process and fate of the nuclear chain after injury in regenerated myofiber. Anat Rec (Hoboken) 291, 122–128. https://doi.org/10.1002/ar.20626

Wagatsuma, A., Kotake, N., Yamada, S., 2011. Muscle regeneration occurs to coincide with mitochondrial biogenesis. Mol Cell Biochem 349, 139–147. https://doi.org/10.1007/s11010-010-0668-2

Wagatsuma, A., Sakuma, K., 2013. Mitochondria as a Potential Regulator of Myogenesis. The Scientific World Journal 2013, e593267. https://doi.org/10.1155/2013/593267

Walker, R.G., Czepnik, M., Goebel, E.J., McCoy, J.C., Vujic, A., Cho, M., Oh, J., Aykul, S., Walton, K.L., Schang, G., Bernard, D.J., Hinck, A.P., Harrison, C.A., Martinez-Hackert, E., Wagers, A.J., Lee, R.T., Thompson, T.B., 2017. Structural basis for potency differences between GDF8 and GDF11. BMC Biology 15, 19. https://doi.org/10.1186/s12915-017-0350-1

Walsh, K., Perlman, H., 1997. Cell cycle exit upon myogenic differentiation. Curr Opin Genet Dev 7, 597–602. https://doi.org/10.1016/s0959-437x(97)80005-6

Wang, J., Helin, K., Jin, P., Nadal-Ginard, B., 1995. Inhibition of in vitro myogenic differentiation by cellular transcription factor E2F1. Cell Growth Differ 6, 1299–1306.

Wang, J., Q, H., W, T., B, N.-G., 1996. E2F1 inhibition of transcription activation by myogenic basic helix-loop-helix regulators. Journal of cellular biochemistry 62. https://doi.org/10.1002/(SICI)1097-4644(199609)62:3%3C405::AID-JCB10%3E3.0.CO;2-H

Wang, J., Walsh, K., 1996. Resistance to apoptosis conferred by Cdk inhibitors during myocyte differentiation. Science 273, 359–361. https://doi.org/10.1126/science.273.5273.359

Wang, N., Stamenovic, D., 2002. Mechanics of vimentin intermediate filaments. J Muscle Res Cell Motil 23, 535–540. https://doi.org/10.1023/a:1023470709071

Wang, N., Wang, M., Zhu, Y.-H., Grosel, T.W., Sun, D., Kudryashov, D.S., Wu, J.-Q., 2015. The Rho-GEF Gef3 interacts with the septin complex and activates the GTPase Rho4 during fission yeast cytokinesis. MBoC 26, 238–255. https://doi.org/10.1091/mbc.E14-07-1196

Wang, S., Reuveny, A., Volk, T., 2015. Nesprin provides elastic properties to muscle nuclei by cooperating with spectraplakin and EB1. J Cell Biol 209, 529–538. https://doi.org/10.1083/jcb.201408098

Wang, X., Fischer, G., Hyvönen, M., 2016. Structure and activation of pro-activin A. Nat Commun 7, 12052. https://doi.org/10.1038/ncomms12052

Wang, Y., Song, J., Liu, X., Liu, J., Zhang, Q., Yan, X., Yuan, X., Ren, D., 2020. Multiple Effects of Mechanical Stretch on Myogenic Progenitor Cells. Stem Cells and Development 29, 336–352. https://doi.org/10.1089/scd.2019.0286

Warner, C.L., Stewart, A., Luzio, J.P., Steel, K.P., Libby, R.T., Kendrick-Jones, J., Buss, F., 2003. Loss of myosin VI reduces secretion and the size of the Golgi in fibroblasts from Snell's waltzer mice. The EMBO Journal 22, 569–579. https://doi.org/10.1093/emboj/cdg055

Wasik, A.A., Dumont, V., Tienari, J., Nyman, T.A., Fogarty, C.L., Forsblom, C., Lehto, M., Lehtonen, E., Groop, P.-H., Lehtonen, S., 2017. Septin 7 reduces nonmuscle myosin IIA activity in the SNAP23 complex and hinders GLUT4 storage vesicle docking and fusion. Exp Cell Res 350, 336–348. https://doi.org/10.1016/j.yexcr.2016.12.010

Watanabe, N., Madaule, P., Reid, T., Ishizaki, T., Watanabe, G., Kakizuka, A., Saito, Y., Nakao, K., Jockusch, B.M., Narumiya, S., 1997. p140mDia, a mammalian homolog of Drosophila diaphanous,is a target protein for Rho small GTPase and is a ligand for profilin. The EMBO Journal 16, 3044–3056. https://doi.org/10.1093/emboj/16.11.3044

Weber, G.F., Menko, A.S., 2005. The Canonical Intrinsic Mitochondrial Death Pathway Has a Non-apoptotic Role in Signaling Lens Cell Differentiation *. Journal of Biological Chemistry 280, 22135–22145. https://doi.org/10.1074/jbc.M414270200

Webster, M.T., Manor, U., Lippincott-Schwartz, J., Fan, C.-M., 2016. Intravital Imaging Reveals Ghost Fibers as Architectural Units Guiding Myogenic Progenitors during Regeneration. Cell Stem Cell 18, 243–252. https://doi.org/10.1016/j.stem.2015.11.005

Weems, A., McMurray, M., 2017. The step-wise pathway of septin hetero-octamer assembly in budding yeast. eLife 6, e23689. https://doi.org/10.7554/eLife.23689

Wei, L., Zhou, W., Croissant, J.D., Johansen, F.-E., Prywes, R., Balasubramanyam, A., Schwartz, R.J., 1998. RhoA Signaling via Serum Response Factor Plays an Obligatory Role in Myogenic Differentiation *. Journal of Biological Chemistry 273, 30287–30294. https://doi.org/10.1074/jbc.273.46.30287

Wei, L., Zhou, W., Wang, L., Schwartz, R.J., 2000. beta(1)-integrin and PI 3-kinase regulate RhoA-dependent activation of skeletal alpha-actin promoter in myoblasts. Am J Physiol Heart Circ Physiol 278, H1736-1743. https://doi.org/10.1152/ajpheart.2000.278.6.H1736

Weirich, C.S., Erzberger, J.P., Barral, Y., 2008. The septin family of GTPases: architecture and dynamics. Nat Rev Mol Cell Biol 9, 478–489. https://doi.org/10.1038/nrm2407

Welle, S., Burgess, K., Mehta, S., 2009. Stimulation of skeletal muscle myofibrillar protein synthesis, p70 S6 kinase phosphorylation, and ribosomal protein S6 phosphorylation by inhibition of myostatin in mature mice. Am J Physiol Endocrinol Metab 296, E567-572. https://doi.org/10.1152/ajpendo.90862.2008

Wells, C., Coles, D., Entwistle, A., Peckham, M., 1997. Myogenic cells express multiple myosin isoforms. J Muscle Res Cell Motil 18, 501–515. https://doi.org/10.1023/a:1018607100730

Wen, Y., Bi, P., Liu, W., Asakura, A., Keller, C., Kuang, S., 2012. Constitutive Notch Activation Upregulates Pax7 and Promotes the Self-Renewal of Skeletal Muscle Satellite Cells. Mol Cell Biol 32, 2300–2311. https://doi.org/10.1128/MCB.06753-11

Weston, C., Gordon, C., Teressa, G., Hod, E., Ren, X.-D., Prives, J., 2003. Cooperative Regulation by Rac and Rho of Agrin-induced Acetylcholine Receptor Clustering in Muscle Cells *. Journal of Biological Chemistry 278, 6450–6455. https://doi.org/10.1074/jbc.M210249200

White, R.B., Biérinx, A.-S., Gnocchi, V.F., Zammit, P.S., 2010. Dynamics of muscle fibre growth during postnatal mouse development. BMC Developmental Biology 10, 21. https://doi.org/10.1186/1471-213X-10-21

Wickham, H., 2016. Introduction, in: Wickham, H. (Ed.), Ggplot2: Elegant Graphics for Data Analysis, Use R! Springer International Publishing, Cham, pp. 3–10. https://doi.org/10.1007/978-3-319-24277-4_1

Wickham, H., François, R., Henry, L., Müller, K., Vaughan, D., Software, P., PBC, 2023. dplyr: A Grammar of Data Manipulation.

Willis, A., Mazon-Moya, M., Mostowy, S., 2016. Chapter 13 - Investigation of septin biology in vivo using zebrafish, in: Gladfelter, A.S. (Ed.), Methods in Cell Biology, Septins. Academic Press, pp. 221–241. https://doi.org/10.1016/bs.mcb.2016.03.019

Willkomm, L., Bloch, W., 2015. State of the Art in Cell–Cell Fusion, in: Pfannkuche, K. (Ed.), Cell Fusion: Overviews and Methods, Methods in Molecular Biology. Springer, New York, NY, pp. 1–19. https://doi.org/10.1007/978-1-4939-2703-6_1

Włoga, D., Strzyżewska-Jówko, I., Gaertig, J., Jerka-Dziadosz, M., 2008. Septins Stabilize Mitochondria in Tetrahymena thermophila. Eukaryotic Cell 7, 1373–1386. https://doi.org/10.1128/ec.00085-08

Wolfman, N.M., McPherron, A.C., Pappano, W.N., Davies, M.V., Song, K., Tomkinson, K.N., Wright, J.F., Zhao, L., Sebald, S.M., Greenspan, D.S., Lee, S.-J., 2003. Activation of latent myostatin by the BMP-1/tolloid family of metalloproteinases. Proc Natl Acad Sci U S A 100, 15842–15846. https://doi.org/10.1073/pnas.2534946100

Woods, B.L., Gladfelter, A.S., 2021. The state of the septin cytoskeleton from assembly to function. Current Opinion in Cell Biology, Cell Architecture 68, 105–112. https://doi.org/10.1016/j.ceb.2020.10.007

Wosczyna, M.N., Rando, T.A., 2018. A Muscle Stem Cell Support Group: Coordinated Cellular Responses in Muscle Regeneration. Developmental Cell 46, 135–143. https://doi.org/10.1016/j.devcel.2018.06.018

Wu, H., Shen, Y., Sivagurunathan, S., Weber, M.S., Adam, S.A., Shin, J.H., Fredberg, J.J., Medalia, O., Goldman, R., Weitz, D.A., 2022. Vimentin intermediate filaments and filamentous actin form unexpected interpenetrating networks that redefine the cell cortex. Proceedings of the National Academy of Sciences 119, e2115217119. https://doi.org/10.1073/pnas.2115217119

Wu, J., Yue, B., 2024. Regulation of myogenic cell proliferation and differentiation during mammalian skeletal myogenesis. Biomedicine & Pharmacotherapy 174, 116563. https://doi.org/10.1016/j.biopha.2024.116563

Wu, L., Li, X., Li, Z., Cheng, Y., Wu, F., Lv, C., Zhang, W., Tang, W., 2021. HtrA serine proteases in cancers: A target of interest for cancer therapy. Biomedicine & Pharmacotherapy 139, 111603. https://doi.org/10.1016/j.biopha.2021.111603

Wu, M., Kwon, H.Y., Rattis, F., Blum, J., Zhao, C., Ashkenazi, R., Jackson, T.L., Gaiano, N., Oliver, T., Reya, T., 2007. Imaging Hematopoietic Precursor Division in Real Time. Cell Stem Cell 1, 541–554. https://doi.org/10.1016/j.stem.2007.08.009

Wu, S., Zhang, Y., You, S., Lu, S., Zhang, N., Sun, Y., 2021. Septin4 promotes cardiomyocytes apoptosis by enhancing the VHL-mediated degradation of HIF-1α. Cell Death Discov. 7, 1–10. https://doi.org/10.1038/s41420-021-00563-4

www.who.int/health-topics/ageing, 2023. www.who.int/health-topics/ageing [WWW Document]. URL https://www.who.int/health-topics/ageing (accessed 8.18.23).

Yang, W., Guo, X., Thein, S., Xu, F., Sugii, S., Baas, P.W., Radda, G.K., Han, W., 2013. Regulation of adipogenesis by cytoskeleton remodelling is facilitated by acetyltransferase MEC-17-dependent acetylation of α-tubulin. Biochem J 449, 605–612. https://doi.org/10.1042/BJ20121121

Yang, W., Hu, P., 2018. Skeletal muscle regeneration is modulated by inflammation. Journal of Orthopaedic Translation 13, 25–32. https://doi.org/10.1016/j.jot.2018.01.002

Yang, Yiting, Qu, R., Fan, T., Zhu, X., Feng, Y., Yang, Yuchao, Deng, T., Peng, Y., Huang, W., Ouyang, J., Dai, J., 2018. Cross-talk between microtubules and the linker of nucleoskeleton complex plays a critical role in the adipogenesis of human adipose-derived stem cells. Stem Cell Research & Therapy 9, 125. https://doi.org/10.1186/s13287-018-0836-y

Yeh, C.-H., Kuo, P.-L., Wang, Y.-Y., Wu, Y.-Y., Chen, M.-F., Lin, D.-Y., Lai, T.-H., Chiang, H.-S., Lin, Y.-H., 2015. SEPT12/SPAG4/LAMINB1 complexes are required for maintaining the integrity of the nuclear envelope in postmeiotic male germ cells. PLoS One 10, e0120722. https://doi.org/10.1371/journal.pone.0120722

Yeh, C.-H., Wang, Y.-Y., Wee, S.-K., Chen, M.-F., Chiang, H.-S., Kuo, P.-L., Lin, Y.-H., 2019. Testis-Specific SEPT12 Expression Affects SUN Protein Localization and is Involved in Mammalian Spermiogenesis. International Journal of Molecular Sciences 20, 1163. https://doi.org/10.3390/ijms20051163

Yeh, Y.-T., Hur, S.S., Chang, J., Wang, K.-C., Chiu, J.-J., Li, Y.-S., Chien, S., 2012. Matrix Stiffness Regulates Endothelial Cell Proliferation through Septin 9. PLOS ONE 7, e46889. https://doi.org/10.1371/journal.pone.0046889

Yi, P., Chew, L.L., Zhang, Z., Ren, H., Wang, F., Cong, X., Zheng, L., Luo, Y., Ouyang, H., Low, B.C., Zhou, Y.T., 2015. KIF5B transports BNIP-2 to regulate p38 mitogen-activated protein kinase activation and myoblast differentiation. MBoC 26, 29–42. https://doi.org/10.1091/mbc.e14-03-0797

Yin, H., Price, F., Rudnicki, M.A., 2013. Satellite cells and the muscle stem cell niche. Physiol Rev 93, 23–67. https://doi.org/10.1152/physrev.00043.2011

Yourek, G., Hussain, M.A., Mao, J.J., 2007. Cytoskeletal Changes of Mesenchymal Stem Cells During Differentiation. ASAIO J 53, 219–228. https://doi.org/10.1097/MAT.0b013e31802deb2d

Yusuf, F., Brand-Saberi, B., 2006. The eventful somite: patterning, fate determination and cell division in the somite. Brain Struct Funct 211, 21–30. https://doi.org/10.1007/s00429-006-0119-8

Zakrzewski, P., Rędowicz, M.J., Buss, F., Lenartowska, M., 2020. Loss of myosin VI expression affects acrosome/acroplaxome complex morphology during mouse spermiogenesis†. Biology of Reproduction 103, 521–533. https://doi.org/10.1093/biolre/ioaa071

Zeng, Y., Cao, Y., Liu, L., Zhao, J., Zhang, T., Xiao, L., Jia, M., Tian, Q., Yu, H., Chen, S., Cai, Y., 2019. SEPT9_i1 regulates human breast cancer cell motility through cytoskeletal and RhoA/FAK signaling pathway regulation. Cell Death Dis 10, 1–16. https://doi.org/10.1038/s41419-019-1947-9

Zent, E., Vetter, I., Wittinghofer, A., 2011. Structural and biochemical properties of Sept7, a unique septin required for filament formation 392, 791–797. https://doi.org/10.1515/BC.2011.082

Zent, E., Wittinghofer, A., 2014. Human septin isoforms and the GDP-GTP cycle. Biological Chemistry 395, 169–180. https://doi.org/10.1515/hsz-2013-0268

Zhang, J., Kong, C., Xie, H., McPherson, P.S., Grinstein, S., Trimble, W.S., 1999. Phosphatidylinositol polyphosphate binding to the mammalian septin H5 is modulated by GTP. Current Biology 9, 1458–1467. https://doi.org/10.1016/S0960-9822(00)80115-3

Zhang, J., Ying, Z., Tang, Z., Long, L., Li, K., 2012. MicroRNA-148a Promotes Myogenic Differentiation by Targeting the ROCK1 Gene. J Biol Chem 287, 21093–21101. https://doi.org/10.1074/jbc.M111.330381

Zhang, L., Noguchi, Y., Nakayama, H., Kaji, T., Tsujikawa, K., Ikemoto-Uezumi, M., Uezumi, A., Okada, Y., Doi, T., Watanabe, S., Braun, T., Fujio, Y., Fukada, S., 2019. The CalcR-PKA-Yap1 Axis Is Critical for Maintaining Quiescence in Muscle Stem Cells. Cell Reports 29, 2154-2163.e5. https://doi.org/10.1016/j.celrep.2019.10.057

Zhang, P., Wong, C., Liu, D., Finegold, M., Harper, J.W., Elledge, S.J., 1999. p21(CIP1) and p57(KIP2) control muscle differentiation at the myogenin step. Genes Dev 13, 213–224. https://doi.org/10.1101/gad.13.2.213

Zhang, Q., Vashisht, A.A., O'Rourke, J., Corbel, S.Y., Moran, R., Romero, A., Miraglia, L., Zhang, J., Durrant, E., Schmedt, C., Sampath, Srinath C., Sampath, Srihari C., 2017. The microprotein Minion controls cell fusion and muscle formation. Nat Commun 8, 15664. https://doi.org/10.1038/ncomms15664

Zhang, S., Zhang, Y., Chen, C., Hu, Q., Fu, Y., Xu, L., Wang, C., Liu, Y., 2022. Identification of Robust and Key Differentially Expressed Genes during C2C12 Cell Myogenesis Based on Multiomics Data. International Journal of Molecular Sciences 23, 6002. https://doi.org/10.3390/ijms23116002

Zhang, Y., Parmigiani, G., Johnson, W.E., 2020. ComBat-seq: batch effect adjustment for RNA-seq count data. NAR Genomics and Bioinformatics 2, lqaa078. https://doi.org/10.1093/nargab/lqaa078

Zheng, S., Zheng, B., Fu, C., 2024. The Roles of Septins in Regulating Fission Yeast Cytokinesis. Journal of Fungi 10. https://doi.org/10.3390/jof10020115

Zhong, W., Feder, J.N., Jiang, M.-M., Jan, L.Y., Jan, Y.N., 1996. Asymmetric Localization of a Mammalian Numb Homolog during Mouse Cortical Neurogenesis. Neuron 17, 43–53. https://doi.org/10.1016/S0896-6273(00)80279-2

Zuvanov, L., Mota, D.M.D., Araujo, A.P.U., DeMarco, R., 2019. A blueprint of septin expression in human tissues. Funct Integr Genomics 19, 787–797. https://doi.org/10.1007/s10142-019-00690-3

6. Appendix

6.1. Expression of Cdc42ep/ Borg proteins in C2C12 cells

Septins oligomerize into complexes that form filaments in mammalian cells (Spiliotis and Nakos, 2021). In this work, we have shown that septins form actin-associated filaments in myoblasts and reorganize into filamentous remnants during myogenic differentiation (Figure 3-13). However, the mechanisms regulating this dynamic reorganization of septin complexes are not well understood. Small RhoGTPase Cdc42 has been demonstrated to modulate the cellular localization of septins, a process requiring Cdc42 effector proteins 1-5 (Cdc42ep1-5)/ Binders of RhoGTPase 1-5 (Borg1-5) (Fig. 6-1A) (Farrugia and Calvo, 2016; Tomasso and Padrick, 2023). Thus, we hypothesized that Borg proteins could potentially mediate the reorganization of septins during myogenic differentiation. Given that the expression of Borg proteins has not been elucidated so far in myoblasts, we aimed to characterize the expression of this gene family and study their interaction and co-localization with Septin9 in C2C12 cells. We designed primers for murine Cdc42ep1-5 (Cep1-5 from here on) and tested the mRNA presence of Borgs by analyzing reverse-transcribed cDNA from C2C12 cells. A semi-quantitative PCR indicated the expression of Cep1/Borg5, Cep3/Borg2, Cep4/Borg4, as well as a faint band at the right molecular size for Cep5/Borg4 (Fig. 6-1B). Next, we tested the ability of Borgs to associate with Septin9 in C2C12 cells. We performed a co-immunoprecipitation with rat Borg1-5-GFP proteins (kindly provided by Prof. Dr. Helge Ewers) (Fig. 6-1C). All introduced Borg constructs precipitated Septin9-Myc, indicating a potential association of Borg proteins with septin filaments in C2C12 cells. Additionally, we tested whether Cdc42 can associate with Septin9 in C2C12 cells. We demonstrated a co-immunoprecipitation of Septin9-Myc with rat WT Cdc42, as well as the constitutively active (CA) and dominant negative (DN) mutants of Cdc42 fused with GFP (also kindly provided by Prof. Dr. Helge Ewers). Hence, Septin9 likely forms a complex with Cdc42 in C2C12 cells, regardless of the RhoGTPase cycling ability (Fig. 6-1D).

Next, we examined the subcellular organization of GFP-Borg1-5 proteins and their co-localization with endogenous Septin9 in C2C12 cells (Fig. 6-2). Overexpressing Borgs resulted in the excessive formation of septin filaments, often spanning the whole cell, as opposed to perinuclear septin filaments observed in control cells (Fig. 6-2A vs Fig. 3-7A). Borg1-5 co-localized with Septin9 and F-actin in C2C12 myoblasts, often resulting in the disruption of

septin filaments (Fig. 6-2B). In some cases, overexpression of Borgs, as depicted for Borg2 and Borg4, resulted in the appearance of curvy septin filaments, never observed in WT C2C12 cell under proliferative conditions (Fig. 6-2B).

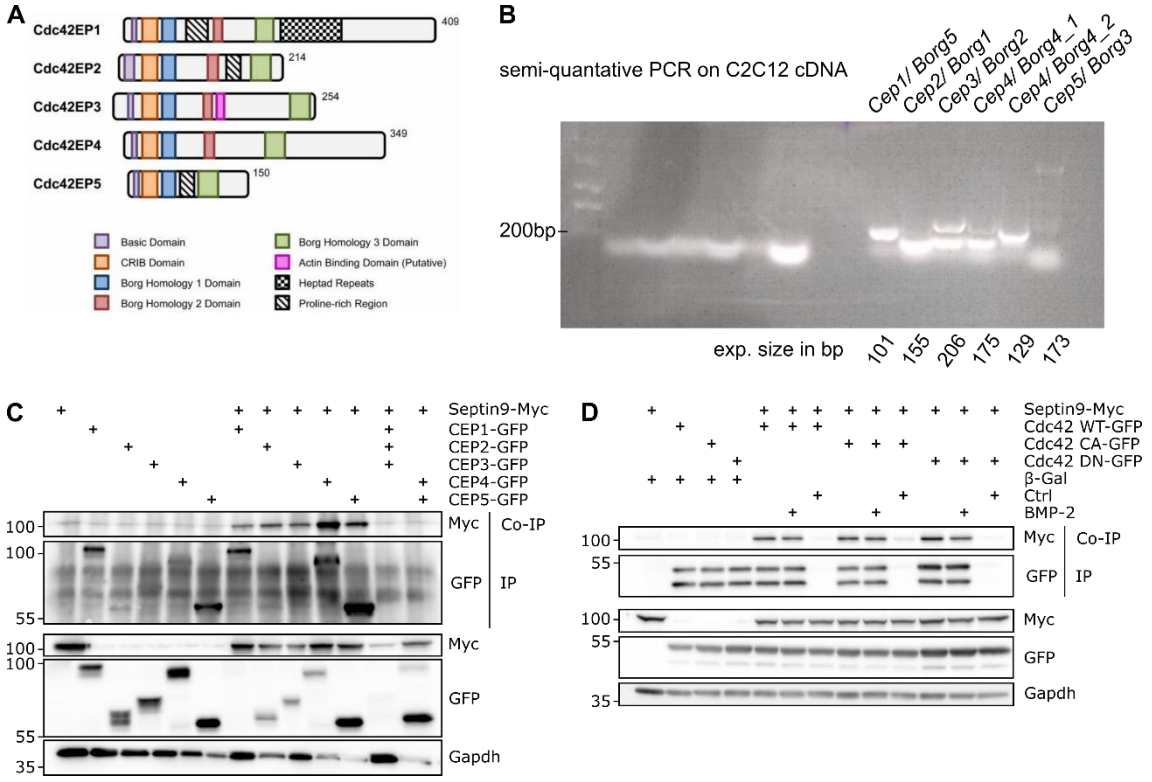

Figure 6-1. Septin9 interacts with Borg proteins and with Cdc42
A Scheme representing domain composition of Cdc42ep/ Borg proteins. Borg Homology 3 (BH3) domain is crucial for the interaction with Septin2/6/7. **B** Semi-quantitative PCR on C2C12 cDNA indicates expression of Cdc42ep1, Cdc42ep3, Cdc42ep4, and potentially Cdc42ep5. **C** Co-Immunoprecipitation in HEK293T cells of Septin9-myc by GFP-fused rat Cdc42 effector proteins. All Cdc42eps interact with Septin9 under these experimental conditions. **D** Co-Immunoprecipitation in HEK293T cells of Septin9-myc by GFP-fused rat Cdc42 mutants. WT, CA, and DN mutant Cdc42 proteins interact with Septin9-myc under these experimental conditions.

Borg1-3 have been demonstrated to bind to septins at the interface between Septin6 and 7, implying an interaction with septin complexes (Castro et al., 2023; Joberty et al., 2001; Sheffield et al., 2003). In this study, we have demonstrated the expression of some Borg proteins in C2C12 cells, including at least Borg2, 4 and 5 (Fig. 6-1). Furthermore, we have provided evidence for the formation of a potential protein complex consisting of Cdc42, Borgs, and septins, as both Cdc42 and Borg proteins co-immunoprecipitated Septin9 from the cell lysate. Additionally, over-expressed GFP-fused Borg proteins co-localized with Septin9 in myoblasts. Moreover, the expression of each Borg paralogue resulted in the formation of ectopic septin filaments, and often led to the disruption of septin organization. Notably, some Borgs, such as Borg 2 and Borg4, resulted in the appearance of distinctly curvy septins, which

are never observed in proliferating myoblasts. Notably, these curvy filaments resemble septin organization observed during myogenic differentiation (Fig.3-15).

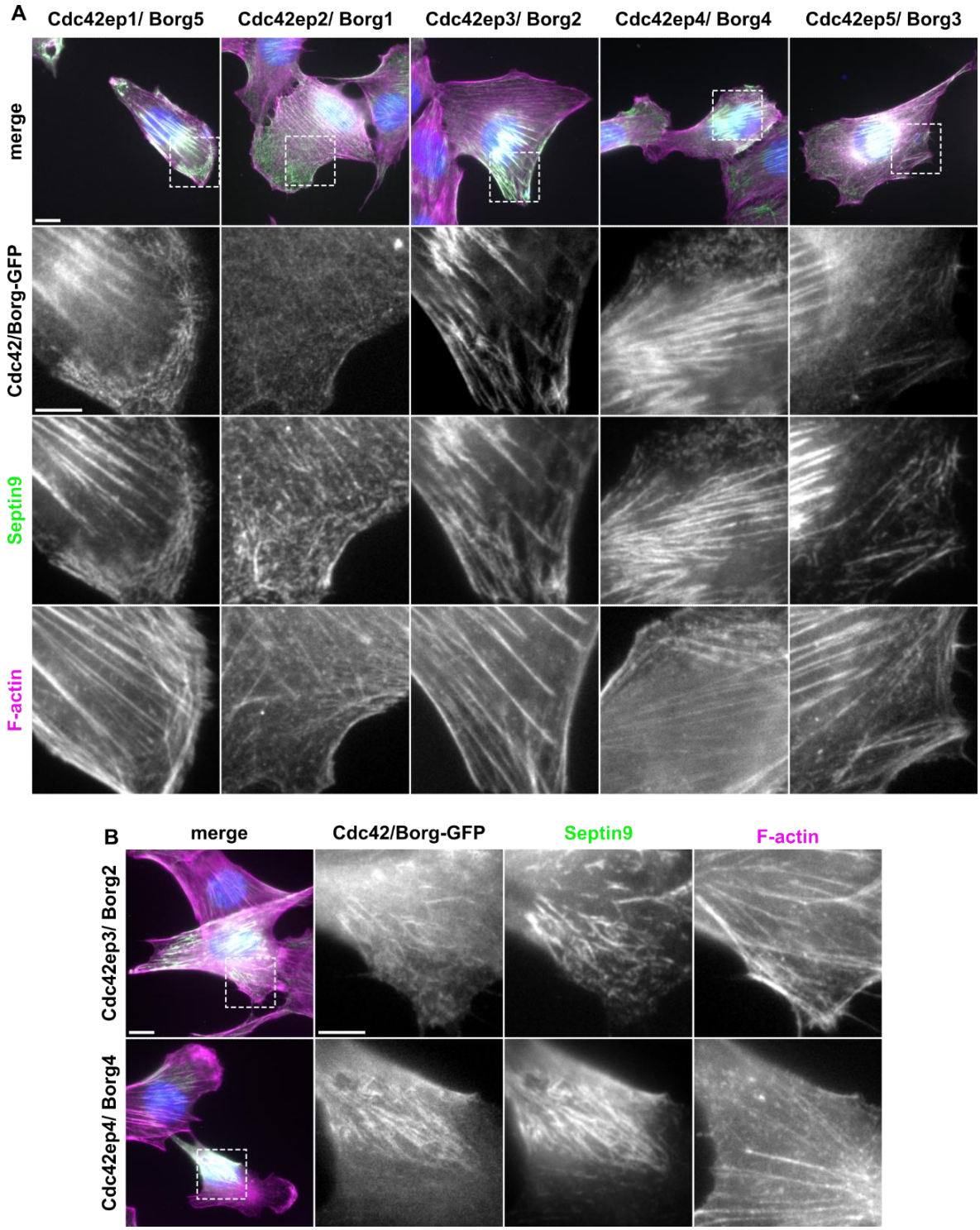

Figure 6-2. Borg proteins co-localize with Septin9 in C2C12 cells and may induce septin filament reorganization

A Representative immunofluorescence images showing Septin9 co-localization with introduced rat Borg proteins in C2C12 cells. GFP-fused Borg1-5 proteins were visualized via GFP, F-actin through Phalloidin AF594 and Septin9 with antibodies using AF647. **B** Overexpression of some Borgs (Borg2 and Borg4) resulted in acquisition of curved Septin9 filaments. Scale bars 10 µm, insets 5µm.

Taken together, we provide evidence for potential regulation exerted by Cdc42/Borg axis on the organization of septin filaments in myoblasts. The appearance of morphologically similar curvy septins upon overexpression of Borgs (Fig. 6-2B) and in differentiating myoblasts (Fig. 3-15A) prompts an intriguing possibility for the involvement of the Cdc42/Borg axis in regulating septin organization during myogenic differentiation.

6.2. Expression of E2F target genes upon Septin9 depletion

In addition to precocious differentiation, the depletion of Septin9 resulted in fewer myoblasts and a lower ratio of EdU-positive cells compared to controls, indicating faulty progression through the DNA synthesis phase of the cell cycle (Fig. 3-27 and 3-28). Pocket protein Rb1 and E2F transcription factors are central regulators in several phases of the cell cycle progression. Rb1 interacts with and inhibits the transcriptional activity of E2F transcription factors (E2f1-E2f7), which heterodimerize with Dp proteins (Dp1 and Dp2). Some E2F members repress (in combination with co-repressors), while others transactivate (in combination with other transcription factors) numerous target genes to ensure orderly progression of cell division (Bracken et al., 2004). Given that terminal myoblast differentiation usually coincides with cell cycle arrest and exit from the division cycle, we aimed to examine the expression of E2F target genes critical for pushing cells into the DNA synthesis phase.

We analyzed the normalized counts extracted from the RNASeq experiments performed in this study in C2C12 and primary myoblasts depleted of Septin9, focusing on E2F target genes summarized by Bracken and colleagues (Bracken et al., 2004). E2F target genes regulating G_1 to S phase transition were not uniformly regulated in Septin9-deficient myoblasts, with some (e.g., *E2F2*) being upregulated and others (e.g., *Tfdp1*) being downregulated (Fig. 6-3A). These strong regulations may indicate an adaptation to deregulated cell cycle exit upon Septin9 depletion. However, E2F target genes expressed in S or G_2 phases of the cell cycle showed a uniform downregulation in both C2C12 and primary myoblasts upon Septin9 depletion, except for the low-expressed Ccna1 (Fig. 6-3B). Instead, E2F target genes specifically involved in DNA synthesis and replication were downregulated in primary myoblasts, while many of these genes showed and opposite regulation in C2C12 cells (Fig. 6-3C).

The regulation of E2F target genes outside of G_1 phase is not very clear, although other transcription factors are proposed to facilitate the delayed de-repression and transactivation downstream of E2F factors (Bracken et al., 2004). Nonetheless, E2F transcription factors

regulate a broad range of factors that function in the S phase and play additional roles in processes such as DNA damage checkpoint and repair. Many of these genes show a functional overlap between these processes. For instance, *Chk1* is an essential component of DNA damage signaling but also accumulates in the S phase in non-stressed cells, ensuring absence of DNA replication mistakes before cells enter the mitotic phase. These features imply that the regulation of some E2F target genes may be another facet of the E2F function in ensuring orderly progression through the cell cycle.

Thus, deregulations of E2F target genes are challenging to interpret. However, the concerted downregulation of S/G_2 target genes in both C2C12 and primary myoblasts in absence of Septin9 indicates a conserved role of organized septins during the orderly progression through the cell cycle. Septin9-deficient myoblasts prematurely enter the differentiation program. It is conceivable that E2F activity could be reduced upon Septin9 depletion, inhibiting the entry into the S phase of the cell division, and allowing cells to commit to the differentiation program. The mechanistic details of this process, however, require further investigation.

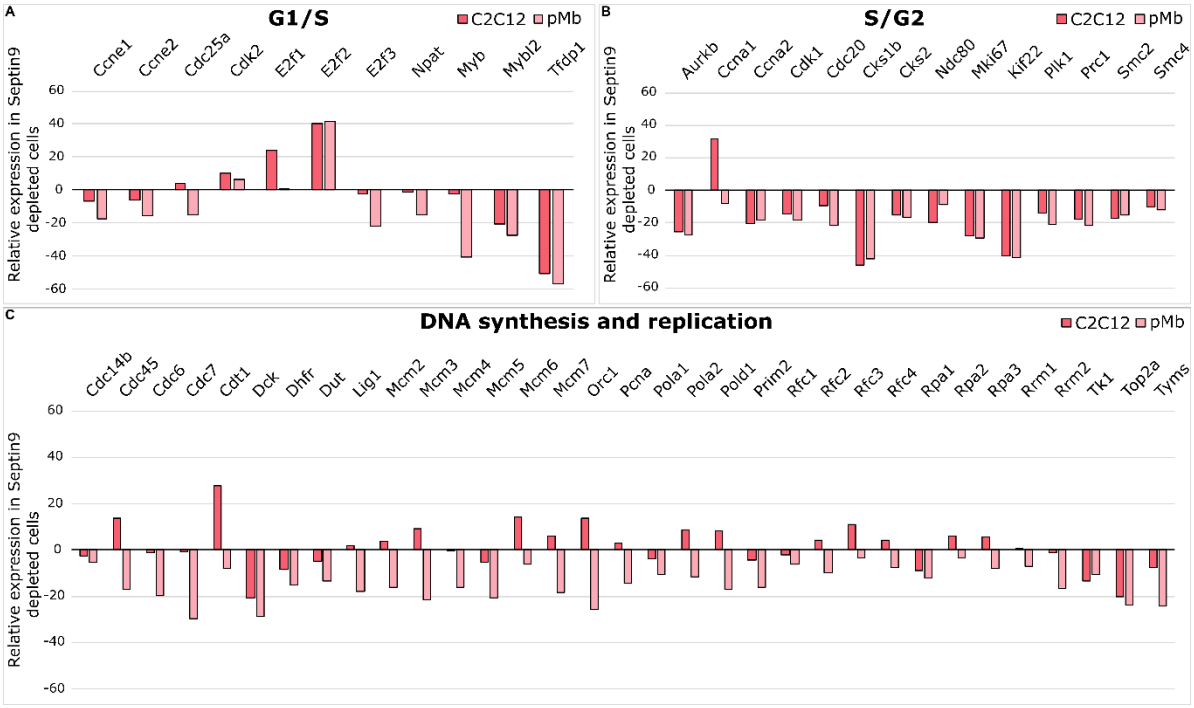

Figure 6-3. Expression of E2F target genes in Septin9-deficient C2C12 and primary myoblasts
Relative mRNA expression of E2F target genes associated with G_1/S transition (**A**), S/G_2 transition (**B**), and DNA synthesis and replication (**C**) upon Septin9 depletion in C2C12 and primary myoblasts. Normalized counts representing knockdown-to-control ratio from two RNASeq experiments performed in this study. E2F target genes are summarized by Bracken *et al.* (Bracken et al., 2004)

6.3. Characterization of actin filaments and focal adhesion organization upon Septin9 depletion

Septin and actin filaments are remarkably interdependent cellular elements, where disruption of one often alters the other (Spiliotis, 2018). Therefore, the observed changes in myogenic differentiation upon Septin9-depletion may arise from changes in actin organization. The nature of the septin-actin interaction is a subject of vigorous investigation, and depletion of septins has been demonstrated to mostly affect contractile actin fibers (Calvo et al., 2015; Dolat et al., 2014a; Joo et al., 2007; Surka et al., 2002). Furthermore, in renal epithelial cells, Septin9 regulates lamellar actin stress fibers, mediating maturation and stability of focal adhesions (Dolat et al., 2014a). Therefore, presence of Septin9 in myoblasts may contribute to actin integrity via regulating the actin bundling, contractility, and force generation at focal adhesions. Hence, we aimed to examine the organization of ventral actin filaments and focal adhesions in Septin9-deficient C2C12 cells.

Given that siRNA-mediated depletion of Septin9 results in disruption of septin filaments in myoblasts (Fig. 3-11), we analyzed organization of perinuclear actin filaments visualized using phalloidin staining (Fig. 6-4). Cells depleted of Septin9 show a complete absence of septin filaments. Additionally, Septin9-deficient cells show lack of organized perinuclear actin filaments, compared to adjacent C2C12 cells still expressing Septin9 (that likely did not receive the siRNA) on the same cover slip. Actin filaments appear more disordered, discontinuous and less bundled (Fig. 6-4). As cytoskeletal reorganization is an essential step in myoblast differentiation and fusion (Lu et al., 2001; Musa et al., 2003; Swailes et al., 2004), it will remain imperative to quantify the changes in actin orientation and bundling, and furthermore study how the F/G actin ratio and actomyosin contractility are influenced by Septin9 depletion.

Focal adhesions attach actin stress fibers to the plasma membrane and extracellular matrix, and, in turn, rely on the integrity of actin filaments (Svitkina, 2018). Therefore, we examined the organization of Zyxin-positive focal adhesions in C2C12 cells depleted of Septin9 (Fig. 6-5). C2C12 cells lacking Septin9 showed less proximal, perinuclear focal adhesions, and smaller distant, nascent focal adhesions. These data indicate a potential problem with maturation of focal adhesion complexes and therefore possible profound changes in mechano-sensation in Septin9-deficient myoblasts. However, focal adhesions parameters such as number and size

have not been quantified in this study. In conclusion, changes in actin and focal adhesion organization may potentially have an impact on myogenic differentiation of Septin9-deficient myoblasts, as cytoskeletal signaling plays important roles in migration, proliferation, differentiation, and fusion of myoblasts (Brondolin et al., 2023; Castellani et al., 2006; Costa, 2014; Noviello et al., 2023).

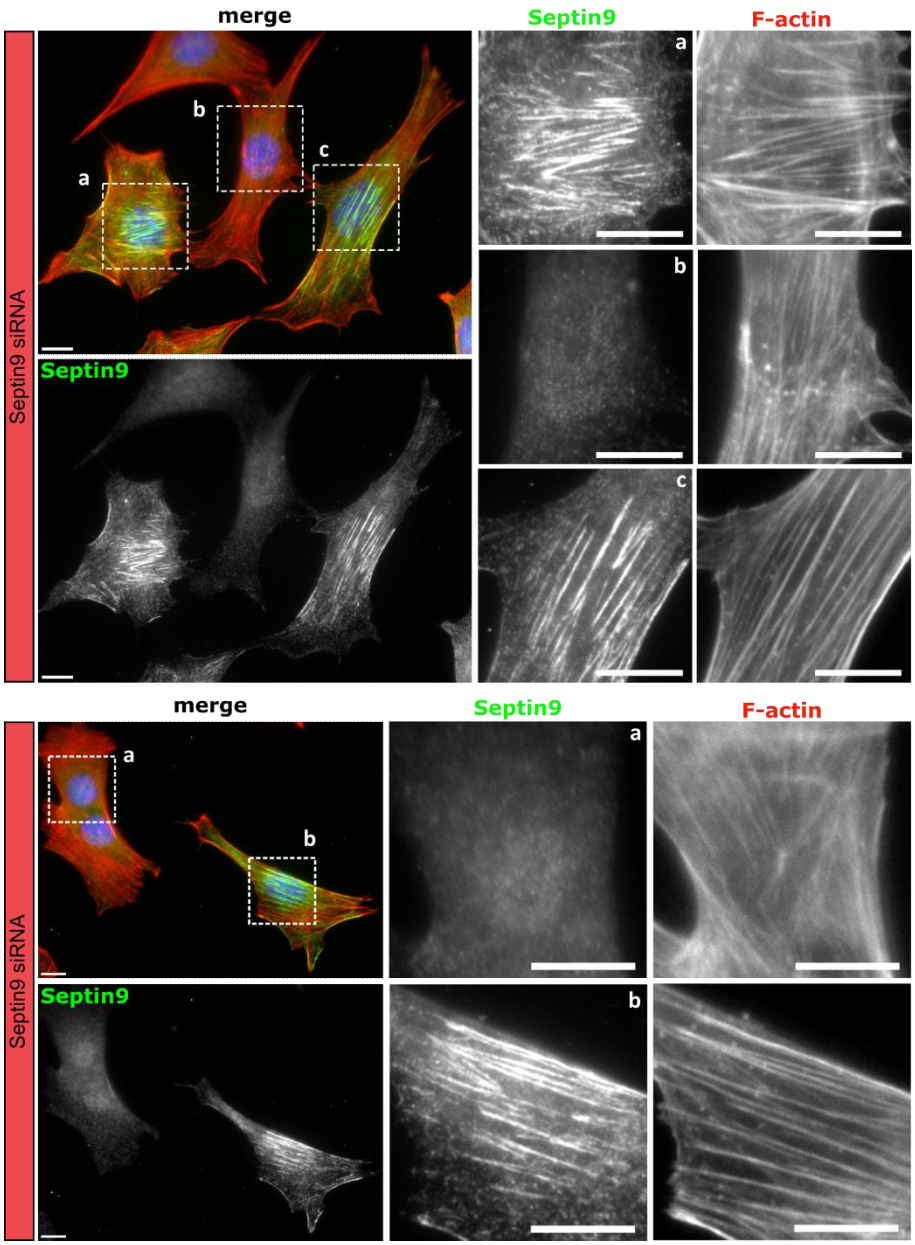

Figure 6-4. Integrity of perinuclear actin fibers in absence of Septin9
Representative immunofluorescence images of Septin9-depleted C2C12 cells, focusing on the ventral and perinuclear contractile stress fibers stained with phalloidin. Disruption of Septin9 leads to altered organization of perinuclear actin filaments in myoblasts. Scale bars 10 µm.

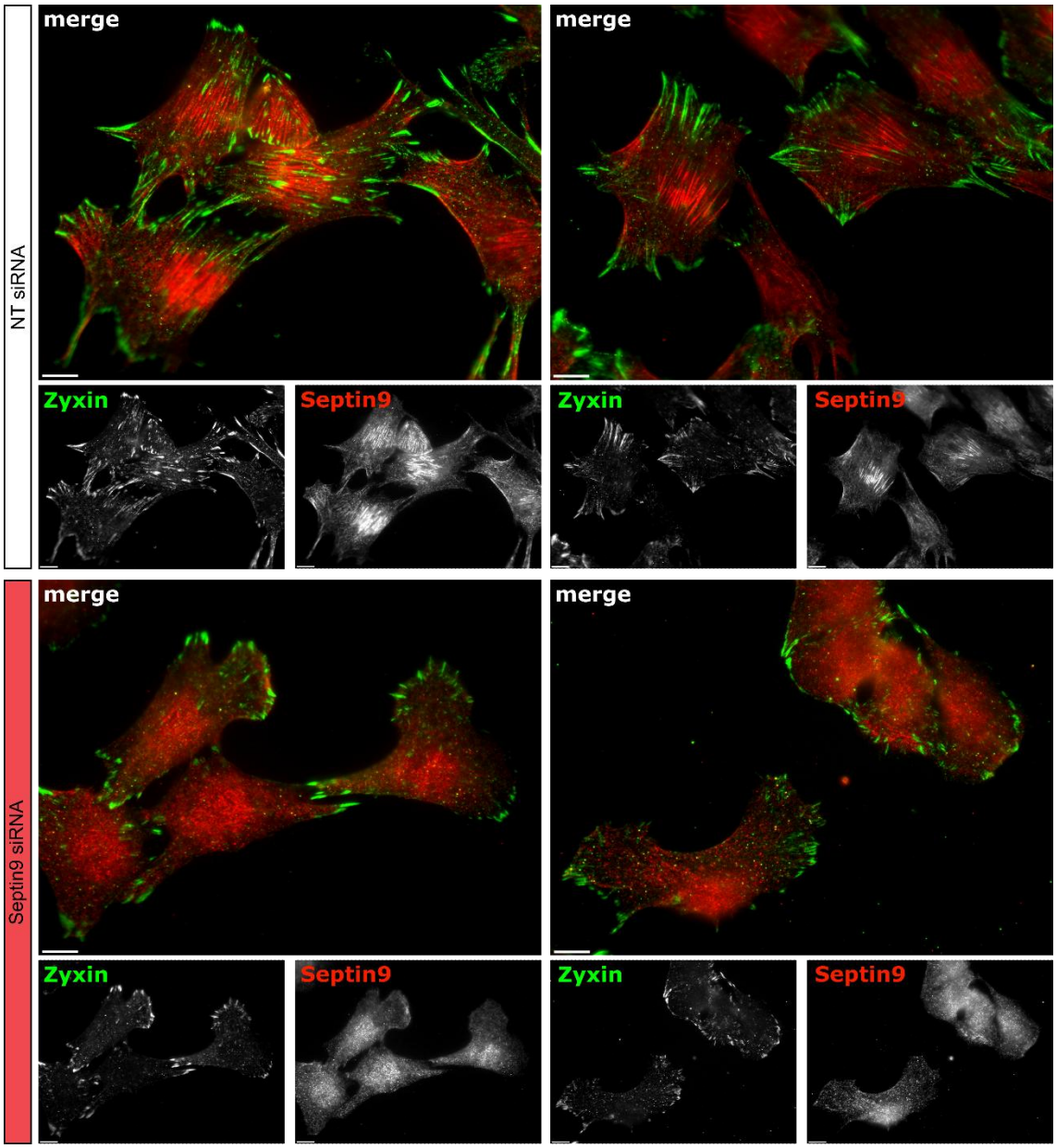

Figure 6-5. Septin9 depletion alters organization of Zyxin-positive focal adhesions
Representative immunofluorescence images showing Zyxin-positive focal adhesions in Septin9-depleted and control C2C12 cells. Disruption of Septin9 leads to a reduction of proximal adhesions and a defect in the maturation of distal focal adhesions in myoblasts. Scale bars 10 µm

6.4. Compartmentalization of BMP signaling pathways by septin scaffolds

Bone morphogenetic proteins (BMPs) are essential dimeric growth factors belonging to the TGF-β superfamily, playing a pivotal role in tissue morphogenesis, architecture, and regeneration by activating complex signaling pathways through transmembrane serine/threonine kinase receptors. These BMP-activated cascades regulate cell division and differentiation and are crucial roles during myogenesis. BMP signaling is initiated through the

binding and hetero-oligomerization of two types of BMP-receptors (Bmprs): type I and type II (Bmpr1 and Bmpr2). Functional signaling receptor complexes are composed of two type I and two type II receptors, where the constitutively active Bmpr2 kinase phosphorylates Bmpr1 upon ligand binding, leading to receptor activation. This receptor oligomerization triggers both Smad-dependent transcriptional responses and non-transcriptional pathways, including cytoskeletal rearrangements. While both pathways are initiated at the cell surface, the molecules involved and the downstream signaling events differ significantly, resulting in distinct cellular outcomes (Bragdon et al., 2011; Horbelt et al., 2012; Nickel and Mueller, 2019).

Previous research from our group demonstrated an interaction between Septin9 Bmpr2, but not with type I receptors such as Alk3 and Alk6 (doctoral thesis of Dr. Agnieszka Denkis). Our goal was to further validate whether this interaction is direct and to identify the subcellular compartment where this interaction occurs.

We expressed of either the long or short form of HA-tagged Bmpr2 (LF or SF, respectively) along with Septin9-Myc in HEK293T cells, followed by immunoprecipitation using antibodies against Myc tag. Our results showed that both splice variants of the receptor interact with exogenous Septin9, and that the addition of BMP2 enhances this pre-existing interaction (Fig. 6-6A-B). However, *in vitro* pulldown experiments using recombinant human SEPTIN9-GST and His-tagged Bmpr2-kinase domain showed no interaction (His pulldown not shown), suggesting that the complex formation between Septin9 and Bmpr2 may be mediated by a bridging protein (Fig. 6-6C).

Additionally, we examined the interaction between Septin9 and other receptors from the TGFβ family, such as Tβr2 and Alk2. Both receptors co-precipitated with exogenous Septin9 in HEK293T cells. Furthermore, the association between Alk2 and Septin9 was enhanced in the presence a ligand (BMP6) (Fig. 6-6D-E).

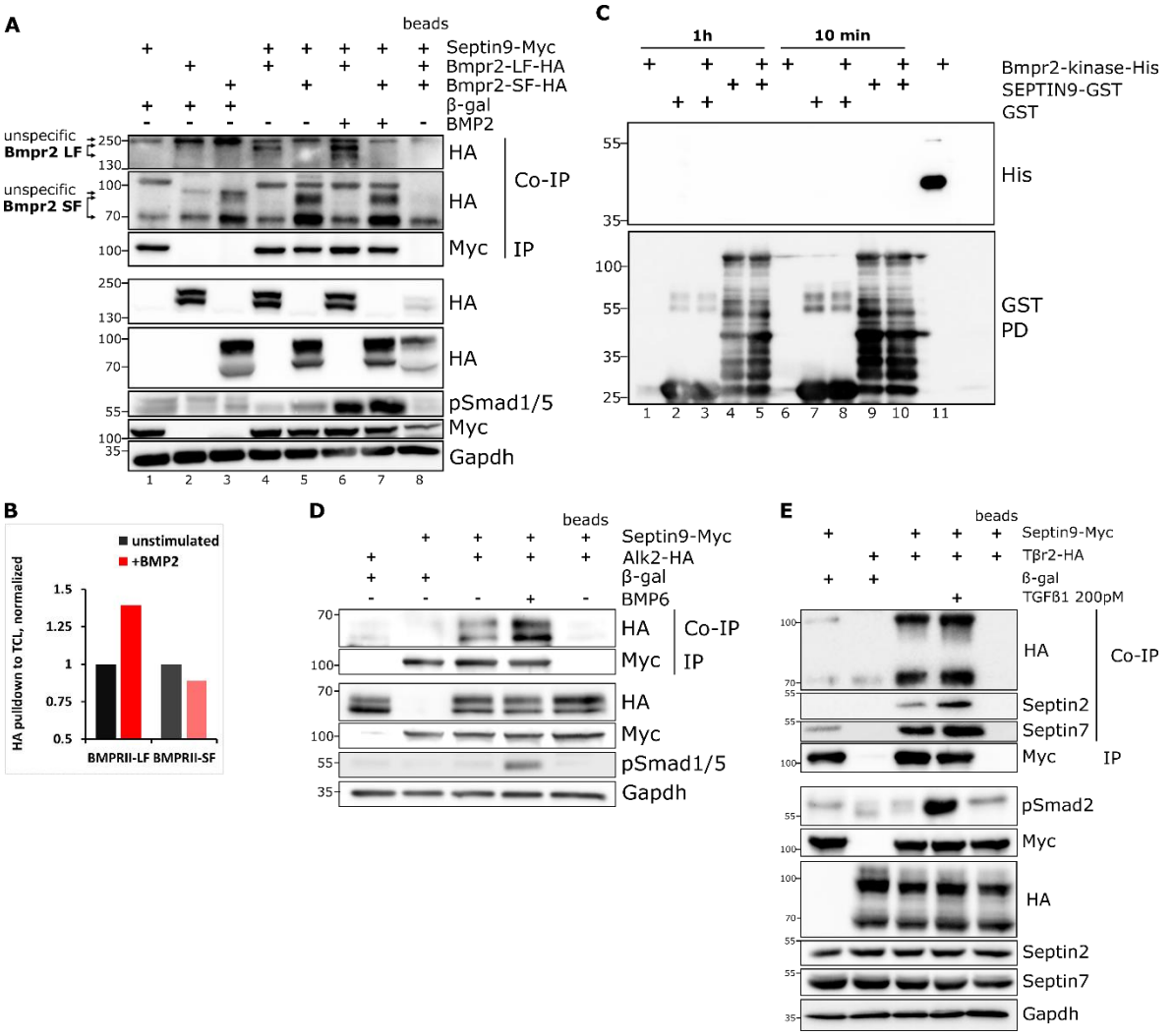

Figure 6-6. Septin9 interacts with Bmpr2, Alk2 and Tβr2

A Co-immunoprecipitation assay in HEK293T cells expressing Septin9-Myc and either the long or short form of Bmpr2-HA (Bmpr2-LF and Bmpr2-SF, respectively), shows that both isoforms of Bmpr2 interact with exogenous Septin9. Notably, stimulation with BMP2 enhanced the interaction with the long isoform only. **B** Quantification of co-precipitated Bmpr2 isoform protein levels normalized to total isoform levels and Gapdh. **C** *In vitro* pulldown assay using recombinant human SEPTIN9-GST and the human kinase domain of Bmpr2 reveals no direct interaction under the conditions tested. **D** Co-immunoprecipitation assay in HEK293T cells expressing Septin9-Myc and Alk2-HA demonstrates that Alk2 interacts with exogenous Septin9 under serum-starved conditions, with the addition of the high affinity ligand BMP6 further enhancing this interaction. **E** Co-immunoprecipitation assay in HEK293T cells expressing Septin9-Myc and Tβr2-HA shows that Septin9 interacts with Tβr2 under serum-deprivation. However, stimulation with TGFβ1 does not alter the interaction under tested conditions. IP: Immunoprecipitation, Co-IP: Co-immunoprecipitation, PD: Pulldown, TCL: Total cell lysate.

To determine whether the interaction between Septin9 and Bmpr2 occurs at the plasma membrane or within the cell, we conducted cell surface biotinylation of HEK293T cells expressing either HA-tagged Bmpr2-LF or Bmpr2-SF. Streptavidin pulldown assays revealed that Septin9-7-2 complexes precipitate with transmembrane proteins and potentially associate with the plasma membrane in both control cells and those expressing Bmpr2 (Fig.

6-7A). Notably, the addition of the ligand enhanced the association of septins with the membrane only in cells expressing the long form of the Bmpr2 (Fig. 6-7A-B), suggesting that the tail region of Bmpr2 may regulate septin oligomerization.

Next, to visualize the interaction between Bmpr2 and Septin9, we performed proximity ligation assays (PLA) using antibodies against the endogenous proteins (Fig. 6-8A-C). The results showed that Septin9 and Bmpr2 interact in serum-deprived C2C12 cells, with ligand stimulation increasing the formation of this complex (Fig. 6-8A-B). Observations under TIRF microscopy, combined with reduced endocytosis through incubation at 4 °C or 13 °C, further emphasized that the interaction between Septin9 and Bmpr2 occurs at the cell surface (Fig. 6-8A and C).

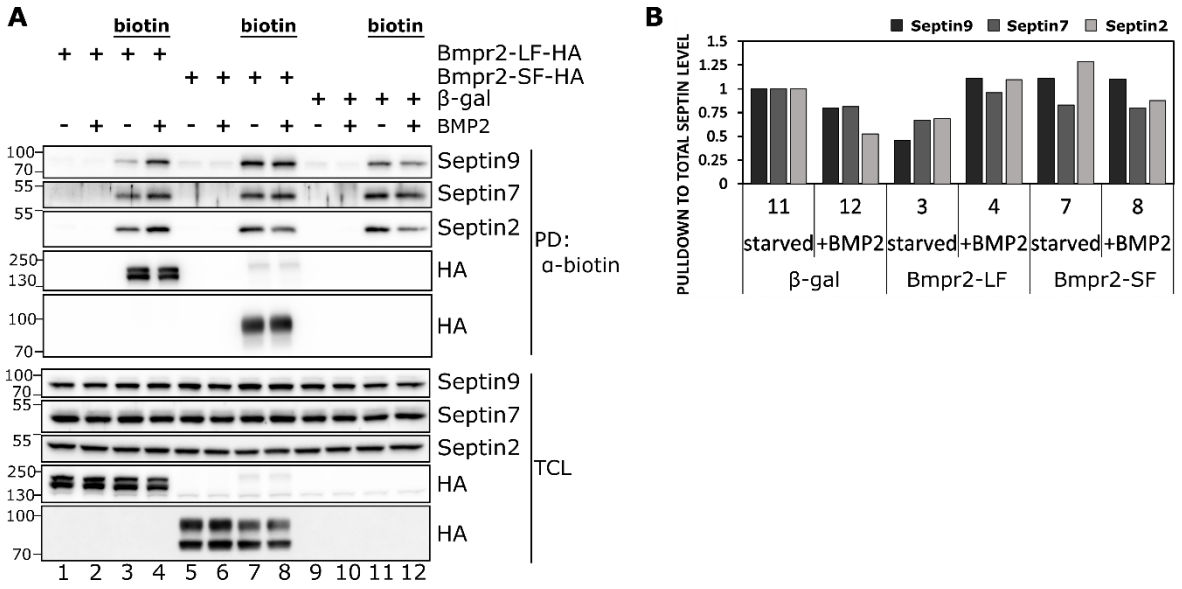

Figure 6-7. Bmpr2 regulates septin organization at the cell surface

A Surface biotinylation assay were performed in HEK293T cells expressing eighter the long (LF) or the short (SF) form of Bmpr2. Streptavidin pulldown was followed by western blot analysis to detect endogenous Septin9, Septin7, Septin2, and HA-tagged Bmpr2. The addition of BMP2 (lanes 2 and 4,) suggests a potential release from auto-inhibition by the tail region of the long Bmpr2 isoform. **B** Quantification of endogenous Septin9, Septin7, and Septin2 levels precipitated with transmembrane proteins after biotinylation, normalized to total septin levels. PD: Pulldown, TCL: Total cell lysate

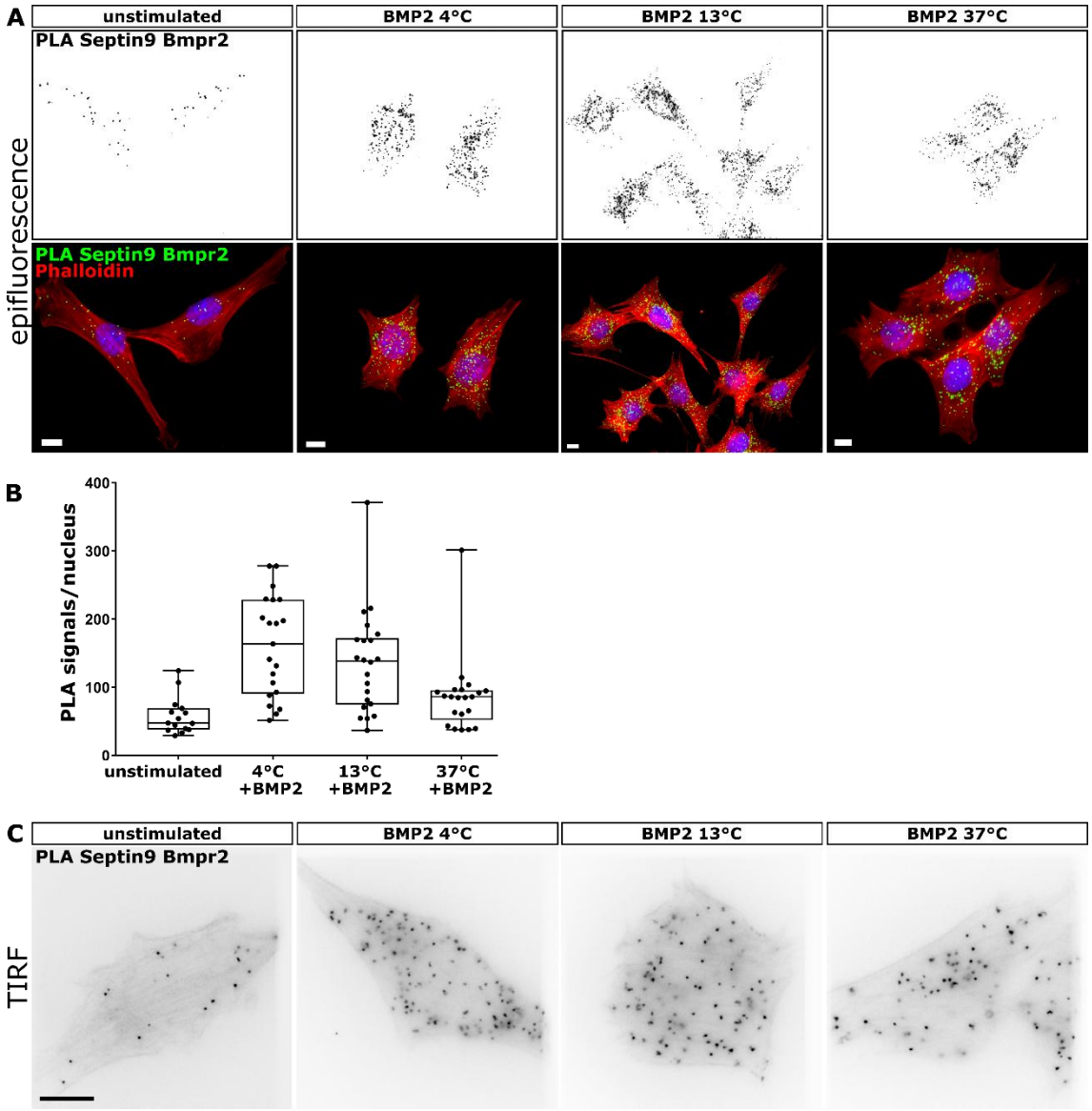

Figure 6-8. Septin9 interacts with Bmpr2 at the plasma membrane
A Representative images from proximity ligation assay between endogenous Septin9 and Bmpr2, illustrating the subcellular localization of the Septin9-Bmpr2 interaction in C2C12 cells at different temperatures. The epifluorescence micrographs show the basal interaction under serum-starved conditions and an increase in interaction upon BMP2 stimulation. **B** Quantification of PLA signals per nucleus from panel A. Slowing or inhibiting endocytosis by lowering the temperature localizes the interaction to the plasma membrane. **C** TIRFM micrographs confirming the interaction between Septin9 and Bmpr2 is localized at the cell surface. Scale bar 10 mµ.

In summary, our study provides spatial insights into Septin9-Bmpr2 interaction, demonstrating that this interaction occurs at the cell surface. The spatiotemporal dynamics and molecular mechanisms underlying this interaction remain to be elucidated. It is plausible that septins act as molecular scaffolds, compartmentalizing the BMP signaling cascade or influencing the distribution and lateral mobility of BMP receptors, which may, in turn, affect the signaling outcome.

6.5. List of DE genes in the transcriptome analysis upon Sepitn9 depletion

Table 6-1. Top 100 DE genes regulated in C2C12 cells following Septin9 knockdown

C2C12			primary myoblasts		
Gene Name	**Log_2FC**	**p-adj. value**	**Gene Name**	**Log_2FC**	**p-adj. value**
Septin9	-1.35	2E-84	Car3	1.41	2E-53
Spp1	0.66	2E-45	C1qtnf3	1.32	2E-35
Mgp	0.86	3E-44	Ogn	1.43	9E-34
Angptl2	-0.79	3E-42	Gm52174	1.35	6E-22
Acta2	-0.58	3E-39	Tfdp1	-1.24	8E-20
Idh1	-0.79	6E-37	Rian	1.04	2E-17
Col18a1	-0.64	2E-35	Rian_1	1.04	2E-17
Gpi1	-0.76	2E-35	H19	0.71	5E-17
Thbs1	-0.56	7E-34	Mir675	0.73	1E-16
Tfdp1	-1.02	6E-32	Septin9	-1.17	7E-16
Ermp1	1.02	1E-29	Ankrd23	1.24	1E-13
Csnk1g2	-0.85	3E-28	Ucp2	1.13	2E-13
Rab31	-0.7	7E-28	Tnnc2	0.95	2E-13
Gprin3	-0.91	2E-24	Septin1	1.02	3E-13
Cyp51	-0.58	1E-21	Htra3	1.26	4E-13
Col6a3	-0.6	3E-19	Actc1	0.96	7E-13
Sel1l	-0.8	4E-19	Myl4	0.96	2E-12
Vcl	-0.51	8E-19	Crkl	-0.91	7E-12
Ets1	-0.85	2E-18	Itm2a	0.8	7E-12
Des	0.48	6E-18	Fxyd6	0.88	1E-11
Tmem65	-0.64	9E-18	Myl1	0.94	3E-11
Atp6v1a	-0.63	4E-17	Itgb1bp2	1.09	4E-11
Actg2	-0.62	1E-16	Kdm4a	-0.82	4E-11
Cdhr1	-0.67	1E-16	Atp6v1a	-0.79	9E-11
Cav1	-0.48	1E-15	Igfbp4	0.77	1E-10
Itfg1	-0.5	2E-15	Hspb7	1.34	2E-10
Csrp1	-0.48	9E-15	Rap1gap2	0.83	2E-10
Dstn	-0.44	2E-14	Csrp3	1.25	2E-10
Ndrg1	-0.53	2E-14	Sypl2	1.65	3E-10
Col12a1	-0.38	4E-14	Myog	0.83	6E-10
Wwtr1	-0.57	5E-14	Trdn	1.08	8E-10
Mir675	0.88	5E-14	Gadd45a	0.65	8E-10
Cks1b	-0.89	2E-13	Gatm	0.82	8E-10
Ctnnb1	-0.42	4E-13	Gatm_1	0.82	9E-10
2510039O18Rik_1	-0.9	1E-12	Gpi1	-0.63	1E-09
Ccnd3	0.56	1E-12	Hif1an	0.72	1E-09
Dhrs3	0.85	1E-12	Scand1	1.46	2E-09
Setd7	-0.56	1E-12	Sel1l	-0.77	2E-09
Tgoln1	-0.65	1E-12	Tnnt2	0.69	2E-09
Hmgcs1	-0.44	2E-12	Tpm2	0.64	2E-09
Malat1	0.37	2E-12	Sntb1	0.97	2E-09
Prss23	-0.4	3E-12	Slc19a2	-0.98	5E-09
Otub1	-0.79	3E-12	Tnnc1	0.76	5E-09
Get1	-1.04	3E-12	E230016M11Rik	0.69	8E-09
Htra3	0.91	7E-12	Tnni1	0.75	9E-09
Prrc2b	-0.5	7E-12	Col18a1	-0.55	9E-09
Fhl1	-0.46	8E-12	Otub1	-0.81	1E-08
Msln	0.41	9E-12	Tnnt3	0.78	1E-08
Rnf150	-0.49	1E-11	Sema3d	0.81	1E-08
Prelp	-0.81	1E-11	Fhod3	1.04	1E-08
Mki67	-0.48	1E-11	Igf2	0.74	2E-08
Sae1	-0.56	1E-11	Fabp3_1	0.88	3E-08
Sfrp2	-0.86	2E-11	Fabp3	0.88	3E-08
Acat2	-0.47	2E-11	Ankrd2	1.41	3E-08
Get1_1	-1.02	3E-11	Cd36	1.03	4E-08

Crabp2	0.91	3E-11	Adssl1	1	5E-08
Idi1	-0.39	5E-11	Hjv	0.97	5E-08
Grem1	-0.53	5E-11	Tmem38a	0.93	5E-08
Crkl	-0.85	5E-11	Mymx	0.78	7E-08
Kdm4a	-0.6	5E-11	Tnni2	0.83	1E-07
Acap2	-0.62	5E-11	Csnk1g2	-0.69	1E-07
Aqp1	-0.47	6E-11	Svbp	0.64	1E-07
Purb	0.36	6E-11	Tnnt1	0.61	2E-07
Myod1	0.54	1E-10	Klhl13	0.75	2E-07
Ywhae	-0.34	2E-10	Pgam2	0.9	2E-07
Lmod1	-1.01	3E-10	Ptgis	0.68	3E-07
Dhcr24	-0.43	4E-10	Jund	0.8	3E-07
Rbm24	1.05	6E-10	Jund_1	0.8	3E-07
Txndc5	-0.38	7E-10	Rn28s1	2.32	3E-07
Kif22	-0.75	1E-09	Des	0.53	3E-07
Slc1a3	-0.76	1E-09	Tnc	-0.69	3E-07
Tuba1a	-0.31	1E-09	Fibin	0.96	4E-07
Ccdc93	-0.8	2E-09	Capn6	1.4	4E-07
Gm38481	-0.39	3E-09	Trim72	0.7	4E-07
Ltbp3	0.34	3E-09	Txndc5	-0.62	5E-07
Synpo2l	1.47	3E-09	Kpna6	-0.61	5E-07
Dmp1	1.08	3E-09	Hes6	0.48	5E-07
Kpnb1	-0.44	3E-09	Bex1	0.9	5E-07
Tagln	-0.51	4E-09	Scx	0.71	7E-07
Map2k1	-0.59	5E-09	H2ac23	0.92	7E-07
Gpd1l	-0.71	5E-09	Fam78a	0.87	7E-07
Kpna6_1	-0.55	6E-09	H2ac24	0.93	8E-07
Prep	-0.4	7E-09	Cnbd2	1.14	8E-07
Stard4	-0.66	7E-09	Wwtr1	-0.63	8E-07
Cenpf	-0.47	9E-09	Jph1	0.83	9E-07
Klf6	-0.42	9E-09	Alg2	-0.98	1E-06
Idh2	-0.46	1E-08	Trip10	-0.76	1E-06
Kctd10	-0.39	1E-08	Rassf3	0.65	1E-06
Arpc1a	-0.58	1E-08	Tceal5	1.19	1E-06
Myog	1.11	1E-08	Stbd1	0.66	1E-06
Ankrd46	-0.59	1E-08	Tgfb3	0.74	1E-06
Irs1	-0.39	2E-08	Mgp	0.58	1E-06
Pten	-0.45	2E-08	Cdkn1a	0.5	2E-06
Hs6st1	-0.48	2E-08	Myl6b	0.59	2E-06
Zfp507	-0.79	3E-08	Tm6sf1	1.14	2E-06
Tsix	-0.7	3E-08	Get1_1	-1.01	2E-06
Timp1	0.42	3E-08	Lmod2	0.89	2E-06
Pcsk7	-0.45	3E-08	Tceal3	1.12	3E-06
Alg2	-0.88	3E-08	Inhba	-0.75	3E-06
Cbr2	-0.57	3E-08	Serpinb1a	1.19	3E-06

Table 6-2. Interactors of Septin2 in myoblasts and myotubes

Proliferating C2C12 S2IP/ IgG day 0					5 days of differentiation S2IP/ IgG day 5				
Protein name	Log_2 IgG_d0	Log_2 S2IP_d0	$-Log_{10}$ p-value	Log_2 FC difference	Protein name	Log_2 IgG_d5	Log_2 S2IP_d5	$-Log_{10}$ p-value	Log_2 FC difference
Neurl4	19.67	24.48	4.08	4.82	Neurl4	19.34	23.83	4.57	4.49
Hexim1	18.66	22.23	4.02	3.56	C1qc	18.80	23.09	3.79	4.30
Herc2	19.34	25.17	3.82	5.82	Map7d1	19.80	21.77	3.62	4.03
Prmt5	19.03	26.02	3.78	6.99	Hexim1	23.54	27.58	3.57	4.49
Aebp1	18.48	21.73	3.67	3.25	Septin6	18.34	22.83	3.19	2.92
Arhgap17	19.23	24.85	3.63	5.61	Septin8	21.05	17.88	3.08	3.42
Septin6	19.80	26.68	3.51	6.89	Gigyf2	23.42	26.34	2.93	3.37
Wdr77	19.51	24.76	3.48	5.25	Herc2	24.55	27.97	2.89	4.57
Cyld	18.73	20.80	3.42	2.07	Sec31a	18.21	21.58	2.76	5.52
Dhx36	18.97	24.04	3.30	5.07	Septin11	19.02	23.59	2.64	3.10
Ccar1	19.25	26.19	3.29	6.93	Tbc1d1	23.75	21.98	2.57	5.23
Larp4b	19.29	21.46	3.21	2.17	Nfat5	26.95	18.29	2.50	4.17
Nfat5	18.96	25.96	3.19	7.00	Septin7	23.67	29.19	2.49	2.93
Atad3	19.17	21.27	3.17	2.10	Larp1	26.79	29.89	2.45	4.89
Naca	19.51	23.34	3.13	3.83	Atxn2l	19.26	24.49	2.34	4.37
Matr3	19.02	22.69	3.11	3.67	Map1b	23.30	22.12	2.33	2.08
Caprin1	20.10	25.93	3.10	5.83	Septin10	19.31	23.47	2.32	3.41
Mov10	19.12	22.79	3.08	3.67	Ubap2l	28.42	31.35	2.28	3.47
C4b	19.05	22.01	3.03	2.97	Septin2	19.01	23.90	2.27	2.66
Sec13	19.01	22.92	2.98	3.91	Srsf7	21.72	18.71	2.26	4.13
Sec23ip	19.35	23.94	2.89	4.58	Septin9	19.06	20.63	2.21	2.66
Atxn2	19.37	22.57	2.82	3.20	Sec13	22.24	21.35	2.12	3.21
C1qc	19.50	22.70	2.68	3.20	Arhgap17	23.39	20.47	2.06	3.46
Atxn2l	19.43	25.26	2.68	5.84	Usp10	21.70	19.78	2.03	3.91
Btf3	18.78	22.77	2.60	4.00	Septin5	19.84	24.20	1.93	3.15
Sec31a	22.18	29.16	2.57	6.98	Dhx29	25.36	24.84	1.83	3.99
Kif1b;Kif1a	18.97	22.32	2.54	3.35	Upf1	19.02	17.91	1.80	2.01
Tax1bp1	20.08	22.70	2.48	2.62	Dhx30	25.63	27.71	1.79	2.51
G3bp2	18.97	22.20	2.48	3.23	Akap13	24.02	27.43	1.71	2.86
Reps1	18.98	22.65	2.46	3.67					
Zcchc6	19.15	21.29	2.40	2.14					
G3bp1	19.18	23.99	2.36	4.80					
Actn1	21.36	27.14	2.36	5.78					
Map7d1	21.04	27.18	2.33	6.14					
Dhx29	19.23	23.93	2.33	4.70					
Usp10	19.46	23.80	2.31	4.35					
Tbc1d1	19.59	23.56	2.28	3.97					
Gigyf2	19.13	23.34	2.24	4.20					
Srsf3	19.01	23.46	2.21	4.45					
Fxr1	19.52	22.05	2.16	2.53					
Farp1	18.87	21.99	2.16	3.13					
Anln	19.71	23.06	2.12	3.35					
Dhx30	19.43	22.86	2.12	3.43					
Rps25	19.47	23.08	2.09	3.61					
Polrmt	18.93	21.33	2.05	2.39					
Tns2	19.26	21.73	2.04	2.47					
Sbf1	19.27	23.39	1.99	4.12					
Aldh2	18.80	21.60	1.96	2.79					
Focad	19.04	21.98	1.95	2.94					
Supt5h	19.36	22.07	1.94	2.70					
Xrn1	18.70	21.71	1.94	3.01					
Septin8	20.87	27.48	1.93	6.61					
Septin11	24.13	29.43	1.92	5.30					
Smarca5	19.06	21.09	1.92	2.03					
Serbp1	19.48	21.75	1.90	2.27					
Larp1	20.99	25.39	1.85	4.40					
Soga1	19.43	22.40	1.85	2.97					
Map1b	24.97	28.63	1.85	3.66					
Clns1a	19.31	21.98	1.78	2.68					
Septin5	19.92	26.75	1.77	6.83					
Septin2	25.54	30.89	1.77	5.35					
Septin7	25.11	31.03	1.77	5.92					
Septin9	23.50	29.14	1.73	5.63					
Wdr60	18.81	21.67	1.73	2.86					
Septin10	20.72	26.81	1.72	6.09					

6.6. List of abbreviations

3D	Three-dimensional	CIP/KIP	CDK interacting protein/Kinase inhibitory protein
Acta1	α-actin 1	CK	Casein Kinase I
ActRIIA	Activin receptor type IIA	cKO	Conditional knock out
ActRIIB	Activin receptor type IIB	Creb	cAMP response element-binding protein
AFM	Atomic force microscopy	CRIK	Citron kinase
Akt	AKR mouse thymoma, Protein kinase B	CRISPR	Clustered regularly interspaced short palindromic repeats
ALK1-7	Activin receptor-like kinase 1-7	CTT	Carboxy-terminal tail
AMHR	Anti-Müllerian hormone receptor type II	Cycs	Cytochrome c
ANOVA	Analysis of variance	*D. melanogaster*	*Drosophila melanogaster,* Fruit fly
Apaf-1	Apoptotic protease activator factor 1	*D. rerio*	*Danio rerio,* Zebrafish
APC	Adenomatous Polyposis Coli	DAPI	4',6-diamidino-2-phenylindole
aPSM	Anterior presomitic mesoderm	Des	Desmin
ArhGAPX	Rho GTPase Activating Protein X	Dhfr	Dyhydrofolate reductase
Arp2/3	Actin-related protein 2/3	DIC/DILC	Dynein intermediate and light chains
ATCC	American type culture collection	DM	Dermomyotome
AtgX	Autophagy related X	DMEM	Dulbecco´s modified Eagle´s medium
ATP	Adenosine triphosphate	DMSO	Dimethyl sulfoxide
BAI1	Brain-specific angiogenesis inhibitor 1	DNA	Desoxyribonucleic acid
Bak1	Bcl2-antagonist/killer 1	Dnm1l/Drp1	Dynamin 1-like/ Dynamin-related protein 1
Bax	Bcl2-associated X protein	dNTP	Deoxynucleotide triphosphates
Bbc3	Bcl2 binding component 3	DPBS	Dulbecco's Phosphate Buffered Saline
Bcl2	B-cell leukemia/lymphoma 2	Duf	Dumbfounded
BH	BORG homology domain	Dvl	Dishevelled
BH3	Bcl2 homology 3	E	Embryonic day
bHLH	Basic helix-loop-helix	*E. coli*	*Escherichia coli,* Coliform bacterium
Bid	Bcl2 homology 3 interacting domain death agonist	E2F/DP1	E2F and DP1 transcription factors
BioID	*E. coli* biotin ligase	Eb1	End-binding protein 1
BMP	Bone morphogenetic protein	ECM	Extracellular matrix
BMPRII	Bone morphogenetic protein receptor type II	EDTA	Ethylenediaminetetraacetic acid
BNIP3	Bcl-2/adenovirus E1B interacting protein 3	Elmo	Engulfment and cell motility
BORG	Binders of Rho GTPases	EM	Electron microscopy
BSA	Bovine serum albumin	EMT	Endothelial to mesenchymal transition
C. elegans	*Caenorhabditis elegans,* Nematode	FA	Focal adhesion
C2C12	myoblast cell line	FACS	Fluorescence-activated cell sorting
C3H/10T1/2	Murine embryonic fibroblast cell line	FAK	Focal adhesion kinase
Ca2+	Calcium	FBS	Fetal bovine serum
Ca^{2+}	Calcium	FC	Founder cell
CAFs	Cancer-associated fibroblasts	FCF	Forchlorfenuron
CAM	Cell adhesion molecule	FCM	Fusion-competent myoblast
CAMKII	Calcium/calmodulin-dependent kinase II	FDB	*m. flexor digitorum brevis*
CaN	Calcineurin	FGF	Fibroblast growth factor
Car3	Enzyme carbonic anhydrase III	FoxO	Forkhead box O
Cas	CRISPR-associated systems	FRAP	Fluorescence recovery after photobleaching
Caspase	Cysteine-aspartic protease	Fst	Follistatin
CBR	Cytoskeletal binding region	Fzd	Frizzled
CC	Coiled-coil	g	Gram
Ccn	Cyclin	GAP	GTPase activating protein
Cdc	Cell division cycle	GDF11	Growth differentiation factor 11
Cdc42Ep	Cdc42 effector protein	GDI	Guanine nucleotide dissociation inhibitor
CDK	Cyclin-dependent kinase	GDP	Guanosine diphosphate
CDS	Coding sequence	GEF	GDP/GTP exchange factor
CE	Convergent extension	GFP/ YFP	Green/ yellow fluorescent protein
CEP170	Centrosomal protein 170	GM	Growth medium
CHP	Cyclic hydrostatic pressure	GO	Gene ontology

GSK3β	Glycogen Synthase Kinase 3β	MOMP	Mitochondrial outer membrane permeabilization
GST	Glutathione S-transferase	MPC	Myogenic progenitor cell
GTP	Guanosine-5´-triphosphate	MRF	Muscle regulatory factors
GTPase	GTP hydrolyzing enzyme	Mrf4	Muscle regulatory factor 4
GUVs	Giant unilamellar vesicles	mRNA	Messenger RNA
H. sapiens	*Homo sapiens,* Modern human	mRNA	Messenger RNA
HA	Human influenza hemagglutinin	Mrtf-A	Myocardin-related transcription factor A
HCC	Hepatocellular carcinoma	MSCs	Mesenchymal stem cells
HDAC6	Histone deacetylase 6	Mstn	Myostatin
HGF	Hepatocyte growth factor	MT	Microtubule
HHL16	Human hepatocyte line 16	MTOC	Microtubule organizing center
Hibris	Hbs	mTOR	Mammalian target of rapamycin
HR	Homology region	MuRF1	Muscle RING finger 1
HRP	Horseradish peroxidase	MuSCs	Skeletal muscle stem cells
Htra2	High temperature requirement protein a2	Myf5	Myogenic factor 5
HUVEC	Human umbilical vein endothelial cells	MyHC	Myosin heavy chain
IAP	Inhibitors of apoptosis	MyhX	Myosin heavy chain
ICB	Intracellular bridge	Myod1	Myogenic determination protein 1
Id3	Inhibitor of differentiation 3	MyoG	Myogenin
IF	Intermediate filament	MyoII	Myosin II
IFN-γ	Interferon-γ	MyoVI	Myo6 Unconventional myosin VI
Ig	Immunoglobulin	NCC	Neural crest cell
IGF1	Insulin like growth factor 1	Nck1	Non-catalytic region of tyrosine kinase 1
IL-1β	Interleukin-1β	NE	Nuclear envelope
IM	Intermediate mesoderm	Nfat	Nuclear factor of activated T-cells
INK4	Inhibitors of CDK4	Nf-κB	Nuclear factor kappa-light-chain-enhancer of activated B cells
IP3	Inositol triphosphate	NPC	Neuronal progenitor cell
IRM	Irre recognition Module	NPF	Nucleation promoting factor
IrreC	Irregular chiasm	NPMs	Neuromesodermal progenitors
IVM	Intravital microscopy	NTE/CTE	Amino- or carboxyl-terminal extension
Jamb	Junctional adhesion molecule B	Opa1	Optic-atrophy 1
JNK	c-Jun N-terminal kinase	OXPHOS	Oxidative phosphorylation
KD	Knockdown	p21	Cdk interacting protein 1/ WT p53-activated fragment 1, protein of 21 kDa
kDa	Kilo Dalton	PA	Polyacrylamide
KIFX	KinesinX	Pak	p21-activated kinase
Kirre	Kin-of-Irregular chiasm	PAR	Polyacidic region
kPa	Kilopascal	Pax3/7	Paired-homeobox 3/7
L	Liter	PB	Polybasic region
LEF	Lymphoid enhancer factor	PCP	Planar cell polarity
LINC	Linker of nucleoskeleton and cytoskeleton	PCR	Polymerase chain reaction
LIV	Low-intensity vibration	PDMS	Polydimethylsiloxane
LPM	Lateral plate mesoderm	PEG	Polyethylene glycol
LRP5/6	Low-density lipoprotein receptor-related protein	PFA	Paraformaldehyde
M. musculus	*Mus musculus,* House mouse	PGC-1	Peroxisome proliferator-activated receptor-gamma coactivator-1
Maldi/LC-MS	Matrix-Assisted Laser Desorption/Ionization /Liquid Chromatography-Mass Spectrometry	PH	Pleckstrin homology
MAP	Microtubule-associated protein	PI	Phosphatidylinositol
Mbc	Myoblast city	PI(3,4)P2	Phosphatidylinositol-3,4-bisphosphate
MBD	Microtubule-binding domain	PKC	Protein kinase C
MCF7	Michigan Cancer Foundation-7, breast ductal carcinoma cell line	PLC	Phospholipase C
MDCK	Madin-Darby canine kidney, epithelial cell line	P-loop	Phosphate-binding loop
mDia1	Mammalian Diaphanous related formin 1	PLS	Podosome-like structures
Mfn1	Mitofusin 1	PM	Plasma membrane
mm	Millimeter	PMSF	Phenylmethylsulphonyl fluoride
mM	Millimolar	pPMS	Posterior presomitic mesoderm
pRb1	Retinoblastoma1	SMAD	Sons of mothers against decapentaplegic

PS	Phosphatidylserine	Sns	Sticks-and-stones
PTM	Post-translational modification	SOCS7	Suppressor of cytokine signaling 7
Ptrh2	Peptidyl-tRNA hydrolase 2	Sqstm1/p62	Sequestosome1
RA	Retinoic acid	SRF	Serum response factor
Rac1	Ras-related C3 botulinum toxin substrate 1	SUE	Septin unique element
RGS	Regulator of G-protein signaling	TA	*m. tibialis anterior*
RhoA	Ras homolog family member A	TAN	Transmembrane actin-associated nuclear
RING	Really interesting new gene	TAZ	WW domain containing transcription regulator 1 (*Wwtr1*)
RNA	Ribonucleic acid	TCF	T cell factor
ROCK	Rho-associated coiled-coiled-containing kinase	TEMED	Tetramethylethylendiamine
ROS	Reactive oxygen species	TGFβ	Transforming growth factor beta
RPE1	Retinal pigment epithelial cells	TIRF	Total internal reflection fluorescence
Rst	Roughest	Tk1	Thymidin kinase1
RT	Room temperature	TNF-α	Tumor necrosis factor-α
S. *cerevisiae*	*Saccharomyces cerevisiae,* Baker's yeast	Tris	Tris(hydroxymethyl)aminomethane
SA	Silicone rhodamine (SiR)-actin	TβRII	TGFβ receptor type II
SA-RhoGEF	Septin-associated RhoGEF	U2OS	Osteosarcoma cell line
SBE	Smad-binding element	WA	Withaferin
SC	Satellite cell	WASP	Wiskott-Aldrich syndrome protein
SDS	Sodium dodecyl sulfate	WAVE	WASP-family verprolin-homologous protein regulatory complex
SDS-PAGE	Sodium dodecyl sulfate-polyacrylamide gel electrophoresis	WHO	World Health Organization
SF	Actin stress fiber	WIP	WASP-interacting protein
sgRNAs	Single guide RNAs	WNT	Wingless and Int-1
Shh	Sonic hedgehog	WT	Wild type
shRNA	Short hairpin RNA	*X. levis*	*Xenopus laevis,* African clawed frog
siRNA	Small interference RNA	XIAP	X-linked inhibitor of apoptosis
Six1/4	Sine oculis–related homeobox	YAP	Yes-associated protein
Sltr	Solitary	αTAT1	α-tubulin acetyltransferase
Smac	Second mitochondria-derived activator of caspase		

6.7. List of publications

Vladimir Ugorets, Paul-Lennard Mendez, Dmitrii Zagrebin, Giulia Russo, Yannic Kerkhoff, Georgios Kotsaris, Jerome Jatzlau, Sigmar Stricker, Petra Knaus. Dynamic remodeling of septin structures fine-tunes myogenic differentiation. iScience (2024). DOI: 10.1016/j.isci.2024.110630

Georgios Kotsaris, Taimoor H. Qazi, Christian H. Bucher, Hafsa Zahid, Sophie Pöhle-Kronawitter, **Vladimir Ugorets**, William Jarassier, Stefan Börno, Bernd Timmermann, Claudia Giesecke-Thiel, Aris N. Economides, Fabien Le Grand, Pedro Vallecillo-García, Petra Knaus, Sven Geissler & Sigmar Stricker. Odd skipped-related 1 controls the pro-regenerative response of fibro-adipogenic progenitors. NPJ Regen. Med. 8, 19 (2023). DOI: 10.1038/s41536-023-00291-6

Maria Reichenbach, Paul-Lennard Mendez, Carolina da Silva Madaleno, **Vladimir Ugorets**, Paul Rikeit, Stefan Boerno, Jerome Jatzlau, Petra Knaus. Differential Impact of Fluid Shear Stress and YAP/TAZ on BMP/TGF-β Induced Osteogenic Target Genes. Adv. Biol. 5, e2000051 (2021). DOI: 10.1002/adbi.202000051

Astrid G Petzoldt, Torsten W B Götz, Jan Heiner Driller, Janine Lützkendorf, Suneel Reddy-Alla, Tanja Matkovic-Rachid, Sunbin Liu, Elena Knoche, Sara Mertel, **Vladimir Ugorets**, Martin Lehmann, Niraja Ramesh, Christine Brigitte Beuschel, Benno Kuropka, Christian Freund, Ulrich Stelzl, Bernhard Loll, Fan Liu, Markus C Wahl, Stephan J Sigrist. RIM-binding protein couples synaptic vesicle recruitment to release sites. J. Cell Biol. 219, e201902059 (2020). DOI: 10.1083/jcb.201902059